



Reduction of Industrial Energy Demand through Sustainable Integration of Distributed Energy Hubs

A thesis submitted to The University of Manchester for

the degree of Doctor of Philosophy

in the School of Science and Engineering

2021

Julia Nataly Jimenez-Romero

School of Engineering

Department of Chemical Engineering and Analytical Science

Table of contents

TABLE OF CONTENTS	1
ABSTRACT	4
LIST OF FIGURES	1
LIST OF TABLES	4
NOMENCLATURE	6
Abbreviations	6
DECLARATION	7
COPYRIGHT STATEMENT	8
ACKNOWLEDGEMENT	9
DEDICATION	10
1 INTRODUCTION	11
1.1 Background	12
1.2 Research motivation.....	13
1.3 Key challenges for industrial decarbonization	14
1.4 Thesis objectives.....	16
1.5 Thesis outline	18
1.6 References.....	19
2 LITERATURE SURVEY	21
2.1 On-site utility systems.....	21
2.2 Mathematical optimization for utility systems.....	24
2.3 Utility systems design optimization	26
2.3.1 Time-dependency models.....	26
2.3.2 Multi-criteria models	28
2.4 Literature gaps	31
2.5 Methodology	32
2.5.1 Synthesis of utility systems considering heat integration	33
2.5.2 Design and operation of flexible industrial utility systems	34
2.5.3 Integration of sustainability criterion	35
3 SYNTHESIS OF INDUSTRIAL UTILITY SYSTEMS	41
3.1 Introduction to Contribution 1	42
3.2 Contribution 1	43
Abstract.....	44
Highlights	45

Keywords.....	45
Nomenclature.....	46
1. Introduction.....	52
2. Literature review.....	55
3. Problem statement and challenges.....	60
4. Problem Formulation.....	61
5. Case studies.....	80
6. Conclusions.....	94
7. Acknowledgments.....	94
8. References.....	95
Supplementary Information P1.....	101
3.3 Introduction to Contribution 2.....	135
3.4 Contribution 2.....	136
Abstract.....	137
Highlights.....	138
Keywords.....	138
Nomenclature.....	139
1. Introduction.....	144
2. State of the art.....	145
3. Problem Statement.....	152
4. Model formulation.....	155
5. MINLP decomposition: Optimization strategy.....	170
6. Case studies.....	184
7. Conclusions.....	195
8. References.....	196
Supplementary Information P2.....	202
4 DESIGN OF FLEXIBLE UTILITY SYSTEMS.....	208
4.1 Contribution 3.....	209
Abstract.....	210
Highlights.....	211
Keywords.....	211
Nomenclature.....	212
1. Introduction.....	216
2. Relevant literature.....	218
3. Problem statement and challenges.....	223
4. Methodology.....	226

5.	Case study definition.....	250
6.	Results and discussion.....	254
7.	Conclusions.....	267
	Supplementary Information P3.....	274
5	INTEGRATION OF SUSTAINABILITY CRITERION IN THE DESIGN OF UTILITY SYSTEMS.....	293
5.1	Contribution 4.....	294
	Abstract.....	295
	Keywords.....	296
	Nomenclature	296
1.	Introduction.....	300
2.	Scope of the paper and contributions	304
3.	Problem statement.....	304
4.	Methodology	306
5.	Case study definition.....	321
6.	Results and discussion.....	322
	References	335
	Supplementary Information P4.....	339
6	CONCLUSIONS AND FUTURE WORK	364
6.1	Conclusions.....	364
6.1.1	Modelling and optimization of industrial energy systems, accounting for heat integration and more realistic and accurate conditions and targets	364
6.1.2	Synthesis of flexible industrial utility system, able to operate under variable demand and supply, accounting for energy price fluctuations	366
6.1.3	Integration of economic and environmental sustainability criteria to the conceptual design of industrial utility systems	367
6.2	Future work.....	367
6.2.1	Incorporation of emerging technologies to the framework	368
6.2.2	Extending the framework to include other end-user sectors.....	369
6.2.3	Extending the framework to take into account location and piping	369
6.2.4	Extending the framework to account uncertainty in the conceptual design of industrial utility systems	369
6.2.5	Integration of other sustainability criteria for the design and optimization of industrial utility systems	369
6.3	Concluding remarks	370

Abstract

The aim of improving resource efficiency while offsetting the environmental impact of industrial processes is directly linked to the optimal management of heat and power flows. The heating requirements of industrial processes are primarily met by the process utility system, or more specifically: steam systems. In most industrial processes, steam systems are also the primary source of electricity generation. Therefore, it is often the case that several processes are linked to a common utility system that generates heat and power. Despite extensive research in this field, most sites' steam systems have developed without basic concerns being addressed, particularly in relation to design and operation. Moreover, if emissions are to be mitigated and driven to zero, fundamental changes in the design and operation of such systems are required. Future process utility systems should not only ensure efficient use of energy, but also shift to low carbon technology alternatives. To make current utility system designs more sustainable, an optimization framework is needed to provide cost-effective pathways to transition from current to future designs. The variety of technologies available, the amount of data, and their strong correlations make energy system design a complex optimization problem.

Furthermore, unlike other energy systems such as district heating, central grids, and local integrated energy systems, process utility systems present additional challenges for decarbonization. First, process industries require high amounts of process heating, usually far more than power: a heat/power ratio between 3.5 to 5.6 (Picón-Núñez and Medina-Flores, 2013). Second, heat at different temperature levels is typically required, especially between 100 400 °C (Fleiter et al., 2016; Naegler et al., 2015). These barriers, coupled with the need for flexible systems to cope with the variable demand and energy price fluctuations (due to renewable energy's unpredictable nature), make developing sustainable utility systems a challenging enterprise. To address this challenge, this thesis provides an optimization framework for the design and operation of process utility systems. It ranges from site-specific data (stream information, energy demands, energy sources and energy market prices) to the thermo-economic modelling of the energy conversion technologies (considering part-load performance), system design, operation strategy while providing an environmental and economic analysis. The framework also includes practical constraints for heat integration and steam system operation, such as steam superheating and desuperheating, selection of steam temperature, pressure distribution levels, and steam temperature constraints. Due to the increasing share of intermittent renewable energy supplies, electrical and thermal energy storage are included in the framework. A range of different energy resources is included (fossil and renewable) to allow an orderly transition from the current framework to a sustainable future. The resulting optimization

problem is complex and multi-objective and utilizes new approaches to solve the resulting nonconvex mixed-integer nonlinear programming problem. A bilevel solution strategy is provided to decompose the original problem in master and slave sub problems, maintaining computational tractability.

Moreover, to capture the short- and long-term dynamic nature of the integrated systems, a multi-period optimization approach is developed based on time-series aggregation of the input data. To address the issue of sustainability, the framework not only allows for cost optimization but also includes life-cycle analysis. The resulting multi-objective problem uses Pareto optimal curves to illustrate the distribution of costs and emissions for different system configurations that satisfy the site energy demand. Finally, the applicability of the methodology is demonstrated in relevant case studies from the industry. These highlight the importance of a holistic optimization approach for the accurate evaluation of the utility system design regarding economic and environmental impact. The methodological framework has the potential to provide informed decisions for the design of a wide range of energy systems that utilize energy integration.

References

- Fleiter, T., Steinbach, J. & Ragwitz, M. (2016) *Mapping and analyses of the current and future (2020 - 2030) heating/cooling fuel deployment (fossil/renewables)*, Germany: European Commission.
- Naegler, T., Simon, S., Klein, M. & Gils, H. C. (2015) 'Quantification of the European industrial heat demand by branch and temperature level', *International Journal of Energy Research*, 39(15), pp. 2019-2030.
- Picón-Núñez, M. & Medina-Flores, J. M. (2013) '16 - Process Integration Techniques for Cogeneration and Trigeneration Systems', in Klemeš, J. J. (ed.) *Handbook of Process Integration (PI)*: Woodhead Publishing, pp. 484-504.

List of Figures

Figure 1-1 Industry share of total energy and process related CO ₂ emissions in 2017. Source: (IRENA, 2020)	12
Figure 1-1 Scheme of a typical site utility system	22
Figure 1-1. Representation of Pareto curve	29
Figure 1-1 Research methodology for the conceptual design of sustainable industrial utility systems	33
Figure 1-1. Schematic representation of STYLE methodology	62
Figure 1-2. Algorithm for process stream data extraction and classification	62
Figure 1-3. Example of heat profile divided into temperature regions (a) heat sources and (b) heat sink processes.	65
Figure 1-4. Schematic representation of the superstructure	66
Figure 1-5. Algorithm for calculating steam mains' superheating	78
Figure 1-6. Procedure to estimate steam turbine outlet enthalpy	79
Figure 1-7. Total site profile of case study 1	81
Figure 1-8. Steam system configurations based on Varbanov et al. (2005) and the design proposed in this work	83
Figure 1-9. Utility system configuration with hot oil circuit.....	84
Figure 1-10. Total site profile of case study 2.....	86
Figure 1-11. Steam system configurations for case study 2	87
Figure 1-12. Steam system configuration for case study 2, integrating flash steam recovery.....	90
Figure 1-13 Effects of the integration hot oil circuit and/or FSR for the synthesis of utility system on: (a) steam and (b) fuel consumption, (c) power generation and (d) costs.	92
Figure 1-14. Effect of steam mains number on the utility system costs.	93
Figure 2-1 Simplified scheme of the superstructure for the synthesis of process utility system	153
Figure 2-2. Schematic representation of the superstructure	157
Figure 2-3. Modelling of capital cost of equipment by multiple linear correlations (PWA).....	159
Figure 2-4. Mass balance for i-th steam main	162
Figure 2-5. Schematic of process steam generation and use	163
Figure 2-6 Temperature – enthalpy representation of HRSG.....	166
Figure 2-7. Algorithm for calculating steam mains' superheating	173
Figure 2-8. STYLE algorithm for synthesis of industrial utility systems taking into account steam mains' operating conditions	173
Figure 2-9. Scheme of optimization strategy 2	184

Figure 2-10. Utility system configuration obtained with a successive MILP strategy or test 6 under scenario 2	190
Figure 2-11. Utility system configuration obtained with the bilevel decomposition strategy for test 6 under scenario 2	191
Figure 2-12. Optimized utility system configuration obtained by fixing the steam main pressures based on the information given by strategy 1.....	191
Figure 2-13 Best utility system configuration for Case Study 3, operating with 3 steam mains	194
Figure 3-1 Schematic representation of the proposed process utility system	224
Figure 3-2 Illustrative example of data set clustering for finding representative periods for the optimization of utility systems.....	227
Figure 3-3 Block diagram of syngas processing	235
Figure 3-4 Block diagram of biogas processing	237
Figure 3-5 Summary of the optimization framework to determine utility system design and operation, considering variable demand and energy price fluctuations.....	248
Figure 3-6 Nominal heating and cooling profile of each plant [based on Contribution 1]	251
Figure 3-7 Production profile of each plant across an operational year with daily resolution [adapted from Bungener et al. (2015) study]	251
Figure 3-8 Electricity profile across the year with hourly resolution	252
Figure 3-9 Electricity and natural gas purchase prices for European countries in 2019 Eurostat (2020).....	253
Figure 3-10 SSE and Silhouette measures as function of the number of typical design days using k-means and k-medoids methods	254
Figure 3-11 Electricity price fluctuation for the different design days.....	255
Figure 3-12 Energy site level across the time horizon for optimized case scenario II	258
Figure 3-13 Thermal site level across the time horizon for optimized case scenario II	260
Figure 3-14 Total (left) and electricity (right) annual costs for a range of electricity/natural gas price ratios from 1 to 7 and two scenarios characterized by interactions with the grid (with and without electricity export)...	260
Figure 3-15 Results for the optimal process utility systems design based on the electricity/natural price and two scenarios characterized by hydrogen storage (HS) investment costs	261
Figure 3-16 Annual site power profile represented by the design time periods at electricity/natural gas price ratio = 7 and three scenarios characterized by hydrogen storage (HS) installed costs	264
Figure 3-17 Results for the optimal systems design for a range of natural gas and electricity price variations (price reference: 24.30 [€·MWh ⁻¹]). Subfigures show the total capacities of the selected technologies (a) packaged boilers, (b) electrode boilers, (c) fluidized bed, (d) stoker boiler, (e) heat recovery steam generators and (f) gas turbines and (g) steam turbines.....	265
Figure 3-18 Annual site primary energy consumption/generation for a range of natural gas and electricity price variations (price reference: 24.30 [€·MWh ⁻¹]).....	267
Figure 4-1 Schematic representation of the proposed process utility system superstructure	305

Figure 4-2 Scheme of the considerations for the industrial utility systems assessment	307
Figure 4-3 Boundaries for the equipment of the utility systems	308
Figure 4-4 System boundaries for the feedstock of the utility system	309
Figure 4-5 European electricity mix IEA (IEA, 2020)	311
Figure 4-6 Load duration curves of site energy demand for a typical year	322
Figure 4-7 TAC oriented optimal design per year of operation: (a) Costs contribution (in m€·y ⁻¹) and (b) electricity and fuel consumption, having as reference Scenario 1 w/o FSR design.	324
Figure 4-8 Environmental lifecycle assessment of best TAC-oriented design (Scenario 2 with FSR), considering a year of operation	325
Figure 4-9 Contribution analysis of: (a) Base case design and (b) TAC- oriented – Scenario 2 + FSR, considering a year of operation (For impact nomenclature see Figure 4-8)	326
Figure 4-10 TAGWP oriented optimal design per year of operation: (a) Costs contribution (in m€·y ⁻¹) and (b) electricity and fuel consumption, having as reference Scenario 1 w/o FSR design.	329
Figure 4-11 Contribution analysis of the TAGWP oriented design (For impact nomenclature see Figure 4-6)	330
Figure 4-12 Life cycle environmental impacts of industrial utility systems per year of operation (For impact nomenclature see Figure 4-6)	331
Figure 4-13 Pareto curve of the multiobjective optimization. Representation of the TAC and TAGWP variation with respect to the best TAC oriented design	332
Figure 4-14 Pareto curve of the multiobjective optimization: (a) thermal generation units capacity (b) Power generation units capacity, at each design point,	333

List of Tables

Table 1-1 Summary of relevant contributions in the synthesis and design of industrial utility systems, considering time-dependency.....	27
Table 2 Summary of research contributions in multi-objective optimization models for the design of utility systems.....	30
Table 3 Lifecycle criteria with their corresponding issues and indicators.....	35
Table 1-1. Temperature specifications for the steam system.....	81
Table 1-2. Steam system targets for the propose methodology in comparison with literature	84
Table 1-3. Comparison of utility system designs including hot oil circuit.....	85
Table 1-4. Comparison of steam system designs for case study 2	88
Table 1-5. Economic and operational effect of hot oil circuit on the steam system design for case study 2....	89
Table 1-6. Economic and operational effect of flash steam recovery on the steam system design for case study 2.....	90
Table 1-7. Comparison of utility system targets including hot oil circuit and/or FSR for case study 2	91
Table 2-1. Main equations of additional utility components	168
Table 2-2. Types of non-linearities in the proposed model.....	169
Table 2-3. <i>Modelling coefficients for the estimation of the isentropic enthalpy change across the steam turbine*</i>	179
Table 2-4. Modelling coefficients for the nonlinear calculation of the superheating temperature at VHP level	180
Table 2-5. Modelling coefficients for the linear estimation of the superheating temperature at VHP level ..	181
Table 2-6 Model parameters and statistics of the six test examples.....	186
Table 2-7. Computational results of the test problems	187
Table 2-8 Comparison of the steam properties values calculated with the presented model against the real values.	192
Table 2-9. Best solution found for 's case study with three steam mains.....	192
Table 3-1 Technical characteristics of energy storage technologies considered in this work	242
Table 3-2. Site specifications for the steam system.....	252
Table 3-3.Scenario specifications for sensitivity analysis	253
Table 3-4. Test levels for electricity and natural gas nominal prices and variations	254
Table 3-5. Costs and equipment capacities for the base case and optimized case under different scenarios .	256
Table 3-6. Utility system costs as a function of the investment costs of.....	263
Table 4-1 Inventory of the main components of the utility system.....	308
Table 4-3 Emissions from fuel combustion.....	311

Table 4-4 By-products from waste biomass	312
Table 4-5 Model coefficients of equipment costs	316
Table 4-6 Model coefficients of energy storage costs	318
Table 4-7 Fuels and resources prices	318
Table 4-7 Optimization results based on minimum total annualized cost (TAC)	323
Table 4-8 Optimization results based on minimal total annual global warming potential (TAGWP)	328

Nomenclature

Abbreviations

EII	Energy-intensive industry
LCA	Life cycle assessment
LP	Linear programming
MIP	Mixed integer programming
MILP	Mixed integer linear programming
MINLP	Mixed integer nonlinear programming
MOO	Multi-objective optimization
NLP	Nonlinear programming
SOO	Single-objective optimization

Declaration

No portion of the work referred to in the thesis has been submitted in support of an application for another degree or qualification of this or any other university or other institute of learning.

Julia Nataly Jimenez Romero

Copyright statement

- i. The author of this thesis (including any appendices and/or schedules to this thesis) owns certain copyright or related rights in it (the "Copyright") and s/he has given The University of Manchester certain rights to use such Copyright, including for administrative purposes.
- ii. Copies of this thesis, either in full or in extracts and whether in hard or electronic copy, may be made only in accordance with the Copyright, Designs and Patents Act 1988 (as amended) and regulations issued under it or, where appropriate, in accordance with licensing agreements which the University has from time to time. This page must form part of any such copies made.
- iii. The ownership of certain Copyright, patents, designs, trademarks and other intellectual property (the "Intellectual Property") and any reproductions of copyright works in the thesis, for example graphs and tables ("Reproductions"), which may be described in this thesis, may not be owned by the author and may be owned by third parties. Such Intellectual Property and Reproductions cannot and must not be made available for use without the prior written permission of the owner(s) of the relevant Intellectual Property and/or Reproductions.
- iv. Further information on the conditions under which disclosure, publication and commercialisation of this thesis, the Copyright and any Intellectual Property and/or Reproductions described in it may take place is available in the University IP Policy (see <http://documents.manchester.ac.uk/DocuInfo.aspx?DocID=487>), in any relevant Thesis restriction declarations deposited in the University Library, The University Librarys regulations (see <http://www.manchester.ac.uk/library/aboutus/regulations>) and in The University's policy on Presentation of Theses.

Acknowledgement

I would like to express my heartfelt gratitude to everyone who has helped me along this way. First and foremost, I would like to thank my supervisors, Professor Robin Smith and Professor Adisa Azapagic, for their kindness and encouragement throughout the process. Their patience and support over the years have been invaluable, especially during the time when I had almost given up hope. I would also like to thank Simon Perry for his kind help from the onset and willingness to share his experience. My deepest gratitude to Professor Truls Gundersen and the Research Council of Norway for the financial support, which made this research possible.

Thanks also to all the staff and friends from the Centre for Process Integration. Without you this journey wouldn't be the same. I will always treasure all the talks, adventures and moments that we spent together. To my friends back home who not only support me during this adventure but also share experiences and support

To David, my partner, who stood by me and supported me throughout this entire experience. Your encouragement and patience thru this rollercoaster ride has given me the strength to persevere and face any inconvenience. There are no words that can express how much I love and appreciate you.

Last but not least, I'd like to thank my family for their patience and support at all times. Especially to my parents, Bernardo and Natividad, because I would not be where I am today without their unconditional love and support. *Gracias familia porque a pesar de la distancia siempre me he sentido acompañada y querida, los amo!*

Dedication

To my family, friends, and David.

CHAPTER 1

Introduction

“The cheapest and cleanest energy choice of all is not to waste it”

Economist (2015)

Overview

The motivation and objectives for the research presented in this thesis, namely reduction of industrial energy demand through the design and optimization of process utility systems, are discussed in this chapter. The increasing need to enhance energy supply and usage efficiency in process industries is inextricably connected to the efficient control of heat and power flows. The majority of industrial operations rely on utility networks to meet their energy requirements. As a result, optimizing the design and operation of such systems is critical for reducing its energy demand and with it, the corresponding greenhouse gas emissions related. Thus, optimum design of process utility systems is crucial for ensuring a sustainable future. Nevertheless, to achieve the optimal utility system design that meets industrial requirements while minimizing environmental effect and costs, new methods and decision-support systems must be developed. The present thesis is focused on creating a broad framework that incorporates various energy sources and technologies in order to help the energy transition from current systems to the future ones in a sustainable basis. Prior to discussing the methodology, this first chapter establishes the background for the issue to being addressed.

1.1 Background

To date, the industrial sector is responsible for 38% of global energy use (IEA, 2018). High-energy consumption, combined with heavy reliance on fossil fuels across the industrial value chain, has resulted in large emissions of a variety of pollutants to the soil, water and air. For instance, industry accounted for 28% of the total CO₂ emissions in 2017 (IRENA, 2020). However, four energy-intensive industries (EII) - iron & steel, (petro) chemicals, cement, and aluminum - accounts for around 75% of total industrial emissions (IRENA, 2020). The (petro) chemical industry alone uses one-third of global energy consumption and generating 3.2 % of the total greenhouse gas emissions (1.2 Gt CO₂ per year), as illustrated in Figure 1-1. Consequently, the process industry is critical for attaining climate neutrality and fulfilling the Paris Agreement's sustainable development objectives. Carbon neutrality requires decarbonization of the process sector.

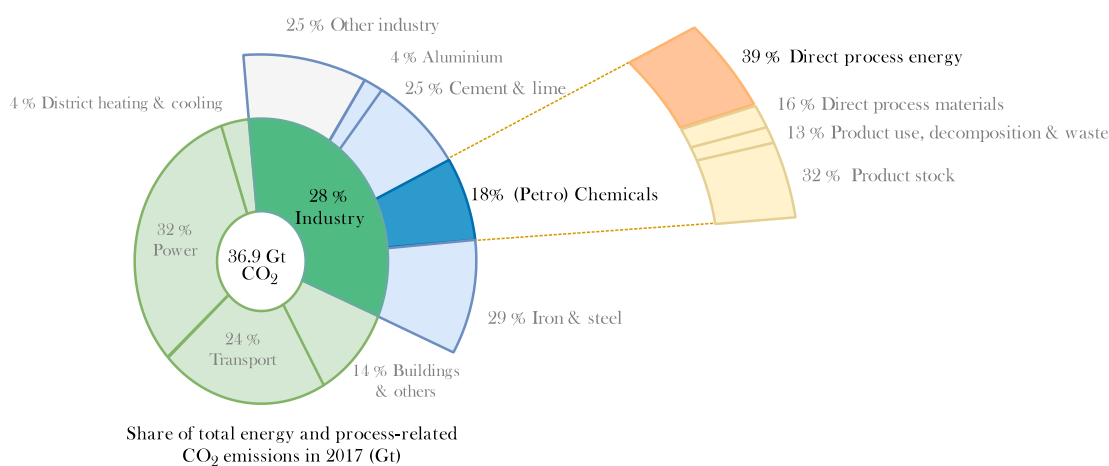


Figure 1-1 Industry share of total energy and process related CO₂ emissions in 2017. Source: (IRENA, 2020)

Approximately 20% of EII emissions are caused by process heating at medium-temperature heat (100-500 °C) provided by gas- or coal-fired steam or heating oil boilers. Moreover, low-temperature heat (below 100 °C) is produced by boilers or derived from high-temperature waste heat (Pee et al., 2018). Apart from EIIs, other energy hogs include food and tobacco, paper and pulp, and nonferrous metals, where the majority of energy consumed (and thus the primary source of emissions) comes from fossil fuels to provide low- and medium-temperature heat, with the exception of the nonferrous metals industry, which relies on electricity to meet its high-temperature heat requirements. Additionally, power imports in these industries account for about one-third of overall energy consumption and nearly half of total CO₂ emissions (indirect emissions). As consequence, industrial utility systems, more specifically, steam systems, are one of the largest energy consumers --when compared against the energy requirements of individual industrial units--, accounting for about 30% of the global energy used in industrial plants (Yang and Dixon, 2012). Therefore, reducing emissions and eventually reaching zero will need substantial efforts on the part of the industrial sector and the utility system.

There are no single or simple solutions to putting the industry on a sustainable path to net-zero emissions. Reducing global CO₂ emissions will require a broad range of different technologies working across all sectors of the economy in various combinations and applications. In this context, a wide variety of new approaches is being explored to minimize the environmental impact of process industry. These include but are not limited to: (i) reducing energy and water demand while improving energy efficiency, (ii) moving away from fossil fuels and towards synthetic and/or renewable carbon feedstock --such as biofuels and green hydrogen--, (iii) electrification of the industrial processes, and (iv) using circular economy concepts to minimize waste. Being the first two of special interest in this research. Note that while reducing energy demand and intensity of use will not result in zero emissions in and of itself, it will help decrease the challenge's overall size and expense and enhance the energy transition to low-carbon technology.

1.2 Research motivation

The urge to enhance industrial processes' energy performance and environmental effect is inextricably connected to the efficient generation and use of heat and power. In this context, steam systems are primarily used to meet the industrial heating requirements at different temperature levels. Steam systems are also the main source of power generation in the majority of industrial processes. As a result, it is very usual for several processes to be connected to a single utility system in order to produce heat and power. Although steam systems are a mature subject, the steam systems at the majority of sites have developed over many years without basic issues about the design and operation of the utility system being addressed (Smith, 2016). This in combination with the increasing environmental limitations and energy supply/demand imbalances call for an ongoing assessment of current utility systems, as well as continuous efforts to enhance their efficiency, operational flexibility, and range of application. Some of the main points to consider are the following:

- (i) Industrial sites (or industrial clusters) are becoming more appealing not only for reducing industrial energy requirements -- through interplant heat use and on-site power generation-- but also as potential sources for other sectors such as district heating and micro grid generation. Although there are numerous studies on site energy integration, the optimal selection of steam levels in terms of number and operating conditions (pressure and temperature) has been generally overlooked/oversimplified, without taking into account the strong interrelationships between the utility system and the site processes and its effect on the energy targets and site performance.
- (ii) The integration of different business areas into industrial sites, each of them operating independently from one another and with different planning (in terms of starting-up, shut-downs, product production, among others), entails to a site with variable energy demand and supply across the time horizon. This, along with greater energy price volatility resulting from the

increasing share of renewables in the power sector, necessitates the development of flexible utility system designs capable of dealing with these variations effectively.

- (iii) Industrial decarbonization is becoming a priority for many process sectors. Under current energy markets, enhancing energy efficiency and decarbonization is critical not only for climate change mitigation but also for maintaining industry competitiveness. Although the market for low-carbon energy sources and technologies is expanding, it is still unclear which technology or combination of technologies is most suited for future utility systems, since the overall environmental and economic impacts are unknown. This, combined with the strong influence of site energy requirements and availability, utility prices, and regulatory framework (in terms of incentives/taxes) on the utility system configuration and operation, leaves unknown the optimal combination of technologies that may become economically viable for a particular industrial site.
- (iv) Finally, analysis of potential modifications to the configuration and/or operation of an existing system to reduce its energy requirements, operating costs, and/or emissions, requires a holistic approach where the different components of the utility system, along with the potential cogeneration and site heat recovery are address simultaneously.

Therefore, to enhance industrial sustainable use of energy taking into account the above-mentioned points, a comprehensive process integration framework that includes different energy sources and technologies options is required. Therefore, this work set out a realistic design framework in which both fossil and low-carbon technologies are considered to facilitate the transition from the present state of high CO₂ emissions to future sustainable utility systems.

1.3 Key challenges for industrial decarbonization

Despite recent efforts, progress in industrial sector decarbonization has been limited to date (IRENA, 2020). The International Renewable Energy Agency (IRENA) and other institutes denote the difficulties of EIIs to be decarbonize. EII transition to climate-neutrality deserve special interest, not only because of their large energy use and CO₂ emissions, but also due to the additional challenges involved, in comparison with other sectors. Some of the main barriers are listed below:

- i. **Heating requirement within industry is often far higher than the power demand.** Site power to heat ratios can vary typically between 0.03 and 3 depending on the nature of the process. For instance, (petro) chemicals has a power to heat ratio of typically between 0.2 and 0.5 but can goes as low as 0.1. (Picón-Núñez and Medina-Flores, 2013; Smith, 2016)
- ii. **Heating requirement and temperature barrier.** Process heating is usually required at medium temperatures (100 – 400 °C) (Fleiter et al., 2016; Naegler et al., 2015). Limiting many of renewable heat technologies due to temperature barrier. Solar collectors and

geothermal sources, for example, can only offer relative low-temperature heat (currently at early stages of technology development >250 °C) and are geographically constrained. Furthermore, the locations of these resources are seldom associated with substantial energy demand centers. Consequently, less than 0.02 % of solar energy is used to meet current industrial heat requirement (IEA, 2020).

In terms of electrification, heat pumps have appeared as a potential alternative. Nevertheless, to date, heat pumps are unable to provide the necessary temperature or amount of heat for industrial processes, and further improvements are still required (IRENA, 2020). Moreover, due to the wide range of temperature at which heat is required. Usually, utilities at different temperatures are used. For instance, steam can be generated at a higher temperature (either by boiler or by process heat recovery) and cascaded down to be used at lower temperatures.

- iii. **EIIs Heterogeneity.** It is still uncertain the technologies that might become more competitive in each of the industry. Early adopters of new unproven technologies with long payback periods risk economic damage if technologies lack maturity or cannot be cost competitive in the long run (Gerres et al., 2019).
- iv. **Absent major technology breakthroughs.** Technologies and other abatement options that could contribute to a further reduction of the carbon intensity in EIIs are not available on commercial scale, yet. Renewable energy technologies in their mature stages struggle to reach competitive costs, a scenario that is exacerbated when early-stage advances are analyzed. Despite the progress being made so far, new technology solutions are at least 5 to 10 years away, which could delay industry investment in low carbon technologies.
- v. **Conservative industry.** Primary process equipment is characterized by high initial investment costs with a long design life of individual equipment of more than 20 years. The EII is closely linked to the metal and construction sector. These industries are considered as more conservative with regard to changes than other industries (Neuhoff et al., 2015). Breakthrough technology innovation in EII sector can take 5–20 years after relevant innovations had reached economic viability, before becoming the dominant new process design, (as shown in the cement and glass industries study by Anderson and Tushman (1990)).

In addition to these challenges, the increasing share of renewables in the power sector and the liberalization of the energy market have increased the complexity of utility system design and operation. As intermittent energy sources like wind and solar grow more common, so does the demand for grid services. Due to the increasing dependence on non-constant resources, power levels may fluctuate often. Power utilities and other system operators are facing a growing and urgent demand for more power to maintain the stability and security of the electric grid. Higher generating capacity comes with at the expense of higher capital investment, therefore looking for cost-effective

ways to guarantee reliability creates an opportunity for industrial sector. On one hand, storage technologies are becoming more widely acknowledged not for only smoothing the intermittent renewable energy sources, but also as flexibility measures to smooth the demand and supply balance. On the other hand, industrial utility systems are also a viable option to increase resiliency and flexibility of energy sector and enhance distributed infrastructures that cut down on transmission losses and allow greater synergy between energy supply and demand by customizing the features of an energy conversion system to better meet end-user requirements. Industrial utility systems are usually sized to meet the site energy demand (or most of it). However, with an additional investment, industrial utility systems may be built with sufficient extra producing capacity to serve the electric grid. Due to the continuous operation of site utility units, they can react quickly if grid services or additional power are required. Aside from the additional revenue, industrial sites with flexible utility systems, can not only save money on energy, but also a better control on plant operations, preventing any power outages, which may interrupt production. Moreover, the availability of low-cost on-site power generation may enable to enhance process electrification. However, the investment decisions strongly depend on energy demand, fuel prices, technical development, governmental interventions and technology acceptability. It is critical, then, that utility facilities be designed and operated in such a manner that energy efficiency is maximized while also considering all operational and environmental limitations, as well as economic factors.

Therefore, the design and operation of utility systems should be supported by methodology, current technologies, availability, industrial requirements and regulatory framework. Identifying realistic enhancements and potential barriers -- techno-economical and environmental, as well as methodological -- to the implementation of integrated systems.

1.4 Thesis objectives

With energy being a non-replaceable and essential industrial component, together with the increasing environmental constraints, requires an efficient use of energy. Additionally, as energy sector become more decentralized and intermittent energy sources become more prevalent, industrial utility systems offer greater opportunities for cost-effective solutions but also becomes more complex. These systems must be flexible enough to handle changing technological, economic, environmental, regulatory, and load conditions. As a result, new technologies (including daily to seasonal storage units) and multiple energy vectors (natural gas, electricity, heat, and biomass) must be integrated and adequately reflected. Additionally, modelling specific market conditions may be beneficial. As a result, approaches that accurately depict such energy systems and offer decision support for its design and optimization are required.

In this context, this project aims to develop a decision-support framework capable of designing and optimizing integrated industrial energy systems in order to assist process industries in reducing their energy consumption and greenhouse gas emissions while taking techno-economic and environmental sustainability criteria into account. The specific objectives of this research work are listed below:

Objective 1

To model and develop a framework for the synthesis of industrial energy systems, accounting for site heat integration and more realistic and accurate conditions and targets.

Questions to address:

- (i) At what temperature and pressure level should steam be generated and used?
- (ii) What are the optimum quantities and levels of heating and cooling utilities?
- (iii) What is the impact of steam main temperature and pressure in the site-wide heat recovery and cogeneration potential?
- (iv) How do the number of steam main and their operating conditions affect the design and configuration of utility system?
- (v) How can heat recovery and cogeneration targets be addressed simultaneously in the design and optimization of industrial utility systems? What methodology approach should be taken to address such issues?

Objective 2

To design a flexible utility system, able to operate under variable demand and supply, accounting for energy price fluctuations.

Questions to address:

- (i) How do the configuration and operation of the energy system change if time-variant energy demand and energy price fluctuations is taken into consideration? How can multi-period optimization aid this decision-making process?
- (ii) How does energy storage impact on the design and operation of utility systems?
- (iii) How the energy price market affects the design and operation of industrial utility system?

Objective 3

To develop a systematic approach to assess the optimal sustainability level for conceptual design of industrial utility systems, accounting for techno-economic and environmental metrics.

Questions to address:

- (i) What are the economic and environmental impacts of industrial utility systems? How can these objectives be reconciled or traded-off?
- (ii) Under current scenario, is carbon neutrality a feasible and cost-effective target for process utility systems?

Despite the application of the methodology is based on industrial processing sites, the proposed framework can be extended to support the design and assessment of any distributed energy system, where heat (steam) is required at multiple levels -- for example, locally integrated energy sectors (LIES). The general framework can be extended to consider other technologies such as waste-to-energy systems, which allows for an impact analysis in relation to the synthesis of future energy system.

1.5 Thesis outline

This thesis is organized following the requirements for the “Journal Format” of The University of Manchester. The thesis contains six chapters that are organized as follows:

Chapter 2 focuses on utility system problems. The findings of the theoretical and bibliographic background are reviewed and discussed. A review of the open research literature on total site energy integration for industrial energy systems is presented, to show the research gaps and the general methodology of the project.

Chapter 3 includes two contributions (Contribution 1 and Contribution 2) of this thesis, which provides two novel and comprehensive superstructure optimization methodologies to synthesize site-wide heat recovery industrial utility systems with the steam network optimal operating conditions, taking into account the interactions between the utility system and the site processes. Both models accounts for more practical and realistic features, such as boiler feedwater preheating, steam superheating and steam de-superheating. Additionally, problems addressing non-isothermal mixing and utility level selection are also considered. In addition, Contribution 2 provides a bilevel decomposition strategy to address large-scale nonlinear mixed integer problems, resulting from the introduction of steam temperature as a design variable.

An extension of the methodology proposed in chapter 3 is applied to time-dependent energy demand and electricity price fluctuations in chapter 4. Contribution 3 adopts a multi-period approach to capture the short- and long-term dynamics of energy demand, storage, and supply while considering the most suitable combination of energy conversion technologies and utility temperature levels to meet the energy requirements across the time. The proposed methodology also includes a time-series aggregation algorithm to reduce the number of time steps while retaining an appropriate level of detail. A set of conventional and low-carbon technology options, as well as both thermal and electrical energy storage, are integrated to the optimization framework.

Chapter 5 presents Contribution 4, which integrates life-cycle environmental assessment to the optimization framework. The decision-support tool brings together the economic and environmental objectives to emphasize holistic design by proposing a methodology for the simultaneous consideration of economic and environmental impact. The different utility system designs under different market scenarios is analyzed.

Lastly, a summary of the main outcomes and limitations of this research work, together with potential improvements and/or future directions are discussed in Chapter 6.

References

- Anderson, P. & Tushman, M. L. (1990) 'Technological Discontinuities and Dominant Designs: A Cyclical Model of Technological Change', *Administrative Science Quarterly*, 35(4), pp. 604-633.
- Economist, T. (2015) 'Invisible fuel', *The Economist*.
- Fleiter, T., Steinbach, J. & Ragwitz, M. (2016) *Mapping and analyses of the current and future (2020 - 2030) heating/cooling fuel deployment (fossil/renewables)*, Germany: European Commission.
- Gerres, T., Chaves Ávila, J. P., Llamas, P. L. & San Román, T. G. (2019) 'A review of cross-sector decarbonisation potentials in the European energy intensive industry', *Journal of Cleaner Production*, 210, pp. 585-601.
- IEA (2018) *CO2 Emissions from Fuel Combustion 2018*: International Energy Agency.
- IEA (2020) *Concentrating Solar Power (CSP)*, Paris: IEA.
- IRENA (2020) *Reaching zero with renewables: Eliminating CO2 emissions from industry and transport in line with the 1.5 C climate goal*, Abu Dhabi: International Renewable Energy Agency.
- Naegler, T., Simon, S., Klein, M. & Gils, H. C. (2015) 'Quantification of the European industrial heat demand by branch and temperature level', *International Journal of Energy Research*, 39(15), pp. 2019-2030.

- Neuhoff, K., Ancygier, A., Ponsard, J.-P., Quirion, P., Sabio, N., Sartor, O., Sato, M. & Schoop, A. (2015) 'Modernization and innovation in the materials sector: Lessons from steel and cement', *DIW Economic Bulletin* 5(28/29), pp. 387-395.
- Pee, A. d., Pinner, D., Roelofsen, O., Somers, K., Speelman, E. & Witteveen, M. (2018) *Decarbonization of industrial sectors: the next frontier*: McKinsey & Company.
- Picón-Núñez, M. & Medina-Flores, J. M. (2013) '16 - Process Integration Techniques for Cogeneration and Trigenation Systems', in Klemeš, J. J. (ed.) *Handbook of Process Integration (PI)*: Woodhead Publishing, pp. 484-504.
- Smith, R. (2016) 'Steam Systems and Cogeneration', *Chemical Process: Design and Integration*. Second ed. Chichester: John Wiley & Sons, Ltd, pp. 583-646.
- Yang, M. & Dixon, R. K. (2012) 'Investing in efficient industrial boiler systems in China and Vietnam', *Energy Policy*, 40, pp. 432-437.

CHAPTER 2

Literature survey

In general, when it comes to industrial energy supply, distributed energy systems are one of the most effective methods for increasing energy efficiency (Liu et al., 2014; Ganschietz, 2021). Distributed energy systems allow industrial processes to utilize locally available resources to meet on-site energy requirements, decreasing their dependence on external energy (particularly electricity), cutting operating costs and improving supply reliability. These benefits, however, may not be achieved unless a comprehensive assessment of the design and operation of the system is performed. To assess the design and operation of distributed/decentralized energy systems, a popular method used in the literature is the 'energy hub' modelling and conceptualization approach (Mohammadi et al., 2017). An 'energy hub' is a self-contained entity that transforms energy from one form to another (or others) to satisfy the energy requirements of users within its boundaries. Therefore, the term 'energy hub' used throughout this thesis refers specifically to on-site utility systems where primary energy (e.g. fuels and electricity grid) is converted to useful forms such as mechanical, thermal or electrical energy.

2.1 On-site utility systems

In most industrial sites, the on-site utility system operates through steam to satisfy process heating, generate power and drive machinery (Brueske et al., 2012). Steam is widely used because of its many features: high heat content (latent heat), wide range of temperature operation, easy control and distribution, non-toxicity, among others (Smith, 2016). Although, site utility system configuration varies greatly, a typical schematic is illustrated in Figure 1-1. In such systems, fuel combustion through boilers or gas turbines coupled with heat recovery steam generators (HRSG) to generate steam at high temperatures. Depending on the heat temperature requirement of the site, steam can be downgraded to lower steam pressures/temperatures through let-down stations or steam turbines (to generate additional power). Noticeably, site utility systems get advantage of higher efficiency when generating both heat and power from the same fuel, also known as cogeneration. However, generation of only heat and power import from the grid can also be found in some cases (Brueske et al., 2012). Utility system has strong interactions within the site processes. These interactions can be exploited to maximize heat recovery, where steam act as intermediate fluid to recover excess heat from one process and supply it to another.

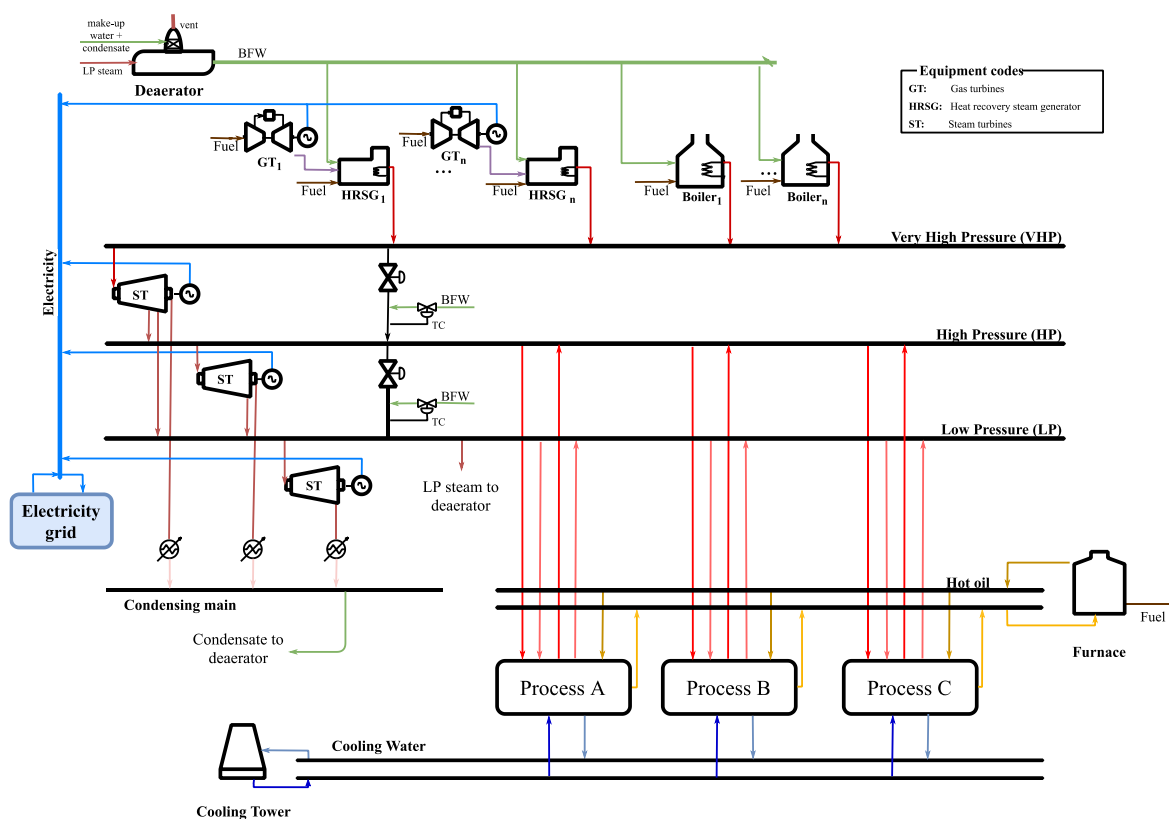


Figure 1-1 Scheme of a typical site utility system

Additionally, as the energy sector evolves to meet technological, economic, and environmental restrictions, process utility systems must do the same. Integration of additional technologies (including energy storage) and energy sources (natural gas, electricity, biomass) necessitates the development of systematic approaches for the synthesis, design, and operation of on-site utility systems that maximizes their benefits and potential. Numerous studies have been conducted in this regard. Whereas the majority of approaches fall into one of three categories -or a combination of them- (Frangopoulos, 2018):

- (i) (Meta)heuristics
- (ii) Insight-based
- (iii) Mathematical programming (superstructures)

Heuristic methods identify feasible configurations by using principles based on engineering expertise and/or physical concepts (Andiappan, 2017; Frangopoulos, 2018). Then, the solution performance can be enhanced via systematic modifications. Modifications may be made using specialized methods or evolutionary algorithms, in which each change is evaluated against an evaluation function (also called fitness function) and the system with the highest performance is selected. In terms of evolutionary algorithms, the most well-known method falls within the category of stochastic algorithms, which search the solution space using a collection of points (Coello et al., 2007).

Although, multiple starting points may theoretically converge to global optimality if run long enough time, there are currently no safeguards against being “stuck” in local optima. Moreover, the degree of optimality cannot be guaranteed.

Insight-based methods integrate thermodynamic and other physical concepts to set energy system targets. Despite its usefulness to define upper and lower limits of feasible configurations, it does not allow to directly screen technology options in a systematic way. Moreover, although some contributions have incorporated economic and environmental indicators, its applicability is still limited to mainly physical targets (such as minimum fuel consumption) (Andiappan, 2017).

Finally, mathematical programming makes use of superstructure that encompasses all possible components and interactions. After that, it is modelled and optimized to identify the optimum solution given an objective function. It is worth noting that, although mathematical methods may offer a more thorough examination of the topology of energy systems and a measure of optimality in comparison to earlier approaches, the optimal configuration is limited by the initial structure provided (Frangopoulos, 2018).

Note that the difference between the three classifications is not always clear. For instance, insight-based approaches can be used as heuristics for meta-heuristic approaches or as targets (boundaries) for mathematical approaches. Moreover, recently developed “superstructure-free synthesis” can be classed as a hybrid of all the classes mentioned above. Superstructure-free methods are often used as two-level decompositions, where the ‘discrete’ decisions are solved in the upper level and the continuous decisions are made in the lower level. For instance, Voll et al. (2012) employed a two-stages method for synthesis of energy systems, where selection options are done through adding, removing or permuting configurations, without the use of integer variables, and therefore, usually speeding up the generation of new candidates. Then the performance of each candidate is assessed through a non-linear programming (NLP) optimization. Nevertheless, strict lower bound cannot be obtained and therefore the degree of optimality is lost. Moreover, its applicability should be studied deeper since although it can speed up the generation of configurations, its benefit could be offset by the computational time required to explore the solution space and convergence guarantee (Mencarelli et al., 2020; Elsidio et al., 2021a).

On previous research, the decision-making process has been mainly formulated as an optimization problem via mathematical programming. Therefore, the following subsections provide a brief overview of key concepts of mathematical optimization for utility systems and the most relevant models proposed for design and operation of process utility systems

2.2 Mathematical optimization for utility systems

A mathematical optimization can be represented concisely by Eq. (1.1), where the decision variables could be continuous like equipment size, load, mass flow rates represented by vector x , or could be discrete choices (0 or 1) to indicate whether a component is selected (1) or not (0), represented by vector y . The objective function f could be minimize (min) or maximize (max), and be subject to fulfilment of some equality constraints (h) expressing energy and mass balances, equipment performance, etc.; and inequality constraints (g), expressing operation and/or economic limits.

$$\begin{aligned} \min_{x,y} f(x,y) & \quad (1.1) \\ \text{s.t.} & \\ & h(x,y) = 0 \\ & g(x,y) \leq 0 \\ & x \in R^n, y \in \{0,1\}^m \end{aligned}$$

Depending on the nature/form of f, g, h, x, y , mathematical problems can be classified as below:

- (i) **Linear program (LP)** if the functions f, g, h are linear and there are no binary variables y .
- (ii) **Mixed-integer linear program (MILP)** if the functions f, g, h are linear.
- (iii) **Nonlinear program (NLP)** if at least one of the functions f, g, h is a nonlinear and there is no binary variables y .
- (iv) **Mixed-integer nonlinear program (MINLP)** if at least one of the functions f, g, h is nonlinear.

Regarding the design and operation of utility systems, mixed integer problems (MIP) are often required due to the need to make discrete decisions about the selection (or not) of specific equipment or its operation (or not) at a given time.

MILP problems are an extension of LP models that allow for the accounting of discrete choices. Consequently, MILP problems have the property that the optimal solution is located at the vertices of the feasible space and that any local optimum found is a global optimum. Nonetheless, they may be difficult to solve owing to the combinatorial aspect provided by integer variables. One of the most often used techniques for addressing MILP problems is branch and bound search (Dakin, 1965), which entails solving a subset of LP sub-problems while searching inside the discrete variables decision tree (Grossmann, 2021). Recent developments, have merged branch and bound techniques with cutting planes, known as branch-and-cut algorithm, to speed up the search and provide rigorous optimum solutions.

MINLP problems, on the other hand, add the combinatorial complexity of optimizing over discrete variable sets with the difficulties inherent in dealing with nonlinear functions. The problem becomes more complex when the nonlinear functions are nonconvex, resulting in many locally optimum

solutions. To solve nonconvex MINLPs, a simple approach is to substitute the nonconvex functions with a set of discrete variables to regulate the nonlinearity. This enables a reasonable trade-off between model precision and computing complexity. However, these methods can only provide lower limits on the true optimization issue, or even worse, due to the approximations it could result in an infeasible solution of the original MINLP problem. The direct solution of nonconvex MINLP problems is closely related to global optimization, which is a subject that also seeks optimal solutions to optimization problems involving nonconvex functions, although global optimization has frequently focused on problems involving only continuous decision variables (Belotti et al., 2013). The most known technique to solve this kind of problems is the spatial branch-and-bound (sBB), which as the branch-and-bound method involves iteratively partitioning the feasible set, producing sets of smaller sub-problems (Tawarmalani and Sahinidis, 2005). These sub-problems are then further analyzed to see if there are no viable or optimum solutions, to find the sub-problems' global optimal solutions, or to further deconstruct the sub-problems for study. In principle, if run long enough, this approach should find the global optimum solution to non-linear problems. While global approaches have improved in performance over the past two decades, for large-scale problems it is still difficult to find the global optimum solution within acceptable computational times (Rebennack et al., 2011; Elsidio et al., 2019).

Moreover, when involving scenarios or periods, solving directly the problem can be intractable due to an exponential increment of the computational time with the number of scenarios/periods. Therefore, decomposition algorithms such as Lagrangean decomposition, outer approximation (Duran and Grossmann, 1986) and generalized Bender decomposition (Geoffrion, 1972) has become popular. On one hand, despite Lagrangean decomposition can provide lower and upper limits, it is consider a heuristic methodology since it cannot ensure closure of the duality gap. On the other hand, outer approximation and extensions of generalized Bender decomposition are alternating problems where there is a master problem (MILP) and a NLP sub-problem. A particular characteristic of these two methodologies is the block structure that are based on. The improvements in these two algorithms could become too technical, thus, for a comprehensive review about improvements in generalized bender decompositions, the interested readers are referred to the review paper (Rahmaniani et al., 2017). Additionally, in some cases exact decomposition, also called bilevel decomposition, for nonconvex MINLP can also be formulated, which similarly to the former algorithms solve iteratively between the master problem (MILP) and a NLP sub-problem, together with integer and/or outer approximation cuts to avoid analysis of suboptimal solutions or solutions already explored. In comparison with Benders decomposition, Lagrangean decomposition and outer approximation method, bilevel decomposition can provide more freedom of how to define the master problem, since the user define the relaxation techniques employed for the master problem. For the same reason, the convergence of these kind of methods highly rely on the quality of the MILP

relaxation and therefore its applicability is specific (Lotero et al., 2016; Lara et al., 2018; Elsidio et al., 2019).

2.3 Utility systems design optimization

Previous research has differentiated the design optimization of energy systems in three levels (Frangopoulos, 2018):

- i. **Synthesis optimization** - referring to the selection of components, size and their interconnections (configuration).
- ii. **Design optimization** - referring to technical specifications of the components selected as well as the properties of the working fluids at the design point.
- iii. **Operation optimization** - referring to given systems, where the synthesis and design are already known, and the operation properties of the components in terms of power output, mass flow rates, pressure, and compositions are defined.

However, if the overall optimal is to be achieved, the levels cannot be treated in isolation (Frangopoulos, 2018). As a result, in this work, design procedures are primarily classified according to their time-dependence ('single'- and 'multi'- period) and objective function ('single'- and 'multi'- objective). It should be noted that additional classifications may include utility system reliability and operation uncertainty. Nonetheless, because they were not part of the scope of this study, they will not be discussed further. The interested readers are referred to review papers (Sahinidis, 2004; Liu and Wang, 2020; Li and Grossmann, 2021) and the optimization book (Hadjidimitriou et al., 2021).

2.3.1 Time-dependency models

In the most fundamental case, the formulation problem is presumed time-independent, which could be modelled by previous formulation (Eq. (1.1)). 'Static' optimizations, or also known as single period optimization, are based on the assumption that the utility system is operating under steady state conditions at a specific time (usually at design/nominal point). As shown in literature, this kind of optimization are particularly useful when performing synthesis and design optimizations of utility systems based on nominal energy demands.

However, analysis of a single (or average) point is not realistic. In reality, industry processes operation changes with time due to multiple factors (e.g. variation of production level, product market, process start-ups, etc.) (Marechal and Kalitventzeff, 2003). Therefore, it is required capturing these variations within the mathematical approaches. One of the most common in the synthesis of utility systems is the multi-period approach. Multi-period optimization involves discretization of the continuous time domain to a certain extent, where process variation is approximated within appropriately chosen time intervals, and where steady-state operation can be assumed in each interval

independently of the others (Frangopoulos, 2018). Multi-period optimization enables the identification of a single feasible solution for a given set of scenarios (periods)(Grossmann and Sargent, 1979).

Table 1-1 summarizes the most relevant research on industrial utility systems, with emphasis on synthesis and design optimization. Additionally, some relevant insight approach models were included. Table 1-1 presents the objective, model type and key features of each methodology. Most of the optimization approaches focus on design variables such as the equipment size, load and efficiency. Noticeably, the majority of studies assumed fixed process steam demands and/or steam mains' conditions, even when site-wide heat integration was accounted for. Despite insight approaches have shown the benefit of considering steam main conditions in the site performance, only a few optimization studies have considered steam main pressure as a design variable for enhancing energy heat recovery from multiple sources. Nonetheless, steam sensible heat (boiler feed water preheat, steam superheat and de-superheat) was neglected.

Table 1-1 Summary of relevant contributions in the synthesis and design of industrial utility systems, considering time-dependency

Authors	Scope	Model type	Objective	Energy demand	Energy integration	Utility level selection	Steam superheating	Fossil fuel based technologies	Renewable based technologies	Thermal energy storage	Electric energy storage	Part-load performance	Multiple component	Start-up constraints
Iyer and Grossmann (1998)	IC	MILP	TAC	FSD	-	-	F	✓	-	-	-	-	-	-
Marechal and Kalitventzeff (2003)	IC	MILP	TOC, TAC	SDB	✓	-	F	✓	-	-	-	✓	✓	-
Varbanov et al. (2005)	IC	MINLP	TAC	FSD	✓	✓	-	✓	-	-	-	✓	✓	-
Aguilar et al. (2007)	IC	MILP	TAC	FSD	-	-	F	✓	-	-	-	✓	✓	-
Aguilar et al. (2008)	IC	MILP	TAC	FSD	-	-	F	✓	-	-	-	✓	✓	-
Varbanov and Klemesš (2011)	LIES	NA	-	SDB	✓	-	-	✓	✓	✓	-	-	-	-
Luo et al. (2012)	IC	MILP	TAC & emissions	FSD	-	-	F	✓	-	-	-	✓	✓	-
Sun and Liu (2015)	IC	MILP	TAC	FSD	-	-	F	✓	-	-	-	✓	✓	✓
Zhang et al. (2015)	IC	MINLP	TAC	SDB	✓	-	F	✓	-	-	-	-	-	-
Mian et al. (2016)	HRS	MILP	TAC	SDB	✓	-	F	✓	-	-	-	-	-	-
Elsido et al. (2017)	UA	MINLP	TOC, TAC	FSD	-	-	F	✓	-	✓	-	✓	-	-
Liew et al. (2017)	LIES	NA	-	SDB	✓	-	-	✓	✓	✓	-	-	-	-
Sun et al. (2017)	IC	MILP	TAC	FSD	-	-	F	✓	-	-	-	✓	✓	-
Gabrielli et al. (2018)	UA	MILP	TAC & CO ₂ emissions	FSD	-	-	-	✓	✓	✓	✓	✓	-	-
Panuschka and Hofmann (2019)	IC	MILP	TOC	FSD	-	-	F	✓	-	✓	-	-	-	-
Jamaluddin et al. (2020)	LIES	NA	-	SDB	✓	-	-	✓	✓	✓	-	-	-	-
Lok et al. (2020)	IC	MILP	TAC & CO ₂ emissions	FSD	-	-	F	✓	✓	-	-	✓	✓	✓
Pérez-Uresti et al. (2020)	UA	MILP	TAC	FSD	-	-	F	-	✓	-	✓	-	-	-
Elsido et al. (2021)	IC & HRS	MINLP	TAC	SDB	✓	-	F	✓	-	✓	-	-	-	-
Yong et al. (2021)	LIES	NA	-	SDB	✓	-	-	✓	✓	✓	✓	-	-	-

Abbreviations:
 Scope: HRS: heat recovery system; IC: Industrial cluster; LIES: Local integrated energy systems; UA: Urban area
 Model: MILP: Mixed integer linear programming; MINLP: Mixed integer non linear programming; NA: Numerical Approach
 Objective: TAC: Total annualized cost; TOC: Total operating costs
 Energy demand: FSD: Fixed steam demand; SDB: Stream data based

2.3.2 Multi-criteria models

As observed in previous section, numerous studies have been conducted using techno-economics and single-objective formulations. While significant improvements in terms of energy and cost savings have been made through cost-effective design, the majority of utility systems continue relying heavily on fossil fuels. New and tighter environmental policies require that utility systems be designed considering environmental impact and limitations. While considering environmental impact, economic cost, and/or other requirements (such as thermodynamic efficiency) complicates the design of utility systems, as these objectives frequently conflict among each other; focusing merely on a single objective without taking into account the broader context may introduce an unintended bias in favor of the selected objective function. To address this issue, multi-objective optimization (MOO) techniques have become increasingly popular in recent years. As a result, the following subsection discusses multi-objective optimization and its application to utility system design and operation.

As implied by its name, MOO optimizes a problem by considering two or more competing objective functions, simultaneously. In this way, a trade-off between the involved objectives is obtained. A concise formulation of the MOO problem comprising k objective functions can be stated as follows:

$$\begin{aligned} \min_{x,y} f(x, y) &= (f_1(x, y), f_2(x, y), \dots, f_k(x, y))^T & (1.1) \\ \text{s.t.} & \\ & h(x, y) = 0 \\ & g(x, y) \leq 0 \\ & x \in R^n, y \in \{0,1\}^m \end{aligned}$$

Where $f(x, y)$ represents the vector of k objective functions and k has an integer value greater or equal than 2 ($k \geq 2$).

Note that for non-trivial MOO problems there is not a single solution but a set of optimal solutions. As long as none of the objective functions values can be enhanced without degrading others, a solution is identified as ‘non-dominated’ or Pareto optimum. The set of Pareto optimum solutions are regarded as equally excellent in the absence of extra subjective preference information, as illustrated in Figure 1-1.

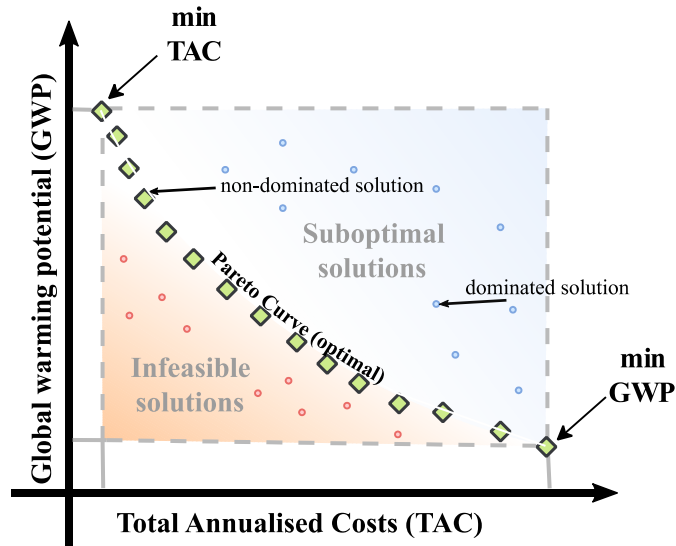


Figure 1-1. Representation of Pareto curve

In contrast to single objective optimizations, MOO comprises two stages: optimization and decision-making. Depending on the order of the stages the methodologies could be classified as follows:

- (i) **A priori methods (decisions before search).** These methods require the knowledge/preference of the decision maker, to specify the relative importance prior search, usually represented in weights assigned to the objective aggregated total. In this way, the MOO problem is transformed to a SOO problem through the use of effective strategies.
- (ii) **A posteriori methods (search before decisions).** In these methods, the decision-making is taken after the analysis of the (preferred) trade-offs of the generated optimal solutions (Pareto curve). The optimal solutions can be obtained based on the Kuhn-Tucker conditions for noninferior solutions (Cohon and Marks, 1975).
- (iii) **Progressive preference articulation (interaction between search and decisions).** These methods require the involvement of the decision maker through the optimization process to guide the search and improve current options.

Despite a priori methods' simplicity and practicality in comparison with the other two categories. In real-world the selection of proper weights is a non-trivial task. Moreover, an "inappropriate" or biased objective prioritization could lead to poor quality or reliability of the results (Coello et al., 2007). Moreover, generation of multiple solutions (pareto optimal) is preferred since it allows the analysis of the trade-offs among all the objective options, and take an informed decision. Note that the analysis of the generated solutions could be a complete task itself, which could be further reviewed in Belton and Stewart (2012).

As mentioned before, a critical aspect in the application of multi-objective optimization to the design of more sustainable energy systems is the evaluation of the system's environmental performance.

Among the different methods for environmental assessment of process energy systems, life cycle assessment (LCA) has lately garnered increased interest. LCA provides a comprehensive methodology for a quantitative evaluation of a system environmental impact throughout its full life cycle. In other words, it considers the emissions and waste generated over different product stages, such as extraction and processing of the required resources, construction and installation of the equipment involved, systems operation and the final waste disposal and equipment decommissioning. The combination of LCA and multi-objective optimization results in a strong quantitative instrument that enables environmentally aware energy system design and operation.

A diverse range of research has been published addressing the design of utility systems by using multi-objective optimization approaches. Broadly, these works differ in the scope, optimization approach and in the environmental criteria considered for the assessment.

Table 2 Summary of research contributions in multi-objective optimization models for the design of utility systems

Authors	Scope*	Model	Optimization approach	Environmental indicator**	Environmental indicator**							
					Time-variation	Part-load efficiency	Utility components	Energy integration	Renewable based technology	LCA resources	LCA technologies	
Chang and Hwang (1996)	IC	MILP	weight sum	Pollutant emissions: CO _x , NO _x and SO _x	-	-	MS	-	-	-	-	-
Oliveira Francisco and Matos (2004)	IC	MILP	ϵ -constraint	Pollutant emissions: CO _x , NO _x and SO _x	✓	✓	MS	-	-	-	-	-
Papandreou and Shang (2008)	IC	MILP	lexicographic	GWP, AP, POCP	-	-	MS	-	-	✓	-	-
Eliceche et al. (2007)	IC	MINLP	weight sum	GWP, AP, EP, POCP, ODP, HTP, ETP	-	-	MS	-	-	✓	-	-
Gutiérrez-Arriaga et al. (2013)	IC	MILP	weight sum	Gas emissions: CO _x , NO _x and SO _x	-	-	FFS	-	✓	-	-	-
Luo et al. (2012)	PP	MILP	-	Pollutant emissions ^f : CO _x , NO _x and SO _x	✓	✓	MS	-	-	-	-	-
Fazollahi et al. (2015)	UA	MINLP	evolutionary algorithm	GWP	✓	-	MS	-	✓	✓	-	-
Hipólito-Valencia et al. (2014)	HRN	MINLP	ϵ -constraint	GWP	✓	-	FFS	✓	✓	✓	-	-
Luo et al. (2014)	IC	MILP	ϵ -constraint	Environmental impact index based on GWP, AP, EP, HTP	✓	✓	MS	-	-	✓	-	-
Vaskan et al. (2014)	IC	MILP	approximation strategy	GWP, AP, EP, POCP, ODP, HTP, ETP	-	-	FFS	-	✓	✓	-	-
Wu et al. (2016)	IC	MILP	ϵ -constraint	Lifecycle single score (Ecoindicator 99)	-	-	MS	-	-	✓	-	-
Isafiade et al. (2017)	HRN	MINLP	ϵ -constraint	Lifecycle single score (Ecoindicator 99)	✓	-	x	✓	✓	✓	-	-
Sun et al. (2017)	IC	MILP	weight method	Gas emissions: CO _x , NO _x and SO _x	✓	✓	MS	-	-	-	-	-
Gabrielli et al. (2018)	UA	MILP	ϵ -constraint	CO ₂ emissions	✓	✓	MS	-	✓	-	-	-
Zheng et al. (2018)	UA	MINLP	weight method	CO ₂ emissions	✓	-	MS	-	✓	-	-	-
Pérez-Uresti et al. (2019)	IC	MINLP	-	GWP ^f	✓	-	MS	-	✓	✓	-	-
Liu and Wang (2020)	HRN	MINLP	ϵ -constraint	Lifecycle single score (Ecoindicator 99)	✓	-	FFS	✓	-	✓	-	-
Xiao et al. (2021)	PP	MINLP	NSGA-II	Environmental impact index based on GWP, AP, EP, HTP	-	✓	MS	-	-	✓	-	-

* HRN: Heat recovery network; IC: Industrial cluster; PP: Power plant; UA: Urban area

** AP: Acidification potential; EP: Eutrophication potential; ETP: Ecotoxicity potential; GWP: Global warming potential; HTP: Human toxicity potential; ODP: Ozone depletion potential; POCP: Photochemical ozone creation potential

*** FFS: Fixed flowsheet structure, MS: Multi-structure, x No specified

^f Emissions are analyzed, but are not part of the optimization

Table 2 outlines some relevant studies for the design of utility systems based on multi-objective criteria. Additional considerations in the models such as time-dependency, energy integration, renewable technology and lifecycle assessment are also analyzed. Due to the increasing concern about CO₂ emissions, it is not a surprise that most environmental studies are mainly focused on gas emissions. Several studies applied a LCA approach; nevertheless, they only focus on the emissions resultant from the use of fuels and electricity. While this is relevant for fossil fuel based systems, since the main source of emissions comes from the fuel combustion, it is not the case for renewable-based technologies and energy storage units, where significant environmental contributions occur at the construction and disassembly stages of the equipment. This may result in underestimating the actual environmental impact of the system components and/or leaking emissions to other stages of the process. It is worth noting that most of studies that incorporate renewable technologies are focused on urban-scale utility systems, revealing a literature gap on industrial-scale networks. Simplifications regarding equipment constant efficiency or fixed.

2.4 Literature gaps

Various studies on the design and operation of energy hubs and/or distributed energy systems have been conducted in recent years, though their primary focus has been on urban areas (residential and commercial) or the power industry. On the other hand, industrial energy systems have additional characteristics that must be considered for their optimal design and operation. Compared to urban energy hubs, industrial hubs require heat at higher temperatures and in a wider range. Moreover, in industrial sites, there is a large amount of waste energy at relatively high temperatures (<150 °C) (Perry et al., 2008) that can be recovered from one site plant to another via an intermediate fluid. As a result, industrial utility systems are not only able to convert and provide energy but also can be used as site heat recovery systems. Even though many process integration studies have demonstrated the value of recovering heat through intermediate fluids such as steam to reduce overall site energy requirements, the majority of these studies were conducted without taking into account the optimal operating conditions – in terms of pressure and temperature – of the site to enhance energy savings. While incorporating steam main pressure and temperature into the synthesis of a utility system increases the problem's complexity, overlooking its impact on the system design and performance may result in misleading energy savings, cogeneration potential, and, as a result, site energy targets. Attempts have been made in the past to include steam main pressure as a design variable, but this was done under the assumption of saturated steam, which may be impractical due to the negligence of the heat required to pre-heat boiler feed water and the minimal degree of superheat required to prevent excessive condensation and the optimum equipment operation. As a result, there is a gap in the literature for a more practical and accurate methodology for optimizing utility energy synthesis, taking into account interactions between the utility system and the site processes, as well as practical features/constraints.

Although daily or seasonal conditions have little effect on industrial energy demand (compared to urban sites) (Bungener et al., 2015), a systematic approach that considers market variations, unforeseen or planned process unit start-ups or shutdowns in utility systems necessitates additional research. Furthermore, the assessment of energy storage integration into the system comprises design-operation linking variables and constraints (also known as complicating variables/constraints), which connect all operational periods and prevent a simple time-wise decomposition of the problem (Elsido et al., 2021b). Consequently, there is a need for methods capable of capturing the short- and long-term dynamics of both energy system and site processes while efficiently using computational resources.

The sustainable growth of both industry and energy sectors has become a primary research focus for industry and academics. While new and innovative technologies/processes can only be developed as a result of paradigm change in science or engineering, the involvement of modelling and optimization of current site components and new developments is critical for comprehending the intricate interactions among the different actors and, consequently, for selecting the appropriate mix of sources and technologies for each scenario. Although mathematical tools have been used to some extent in research, their use to inform and assist policymaking remains limited.

Finally, despite the development of different frameworks to assess the environmental impact of energy systems in recent years, several studies have looked at single objective functions based on emissions taxes or penalty costs, and others have employed Pareto frontiers. However, most research on utility systems has focused on emissions generated during the production stage and fuel combustion, ignoring emissions throughout the entire lifecycle. This may result in underestimating the actual environmental impact of the system components and/or leaking emissions to other stages of the process. It is critical to examine energy resources entire life cycle to assess its environmental impact accurately.

2.5 Methodology

Based on the gaps in the literature identified in the preceding section, this thesis addresses sustainable development in process industries by developing a decision-support tool for conceptual design and optimization of industrial utility systems that considers a variety of energy sources and technologies (both fossil and renewable) in order to facilitate a systematic transition from the current state to a more sustainable one. Figure 1-1 depicts a high-level overview of the proposed general methodology and its primary outputs.

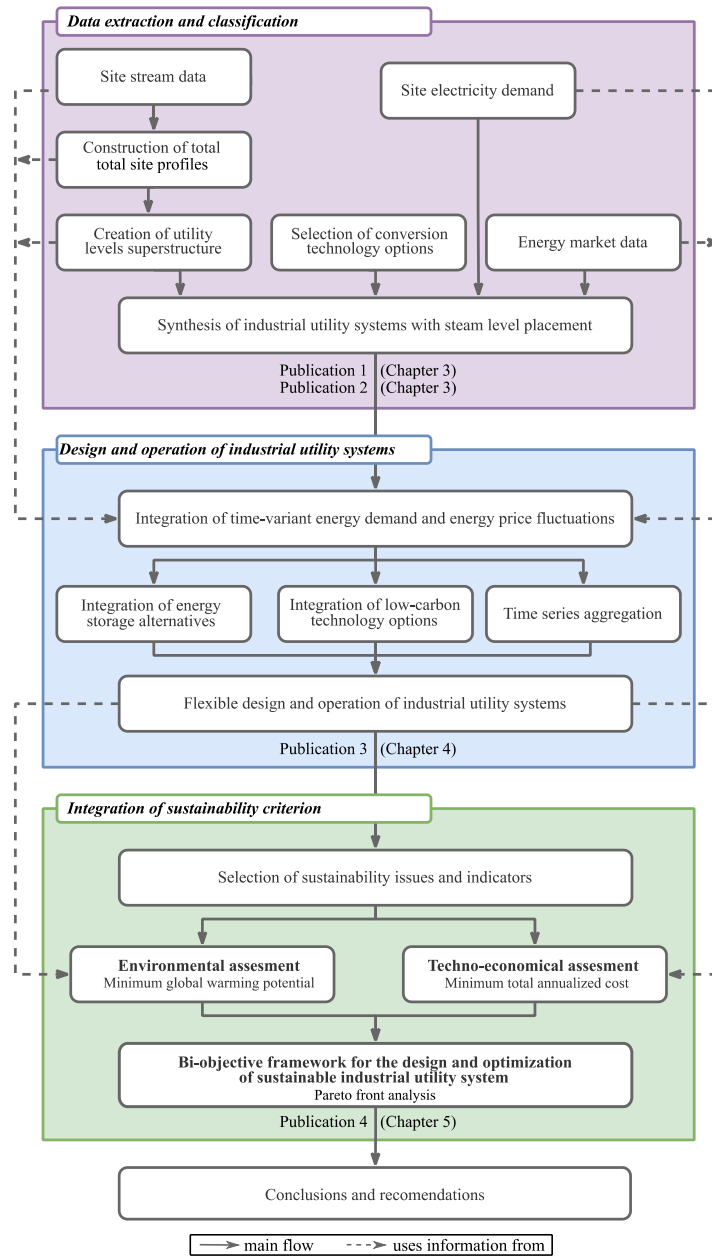


Figure 1-1 Research methodology for the conceptual design of sustainable industrial utility systems

2.5.1 Synthesis of utility systems considering heat integration

The proposed framework starts with the formulation of a synthesis problem for steam systems that takes into account site-wide heat integration. The framework includes a number of previously unaddressed practical issues, such as steam sensible heat (e.g. boiler feed water preheat and steam superheat and de-superheat), equipment part-load performance, and utility components such as flash steam recovery, let-down stations, and deaerators. In order to provide the most cost-effective design options and maximize potential energy savings through indirect heat recovery, the methodology also considers steam main operating conditions (in terms of temperature and pressure) as a design variable. As a result, the methodology leads to a good trade-off between steam loads and costs, while also taking into account the impact on site heat recovery and energy targets.

The assumption of steam main operating conditions as design variable results in a nonconvex mixed-integer nonlinear problem (MINLP). Due to the combinatorial nature of the synthesis problem, its direct solve for large-scale problems with state-of-the-art-general purpose solvers such as BARON (Tawarmalani and Sahinidis, 2005) may become intractable. As a result, we propose a solution pool-based bilevel optimization strategy based on linear relaxations (i.e. McCormick, piece-wise linearization) for evaluating economically viable technologies while minimizing computational time. Detailed information about the optimization strategy can be found in Chapter 3.

- *Selection of conversion technologies*

For steam generation, this study considers all major existing technology options such as fuel gas biomass and electrode boilers, also heat recovery steam generators. Although solar thermal technologies for industrial heating (150°C to 400 °C) is an upcoming technology, they have been excluded from the scope due to its early stage of technology development and commercialization for energy-intensive industries (Sanchez, 2020), being less than 0.02 % of solar energy used to meet current industrial heat requirement (IEA, 2020). Thermal storage units such as steam accumulator and molten salt system have been included due to its maturity in the market.

For power generation, backpressure and condensing turbines as well as gas turbines (operating with renewable and non-renewable fuels) were considered. While for electric energy storage, Sodium-Sulphur and Lithium-ion batteries are considered due to its maturity in the market (Mongird et al., 2019). In addition, for seasonal storage hydrogen storage system has been included in the analysis, which comprises electrolyzer, hydrogen storage tank and fuel cell. Note that, the use of solar and wind electricity for industrial implementation was not considered, since its mainly deployment is related to the grid to decarbonize the power sector (González-Garay et al., 2021). Therefore, its impact was consider indirectly through the analysis of (renewable) electricity import to the system.

Regarding biomass, the three most well know alternatives for energy conversion: anaerobic digestion (biogas), direct combustion (solid biomass) and gasification (syngas) are considered.

2.5.2 Design and operation of flexible industrial utility systems

To incorporate flexibility to the utility system design, the framework accounts for time-varying energy demand and fluctuating power tariffs. Power and heat storage are also included as potential solutions for balancing the mismatch between energy demand and supply. The integration of time-dependency and energy storage requires also considering time-series aggregation algorithm to maintain an appropriate level of detail without sacrificing tractability.

2.5.3 Integration of sustainability criterion

Finally, the framework incorporates environmental life-cycle analysis to address concerns about sustainability. The resulting multi-objective synthesis problem is solved using a constraint approach. In this way, the trade-off between cost and environmental impact can thus be investigated, and design options with significant environmental improvement at a marginal cost can be identify. It is important to note that environmental lifecycle assessment entails taking into account a variety of indicators. Nonetheless, based on the scope of this study and the available literature (Vaskan et al., 2014), global warming potential is chosen as the environmental criterion for design optimization, while other environmental impacts (e.g. water depletion and acidification) are still taken into account for analysis.

- Selection of sustainability issues and indicators

Indicators in sustainability assessments are quantified measures of issues that are recognized to be relevant to the stakeholders. In this project, indicators used in life cycle assessment (LCA) and life cycle costing (LCC) that reflect issues industrial systems are proposed (Table 3).

Table 3 Lifecycle criteria with their corresponding issues and indicators

Criteria	Issue	Indicator
Economic	Costs	Annualized capital costs
		Operating and maintenance costs
		Total annualized costs
Environmental	Climate change	Global warming potential (GWP)
	Air pollution	Ozone depletion potential (ODP)
		Particulate matter formation potential (PMFP)
	Water and soil pollution	Freshwater eutrophication potential (FEP)
		Marine eutrophication potential (MEP)
		Terrestrial acidification potential (TAP)
	Ecotoxicity	Freshwater ecotoxicity potential (FETP)
		Marine ecotoxicity potential (METP)
		Terrestrial ecotoxicity potential (TETP)
	Resource depletion	Fossil depletion potential (FDP)
Mineral depletion potential (MDP)		
Human health	Water depletion potential (WDP)	
	Human toxicity potential (HTP)	

Life cycle environmental impacts are calculated using ReCiPe 2016 v1.1, the state-of-the-art life cycle impact assessment methodology (Huijbregts et al., 2017). ReCiPe was chosen for its ability to reconcile midpoint (problem-oriented) and endpoint (damage-oriented) characterization levels. Midpoint approach is used for indicators because to its reduced uncertainty and higher acceptability (Huijbregts et al., 2017). Finally, a hierarchical viewpoint (100 years) is employed.

For the economic aspects, three main economic indicators are used to measure economic sustainability: annualized capital costs, operating and maintenance costs, and total costs of utilities. Capital expenses consider the construction and installation costs (including transport), while operating and maintenance expenses comprise costs incurred during the useful life of the plant. Finally, the total annualized costs indicator enables a trade-off between capital and operating costs over its entire life and, in this way, define the cost-effectiveness of the design options under similar lifespans.

- *Decision analysis*

Currently, environmental and economic criteria are conflicting goals. Thus, multi-objective optimization tools are required to incorporate both criteria, take advantage of potential trade-offs, and identify cost-effective and environmentally sustainable solutions. To this end, an ϵ -constraint approach is implemented, based on the problem formulation. Additionally, in order to reduce the problem's complexity and focus on the goal of reduce climate change impact, the decision criteria is based on total annualized costs and global warming potential as economic and environmental decision criteria, respectively.



References

- Aguilar, O., Kim, J.-K., Perry, S. & Smith, R. (2008) 'Availability and reliability considerations in the design and optimisation of flexible utility systems', *Chemical Engineering Science*, 63(14), pp. 3569-3584.
- Aguilar, O., Perry, S., Kim, K. & Smith, R. (2007) 'Design and Optimization of flexible utility systems subject to variable conditions. Part 1: Modelling Framework', *Chemical Engineering Research and Design*, 85(8), pp. 1136-1148.
- Andiappan, V. (2017) 'State-Of-The-Art Review of Mathematical Optimisation Approaches for Synthesis of Energy Systems', *Process Integration and Optimization for Sustainability*, 1(3), pp. 165-188.
- Belotti, P., Kirches, C., Leyffer, S., Linderoth, J., Luedtke, J. & Mahajan, A. (2013) 'Mixed-integer nonlinear optimization', *Acta Numerica*, 22, pp. 1-131.
- Belton, V. & Stewart, T. (2012). *Multiple criteria decision analysis: an integrated approach*: Springer.
- Brueske, S., Sabouni, R., Zach, C. & Andres, H. (2012) *U.S. MANUFACTURING ENERGY USE AND GREENHOUSE GAS EMISSIONS ANALYSIS*, Columbia, Maryland: ENERGETICS INCORPORATED/DORN/2012/504).
- Bungener, S., Hackl, R., Van Eetvelde, G., Harvey, S. & Marechal, F. (2015) 'Multi-period analysis of heat integration measures in industrial clusters', *Energy*, 93, pp. 220-234.

- Chang, C.-T. & Hwang, J.-R. (1996) 'A multiobjective programming approach to waste minimization in the utility systems of chemical processes', *Chemical Engineering Science*, 51(16), pp. 3951-3965.
- Coello, C. A. C., Lamont, G. B. & Veldhuizen, D. A. V. (2007). *Evolutionary Algorithms for Solving Multi-Objective Problems* (2nd ed.): Springer.
- Cohon, J. L. & Marks, D. H. (1975) 'A review and evaluation of multiobjective programming techniques', *Water Resources Research*, 11(2), pp. 208-220.
- Dakin, R. J. (1965) 'A tree-search algorithm for mixed integer programming problems', *The Computer Journal*, 8(3), pp. 250-255.
- Duran, M. A. & Grossmann, I. E. (1986) 'An outer-approximation algorithm for a class of mixed-integer nonlinear programs', *Mathematical Programming*, 36(3), pp. 307-339.
- Eliceche, A. M., Corvalán, S. M. & Martínez, P. (2007) 'Environmental life cycle impact as a tool for process optimisation of a utility plant', *Computers & Chemical Engineering*, 31(5), pp. 648-656.
- Elsido, C., Bischi, A., Silva, P. & Martelli, E. (2017) 'Two-stage MINLP algorithm for the optimal synthesis and design of networks of CHP units', *Energy*, 121, pp. 403-426.
- Elsido, C., Cremonesi, A. & Martelli, E. (2021a) 'A novel sequential synthesis algorithm for the integrated optimization of Rankine cycles and heat exchanger networks', *Applied Thermal Engineering*, 192, pp. 116594.
- Elsido, C., Martelli, E. & Grossmann, I. E. (2019) 'A bilevel decomposition method for the simultaneous heat integration and synthesis of steam/organic Rankine cycles', *Computers & Chemical Engineering*, 128, pp. 228-245.
- Elsido, C., Martelli, E. & Grossmann, I. E. (2021b) 'Multiperiod optimization of heat exchanger networks with integrated thermodynamic cycles and thermal storages', *Computers & Chemical Engineering*, 149, pp. 107293.
- Fazlollahi, S., Becker, G., Ashouri, A. & Maréchal, F. (2015) 'Multi-objective, multi-period optimization of district energy systems: IV – A case study', *Energy*, 84, pp. 365-381.
- Frangopoulos, C. A. (2018) 'Recent developments and trends in optimization of energy systems', *Energy*, 164, pp. 1011-1020.
- Gabrielli, P., Gazzani, M., Martelli, E. & Mazzotti, M. (2018) 'Optimal design of multi-energy systems with seasonal storage', *Applied Energy*, 219, pp. 408-424.
- Ganschinietz, D. C. (2021) 'Design of on-site energy conversion systems for manufacturing companies – A concept-centric research framework', *Journal of Cleaner Production*, 310, pp. 127258.
- Geoffrion, A. M. (1972) 'Generalized Benders decomposition', *Journal of Optimization Theory and Applications*, 10(4), pp. 237-260.
- González-Garay, A., Mac Dowell, N. & Shah, N. (2021) 'A carbon neutral chemical industry powered by the sun', *Discover Chemical Engineering*, 1(1), pp. 2.
- Grossmann, I. E. (2021). *Advanced Optimization for Process Systems Engineering*. Cambridge: Cambridge University Press.

- Grossmann, I. E. & Sargent, R. W. H. (1979) 'Optimum Design of Multipurpose Chemical Plants', *Industrial & Engineering Chemistry Process Design and Development*, 18(2), pp. 343-348.
- Gutiérrez-Arriaga, C. G., Serna-González, M., Ponce-Ortega, J. M. & El-Halwagi, M. M. (2013) 'Multi-objective optimization of steam power plants for sustainable generation of electricity', *Clean Technologies and Environmental Policy*, 15(4), pp. 551-566.
- Hadjidimitriou, S., Frangioni, A., Koch, T. & Lodi, A. (2021). *Mathematical Optimization for Efficient and Robust Energy Networks* (Vol. 4): Springer International Publishing.
- Hipólito-Valencia, B. J., Lira-Barragán, L. F., Ponce-Ortega, J. M., Serna-González, M. & El-Halwagi, M. M. (2014) 'Multiobjective design of interplant trigeneration systems', *AIChE Journal*, 60(1), pp. 213-236.
- Huijbregts, M. A. J., Steinmann, Z. J. N., Elshout, P. M. F., Stam, G., Verones, F., Vieira, M. D. M., Hollander, A., Zijp, M. & Zelm, R. v. (2017) *Recipe 2016 v1.1* RIVM Report 2016-0104a).
- IEA (2020) *Concentrating Solar Power (CSP)*, Paris: IEA.
- Isafiade, A. J., Short, M., Bogataj, M. & Kravanja, Z. (2017) 'Integrating renewables into multi-period heat exchanger network synthesis considering economics and environmental impact', *Computers & Chemical Engineering*, 99, pp. 51-65.
- Iyer, R. R. & Grossmann, I. E. (1998) 'Synthesis and operational planning of utility systems for multiperiod operation', *Computers & Chemical Engineering*, 22(7), pp. 979-993.
- Jamaluddin, K., Wan Alwi, S. R., Hamzah, K. & Klemeš, J. J. (2020) 'A Numerical Pinch Analysis Methodology for Optimal Sizing of a Centralized Trigeneration System with Variable Energy Demands', *Energies*, 13(8).
- Lara, C. L., Trespalacios, F. & Grossmann, I. E. (2018) 'Global optimization algorithm for capacitated multi-facility continuous location-allocation problems', *Journal of Global Optimization*, 71(4), pp. 871-889.
- Li, C. & Grossmann, I. E. (2021) 'A Review of Stochastic Programming Methods for Optimization of Process Systems Under Uncertainty', *Frontiers in Chemical Engineering*, 2(34).
- Liew, P. Y., Theo, W. L., Wan Alwi, S. R., Lim, J. S., Abdul Manan, Z., Klemeš, J. J. & Varbanov, P. S. (2017) 'Total Site Heat Integration planning and design for industrial, urban and renewable systems', *Renewable and Sustainable Energy Reviews*, 68, pp. 964-985.
- Liu, B. & Wang, Y. (2020) '6 - Energy system optimization under uncertainties: A comprehensive review', in Ren, J., Wang, Y. & He, C. (eds.) *Towards Sustainable Chemical Processes*: Elsevier, pp. 149-170.
- Liu, M., Shi, Y. & Fang, F. (2014) 'Combined cooling, heating and power systems: A survey', *Renewable and Sustainable Energy Reviews*, 35, pp. 1-22.
- Lok, W. J., Ng, L. Y. & Andiappan, V. (2020) 'Optimal decision-making for combined heat and power operations: A fuzzy optimisation approach considering system flexibility, environmental emissions, start-up and shutdown costs', *Process Safety and Environmental Protection*, 137, pp. 312-327.
- Lotero, I., Trespalacios, F., Grossmann, I. E., Papageorgiou, D. J. & Cheon, M.-S. (2016) 'An MILP-MINLP decomposition method for the global optimization of a source based model of the multiperiod blending problem', *Computers & Chemical Engineering*, 87, pp. 13-35.

- Luo, X., Hu, J., Zhao, J., Zhang, B., Chen, Y. & Mo, S. (2014) 'Multi-objective optimization for the design and synthesis of utility systems with emission abatement technology concerns', *Applied Energy*, 136, pp. 1110-1131.
- Luo, X., Zhang, B., Chen, Y. & Mo, S. (2012) 'Operational planning optimization of multiple interconnected steam power plants considering environmental costs', *Energy*, 37, pp. 549-561.
- Marechal, F. & Kalitventzeff, B. (2003) 'Targeting the integration of multi-period utility systems for site scale process integration', *Applied Thermal Engineering*, 23(14), pp. 1763-1784.
- Mencarelli, L., Chen, Q., Pagot, A. & Grossmann, I. E. (2020) 'A review on superstructure optimization approaches in process system engineering', *Computers & Chemical Engineering*, 136, pp. 106808.
- Mian, A., Martelli, E. & Maréchal, F. (2016) 'Framework for the Multiperiod Sequential Synthesis of Heat Exchanger Networks with Selection, Design, and Scheduling of Multiple Utilities', *Industrial & Engineering Chemistry Research*, 55(1), pp. 168-186.
- Mohammadi, M., Noorollahi, Y., Mohammadi-ivatloo, B. & Yousefi, H. (2017) 'Energy hub: From a model to a concept – A review', *Renewable and Sustainable Energy Reviews*, 80, pp. 1512-1527.
- Mongird, K., Fotedar, V., Viswanathan, V., Koritarov, V., Balducci, P., Hadjerioua, B. & Alam, J. (2019) *Energy Storage Technology and Cost Characterization Report*: Pacific Northwest National Laboratory (PNNL-28866, PNNL-28866).
- Oliveira Francisco, A. P. & Matos, H. A. (2004) 'Multiperiod synthesis and operational planning of utility systems with environmental concerns', *Computers & Chemical Engineering*, 28(5), pp. 745-753.
- Panuschka, S. & Hofmann, R. (2019) 'Impact of thermal storage capacity, electricity and emission certificate costs on the optimal operation of an industrial energy system', *Energy Conversion and Management*, 185, pp. 622-635.
- Papandreou, V. & Shang, Z. (2008) 'A multi-criteria optimisation approach for the design of sustainable utility systems', *Computers & Chemical Engineering*, 32(7), pp. 1589-1602.
- Pérez-Uresti, S. I., Martín, M. & Jiménez-Gutiérrez, A. (2019) 'Superstructure approach for the design of renewable-based utility plants', *Computers & Chemical Engineering*, 123, pp. 371-388.
- Pérez-Uresti, S. I., Martín, M. & Jiménez-Gutiérrez, A. (2020) 'A Methodology for the Design of Flexible Renewable-Based Utility Plants', *ACS Sustainable Chemistry & Engineering*, 8(11), pp. 4580-4597.
- Perry, S., Klemeš, J. & Bulatov, I. (2008) 'Integrating waste and renewable energy to reduce the carbon footprint of locally integrated energy sectors', *Energy*, 33(10), pp. 1489-1497.
- Rahmaniani, R., Crainic, T. G., Gendreau, M. & Rei, W. (2017) 'The Benders decomposition algorithm: A literature review', *European Journal of Operational Research*, 259(3), pp. 801-817.
- Rebennack, S., Kallrath, J. & Pardalos, P. M. (2011) 'Optimal storage design for a multi-product plant: A non-convex MINLP formulation', *Computers & Chemical Engineering*, 35(2), pp. 255-271.

- Sahinidis, N. V. (2004) 'Optimization under uncertainty: state-of-the-art and opportunities', *Computers & Chemical Engineering*, 28(6), pp. 971-983.
- Sanchez, R. (2020) *Integrating National Research Agendas on Solar Heat for Industrial Processes. Project Deliverable 6.5: Mid-Term Report On The Infrastructure Access Scheme*: CIEMAT.
- Smith, R. (2016) 'Steam Systems and Cogeneration', *Chemical Process: Design and Integration*. Second ed. Chichester: John Wiley & Sons, Ltd, pp. 583-646.
- Sun, L., Gai, L. & Smith, R. (2017) 'Site utility system optimization with operation adjustment under uncertainty', *Applied Energy*, 186, pp. 450-456.
- Sun, L. & Liu, C. (2015) 'Reliable and flexible steam and power system design', *Applied Thermal Engineering*, 79, pp. 184-191.
- Tawarmalani, M. & Sahinidis, N. V. (2005) 'A polyhedral branch-and-cut approach to global optimization', *Mathematical Programming*, 103(2), pp. 225-249.
- Varbanov, P., Perry, S., Klemeš, J. & Smith, R. (2005) 'Synthesis of industrial utility systems: cost-effective de-carbonisation', *Applied Thermal Engineering*, 25(7), pp. 985-1001.
- Varbanov, P. S. & Klemeš, J. J. (2011) 'Integration and management of renewables into Total Sites with variable supply and demand', *Computers & Chemical Engineering*, 35(9), pp. 1815-1826.
- Vaskan, P., Guillén-Gosálbez, G., Turkay, M. & Jiménez, L. (2014) 'Multiobjective Optimization of Utility Plants under Several Environmental Indicators Using an MILP-Based Dimensionality Reduction Approach', *Industrial & Engineering Chemistry Research*, 53(50), pp. 19559-19572.
- Voll, P., Lampe, M., Wrobel, G. & Bardow, A. (2012) 'Superstructure-free synthesis and optimization of distributed industrial energy supply systems', *Energy*, 45(1), pp. 424-435.
- Wu, L., Liu, Y., Liang, X. & Kang, L. (2016) 'Multi-objective optimization for design of a steam system with drivers option in process industries', *Journal of Cleaner Production*, 136, pp. 89-98.
- Xiao, W., Cheng, A., Li, S., Jiang, X., Ruan, X. & He, G. (2021) 'A multi-objective optimization strategy of steam power system to achieve standard emission and optimal economic by NSGA-II', *Energy*, 232, pp. 120953.
- Yong, W. N., Liew, P. Y., Woon, K. S., Wan Alwi, S. R. & Klemeš, J. J. (2021) 'A pinch-based multi-energy targeting framework for combined chilling heating power microgrid of urban-industrial symbiosis', *Renewable and Sustainable Energy Reviews*, 150, pp. 111482.
- Zhang, B. J., Liu, K., Luo, X. L., Chen, Q. L. & Li, W. K. (2015) 'A multi-period mathematical model for simultaneous optimization of materials and energy on the refining site scale', *Applied Energy*, 143, pp. 238-250.
- Zheng, X., Wu, G., Qiu, Y., Zhan, X., Shah, N., Li, N. & Zhao, Y. (2018) 'A MINLP multi-objective optimization model for operational planning of a case study CCHP system in urban China', *Applied Energy*, 210, pp. 1126-1140.

Synthesis of Industrial Utility Systems

Overview

To achieve cost-effective decarbonization, industrial energy systems must operate at maximum efficiency. More efficient systems not only meet lower energy targets, but they also produce fewer emissions. Typically, the performance of an energy system is determined by its configuration and operational load. However, there is the potential for heat recovery in industrial utility systems, where excess heat from one plant can be used to meet the heating requirements of another. Interplant heat recovery can take a variety of forms (direct, indirect, a combination of both). (Wang and Feng, 2017) findings shown that using intermediate fluids (steam) to transfer heat between plants is more economically beneficial for independent plants, especially when located at long distances. In this context, steam mains pressure and superheating are critical not only for equipment performance optimization but also for site energy integration, affecting the overall performance of the site. Thus, designing energy-efficient utility systems requires optimizing the configuration of utility components considering the operating conditions of steam mains.

However, including the operating condition of steam mains in the optimization framework generally results in difficult-to-solve MINLP problems. As a result, total site integration and process utility system design are typically performed with fixed steam main operating conditions (temperature and pressure) and/or with the assumption of saturated conditions. The resulting inaccurate energy targets may not only miss energy savings opportunities, but may also increase capital investment due to oversizing of several utility components.

To address the limitations of previous research, this Chapter presents a superstructure-based model for the synthesis of utility systems with steam main selection. This chapter includes two manuscripts, referred as Contribution 1 and Contribution 2 that propose two solution strategies for the resulting non-convex MINLP problem. The first strategy used a sequential approach of MILP and simulation stages (described in detail in Contribution 1), whereas the second strategy used a solution pool-based bilevel decomposition (explained in Contribution 2).

3.1 Introduction to Contribution 1

This section discusses a manuscript submitted to the journal "Applied Energy" that describes a comprehensive and holistic framework for process utility system synthesis. The framework includes site-wide heat recovery, heat and power generation, and steam level selection. To provide more robust framework, the model considers steam sensible heat, such as boiler feed water preheating, steam superheating (for process steam generation), and steam de-superheating (for process steam use). Incorporating these elements into the optimization framework, as demonstrated later in the results section, allows for more precise calculation of process steam generation and use loads, and thus of heat recovery and utility steam requirements.

The formulation of the superstructure of utility system components with the steam operating conditions requires several discrete (e.g. utility components selections) and continuous decisions (e.g. utility component size and load, steam mass flowrate and enthalpies). Moreover, nonlinearities are introduced by using steam main conditions as design variables. To address the resultant nonconvex MINLP problem, a sequential MILP method is employed. The methodology, determines steam main pressures based on a set of the most promising pressure levels derived from the total site profile kinks. Whereas, steam enthalpy is treated as a fixed pseudo-parameter. Steam enthalpy is assumed as a defined value during the MILP optimization, which is later recalculated using an algorithm that takes into account steam property functions and nonlinear effects on system performance. Once calculated the real steam main condition, steam enthalpies are updated for the next iteration.

Overall, this first contribution addresses major shortcomings of previous research, improving the practicality and accuracy of process utility system synthesis. Furthermore, the findings of this study not only highlight the impact of steam operating conditions in improving site performance, but also in achieving significant energy and cost savings. Furthermore, the effect of the number of steam mains and the integration of utility components such as hot oil systems and flash steam recovery on the synthesis of utility systems and energy requirement is investigated in this work.

3.2 Contribution 1

Title: STYLE: A new optimization model for Synthesis of uTility sYtems with steam Level placEment

Authors: Julia Jimenez-Romero, Adisa Azapagic and Robin Smith

Submitted to: Applied Energy

Year: 2021

STYLE: A new optimization model for Synthesis of uTility sYstems with steam LEvel placement

Julia Jiménez-Romero^{a,b,*}, Adisa Azapagic^b, Robin Smith^a

^a Centre for Process Integration, Department of Chemical Engineering and Analytical Science, University of Manchester, Manchester, M13 9PL, United Kingdom

^b Sustainable Industrial Systems Group, Department of Chemical Engineering and Analytical Science, University of Manchester, Manchester, M13 9PL, United Kingdom

* Julia Jiménez-Romero. Email: julia.jimenezromero@manchester.ac.uk

Abstract

Moving industrial production to a more sustainable basis requires a step change in the efficiency of site steam and cogeneration systems and, in the long term, a switch away from fossil fuels to renewable energy sources. Previous approaches to the design and optimization of steam and cogeneration systems have simplified the problem to the extent that many important practical issues have been neglected, restricting the scope of the options included. The use of grossly simplified models has been prompted by the mathematical difficulties of optimizing such complex energy systems. To overcome limitations in previous work, this paper proposes a new superstructure-based optimization model for the optimization of utility systems, accounting for optimum steam level placement. The latter is important for improving systems efficiency and reducing energy consumption. The optimization problem involves the selection of more realistic operating conditions of the steam mains (superheating and pressure). The model accounts for water preheating, as well as superheating and de-superheating for process steam generation and use. Hot oil circuits are also included as hot utility option to overcome potential steam temperature and/or pressure limitations at high temperatures, and with it provide more flexibility in the framework. The general problem requires making several continuous and discrete decisions, where non-linearities and non-convexities from underlying physics and binary decisions exacerbate the complex nature of the problem, yielding a nonconvex Mixed Integer Non-Linear Programming (MINLP) formulation. However, MINLP formulations could become computationally intractable to solve. Thus, to guarantee tractability and fast conversion, STYLE model, a successive Mixed Integer Linear Programming formulation, is developed and presented in this work. STYLE methodology is applied to two case studies to illustrate the advantages of the synthesis method and the benefits of optimizing steam levels for the reduction of overall energy consumption at industrial sites. The proposed approach addresses major shortcomings inherent in previous research and provides a foundation for future work to explore the next generation of sustainable utility systems.

Highlights

- The optimization model includes more realistic conditions for steam generation and use.
- Steam main pressure and superheating temperatures are used as design variables.
- A more cost-effective and practical design of industrial utility systems can be achieved.
- The influence of both number of steam mains and operating conditions is analyzed.
- Illustrative case studies demonstrate fuel savings between 15.8 and 32.2 %.

Keywords

- Superstructure, Mixed Integer Linear Programming, indirect heat recovery, industrial energy systems, steam systems.

Nomenclature**Abbreviations**

ACC	Annualized Capital Cost
b	Boiler
BFW	Boiler feed water
BP-ST	Back-Pressure steam turbine
cond	Condensate
C-ST	Condensing steam turbine
cw	Cooling water
Deae	Deaerator
DEM	Demand
e	Electricity
Eq	Equipment
EXP	Export
f	Fuel
FSR	Flash steam recovery
GEN	Generation
grid	Electricity grid
gt	Gas turbine
HO	Hot oil
HP	High-pressure
HRSG	Heat recovery steam generator
IMP	Import
In	Input
is	Isentropic
ISO	International Standards Organization
ISO conditions	Reference temperature, humidity and pressure conditions established by the International Standards Organization
LD	Let-down
lim	Limit
M	Mass flowrate
main	Maintenance cost
MP	Medium-pressure
nEq	Number of equipment
NHV	Net heat value
OC	Operating costs
op	Operating
out	Output
SF	Supplementary firing
sh	Superheated
st	Steam turbine
UF	Unfired
vent	Vent
VHP	Very High Pressure
w	Treated water

WH Waste heat

Sets

C	Set of cold streams
F	Set of site fuels
F_b, F_{gt}	Set of boiler and gas turbine fuels (subset of site fuels)
H	Set of hot streams
I	Set of steam mains
IJ_s	Set of steam levels j_s that belong to steam main i
J	Set of temperature intervals
J_{HO}	Set of temperature intervals for hot oil (subset of temperature intervals)
J_s	Set of temperature intervals for steam main (subset of temperature intervals)
J_{WH}	Set of temperature intervals for waste heat (subset of temperature intervals)
N_b, N_{gt}, N_{st}	Set of boilers, gas turbines, steam turbines number of units available, respectively
N_{HRSG}	Set of HRSG units available (subset of gas turbines)
T_b, T_{gt}	Set of boiler and gas turbine types
v	Set of VHP steam levels

Parameters

α	Proportion of steam vented	-
β	Condensate return rate	-
$\Delta h_{j_s}^C$	Enthalpy difference of process steam use at steam level j_s	MWh t^{-1}
$\Delta h_{j_s}^H$	Enthalpy difference of process steam generation at steam level j_s	MWh t^{-1}
γ	Boiler blowdown fraction of the boiler steam output	-
$\sigma_{n_{gt}, t_{gt}, f_{gt}}^{gt}, \sigma_{\theta}^{st}$	minimum load fraction of gas and steam turbine	-
$\Omega_{min}, \Omega_{max}$	minimum and maximum equipment capacity, in terms of flow rate	$t h^{-1}$
θ_e^{dem}	Power demand	MW
a,b,c	Modelling coefficients of steam turbines in the algorithm for calculating steam mains' superheating	-
$a_{\theta}^{st}, b_{\theta}^{st}, c_{\theta}^{st}$	Modelling coefficients of steam turbines operating at θ conditions	-
$a_{t_{gt}}^{gt}, b_{t_{gt}}^{gt}$	Modelling coefficients of gas turbine n_{gt} type t_{gt}	-
$L_{n_{gt}, t_{gt}, f_{gt}}^{gt}$		
C_{nEq}^A	Variable cost of equipment, depending on its size	
C_{nEq}^B	Fixed cost of equipment selection	m€
CP_c, CP_h	Heat capacity of cold streams c and hot streams h , respectively	MW $^{\circ}C^{-1}$
cp_{exh}	Specific heat capacity of exhausts gases	MWh t^{-1} $^{\circ}C^{-1}$
F_{IEq}^{ann}	Annualization factor	
F_{IEq}^{inst}	Installation factor	
f_T^{GT}, f_{Teff}^{GT}	Gas turbine correction factors that account for the ambient temperature influence	-
$h_{j_s}, h_{v_{j_s}}$	Enthalpy of saturated liquid and vapor at steam level j_s , respectively	MWh t^{-1}
h_{v}^{VHP}, h_{v}^{VHP}	Enthalpy of saturated liquid and vapor at VHP steam level v , respectively	MWh t^{-1}
h^{BFW}	Enthalpy of boiling feed water	MWh t^{-1}

$h_{j_s}^C$	Enthalpy of saturated liquid of process steam use at steam level j_s	MWh t^{-1}
h_{sh,j_s}^C	Enthalpy of superheated process steam use at steam level j_s	MWh t^{-1}
h_{sh,j_s}^H	Enthalpy of superheated process steam generation at steam level j_s	MWh t^{-1}
L^H, L^C	Heat losses due to distribution at the source and sink side, respectively	-
NHV	Net heat value of fuel	MWh t^{-1}
η_{eff}^{HRSG}	Thermal efficiency of HRSG	-
η_{mec}	Mechanical efficiency of steam turbines	-
η_t	Efficiency of electricity transmission	-
P_{imp}^e, P_{exp}^e	Unit price of electricity imported and exported from/to the grid, respectively	€ MWh $^{-1}$
P_{fEq}^f	Unit price of fuel consumed by equipment	€ MWh $^{-1}$
P^{CW}	Unit price of cooling water consumed by site	€ MWh $^{-1}$
P^W	Unit price of treated water consumed by site	€ t^{-1}
$q_{h,j}^H$	Heat content of hot stream h involved in temperature interval j	MW
$q_{c,j}^C$	Heat content of cold stream c involved in temperature interval j	MW
$Q_{j_s}^{Cout}$	Process heat source at steam level j_s	MW
$Q_{j_s}^{Hin}$	Process heat source at steam level j_s	MW
$Q_{j_{wh}}^{Hin}$	Process heat source at waste heat level j_s	MW
T_{amb}	Ambient temperature	°C
T_j	Temperature level j	°C
T_{max}	Maximum temperature allowed for steam generation	°C
T_s^{HO}	Supply temperature of hot oil	°C
T_i^{MIN}	Minimum superheat temperature of steam main i	°C
T_{max}^{SF}	Maximum temperature reached by exhaust gases with supplementary firing	°C
T_c^s, T_c^t	Supply and target temperature of cold stream c	°C
T_h^s, T_h^t	Supply and target temperature of hot stream h	°C
T_{max}^{UF}	Maximum temperature reached by exhaust gases unfired	°C
U	Upper bound	
\overline{W}^{EXP}	Maximum electricity export	MW
\overline{W}^{IMP}	Maximum electricity import	MW

Pseudo-parameters

ΔH_θ^{IS}	Isentropic enthalpy difference of steam turbine operating at θ conditions	MWh t^{-1}
h_{sh,i,j_s}^{main}	Enthalpy of superheated steam at steam main i operating at j_s conditions	MWh t^{-1}
$h_{sh_v}^{VHP}$	Enthalpy of superheated steam at VHP steam main operating at v conditions	MWh t^{-1}

Variables

C_{op}^e	Operating costs of electricity	m€ y^{-1}
OC	Total operating costs	m€ y^{-1}
TAC	Total annualized costs	m€ y^{-1}
W^{grid}	Electricity from/to the grid	MW

Positive variables

ACC	Annualized capital cost	$m\text{€ } y^{-1}$
$C_{\text{main}}^{\text{Eq}}$	Maintenance cost of each equipment	$m\text{€ } y^{-1}$
C_{op}^f	Operating costs of fuel	$m\text{€ } y^{-1}$
$C_{\text{op}}^{\text{cw}}$	Operating costs of cooling water	$m\text{€ } y^{-1}$
C_{op}^w	Operating costs of water	$m\text{€ } y^{-1}$
$m_{\text{air}n_{\text{gt}}}$	Air mass flowrate used in the gas turbine n_{gt}	$t \text{ h}^{-1}$
$M_{n_b, t_b, v}^b$	Steam mass flow rate from unit n_b boiler type t_b , operating at v conditions	$t \text{ h}^{-1}$
M_{i, j_s}^{BFW}	BFW mass flow rate for steam main i operating at j_s conditions	$t \text{ h}^{-1}$
M_{i, j_s}^{BFWC}	BFW mass flow rate injected to de-superheat process steam prior its use at level j_s	$t \text{ h}^{-1}$
M_T^{BFW}	Total mass flow rate of BFW	$t \text{ h}^{-1}$
$m_{n_{\text{st}}, i, j_s, j_s'}^{\text{BP-ST}}$	Steam mass flow rate of BP turbine n_{st} operating from level j_s to level j_s'	$t \text{ h}^{-1}$
$M_{i, j_s}^{\text{BP-STin}}$	Steam mass flow rate of BP turbines entering to steam main i operating at j_s conditions	$t \text{ h}^{-1}$
$M_{i, j_s}^{\text{BP-STout}}$	Steam mass flow rate of BP turbines leaving steam main i operating at j_s conditions	$t \text{ h}^{-1}$
M_{i, j_s}^{Cin}	Steam mass flow rate for process heating at steam level j_s	$t \text{ h}^{-1}$
$M_{i, j_s}^{\text{Cmain}}$	Steam mass flow rate from steam main i operating at j_s conditions	$t \text{ h}^{-1}$
M^{Cond}	Mass flowrate of returned condensate	
$M_{i, j_s}^{\text{C-STout}}$	Steam mass flow rate of condensing turbines from steam main i operating at j_s conditions	$t \text{ h}^{-1}$
$m_{n_{\text{st}}, i, j_s}^{\text{C-ST}}$	Steam mass flow rate of condensing turbine n_{st} from steam main i operating at j_s conditions	$t \text{ h}^{-1}$
$M_{j_s}^{\text{Deae}}$	Steam mass flow rate entering to deaerator from steam level j_s	$t \text{ h}^{-1}$
$M_{n_{\text{Eq}}, t_{\text{Eq}}}^{\text{Eq}}$	Variable vector representing mass load of unit n_{Eq} of equipment type t_{Eq} at the general MILP formulation	
$m_{\text{exh}n_{\text{gt}}}$	Exhausts mass flow rate from gas turbine n_{gt}	$t \text{ h}^{-1}$
m_{n_b, t_b, f_b}^f	Mass flowrate of fuel f_b consumed in boiler unit n_b of type t_b	$t \text{ h}^{-1}$
M_{i, j_s}^{FSR}	Flashed steam mass flow rate fed to the mixer i operating at j_s conditions	$t \text{ h}^{-1}$
$M_{\text{in}i, j_s}^{\text{FSR}}$	Inlet mass flow rate at FSR drum i	$t \text{ h}^{-1}$
$m_{i, j_s, j_s'}^{\text{FSR}}$	Liquid mass flow rate of FSR i operating from pressure j_s to j_s'	$t \text{ h}^{-1}$
$m_{s, i, j_s, j_s'}^{\text{FSR}}$	Steam mass flow rate of FSR i operating from pressure j_s to pressure j_s'	$t \text{ h}^{-1}$
$m_{n_{\text{gt}}, t_{\text{gt}}, f_{\text{gt}}}^{\text{gt}}$	Mass flowrate of fuel f_{gt} consumed in gas turbine n_{gt} , type t_{gt}	$t \text{ h}^{-1}$
$m_{\text{fmax}n_{\text{gt}}, t_{\text{gt}}, f_{\text{gt}}}^{\text{gt}}$	Maximum mass flowrate of fuel f_{gt} consumed in gas turbine n_{gt} , type t_{gt}	$t \text{ h}^{-1}$
M_{i, j_s}^{H}	Mass flow rate of process steam generation for steam main i operating at j_s conditions	$t \text{ h}^{-1}$
$m_{\text{exh}n_{\text{gt}}}^{\text{HRSG}}$	Exhausts mass flow rate entering HRSG n_{gt}	$t \text{ h}^{-1}$
$M_{n_{\text{HRSG}}, v}^{\text{HRSG}}$	Steam mass flow rate from unit n_{HRSG} , operating at v conditions	$t \text{ h}^{-1}$
$M_{i, j_s}^{\text{in}}, M_{i, j_s}^{\text{out}}$	Variable vectors representing inlet and outlet mass flow rates at steam main i operating at j_s conditions at the general MILP formulation	$t \text{ h}^{-1}$
$m_{i, j_s, j_s'}^{\text{LD}}$	Mass flow rate of let-down passing from steam main i operating at level j_s to steam level j_s'	$t \text{ h}^{-1}$

M_{i,j_s}^{LDin}	Let-down mass flow rate entering to steam main i operating at j_s conditions	$t h^{-1}$
M_{i,j_s}^{LDout}	Let-down mass flow rate leaving steam main i operating at j_s conditions	$t h^{-1}$
m_{θ}^{st}	Steam mass flow rate of steam turbine operating at θ conditions	$t h^{-1}$
$m_{\max \theta}^{st}$	Maximum steam mass flow rate of steam turbine operating at θ conditions	$t h^{-1}$
$m_{n_{gt},f_{gt}}^{SF}$	Mass flowrate of fuel f_{gt} of supplementary firing	$t h^{-1}$
$M_{T_v}^{VHP}$	Total steam mass flow rate produce at VHP main header operating at v conditions	$t h^{-1}$
$m_{n_{st},v,j_s}^{VHP BP-ST}$	Steam mass flow rate of BP turbine n_{st} operating from VHP level v to level j_s	$t h^{-1}$
$m_{n_{st},v,j_s}^{VHP C-ST}$	Steam mass flow rate of condensing turbine n_{st} operating from VHP level v	$t h^{-1}$
$m_{v,j_s}^{VHP LD}$	Let-down mass flow rate passing from VHP main level v to steam level j_s	$t h^{-1}$
m_{DA}^W	Treated water mass flow rate consumed in the deaerator	$t h^{-1}$
Output	Variable vector representing the energy output of each utility component at the general MILP formulation	
Q_{i,j_s}^{BP-ST}	Heat of BP turbine exhausts entering to steam main i operating at j_s conditions	MW
Q_{i,j_s}^{Cin}	Heat available for process heating from steam main i operating at j_s conditions	MW
$Q_{CW}^{C-ST}, Q_{CW}^{VHP C-ST}$	Heat duties of cooling water from the turbine condensers	MW
$Q_{process}^{CW}, Q_{Utility}^{CW}$	Heat rejected to cooling water from the process and the utility system	MW
$Q_{exh n_{gt}}^{gt}$	Heat available in the gas exhausts of turbine n_{gt}	MW
$Q_{t_{Eq},f_{Eq}}^f$	Fuel energy consumed by type of equipment t_{Eq}	MW
Q_{n_b,t_b}^f	Fuel consumption from unit boiler n_b , type t_b	MW
$Q_{n_{gt},v}^{sh}, Q_{n_{gt},v}^{vap}, Q_{n_{gt},v}^{pre}$	Heat available in the different HRSG sections: superheating (sh), evaporation (vap) and pre heating (pre) to generate steam at v conditions	MW
$Q_{j_s}^{Hout}$	Process heat available at steam level j_s	MW
Q^{HO}	Process heating requirements that cannot be used/satisfied by steam	MW
Q_s^{HO}	Process heating provided by hot oil system at steam temperature range	MW
Q_T^{HO}	Total process heating provided by hot oil system	MW
$Q_{T_{n_{gt},v}}^{HRSG}$	Total heat used in the HRSG unit to generate steam at v conditions	MW
$Q_{i,j_s}^{in}, Q_{i,j_s}^{out}$	Variable vectors representing inlet and outlet heat flow at steam main i operating at j_s conditions at the general MILP formulation	MW
Q_{i,j_s}^{LD}	Heat from let-down station of steam main i operating at j_s conditions	MW
Q^{VHP}	Total heat provided at VHP header	MW
$R_{j_s}^C$	Residual sink heat at steam level j_s	MW
$R_{j_s}^H$	Residual source heat at steam level j_s	MW
T_i^{GUESS}	Estimated superheat temperature of steam main i , in the algorithm for calculating steam mains' superheating	$^{\circ}C$
$W_{i,j_s,j_s'}^{BP-ST}$	Power generated by BP turbine from steam main i operating from steam level j_s to steam level j_s'	MW
W_{v,j_s}^{BP-ST}	Power generated by BP turbine from VHP steam main operating from VHP main level v to steam level j_s	MW

W^{Eq}	Variable vector representing power generated by equipment Eq in the general MILP formulation	MW
W^{EXP}	Power exported to the grid	MW
$W_{n_{gt}}^{gt}$	Power generated by gas turbine n_{gt}	MW
$W_{max_{n_{gt}, t_{gt}}}^{GT}$	Maximum power generated by gas turbine operating at ISO conditions	MW
W^{IMP}	Power imported from the grid	MW
W_{θ}^{st}	Power generated by steam turbine operating at θ conditions	MW
x	Variable vector representing continuous variables in the general MILP formulation	
$x_{n_{gt}, t_{gt}, f_{gt}}^{gt}$	Load fraction of fuel consumed by gas turbine n_{gt} of type t_{gt}	-
x_{θ}^{st}	Load fraction of steam turbine operating at θ conditions	-
$y_{i,j_s, j_s'}^{L-L}$	existence of connection between level j_s and level j_s' , $[0, 1]$	
y_{v, j_s}^{VHP-L}	existence of connection between VHP level v and level j_s , $[0, 1]$	
$Z_{n_{Eq}, t_{Eq}}^{Eq}$	Variable vector representing size of unit n_{Eq} of equipment type t_{Eq} at the general MILP formulation	

Binary variables

y_v^{VHP}	Selection of VHP steam operating at condition v
y_{i,j_s}^L	Selection of steam level i operating at condition j_s
$y_{n_{Eq}, t_{Eq}}^{Eq}$	Selection of unit n_{Eq} of equipment type t_{Eq}
$y_{n_b, t_b, v}^b$	Selection of unit n_b of boiler type t_b , operating at condition v
$y_{n_b, t_b, f_b}^{F_b}$	Selection of fuel f_b for boiler unit n_b, t_b
$y_{n_{st}, v, j_s}^{VHP BP-ST}$	Selection of unit n_{st} of back pressure steam turbine operating between v (inlet pressure) and j_s (outlet pressure)
$y_{n_{st}, i, j_s, j_s'}^{BP-ST}$	Selection of unit n_{st} of back pressure steam turbine operating between j_s (inlet pressure) and j_s' (outlet pressure)
$y_{n_{st}, v}^{VHP C-ST}$	Selection of unit n_{st} of condensing steam turbine operating at v (inlet pressure)
$y_{n_{st}, i, j_s}^{C-ST}$	Selection of unit n_{st} of condensing steam turbine operating at j_s (inlet pressure)
$y_{n_{gt}, t_{gt}}^{gt}$	Selection of unit n_{gt} of condensing steam turbine operating at j_s (inlet pressure)
$y_{n_{gt}, t_{gt}, f_{gt}}^{F_{gt}}$	Selection of fuel f_{gt} for gas turbine unit n_{gt}, t_{gt}
$y_{n_{gt}, v}^{HRSG}$	Selection of unit n_{gt} of HRSG operating at condition v
$y_{n_{gt}, f_{gt}}^{F_{HRSG}}$	Fuel f_{gt} usage status for supplementary firing of HRSG unit n_{gt}

1. Introduction

Sustainable use of energy is necessary to mitigate climate change and avoid other environmental impacts associated with conversion and use of energy. The industrial sector was responsible for the 37 % (157 EJ) of global energy use as of 2018 (International Energy Agency, 2018; IEA, 2020b), and the share is further increasing. Industrial energy consumption has been driven by a long-term trend of incremental rises in demand for materials in energy-intensive industry subsectors, which is a consequence of both population growth and economic expansion. Three-quarters of the energy used in industry is for process heating purposes, with around 50% of the requirement in the form of heat up to 400 °C (Fleiter et al., 2016; Naegler et al., 2015). Moreover, only 10 % of the heat used comes from renewables, which are mostly biomass and waste (IRENA, 2015). This reflects industry's heavy reliance on the combustion of fossil fuels, meaning that increased demand for energy over past decades has been accompanied by rising CO₂ emissions (IEA, 2018). Therefore, reducing greenhouse gas emissions depends, to a large extent, on changes and developments in industry.

According to the International Energy Agency (IEA, 2020a), electricity and heat generation accounted for 41 % of global CO₂ emissions. When analyzing the emissions produced by the consumption of electricity and heat, industry was the largest emitter with 43 % (12 billion t/y). In most of the process industries the largest energy consumer is the utility system itself, where energy is supplied mainly by the combustion of fossil fuels to produce steam for both heat and power generation. Moreover, the performance of process utility systems directly influences the operation of the plants. For this reason, synthesis of energy-efficient utility systems is becoming a key area in relation to energy use, contributing to a transition from the existing to more sustainable energy systems (Broberg Viklund, 2015). In order to achieve this, process utility systems will need to reduce their energy intensity by fuel shifting and improved efficiency, integration of renewable energy sources, electrification of processes, and the use of carbon capture and storage (CSS) (HM Government, 2011). In the long term, this will lead to a paradigm shift in the way such utility systems are designed and operated.

However, before switching to low carbon fuels and/or the integration of different energy technologies, the main opportunities for industrial utility systems to embrace cost-effective decarbonization arise from operating at optimum conditions. The relative abatement potential is influenced by the carbon intensity of the energy carrier used, as well as the thermal efficiency of the system. Hence, the amount of emissions savings will further increase if the energy demand is reduced. In order to provide an assessment of improvement potential, it is necessary to first understand and establish a baseline of the energy requirement.

Energy targets for process utility system design and operation require addressing potential energy savings via energy integration. Energy integration comprises both direct and indirect heat recovery, as well as the cogeneration potential. The amount of heat recovery and cogeneration potential are strongly interrelated with the configuration and operation of the energy distribution systems in an industrial site where steam, that is usually used as an intermediate heat carrier, is distributed around sites at different pressures and temperatures. Steam pressure is an important design variable as it can be tuned to exploit heat recovery across the site, and with it reduce fuel consumption. It can also be set to enhance on site power generation from steam expansion through steam turbines. Thus, the selection of steam levels in the design of process utility systems is crucial to ensure the cost-effective generation of heat and power and its distribution on the site.

Although steam heating is most efficiently carried out using the latent heat (defined by its pressure), steam superheating is required to avoid excessive condensation in the mains and/or machines, e.g. steam turbines. While a small amount of condensation could be acceptable, over condensation can lead to equipment damage. Therefore, a degree of superheat, usually between 10 to 20 °C above saturation are required at each steam level, being the most critical point of superheating is usually at the lowest steam main – low pressure (LP) level (Smith, 2016). In order to achieve the superheat at the LP main, the most practical option is to increase the temperature of the utility steam at higher pressure levels, especially at the very high pressure (VHP) steam main (Sun et al., 2015). However, this superheating temperature is restricted by the limitations of the materials used in equipment, such as boilers, steam turbines, and pipework. All these constraints need to be considered for the system design and operation.

The superheating affects several aspects of the steam system performance, including heat recovery, power generation and process heating. In relation to process steam generation (heat recovery), superheating introduces additional constraints for the amount of steam that can be recovered (due to temperature limitations) or involves additional complexities in its design. In terms of power generation, higher steam temperatures are directly linked with higher shaft power generation potential. A significant consideration, however, is that high steam temperatures might not be always optimal, because of loss of cogeneration potential due to a temperature reduction in turbine exhausts. Consequently, there is a need for steam let down to both control the pressure and temperature of the mains. Lastly, although superheating is beneficial for greater power generation potential, superheating is not desirable for process heating. Superheated steam would cause poor heat transfer until saturation is reached. Hence, boiler feed water (BFW) may need to be injected locally into the steam (de-superheating) prior to its use for process heating, altering the steam flowrate required and site fuel consumption. Another important aspect to consider is that the degree of superheat for steam generation and use may not be the same (leading to non-isothermal mixing). While the superheat for

the steam generation could be easily defined, since it is a design matter, the temperature (and flow) of steam use is not as straightforward to determine. Both depend on the superheating and de-superheating in the steam mains. The former relies on several factors, such as the temperature of both the utility steam and process steam generation, the efficiency of the steam turbines, and amount of let-down between the mains (Sun et al., 2015). Therefore, steam superheating should be considered in the system analysis to analyze its effect on the system performance and to provide more accurate and realistic energy targeting.

Despite the influence of steam superheating on the overall system performance, as discussed in the next section, only the latent heat of steam has been usually considered in the literature for steam distribution systems. The sensible heat of both utility and process steam at different superheating conditions has not been fully considered yet. Moreover, while several efficient optimization approaches have been devised for the synthesis of utility systems, the optimum operating conditions (temperature and pressure) and number of steam mains have received little attention. To address this gap, this work presents a new optimization model for the synthesis of utility systems with optimum steam level placement, considering both practical and realistic steam operating conditions. The proposed model takes into account boiler feed water preheating, as well as superheating and de-superheating for process steam generation and use, rather than only steam at saturated conditions. This is combined with an evaluation of the interactions between steam mains conditions (pressure and superheat) and the system performance. The effect of process steam generation at a different temperature from the steam mains (non-isothermal mixing), as well as the efficiency and the exhaust temperature of the steam turbines based on steam conditions (superheating) and load, are also included to provide a realistic analysis of heat recovery and power generation. Furthermore, the integration of additional utility options (e.g. hot oil) and other utility components (e.g. deaerator, flash steam recovery) allows a more complete evaluation.

To address these challenges, a mixed integer linear programming (MILP) superstructure is applied that allows for simultaneous (1) optimal selection of utilities, (2) optimum configuration (equipment selection, size and load) of the industrial energy system, and (3) appropriate number of steam mains together with mains operating conditions. To reduce the computational effort (especially when dealing with industrial size problems), as well as take advantage of robust linear optimization solvers without compromising on the accuracy of the models, the problem formulation is approached by a successive MILP problem.

The next section provides an overview of the extant literature on the topic, followed in Section 3 by the problem formulation and the principal assumptions considered in this work. Section 4 presents the modelling framework and the proposed algorithm. The applicability of the proposed framework

is demonstrated in Section 5 through two illustrative case studies. Finally, conclusions of this study are presented in Section 6.

2. Literature review

Several studies have focused on increasing the accuracy of estimating the cogeneration potential and synthesis of utility systems. The contributions vary from mostly heuristic methods to approaches employing superstructures and mathematical optimization. Dhole and Linnhoff (1993) extended the principle of Pinch Analysis and introduced the concept of “Total Sites Profiles” for targeting fuel consumption, cogeneration, emissions, and cooling of several processes linked to a central utility system. Their model is based on the following assumptions: steam turbine performance (efficiency) is independent of the load and the inlet-outlet conditions and steam conditions can be estimated based on the saturated steam properties (superheat was neglected). This research was further enhanced by Raissi (1994), introducing a graphical tool known as Site Utility Grand Composite Curve (SUGCC). The researchers established that the area enclosed by the SUGCC is proportional to the site power generation potential – denoted as ‘the Temperature-Enthalpy (T-H) model’. In Klemeš et al. (1997), a targeting and design methodology is presented for reducing industrial energy demands. The authors combine the concepts of Total Site Integration and SUGCCs with optimization tools to evaluate the trade-offs between operating and capital costs. The cogeneration potential is estimated based on a Carnot factor – Enthalpy plot. Although previous models provide a general idea of the shaft power potential, in reality, the cogeneration target is overestimated. This is due to the assumption of steam heat generation and consumption as latent heat only, as well as the omission of the effect of the inlet and outlet conditions in the turbine performance. Hui and Ahmad (1997) suggested a method to integrate the design of several heat exchanger networks (HEN) from different processes, employing the site utility steam mains as a vehicle to exchange heat among all plants. A simple boiler-turbine configuration is assumed and no quantitative criteria are provided (only heuristics) for selecting the final steam levels.

Graphical targeting methods are effective for maximizing the thermal efficiency, as well as understanding the physical insights of the problem. However, they cannot provide a general framework, nor a systematic decision-making approach to solving the problem. Moreover, the use of graphical methods for industrial size problems without commercial software packages can be complex. Furthermore, these kinds of methodologies cannot guarantee optimal solutions (Papoulias and Grossmann, 1983). To take into account a general framework as well as an optimal capital and energy trade-off, Bruno et al. (1998) present a mathematical method to synthesize the utility system, with possible configurations included within a superstructure. A more rigorous approach is adopted to calculate steam conditions; but nevertheless, the superheating effect and variation of the turbine efficiency in relation to the load are absent. Maréchal and Kalitventzeff (1998) developed a MILP

model considering the grand composite curve (GCC) and steam superheating. However, the degree of superheating of the steam mains and equipment efficiency are considered as given values and are not part of the optimization variables.

To incorporate efficiency variation of energy system components into the design problem, Mavromatis and Kokossis (1998) introduced the thermodynamic model known as Turbine Hardware Model (THM), based on the energy balance for energy target and a simplified level optimization. The THM coefficients were later improved and extended to condensing turbines by Varbanov (2004). Nevertheless, both models considered only the effect of latent heat across the turbine. This neglects the effect of steam sensible heat at the inlet and outlet of steam turbines, as well as the steam mains, leading to inaccurate results. Shang and Kokossis (2004) integrated pinch and thermodynamic analysis with MILP optimization to address the design of utility systems with optimal steam levels. The study considers the interactions between the various levels of steam and the performance of turbines (THM) for different scenarios. However, the proposed methodology is based only on heat balances, without any distinction between available and useful heat, while neglecting potential limitations related to the mass balance. In heat sink cascade, this rough assumption may lead to impractical scenarios or to more complex designs. Additionally, the number of steam header candidates is assumed to be fixed and there is no systematic criterion for the allocation of the steam level candidates to each steam main. To overcome some of these issues, Varbanov et al. (2005) present improved models for utility system components and propose a successive MILP (sMILP) formulation to avoid local optimality of the (mixed integer non-linear programming, MINLP) problem formulation. Later, Beangstrom and Majozi (2016) developed a MINLP model to optimize the steam systems with multiple steam levels and the power generation simultaneously. Nevertheless, this work focuses only on the demands of cold streams, neglecting the effect of the process heat sources in the selection of the steam main operating conditions and any heat recovery potential. One limitation in the previous works is that the degree of superheat is often overlooked, along with its effect on the potential shaft power generated, and heat recovery.

In addition to these models, Kundra (2005) and Ghannadzadeh et al. (2012) presented targeting approaches, in which both sensible and latent heat of steam were considered, but the effect of the size and variation of turbines efficiency was not taken into account. To overcome this drawback, a cogeneration potential targeting method was developed by Khoshgoftar Manesh et al. (2013). Recently, Pirmohamadi et al. (2019) proposed a methodology for targeting cogeneration potential by using an exergy approach. However, previous methodologies have assumed fixed steam mains pressure, usually based on heuristics. This neglects the close interrelation between the processes and the system and its subsequent implications. Moreover, the superheat for both the steam generation and use has been assumed to be the same. This premise might lead to solutions that are

thermodynamically unfeasible or difficult to implement in practice due to limitations of the materials of construction or design complexity.

Sun et al. (2015) proposed a practical graphical approach to overcome the shortcomings, assessing cogeneration potential and enhancing site-wide heat recovery methodically. This gives useful insights both thermodynamically and physically for understanding some of the interactions within the system. Yet, it does not provide a systematic decision-making approach to determine the optimum utility system performance since it does not allow for analysis of the trade-off between the cost of the additional steam generation and the profit from power generation. To take into account the economic evaluation, Goh et al. (2016) proposed an algorithm for the synthesis of the heat exchanger network with utility systems, considering the interaction between the process and utility system via cascade automated targeting. The targeting method permits to reduce the total operating cost, though, the methodology does not account the synthesis of utility system. Ng et al. (2017) presented two targeting approaches, known as Steam Cascade Analysis (SCA) and automated Targeting Model (ATM), to determine both cogeneration potential and economics. While SCA employs algebraic techniques to targeting the cogeneration potential of single and multiple steam sources, the ATM extended the concept into an optimisation framework to allow cost optimisation and account for system constraints. Previous works presented inaccurate cogeneration and economic targets, since neither the system configuration nor variable efficiency of the units and their effect are considering in the framework.

As mentioned before, the main trade-offs in designing and optimizing energy systems is the one between energy saving and total costs (both OPEX and CAPEX). The outcome of this trade-off strongly depends on the utility system configuration, not only in terms of equipment selection and operation, but also in terms of number of units required. The utility system configuration involves taking several discrete and continuous decisions. Moreover, strict energy balances, along with nonlinear part-load performance models of each component, result in a nonconvex MINLP. In terms of optimization, significant work has been done exploring different optimization approaches for MINLP. One of the first MINLP models for synthesis of energy systems was presented by Bruno et al. (1998). Due to the complexity of the problem, only one component (operating at full load) of each technology was included in the superstructure. Later, Chen and Lin (2011) introduced an MINLP formulation for a utility system solved directly by the SBB solver. However, the model is applied to small-scale examples and the effect of part-load in equipment performance is not analyzed in detail. In more recent studies, Li et al. (2018) presented a block-superstructure framework to solve mass and energy balances, applying a MINLP formulation. Li et al. (2018) suggested that the methodology could be applied to different uses, yet acknowledged that without simplifying decisions, larger problems may become computationally expensive. According to Kantor et al. (2015), academic case-

study solutions required up to 24 hours for computation, while for larger problems 7 to 10 days may be required (if converged). Therefore, employing MINLP formulations could become intractable, stressing the value of fast conversion and global MILP solvers. To provide a more rigorous optimization, linearized methods have been also considered, with the drawback of approximated solutions. For example, Varbanov et al. (2005) published an improved model, where multiple and more detailed models (accounting for part-load) in which some of the non-linearities introduced by the equipment performance models are solved by an iterative process (sMILP). Aguilar et al. (2007b) presented a model formulation to address the synthesis of the utility network, where the performance model of equipment was able to estimate the efficiency at different operating conditions. The model of Aguilar et al. (2007b) required that some operating conditions were pre-specified, as for example the operating temperatures of turbines, boilers and the steam mains. Sun et al. (2017), presented a mathematical model to optimized utility systems operation under variable demand. In their work, the effect of steam mains superheating on steam distribution and power generation is underlined through a sensitivity analysis. The papers mentioned above mainly focus on the selection, size and load of the equipment use in the utility system for maximizing profit or minimizing costs. However, most of them have assumed pre-specified steam demands and steam operating conditions, thus, overlooking the interactions between the steam levels and the site processes and its effect on the operation of the utility system.

In recent years, scientific contributions about energy systems have addressed environmental issues due to extensive use of fossil fuels at the industrial level, triggering research about other energy sources and energy conversion units, as well as energy integration of the industrial sector with commercial and residential areas. For example, Perry et al. (2008) proposed a method to satisfy heat and power demands of locally integrated energy sectors (LIES), which usually involve industrial, commercial and domestic areas. Moreover, Varbanov and Klemeš (2010) presented an algebraic method that integrated renewable energy into a total site energy systems with fossil fuels. Similarly, Ong et al. (2017) developed a P-graph method where multiple utilities in industrial sites are considered for the total site integration and optimization is considered. Lee et al. (2020) extended LIES integration approach to optimize heat and power systems operating with steam turbines. While this and previous research contributed to the study of industrial decarbonization options, neither accounted for the system configuration nor utility-level optimization. Moreover, only the useful energy of utilities was accounted for the energy integration.

Even though total site integration and utility systems have been widely analyzed and used in numerous studies for improving energy efficiency demonstrating economic and environmental advantages at industrial sites, several issues remain unresolved. Addressing such problems is

imperative to further improve energy integration (particularly in industrial clusters) and reduce fossil fuel use. From the abovementioned literature, the following observations are apparent:

- i. Estimation of cogeneration potential and heat recovery is necessary to set energy targets as well as heat and power generation. However, due to the high level of interactions between the processes and the utility system, a comprehensive design and operation framework is crucial to estimate supply and demand sides and to analyze the energy-cost trade-offs. Therefore, practical arrangements, including plant layout, number of utility components (energy conversion technologies and steam mains), as well as their appropriate operation, need to be considered when analyzing potential energy integration.
- ii. Graphical targeting methods provide valuable insights for understanding the interactions within the total site. However, to guarantee optimal industrial symbiosis with cost effective infrastructure, the application of optimization methods is required. At present, a holistic framework to systematically identify the configuration and operation of utility systems for optimal symbiosis is still lacking.
- iii. The steam pressure levels in steam distribution system are key to maximizing energy integration within and between industrial sites and to improve utility system performance. However, the identification of the correct compromise in steam pressure levels and loads is challenging. Little work has been carried out on implementing simultaneous process integration and steam levels selection when synthesizing total site utility systems. At present, the main systematic attempts to address simultaneously cogeneration and utility levels optimization (Mavromatis and Kokossis, 1998; Shang and Kokossis, 2004; Varbanov et al., 2005) have simplified the problem to such an extent that they consider only the latent heat of steam, omitting relevant utility components and constraints.
- iv. Several methods have focused on optimizing heat and power cogeneration systems. However, the degree of the steam superheat required at different steam levels as a design variable has usually been overlooked.
- v. The appropriate number of steam levels (mains) required and its effect on heat recovery and cogeneration potential, has been paid little attention to.
- vi. Superstructure-based MINLP formulations for the synthesis of utility systems operating at optimum conditions are usually large-scale and time consuming.

The above-identified research gaps regarding total site integration practical considerations, as well as simultaneous optimization of utility system configuration and operating conditions, highlight a lack of a rigorous optimization framework to consider complex industrial symbiosis. This work, therefore, presents a comprehensive and holistic energy integration framework that not only forms a powerful basis for synthesis of energy systems and industrial symbiosis problems but also provides

the basis to incorporate efficiently many other energy sources and technologies into the analysis. This work provides for the first time a successive MILP formulation as a decision-support tool for designing cost-effective utility systems with a comparatively small computational effort.

3. Problem statement and challenges

The optimization problem related to utility system synthesis with steam level placement is stated below.

The following needs to be determined by minimizing an objective function (e.g. total annualized cost, operating cost), while satisfying both thermal and power demand:

- i. **utility system configuration:** size and load of the selected units along with the values of their operative variables;
- ii. **energy use of the utility system:** total site fuel consumption, power generation and cooling water consumption;
- iii. the appropriate combination of hot utilities (if applicable); and
- iv. **steam mains' operating conditions:** suitable number of steam mains and their operating conditions in relation to pressure levels and superheating.

The following is known:

- i. a structure for different chemical sites (or process within each plant) to be integrated on a site; sets of process streams with their supply and target temperatures, flow heat capacities, as well as specific minimum temperature approach for each process;
- ii. degree of superheating for steam generation and steam usage;
- iii. list of potential technologies (and types) available with a range of feasible sizes and loads (e.g. aero-derivative and industrial gas turbines, field erected and package boilers, condensing and back-pressure steam turbines, and other relevant technologies);
- iv. market data, list of fuels (e.g. natural gas, fuel gas) and utilities options (e.g. hot oil) available with their corresponding prices, in addition to import and export electricity costs; and
- v. expected lifetime of the network and the relevant economic parameters.

3.1. Assumptions

The subsequent assumptions are considered for the problem formulation:

- i. Process streams have constant specific heat capacities.
- ii. The specific approach temperature of each process is specified as an input.

- iii. Process source heat is used to generate steam at different steam levels, from BFW conditions to superheating. The latter is a designer variable and is restricted by the source profile and the heat exchanger equipment.
- iv. Heat integration between processes is considered indirectly. Heat flows from the process sources to sinks through intermediate fluids such as water, steam or hot oil.
- v. Cooling demand is satisfied by cooling water (CW) as cold utility.
- vi. Steam main operating pressure and temperature (enthalpy) are degrees of freedom for the optimization. The enthalpies of both process steam generation and process steam usage are set as parameters, defined by the degree of superheat required.
- vii. Utility steam is raised at VHP conditions and distributed to the different headers by either passing through steam turbines or let down stations.
- viii. Process sink heat demand can be satisfied by either hot oil or de-superheated steam.
- ix. Non-isothermal mixing at the inlet of each steam main can occur.
- x. There is only one deaerator in the utility system, and it works with steam from the lowest pressure main. In practice, despite the fact more than one de-aerator can be used, the contribution of the deaerator cost to the system total annual costs (TAC) is relatively small (Varbanov, 2004).
- xi. The gas turbine energy losses can be expressed as a fixed fraction- of the generated power (Varbanov, 2004).
- xii. If a condensing steam turbine is selected, it operates with water-cooled condensers.
- xiii. Heat Exchanger Network (HEN) design is out of scope of this work.

4. Problem Formulation

To include all the design alternatives including their corresponding operating conditions, a superstructure based framework is proposed. The framework developed in this work and shown in Figure 1-1 uses a sequence of MILP optimization and simulation stages. This is to exploit the strengths of linear optimization techniques (compared to MINLP formulations) while considering the non-linearities. To ‘simplify’ the original (MINLP) problem formulation, some system properties, such as temperatures and enthalpies, are specified as fixed values during the optimization. After each optimization step, the steam main temperatures, as well as steam system properties, are re-calculated to account for the non-linear effects in the system and to define the actual steam boiler temperature required. This process is repeated until the assumed and actual properties values converge. The simulation stage is carried out in VBA – Excel®, while the MILP optimization is solved using CPLEX 12.10.0 in GAMS 30.3.0. The following subsections provide a summary of these steps.

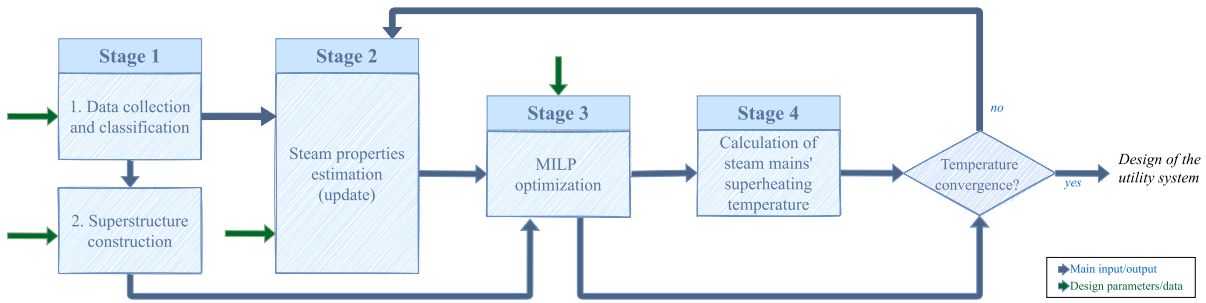


Figure 1-1. Schematic representation of STYLE methodology

4.1. Stage 1 – Data collection and superstructure construction

4.1.1. Process stream data collection and classification

This section explains the data collection and classification procedure for the optimization. This stage comprises three main steps: data collection, construction of total site profiles, and selection and classification of temperature intervals, as illustrated in Figure 1-2.

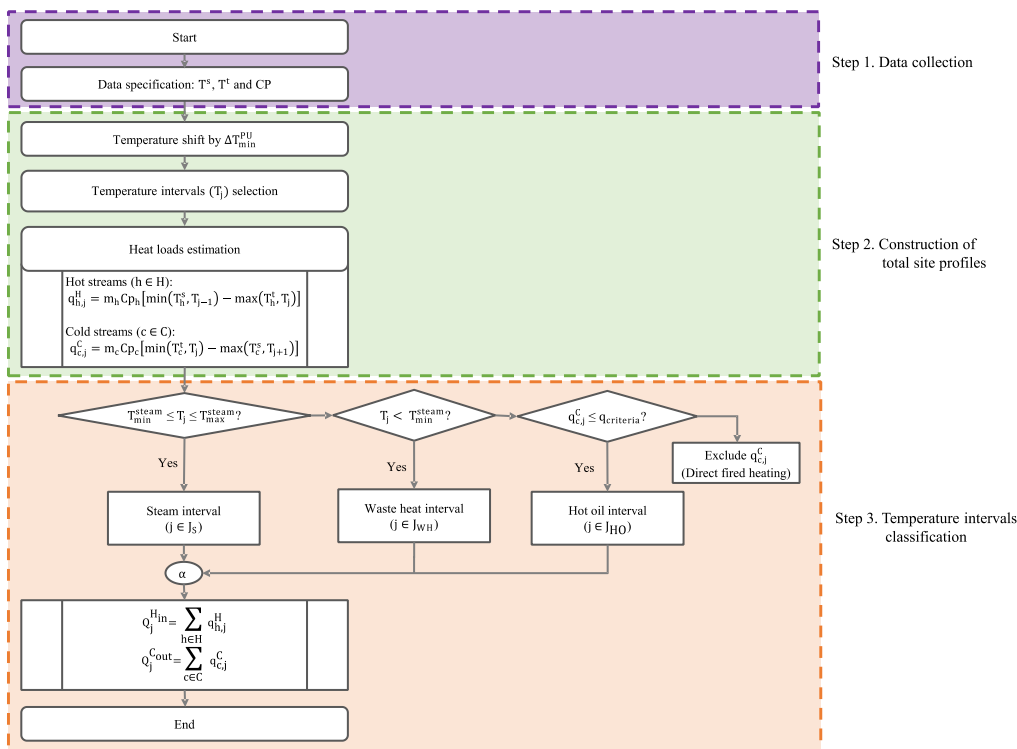


Figure 1-2. Algorithm for process stream data extraction and classification

i. Step 1. Data collection

The data collection involves extracting the data from the processes to characterize the industrial site and its specifics. In this stage, process streams along with the supply and target temperatures (T^s and T^t), and heat capacity flowrate (CP) need to be determined to analyze the potential heat recovery through the utility system. It is important to mention that further heat recovery (HR) could be

obtained if in-process HR is considered. However, in large sites, where several processes/plants are involved, direct HR is not always practical to realize due to limitations, such as distance, safety, controllability, flexibility and/or other operational issues. Therefore, in this work the autonomy of each individual process (whether maximized or not) is considered, focusing on inter-process HR via a total site utility system (Smith, 2016). This approach is also beneficial if the stream data collection is complex. This is because it only requires the information of the streams involving heat exchange with the utility system rather than data from all the heat sources and sinks involved in each process (Smith, 2016). In addition, site specifications regarding technical design limitations (e.g. material temperature constraints, minimum superheating requirement across the site, maximum import and export electricity, etc.), as well as power requirements need to be included.

In reality, it is most likely that the heat supply and the heat demand on the site do not match. The additional required (utility) steam is generated at the highest-pressure main, for example the VHP header. By problem definition, the VHP main is at temperatures/pressures higher than any process heat sink or source. VHP levels (v) are chosen from a set of discrete pressure levels, which are specified by the designer, while the superheat temperature offers a degree of freedom.

In addition to the VHP steam level and temperature specifications and/or constraints across the site, the number of steam mains is required for the design procedure. Also, a list of suitable energy conversion units (e.g. boilers, steam turbines, gas turbines, etc.) with their corresponding economic data, performance at full and part load and technical limitations is required. Furthermore, market conditions and utility prices need to be specified before the optimization.

ii. Step 2. Construction of total site profiles

To provide an overview of the energy demand and to set the potential heat recovery across plants, stream data are translated to a site utility form through total site profiles (TSPs) (Dhole and Linnhoff, 1993). TSPs are temperature-enthalpy plots that focus on exploiting the utility system to recover heat across the whole site. The TSPs combine the heat loads of different processes streams at the same temperature interval to provide an overall view of the heat sources and sinks on the site, in terms of quantity (load) and quality (temperature). The total site profiles are plotted by shifting process stream temperature scales based on a minimum temperature difference for process-to-utility heat transfer ($\Delta T_{\min}^{\text{PU}}$). Heat source temperatures are shifted by $-\Delta T_{\min}^{\text{PU}}$, while heat sink temperatures have $\Delta T_{\min}^{\text{PU}}$ added. Note that different values of $\Delta T_{\min}^{\text{PU}}$ apply to different processes/plants, therefore specific $\Delta T_{\min}^{\text{PU}}$ for each process should be given before the streams are combined for the construction of the total site profiles.

As mentioned in the introduction, heat recovery and cogeneration targets depend on the selection of utility temperature/pressure levels. The identification (selection) of the most relevant temperature intervals (T_j) is a crucial step to define the superstructure that embeds all the design alternatives considered. For instance, in the steam region, temperature intervals (and their corresponding saturated pressure) denote the potential steam levels. To assess all the possible options, ideally the temperature could be defined by uniform partitioning of the site-wide temperature range. Although this approach could be more robust and systematic, it will unnecessarily increase the number of binary variables and the size of the optimization problem. To keep the formulation robust and not to add avoidable complexity, the temperature intervals are defined initially by the kinks (turning points) of both heat sink and source profiles. The kinks, which correspond to the inlet or outlet temperature of each stream, are extracted and ordered from higher (j) to lower ($j+1$) to generate a set of temperature intervals (T_j).

Once a set of the temperature intervals has been defined, the heat content q of hot stream h and cold stream c involved in temperature interval j can be calculated by the following expressions:

$$q_{h,j}^H = CP_h [\min(T_h^s, T_{j-1}) - \max(T_h^t, T_j)] \quad \forall h \in H \quad (1.1)$$

$$q_{c,j}^C = CP_c [\min(T_c^t, T_j) - \max(T_c^s, T_{j+1})] \quad \forall c \in C$$

where T_h^s , T_c^s , T_h^t , T_c^t are the shifted supply and target stream process temperatures.

iii. Step 3 - Temperature intervals classification

Based on the site temperature intervals and the utilities constraints, the TSPs are divided into temperature regions, as illustrated in Figure 1-3. For example, steam distribution is constrained by either the minimum/maximum allowed temperature to generate/use steam or by limitations of materials of construction, defined by the terms T_{\min}^{steam} and T_{\max}^{steam} . Consequently, auxiliary cooling and heating are required. Process heat source temperatures below the minimum allowed temperature for steam generation (specified in this work at 130 °C) can reject heat to BFW (for preheating) or to cool water, as illustrated in Figure 1-3(a). On the other hand, process heat sink temperatures that are above the maximum allowed temperature for steam distribution are satisfied by fired heat (Figure 1-3(b)). In this work, it is assumed that steam can satisfy process heating demands up to 250 °C (saturated conditions). Steam at high pressures is likely to be prohibitively expensive due to the requirement of expensive materials for construction (Smith, 2016) and will prove unsafe for distribution (Towler and Sinnott, 2013).

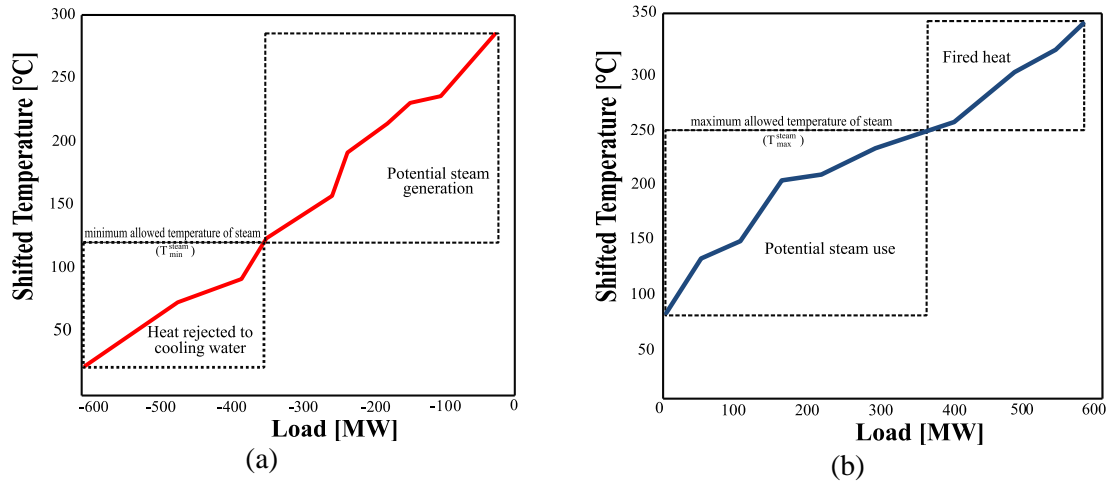


Figure 1-3. Example of heat profile divided into temperature regions (a) heat sources and (b) heat sink processes.

Fired heat can be used for heating directly the streams, or indirectly through hot oil systems. Hot oil systems may be more economically attractive to implement due to the potential for meeting several relatively small high-temperature heat requirements at a reduced financial cost (Towler and Sinnott, 2013). In the case of large amounts of high-temperature duties greater than a minimum amount (in this work assumed at 5 MW), the use of local fired heaters is considered. Ultimately, the minimum amount of heat is dependent on the capacity of technology options.

Once the potential steam levels (j_s) are defined, they are grouped into candidate intervals based on the number of steam mains required (i). Each steam main is defined by a pressure range (boundaries), which is related to the saturated conditions of the steam. The steam mains are sorted in descending order, without considering the utility steam generation (VHP level). This implies that $i = 1, 2, \dots, i_n$ corresponds to the mains ranging from high pressure (HP) to low pressure (LP), respectively. Thus, the temperature intervals involved in each steam main are then defined as (i, j_s) .

The utility steam generation (VHP) levels are considered as a separate set. Finally, steam levels for potential VHP steam levels are indexed as ν , which involve any steam saturation pressures/temperatures above any sink and source heat temperature, as defined by the designer. In a similar way, the number of steam mains and their corresponding pressure ranges are considered as designer parameters.

4.1.2. Superstructure construction

The general superstructure modelling framework for the industrial utility system is illustrated in Figure 1-4 which consists of the following components:

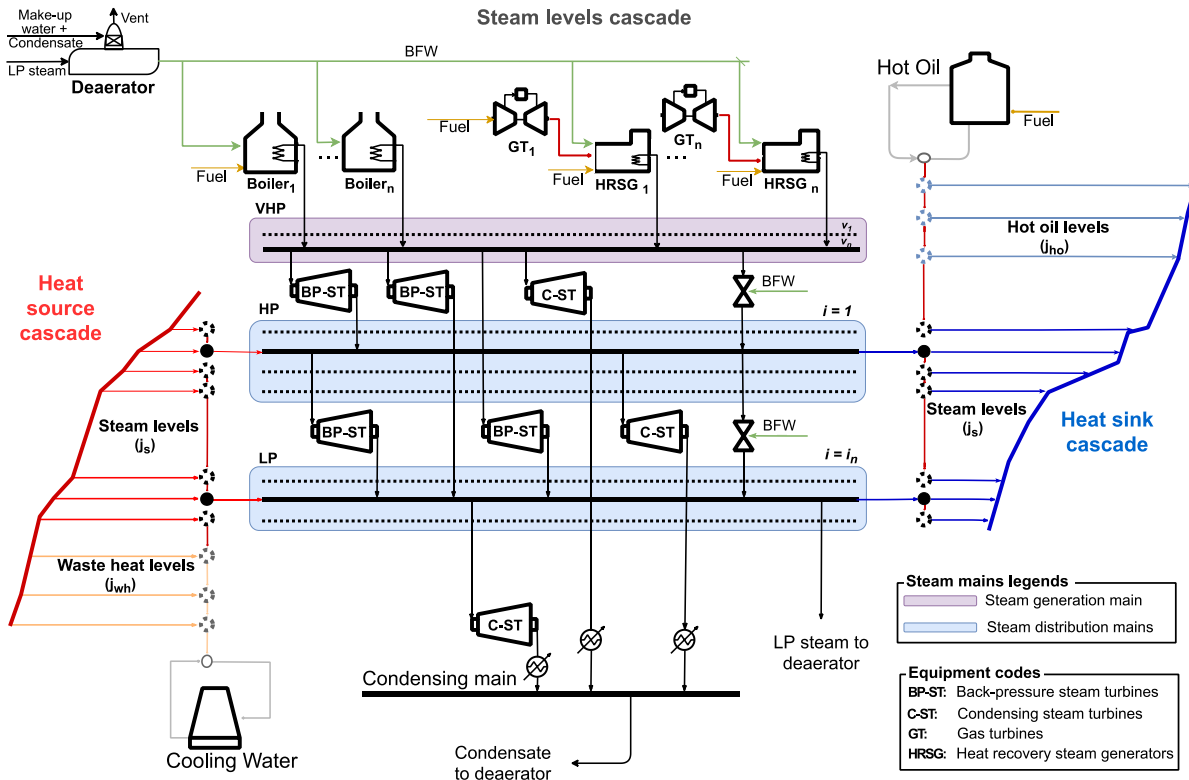


Figure 1-4. Schematic representation of the superstructure (BFW: boiling feed water, HP: High pressure; LP: Low pressure VHP: Very high pressure)

- Temperature intervals, indexed as j in descending order, classified by temperature range and operational constraints (i.e. minimum/maximum temperature for utility and process steam generation)
 - o High-temperature intervals or hot oil levels, indexed as j_{ho} , which represent the temperature intervals that require indirect fired heat
 - o Steam temperature intervals or potential steam levels, indexed as j_s , which represent the potential steam levels
 - o Low-temperature intervals or waste heat levels, indexed as j_{wh} , which represent the temperature intervals for cooling
- n given steam mains, listed as i , from higher to lower pressure, without considering the main for utility steam generation (VHP level).
- Potential VHP steam levels are indexed as v that involve any steam saturation pressures/temperatures above any sink and source heat temperature.
- Superstructure of energy conversion units such as boilers, heat recovery steam generators (HRSGs), gas turbines and steam turbines, furnaces. In addition, utility components, as for example let-down stations.

The utility system is required to meet the heating and power site demand. Heat demand is mainly satisfied by a steam system. Additionally, cooling water systems and hot oil circuits are considered

for auxiliary cooling and heating, respectively. Utility steam is raised at VHP level, by either boilers or heat recovery steam generators (HRSGs). Two types of boiler, i.e. packaged and field-erected, firing fossil fuels are considered for steam generation. HRSGs are driven by the waste gases from gas turbines and supplementary firing (if required). As shown in Figure 1-4, steam is distributed to the different steam levels (headers) by either passing through (back-pressure) steam turbines or let-down stations. In addition, process steam can also be recovered/generated at the different steam levels, depending on the utility level selected. To satisfy the power demand, gas turbines (either aero-derivative or industrial frame), back-pressure turbines and condensing turbines are considered. In case of power imbalance, electricity can be imported or exported from/to the local grid (if allowed). Other utility components, such as deaerators and flash steam recovery systems, are also considered in the modelling framework.

4.2. Stage 2 – Steam properties estimation/update

Steam properties are defined from steam tables based on experimental measurements. Steam tables can be numerically approximated by a set of second or higher-order polynomial regressions. The different correlations comprise several terms involving floating-point powers and natural logarithms, varying according to the water phase region. Due to the high non-linearity and/or requirement of external functions, a non-linear programming (NLP) formulation based on steam temperature optimization could prove challenging to solve, or even intractable with state-of-the-art solvers. Therefore, to avoid non-linearities related with the bilinear terms – resulting from the multiplication between mass flowrates and enthalpies – and to obtain an MILP formulation, steam temperature and enthalpy, alongside isentropic enthalpy difference, are defined as pseudo-parameters. Put simply, they are defined as fixed values (parameters) during the optimization steps, while they are calculated/updated in Stages 4 and 2. In this work, the Excel add-in Steam97® is used, based on the IAPWS-97 equation-of-state model for water (Wagner et al., 2000).

In general, to define steam properties only two variables are required (e.g. pressure and temperature, temperature and enthalpy, enthalpy and pressure, etc.). In this work, steam operating conditions are defined by pressure and enthalpy. As mentioned previously, to reduce the complexity of the problem, a discrete number of pressure levels have been assumed. Therefore, superheating temperature is included as a continuous variable of enthalpy. Moreover, the steam turbine models rely on the isentropic enthalpy change across the steam turbine (ΔH_0^{IS}). ΔH_0^{IS} depends on the actual inlet superheating temperature and the inlet and outlet pressures. While the virtual steam level pressures are defined parameters, the actual inlet temperature/enthalpy is a design variable. In comparison with other work, consideration of superheat temperature as a variable allows to have an overview of the main limitations/restrictions for heat recovery across the site while exploiting the trade-off between heat recovery and cogeneration potential, a more accurate and realistic energy targeting and

performance of the utility system can be achieved. In this approach, the trade-offs between heat recovery and cogeneration potential with the steam level placement can be analysed without compromising the computational effort.

Based on the potential steam level pressures and the site requirements (i.e. minimum steam main superheating, and degree of superheating for both process steam generation and process heating), the enthalpy of steam at every level is defined in the first instance. In addition, the ΔH_0^{IS} for all the potential combinations for steam turbines are calculated/updated in this stage.

4.3. Stage 3 – MILP optimization

The MILP formulation is based on, what is termed here as the Total Site Heat and Mass Cascades (TSHMC) employing a transshipment model. An extension of the Shang and Kokossis (2004) superstructure representation enables to include more accurate energy and mass balances among process source/sink streams and potential steam levels. The TSHMC are formulated by the temperature intervals and comprise three cascades: source, steam, and sink. Process streams act as steam sources or sinks, where the (residual) heat that cannot be used in the interval for either steam generation or use is going to the next lower temperature level, at the respective cascade.

The detailed MILP model accounting for part-load behavior and minimal loads is presented in Supplementary Information P1.A. For brevity, a simplified formulation of the problem (Eqs. (1.2)-(1.16)) is presented in this section.

$$\text{Objective function} \quad \{\min \text{TAC} = \text{ACC} + \text{OC} \quad (1.2)$$

$$\text{Annualized capital cost} \quad \left\{ \text{ACC} = \sum_{\text{Eq}} \sum_{t_{\text{Eq}}} F_{t_{\text{Eq}}}^{\text{ann}} \sum_{n_{\text{Eq}}} F_{n_{\text{Eq}}}^{\text{inst}} \left(C_{n_{\text{Eq}}}^{\text{A}} \cdot Z_{n_{\text{Eq}}, t_{\text{Eq}}}^{\text{Eq}} + C_{n_{\text{Eq}}}^{\text{B}} \cdot y_{n_{\text{Eq}}, t_{\text{Eq}}}^{\text{Eq}} \right) \quad (1.3)$$

$$\text{Operating cost} \quad \{\text{OC} = C_{\text{main}}^{\text{Eq}} + C_{\text{op}}^{\text{f}} + C_{\text{op}}^{\text{cw}} + C_{\text{op}}^{\text{w}} + C_{\text{op}}^{\text{e}} \quad (1.4)$$

Subject to:

$$\text{Source cascade} \quad \begin{cases} Q_{j_s}^{\text{H}_{\text{in}}} + R_{j_s-1}^{\text{H}} = Q_{j_s}^{\text{H}_{\text{out}}} + R_{j_s}^{\text{H}} & \forall j_s \in J_s \\ (1-L^{\text{H}}) Q_{j_s}^{\text{H}_{\text{out}}} = M_{i,j_s}^{\text{H}} \cdot \Delta h_{j_s}^{\text{H}} & \forall i \in I, (i,j_s) \in IJ_s \end{cases} \quad (1.5)$$

$$\text{Steam level cascade} \quad \begin{cases} \sum_{\text{in}} Q_{i,j_s}^{\text{in}} = \sum_{\text{out}} Q_{i,j_s}^{\text{out}} & \forall i \in I, (i,j_s) \in IJ_s \\ \sum_{\text{in}} M_{i,j_s}^{\text{in}} = \sum_{\text{out}} M_{i,j_s}^{\text{out}} & \forall i \in I, (i,j_s) \in IJ_s \end{cases} \quad (1.7)$$

$$\text{Sink cascade} \quad \begin{cases} Q_{i,j_s}^{\text{C}_{\text{in}}} + R_{j_s-1}^{\text{C}} = Q_{j_s}^{\text{C}_{\text{out}}} + R_{j_s}^{\text{C}} & \forall j_s \in J_s \\ Q_{i,j_s}^{\text{C}_{\text{in}}} = M_{i,j_s}^{\text{C}_{\text{in}}} \cdot \Delta h_{j_s}^{\text{C}} & \forall i \in I, (i,j_s) \in IJ_s \end{cases} \quad (1.9)$$

$$\text{Electricity balance} \quad \left\{ W^{\text{grid}} + \sum_{\text{Eq}} W^{\text{Eq}} = \theta_{\text{e}}^{\text{dem}} \quad (1.11)$$

$$\begin{array}{l} \text{Equipment performance} \\ \text{(if selected)} \end{array} \left\{ \begin{array}{l} \text{Output} = \tilde{A}_{11} \begin{bmatrix} Z_{n_{Eq}, t_{Eq}}^{Eq} \\ M_{n_{Eq}, t_{Eq}}^{Eq} \end{bmatrix} + \tilde{A}_{12} y_{n_{Eq}, t_{Eq}}^{Eq} \\ \forall n_{Eq} \in N_{Eq}, t_{Eq} \\ \in T_{Eq} \end{array} \right. \quad (1.12)$$

$$\begin{array}{l} \text{Size and load equipment} \\ \text{constraints (if selected)} \end{array} \left\{ \begin{array}{l} \tilde{A}_{21} \begin{bmatrix} Z_{n_{Eq}, t_{Eq}}^{Eq} \\ M_{n_{Eq}, t_{Eq}}^{Eq} \end{bmatrix} + \tilde{A}_{22} y_{n_{Eq}, t_{Eq}}^{Eq} \leq b_1 \\ \forall n_{Eq} \in N_{Eq}, t_{Eq} \\ \in T_{Eq} \end{array} \right. \quad (1.13)$$

$$\begin{array}{l} \text{Existence of steam main} \\ \text{i operating at condition js} \end{array} \left\{ \begin{array}{l} \tilde{A}_{31} \begin{bmatrix} M_{i,j_s}^{in} \\ M_{i,j_s}^{out} \end{bmatrix} + \tilde{A}_{32} y_{i,j_s}^L \leq b_2 \\ \forall i \in I, (i,j_s) \in IJ_s \end{array} \right. \quad (1.14)$$

$$\begin{array}{l} \text{Electricity import/export} \\ \text{constraint} \end{array} \left\{ |W^{grid}| \leq \tilde{W}_{max}^{grid} \quad (1.15)$$

$$\begin{array}{l} \text{Additional constraints to} \\ \text{avoid infeasibilities} \end{array} \left\{ \tilde{A}_{41} x + \tilde{A}_{42} y \leq b_3 \quad (1.16)$$

$$\begin{array}{l} \text{Variables definition} \end{array} \left\{ \begin{array}{l} y_{n_{Eq}, t_{Eq}}^{Eq}, y_{i,j_s}^L, y \in \{0,1\} \\ M_{i,j_s}^{in}, Q_{i,j_s}^{in}, M_{i,j_s}^{out}, Q_{i,j_s}^{out}, W^{Eq}, Z_{n_{Eq}, t_{Eq}}^{Eq}, M_{n_{Eq}, t_{Eq}}^{Eq}, x \in \mathbb{R}^+ \\ W^{grid} \in \mathbb{R} \end{array} \right.$$

The MILP formulation is based on the minimum total annualized costs (TAC) as the objective function, consisting of the annualized capital (ACC) and operational (OC) expenditures. The capital cost (CC) comprises the sum of the cost of each unit (n_{Eq}) of the different types of equipment available (t_{Eq}), such as furnaces, boilers, back-pressure steam turbines, condensing turbines, gas turbines with HRSGs, condensers, flash tanks and a deaerator. The cost functions are modelled as the sum of a fixed cost for each device ($C_{n_{Eq}}^B$) and a variable cost ($C_{n_{Eq}}^A$), depending on the device size ($Z_{n_{Eq}, t_{Eq}}^{Eq}$). The CC is obtained by including the installation factor ($F_{t_{Eq}}^{inst}$) to account for the construction, installation, contingencies and other associated costs. Additionally, the annualized factor ($F_{t_{Eq}}^{ann}$) is used to spread the CC over the lifetime of the device. The OC includes maintenance costs (C_{main}^{Eq}), in addition to the operating costs of fuel (C_{op}^f), cooling water (C_{op}^{cw}), treated water (C_{op}^w), and electricity (C_{op}^e).

The heat integration is constrained by three heat cascade layers: source, steam level and source. The heat cascades implement the first and second laws of thermodynamics. Eqs. (1.6)-(1.8) and (1.10) satisfy mass and energy balance at each cascade layer (the first law). Meanwhile, Eqs. (1.5) and (1.9) guarantee heat transfer from higher to lower temperatures (the second law).

Further equality constraints involve electricity balance, given by Eq. (1.11). This constraint ensures that the power generated on-site (W^{Eq}) added to grid electricity (W^{grid}) -- either import or export -- meets the power demand (θ_e^{dem}). For reference, Eq. (1.15) restricts the electricity import/export from/to the grid. Equality constraint (1.12) represents the operating performance model of each utility component (i.e. boilers, HRSG and gas and steam turbines), accounting for full and part-load operation.

The linear inequalities, expressed by Eqs. (1.13) and (1.14), with coefficient matrices \tilde{A} and the parameter vectors b , denote the existence of steam main i (operating at j_s conditions) through discrete variable y_{i,j_s}^L , along with the selection of components (i.e. boilers, HRSG, gas and steam turbines) by the binary variable $y_{n_{Eq}, t_{Eq}}^{Eq}$. Moreover, Eq. (1.13) and (1.14) involve logical constraints, such as minimum and maximum: load ($M_{n_{Eq}, t_{Eq}}^{Eq}$)/size ($Z_{n_{Eq}, t_{Eq}}^{Eq}$)/mass flowrate (M_{i,j_s}^{in} and M_{i,j_s}^{out}) for each component (if selected). Further inequalities are summarized in Eq. (1.16), where additional continuous and binary variables of the original problem are represented by vector x and y , respectively.

4.3.1. Main innovations in the MILP formulation

i. Source cascade

Previous methodologies in this field assume only latent heat to determine (process) steam generation. Furthermore, others do not consider the energy required for either boiler feed water preheating or steam superheating. To overcome this drawback, Eq. (1.6a) presents a new modification that addresses the shortcomings of previous work:

$$(1-L^H) Q_{j_s}^{H_{out}} = M_{i,j_s}^H \cdot (h_{sh_{j_s}}^H - h^{BFW}) \quad \forall i \in I, (i,j_s) \in IJ_s \quad (1.6a)$$

Indeed, this work introduces the enthalpy of superheated process steam ($h_{sh_{j_s}}^H$) as a design parameter, whose value is not necessarily the same as the enthalpy of the corresponding steam main ($h_{j_s}^{main}$). Whilst high superheat temperatures could be required for the optimum operation of utility system and its components (i.e. steam turbines), it may not be ideal for the process steam generation and its heat exchanger design. High amounts of superheat in steam can be a problem in heat exchanger design because of its resulting low heat transfer coefficient. Crucially, in the model presented in this work process steam can be produced at a different temperature from the steam main. To be precise, the value defined for $h_{sh_{j_s}}^H$ is independent of $h_{j_s}^{main}$. Importantly, $h_{sh_{j_s}}^H$ is defined/restricted by the steam main pressure, the source profile temperatures, and the heat exchanger equipment constraints. Additional losses -- due to steam distribution from the users to the utility system -- are accounted for in the parameter L^H .

i. Steam level cascade

Heat flows into the steam level from steam generation (M^H), with steam passing through either the back pressure steam turbines (BP-ST) or let-down stations (LD) and BFW. Steam may be used for:

(1) process heating ($M_{i,j}^{C_{main}}$), (2) power generation through steam expansion via a back-pressure ($M_{i,j}^{BP-ST_{out}}$) or a condensing steam turbine ($M_{i,j}^{C-ST_{out}}$), or (3) for temperature/ pressure control in the steam mains by passing it to a let-down station ($M_{i,j}^{LD_{out}}$). Eq. (1.7a) corresponds to the generic energy balance around each steam header with exception of the bottom steam header. The bottom steam header (i_n) can only expand steam to a vacuum condition and has an additional steam output which feeds the deaerator ($M_{j_s}^{Deae}$), as stated in Eq. (1.7b):

$$M_{i,j_s}^H \cdot h_{sh_{j_s}}^H + Q_{i,j_s}^{BP-ST} + Q_{i,j_s}^{LD} + M_{i,j_s}^{BFW} \cdot h^{BFW} = \left(M_{i,j_s}^{C_{main}} + M_{i,j_s}^{BP-ST_{out}} + M_{i,j_s}^{C-ST_{out}} + M_{i,j_s}^{LD_{out}} \right) \cdot h_{sh_{i,j_s}}^{main} \quad \forall i < i_n, (i,j_s) \in IJ_s \quad (1.7a)$$

$$M_{i,j_s}^H \cdot h_{sh_{j_s}}^H + Q_{i,j_s}^{BP-ST} + Q_{i,j_s}^{LD} + M_{i,j_s}^{BFW} \cdot h^{BFW} = \left(M_{i,j_s}^{C_{main}} + M_{j_s}^{Deae} + M_{i,j_s}^{C-ST_{out}} + M_{i,j_s}^{LD_{out}} \right) \cdot h_{sh_{i,j_s}}^{main} \quad \forall i = i_n, (i,j_s) \in IJ_s \quad (1.7b)$$

A significant development in this research is the increased combinations available in the design options which allows a more realistic analysis. The proposed superstructure considers all the possible combinations of inlet/outlet conditions for steam turbines and let-down stations, based on the potential pressure levels of every steam main. The superstructure also includes the potential combinations with the different conditions of the VHP header. Due to the flexible consideration in the inlet streams from steam turbines and let-down stations, their terms are abbreviated as (Q_{i,j_s}^{BP-ST}) and (Q_{i,j_s}^{LD}). All the feasible possibilities mentioned above are defined by Eqs. (1.17) and (1.18):

$$Q_{i,j_s}^{LD} = \sum_{i' < i} \sum_{(i',j_s') \in IJ_s} \left(m_{i',j_s'}^{LD} \cdot h_{j_s'}^{main} \right) + \sum_{v \in V} \left(m_{v,j_s}^{LD} \cdot h_{sh_v}^{VHP} \right) \quad \forall i \in I, \quad (i,j_s) \in IJ_s \quad (1.17)$$

$$Q_{i,j_s}^{BP-ST} = \sum_{n_{st} \in N_{st}} \sum_{i' < i} \sum_{(i',j_s') \in IJ_s} \left(m_{n_{st},i',j_s'}^{BP-ST} \cdot h_{sh_{j_s'}}^{main} - \frac{W_{n_{st},i',j_s'}^{BP-ST}}{\eta_{mec}} \right) + \sum_{n_{st} \in N_{st}} \sum_{v \in V} \left(m_{n_{st},v,j_s}^{VHP} \cdot h_{sh_v}^{VHP} - \frac{W_{n_{st},v,j_s}^{VHP}}{\eta_{mec}} \right) \quad \forall i \in I, \quad (i,j_s) \in IJ_s \quad (1.18)$$

Where indices i' and j_s' are aliases of position sets I and J_s , respectively, and used to restrict heat transfer from higher to lower levels only. For instance, in Eq. (1.17) the heat content of the steam let-down entering at steam main i (operating at j_s conditions) is limited to steam coming from either steam mains operating at higher temperatures/pressures (i', j_s') or the VHP level v .

Additionally, the mass balance at each steam main is expressed by Eq. (1.8):

$$M_{i,j_s}^H + M_{i,j_s}^{BP-ST_{in}} + M_{i,j_s}^{LD_{in}} + M_{i,j_s}^{BFW} = M_{i,j_s}^{C_{main}} + M_{i,j_s}^{BP-ST_{out}} + M_{i,j_s}^{Cond-ST_{out}} + M_{i,j_s}^{LD_{out}} \quad \forall i < i_n, (i,j_s) \in IJ_s \quad (1.8)$$

$$M_{i,j_s}^H + M_{i,j_s}^{BP-ST_{in}} + M_{i,j_s}^{LD_{in}} + M_{i,j_s}^{BFW} = M_{i,j_s}^{C_{main}} + M_{j_s}^{Deae} + M_{i,j_s}^{Cond-ST_{out}} + M_{i,j_s}^{LD_{out}} \quad i = i_n, (i,j_s) \in IJ_s$$

Due to the above defined superstructure, Eqs. (1.19) - (1.22) ensure that the total amount of steam from the let-down stations and steam turbines entering the headers equals that leaving:

$$M_{i,j_s}^{\text{BP-ST in}} = \sum_{n_{st} \in N_{st}} \sum_{i' < i} \sum_{(i', j_s') \in IJ_s} m_{n_{st}, i', j_s', j_s}^{\text{BP-ST}} + \sum_{n_{st} \in N_{st}} \sum_{v \in V} m_{n_{st}, v, j_s}^{\text{VHP BP-ST}} \quad \forall i \in I, (i, j_s) \in IJ_s \quad (1.19)$$

$$M_{i,j_s}^{\text{BP-ST out}} = \sum_{n_{st} \in N_{st}} \sum_{j_s > j_s'} m_{n_{st}, i, j_s, j_s'}^{\text{BP-ST}} \quad \forall i \in I, (i, j_s) \in IJ_s \quad (1.20)$$

$$M_{i,j_s}^{\text{LD in}} = \sum_{i' < i} \sum_{(i', j_s') \in IJ_s} m_{i', j_s', j_s}^{\text{LD}} + \sum_{v \in V} m_{v, j_s}^{\text{VHP LD}} \quad \forall i \in I, (i, j_s) \in IJ_s \quad (1.21)$$

$$M_{i,j_s}^{\text{LD out}} = \sum_{j_s > j_s'} m_{i, j_s, j_s'}^{\text{LD}} \quad \forall i \in I, (i, j_s) \in IJ_s \quad (1.22)$$

ii. Sink energy balance

As outlined in the introduction section, superheating may not be ideal for heating purposes. For this reason, steam desuperheating prior to its use is included as an option, as expressed by Eq. (1.10a):

$$Q_{i,j_s}^{\text{C in}} = M_{i,j_s}^{\text{C in}} \cdot (h_{sh, j_s}^{\text{C}} - h_{l, j_s}^{\text{C}}) \quad \forall i \in I, (i, j_s) \in IJ_s \quad (1.10a)$$

Desuperheating is usually achieved by mixing the steam locally with BFW. Because of this there is a further addition of the variable M_{i,j_s}^{BFWC} in the mass and energy balance of the sink cascade, as expressed in Eqs. (1.23) and (1.24):

$$(1-L^{\text{C}}) \cdot M_{i,j_s}^{\text{C main}} \cdot h_{sh, j_s}^{\text{main}} + M_{i,j_s}^{\text{BFWC}} \cdot h^{\text{BFW}} = M_{i,j_s}^{\text{C in}} \cdot (h_{sh, j_s}^{\text{C}} - h_{l, j_s}^{\text{C}}) \quad \forall i \in I, (i, j_s) \in IJ_s \quad (1.23)$$

$$M_{i,j_s}^{\text{C main}} + M_{i,j_s}^{\text{BFWC}} = M_{i,j_s}^{\text{C in}} \quad \forall i \in I, (i, j_s) \in IJ_s \quad (1.24)$$

Similar to the source cascade, the enthalpy of steam use (h_{sh, j_s}^{C}) is a specified design parameter that may differ from $h_{sh, j_s}^{\text{main}}$. Additional losses caused by steam distribution from the site to the steam users are included in the parameter L^{C} .

iii. Flash steam recovery (FSR) integration

For large heat transfer loads, recovering the steam that is flashed as the condensate pressure is reduced can improve the thermal efficiency of the system. In this work, FSR is assumed to be only used for heating purposes and not considered for steam cascade and with it, power generation. Despite the potential benefit of the power generation potential, the recovery of saturated steam into the main (at superheated conditions) may lead to a higher energy requirement to balance the headers and avoid excessive condensation. If FSR is included, Eqs. (1.23) and (1.24) are replaced by Eqs. (1.23a) and (1.24a):

$$(1-L^{\text{C}}) \cdot M_{i,j_s}^{\text{C main}} \cdot h_{sh, j_s}^{\text{main}} + M_{i,j_s}^{\text{BFWC}} \cdot h^{\text{BFW}} + M_{i,j_s}^{\text{FSR}} \cdot h_{v, j_s} = M_{i,j_s}^{\text{C in}} \cdot (h_{sh, j_s}^{\text{C}} - h_{l, j_s}^{\text{C}}) = Q_{i,j_s}^{\text{C in}} \quad \forall i \in I, (i, j_s) \in IJ_s \quad (1.23a)$$

$$M_{i,j_s}^{\text{C main}} + M_{i,j_s}^{\text{BFWC}} + M_{i,j_s}^{\text{FSR}} = M_{i,j_s}^{\text{C in}} \quad \forall i \in I, (i, j_s) \in IJ_s \quad (1.24a)$$

M_{i,j_s}^{FSR} represents the flashed steam fed to the mixer i operating at j_s conditions and h_{v,j_s} is the specific enthalpy of saturated steam at pressure level j_s .

The amount of flashed steam is determined by the mass and energy balance given in the FSR, as shown below:

$$M_{i,j_s}^{\text{FSR}} = \sum_{i' < i} \sum_{(i',j_s') \in \text{IJ}_s} m_{s,i',j_s',j_s}^{\text{FSR}} \quad \forall i \in I, (i, j_s) \in \text{IJ}_s, \text{FSR} = 1 \quad (1.25)$$

$$M_{i,j_s}^{\text{FSR}} = 0 \quad \forall i \in I, (i, j_s) \in \text{IJ}_s, \text{FSR} = 0 \quad (1.26)$$

$$\beta \cdot M_{i,j_s}^{\text{C}_{in}} + \sum_{i' < i} \sum_{(i',j_s') \in \text{IJ}_s} m_{l,i',j_s',j_s}^{\text{FSR}} = m_{in,i,j_s}^{\text{FSR}} \quad \forall i \in I, (i, j_s) \in \text{IJ}_s \quad (1.27)$$

$$\sum_{j_s' \in \text{J}_s} (m_{s,i,j_s,j_s'}^{\text{FSR}} + m_{l,i,j_s,j_s'}^{\text{FSR}}) = M_{in,i,j_s}^{\text{FSR}} \quad \forall i \in I, (i, j_s) \in \text{IJ}_s \quad (1.28)$$

$$\sum_{j_s' > j_s} (m_{s,i,j_s,j_s'}^{\text{FSR}} \cdot h_{v,j_s'} + m_{l,i,j_s,j_s'}^{\text{FSR}} \cdot h_{l,j_s'}) = M_{in,i,j_s}^{\text{FSR}} \cdot h_{l,j_s} \quad \forall i \in I, (i, j_s) \in \text{IJ}_s \quad (1.29)$$

where $m_{s,i,j_s,j_s'}^{\text{FSR}}$ and $m_{l,i,j_s,j_s'}^{\text{FSR}}$ are the steam and liquid amount recovered at pressure j_s' , based on the condensate at the drum inlet ($M_{in,i,j_s}^{\text{FSR}}$). Additionally, β represents the rate of steam condensate return. The condensate recycle may depend on the steam use (direct steam injection, indirect heating) and potential losses (i.e. contamination, leaks or economic viability). Condensate return (if recovered) could be as high as 90%. Higher return rates are plausible but may be prohibitively expensive due to the cost of the pipework needed (Smith, 2016).

iv. Steam temperature constraints and hot oil circuit integration

While steam at 90 – 110 bars may be used for power generation, the use of steam for heating purposes above 40 bar ($T_{\text{sat}} = 250 \text{ }^\circ\text{C}$) is unlikely (Towler and Sinnott, 2013). This is because -- as previously mentioned -- steam at very high pressures is likely to be prohibitively expensive and unsafe for distribution (Smith, 2016). Therefore, in this work steam is assumed to satisfy process heating demands of up to 250 °C (saturated conditions). Above this temperature fired heat is required. Fired heat can be used for heating directly the streams, or indirectly through hot oil systems. The latter is favored in this work due to its potential for meeting several relatively small amounts of high-temperature heat at a lower economic cost (Towler and Sinnott, 2013), but restricted to a maximum of 400 °C. However, in the case of large amounts of high-temperature duties the use of local fired heaters should be considered.

The heat provided above the maximum steam temperature (T_{max}) is defined by Eq. (1.30):

$$Q^{\text{HO}} = \sum_{j \in J, T_j \geq T_{\text{max}}} Q_j^{\text{C}_{out}} \quad (1.30)$$

Below the maximum steam temperature, heat demand can be provided by either steam usage from the corresponding interval or from hot oil. To represent this, at the highest steam level, heat flow from hot oil is allowed, as expressed by Eq. (1.31).

$$Q_{i,j_s}^{C_{in}} + Q_s^{HO} = Q_{j_s}^{C_{out}} + R_{j_s}^C \quad i=1, j_s=1 \quad (1.31)$$

Within the steam temperature range, the heat supplied by hot oil is restricted to the levels where the use of hot oil is favored by the optimization ($y_{j_s}^{HO} = 1$), as given by Eq. (1.32):

$$Q_s^{HO} = \sum_{j_s \in J_s, T_{j_s} > T_t^{HO}} (Q_{j_s}^{C_{out}} \cdot y_{j_s}^{HO}) \quad (1.32)$$

Total fired heating utility (Q_T^{HO}) can be modelled as a sum of the heat duties above the steam temperature range, added to all the process heating requirements that cannot be used/satisfied by steam, as shown in Eq. (1.33):

$$Q_T^{HO} = Q_s^{HO} + Q^{HO} \quad (1.33)$$

Finally, the overall energy balance in the heat sink cascade is considered via Eq. (1.34):

$$\sum_{i \in I} \sum_{j_s \in I_{j_s}} Q_{i,j_s}^{C_{in}} + Q_T^{HO} = \sum_{j \in J} Q_j^{C_{out}} \quad (1.34)$$

A further vital point is that the hot oil mass flowrate is not relevant in this mathematical formulation since the working fluid is recirculated within the system. As examined in literature (Towler and Sinnott, 2013), the initial cost of the fluid has a limited impact on the overall cost of the hot oil system and instead the operating cost is mainly due to the fuel needed to re-heat the working fluid. Therefore, the design variable is the heat load of hot oil required.

Additional constraints are added to ensure: (1) hot oil (if required) is used first at higher temperatures (Eq. (1.35)), (2) the use of only one utility at each temperature interval (Eq. (1.36)):

$$y_{j_s}^{HO} - y_{j_s-1}^{HO} \leq 0 \quad j_s > 1 \quad (1.35)$$

$$y_{j_s}^{HO} + y_{i,j_s}^L \leq 1 \quad \forall i \in I, (i,j_s) \in I_{j_s} \quad (1.36)$$

v. VHP steam level

As noted earlier, the highest-pressure (VHP) main receives steam from the operating utility boilers ($M_{nb, t_b, v}^b$) and the heat recovery steam generators ($M_{n_{HRSG}, v}^{HRSG}$). From the problem definition, VHP level conditions are always located at temperatures higher than any process heat sink or source. In this work, different VHP level conditions can be assessed simultaneously, by the addition of the set v , which represents the pressure at which the generator units will be producing steam. The balance

equations for the VHP level candidates are the usual mass and energy balances, involving the corresponding inlet and outlet steam flows. The mass balance around the VHP steam level is expressed by Eq. (1.37) where the $M_{T_v}^{\text{VHP}}$ term comprises the overall utility steam requirement at v conditions:

$$\begin{aligned} \sum_{\text{in}} M_v^{\text{in}} &= \sum_{\text{out}} M_v^{\text{out}} & \forall v \in V & \quad (1.37) \\ \sum_{n_b \in N_b} \sum_{t_b \in T_b} M_{n_b, t_b, v}^b + \sum_{n_{\text{HRSG}}} M_{n_{\text{HRSG}}, v}^{\text{HRSG}} &= M_{T_v}^{\text{VHP}} & \forall v \in V & \\ M_{T_v}^{\text{VHP}} &= \sum_{n_{\text{st}}} \sum_{j_s \in J_s} m_{n_{\text{st}}, v, j_s}^{\text{VHP BP-ST}} + \sum_{n_{\text{st}} \in N_{\text{st}}} m_{n_{\text{st}}, v}^{\text{VHP C-ST}} + \sum_{j_s \in J_s} m_{v, j_s}^{\text{VHP LD}} & \forall v \in V & \end{aligned}$$

For the heat balance in the VHP steam level, iso-thermal mixing is assumed. As expressed in Eq. (1.38), any boiler or HRSG unit generates steam at v conditions (temperature and pressure).

$$M_{T_v}^{\text{VHP}} \cdot h_{\text{sh}_v}^{\text{VHP}} = \left[\sum_{j_s \in J_s} \left(m_{v, j_s}^{\text{VHP BP-ST}} + m_{v, j_s}^{\text{VHP LD}} \right) + m_v^{\text{VHP C-ST}} \right] \cdot h_{\text{sh}_v}^{\text{VHP}} \quad \forall v \in V \quad (1.38)$$

VHP steam level is linked to the steam distribution system through the steam expanded by either back-pressure steam turbines ($m_{n_{\text{st}}, v, j_s}^{\text{VHP BP-ST}}$) or let-down stations ($m_{v, j_s}^{\text{VHP LD}}$), involved in Eqs. (1.19), (1.21), (1.37), (1.38), (1.42) and (1.44).

vi. Equipment models

The operating performance for boilers (Varbanov, 2004), HRSG, gas turbines (Shang, 2000; Varbanov, 2004; Aguilar et al., 2007a), and steam turbines (Sun and Smith, 2015) is estimated by employing models that account for full and part-load operation. Regarding gas and steam turbines performance, shaft power (W_{θ}^{st}) can be linearly related to its load (m_{θ}^{st}) through Willans's correlation (Willans, 1888), as given by Eq. (1.39). The terms $\eta_{\theta}^{\text{st}}$ and $W_{\text{int}_{\theta}}^{\text{st}}$ denote the slope and the intercept of the Willans' line, respectively. A compact formulation to describe the calculation of steam turbine shaft-work is given below.

$$W_{\theta}^{\text{st}} = \eta_{\theta}^{\text{st}} \cdot m_{\theta}^{\text{st}} - W_{\text{int}_{\theta}}^{\text{st}} \cdot y_{\theta}^{\text{st}} \quad (1.39)$$

$$\eta_{\theta}^{\text{st}} = \frac{1 + c_{\theta}^{\text{st}}}{a_{\theta}^{\text{st}}} \left(\Delta H_{\theta}^{\text{IS}} - \frac{b_{\theta}^{\text{st}}}{m_{\text{max}_{\theta}}^{\text{st}}} \right) \quad (1.40)$$

$$W_{\text{int}_{\theta}}^{\text{st}} = \frac{c_{\theta}^{\text{st}}}{a_{\theta}^{\text{st}}} \left(\Delta H_{\theta}^{\text{IS}} \cdot m_{\text{max}_{\theta}}^{\text{st}} - b_{\theta}^{\text{st}} \right) \quad (1.41)$$

The sub-index θ represents the different alternative options:

$$\theta = n_{\text{st}, i, j_s, j'_s} \quad \text{for back-pressure steam turbine } n_{\text{st}} \text{ operating between headers } (i, j_s) \text{ and } (i', j'_s).$$

- $\theta = n_{st}, v, i, j_s$ for back-pressure steam turbine n_{st} operating between VHP header v and steam main (i, j) .
- $\theta = n_{st}, i, j_s$ for condensing turbine n_{st} operating at inlet pressure j_s .
- $\theta = n_{st}, v$ for condensing turbine n_{st} operating at inlet pressure v .

Modelling coefficients a_θ^{st} , b_θ^{st} and c_θ^{st} are turbine parameters, defined by inlet and outlet pressure, as well as the turbine type (Sun and Smith, 2015).

Replacing Eqs (1.40) and (1.41) in Eq. (1.39) and rearranging gives:

$$W_\theta^{st} = \frac{1+c_\theta^{st}}{a_\theta^{st}} \left(\Delta H_\theta^{IS} \cdot m_\theta^{st} - b_\theta^{st} \frac{m_\theta^{st}}{m_{\max \theta}^{st}} \right) - \frac{c_\theta^{st}}{a_\theta^{st}} (\Delta H_\theta^{IS} \cdot m_{\max \theta}^{st} - b_\theta^{st} \cdot y_\theta^{st}) \quad (1.42)$$

The turbine models comprise non-linear features arising from the correlation between the equipment capacity and load $\left(\frac{m_\theta^{st}}{m_{\max \theta}^{st}} \right)$, as expressed in Eq. (1.42). The correlation can be expressed as a fraction, represented by variable x_θ^{st} . Alternatively, the fraction can be expressed as a product (see Eq. (1.43)). The nonconvex term can be relaxed into a convex expression, by widely used methodologies, such as McCormick convex envelopes (Eq. (1.44)).

$$x_\theta^{st} = \frac{m_\theta^{st}}{m_{\max \theta}^{st}} \text{ or } m_\theta^{st} = x_\theta^{st} \cdot m_{\max \theta}^{st} \quad (1.43)$$

$$\begin{aligned} m_\theta^{st} &\geq \sigma_\theta^{st} \cdot m_{\max \theta}^{st} + \Omega_{\min \theta}^{st} \cdot x_\theta^{st} - \sigma_\theta^{st} \cdot \Omega_{\min \theta}^{st} \cdot y_\theta^{st} \\ m_\theta^{st} &\leq m_{\max \theta}^{st} + \Omega_{\min \theta}^{st} \cdot x_\theta^{st} - \Omega_{\min \theta}^{st} \cdot y_\theta^{st} \\ m_\theta^{st} &\geq m_{\max \theta}^{st} + \Omega_{\max \theta}^{st} \cdot x_\theta^{st} - \Omega_{\max \theta}^{st} \cdot y_\theta^{st} \\ m_\theta^{st} &\leq \sigma_\theta^{st} \cdot m_{\max \theta}^{st} + \Omega_{\max \theta}^{st} \cdot x_\theta^{st} - \sigma_\theta^{st} \cdot \Omega_{\max \theta}^{st} \cdot y_\theta^{st} \end{aligned} \quad (1.44)$$

where σ_θ^{st} represents the minimum load fraction of steam turbine operating at θ conditions; $\Omega_{\min \theta}^{st}$ and $\Omega_{\max \theta}^{st}$ define the minimum and maximum equipment capacity in terms of flowrate, respectively.

Additional, logical constraints to ensure the range of the variable x_θ^{st} are included in Eq. (1.45) and (1.46):

$$x_\theta^{st} \geq \sigma_\theta^{st} \cdot y_\theta^{st} \quad (1.45)$$

$$x_\theta^{st} \leq y_\theta^{st} \quad (1.46)$$

Based on the above mentioned modification, Eq. (1.42) can be written as:

$$W_\theta^{st} = \frac{1+c_\theta^{st}}{a_\theta^{st}} (\Delta H_\theta^{IS} \cdot m_\theta^{st} - b_\theta^{st} \cdot x_\theta^{st}) - \frac{c_\theta^{st}}{a_\theta^{st}} (\Delta H_\theta^{IS} \cdot m_{\max \theta}^{st} - b_\theta^{st} \cdot y_\theta^{st}) \quad (1.42a)$$

This arrangement allows for an approximation of the equipment performance at part-load. Based on the obtained results, the size boundaries $(\Omega_{\min\theta}^{st}, \Omega_{\max\theta}^{st})$ are updated within the optimization, resulting in tighter envelopes. Tighter relaxation guarantees convexity while its outcome is closer to the global solution. Due to the nature of the variables involved and their high interrelation, the computational time required to converge to the optimal solution can be considered negligible. The presented approach allows the definition of equipment size as a variable without requiring a decision by the designer prior to utilization. The adjustment is only required if the equipment capacity under analysis is unknown a priori, or if the entire range of options is under analysis. If the designer has a set of defined equipment sizes that they seek to evaluate, the equipment size becomes a parameter and Eq. (1.42) does not involve any non-linearity. However, Eq. (1.44) is still valid by simply defining $\Omega_{\min\theta}^{st} = \Omega_{\max\theta}^{st} = m_{\max\theta}^{st}$.

4.4. Stage 4 - Calculation of steam main superheating temperature

As mentioned previously, most previous work has assumed fixed steam operating conditions (pressure and temperature). Some researchers (Shang and Kokossis, 2004; Varbanov et al., 2005) that attempted to address this problem had assumed variable pressure, but considered only saturated steam temperature. More importantly, in their work the VHP operating conditions have been assumed as a given parameter. By contrast, this work ensures that not only the optimum pressure levels of the main for steam distribution are determined by the model, but also allows for the selection of VHP levels. Additionally, it estimates steam superheated temperature required in both VHP and steam distribution mains. Figure 1-5 shows the general methodology developed in this work to calculate the superheating temperature at each steam main, using the Steam97® Excel Add-In, as explained in more detail below.

As shown in Figure 1-5, the calculations of superheating temperatures require top-down iterations that start with the utility steam main ($i = 1$) and work down through the cascade. The calculations progress from high to low pressure levels until the superheating constraint is satisfied by all the steam mains (described below). The following steps are involved:

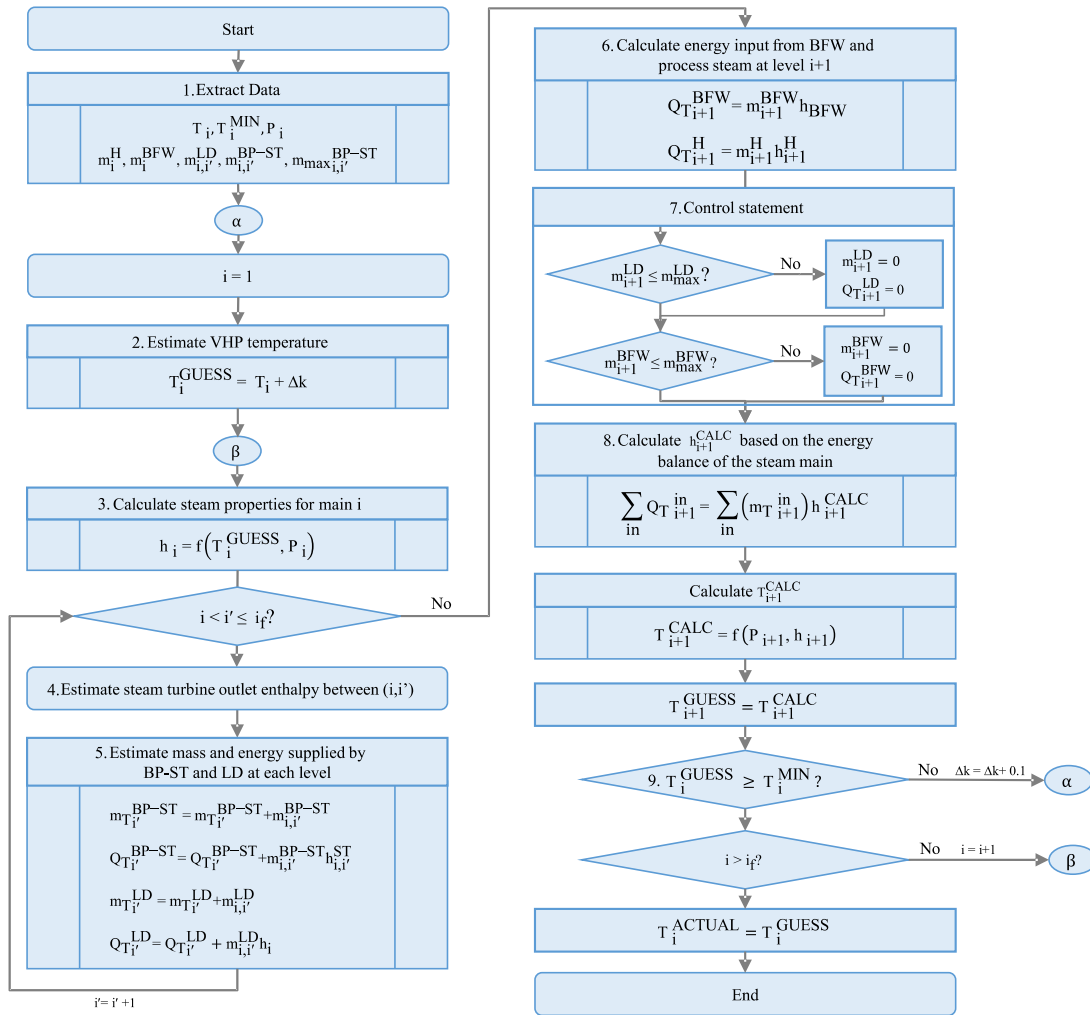


Figure 1-5. Algorithm for calculating steam mains' superheating

Step 1: Data extraction. Once the optimum steam level placement (saturated temperature/pressure) has been obtained, the mass flowrates, pressures (P_i) and minimum superheat temperature (T_i^{MIN}) are set as input data. If either let-down or back pressure connections are selected, their corresponding inlet or outlet pressures must be defined at the beginning of the algorithm. Additionally, if back-pressure turbines are selected, its capacity (m_{max}^{BP-ST}) must also be specified. Importantly, this is required for the calculation of the outlet conditions of the steam turbine, carried out later in Step 5.

Step 2: Initial estimation of VHP superheating temperature ($T_{i=1}^{GUESS}$).

Step 3: Estimation of the enthalpy at steam conditions. The actual enthalpy at each level is given by the IAPWS95 function (Wagner et al., 2000), based on the estimated temperature (T_i^{GUESS}) and the steam pressure (P_i) at each level.

Steps 4 and 5: Determination of mass and heat flows passing from steam main i into steam level i' , through either the steam turbines or let-down stations. In this work, the model accounts for different arrangements of inlet/outlet conditions for steam turbines and let-down stations. Due to this

consideration, these stages determine the mass and heat flows coming from different levels into steam main i' . This addresses previous limitations of steam turbines placed only in series, in addition to the consideration of let-down flow to satisfy superheat requirement.

To calculate the heat available at the outlet of the steam turbine, it is required to estimate the turbine exhaust properties. Turbine exhaust properties (Step 4) are obtained using the Willans' model presented in Sun and Smith (2015). Their pressure-based method can predict the steam outlet conditions, as well as the isentropic efficiency, based on the load of a given turbine capacity with fixed steam pressure drop, following the steps detailed in Figure 1-6. For the let-down heat calculation, isenthalpic expansion is assumed.

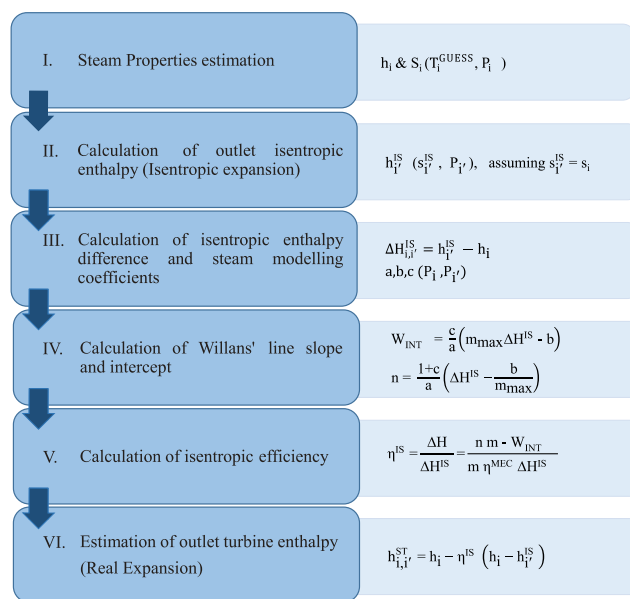


Figure 1-6. Procedure to estimate steam turbine outlet enthalpy

Step 6: In this stage the mass and energy flows of BFW and process steam entering the level ($i+1$) are estimated. It is important to note that process steam enthalpy (h_i^{H}) is a pre-defined input and independent of the steam main temperature calculation.

Step 7: Control statement. If the amount of let-down ($m_{T_i}^{\text{LD}}$) in any of the steam mains is higher than the preferred one (value defined by the designer), the let-down mass ($m_{T_i}^{\text{LD}}$) and heat ($Q_{T_i}^{\text{LD}}$) flows are set to zero. This is to estimate the VHP temperature increase required to obtain the minimum superheated temperature at each level without the “excessive” let-down heat contribution. Although such an event is rare, large amounts of let-down are most likely in the first iteration of the optimization when additional let-down may be necessary to balance the initially assumed header temperature. A similar constraint is added for the BFW mass flowrate (m_i^{BFW}).

Step 8: Calculation of superheating temperature. The actual enthalpy at (h_{i+1}) is calculated through the energy balance at steam main level ($i+1$). The superheating temperature at the ($i+1$) level is determined via the IAPWS95 function.

Step 9: The calculated temperature ($T_{i=1}^{\text{GUESS}}$) is compared against the minimum superheating temperature at i level. If the temperature is above the minimum allowed, Steps 3 to 8 are repeated for the next lower level. Otherwise the VHP temperature is increased and the algorithm is restarted. The process is repeated until the superheating constraint is satisfied by all the steam mains.

Finally, Stage 2 to 4 are repeated until convergence between the assumed temperature and the real temperature of the steam mains is achieved.

It is worth noting that in comparison with existing models (Kundra, 2005; Khoshgoftar Manesh et al., 2013; Ghannadzadeh et al., 2012), the proposed algorithm for calculating the actual temperature of each steam main takes into account process steam generation at different temperatures (than the steam mains), steam expansion through letdown stations and injection of BFW, which are practical features found when balancing steam mains. Despite steam expansion through let-down valves reducing the cogeneration efficiency, its use is essential for providing flexibility to the utility system and/or achieving the minimum degree of superheat for every steam main without violating the maximum temperature constraints. A key limitation of the models of Kundra (2005) and Ghannadzadeh et al. (2012) is that they assume constant isentropic turbine efficiency, neglecting the effect of steam turbines operating at part-load on the actual temperature of steam mains. Additionally, previous studies considered only steam expansion (by either steam turbines or letdown stations) between two consecutive steam mains, oversimplifying the problem and resulting in misleading steam main temperatures and energy targets.

In summary, the overall methodology provides a systematic procedure for designing utility systems accounting for steam level selection and more accurate and realistic operating conditions.

5. Case studies

This section uses two different case studies taken from literature and real-world cases to illustrate the application of the proposed methodology to optimize the utility system design and the steam mains operating conditions. The proposed algorithms are solved using CPLEX v.12.6.1 as solver for the MILP problem. The objective function (TAC) values obtained for the best solutions are also compared to the values obtained by other methods available in the literature.

5.1. Case Study 1

For the first case, site data were adapted from an example available in the literature (Varbanov et al., 2005). Site sink and source profiles are shown in Figure 1-7. Power site demand is 25 MW. The site electricity demand can be provided by either the site or the electricity grid, and up to 10 MW of electricity can be exported. There is no steam imported or exported to or from the system. The utility system comprises boilers, a deaerator, expansion valves, steam turbines, gas turbines, a single cold utility (cooling water). Stream data and additional site specifications are detailed in Supplementary Information P1.C. In addition, thermal oil is included as hot utility if required. The utility steam is generated in the boiler house at the VHP main conditions (90 bar). The header conditions are estimated to minimize the TAC. Operating costs include the price of all the utilities consumed: fuel, electricity, demineralized water and cooling water, in addition to hot oil if it is required. Capital costs comprise the costs of boilers, steam turbines, gas turbines, HRSG, deaerator and hot oil furnace. In order to assess the benefit of the methodology, the optimized system configuration is compared against the work of Varbanov et al. (2005) under the same operating parameters and costs. Additionally, temperature specifications, as well as constraints, are defined (Table 1-1) to identify the potential steam levels and to calculate steam mains' superheating temperature.

Table 1-1. Temperature specifications for the steam system

Constraints	Temperature [°C]
Maximum boiler steam superheated temperature	570
Maximum process steam usage temperature (saturation)	250
Minimum process steam generation temperature (saturation)	134
Minimum steam main superheating	20
Degree of superheating for process steam generation	20
Degree of superheating for process heating	3

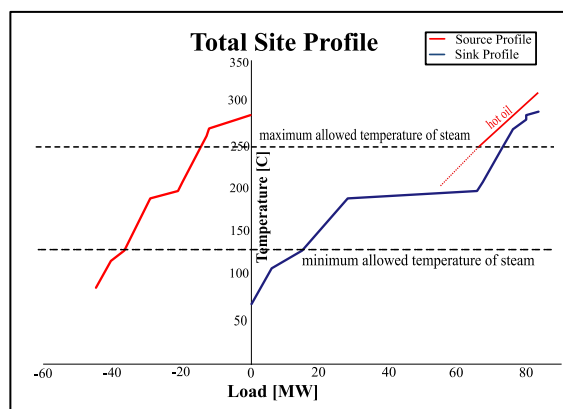
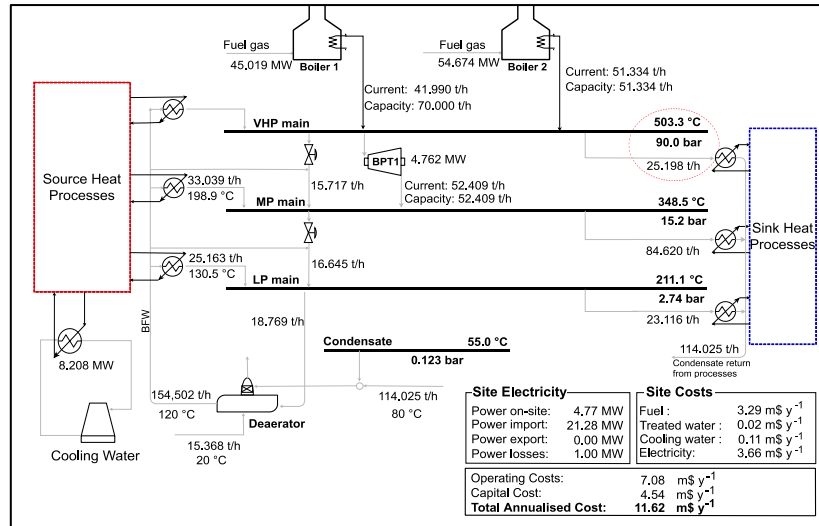


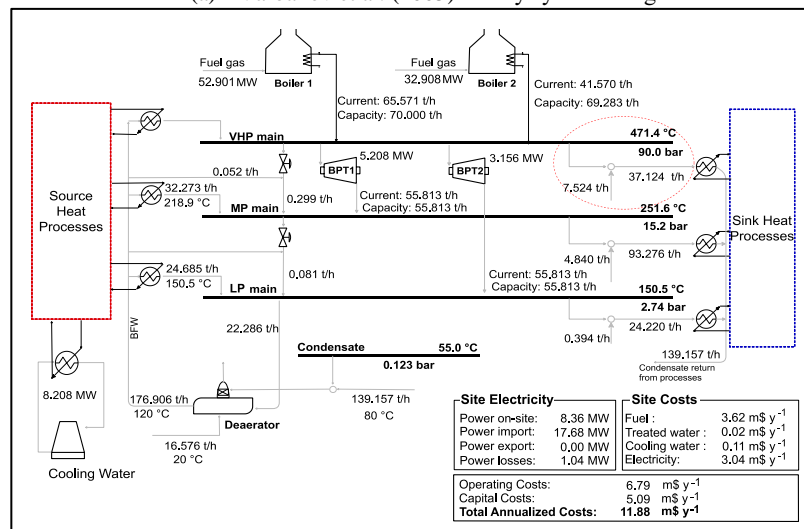
Figure 1-7. Total site profile of case study 1

Figure 1-8 compares the proposed methodology with the methodology proposed in the work of Varbanov et al. (2005). For the purpose of comparison, the constraint of maximum temperature for steam generation and distribution (discussed later in this section) is relaxed to evaluate the system design of the two methodologies under the same conditions. As expected, both systems select the same pressures for the optimized system configurations. This is explained by the shape of total site profile, where a large heat requirement is given at 15.2 bar ($T_{\text{sat}} = 198.9 \text{ }^{\circ}\text{C}$). Therefore, it is ideal to have a steam main at those conditions to satisfy the demand. Since there is no other critical point with a high steam requirement or generation, it is reasonable that the LP steam main is at the minimum pressure (temperature) possible in order to increase the heat recovery within the system and to increase the pressure difference for power generation. In addition, none of the optimal designs selects either gas turbines or condensing turbines in their configuration.

Although both methodologies select the same pressures for the steam mains operating conditions, there are several differences in the system configuration. Regarding steam generation and usage, the difference in the amount of steam can be neglected (error around 2 %). This is due to the sensible heat for 20 °C of superheating steam is around 2 - 4 % of the total heat required to raise steam. However, its consideration is important later for determining the superheating temperature of header and thus the steam usage. While the difference for the steam generation is not significant, it is not the same case for process steam usage. In that case, the header steam flow varies up to 4.4 t h⁻¹, due to the injection of BFW for de-superheating. Moreover, de-superheating steam increases the utility boiler demand. This is caused by the requirement to heat up the BFW to the same conditions and the reduction of the content heat in the utility steam. Furthermore, the increment in the boiler duty entails a rise of the BFW flowrate, consequently increasing the deaeration steam (3.51 t h⁻¹). Hence, the omission of the steam superheating and de-superheating may result in misleading steam boiler targeting (12.9 %), and therefore inaccuracies in the operating and capital costs, as observed in Figure 1-8. It should be noted that the design costs are not comparable due to the different considerations in each design model. However, the increment of 2.2 % in the total annualized cost of the proposed design (when compared to the literature design) can be explained by the higher boiler duty/capacity (and additional steam turbine) required to meet the site energy demands when considering steam superheating and de-superheating.



(a) Varbanov et al. (2005)' utility system design



(b) Proposed utility system design

Figure 1-8. Steam system configurations based on Varbanov et al. (2005) and the design proposed in this work

(VHP: very high pressure; MP: medium pressure; LP: low pressure; BPT: back-pressure turbine)

In relation to superheated steam temperature, Table 1-2 lists the flowrates of both boiler and let-down, as well as the power generated and the power generation per unit of boiler steam flow. The latter is used as a basis of comparison between the two methodologies. Despite both systems having low cogeneration potential (due to the power import/export constraint and the relatively low power price/expensive capital), the proposed methodology presents a 34.7 % higher power generation per unit of boiler flow than that of Varbanov et al. (2005). Superheating steam temperature might reduce the boiler fuel consumption due to a higher content heat in the utility steam. However, a higher steam temperature may lead to a greater amount of steam passing through let-down stations to balance the header temperature. Nonetheless, this may be at the cost of power potential, as observed in Figure 1-8.

Table 1-2. Steam system targets for the propose methodology in comparison with literature

Methodology	Utility steam temperature [°C]	Boiler flowrate [t h ⁻¹]	Let-down flowrate [t h ⁻¹]	Power generation [MW]	Power generation per unit boiler flow [MWh t ⁻¹]
Varbanov et al. (2005)	503*	93.324	16.645	4.762	0.051
Authors	471**	107.140	0.036	8.364	0.078

*The boiler temperature is a specified parameter.

** Calculated by the model.

An alternative superstructure is also considered with the use of an additional steam main (if necessary) and a hot oil circuit with a supply temperature of 300 °C and an operating temperature range (ΔT_{in-out}) of 90 °C (KLM Technology Group, 2011). This is to define the lower temperature bound of hot oil use and allow the framework to optimize the selection and use of utility (hot oil or steam) in that temperature range. As noted in Section 4.3.1, the main cost for the hot oil circuit comes from the fuel required to heat up the oil. Hot oil is heated up in fired heaters which usually use natural gas as fuel and are 80 – 85 % efficient (Towler and Sinnott, 2013). Therefore, in this study an efficiency of 83 % has been assumed. Figure 1-9 demonstrates the optimized design when taking into account hot oil circuit. The system comprises two fired steam boilers, four steam turbines and a hot oil circuit.

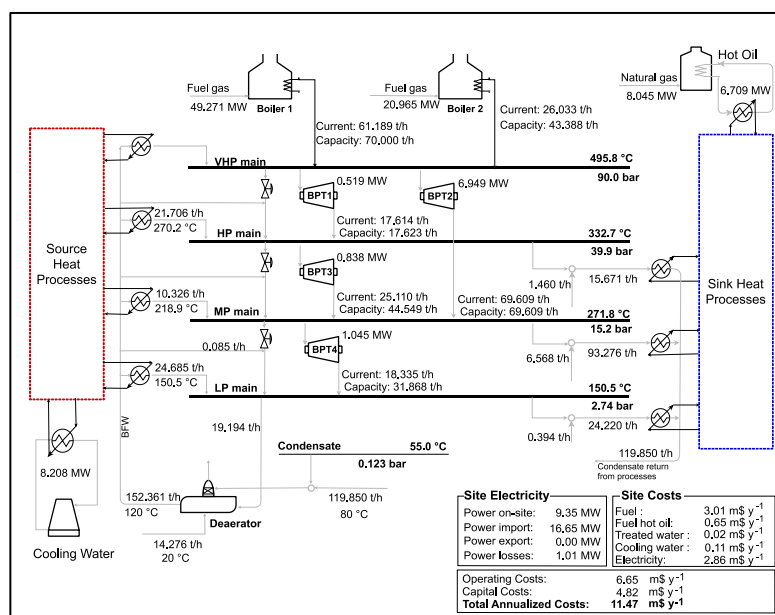


Figure 1-9. Utility system configuration with hot oil circuit

(VHP: very high pressure; MP: medium pressure; LP: low pressure; BPT: back-pressure turbine)

Table 1-3 compares the economic performance of two options of utility system design including a hot oil circuit. The first option is a utility system with an additional steam main that includes the maximum pressure for steam distribution and the hot oil circuit, as seen in Figure 1-9. The second option uses only the hot oil to satisfy the high temperature energy demand that steam cannot provide. It can be seen in Table 1-3 that MP steam pressure change is caused by the trade-off between fuel

consumption (by both boilers and fired heaters) and potential power generation by steam expansion. The power generation rises when three steam mains are selected. This can be explained by the additional expansion zone available and the additional steam flows to satisfy the heat demand at the HP level (15.671 t h⁻¹). The larger steam demand increases the boiler capital cost and the fuel consumption from the boilers. However, the increment in the steam demand leads to a higher power generation on site, which in turn offsets some power import costs. The utility systems that add only the hot oil circuit reduce the fuel demand from the boilers, at the cost of power generation. Moreover, the fuel saved in the boiler is used in the fired heater using natural gas (more expensive fuel). Overall, the utility system with hot oil circuit and additional steam main is \$0.2 M (per year) cheaper than one that utilizes only the hot oil circuit.

Table 1-3. Comparison of utility system designs including hot oil circuit

Parameter	Hot oil circuit and additional steam main	Hot oil circuit
Pressure [bar] (MP / LP)	15.2 / 2.7	18.8 / 2.7
Boiler flowrate	87.22	75.90
Power generation	9.35	7.38
Operating costs [m\$ y ⁻¹]		
Boiler fuel cost	3.01	2.59
Hot Oil fuel cost	0.65	1.22
Power cost	2.86	3.18
Cooling cost	0.11	0.11
Treated water cost	0.02	0.02
Total operating cost	6.64	7.12
Capital costs [m\$ y ⁻¹]		
Boilers	3.99	3.58
Hot oil circuit	0.33	0.56
Steam turbines	0.43	0.35
Deaerator	0.06	0.06
Total Capital Cost	4.83	4.55
Total Annualized Cost [m\$ y⁻¹]	11.47	11.67

5.2. Case study 2

This case relies on the site data reported by Sun et al. (2015). The number of streams and $\Delta T_{\min}^{\text{PU}}$ for each process are detailed in Supplementary Information P1.D. Site sink and source profiles are shown in Figure 1-10. Site power demand is 40 MW. The site energy requirement is satisfied using a steam system comprising a natural gas boiler, three steam distribution mains, a deaerator, let down valves, steam and gas turbines, and a single cold utility (cooling water). The utility steam is generated in the boiler house at the VHP main conditions (100 bar). The inlet temperature of the cooling water is 20

°C. Electricity can be generated by single back-pressure and by condensing steam turbines, in addition to gas turbines. The site allows a maximum electricity import and export of 1 and 5 MW, respectively. The HP, MP and LP steam mains operating conditions are estimated to minimize the total annualized cost.

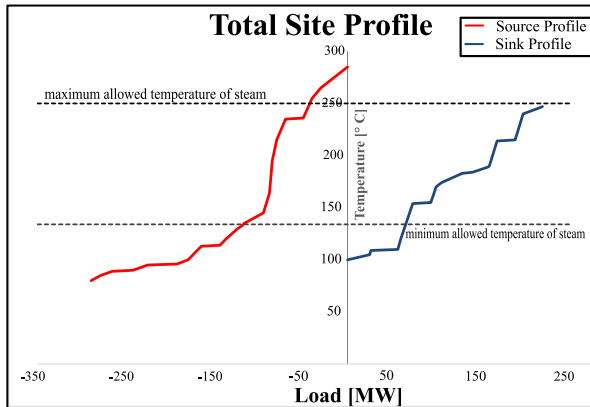


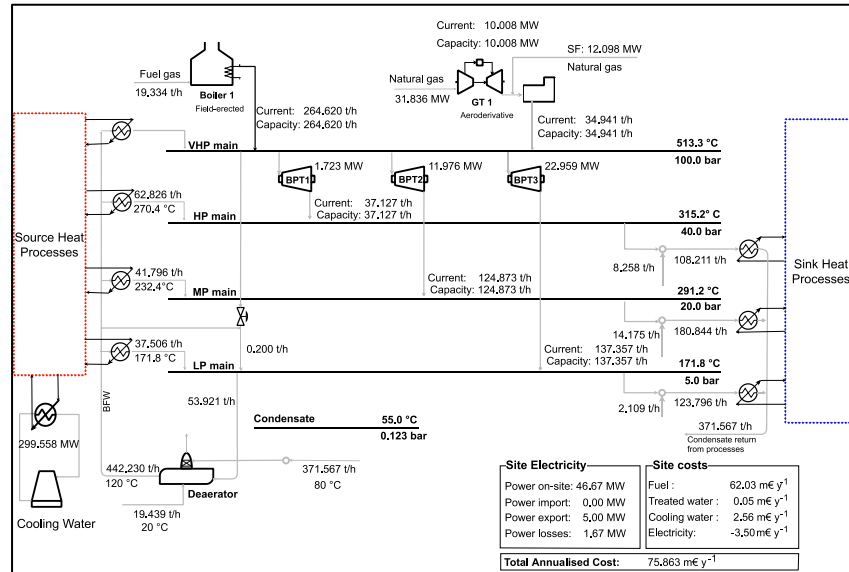
Figure 1-10. Total site profile of case study 2

5.2.1. Comparison with conventional system design

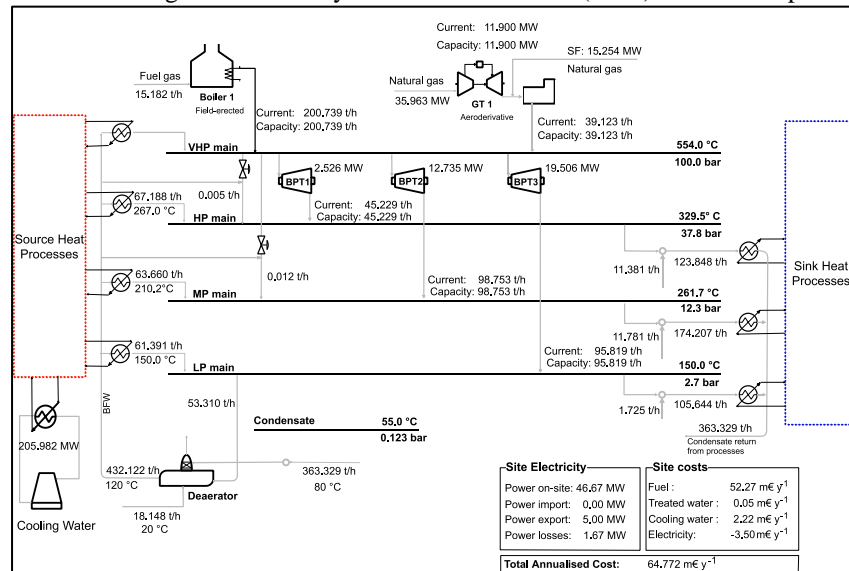
To assess the impact of the steam main conditions on the operational performance of the site, the results of this methodology are compared against a base case system, termed here as conventional design. The conventional design is obtained by the optimization model proposed in this work, but maintains the steam main pressures suggested by Sun et al. (2015) for the petrochemical plant. The steam main pressure for the HP, MP and LP mains are 40, 20 and 5 bar_a respectively. Figure 1-11 and Table 1-4 compare the two steam system configurations. Both systems were obtained under the temperature specifications presented previously in Table 1-1.

For reference, a comparison without hot oil circuit is made first. However, hot oil circuit integration is further analyzed later in this section. The steam main pressures for the optimized system configuration are 37.8, 12.3 and 2.7 bar_a, as shown in Figure 1-11(b). The optimal steam mains pressures are determined by establishing the process steam generation and use loads, ensuring an appropriate trade-off between heat integration and power generation.

Additionally, it is noted that steam main superheating is reliant on turbine exhausts and any let-down. Steam passing through let-downs is required to achieve steam balance and to maintain the minimum superheat (20 °C) in each steam main, especially at the lowest level. Increasing the steam passing by steam turbines would reduce the superheating due to higher power generation.



(a) Conventional design for case study 2 based on Sun et al. (2015) steam main pressure levels



(b) Optimized design for case study 2 determined using the methodology proposed in this work

Figure 1-11. Steam system configurations for case study 2

(BPT: back-pressure turbine; GT: gas turbine; SF: supplementary firing)

Table 1-4 summarizes the main results of the proposed design. For this particular example, the proposed design reduces fuel and cooling water consumption by 15.8 % and 13.3%, when compared with the conventional design. This reduction is due to higher (indirect) heat integration between the processes. The decrease of the boiler steam demand leads to lower sizes for the steam generation units. Although the utility steam demands decreases by 19.9 %, the power generation remains the same. This results in an increase of 24.6 % power generation per unit of utility steam produced and achieving an overall energy reduction of 15.8 %. Regarding costs, the proposed design decreases operating and capital costs by 16.5 % and 7.9 %, respectively; leading to an overall cost reduction of 14.6 %.

Table 1-4. Comparison of steam system designs for case study 2

Parameter	Conventional design*	Proposed design w/o hot oil	Difference [%]
Steam mass flowrate [t h ⁻¹]			
Boiler steam	264.62	200.74	-24.1
HRSB steam	34.94	39.12	12.0
Total utility steam	299.56	239.86	-19.9
Process steam generation	142.13	192.24	35.3
Fuel consumption [MW]			
Boiler	251.93	197.82	-21.5
Gas turbine + HRSB	43.93	51.22	16.6
Total fuel consumption	295.86	249.03	-15.8
Power generation [MW]			
BP steam turbines	36.66	34.77	-5.2
Gas turbines	10.01	11.9	18.9
Total power generated	46.67	46.67	0.0
Operating costs [m€ y ⁻¹]			
Fuel cost	62.03	52.27	-15.7
Power cost	-3.5	-3.5	0.0
Cooling cost	2.56	2.22	-13.3
Treated water cost	0.05	0.05	0.0
Total operating cost	61.14	51.04	-16.5
Capital costs [m€ y ⁻¹]			
Boilers	5.71	4.56	-20.1
HRSBs	0.5	0.57	14.0
Gas turbines	1.85	2.15	16.2
Steam turbines	4.87	4.63	-4.9
Deaerator	0.08	0.07	-12.5
Total Capital Cost	13.01	11.98	-7.9
Maintenance costs [m€ y ⁻¹]	1.71	1.75	2.3
Total Annualized Cost [m€ y⁻¹]	75.86	64.77	-14.6

*Optimized design obtained based on Sun et al. (2015) stream data and (fixed) pressure levels.

5.2.2. Effect of hot oil circuit on the utility system design

When only the hot oil circuit integration option is included, the use of hot oil to satisfy heat requirements at high temperatures (>200 °C) is favored by the optimization algorithm. The optimization favors a two steam main system coupled with a hot oil system. This is because the hot oil circuit not only decrease user heat demand at high temperatures, but also allows for the generation of more process steam at a lower level. Overall, this results in a reduction of the thermal generators duty and consequently, capital and operating costs decrease of 9.0 % and 11.4 %, respectively.

Importantly, the power generation in both cases is the same because the reduced amount of steam passing through steam turbines is compensated by a higher power generation via gas turbines. In summary, this leads to a further 12.2 % energy saving and a 9.1 % reduction of the total costs relative to the optimized design without hot oil circuit, as shown in Table 1-5.

Table 1-5. Economic and operational effect of hot oil circuit on the steam system design for case study 2

Parameter	Optimized Design w/o HO	Optimized Design w/ HO	Difference [%]
Steam mains	VHP/HP/MP/LP	VHP/MP / LP	-
Pressure [bar]	100.0/37.8 / 12.3 / 2.7	100.0/14.0 / 2.7	-
Temperature [°C]	554.0/ 329.5/261.7/150.0	536.0/245.4/150.0	-
Fuel consumption [MW]	249.03	218.75	-12.2
Power Generation [MW]	46.67	46.67	-
Operating Cost [m€ y ⁻¹]	51.03	45.24	-11.4
Maintenance Cost [m€ y ⁻¹]	1.76	2.71	54.1
Capital Cost [m€ y ⁻¹]	11.98	10.90	-9.0
Total Annualized Cost [m€ y⁻¹]	64.77	58.85	-9.1

5.2.3. Effect of flash steam recovery on the utility system design

For large heat transfer loads, recovering the steam that is flashed as the condensate pressure is reduced can improve the thermal efficiency of the system. This measure could also decrease the fuel consumption and the overall costs of the energy system. In this design, the impact of a 90 % flash steam recovery on the utility system design and performance is analyzed. Figure 1-12 shows the system configuration and nominal operating conditions of the energy system with flash steam recovery integration. A summary of the relevant variables is presented in Table 1-6. Further details of the techno-economic impact of flash steam recovery integration can be found in Supplementary Information P1.E.

FSR integration is favored by the optimization algorithm, as shown in Figure 1-12. In the optimization, the same pressures for the steam mains are preferred. The use of recovered flash steam results in both a reduction in the utility steam requirement and in a decrease in the amount of BFW needed to de-superheat steam for process heating purposes. The reduction in the boiler duties causes a lower steam availability for power generation via steam turbines. Therefore, the gas turbine capacity is increased to satisfy the site power demand. Overall, the integration of FSR leads to 15.7 % energy saving and 13.4 % reduction of the total annualized costs when compared to the conventional design.

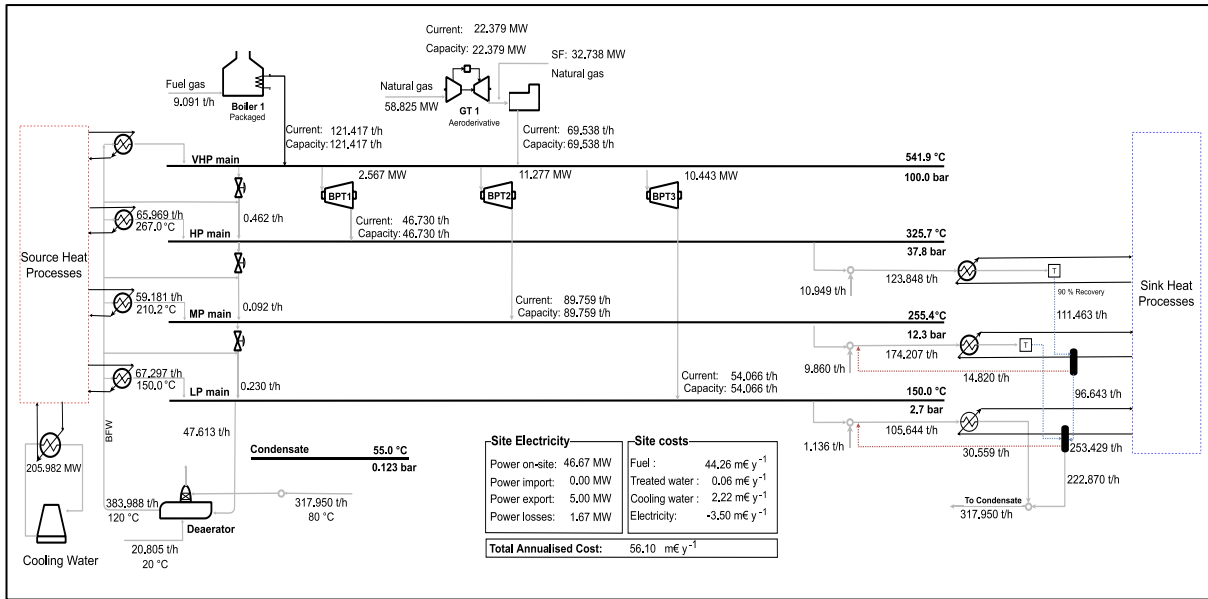


Figure 1-12. Steam system configuration for case study 2, integrating flash steam recovery (BPT: back-pressure turbine; GT: gas turbine; SF: supplementary firing)

Table 1-6. Economic and operational effect of flash steam recovery on the steam system design for case study 2

Parameter	Optimized Design w/o FSR	Optimized Design w/ FSR	Difference [%]
Steam mains	VHP/HP/MP/LP	VHP/HP/MP/LP	-
Pressure [bar]	100.0 / 37.8 / 12.3 / 2.7	100.0 / 37.8 / 12.3 / 2.7	-
Temperature [°C]	554.0 / 329.5 / 261.7 / 150.0	541.9 / 325.7 / 255.4 / 150.0	-
Fuel consumption [MW]	249.03	210.02	-15.7%
Power Generation [MW]	46.67	46.67	0.0%
Operating Cost [m€ y ⁻¹]	51.03	43.03	-15.7%
Maintenance Cost [m€ y ⁻¹]	1.76	2.00	13.5%
Capital Cost [m€ y ⁻¹]	11.98	11.07	-7.6%
Total Annualized Cost [m€ y⁻¹]	64.77	56.10	-13.4%

5.2.4. Integration of hot oil circuit and FSR in case study 2

So far, the influence of two integration options (hot oil circuit and FSR) has been considered separately. However, an analysis of the system design including all the options is required to determine the overall effect in the utility system configuration and performance. The results of the analysis for the design of a utility system with three steam distribution mains available are reported in Table 1-7 and Figure 1-13. It is important to note that despite three steam mains are available for the optimization, when hot oil system is available, the optimization algorithm favors a system configuration with only two steam mains.

Table 1-7. Comparison of utility system targets including hot oil circuit and/or FSR for case study 2

Parameter	Utility system with three steam distribution mains available			
	w/o hot oil circuit		w/ hot oil circuit	
	w/o FSR	w/ FSR	w/o FSR	w/ FSR
VHP pressure [bar]	100.0	100.0	100.0	100.0
VHP temperature [°C]	554.0	541.9	536.0	536.0
Steam mains	HP/MP/LP	HP/MP/LP	- /MP/LP	- /MP/LP
Pressure [bar]	37.8 / 12.3 / 2.7	37.8 / 12.3 / 2.7	- / 14.0 / 2.7	- / 14.0 / 2.7
Temperature [°C]	329.5 / 261.7 / 150.0	325.7 / 255.4 / 150.0	- / 245.4 / 150.0	- / 236.8 / 150.0
FSR flow [t h⁻¹]	-	- / 14.82 / 30.56	-	- / - / 21.04
Utility steam flow [t h⁻¹]	239.86	190.96	118.84	97.46
Boiler steam	200.74	121.42	29.97	-
HRSG steam	39.12	69.54	88.86	97.46
Fuel consumption [MW]	249.03	210.02	218.75	201.13
Boiler	197.82	118.45	29.10	-
Gas turbine + HRSG SF*	51.22	91.56	116.95	128.43
Hot oil circuit	-	-	72.70	72.70
Power generation [MW]	46.67	46.67	46.67	46.67
Gas turbines	11.90	22.38	28.97	31.96
BP steam turbines	34.77	24.29	17.69	14.71
Condensing turbines	-	-	-	-

* HRSG SF: Supplementary firing of heat recovery steam generator

For cases incorporating a hot oil circuit and/or an FSR, all options lead to lower total annualized costs compared to the system configuration without integration. Nevertheless, the utility system with FSR integration presents the lowest fuel consumption and total annualized cost.

It is essential to note that the two utility options will only reduce thermal site demand while leaving power requirements remain unaltered. Besides that, the integration options could limit steam turbine power generation (due to a reduced utility steam flow rate). This, combined with the higher heat to power ratio of gas turbines, explains why the optimization favors the deployment of gas turbines coupled with HRSG, and the shifting of thermal duties from boilers to HRSGs when thermal demand is reduced.

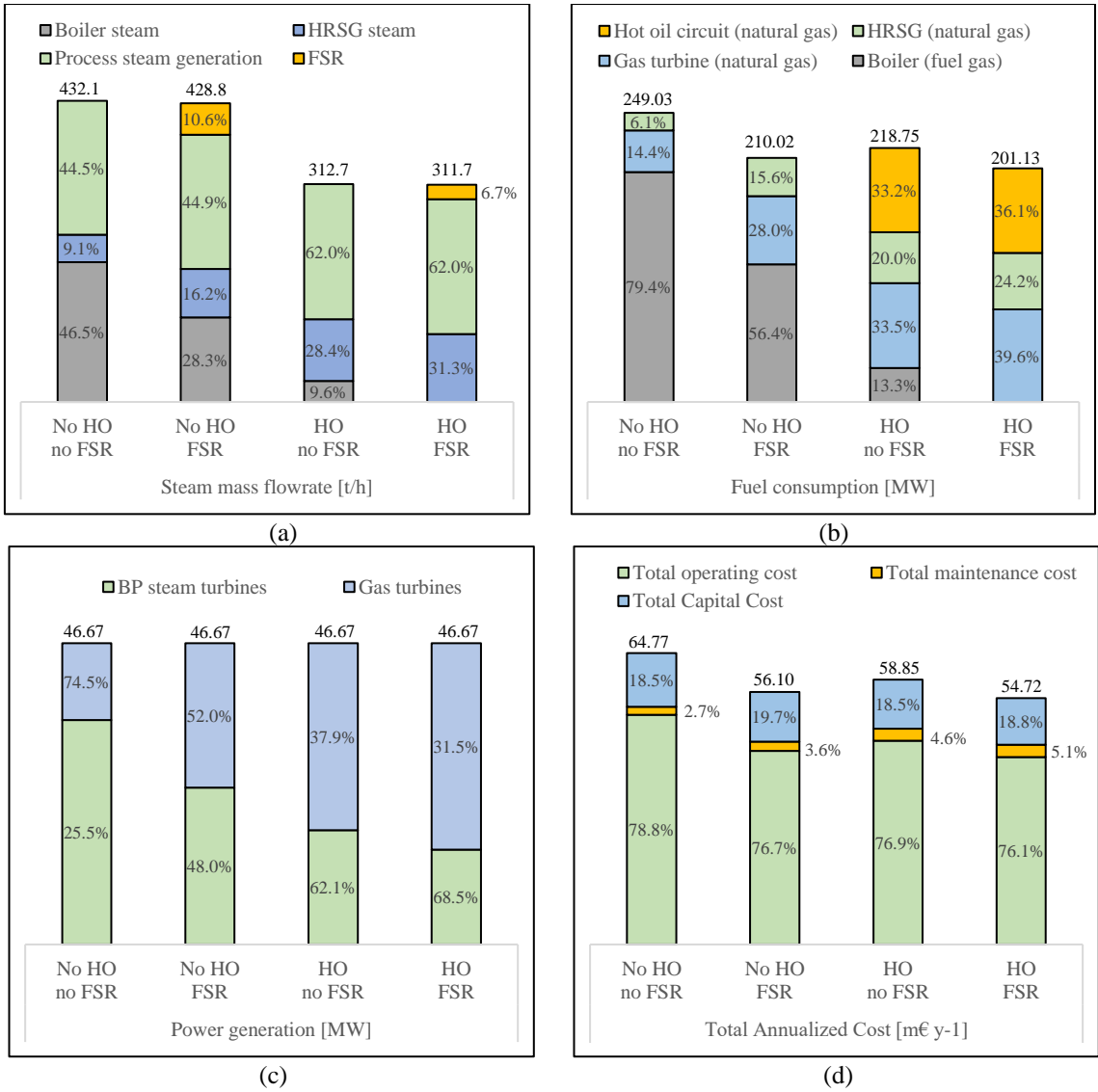


Figure 1-13 Effects of the integration hot oil circuit and/or FSR for the synthesis of utility system on: (a) steam and (b) fuel consumption, (c) power generation and (d) costs. (HO: Hot oil circuit; FSR: flash steam recovery)

Overall, for this case study, the most economical and energy efficient design incorporates both a hot oil system and a flash tank. The proposed integrated utility system design can further reduce site energy consumption through a combination of flashed steam recovered at the lowest steam main and appropriate utility selection to satisfy site heat demands at different temperatures. The integration of both utility components results in an additional 4.5 % (8.3 %) reduction in fuel consumption when compared to a utility system with only a FSR (HO) system. Compared to the optimized utility system without integration, this results in 19.5 % fuel savings and a 15.5 % cost reduction. While compared to the base case (noted as conventional design), the integration could lead to an overall 32.2 % fuel savings and a 27.7 % cost reduction.

5.2.5. Effect of the number of steam mains on the system performance

Finally, the addition of intermediate steam mains could further increase heat recovery potential, resulting in additional savings of fuel fired in the utility boilers. Therefore, the effect of the number of steam mains is analyzed in this section. However, the additional cost of pipes involved with the increasing number of steam mains is not taken into account due to difficulty of producing an accurate economic assessment of the capital costs involved, at this design stage. The main purpose of this work is to assess the potential benefit of increasing the number of steam mains, paying particular attention to energy efficiency and the potential cost trade-off. A summary of the design costs is presented in Figure 1-14. Further details can be found in Supplementary Information P1.E.

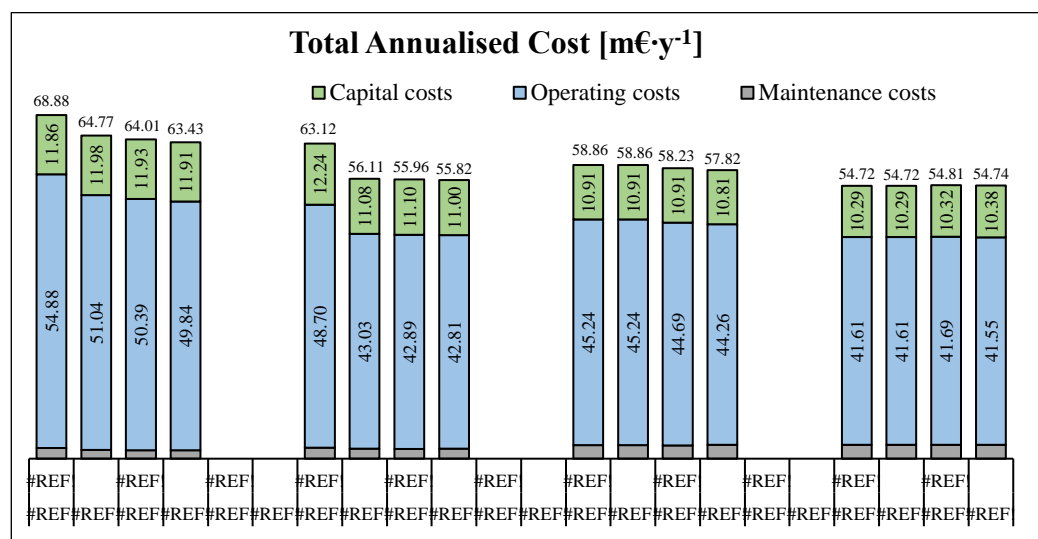


Figure 1-14. Effect of steam mains number on the utility system costs.
(HO: Hot oil circuit; FSR: flash steam recovery)

Figure 1-14 shows a decrease in both capital and operating costs in relation to the number of steam mains in each scenario. Overall, the total costs are dominated by the operating costs. As a result, increasing the number of steam mains can result in higher (indirect) heat integration, thus reducing both the operating costs and the duty of steam generation units. However, it should be noted that as the number of steam mains increases, the economic benefit decreases. The amount of energy saved is limited by the amount of process heat recovered via steam. According to the case study presented, a utility system with three steam mains could result in a cost savings of 6% compared to a system with only two distribution steam mains. However, further increase of the number of steam mains will only result in a 2% reduction in overall costs. Moreover, it is important to keep in mind, that a higher number of steam mains increases the complexity of the system and the indirect costs involved. As a result, additional expenses such as piping costs may offset the energy savings. With respect to the integration options, a similar trend to the one outlined in the earlier analysis – relating to the three steam mains system – can be observed (see Table 1-7). However, the economic benefits from additional steam mains (and higher heat integration) are considerably reduced.

In general, the optimization favors the integration of both FSR and HO systems. If only one utility component can be selected (FSR or HO system), the integration of flash tanks provide further costs savings than the deployment of a hot oil circuit. An exception to this trend is for the two steam distribution mains utility system, where the integration of HO circuit can provide an additional 6.2 % costs savings in comparison with a steam system with only FSR selected. This is likely due to the lower potential of FSR within a system with only two steam mains.

6. Conclusions

This paper offers additional practicality and accuracy in synthesizing utility systems at optimum conditions. The proposed methodology considers boiler feed water preheating and steam superheating and de-superheating instead of only steam operating at saturated conditions. The model also explores the impact of process steam generation at a different temperature from the steam headers on the system operating conditions and performance while also considering full and part-load equipment operation. Additionally, the model incorporates additional utility options (hot oil) and other utility components (deaerator, flash steam recovery) to enable a more complete evaluation. These issues have not been included in the mathematical models in previous studies.

Given fixed processes requirements, the methodology provides the system configuration (size and load) and optimum operating conditions. The optimization is based on a superstructure approach. The study demonstrates the close relationship between steam level selection and heat recovery and power generation enhancement. Steam mains selection affects both process steam generation and use loads and, therefore, the heat recovery and utility steam requirement. Additionally, the integration of more practical constraints (steam superheating and de-superheating, steam temperature limitation) and utility components (hot oil circuit, FSR) into the design options allows to explore further the energy targets of the utility system. In illustrative examples, the new model shows the impact of the steam main conditions on the system configuration and its operational performance. This proves that the energy requirement can be further reduced by a holistic optimization of the steam mains operating conditions and of site heat recovery and cogeneration.

7. Acknowledgments

This work has been funded by the Norwegian Research Council through HighEFF (project no. 257632). The authors gratefully acknowledge the financial support from the Research Council of Norway and user partners of HighEFF. Also, a special gratitude to the National Secretariat for Higher Education Science, Technology and Innovation of Ecuador (SENESCYT) for its support.

References

- Aguilar, O., Perry, S. J., Kim, J. K. & Smith, R. (2007) 'Design and Optimization of Flexible Utility Systems Subject to Variable Conditions: Part 2: Methodology and Applications', *Chemical Engineering Research and Design*, 85(8), pp. 1149-1168.
- Al-Khayyal, F. A. & Falk, J. E. (1983) 'Jointly Constrained Biconvex Programming', *Mathematics of Operations Research*, 8(2), pp. 273-286.
- Andiappan, V. (2017) 'State-Of-The-Art Review of Mathematical Optimisation Approaches for Synthesis of Energy Systems', *Process Integration and Optimization for Sustainability*, 1(3), pp. 165-188.
- Beangstrom, S. G. & Majozzi, T. (2016) 'Steam system network synthesis with hot liquid reuse: II. Incorporating shaft work and optimum steam levels', *Computers & Chemical Engineering*, 85, pp. 202-209.
- Belotti, P., Kirches, C., Leyffer, S., Linderoth, J., Luedtke, J. & Mahajan, A. (2013) 'Mixed-integer nonlinear optimization', *Acta Numerica*, 22, pp. 1-131.
- Brandoni, C. & Renzi, M. (2015) 'Optimal sizing of hybrid solar micro-CHP systems for the household sector', *Applied Thermal Engineering*, 75, pp. 896-907.
- Bruno, J. C., Fernandez, F., Castells, F. & Grossmann, I. E. (1998) 'A Rigorous MINLP Model for the Optimal Synthesis and Operation of Utility Plants', *Chemical Engineering Research and Design*, 76(3), pp. 246-258.
- Casisi, M., Pinamonti, P. & Reini, M. (2009) 'Optimal lay-out and operation of combined heat & power (CHP) distributed generation systems', *Energy*, 34(12), pp. 2175-2183.
- Chen, C.-L. & Lin, C.-Y. (2011) 'A flexible structural and operational design of steam systems', *Applied Thermal Engineering*, 31(13), pp. 2084-2093.
- Corporation, I. (2017). V12. 8: IBM ILOG CPLEX Optimization Studio CPLEX User's Manual: International Business Machines Corporation.
- Dhole, V. R. & Linnhoff, B. (1993) 'Total site targets for fuel, co-generation, emissions, and cooling', *Comput Chem Eng.*, 17, pp. 101-109.
- Dogan, M. E. & Grossmann, I. E. (2006) 'A Decomposition Method for the Simultaneous Planning and Scheduling of Single-Stage Continuous Multiproduct Plants', *Industrial & Engineering Chemistry Research*, 45(1), pp. 299-315.
- Drud, A. (1985) 'CONOPT: A GRG code for large sparse dynamic nonlinear optimization problems', *Mathematical Programming*, 31(2), pp. 153-191.
- Elsido, C., Bischi, A., Silva, P. & Martelli, E. (2017) 'Two-stage MINLP algorithm for the optimal synthesis and design of networks of CHP units', *Energy*, 121, pp. 403-426.

- Elsido, C., Martelli, E. & Grossmann, I. E. (2019) 'A bilevel decomposition method for the simultaneous heat integration and synthesis of steam/organic Rankine cycles', *Computers & Chemical Engineering*, 128, pp. 228-245.
- Ghannadzadeh, A., Perry, S. & Smith, R. (2012) 'Cogeneration targeting for site utility systems', *Applied Thermal Engineering*, 43, pp. 60-66.
- Goderbauer, S., Bahl, B., Voll, P., Lübbecke, M. E., Bardow, A. & Koster, A. M. C. A. (2016) 'An adaptive discretization MINLP algorithm for optimal synthesis of decentralized energy supply systems', *Computers & Chemical Engineering*, 95, pp. 38-48.
- Gomes, F. R. A. & Mateus, G. R. (2017) 'Improved Combinatorial Benders Decomposition for a Scheduling Problem with Unrelated Parallel Machines', *Journal of Applied Mathematics*, 2017, pp. 9452762.
- Gounaris, C. E., Misener, R. & Floudas, C. A. (2009) 'Computational Comparison of Piecewise-Linear Relaxations for Pooling Problems', *Industrial & Engineering Chemistry Research*, 48(12), pp. 5742-5766.
- Hackl, R., Andersson, E. & Harvey, S. (2011) 'Targeting for energy efficiency and improved energy collaboration between different companies using total site analysis (TSA)', *Energy*, 36(8), pp. 4609-4615.
- Hawkes, A. D. & Leach, M. A. (2009) 'Modelling high level system design and unit commitment for a microgrid', *Applied Energy*, 86(7), pp. 1253-1265.
- Iyer, R. R. & Grossmann, I. E. (1998) 'A Bilevel Decomposition Algorithm for Long-Range Planning of Process Networks', *Industrial & Engineering Chemistry Research*, 37(2), pp. 474-481.
- Jimenez-Romero, J., Azapagic, A. & Smith, R. (2022). *STYLE: A new optimization model for Synthesis of uTility sYstems with steam LLevel placement*. Manchester: University of Manchester.
- Kermani, M., Wallerand, A. S., Kantor, I. D. & Maréchal, F. (2018) 'Generic superstructure synthesis of organic Rankine cycles for waste heat recovery in industrial processes', *Applied Energy*, 212, pp. 1203-1225.
- Khoshgoftar Manesh, M. H., Abadi, S. K., Amidpour, M. & Hamed, M. H. (2013) 'A new targeting method for estimation of cogeneration potential and total annualized cost in process industries', *Chemical Engineering Research and Design*, 91(6), pp. 1039-1049.
- Klemeš, J., Dhole, V. R., Raissi, K., Perry, S. J. & Puigjaner, L. (1997) 'Targeting and design methodology for reduction of fuel, power and CO₂ on total sites', *Applied Thermal Engineering*, 17(8), pp. 993-1003.
- Klemeš, J. J., Varbanov, P. S., Walmsley, T. G. & Foley, A. (2019) 'Process Integration and Circular Economy for Renewable and Sustainable Energy Systems', *Renewable and Sustainable Energy Reviews*, 116, pp. 109435.

- Klemeš, J. J., Varbanov, P. S., Walmsley, T. G. & Jia, X. (2018) 'New directions in the implementation of Pinch Methodology (PM)', *Renewable and Sustainable Energy Reviews*, 98, pp. 439-468.
- Lara, C. L., Trespalacios, F. & Grossmann, I. E. (2018) 'Global optimization algorithm for capacitated multi-facility continuous location-allocation problems', *Journal of Global Optimization*, 71(4), pp. 871-889.
- Lee, P. Y., Liew, P. Y., Walmsley, T. G., Wan Alwi, S. R. & Klemeš, J. J. (2020) 'Total Site Heat and Power Integration for Locally Integrated Energy Sectors', *Energy*, 204, pp. 117959.
- Liew, P. Y., Theo, W. L., Wan Alwi, S. R., Lim, J. S., Abdul Manan, Z., Klemeš, J. J. & Varbanov, P. S. (2017) 'Total Site Heat Integration planning and design for industrial, urban and renewable systems', *Renewable and Sustainable Energy Reviews*, 68, pp. 964-985.
- Liew, P. Y., Wan Alwi, S. R., Ho, W. S., Abdul Manan, Z., Varbanov, P. S. & Klemeš, J. J. (2018) 'Multi-period energy targeting for Total Site and Locally Integrated Energy Sectors with cascade Pinch Analysis', *Energy*, 155, pp. 370-380.
- Lin, Y. & Schrage, L. (2009) 'The global solver in the LINDO API', *Optimization Methods and Software*, 24(4-5), pp. 657-668.
- Linnhoff, B. & Vredeveld, R. (1984) 'Pinch technology has come of age', *Chemical Engineering Progress*, 80, pp. 33-40.
- Lotero, I., Trespalacios, F., Grossmann, I. E., Papageorgiou, D. J. & Cheon, M.-S. (2016) 'An MILP-MINLP decomposition method for the global optimization of a source based model of the multiperiod blending problem', *Computers & Chemical Engineering*, 87, pp. 13-35.
- Luo, X., Hu, J., Zhao, J., Zhang, B., Chen, Y. & Mo, S. (2014) 'Multi-objective optimization for the design and synthesis of utility systems with emission abatement technology concerns', *Applied Energy*, 136, pp. 1110-1131.
- Luo, X., Zhang, B., Chen, Y. & Mo, S. (2011) 'Modeling and optimization of a utility system containing multiple extractions steam turbines', *Energy*, 36(5), pp. 3501-3512.
- Ma, J., Chang, C., Wang, Y. & Feng, X. (2018) 'Multi-objective optimization of multi-period interplant heat integration using steam system', *Energy*, 159, pp. 950-960.
- Maréchal, F. & Kalitventzeff, B. (1998) 'Process integration: Selection of the optimal utility system', *Computers & Chemical Engineering*, 22, pp. S149-S156.
- Matsuda, K., Tanaka, S., Endou, M. & Iiyoshi, T. (2012) 'Energy saving study on a large steel plant by total site based pinch technology', *Applied Thermal Engineering*, 43, pp. 14-19.
- McCormick, G. P. (1976) 'Computability of global solutions to factorable nonconvex programs: Part I — Convex underestimating problems', *Mathematical Programming*, 10(1), pp. 147-175.

- Misener, R. & Floudas, C. A. (2010) 'Global Optimization of Large-Scale Generalized Pooling Problems: Quadratically Constrained MINLP Models', *Industrial & Engineering Chemistry Research*, 49(11), pp. 5424-5438.
- Misener, R. & Floudas, C. A. (2014) 'ANTIGONE: Algorithms for coNTinuous / Integer Global Optimization of Nonlinear Equations', *Journal of Global Optimization*, 59(2), pp. 503-526.
- Mitra, S., Sun, L. & Grossmann, I. E. (2013) 'Optimal scheduling of industrial combined heat and power plants under time-sensitive electricity prices', *Energy*, 54, pp. 194-211.
- Nemet, A. & Kravanja, Z. (2017) 'Synthesis of More Sustainable Total Site', *CHEMICAL ENGINEERING TRANSACTIONS*, 56, pp. 19-24.
- Oluleye, O. (2015) *Integration of Waste Heat Recovery in Process Sites*. PhD, University of Manchester, Manchester.
- Omu, A., Choudhary, R. & Boies, A. (2013) 'Distributed energy resource system optimisation using mixed integer linear programming', *Energy Policy*, 61, pp. 249-266.
- Papoulias, S. A. & Grossmann, I. E. (1983) 'A structural optimization approach in process synthesis—I: Utility systems', *Computers & Chemical Engineering*, 7(6), pp. 695-706.
- Picón-Núñez, M. & Medina-Flores, J. M. (2013) '16 - Process Integration Techniques for Cogeneration and Trigeneration Systems', in Klemeš, J. J. (ed.) *Handbook of Process Integration (PI)*: Woodhead Publishing, pp. 484-504.
- Pyrgakis, K. A. & Kokossis, A. C. (2020) 'Total Site Synthesis: Selection of Processes to Save Energy and Boost Cogeneration', in Pierucci, S., Manenti, F., Bozzano, G. L. & Manca, D. (eds.) *Computer Aided Chemical Engineering*: Elsevier, pp. 1345-1350.
- Rieder, A., Christidis, A. & Tsatsaronis, G. (2014) 'Multi criteria dynamic design optimization of a small scale distributed energy system', *Energy*, 74, pp. 230-239.
- Sanaei, S. M. & Nakata, T. (2012) 'Optimum design of district heating: Application of a novel methodology for improved design of community scale integrated energy systems', *Energy*, 38(1), pp. 190-204.
- Serra, L. M., Lozano, M.-A., Ramos, J., Ensinas, A. V. & Nebra, S. A. (2009) 'Polygeneration and efficient use of natural resources', *Energy*, 34(5), pp. 575-586.
- Shang, Z. (2000) *Analysis and Optimisation of Total Site Utility Systems*. Ph.D, Manchester, U.K.
- Shang, Z. & Kokossis, A. (2004) 'A transshipment model for the optimisation of steam levels of total site utility system for multiperiod operation', *Computers & Chemical Engineering*, 28(9), pp. 1673-1688.
- Singh, H. (1997) *Flue Gas Minimisation From Total Sites*. Ph.D., UK.
- Smith, R. (2016a). *Chemical Process Design and Integration* (2nd ed. ed.): Wiley.

- Smith, R. (2016b) 'Steam Systems and Cogeneration', *Chemical Process: Design and Integration*. Second ed. Chichester: John Wiley & Sons, Ltd, pp. 583-646.
- Sun, L., Doyle, S. & Smith, R. (2015) 'Heat recovery and power targeting in utility systems', *Energy*, 84, pp. 196-206.
- Sun, L., Gai, L. & Smith, R. (2017) 'Site utility system optimization with operation adjustment under uncertainty', *Applied Energy*, 186, pp. 450-456.
- Sun, L. & Liu, C. (2015) 'Reliable and flexible steam and power system design', *Applied Thermal Engineering*, 79, pp. 184-191.
- Sun, L. & Smith, R. (2015) 'Performance Modeling of New and Existing Steam Turbines', *Industrial & Engineering Chemistry Research*, 54(6), pp. 1908-1915.
- Tawarmalani, M. & Sahinidis, N. V. (2001) 'Semidefinite Relaxations of Fractional Programs via Novel Convexification Techniques', *Journal of Global Optimization*, 20(2), pp. 133-154.
- Tawarmalani, M. & Sahinidis, N. V. (2005) 'A polyhedral branch-and-cut approach to global optimization', *Mathematical Programming*, 103(2), pp. 225-249.
- Towler, G. & Sinnott, R. (2013) 'Utilities and Energy Efficient Design', *Chemical engineering design, principles, practice and economics of plant and process design*. Second ed. Oxford, UK: Elsevier, pp. 103-160.
- Trespalacios, F. & Grossmann, I. E. (2014) 'Review of Mixed-Integer Nonlinear and Generalized Disjunctive Programming Methods', *Chemie Ingenieur Technik*, 86(7), pp. 991-1012.
- Varbanov, P., Perry, S., Klemeš, J. & Smith, R. (2005) 'Synthesis of industrial utility systems: cost-effective de-carbonisation', *Applied Thermal Engineering*, 25(7), pp. 985-1001.
- Varbanov, P., Perry, S., Makwana, Y., Zhu, X. X. & Smith, R. (2004) 'Top-level Analysis of Site Utility Systems', *Chemical Engineering Research and Design*, 82(6), pp. 784-795.
- Varbanov, P. S. D., S.; Smith, R. (2004) 'Modelling and Optimization of Utility Systems', *Chem. Eng. Res. Des.*, 82, pp. 561-578.
- Voll, P., Klaffke, C., Hennen, M. & Bardow, A. (2013) 'Automated superstructure-based synthesis and optimization of distributed energy supply systems', *Energy*, 50, pp. 374-388.
- Wagner, W., Cooper, J., Dittmann, A., Kijima, J., Kretzschmar, H.-J., Kruse, A., Mareš, R., Oguchi, K., Sato, H., Stoecker, I., Šifner, O. & Takaishi, Y. (2000) 'The IAPWS Industrial Formulation 1997 for the Thermodynamic Properties of Water and Steam', *Journal of Engineering for Gas Turbines and Power-transactions of The Asme - J ENG GAS TURB POWER-T ASME*, 122.
- Wang, H., Yin, W., Abdollahi, E., Lahdelma, R. & Jiao, W. (2015) 'Modelling and optimization of CHP based district heating system with renewable energy production and energy storage', *Applied Energy*, 159, pp. 401-421.

- Wang, L., Yang, Z., Sharma, S., Mian, A., Lin, T.-E., Tsatsaronis, G., Maréchal, F. & Yang, Y. (2019) 'A Review of Evaluation, Optimization and Synthesis of Energy Systems: Methodology and Application to Thermal Power Plants', *Energies*, 12(1), pp. 73.
- Wicaksono, D. S. & Karimi, I. A. (2008) 'Piecewise MILP under- and overestimators for global optimization of bilinear programs', *AIChE Journal*, 54(4), pp. 991-1008.
- Wouters, C., Fraga, E. S. & James, A. M. (2015) 'An energy integrated, multi-microgrid, MILP (mixed-integer linear programming) approach for residential distributed energy system planning – A South Australian case-study', *Energy*, 85, pp. 30-44.
- Xu, A. Z., Mu, L. X., Wu, X. H., Fan, Z. F. & Zhao, L. (2013) 'Superiority of Superheated Steam Flooding in Development of High Water-Cut Heavy Oil Reservoir', *Advanced Materials Research*, 616-618, pp. 992-995.
- Zamora, J. M. & Grossmann, I. E. (1998) 'A global MINLP optimization algorithm for the synthesis of heat exchanger networks with no stream splits', *Computers & Chemical Engineering*, 22(3), pp. 367-384.
- Zhang, B. J., Liu, K., Luo, X. L., Chen, Q. L. & Li, W. K. (2015a) 'A multi-period mathematical model for simultaneous optimization of materials and energy on the refining site scale', *Applied Energy*, 143, pp. 238-250.
- Zhang, D., Evangelisti, S., Lettieri, P. & Papageorgiou, L. G. (2015b) 'Optimal design of CHP-based microgrids: Multiobjective optimisation and life cycle assessment', *Energy*, 85, pp. 181-193.
- Zhao, H., Rong, G. & Feng, Y. (2015) 'Effective Solution Approach for Integrated Optimization Models of Refinery Production and Utility System', *Industrial & Engineering Chemistry Research*, 54(37), pp. 9238-9250.
- Zidan, A., Gabbar, H. A. & Eldessouky, A. (2015) 'Optimal planning of combined heat and power systems within microgrids', *Energy*, 93, pp. 235-244.

SUPPLEMENTARY INFORMATION P1

STYLE: A new optimization model for Synthesis of uTility sYstems with steam LLevel placement

Julia Jiménez-Romero^{a,b,*}, Adisa Azapagic^b, Robin Smith^a

^a Centre for Process Integration, Department of Chemical Engineering and Analytical Science, University of Manchester, Manchester, M13 9PL, United Kingdom

^b Sustainable Industrial Systems Group, Department of Chemical Engineering and Analytical Science, University of Manchester, Manchester, M13 9PL, United Kingdom

* Julia Jiménez-Romero. Email: julia.jimenezromero@manchester.ac.uk, nataly.jimenezr@hotmail.com

SUPPLEMENTARY INFORMATION P1.A

Detailed MILP formulation

Nomenclature

Abbreviations

ACC	Annualized Capital Cost
BFW	Boiler feed water
BP-ST	Back-pressure steam turbine
C-ST	Condensing steam turbine
cw	Cooling water
Deae	Deaerator
dem	demand
e	electricity
Eq	Equipment
f	Fuel
FSR	Flash steam recovery
grid	Electricity grid
HO	Hot oil
HRSG	Heat recovery steam generator
i_f	Last steam main i
IS	isentropic
LD	Let-down
M	Mass flowrate
main	Maintenance cost
nEq	Number of equipment
OC	Operating costs
op	Operating
Q	Heat flow
sh	superheated
TAC	Total Annualized Cost
tEq	Type of equipment
TSP	Total site profile
VHP	Very High Pressure
w	Treated water

Sets

C	Set of cold streams
H	Set of hot streams
I	Set of steam mains
I_j s	Set of steam levels j s that belong to steam main i
J	Set of temperature/pressure intervals
J_{HO}	Set of temperature/pressure intervals for hot oil (subset of temperature intervals)
J_s	Set of temperature/pressure intervals for steam main (subset of temperature intervals)
J_{WH}	Set of temperature/pressure intervals for waste heat (subset of temperature intervals)
N_b, N_{HRSG}, N_{st}	Set of boilers, HRSG, steam turbines number of units available, respectively.
T_b	Set of boiler types

v Set of VHP steam levels

Variables

C_{op}^e Operating costs of electricity
 OC Total operating costs
 TAC Total annualized costs
 W^{grid} Electricity from/to the grid

Positive variables

ACC Annualized capital cost
 C_{main}^{Eq} Maintenance cost of each equipment
 C_{op}^f Operating costs of fuel
 C_{op}^{cw} Operating costs of cooling water
 C_{op}^w Operating costs of water
 $M_{nb, tb, v}^b$ Steam mass flow rate from unit nb boiler type tb, operating at v conditions
 M_{i, j_s}^{BFW} BFW mass flow rate for steam main i operating at j_s conditions
 M_{i, j_s}^{BFWC} BFW mass flow rate injected to desuperheat process steam prior its use at level js
 $m_{nst, i, j_s, j_s'}^{BP-ST}$ Steam mass flow rate of BP turbine nst operating from level j_s to level j_s'
 $M_{i, j_s}^{BP-STin}$ Steam mass flow rate of BP turbines entering to steam main i operating at j_s conditions
 $M_{i, j_s}^{BP-STout}$ Steam mass flow rate of BP turbines leaving steam main i operating at j_s conditions
 M_{i, j_s}^{Cin} Steam mass flow rate for process heating at steam level j_s
 M_{i, j_s}^{Cmain} Steam mass flow rate from steam main i operating at j_s conditions
 $M_{i, j_s}^{C-STout}$ Mass flow rate of condensing turbines from steam main i operating at j_s conditions
 $m_{nst, i, j_s}^{C-STout}$ Mass flow rate of condensing turbine nst from steam main i operating at j_s conditions
 $M_{j_s}^{Deae}$ Mass flow rate to deaerator from steam level j_s
 $M_{nEq, tEq}^{Eq}$ Variable vector representing mass load of unit nEq of equipment type tEq at the general MILP formulation
 M_{i, j_s}^{FSR} Flashed steam mass flow rate fed to the mixer i operating at j_s conditions
 M_{in, i, j_s}^{FSR} Inlet mass flow rate at FSR drum i
 $m_{i, j_s, j_s'}^{FSR}$ Liquid mass flow rate of FSR i operating from pressure j_s to j_s'
 $m_{s, i, j_s, j_s'}^{FSR}$ Steam mass flow rate of FSR i operating from pressure j_s to j_s'
 M_{i, j_s}^H Mass flow rate of process steam generation for steam main i operating at j_s conditions
 $M_{nHRSG, v}^{HRSG}$ Steam mass flow rate from unit nHRSG, operating at v conditions
 $M_{i, j_s}^{in}, M_{i, j_s}^{out}$ Variable vectors representing inlet and outlet mass flow rates at steam main i operating at j_s conditions at the general MILP formulation
 $m_{i, j_s, j_s'}^{LD}$ Mass flow rate of let-down passing from steam main i operating at j_s to steam level j_s'
 M_{i, j_s}^{LDin} Let-down mass flow rate entering to steam main i operating at j_s conditions
 M_{i, j_s}^{LDout} Let-down mass flow rate leaving steam main i operating at j_s conditions
 m_{θ}^{st} Steam mass flow rate of steam turbine operating at θ conditions
 $m_{max, \theta}^{st}$ Maximum steam mass flow rate of steam turbine operating at θ conditions
 $M_{\Gamma, v}^{VHP}$ Total steam mass flow rate produce at VHP main header operating at v conditions

$m_{nst,v,j_s}^{VHP\ BP-ST}$	Steam mass flow rate of BP turbine nst operating from VHP level v to level js
$m_{nst,v,j_s}^{VHP\ C-ST}$	Steam mass flow rate of condensing turbine nst operating from VHP level v
$m_{v,j_s}^{VHP\ LD}$	Let-down mass flow rate passing from VHP main level v to steam level js
Output	Variable vector representing the energy output of each utility component at the general MILP formulation
Q_{i,j_s}^{BP-ST}	Heat from back-pressure steam turbine of steam main i operating at js conditions
Q_{i,j_s}^{Cin}	Heat available for process heating from steam main i operating at js conditions
$Q_{j_s}^{Hout}$	Process heat available at steam level js
Q_s^{HO}	Process heating requirements that cannot be used/satisfied by steam
Q_s^{HO}	Process heating provided by hot oil system at steam temperature range
Q_T^{HO}	Total process heating provided by hot oil system
$Q_{i,j_s}^{in}, Q_{i,j_s}^{out}$	Variable vectors representing inlet and outlet heat flow at steam main i operating at js conditions at the general MILP formulation
Q_{i,j_s}^{LD}	Heat from let-down station of steam main i operating at js conditions
$R_{j_s}^C$	Residual sink heat at steam level js
$R_{j_s}^H$	Residual source heat at steam level js
T_i^{GUESS}	Estimated superheat temperature of steam main i, in the algorithm for calculating steam mains' superheating
$W_{i,j_s,j_s'}^{BP-ST}$	Power generated by BP turbine from steam main i operating from steam level js to steam level js'
W_{v,j_s}^{BP-ST}	Power generated by BP turbine from VHP steam main operating from VHP main level v to steam level js
W^{Eq}	Variable vector representing power generated by equipment Eq in the general MILP formulation
W_θ^{st}	Power generated by steam turbine operating at θ conditions
x	Variable vector representing continuous variables in the general MILP formulation
x_θ^{st}	Load fraction of steam turbine operating at θ conditions
$Z_{n_{Eq}, t_{Eq}}^{Eq}$	Variable vector representing size of unit n_{Eq} of equipment type t_{Eq} at the general MILP formulation

Binary variables

y	Variable vector representing binary variables at the general MILP formulation
$y_{n_{Eq}, t_{Eq}}^{Eq}$	Vector representing binary variables that denote the selection of unit n_{Eq} of equipment type t_{Eq}
$y_{j_s}^{HO}$	Binary variables to denote the selection of hot oil at steam level js
y_{i,j_s}^I	Binary variables to denote the selection of steam level i operating at condition js
y_θ^{st}	Binary variables to denote the selection of steam turbines operating at θ conditions

Parameters

β	condensate return rate
$\Delta h_{j_s}^C$	Enthalpy difference of process steam use at steam level js
$\Delta h_{j_s}^H$	Enthalpy difference of process steam generation at steam level js
σ_θ^{st}	minimum load fraction of steam turbine operating at θ conditions
$\Omega_{min_\theta}^{st}, \Omega_{max_\theta}^{st}$	minimum and maximum equipment steam turbine capacity, in terms of flow rate
θ_e^{dem}	Power demand

a, b, c	Steam modelling coefficients of steam turbines in the algorithm for calculating steam mains' superheating
$a_{\theta}^{st}, b_{\theta}^{st}, c_{\theta}^{st}$	Steam modelling coefficients of steam turbines operating at θ conditions
\tilde{A}_{x1}	Coefficient matrices of the continuous variables at the general MILP formulation
\tilde{A}_{x2}	Coefficient matrices of the binary variables at the general MILP formulation
b_x	parameter vectors on the right side at the general MILP formulation
C_{nEq}^A	Variable cost of equipment depending on its size, in the general MILP formulation
C_{nEq}^B	Fixed cost of equipment selection, in the general MILP formulation
F_{tEq}^{ann}	Annualization factor
F_{tEq}^{inst}	Installation factor
h_i	Enthalpy at operating conditions of steam main i , in the algorithm for calculating steam mains' superheating
$h_{l j_s}$	Enthalpy of saturated liquid at steam level j_s
$h_{v j_s}$	Enthalpy of saturated vapor at steam level j_s
h^{BFW}	Enthalpy of boiling feed water
h^{Cond}	Enthalpy of returned condensate
$h_{j_s}^C$	Enthalpy of saturated liquid of process steam use at steam level j_s
$h_{sh j_s}^C$	Enthalpy of superheated process steam use at steam level j_s
$h_{sh j_s}^H$	Enthalpy of superheated process steam generation at steam level j_s
h^{vent}	Enthalpy of steam vented
h^W	Enthalpy of treated water
L^H, L^C	Heat losses due to distribution at the source and sink side, respectively
η^{IS}	Isentropic efficiency of steam turbine in the algorithm for calculating steam mains' superheating
η_{mec}	Mechanical efficiency of steam turbines
P_i	Steam pressure of steam main i
$Q_{j_s}^{Cout}$	Process heat source at steam level j_s
$Q_{j_s}^{Hin}$	Process heat source at steam level j_s
s_i	Entropy at operating conditions of steam main i , in the algorithm for calculating steam mains' superheating
s_i^{IS}	Isentropic entropy at steam operating conditions of steam main i in the algorithm for calculating steam mains' superheating
T_{max}	Maximum temperature allowed for steam generation
T_s^{HO}	Supply temperature of hot oil
T_i^{MIN}	Minimum superheat temperature of steam main i
$\overline{W}_{max}^{grid}$	Upper bound of import/export electricity

A.I.1. Pseudo-parameters

ΔH_{θ}^{IS}	Isentropic enthalpy difference of steam turbine operating at θ conditions
$h_{sh i j_s}^{main}$	Enthalpy of superheated steam at steam main i operating at j_s conditions
$h_{sh v}^{VHP}$	Enthalpy of superheated steam at VHP steam main operating at v conditions

A.II. Objective function

The steam system is designed to achieve the optimal economic performance in relation to the total annualized cost (TAC), which comprises the annualized cost of investment (ACC) and operating costs (OC) - as given in Eq. (P1.A. 1). To keep the formulation concise, the general expression used to calculate the ACC of the energy system is presented in Eq. (P1.A. 2). The sum of the capital cost (CC) comprises of the cost of each unit (n_{Eq}) of the equipment available (t_{Eq}), such as furnaces, boilers, back-pressure steam turbines, condensing turbines, gas turbines with HRSGs, condensers, flash tanks and deaerator. The cost functions are modelled as the sum of a fixed cost for each device (C_{nEq}^B) and a variable cost (C_{nEq}^A), which depends on the device size ($Z_{nEq, tEq}^{Eq}$). The total capital cost is obtained by including the installation factor (F_{tEq}^{inst}) to account for the construction, installation, contingencies and other associated costs. Finally, an annualization factor (F_{tEq}^{ann}) is used to spread the cost over the lifetime of the devices.

$$\min TAC = ACC + OC \quad (P1.A. 1)$$

$$ACC = F_{tEq}^{ann} \left(\sum_{Eq} \sum_{tEq} F_{tEq}^{inst} \sum_{nEq} \left(C_{nEq}^A \cdot Z_{nEq, tEq}^{Eq} + C_{nEq}^B \cdot y_{nEq, tEq}^{Eq} \right) \right) \quad (P1.A. 2)$$

$$OC = C_{main}^{Eq} + C_{op}^f + C_{op}^{cw} + C_{op}^w + C_{op}^e \quad (P1.A. 3)$$

The operating costs (OC) based on Eq. (P1.A. 3), comprises the maintenance cost of equipment (C_{main}^{Eq}), and the costs of fuels (C_{op}^f), cooling water (C_{op}^{cw}), treated water (C_{op}^w) and electricity (C_{op}^e). The latter involves the costs of power import minus the revenue from power export, as shown in Eq. (P1.A. 4) P_{imp}^e and P_{exp}^e are the electric power import and export tariff, respectively.

$$C_{op}^e = W^{IMP} P_{imp}^e - W^{EXP} P_{exp}^e \quad (P1.A. 4)$$

The fuel cost is associated with the fuel consumed in the site of the cogeneration system (boilers, gas turbines and HRSGs) and any auxiliary equipment such as the fired heaters (if required), for high temperature process heating that cannot be satisfied via steam.

$$C_{op}^f = \sum_{tEq} \sum_{fEq} Q_{tEq, fEq}^f P_{fEq}^f \quad (P1.A. 5)$$

In this analysis, P_{fEq}^f denotes the unit price of the fuel consumed by each device in the utility system. Additionally, cooling water costs involve the consumption of both site processes ($Q_{process}^{CW}$) and the utility system i.e. steam turbine condensers ($Q_{Utility}^{CW}$), while treated water is based on the make-up

water requirements of the deaerator (m_{DA}^W), as shown below. P^{CW} and P^W are the unit price of cooling water and water, respectively.

$$C_{op}^{CW} = (Q_{process}^{CW} + Q_{Utility}^{CW}) P^{CW} \tag{P1.A. 6}$$

$$C_{op}^W = m_{DA}^W \cdot P^W \tag{P1.A. 7}$$

A.III. Design constraints

The constraints of the problem are described in the following Eqs. (P1.A. 8) - (P1.A. 121).

A.III.1. Heat integration

To assess the heat integration between the processes and the utility system three heat cascades are constructed based on heat cascades (and the transshipment problem), as shown in . The heat cascades comply with the first and second thermodynamic laws by ensuring that the energy balance is satisfied (first law). Heat is only transmitted from higher to lower temperatures (second law). The problem formulation comprises three cascades: source, steam and sink.

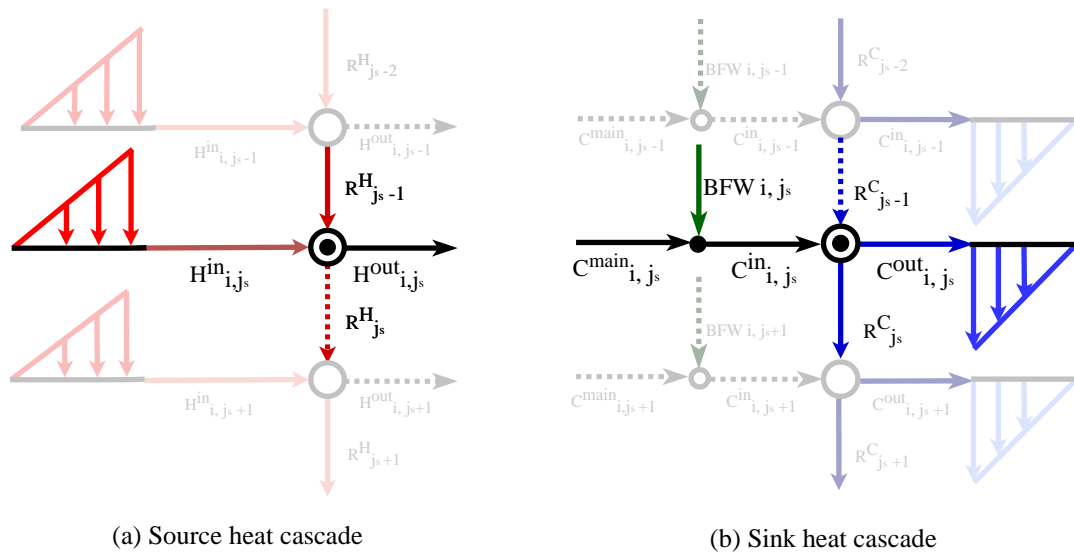


Figure P1. A. 1. Heat cascade diagram

A.III.1.1. Source cascade

Heat from the process sources ($Q_j^{H_{in}}$) flows into the temperature interval to raise steam at superheated conditions. Heat that cannot be used in a particular interval flows to the next lower interval as residual heat (R^H). The energy balance for each temperature interval in the source cascade is illustrated in , while the formulations are given by Eqs.(P1.A. 8) and (P1.A. 9). Note that any heat source above the topmost steam level candidate (1, 1) is cascaded to the first steam main, as shown in Eq. (P1.A. 8).

In addition, any residual heat from the bottom-most steam level candidate is added to the site utility cooling demand. The site utility cooling is discussed later in the “cooling utility” section of this work.

$$\sum_{j \in J, \bar{T}_j \geq \bar{T}_{j_s}} Q_j^{H_{in}} = Q_{i,j_s}^{H_{out}} + R_{j_s}^H \quad \forall i=1, (i,j_s) \in IJ_s, j_s=1 \quad (P1.A. 8)$$

$$Q_{j_s}^{H_{in}} + R_{j_s-1}^H = Q_{j_s}^{H_{out}} + R_{j_s}^H \quad \forall i=1, (i,j_s) \in IJ_s, j_s > 1 \quad (P1.A. 9)$$

A.III.1.2. Constraints for steam level selection

If a steam level candidate is selected, the heat available ($Q_j^{H_{out}}$) is used to produce superheated steam ($M_{i,j}^H$), and no residual heat is cascaded downwards, as expressed in Eqs. (P1.A. 10) and (P1.A. 11). L^H is a parameter set to consider heat losses.

$$(1-L^H) Q_{j_s}^{H_{out}} = M_{i,j_s}^H \cdot (h_{sh_{j_s}}^H - h^{BFW}) \quad \forall i \in I, (i,j_s) \in IJ_s \quad (P1.A. 10)$$

$$R_{j_s}^H - U_{j_s}^H \cdot (1-y_{i,j_s}^L) \leq 0 \quad \forall i \in I, (i,j_s) \in IJ_s \quad (P1.A. 11)$$

Additionally, Eqs. (P1.A. 12) and (P1.A. 13) are logical constraints to prevent non-zero flows for non-existing steam level candidates.

$$Q_{j_s}^{H_{out}} - U_{j_s}^H \cdot y_{i,j_s}^L \leq 0 \quad \forall i \in I, (i,j_s) \in IJ_s \quad (P1.A. 12)$$

$$M_{i,j_s}^H \cdot h_{sh_{j_s}}^H - U_{j_s}^H \cdot y_{i,j_s}^L \leq 0 \quad \forall i \in I, (i,j_s) \in IJ_s \quad (P1.A. 13)$$

Where U_{i,j_s}^H is the maximum heat that can be transferred from the heat sources at level j . To obtain a tight problem formulation, U_{i,j_s}^H can be set as the cumulative heat at interval j , as expressed below.

$$U_{j_s}^H = \sum_{j \in J, \bar{T}_j \geq \bar{T}_{j_s}} Q_j^{H_{in}} \quad \forall j_s \in J_s \quad (P1.A. 14)$$

A.III.1.3. Steam level cascade

Eq. (P1.A. 15) represents the energy balance for each steam main i , operating at j conditions. The equation assumes adiabatic mixing. Heat flows into the steam level from steam generation (M^H), with steam passing through either the steam turbines (BP-ST) or let-down stations (LD) and BFW. Steam may be used for: (1) process heating ($M_{i,j}^{C_{main}}$), (2) power generation through steam expansion via a back-pressure ($M^{BP-ST_{out}}$) or a condensing steam turbine ($M^{C-ST_{out}}$), or (3) for temperature/pressure control in the steam mains by passing it to a let-down station ($M^{LD_{out}}$). As stated in Eq. (P1.A. 15), the bottom steam header i_n can only expand steam to vacuum condition and has an additional steam output which feeds the deaerator.

$$M_{i,j_s}^H \cdot h_{sh_{j_s}}^H + Q_{i,j_s}^{BP-ST} + Q_{i,j_s}^{LD} + M_{i,j_s}^{BFW} \cdot h^{BFW} = \left(M_{i,j_s}^C + M_{i,j_s}^{BP-ST_{out}} + M_{i,j_s}^{C-ST_{out}} + M_{i,j_s}^{LD_{out}} \right) \cdot h_{sh_{i,j_s}}^{main} \quad \forall i \in I, \quad (i,j_s) \in IJ_s \quad (P1.A. 15)$$

$$M_{i,j_s}^H \cdot h_{sh_{j_s}}^H + Q_{i,j_s}^{BP-ST} + Q_{i,j_s}^{LD} + M_{i,j_s}^{BFW} \cdot h^{BFW} = \left(M_{i,j_s}^C + M_{i,j_s}^{Deac} + M_{i,j_s}^{C-ST_{out}} + M_{i,j_s}^{LD_{out}} \right) \cdot h_{sh_{i,j_s}}^{main} \quad \forall i \in I, \quad (i,j_s) \in IJ_s$$

Due to the flexible consideration in the inlet streams from steam turbines and let-down stations, their terms are abbreviated as (Q_{i,j_s}^{BP-ST}) and (Q_{i,j_s}^{LD}) and expressed by Eqs. (P1.A. 16) and (P1.A. 17).

$$Q_{i,j_s}^{LD} = \sum_{i' < i} \sum_{(i',j_s') \in IJ_s} \left(m_{i',j_s',j_s}^{LD} \cdot h_{j_s'}^{main} \right) + \sum_{v \in V} \left(m_{v,j_s}^{LD} \cdot h_{sh_v}^{VHP} \right) \quad \forall i \in I, \quad (i,j_s) \in IJ_s \quad (P1.A. 16)$$

$$Q_{i,j_s}^{BP-ST} = \sum_{n_{st} \in N_{st}} \sum_{i' < i} \sum_{(i',j_s') \in IJ_s} \left(m_{n_{st},i',j_s',j_s}^{BP-ST} \cdot h_{sh_{j_s'}}^{main} - \frac{W_{n_{st},i',j_s',j_s}^{BP-ST}}{\eta_{mec}} \right) + \sum_{n_{st} \in N_{st}} \sum_{v \in V} \left(m_{n_{st},v,j_s}^{VHP \ BP-ST} \cdot h_{sh_v}^{VHP} - \frac{W_{n_{st},v,j_s}^{VHP \ BP-ST}}{\eta_{mec}} \right) \quad \forall i \in I, \quad (i,j_s) \in IJ_s \quad (P1.A. 17)$$

Eq. (P1.A. 18) show the mass balance at each steam main.

$$M_{i,j_s}^H + M_{i,j_s}^{BP-ST_{in}} + M_{i,j_s}^{LD_{in}} + M_{i,j_s}^{BFW} = M_{i,j_s}^C + M_{i,j_s}^{BP-ST_{out}} + M_{i,j_s}^{C-ST_{out}} + M_{i,j_s}^{LD_{out}} \quad \forall i < i_n, (i,j_s) \in IJ_s \quad (P1.A. 18)$$

$$M_{i,j_s}^H + M_{i,j_s}^{BP-ST_{in}} + M_{i,j_s}^{LD_{in}} + M_{i,j_s}^{BFW} = M_{i,j_s}^C + M_{i,j_s}^{Deac} + M_{i,j_s}^{C-ST_{out}} + M_{i,j_s}^{LD_{out}} \quad i = i_n, (i,j_s) \in IJ_s$$

Eqs. (P1.A. 19) - (P1.A. 23) ensure that the total amount of steam from the let-down stations and steam turbines entering the headers equals that leaving.

$$M_{i,j_s}^{BP-ST_{in}} = \sum_{n_{st} \in N_{st}} \sum_{i' < i} \sum_{(i',j_s') \in IJ_s} m_{n_{st},i',j_s',j_s}^{BP-ST} + \sum_{n_{st} \in N_{st}} \sum_{v \in V} m_{n_{st},v,j_s}^{VHP \ BP-ST} \quad \forall i \in I, (i,j_s) \in IJ_s \quad (P1.A. 19)$$

$$M_{i,j_s}^{BP-ST_{out}} = \sum_{n_{st} \in N_{st}} \sum_{j_s > j_s'} m_{n_{st},i,j_s,j_s'}^{BP-ST} \quad \forall i \in I, (i,j_s) \in IJ_s \quad (P1.A. 20)$$

$$M_{i,j_s}^{C-ST_{out}} = \sum_{n_{st} \in N_{st}} m_{n_{st},i,j_s}^{C-ST} \quad \forall i \in I, (i,j_s) \in IJ_s \quad (P1.A. 21)$$

$$M_{i,j_s}^{LD_{in}} = \sum_{i' < i} \sum_{(i',j_s') \in IJ_s} m_{i',j_s',j_s}^{LD} + \sum_{v \in V} m_{v,j_s}^{VHP \ LD} \quad \forall i \in I, (i,j_s) \in IJ_s \quad (P1.A. 22)$$

$$M_{i,j_s}^{LD_{out}} = \sum_{j_s > j_s'} m_{i,j_s,j_s'}^{LD} \quad \forall i \in I, (i,j_s) \in IJ_s \quad (P1.A. 23)$$

a) Constraints for steam level selection

When a certain steam level j_s is selected for a given steam header i , the input and output flowrates from that particular level are enabled. Otherwise, they are forbidden. A simplified version of feasibility constraints are represented by Eqs. (P1.A. 24) and (P1.A. 27).

$$M_{i,j_s}^{in} - U^m \cdot y_{i,j_s}^L \leq 0 \quad \forall i \in I, (i,j_s) \in IJ_s \quad (P1.A. 24)$$

$$M_{i,j_s}^{out} - U^m \cdot y_{i,j_s}^L \leq 0 \quad \forall i \in I, (i,j_s) \in IJ_s \quad (P1.A. 25)$$

$$Q_{i,j_s}^{\text{in}} - U^Q \cdot y_{i,j_s}^L \leq 0 \quad \forall i \in I, (i,j_s) \in IJ_s \quad (\text{P1.A. 26})$$

$$Q_{i,j_s}^{\text{out}} - U^Q \cdot y_{i,j_s}^L \leq 0 \quad \forall i \in I, (i,j_s) \in IJ_s \quad (\text{P1.A. 27})$$

where U^m and U^Q are the upper bound for mass and heat flowrate for the steam system. These parameters are set based on the problem specifications. Importantly, if there is a non-zero lower bound, then this is determined later by the relevant equipment specifications.

b) Sink cascade

The utility system (steam level cascade) relates to the sink processes through the steam usage ($M_{i,j_s}^{C,\text{main}}$). It is important to note that steam is desuperheated prior its use for process heating, which is achieved by mixing the steam locally with BFW (see). Note that process steam use is assumed to be used at the degree of superheat required (h_{sh,j_s}^C) until saturated liquid conditions of the corresponding level (h_{l,j_s}^C). The sensible heat of condensing water is not considered.

$$M_{i,j_s}^{C,\text{main}} + M_{i,j_s}^{\text{BFWC}} = M_{i,j_s}^{C,\text{in}} \quad \forall i \in I, (i,j_s) \in IJ_s \quad (\text{P1.A. 28})$$

$$(1-L^C) \cdot M_{i,j_s}^{C,\text{main}} \cdot h_{\text{sh},j_s}^{\text{main}} + M_{i,j_s}^{\text{BFWC}} \cdot h^{\text{BFW}} = M_{i,j_s}^{C,\text{in}} \cdot (h_{\text{sh},j_s}^C - h_{l,j_s}^C) = Q_{i,j_s}^{C,\text{in}} \quad \forall i \in I, (i,j_s) \in IJ_s \quad (\text{P1.A. 29})$$

Heat used ($Q_{i,j_s}^{C,\text{in}}$) is calculated based on the process heat requirement at the different temperature intervals of the heat sink cascade. The heat provided can be used within the process sinks involved in the interval ($Q_j^{C,\text{out}}$) or cascaded down to the next lower temperature heat sink interval (R_j^C). Process heat demand can be provided by either steam usage from the corresponding interval or from hot oil (Q_s^{HO}). Consequently, at the topmost steam level, heat flow from hot oil is allowed (Eq. (P1.A. 30)). Hot oil system and its constraints are detailed in the section ‘Fired heat utility’.

$$Q_{i,j_s}^{C,\text{in}} + Q_s^{\text{HO}} = Q_j^{C,\text{out}} + R_j^C \quad i = 1, j_s = 1 \quad (\text{P1.A. 30})$$

$$Q_{i,j_s}^{C,\text{in}} + R_{j_s-1}^C = Q_j^{C,\text{out}} + R_j^C \quad i=i_n, (i,j_s) \in IJ_s \quad (\text{P1.A. 31})$$

The last steam main (i_n) needs to satisfy the heat requirement at that level and below (if it is the case). Therefore, the “residual” heat is constrained to be equal to the heat sinks below the last steam level (j_{s_n}).

$$R_{j_s}^C = \sum_{j \in I, T_j < T_{j_s}} Q_j^{C,\text{out}} \quad i=i_n, j_s=j_{s_n} \quad (\text{P1.A. 32})$$

The overall energy balance in the heat sink cascade is considered by Eq. (P1.A. 33)

$$\sum_{i \in I} \sum_{j_s \in I_{j_s}} Q_{i,j_s}^{C_{in}} + Q_T^{HO} = \sum_{j \in J} Q_j^{C_{out}} \quad (\text{P1.A. 33})$$

c) Constraints for steam level selection

When a steam level j_s is selected for a given steam header i , the heat flow rate from that level is allowed. Otherwise, it is forbidden. Moreover, heat sink intervals can accept cascaded heat -- if and only if -- their corresponding steam level candidate is not selected. This guarantees that no heat flows across steam mains at the sink cascade. For reference, the feasibility constraints are given in Eqs. (P1.A. 34) - (P1.A. 37).

$$Q_{j_s}^{C_{in}} - U_{j_s}^C \cdot y_{i,j_s}^L \leq 0 \quad \forall i \in I, (i,j_s) \in I_{j_s} \quad (\text{P1.A. 34})$$

$$Q^{HO} - U_{j_s}^C \cdot (1 - y_{i,j_s}^L) \leq 0 \quad i = 1, j_s = 1 \quad (\text{P1.A. 35})$$

$$R_{j_s-1}^C - U_{j_s}^C \cdot (1 - y_{i,j_s}^L) \leq 0 \quad \forall i \in I, (i,j_s) \in I_{j_s}, j_s > 1 \quad (\text{P1.A. 36})$$

Where $U_{j_s}^C$ is the maximum heat that can be transferred to the heat sink at level j_s . $U_{j_s}^C$ can be set to the cumulative heat at interval j_s , as expressed below.

$$U_{j_s}^C = \sum_{j \in J, T_j \leq T_{j_s}} Q_j^{C_{out}} \quad \forall j_s \in J_s \quad (\text{P1.A. 37})$$

A.III.2. VHP steam level

As noted, the highest-pressure (VHP) main receives steam from the operating boilers ($M_{n_b, t_b, v}^b$) and the heat recovery steam generators ($M_{n_{HRSG}, v}^{HRSG}$). By the problem definition, VHP level conditions are always located at temperatures higher than any process heat sink or source. The balance equations for the VHP level candidates are the usual mass and energy balances, involving the corresponding inlet and outlet steam flows. The mass balance around the VHP steam level is expressed by Eq. (P1.A. 38). Moreover, the $M_{T_v}^{VHP}$ term comprises the overall utility steam requirement at v conditions.

$$\sum_{n_b} \sum_{t_b} M_{n_b, t_b, v}^b + \sum_{n_{HRSG}} M_{n_{HRSG}, v}^{HRSG} = M_{T_v}^{VHP} \quad \forall v \in V \quad (\text{P1.A. 38})$$

$$M_{T_v}^{VHP} = \sum_{n_{st}} \sum_{j_s \in J_s} m_{n_{st}, v, j_s}^{VHP \text{ BP-ST}} + \sum_{n_{st} \in N_{st}} m_{n_{st}, v}^{VHP \text{ C-ST}} + \sum_{j_s \in J_s} m_{v, j_s}^{VHP \text{ LD}} \quad \forall v \in V$$

For the heat balance in the VHP steam level, iso-thermal mixing is assumed. In short, any boiler or HRSG unit generates steam at v conditions (temperature and pressure).

$$M_{T_v}^{VHP} \cdot h_{sh_v}^{VHP} = \left[\sum_{j_s \in J_s} \left(m_{v,j_s}^{VHP \text{ BP-ST}} + m_{v,j_s}^{VHP \text{ LD}} \right) + m_v^{VHP \text{ C-ST}} \right] \cdot h_{sh_v}^{VHP} \quad \forall v \in V \quad (\text{P1.A. 39})$$

VHP steam level is linked to the steam distribution system through the steam expanded by either back-pressure steam turbines ($m_{n_{st,v},j_s}^{VHP \text{ BP-ST}}$) or let-down stations ($m_{v,j_s}^{VHP \text{ LD}}$), involved in Eqs.(P1.A. 16), (P1.A. 17), (P1.A. 19), (P1.A. 22), (P1.A. 69a) and (P1.A. 71). On a similar note to the steam levels, only when VHP steam main is operating at condition v , the input and output flowrates from that particular level are enabled. Otherwise, they are forbidden. For reference purposes, a generalized form of the practical constrains is represented below.

$$M_{T_v}^{VHP} h_{sh_v}^{VHP} - U_Q^{VHP} \cdot y_v^{VHP} \leq 0 \quad \forall v \in V \quad (\text{P1.A. 40})$$

$$M_m^{VHP} - U_m^{VHP} \cdot y_v^{VHP} \leq 0 \quad \forall v \in V \quad (\text{P1.A. 41})$$

$$M_{out}^{VHP} - U_m^{VHP} \cdot y_v^{VHP} \leq 0 \quad \forall v \in V \quad (\text{P1.A. 42})$$

Where U_Q^{VHP} and U_m^{VHP} are the upper bound for heat and mass flowrates for the steam system, which must be set based on the problem specifications. Note that if there is a non-zero lower bound, this is determined later by each equipment specifications.

A.III.2.1. Constraints for steam level selection

Each steam main works at a single operating condition, as shown in Eqs. (P1.A. 43) and (P1.A. 44). Additionally, It should also be noted that connections only exist between selected steam levels. To account for this constraint without increasing the number of binary variables, variables y_{i,j_s}^{L-L} , and y_{v,j_s}^{VHP-L} are defined as continuous variables with a range between [0, 1] constrained by Eqs. (P1.A. 45)-(P1.A. 48).

$$\sum_{j_s \in J_s} y_{i,j_s}^L \leq 1 \quad \forall i \in I \quad (\text{P1.A. 43})$$

$$\sum_{v \in V} y_v^{VHP} = 1 \quad \forall v \in V \quad (\text{P1.A. 44})$$

$$y_{i,j_s}^{L-L} \geq y_{i,j_s}^L + y_{i',j_s}^L - 1 \quad \forall i \in I, i' > i, (i,j_s) \text{ and } (i',j_s) \in IJ_s \quad (\text{P1.A. 45})$$

$$y_{i,j_s}^{L-L} \leq y_{i,j_s}^L \text{ and } y_{i,j_s}^{L-L} \leq y_{i',j_s}^L, \quad \forall i \in I, i' > i, (i,j_s) \text{ and } (i',j_s) \in IJ_s \quad (\text{P1.A. 46})$$

$$y_{v,j_s}^{VHP-L} \geq y_v^{VHP} + y_{i,j_s}^L - 1 \quad \forall v \in V, i \in I, (i,j_s) \in IJ_s \quad (\text{P1.A. 47})$$

$$y_{v,j_s}^{VHP-L} \leq y_v^{VHP} \text{ and } y_{v,j_s}^{VHP-L} \leq y_{i,j_s}^L \quad \forall v \in V, i \in I, (i,j_s) \in IJ_s \quad (\text{P1.A. 48})$$

Only actual steam level candidates j_s of each steam main can be selected. Therefore, for any “forbidden” operating condition (i, j_s) , y_{i, j_s}^L is fixed as zero.

$$y_{i, j_s}^L = 0 \quad \forall i \in I, (i, j_s) \notin IJ_s \quad (\text{P1.A. 49})$$

Eqs.(P1.A. 50)-(P1.A. 53) are logical constraints to prevent non-zero flows for non-existing steam level candidates.

$$m_{i, j_s, j_s}^{\text{LD}} - U^{\text{LD}} \cdot y_{i, j_s, j_s}^{\text{L-L}} \leq 0 \quad \forall i \in I, (i, j_s) \in IJ_s \quad (\text{P1.A. 50})$$

$$m_{s, i, j_s, j_s}^{\text{FSR}} - U_{j_s}^{\text{FSR}} \cdot y_{i, j_s, j_s}^{\text{L-L}} \leq 0 \quad \forall i \in I, (i, j_s) \in IJ_s \quad (\text{P1.A. 51})$$

$$m_{i, i, j_s, j_s}^{\text{FSR}} - U_{j_s}^{\text{FSR}} \cdot y_{i, j_s, j_s}^{\text{L-L}} \leq 0 \quad \forall i \in I, (i, j_s) \in IJ_s \quad (\text{P1.A. 52})$$

$$M_{i, j_s}^{\text{FSR}} - U_{j_s}^{\text{FSR}} \cdot y_{i, j_s}^{\text{L}} \leq 0 \quad \forall i \in I, (i, j_s) \in IJ_s \quad (\text{P1.A. 53})$$

A.III.3. Other Utilities

A.III.3.1. Cooling utility

Heat sources are recovered to generate steam. Nevertheless, it is most likely that some of the source heat temperatures are lower than the minimum allowed temperature for steam generation at the lowest steam level. Thus, a cooling utility is required to satisfy the remaining process cooling demand. Moreover, condensing turbines (if applicable) involves a condenser to reject the residual heat of the exhausts (via a cooling utility) and condensate. The heat load of the turbine condensers ($Q_{\text{CW}}^{\text{VHP C-ST}}$ and $Q_{\text{CW}}^{\text{C-ST}}$) can be calculated by Eqs. (P1.A. 55) and (P1.A. 56). Therefore, the total cooling utility (Q^{CW}) is calculated as a sum of the heat duties on the turbine condensers, plus all remaining process cooling demands that cannot be used/satisfied by steam generation, as shown in Eq. (P1.A. 54).

$$Q^{\text{CW}} = \sum_{j_{\text{wh}} \in I_{\text{WH}}} Q_{j_{\text{wh}}}^{\text{H}_{\text{in}}} + R_{j_s}^{\text{H}} + Q_{\text{CW}}^{\text{VHP C-ST}} + Q_{\text{CW}}^{\text{C-ST}} \quad j_s = J_s \quad (\text{P1.A. 54})$$

$$Q_{\text{CW}}^{\text{C-ST}} = \sum_{n_{\text{st}}} \sum_{i \in I} \sum_{j_s \in IJ_s} \left[m_{n_{\text{st}}, i, j_s}^{\text{C-ST}} (h_{\text{sh}_{j_s}}^{\text{main}} - h_1^{\text{vac}}) - \frac{W_{n_{\text{st}}, i, j_s}^{\text{C-ST}}}{\eta_{\text{mec}}} \right] \quad \forall i \in I, (i, j_s) \in IJ_s \quad (\text{P1.A. 55})$$

$$Q_{\text{CW}}^{\text{VHP C-ST}} = \sum_{n_{\text{st}}} \sum_{v \in V} \left[m_{n_{\text{st}}, v}^{\text{VHP C-ST}} (h_{\text{sh}_v}^{\text{VHP}} - h_1^{\text{vac}}) - \frac{W_{n_{\text{st}}, v}^{\text{VHP C-ST}}}{\eta_{\text{mec}}} \right] \quad \forall i \in I, (i, j_s) \in IJ_s \quad (\text{P1.A. 56})$$

A.III.3.2. Fired heat utility

The heat provided by hot oil above the maximum steam temperature (T_{max}) is defined by Eq. (P1.A. 57)

$$Q^{HO} = \sum_{j \in I, T_j \geq T_{\max}} Q_j^{C_{out}} \quad (P1.A. 57)$$

Below the maximum steam temperature, heat demand can be provided by either steam usage from the corresponding interval or from hot oil. To represent this, at the topmost steam level, heat flow from hot oil is allowed, as expressed by Eq. (P1.A. 58). Within the steam temperature range, the heat supplied by hot oil is restricted to the levels where the use of hot oil is favored by the optimization ($y_{j_s}^{HO} = 1$), as given by Eq. (P1.A. 59)

$$Q_{i,j_s}^{C_{in}} + Q_s^{HO} = Q_{j_s}^{C_{out}} + R_{j_s}^C \quad i=1, j_s=1 \quad (P1.A. 58)$$

$$Q_s^{HO} = \sum_{j_s \in I_s, T_{j_s} < T_s^{HO}} (Q_{j_s}^{C_{out}} \cdot y_{j_s}^{HO}) \quad (P1.A. 59)$$

Total fired heating utility (Q_T^{HO}) can be modelled as a sum of the heat duties above the steam temperature range, added to all the process heating requirements that cannot be used/satisfied by steam, as shown in Eq. (P1.A. 60).

$$Q_T^{HO} = Q_s^{HO} + Q^{HO} \quad (P1.A. 60)$$

A further vital point is that the hot oil mass flowrate is not relevant in this mathematical formulation. The working fluid is recirculated within the system. As examined in literature, the initial cost of the fluid has a limited impact on the overall cost of the hot oil system. The main operating costs results from the fuel needed to re-heat the working fluid. Therefore, the calculation of hot oil mass flowrate is not required. The design variable is the heat load of hot oil required.

Additional constraints are added to ensure: (1) hot oil (if required) is used first at higher temperatures (Eqs.(P1.A. 61)), (2) the use of only one utility at each temperature interval (Eq. (P1.A. 62)).

$$y_{j_s}^{HO} - y_{j_s-1}^{HO} \leq 0 \quad j_s > 1 \quad (P1.A. 61)$$

$$y_{j_s}^{HO} + y_{i,j_s}^L \leq 1 \quad \forall i \in I, (i,j_s) \in IJ_s \quad (P1.A. 62)$$

A.III.4. Utility system hardware models

A.III.4.1. Boiler

Boiler fuel consumption can be described in two ways: based on a constant efficiency or variable efficiency model. In this work a variable efficient model is considered. Eq.(P1.A. 63) gives the fuel consumption based on the modified BHM model of Varbanov (2004), which accounts for full and part-load operating performance and boiler blowdown losses. The blowdown is assumed as a fixed fraction of the boiler steam output (γ).

$$Q_{b_{n_b, t_b}}^f = \sum_{v \in V} \sum_{t_b \in T_b} [(h_{sh_v}^{VHP} - h^{BFW})(a_{t_b}^b \cdot Z_{n_b, t_b, v}^b + (1 + b_{t_b}^b) m_{n_b, t_b, v}^b) + \gamma \cdot m_{n_b, t_b, v}^b (h_{l_v}^{VHP} - h^{BFW})] \quad (P1.A. 63)$$

Where $m_{n_b, t_b, v}^b$ and $Z_{n_b, t_b, v}^b$ terms represent the boiler mass flow rate (load) and size, respectively. Both terms are degrees of freedom in the optimization.

Logical constraints

Several decisions regarding boilers need to be addressed: (1) type of boiler required, (2) boiler fuel, and (3) operating conditions. Regarding the boiler's type, there are two broad types of steam boilers in industry: field-erected and packaged. Both have different sizes and different capital costs. For example, field-erected boilers are available in a larger range than the packaged ones. However, field erected boilers require a higher capital costs due to increased on-site work (Varbanov, 2004). Moreover, different types of boilers give different performances. In relation to the type of fuel, boilers may be able to burn different type of fuels simultaneously. The latter statement, can be represented by Eq. (P1.A. 64).

$$Q_{b_{n_b, t_b}}^f = \sum_{f_b \in F_b} (m_{n_b, t_b, f_b}^{f_b} \cdot NHV_{f_b}) \quad \forall n_b \in N_b, t_b \in T_b \quad (P1.A. 64)$$

Each boiler can only operate at selected condition v , and can be either package or field-erected but not both:

$$\sum_{t_b} y_{n_b, t_b, v}^b \leq y_v^{VHP} \quad \forall n_b \in N_b, v \in V \quad (P1.A. 65)$$

Where $y_{n_b, t_b, v}^b$ is a binary variable reflecting the boiler selection.

A.III.4.2. Steam turbines

There are two types of steam turbines used in this work, which are back-pressure turbines and condensing turbines. While condensing turbines expand steam into a partially condensed state, back-pressure turbines expand steam to a specified pressure, where the outlet steam can be used for heating purposes or further expanded by either another turbine or let-down valves. Steam turbine performance is affected by numerous factors. The most significant are the turbine size, the pressure drop of the steam expansion and the current load (Varbanov et al., 2005). Power output (W_{θ}^{st}) and steam load (m_{θ}^{st}) can be linearly related through Willans line correlation (Willans, 1888) and given by Eq. (P1.A. 66). Where the terms η_{θ}^{st} and $W_{int_{\theta}}^{st}$ denote the slope and the intercept of the Willans line, respectively. The terms are derived from the maximum power output, the change in isentropic enthalpy, and pressure difference. Significantly, for a given design and operation of steam turbines

(or manufacturer data), Willans' line parameters can be easily determined, without requiring thermodynamic correlations, expressed in Eqs (P1.A. 67) and (P1.A. 65). To summarize this, a compact formulation to describe turbines shaft-work calculation is given.

$$W_{\theta}^{\text{st}} = \eta_{\theta}^{\text{st}} \cdot m_{\theta}^{\text{st}} - W_{\text{int}\theta}^{\text{st}} \cdot y_{\theta}^{\text{st}} \quad (\text{P1.A. 66})$$

$$\eta_{\theta}^{\text{st}} = \frac{1 + c_{\theta}^{\text{st}}}{a_{\theta}^{\text{st}}} \left(\Delta H_{\theta}^{\text{IS}} - \frac{b_{\theta}^{\text{st}}}{m_{\text{max}\theta}^{\text{st}}} \right) \quad (\text{P1.A. 67})$$

$$W_{\text{int}\theta}^{\text{st}} = \frac{c_{\theta}^{\text{st}}}{a_{\theta}^{\text{st}}} (\Delta H_{\theta}^{\text{IS}} \cdot m_{\text{max}\theta}^{\text{st}} - b_{\theta}^{\text{st}}) \quad (\text{P1.A. 68})$$

The sub-index θ represents the different alternative options:

- $\theta = n_{\text{st},i,j_s,j'_s}$ for back-pressure steam turbine n_{st} operating between headers (i, j_s) and (i', j'_s) .
- $\theta = n_{\text{st},v,i,j_s}$ for back-pressure steam turbine n_{st} operating between VHP header v and steam main (i, j) .
- $\theta = n_{\text{st},i,j_s}$ for condensing turbine n_{st} operating at inlet pressure j_s .
- $\theta = n_{\text{st},v}$ for condensing turbine n_{st} operating at inlet pressure v .

Modelling coefficients a_{θ}^{st} , b_{θ}^{st} and c_{θ}^{st} are turbine parameters, defined by inlet and outlet pressure, as well as the turbine type (Sun and Smith, 2015).

Replacing Eqs. (P1.A. 67) and (P1.A. 65) in Eq. (P1.A. 66), and rearranging gives:

$$W_{\theta}^{\text{st}} = \frac{1 + c_{\theta}^{\text{st}}}{a_{\theta}^{\text{st}}} \left(\Delta H_{\theta}^{\text{IS}} \cdot m_{\theta}^{\text{st}} - b_{\theta}^{\text{st}} \frac{m_{\theta}^{\text{st}}}{m_{\text{max}\theta}^{\text{st}}} \right) - \frac{c_{\theta}^{\text{st}}}{a_{\theta}^{\text{st}}} (\Delta H_{\theta}^{\text{IS}} \cdot m_{\text{max}\theta}^{\text{st}} - b_{\theta}^{\text{st}} \cdot y_{\theta}^{\text{st}}) \quad (\text{P1.A. 69})$$

The turbine models comprise non-linear features arising from the correlation between the equipment capacity and load $\left(\frac{m_{\theta}^{\text{st}}}{m_{\text{max}\theta}^{\text{st}}} \right)$, as expressed in Eq. (P1.A. 69). The correlation can be expressed as a fraction, represented by variable x_{θ}^{st} . Alternatively, the fraction can be expressed as a product (see Eq. (P1.A. 70)) The nonconvex term can be relaxed into a convex expression, by widely used methodologies, such as McCormick convex envelopes, (Eq. (P1.A. 71)).

$$x_{\theta}^{\text{st}} = \frac{m_{\theta}^{\text{st}}}{Z_{\theta}^{\text{st}}} \text{ or } m_{\theta}^{\text{st}} = x_{\theta}^{\text{st}} \cdot m_{\text{max}\theta}^{\text{st}} \quad (\text{P1.A. 70})$$

$$m_{\theta}^{\text{st}} \geq \sigma_{\theta}^{\text{st}} \cdot m_{\text{max}\theta}^{\text{st}} + \Omega_{\text{min}\theta}^{\text{st}} \cdot x_{\theta}^{\text{st}} - \sigma_{\theta}^{\text{st}} \cdot \Omega_{\text{min}\theta}^{\text{st}} \cdot y_{\theta}^{\text{st}} \quad (\text{P1.A. 71a})$$

$$m_{\theta}^{\text{st}} \leq m_{\text{max}\theta}^{\text{st}} + \Omega_{\text{min}\theta}^{\text{st}} \cdot x_{\theta}^{\text{st}} - \Omega_{\text{min}\theta}^{\text{st}} \cdot y_{\theta}^{\text{st}} \quad (\text{P1.A. 71b})$$

$$m_{\theta}^{\text{st}} \geq m_{\text{max}\theta}^{\text{st}} + \Omega_{\text{max}\theta}^{\text{st}} \cdot x_{\theta}^{\text{st}} - \Omega_{\text{max}\theta}^{\text{st}} \cdot y_{\theta}^{\text{st}} \quad (\text{P1.A. 71c})$$

$$m_{\theta}^{\text{st}} \leq \sigma_{\theta}^{\text{st}} \cdot m_{\text{max}\theta}^{\text{st}} + \Omega_{\text{max}\theta}^{\text{st}} \cdot x_{\theta}^{\text{st}} - \sigma_{\theta}^{\text{st}} \cdot \Omega_{\text{max}\theta}^{\text{st}} \cdot y_{\theta}^{\text{st}} \quad (\text{P1.A. 71d})$$

Where σ_0^{st} represents the steam turbine minimum load, in fraction. $\Omega_{\min\theta}^{st}$ and $\Omega_{\max\theta}^{st}$ define the minimum and maximum equipment capacity in terms of flowrate, respectively.

Additional, logical constraints to ensure the range of the variable x_0^{st} are included in Eq. (P1.A. 72) and (P1.A. 73).

$$x_0^{st} \geq \sigma_0^{st} \cdot y_0^{st} \quad (\text{P1.A. 72})$$

$$x_0^{st} \leq y_0^{st} \quad (\text{P1.A. 73})$$

Based on the above mentioned modification, Eq. (P1.A. 69) can be written as:

$$W_\theta^{st} = \frac{1+c_\theta^{st}}{a_\theta^{st}} (\Delta H_\theta^{IS} \cdot m_\theta^{st} - b_\theta^{st} \cdot x_\theta^{st}) - \frac{c_\theta^{st}}{a_\theta^{st}} (\Delta H_\theta^{IS} \cdot m_{\max\theta}^{st} - b_\theta^{st} \cdot y_\theta^{st}) \quad (\text{P1.A. 69a})$$

a) *Logical constraints*

As a result of the selection of different header pressure levels, some alternatives of each steam turbine option may be permitted and others excluded. First, among the alternatives corresponding to a given condensing turbine option, a unit can be selected only if the corresponding steam header is activated. Further to this, for back pressure steam turbines it is required that both inlet and outlet steam headers are chosen. Eqs. (P1.A. 74) and (P1.A. 75) define these limitations, where Eqs. (a) constraint the turbines involving only steam distribution mains and (b) the connexions with VHP header.

$$y_{n_{st},i,j_s}^{C-ST} \leq y_{i,j_s}^L \quad \forall n_{st} \in N_{ST}, (i,j_s) \in IJ_s \quad (\text{P1.A. 74a})$$

$$y_{n_{st},v}^{VHP C-ST} \leq y_v^{VHP} \quad \forall n_{st} \in N_{ST}, v \in V \quad (\text{P1.A. 74b})$$

$$y_{n_{st},i,j_s,j'_s}^{BP-ST} \leq \frac{y_{i,j_s}^L + y_{i',j'_s}^L}{2} \quad \forall n_{st} \in N_{ST}, i \text{ and } i' \in I, i' > i, (i,j_s) \text{ and } (i',j'_s) \in IJ_s \quad (\text{P1.A. 75a})$$

$$y_{n_{st},v,i,j_s}^{VHP BP-ST} \leq \frac{y_v^{VHP} + y_{i,j_s}^L}{2} \quad \forall n_{st} \in N_{ST}, v \in V, (i,j_s) \in IJ_s \quad (\text{P1.A. 75b})$$

A.III.4.3. *Gas turbines with heat recovery steam generator (HRSG)*

Gas turbines generate power and the residual heat of the exhaust gas is used to produce steam in a HRSG. In a similar vein to steam turbines, the relationship between shaft power and fuel input for a part-load performance can be described by a Willans Line (Shang, 2000; Varbanov, 2004; Aguilar et al., 2007). The equipment model is adopted from Varbanov (2004), which allows for the preservation of linearity while concurrently taking into account operating performance. Its coefficients are based on industrial gas turbines data from Brooks (2000) and Gas Turbine World (2001), referenced by Del Nogal (2006). However, in practice such parameters and correlations depend on the design and operation of the gas turbines, in addition to the manufacturer.

$$W_{n_{gt}}^{gt} = \sum_{t_{gt}} \sum_{f_{gt}} \left[\eta_{n_{gt}, t_{gt}, f_{gt}}^{gt} \cdot m_{f_{n_{gt}, t_{gt}, f_{gt}}}^{gt} - W_{int_{n_{gt}, t_{gt}, f_{gt}}}^{gt} \right] \quad (P1.A. 76)$$

$$\eta_{n_{gt}, t_{gt}, f_{gt}}^{gt} = \frac{(1 + L_{n_{gt}, t_{gt}, f_{gt}}^{gt})}{b_{f_{gt}}^{gt}} \left(NHV_{f_{gt}} - \frac{a_{t_{gt}}^{gt}}{m_{f_{max_{n_{gt}, t_{gt}, f_{gt}}}^{gt}}} \right) \quad \forall n_{gt} \in N_{GT}, \quad (P1.A. 77)$$

$$t_{gt} \in T_{GT}, f_{gt} \in F_{GT}$$

$$W_{int_{n_{gt}, t_{gt}, f_{gt}}}^{gt} = \frac{L_{n_{gt}, t_{gt}, f_{gt}}^{gt}}{b_{f_{gt}}^{gt}} \left(NHV_{f_{gt}} \cdot m_{f_{max_{n_{gt}, t_{gt}, f_{gt}}}^{gt}} - a_{t_{gt}}^{gt} \cdot y_{n_{gt}, t_{gt}, f_{gt}}^{f_{gt}} \right) \quad \forall n_{gt} \in N_{GT}, \quad (P1.A. 78)$$

$$t_{gt} \in T_{GT}, f_{gt} \in F_{GT}$$

Analogue to the steam turbine model, a non-linear term may be involved if the equipment capacity under analysis is unknown, or if the entire range of options is under analysis. This is due to the correlation between equipment capacity and load contained in Eq.(P1.A. 76). Therefore, Eqs.(P1.A.

80) - (P1.A. 82) are added to linearize the potential non-convex term $\frac{m_{f_{n_{gt}, t_{gt}, f_{gt}}}^{gt}}{m_{f_{max_{n_{gt}, t_{gt}, f_{gt}}}^{gt}}}$.

$$W_{n_{gt}}^{gt} = \sum_{t_{gt}} \sum_{f_{gt}} \left[\frac{(1 + L_{n_{gt}, t_{gt}, f_{gt}}^{gt})}{b_{f_{gt}}^{gt}} \left(NHV_{f_{gt}} \cdot m_{f_{n_{gt}, t_{gt}, f_{gt}}}^{gt} - a_{t_{gt}}^{gt} \cdot x_{n_{gt}, t_{gt}, f_{gt}}^{gt} \right) - \frac{L_{n_{gt}, t_{gt}, f_{gt}}^{gt}}{b_{f_{gt}}^{gt}} \left(NHV_{f_{gt}} \cdot m_{f_{max_{n_{gt}, t_{gt}, f_{gt}}}^{gt}} - a_{t_{gt}}^{gt} \cdot y_{n_{gt}, t_{gt}, f_{gt}}^{f_{gt}} \right) \right] \quad (P1.A. 76a)$$

$$x_{n_{gt}, t_{gt}, f_{gt}}^{gt} = \frac{m_{f_{n_{gt}, t_{gt}, f_{gt}}}^{gt}}{m_{f_{max_{n_{gt}, t_{gt}, f_{gt}}}^{gt}}} \text{ or } m_{f_{n_{gt}, t_{gt}, f_{gt}}}^{gt} = x_{n_{gt}, t_{gt}, f_{gt}}^{gt} \cdot m_{f_{max_{n_{gt}, t_{gt}, f_{gt}}}^{gt}} \quad (P1.A. 79)$$

$$m_{f_{n_{gt}, t_{gt}, f_{gt}}}^{gt} \geq \sigma_{n_{gt}, t_{gt}, f_{gt}}^{gt} \cdot m_{f_{max_{n_{gt}, t_{gt}, f_{gt}}}^{gt}} + \Omega_{min_{n_{gt}, t_{gt}, f_{gt}}}^{gt} \cdot x_{n_{gt}, t_{gt}, f_{gt}}^{gt} - \sigma_{n_{gt}, t_{gt}, f_{gt}}^{gt} \cdot \Omega_{min_{n_{gt}, t_{gt}, f_{gt}}}^{gt} \cdot y_{n_{gt}, t_{gt}, f_{gt}}^{st} \quad (P1.A. 80)$$

$$m_{f_{n_{gt}, t_{gt}, f_{gt}}}^{gt} \leq m_{f_{max_{n_{gt}, t_{gt}, f_{gt}}}^{gt}} + \Omega_{min_{n_{gt}, t_{gt}, f_{gt}}}^{st} \cdot x_{n_{gt}, t_{gt}, f_{gt}}^{gt} - \Omega_{min_{n_{gt}, t_{gt}, f_{gt}}}^{gt} \cdot y_{\theta}^{st}$$

$$m_{f_{n_{gt}, t_{gt}, f_{gt}}}^{gt} \geq m_{f_{max_{n_{gt}, t_{gt}, f_{gt}}}^{gt}} + \Omega_{max_{n_{gt}, t_{gt}, f_{gt}}}^{st} \cdot x_{n_{gt}, t_{gt}, f_{gt}}^{gt} - \Omega_{max_{n_{gt}, t_{gt}, f_{gt}}}^{gt} \cdot y_{n_{gt}, t_{gt}, f_{gt}}^{st}$$

$$m_{f_{n_{gt}, t_{gt}, f_{gt}}}^{gt} \leq \sigma_{n_{gt}, t_{gt}, f_{gt}}^{gt} \cdot m_{f_{max_{n_{gt}, t_{gt}, f_{gt}}}^{gt}} + \Omega_{max_{n_{gt}, t_{gt}, f_{gt}}}^{st} \cdot x_{n_{gt}, t_{gt}, f_{gt}}^{gt} - \sigma_{n_{gt}, t_{gt}, f_{gt}}^{gt} \cdot \Omega_{max_{n_{gt}, t_{gt}, f_{gt}}}^{gt} \cdot y_{n_{gt}, t_{gt}, f_{gt}}^{st}$$

$$x_{n_{gt}, t_{gt}, f_{gt}}^{gt} \geq \sigma_{n_{gt}, t_{gt}, f_{gt}}^{gt} \cdot y_{n_{gt}, t_{gt}, f_{gt}}^{st} \quad (P1.A. 81)$$

$$x_{n_{gt}, t_{gt}, f_{gt}}^{gt} \leq y_{n_{gt}, t_{gt}, f_{gt}}^{st} \quad (P1.A. 82)$$

$\sigma_{n_{gt}, t_{gt}, f_{gt}}^{gt}$ denotes the gas turbine minimum fuel load, in fraction. $\Omega_{min_{n_{gt}, t_{gt}, f_{gt}}}^{st}$ and $\Omega_{max_{n_{gt}, t_{gt}, f_{gt}}}^{st}$ define the minimum and maximum equipment capacity in terms of fuel flowrate, respectively.

The maximum fuel flowrate $\left(m_{f_{max_{n_{gt}, t_{gt}, f_{gt}}}^{gt}} \right)$ is defined by Eq. (P1.A. 83). The gas turbine performance model is usually specified at ISO conditions (15 °C, 1.013 bar and 60% relative

humidity). Thus, f_T^{GT} and $f_{T_{eff}}^{GT}$ are correction factors that account for the ambient temperature influence, which are equal to 1 at 15 °C (Smith, 2016). For this work, the correlating parameters are based on the data presented in Brooks (2000). The coefficients used in this work are detailed in Supplementary Information P1.B, but as noted, these factors also depend on specific gas turbine model used.

$$\sum_{f_{gt}} \left[m_{f_{max_{n_{gt}, t_{gt}, f_{gt}}}^{gt}} \cdot NHV_{f_{gt}} \right] = \left(a_{t_{gt}}^{gt} \cdot W_{max_{n_{gt}, t_{gt}}}^{GT} + y_{n_{gt}, t_{gt}}^{gt} \cdot b_{t_{gt}}^{gt} \right) \cdot \frac{f_T^{GT}}{f_{T_{eff}}^{GT}} \quad \forall n_{gt} \in N_{GT}, t_{gt} \in T_{GT} \quad (P1.A. 83)$$

$$f_T^{GT} = \frac{W^{GT}}{W_{GT15}^{GT}} = e^{gt} + f^{gt} \cdot T_{amb} \quad (P1.A. 84)$$

$$f_{T_{eff}}^{GT} = \frac{Eff^{GT}}{Eff_{GT15}^{GT}} = g^{gt} + h^{gt} \cdot T_{amb}, \quad \text{where: } Eff^{GT} = \frac{Q_f^{GT}}{W^{GT}} \quad (P1.A. 85)$$

Gas turbine exhausts are sent to the HRSG unit as heat input/ The corresponding relations are derived from the mass and energy balance in the equipment, where Eqs. (P1.A. 86) - (P1.A. 100) are derived to consider temperature feasibility constraints through heat flow constraints. HRSG can operate with or without supplementary firing. The main purpose of supplementary firing is raising the flue gas temperature by combustion of additional fuel. Crucially, supplementary firing decreases the overall energy efficiency since the added heat is only used by the steam turbines (if used).

$$Q_{exh_{n_{gt}}}^{gt} = \sum_{t_{gt} \in T_{gt}} \sum_{f_{gt} \in F_{gt}} \left[m_{f_{n_{gt}, t_{gt}, f_{gt}}}^{gt} \cdot NHV_{f_{gt}} \right] - W_{n_{gt}}^{gt} \quad \forall n_{gt} \in N_{GT} \quad (P1.A. 86)$$

$$m_{air_{n_{gt}}} = \sum_{t_{gt} \in T_{gt}} \left[c_{n_{gt}, t_{gt}}^{GT} \cdot W_{max_{n_{gt}, t_{gt}}}^{GT} + y_{n_{gt}, t_{gt}}^{gt} \cdot d_{n_{gt}, t_{gt}}^{GT} \right] \quad \forall n_{gt} \in N_{GT} \quad (P1.A. 87)$$

$$m_{exh_{n_{gt}}} = m_{air_{n_{gt}}} + \sum_{t_{gt} \in T_{gt}} \sum_{f_{gt} \in F_{gt}} m_{f_{n_{gt}, t_{gt}, f_{gt}}}^{gt} \quad \forall n_{gt} \in N_{GT} \quad (P1.A. 88)$$

$$Q_{exh_{n_{gt}}}^{in} = Q_{exh_{n_{gt}}}^{gt} + Q_{n_{gt}}^{SF} \quad \forall n_{gt} \in N_{GT} \quad (P1.A. 89)$$

$$\sum_{v \in V} m_{exh_{n_{gt}, v}}^{HRSG} = m_{exh_{n_{gt}}} + \sum_{f_{gt} \in F_{gt}} m_{n_{gt}, f_{gt}}^{SF} \quad \forall n_{gt} \in N_{GT} \quad (P1.A. 90)$$

$$Q_{n_{gt}}^{SF} = \sum_{f_{gt} \in F_{gt}} \left[m_{n_{gt}, f_{gt}}^{SF} \cdot NHV_{f_{gt}} \right] \quad \forall n_{gt} \in N_{GT} \quad (P1.A. 91)$$

$$Q_{exh_{n_{gt}}}^{gt} \leq m_{exh_{n_{gt}}} \cdot cp_{exh} (T_{max}^{UF} - T_{amb}) \quad \forall n_{gt} \in N_{GT} \quad (P1.A. 92)$$

$$Q_{exh_{n_{gt}, v}}^{in} \leq m_{exh_{n_{gt}, v}}^{HRSG} \cdot cp_{exh} (T_{max}^{SF} - T_{amb}) \quad \forall n_{gt} \in N_{GT}, v \in V \quad (P1.A. 93)$$

$$Q_{exh_{n_{gt}, v}}^{in} - Q_{n_{gt}, v}^{sh} - Q_{n_{gt}, v}^{vap} \geq m_{exh_{n_{gt}, v}}^{HRSG} \cdot cp_{exh} (T_v^{sat} + \Delta T_{min}^{HRSG} - T_{amb}) \quad \forall n_{gt} \in N_{GT}, v \in V \quad (P1.A. 94)$$

$$Q_{exh_{n_{gt}, v}}^{in} \geq m_{exh_{n_{gt}, v}}^{HRSG} \cdot cp_{exh} (T_v^{VHP} + \Delta T_{min}^{HRSG} - T_{amb}) \quad \forall n_{gt} \in N_{GT}, v \in V \quad (P1.A. 95)$$

$$Q_{exh_{n_{gt}, v}}^{in} - Q_{T_{n_{gt}, v}}^{HRSG} \geq m_{exh_{n_{gt}, v}}^{HRSG} \cdot cp_{exh} (T_{min}^{BFW} + \Delta T_{min}^{HRSG} - T_{amb}) \quad \forall n_{gt} \in N_{GT}, v \in V \quad (P1.A. 96)$$

$$Q_{T_{n_{gt},v}}^{HRSG} = Q_{n_{gt},v}^{sh} + Q_{n_{gt},v}^{vap} + Q_{n_{gt},v}^{pre} \quad \forall n_{gt} \in N_{GT}, v \in V \quad (P1.A. 97)$$

$$\sum_{n_{gt} \in N_{gt}} Q_{n_{gt},v}^{sh} = \frac{1}{\eta_{eff}^{HRSG}} [(h_{sh_v}^{VHP} - h_{v_v}^{VHP}) M_v^{HRSG}] \quad v \in V \quad (P1.A. 98)$$

$$\sum_{n_{gt} \in N_{gt}} Q_{n_{gt},v}^{vap} = \frac{1}{\eta_{eff}^{HRSG}} [(h_{v_v}^{VHP} - h_{1_v}^{VHP}) M_v^{HRSG}] \quad v \in V \quad (P1.A. 99)$$

$$\sum_{n_{gt} \in N_{gt}} Q_{n_{gt},v}^{pre} = \frac{1}{\eta_{eff}^{HRSG}} [(h_{1_v}^{VHP} - h^{BFW})(1 + \gamma) M_v^{HRSG}] \quad v \in V \quad (P1.A. 100)$$

Logical constraints

Eqs. (P1.A. 101) and (P1.A. 102) ensure that only one type of fuel and gas turbine can be selected.

Constraints (P1.A. 103) and (P1.A. 104) link the binary variables related of the supplementary firing with the additional fuel required.

$$\sum_{t_{gt}} y_{n_{gt},t_{gt}}^{gt} \leq 1 \quad \forall n_{gt} \in N_{GT} \quad (P1.A. 101)$$

$$\sum_{f_{gt}} y_{n_{gt},t_{gt},f_{gt}}^{f_{gt}} = y_{n_{gt},t_{gt}}^{gt} \quad \forall n_{gt} \in N_{GT}, t_{gt} \in T_{GT} \quad (P1.A. 102)$$

$$\sum_{f_{gt}} y_{n_{gt},f_{gt}}^{SF} \leq \sum_{t_{gt}} y_{n_{gt},t_{gt}}^{gt} \quad \forall n_{gt} \in N_{GT}, t_{gt} \in T_{GT} \quad (P1.A. 103)$$

$$m_{n_{gt},f_{gt}}^{SF} \leq U_{max}^{SF} y_{n_{gt},f_{gt}}^{SF} \quad \forall n_{gt} \in N_{GT}, t_{gt} \in T_{GT} \quad (P1.A. 104)$$

Eqs. (P1.A. 105) and (P1.A. 106) guarantee that mass and heat flows from HRSG exhaust gases are connected to only one VHP header

$$m_{exh_{n_{gt},v}}^{HRSG} \leq U_{exh}^{mHRSG} y_v^{VHP} \quad \forall n_{gt} \in N_{GT}, v \in V \quad (P1.A. 105)$$

$$Q_{exh_{n_{gt},v}}^{\mu} \leq U_{exh}^{QHRSG} y_v^{VHP} \quad \forall n_{gt} \in N_{GT}, v \in V \quad (P1.A. 106)$$

The sub-index μ represents the different HRSG sections, superheating (sh), evaporation (vap) and pre heating (pre).

A.III.4.4. Deaerator

Eqs. (P1.A. 107) and (P1.A. 108) set the deaerator steam requirement (M^{Deac}) ensuring the BFW is at saturated liquid conditions. In the deaerator, the inlet streams may come from LP steam, condensate return, and/or treated water make-up. The condensate return depends on the site feed water requirement, as shown in Eq. (P1.A. 109). The site feed water requirement based on Eq. (P1.A. 110) consists of the water used for steam generation and any injected for desuperheating of both steam headers and let-down stations.

$$m_{DA}^W = M_T^{BFW} - M^{Cond} - (1-\alpha) \sum_{j_s \in J_s} M_{j_s}^{Deae} \quad (P1.A. 107)$$

$$M_T^{BFW} \cdot h^{BFW} + \alpha \sum_{j_s \in J_s} M_{j_s}^{Deae} \cdot h^{vent} = M^{Cond} \cdot h^{Cond} + m_{DA}^W \cdot h^W + \sum_{j_s \in J_s} (M_{j_s}^{Deae} \cdot h_{sh_{j_s}}^{main}) \quad (P1.A. 108)$$

$$M^{Cond} = \beta \cdot M_T^{BFW} \quad (P1.A. 109)$$

$$M_T^{BFW} = \sum_{icl} \sum_{j_s \in J_s} (M_{i,j_s}^H + M_{i,j_s}^{BFWC} + M_{i,j_s}^{BFW}) + \sum_v (M_v^{boi} + M_v^{HRSG}) \quad (P1.A. 110)$$

Where:

$$Q^{VHP} = \sum_{v \in V} [M_v^{VHP} \cdot h_{sh\ v}^{VHP} + M_{i,j}^{BFWC} \cdot h^{BFW}] = (M_v^{VHP} + M_{i,j}^{BFWC}) \cdot (h_{sh\ j}^C - h_{l\ j}^C) \quad \forall i=1, j=1 \quad (P1.A. 111)$$

A.III.4.5. Flash steam recovery

In addition, any flash steam recovery (FSR) can be taken into account. FSR is assumed to be only used for heating purposes and not consider for steam cascade and with it, power generation. Despite the potential benefit of the power generation potential, the recovery of saturated steam into the mains (at superheated conditions) may lead to a higher energy requirement to balance the headers and avoid excessive condensation. If FSR is included Eqs. (P1.A. 28) and (P1.A. 29) are replaced by Eqs. (P1.A. 28a) and (P1.A. 29a). $h_{v\ j_s}$ is the specific enthalpy of steam saturated at pressure level j_s .

$$M_{i,j_s}^C + M_{i,j_s}^{BFWC} + M_{i,j_s}^{FSR} = M_{i,j_s}^{Cin} \quad \forall i \in I, (i, j_s) \in IJ_s \quad (P1.A. 28a)$$

$$(1-L^C) \cdot M_{i,j_s}^C \cdot h_{sh\ j_s}^{main} + M_{i,j_s}^{BFWC} \cdot h^{BFW} + M_{i,j_s}^{FSR} \cdot h_{v\ j_s} = M_{i,j_s}^{Cin} \cdot (h_{sh\ j_s}^C - h_{l\ j_s}^C) = Q_{i,j_s}^{Cin} \quad \forall i \in I, (i, j_s) \in IJ_s \quad (P1.A. 29a)$$

The amount of flashed steam is determined by the mass and energy balance given in the FSR, as shown below:

$$M_{i,j_s}^{FSR} = \sum_{i' < i} \sum_{(i', j_s') \in IJ_s} m_{s\ i', j_s', j_s}^{FSR} \quad \forall i \in I, (i, j_s) \in IJ_s, FSR = 1 \quad (P1.A. 112)$$

$$M_{i,j_s}^{FSR} = 0 \quad \forall i \in I, (i, j_s) \in IJ_s, FSR = 0 \quad (P1.A. 113)$$

$$\beta \cdot M_{i,j_s}^{Cin} + \sum_{i' < i} \sum_{(i', j_s') \in IJ_s} m_{l\ i', j_s', j_s}^{FSR} = m_{in\ i,j_s}^{FSR} \quad \forall i \in I, (i, j_s) \in IJ_s \quad (P1.A. 114)$$

$$\sum_{j_s' \in J_s} (m_{s\ i,j_s,j_s'}^{FSR} + m_{l\ i,j_s,j_s'}^{FSR}) = M_{in\ i,j_s}^{FSR} \quad \forall i \in I, (i, j_s) \in IJ_s \quad (P1.A. 115)$$

$$\sum_{j_s' > j_s} (m_{s\ i,j_s,j_s'}^{FSR} \cdot h_{v\ j_s'} + m_{l\ i,j_s,j_s'}^{FSR} \cdot h_{l\ j_s'}) = M_{in\ i,j_s}^{FSR} \cdot h_{l\ j_s} \quad \forall i \in I, (i, j_s) \in IJ_s \quad (P1.A. 116)$$

Where $m_{s\ i,j_s,j_s'}^{FSR}$ and $m_{l\ i,j_s,j_s'}^{FSR}$ are the steam and liquid amount recovered at pressure j_s' , based on the condensate at the drum inlet ($M_{in\ i,j_s}^{FSR}$). Additionally, $cond_{ret}$ represents the rate of steam condensate return. The condensate recycled may depend on the steam use (direct steam injection, indirect heating) and potential losses (i.e. contamination or leaks). Condensate return (if recovered) could be as high as 90%. Higher return rates are plausible but may be prohibitively expensive due to the cost of the pipework needed (Smith, 2016).

A.III.5. Electrical Energy balance

The cost of electricity imported or exported on a site on the overall operating cost is determined by the electrical energy balance.

$$\eta_t(W^{\text{IMP}} + W^{\text{GEN}} - W^{\text{EXP}}) = W^{\text{DEM}} \quad (\text{P1.A. 117})$$

The electricity generation (W^{GEN}) from the site utility system can be provided by the back-pressure and condensing steam turbine, as well as gas turbines. Site constraints in Eq. (P1.A. 118) limit electricity import or export.

$$W^{\text{EXP}} \leq \overline{W}^{\text{EXP}}, \quad W^{\text{IMP}} \leq \overline{W}^{\text{IMP}} \quad (\text{P1.A. 118})$$

A.III.6. Operation and sizing

Depending on the capacity of units, equipment size constraints are imposed in Eqs. (P1.A. 119) - (P1.A. 121).

$$\Omega_{\min_{n_{\text{Eq}}}} \cdot y_{n_{\text{Eq}}} \leq Z_{n_{\text{Eq}}} \leq \Omega_{\max_{n_{\text{Eq}}}} \cdot y_{n_{\text{Eq}}} \quad (\text{P1.A. 119})$$

$$\Omega_{\min_{n_{\text{Eq}}}} \cdot y_{n_{\text{Eq}}} \leq m_{n_{\text{Eq}}} \leq \Omega_{\max_{n_{\text{Eq}}}} \cdot y_{n_{\text{Eq}}} \quad (\text{P1.A. 120})$$

$$\sigma_{n_{\text{Eq}}} \cdot Z_{n_{\text{Eq}}} \leq m_{n_{\text{Eq}}} \leq Z_{n_{\text{Eq}}} \quad (\text{P1.A. 121})$$

Where $\Omega_{\min_{n_{\text{Eq}}}}$ and $\Omega_{\max_{n_{\text{Eq}}}}$ are the minimum and maximum capacities of each equipment. Additionally, $Z_{n_{\text{Eq}}}$ and $m_{n_{\text{Eq}}}$ terms represent the size and load of each unit. Lastly, $\sigma_{n_{\text{Eq}}}$ denotes minimum load requirements.

References

- Aguilar, O., Perry, S., Kim, K. & Smith, R. (2007) 'Design and Optimization of flexible utility systems subject to variable conditions. Part 1: Modelling Framework', *Chemical Engineering Research and Design*, 85(8), pp. 1136-1148.
- Brooks, F. J. (2000) *Gas Turbine Performance Characteristics*, Schenectady, NY: GE Power SystemsGER-3567H).
- Del Noyal, F. L. (2006) *Optimal design and integration of re Fridgeration and power systems*. University of Manchester, Manchester.
- Gas Turbine World. (2001). *2000-2001 GTW Handbook* (Vol. 21). Fairfield,CT,USA: Pequot Publishing Inc.

- Shang, Z. (2000) Analysis and Optimisation of Total Site Utility Systems. Ph.D, Manchester, U.K.
- Smith, R. (2016) 'Steam Systems and Cogeneration', *Chemical Process: Design and Integration*. Second ed. Chichester: John Wiley & Sons, Ltd, pp. 583-646.
- Sun, L. & Smith, R. (2015) 'Performance Modeling of New and Existing Steam Turbines', *Industrial & Engineering Chemistry Research*, 54(6), pp. 1908-1915.
- Varbanov, P., Perry, S., Klemeš, J. & Smith, R. (2005) 'Synthesis of industrial utility systems: cost-effective de-carbonisation', *Applied Thermal Engineering*, 25(7), pp. 985-1001.
- Varbanov, P. S. D., S.; Smith, R. (2004) 'Modelling and Optimization of Utility Systems', *Chem. Eng. Res. Des.*, 82, pp. 561-578.
- Willans, P. W. (1888) 'ECONOMY TRIALS OF A NON-CONDENSING STEAM-ENGINE: SIMPLE, COMPOUND AND TRIPLE. (INCLUDING TABLES AND PLATE AT BACK OF VOLUME)', *Minutes of the Proceedings of the Institution of Civil Engineers*, 93(1888), pp. 128-188.

SUPPLEMENTARY INFORMATION P1.B

Gas turbine model coefficients

Table P1.B. 1. Gas turbine modelling coefficients at full-load

Modelling coefficients	Industrial	Aero derivative
Coefficients for full-load		
$a_{t_{gt}}^{gt}$, [kW kW ⁻¹]	2.5948	2.1816
$b_{t_{gt}}^{gt}$, [kW]	30093	10002
Coefficients for air mass flowrate		
c^{GT} , [kg kW ⁻¹]	0.0028	0.0029
d^{GT} , [kg s ⁻¹]	18.444	5.538

Source: Coefficients based on data extracted from Brooks (2000) and Gas Turbine World (2000-2001)

Table P1.B. 2. Gas turbine correction factors by ambient temperature and pressure

Correction factors	Value
Ambient temperature	
e^{GT} , [-]	1.02
f^{GT} , [°C ⁻¹]	$1.33 \cdot 10^{-3}$
g^{GT} , [-]	1.1
h^{GT} , [°C ⁻¹]	$6.66 \cdot 10^{-3}$

Source: Coefficients based on data extracted from Brooks (2000)

Table P1.B. 3. Gas turbine modelling coefficients at part-load

Coefficients for part-load (L)	Natural Gas	Distillate Oil
$a_{f_{gt}}^L$, [-]	0.152	0.144
$b_{f_{gt}}^L$, [MW ⁻¹]	-0.00142	-0.00153

Source: Varbanov (2004)

In this work, $L_{n_{gt}, t_{gt}, f_{gt}}^{gt}$ is assumed to be described by Varbanov's correlation, shown below. Nevertheless, in practice, such parameters and correlation depend on the design and operation of the gas turbines and the manufacturer.

$$L_{n_{gt}, t_{gt}, f_{gt}}^{gt} = a_{f_{gt}}^L + b_{f_{gt}}^L \cdot \ln\left(\Omega_{\max_{n_{gt}, t_{gt}, f_{gt}}}^{gt}\right) \quad \begin{matrix} \forall n_{gt} \in N_{GT}, \\ t_{gt} \in T_{GT}, f_{gt} \in F_{GT} \end{matrix} \quad (P1.B.1)$$

References

- Brooks, F. J. (2000) *Gas Turbine Performance Characteristics*, Schenectady, NY: GE Power SystemsGER-3567H).
- Gas Turbine World. (2000-2001). *GTW Handbook* (Vol. 21). USA: Pequot Publishing Inc.
- Varbanov, P. S. D., S.; Smith, R. (2004) 'Modelling and Optimization of Utility Systems', *Chem. Eng. Res. Des.*, 82, pp. 561-578.

SUPPLEMENTARY INFORMATION P1.C

Case Study 1

Supplementary data for case study 1.

Table P1.C. 1. Site configuration and operating conditions of case study 1

Parameter	Value
Site power demand [MW]	25
Max export allowed [MW]	10
Working hours [$\text{h}\cdot\text{y}^{-1}$]	8600
Interest rate [%]	8
Plant life [y]	25
Capital installation factor [-]	4.0
ΔT_{CW} [$^{\circ}\text{C}$]	10
T_{BFW} [$^{\circ}\text{C}$]	120
P_{VHP} [bar(a)]	90
$\Delta T_{\text{VHP,SH}}$ [$^{\circ}\text{C}$]	200*

*Fixed parameter for Varbanov study

Table P1.C. 2. Resources data of case study 1

Resource	LHV [$\text{MWh}\cdot\text{t}^{-1}$]	Cost [$\text{\$}\cdot\text{MWh}^{-1}$]
Natural gas	13.876	9.369
Distillate oil	11.179	10.734
Fuel gas	9.029	4.984
Fuel oil	12.097	6.226
Electricity (Import and Export)	-	20.000
Cooling water		1.589
Treated water		0.200*

*Cost per ton [$\text{\$}\cdot\text{t}^{-1}$]

Table P1.C. 3. Stream data of case study 1

Stream	Type	Supply Temperature T_s [°C]	Target temperature T_t [°C]	Heat Load ΔH [MW]	Heat capacity CP [MW·°C ⁻¹]
S1-1	hot	296.07	290.94	5.626	1.0967
S1-2	hot	290.94	280.68	8.000	0.7797
S1-3	hot	280.68	279.83	0.070	0.0824
S1-4	hot	279.83	272.14	0.630	0.0819
S1-5	hot	272.14	260.17	1.581	0.1321
S1-6	hot	260.17	219.15	5.419	0.1321
S1-7	hot	219.15	208.89	1.300	0.1267
S1-8	hot	208.89	200.34	8.000	0.9357
S1-9	hot	200.34	140.51	7.500	0.1254
S1-10	hot	140.51	128.55	3.900	0.3261
S1-11	hot	128.55	97.78	4.310	0.1401
S2-1	cold	276.07	280.00	3.175	0.8079
S2-2	cold	260.68	270.94	3.175	0.3095
S2-3	cold	259.83	260.68	0.265	0.3118
S2-4	cold	252.14	259.83	0.857	0.1114
S2-5	cold	240.17	252.14	1.332	0.1113
S2-6	cold	199.15	240.17	3.502	0.0854
S2-7	cold	188.89	199.15	1.501	0.1463
S2-8	cold	180.34	188.89	34.396	4.0229
S2-9	cold	120.51	180.34	9.381	0.1568
S2-10	cold	100.00	120.51	6.822	0.3326
S2-11	cold	58.97	100.00	3.810	0.0929

SUPPLEMENTARY INFORMATION P1.D

Case Study 2

Supplementary data for case study 2.

Table P1.D. 1. Site configuration and operating conditions of case study 2

Parameter	Value
Site power demand [MW]	40
Max export allowed [MW]	10
Working hours [h·y ⁻¹]	8600
Interest rate [%]	8
Plant life [y]	25
Capital installation factor [-]	4
Δ TCW [°C]	10
TBFW [°C]	120
PVHP [bar(a)]	100

Table P1.D. 2. Site configuration and operating conditions of case study 2

Parameter	Value
CEPCI 2000 [-]	394.1
CEPCI 2008 [-]	575.4
CEPCI 2010 [-]	532.9
CEPCI 2014 [-]	576.1
CEPCI 2019 [-]	607.5
Energy CPI 2002 [-]	59.2
Energy CPI 2019 [-]	109.3
USD to EURO 2019	0.8931

Table P1.D. 3. Linear model coefficients of equipment capital cost

Resource	Variable/units	C_{nEq}^A [€/unit]	C_{nEq}^B [€]	Range	Reference
Boiler					
Packaged	$m_{nb,fb,fb,v}^b$ [t/h]	46,432.32	318,715.66	50 - 350	Smith (2016)
Field-erected	$m_{nb,fb,fb,v}^b$ [t/h]	57,059.40	843,282.30	20 - 154.2	Smith (2016)
		40,411.71	3,948,425.00	154.2 - 800	
Steam turbine	W_{θ}^{st} [MW]	345,101.63	44,057.43	1 - 200	Fleiter et al. (2016)
Gas turbine					
Aeroderivative	W_{ngt}^{gt} [MW]	417,061.85	764,213.50	2 - 13.1	Pauschert (2009)
		299,924.77	2,497,065.00	13.1 - 51	
Industrial	W_{ngt}^{gt} [MW]	282,115.02	1,463,097.00	6 - 34.1	Pauschert (2009)
		204,104.04	4,439,144.00	34.1 - 125	
HRSG	m_{exh}^{HRSG} [t/h]	2,894.08	266.54	< 85	Luo et al. (2014)
		22,895.56	135.33	> 85	
HO Furnace	Q^{HO} [MW]	44,447.73	403,443.62	5 - 60	Towler and Sinnott (2013)

Note: costs adjusted to 2019

Table P1.D. 4. Resources data of case study 2

Resource	LHV ^a [MWh·t ⁻¹]	Cost [€·MWh ⁻¹]	Reference
Natural gas	13.08	24.30 ^b	Eurostat (2020)
Distillate oil	11.28	39.65	Comission (2019)
Fuel gas	13.03	23.87	Author's estimation ^d
Fuel oil	10.83	39.40	Comission (2019)
Hot oil	-	30.40	Author's estimation ^e
Electricity import	-	88.65 ^b	
Electricity export	-	79.79	Author's estimation ^f
Cooling water		1.230	Turton et al. (2018)
Treated water		0.301 ^c	Turton et al. (2018)

^a Source :^b Prices for XL scale industries: Band I6 for natural gas (>4 000 000 MWh y⁻¹)Band IG for electricity (>150 000 MWh y⁻¹)^c Cost per ton [€·t⁻¹]^d Based on energy inflation (CPI)^e Assuming 10 % of distribution losses^f Price related to the furnace fuel (Natural gas). Assuming 80 % efficiency

Table D. 5. Stream data of Case Study 2

Stream	Type	Supply Temperature T_s [°C]	Target temperature T_t [°C]	Heat Load ΔH [MW]	Heat capacity CP [MW·°C ⁻¹]	Temperature difference ΔT_{\min} [°C]
Process A						
A-1	Hot	300	280	30.000	1.500	15
A-2	Hot	148	135	10.000	0.769	
A-3	Hot	135	110	20.000	0.800	
A-4	Hot	110	100	10.000	1.000	
Process B						
B-1	Hot	270	260	10.000	1.000	5
B-2	Hot	260	241	10.000	0.526	
B-3	Hot	241	240	20.000	20.000	
B-4	Hot	240	220	10.000	0.500	
B-5	Hot	220	200	5.000	0.250	
B-6	Hot	200	150	5.000	0.100	
B-7	Hot	150	135	10.000	0.667	
B-8	Hot	135	90	10.000	0.222	
Process C						
C-1	Cold	169	174	10.000	2.000	15
C-2	Cold	168	169	10.000	10.000	
C-3	Cold	159	168	10.000	1.111	
C-4	Hot	179	160	5.000	0.263	
C-5	Hot	160	150	15.000	1.500	
C-6	Hot	150	135	5.000	0.333	
C-7	Hot	135	90	5.000	0.111	
C-8	Hot	90	85	8.000	1.600	
C-9	Hot	85	84	12.000	12.000	
Process D						
D-1	Cold	209	210	20.000	20.000	5
D-2	Cold	149	150	20.000	20.000	
D-3	Cold	104	105	30.000	30.000	
D-4	Hot	119	118	20.000	20.000	
D-5	Hot	101	100	30.000	30.000	
D-6	Hot	95	94	20.000	20.000	
Process E						
E-1	Cold	235	237	5.714	2.857	10
E-2	Cold	230	235	16.104	3.221	
E-3	Cold	180	230	18.182	0.364	
E-4	Cold	160	180	30.000	1.500	
E-5	Cold	110	160	20.000	0.400	

Stream	Type	Supply Temperature T_s [°C]	Target temperature T_t [°C]	Heat Load ΔH [MW]	Heat capacity CP [MW·°C ⁻¹]	Temperature difference ΔT_{\min} [°C]
E-6	Cold	95	110	5.000	0.333	
E-7	Cold	90	95	25.000	5.000	
E-8	Hot	110	90	40.000	2.000	
E-9	Hot	90	80	20.000	2.000	

References

- Comission, E. (2019) *Consumer prices of petroleum products inclusive of duties and taxes: European Comission*. Available at: https://ec.europa.eu/energy/observatory/reports/2019_01_07_with_taxes_1933.pdf.
- Eurostat (2020) 'Gas prices for non-household consumers - bi-annual data (from 2007 onwards)'. Available at: https://ec.europa.eu/eurostat/databrowser/view/NRG_PC_203_custom_494286/default/table?lang=en [Accessed 2021].
- Fleiter, T., Steinbach, J. & Ragwitz, M. (2016) Mapping and analyses of the current and future (2020 - 2030) heating/cooling fuel deployment (fossil/renewables), Germany: European Commission.
- Luo, X., Hu, J., Zhao, J., Zhang, B., Chen, Y. & Mo, S. (2014) 'Multi-objective optimization for the design and synthesis of utility systems with emission abatement technology concerns', *Applied Energy*, 136, pp. 1110-1131.
- Pauschert, D. (2009) *Study of Equipment Prices in the Power Sector*, Washington, D.C.: Energy Sector Management Assistance ProgramESMAP Technical Paper 122/09).
- Smith, R. (2016). *Chemical Process Design and Integration* (2nd ed. ed.): Wiley.
- Towler, G. & Sinnott, R. (2013) 'Utilities and Energy Efficient Design', *Chemical engineering design, principles, practice and economics of plant and process design*. Second ed. Oxford, UK: Elsevier, pp. 103-160.
- Turton, R., Shaeiwitz, J. , Bhattacharyya, D. & Whiting, W. (2018) *Analysis, Synthesis, and Design of Chemical Processes*. Pearson

SUPPLEMENTARY INFORMATION P1.E
Detailed results of case study 2 assessment

Parameter	2 mains				3 mains				4 mains				5 mains			
			Hot Oil circuit				Hot Oil circuit				Hot Oil circuit				Hot Oil circuit	
	w/o FSR	w/ FSR	w/o FSR	w/ FSR	w/o FSR	w/ FSR	w/o FSR	w/ FSR	w/o FSR	w/ FSR	w/o FSR	w/ FSR	w/o FSR	w/ FSR	w/o FSR	w/ FSR
Utility steam [t h⁻¹]	246.63	214.36	118.83	97.46	239.86	190.96	118.83	97.46	239.93	187.01	119.12	97.38	238.64	185.05	114.54	97.75
Boiler steam	154.02	121.51	29.97	-	200.74	121.42	29.97	-	207.43	121.76	39.49	-	208.46	115.77	20.00	-
HRSG steam	92.61	92.85	88.86	97.46	39.12	69.54	88.86	97.46	32.50	65.25	79.63	97.38	30.18	69.28	94.54	97.75
Process steam [t h⁻¹]	194.69	182.85	193.91	193.24	192.24	192.45	193.91	193.24	192.05	193.14	193.53	194.08	192.22	193.21	194.86	194.36
FSR [t h⁻¹]	-	67.01	-	21.04	-	45.38	-	21.04	-	41.12	-	17.88	-	41.51	-	16.12
Power generation [MW]	46.66	46.67	46.66	46.67	46.67	46.67	46.66	46.67	46.67	46.66	46.66	46.43	46.67	46.66	46.67	46.67
BP steam turbines	16.99	12.70	17.69	14.71	34.77	24.29	17.69	14.71	37.13	25.25	20.77	14.43	38.05	23.81	16.34	14.78
Condensing turbines	-	4.21	-	-	-	-	-	-	-	-	-	-	-	-	-	-
Gas turbines	29.67	29.76	28.97	31.96	11.90	22.38	28.97	31.96	9.54	21.41	25.89	32.00	8.62	22.85	30.33	31.89
Operating costs [m€ y⁻¹]																
Fuel cost	56.15	49.74	30.98	27.34	52.27	44.26	30.98	27.34	51.61	44.12	30.42	27.25	51.06	44.05	29.99	27.28
Boiler	30.68	41.36	6.08	-	41.36	24.77	6.08	-	42.64	25.42	8.05	-	42.80	24.17	3.98	-
GT + HRSG	25.47	10.90	24.89	27.34	10.90	19.49	24.89	27.34	8.97	18.70	22.37	27.25	8.26	19.88	26.01	27.28
HO fuel cost	-	-	15.49	15.49	-	-	15.49	15.49	-	-	15.49	15.49	-	-	15.49	15.49
Power cost	- 3.50	- 3.50	- 3.50	- 3.50	- 3.50	- 3.50	- 3.50	- 3.50	- 3.50	- 3.50	- 3.50	- 3.50	- 3.50	- 3.50	- 3.50	- 3.50
Cooling cost	2.22	2.44	2.22	2.22	2.22	2.22	2.22	2.22	2.22	2.22	2.22	2.22	2.22	2.22	2.22	2.22
Treated water cost	0.01	0.02	0.05	0.06	0.05	0.05	0.05	0.06	0.06	0.05	0.06	0.06	0.06	0.04	0.06	0.06
Total cost	54.88	48.70	45.24	41.61	51.04	43.03	45.24	41.61	50.39	42.89	44.69	41.69	49.84	42.81	44.26	41.55
Maintenance costs	2.14	2.18	2.71	2.81	1.75	2.00	2.71	2.81	1.69	1.97	2.63	2.80	1.68	2.01	2.75	2.81
Capital costs [m€ y⁻¹]																
Hot oil furnace	-	-	1.78	1.78	-	-	1.78	1.78	-	-	1.78	1.78	-	-	1.78	1.78
Boilers	3.64	2.94	0.97	-	4.56	2.94	0.97	-	4.66	2.95	1.17	-	4.68	2.82	0.75	-
HRSGs	1.21	1.22	1.19	1.30	0.57	0.95	1.19	1.30	0.49	0.92	1.08	1.30	0.46	0.97	1.24	1.29
Gas turbines	4.64	4.65	4.53	4.99	2.15	3.50	4.53	4.99	1.78	3.35	4.05	5.00	1.65	3.57	4.74	4.98
Steam turbines	2.29	2.36	2.38	1.99	4.63	3.27	2.38	1.99	4.93	3.40	2.77	1.95	5.05	3.21	2.24	2.00
BP steam	-	-	-	-	-	-	-	-	-	-	-	-	-	-	-	-
Condensing	-	0.64	-	-	-	-	-	-	-	-	-	-	-	-	-	-
Condenser	-	0.08	-	-	-	-	-	-	-	-	-	-	-	-	-	-
Deaerator	0.08	0.07	0.06	0.06	0.07	0.07	0.06	0.06	0.07	0.07	0.06	0.06	0.07	0.07	0.06	0.06
FSR	-	0.28	-	0.17	-	0.35	-	0.17	-	0.41	-	0.23	-	0.36	-	0.27
Total Capital Cost	11.86	12.24	10.91	10.29	11.98	11.08	10.91	10.29	11.93	11.10	10.91	10.32	11.91	11.00	10.81	10.38
TAC [m€ y⁻¹]	68.88	63.12	58.86	54.72	64.77	56.11	58.86	54.72	64.01	55.96	58.23	54.81	63.43	55.82	57.82	54.74

Table PI.E. 1. Comparison of system configuration and performance for different utility options

3.3 Introduction to Contribution 2

Based on the promising results obtained in Contribution 1 for the synthesis of utility systems considering steam level placement, a solution pool based bilevel algorithm is developed to optimize the steam main operating conditions and tackle the challenging non convex MINLP problem.

The bilevel decomposition consists of a linearized mixed-integer master problem and a nonlinear sub problem. The master problem is linearized using a variety of techniques. For instance, piecewise relaxation of bilinear components in energy balancing constraints, convex envelopes for dependent variables, and linearization of steam characteristics within the superheating zone have been explored. Additionally, the algorithm's performance is enhanced by the inclusion of a solution pool, which allows for the exploration of several plausible solutions during each iteration. Due to the good solution quality obtained with STYLE methodology, it is used to generate good initial points at a low computational effort.

The proposed methodology was assessed three different case studies under different scenarios (24 case tests in total). The results were compared against state-of-the-art commercial solver BARON, employing . The results shown that while for a small case studies the problem may be able to be solved with commercial solvers, as the problem increases in size and especially for real-world cases, the problem may become intractable if approached directly with commercial solvers. Thus, it is of fundamental importance to develop strategies to address the synthesis of utility systems.

Furthermore, the presented work reveals that one of the challenges of such problems is the high combinatorial nature of the system, where not only different equipment configurations, but also enthalpy-pressure combinations, and strong interactions among the system and the site processes could result in different near-optimal solutions. In fact, the near-optimal solutions differ only marginally with respect to the objective function, and could be considered equally good.

Overall, Contribution 2 presents a systematic methodology to allow not only the design of efficient and cost-effective process utility systems but also considers: (i) the optimal steam conditions for heat integration at multiple temperature levels, (ii) interactions between the on-site utility system and processes (industrial clusters) (iii) alongside more practical issues such as steam sensible heat and part-load efficiency of utility components, (iv) with a rapid convergence and good solution quality.

3.4 Contribution 2

Title: BEELINE: BiLevel dEcomposition aLgorithm for synthesis of Industrial eNergy systEms

Authors: Julia Jimenez-Romero, Adisa Azapagic and Robin Smith

To be submitted to: Energy

Year: 2021

BEELINE: Bilevel Decomposition Algorithm for synthesis of Industrial Energy systems

Julia Jiménez-Romero^{a,b,*}, Adisa Azapagic^b, Robin Smith^a

^a Centre for Process Integration, Department of Chemical Engineering and Analytical Science, University of Manchester, Manchester, M13 9PL, United Kingdom

^b Sustainable Industrial Systems Group, Department of Chemical Engineering and Analytical Science, University of Manchester, Manchester, M13 9PL, United Kingdom

* Julia Jiménez-Romero. Email: julia.jimenezromero@manchester.ac.uk

Abstract

Energy transition is the most significant and complex challenge facing industry. On most industrial sites, the largest single energy user is the utility system that produces the heat and power necessary for the site. The heavy reliance of current utility systems on fossil fuels and the requirement of strategic measures to ensure a sustainable future has prompted researchers to explore different energy sources, technologies and pathways for evolving existing systems to a sustainable basis for future utility systems. Nevertheless, prior to any substantial change, providing energy-efficient systems based on renewable or non-renewable energy sources is essential to minimize fuel demand and mitigate emissions. The present work focuses on developing cost-effective solutions for the synthesis of process utility systems, considering site-wide energy integration. Utility system performance is generally determined by system setup and operational load. Steam mains selection, in terms of pressures and superheating have an essential role in the utility system performance and site energy integration. Therefore, the synthesis of energy-efficient utility systems involves optimizing utility components configuration and steam mains operating conditions simultaneously. Due to nonlinearities and non-convexities from underlying physics and binary decisions involved, the resulting Mixed-Integer Non-Linear Problem (MINLP) presents challenges for advanced state-of-art solvers for real-world problems. In past work, a number of important practical issues (e.g. boiler feed water preheat and steam superheat) have been oversimplified in order to make the solution tractable. However, the oversimplifications also lead to misleading results. In this research, a mathematical formulation for simultaneous optimization of comprehensive utility system configurations and operating conditions is for the first time combined with more realistic steam operating conditions (superheating and desuperheating) to represent the utility systems. Its framework is constructed via a bilevel decomposition algorithm based on piecewise MILP relaxation, McCormick relaxation, and linearization of steam properties at the superheated stage. In addition, the solution pool feature of

CPLEX solver is incorporated to enhance the performance and convergence of the algorithm. This work presents the fundamental problem formulation that has not been sufficiently addressed previously. Indeed, this methodology sets out the basis for synthesizing energy-efficient utility systems for the future and allows for many energy conversion technologies and sources to be added to the framework that have previously not been possible to include.

Highlights

- Cost-effective solution for synthesis of utility systems considering steam levels operating conditions.
- Steam sensible heat has been included to provide more realistic and accurate energy targets.
- The nonconvex MINLP is solved using a solution pool based bilevel decomposition algorithm.
- Accurate MINLP and an MILP model are proposed and compared.
- Improvement in CPU time over state-of-the-art MINLP solver.
- New framework to screen different conversion technologies considering multiple heating levels.

Keywords

- Superstructure, nonconvex mixed integer nonlinear programming model, bilevel decomposition, mixed integer linear relaxation, heat recovery, process steam systems, steam networks.

Nomenclature

Abbreviations

BFW	Boiler feed water
BP-ST	Back-pressure steam turbine
C	Heat sinks
cmdty	Commodity
cw	Cooling water
Deae	Deaerator
E	Electricity
eq	Equipment
F	Fuel
FSR	Flash steam recovery
grid	Electricity grid
H	Heat sources
HO	Hot oil
HRSG	Heat recovery steam generator
i_n	Last steam main i
IS	Isentropic
LD	Let-down
M	Mass flowrate
main	Maintenance cost
MILP	Mixed integer linear programming
MINLP	Mixed integer non liner programming
ns_{eq}	Linear segment for cost calculation of equipment
NHV	Net heat value
op	Operating
Q	Heat flow
sh	superheated
ST	Steam turbine
TAC	Total Annualized Cost
UC	Utility components
VHP	Very High Pressure
w	Treated water

Sets

cmdty	Set of utility commodities
C	Set of cold streams
EQ	Set of utility equipment for thermal and/or power generation
F	Set of fuels
GT_F	Set of fuels for gas turbines
I	Set of steam mains
IJ	Set of steam levels j_s that belong to steam main i (i, j_s)
J	Set of temperature/pressure intervals
J_{HO}	Set of temperature/pressure intervals for hot oil (subset of temperature intervals)
J_s	Set of temperature/pressure intervals for steam main (subset of temperature intervals)
J_{WH}	Set of temperature/pressure intervals for waste heat (subset of temperature intervals)
N	Set of segments for linearization of steam enthalpy
S_{eq}	Set of segments for linearization of capital cost for each equipment
S_x	Set of segments for the linearization of steam superheat temperature

UC	Set of utility components
VHP _L	Set of VHP steam levels

Variables

$C_{\text{comdty}}^{\text{op}}$	Operating costs of commodities
TAC	Total annualized costs

Positive variables

$\Delta H_{\theta}^{\text{IS}}$	Isentropic enthalpy difference of steam turbine operating at θ conditions for the original MINLP problem and strategy 2
$\Delta m_{n,i,j_s}^{C_{\text{steam}}}$	Place holders for mass flow rates $m_{n,i,j_s}^{C_{\text{steam}}}$ in the piecewise linearization in strategy 2
$\mu_{\text{eq}, \theta}$	Auxiliary variable to replace the mixed-integer binary term $\Delta H_{\theta}^{\text{IS}} y_{\text{eq}, \theta}$ in strategy 2
$C_{\text{eq}}^{\text{inv}}$	Investment cost of equipment
$C_{\text{eq}}^{\text{main}}$	Maintenance cost of each equipment
$h_{\text{sh}j_s}$	Enthalpy of of superheated steam at steam level j_s for the original MINLP problem and strategy 2
$h_{\text{sh}v}$	Enthalpy of superheated steam at VHP steam main operating at v conditions for the original MINLP problem and strategy 1
m	Variable representing mass flowrates
$m_{\text{eq},i',j_s',j_s}^{\text{BP-ST}}$	Steam mass flow of back-pressure turbine eq passing from steam level j_s' to level j_s
m_{i,j_s}^{CBFW}	Steam mass flow rate of BFW injected to desuperheated steam operating at j_s conditions
m_{i,j_s}^{CFSR}	Steam mass flow rate of FSR injected to desuperheated steam operating at j_s conditions
$m_{i,j_s}^{C_{\text{steam}}}$	Process steam use at steam main i instant operating at level j_s
$m_{i,j_s}^{C_{\text{T}}}$	Process steam use at the process use instant at level j_s
m_{i,j_s}^{H}	Process steam generation at steam main i instant operating at level j_s
$m_{i,j_s',j_s}^{\text{LD}}$	Steam mass flow passing through let-down valve from steam level j_s' to level j_s
$m_{\text{UC},i,j_s}^{\text{in}}$	Variable representing mass flows from unit component UC to steam main i (operating at j_s)
$m_{\text{UC},i,j_s}^{\text{out}}$	Variable representing mass flows from steam main i (operating at j_s) to unit component UC
$m_{\text{in},i,j_s}^{\text{FSR}}$	Inlet mass flow rate at FSR drum i operating at j_s conditions
$m_{i,j_s,j_s'}^{\text{FSR}}$	Liquid mass flow rate of FSR i operating from pressure j_s to j_s'
$m_{s,i,j_s,j_s'}^{\text{FSR}}$	Steam mass flow rate of FSR i operating from pressure j_s to j_s'
$m_{j_s}^{\text{H}}$	Mass flow rate of process steam generation for steam level j_s
$m_{\text{exh}, \text{eq}, v}^{\text{HRSG}}$	Mass flow rate of gas exhausts of unit eq , to generate steam in a HRSG operating at v conditions
$m_{i,j_s}^{\text{in}}, m_{i,j_s}^{\text{out}}$	Variable vectors representing inlet and outlet mass flow rates at steam main i operating at j_s conditions at the general MILP formulation
$m_{i,j_s,j_s'}^{\text{LD}}$	Mass flow rate of let-down passing from steam main i operating at j_s to steam level j_s'
m_{i,j_s}^{LDin}	Let-down mass flow rate entering to steam main i operating at j_s conditions
$m_{\text{eq},v,j_s}^{\text{VHP BP-ST}}$	Steam mass flow rate of BP turbine n_{st} operating from VHP level v to level j_s
$m_{v,j_s}^{\text{VHP LD}}$	Mass flow rate of let-down passing from VHP main operating at v conditions to steam level j_s
m^{W}	Mass flow rate of treated water
$n_{\text{eq}, \theta}$	Slope of Willans line correlation

Q_{eq,j_s',j_s}^{BP-ST}	Heat from back-pressure steam turbine eq operating between level j_s' and level j_s
$Q_{eq,v,j_s}^{VHP BP-ST}$	Heat from back-pressure steam turbine eq operating between VHP level v and steam level j_s
Q_{i,j_s}^{Cin}	Heat available for process heating from steam main i operating at j_s conditions
Q_{i,j_s}^{Csteam}	Auxiliary variable to replace the bilinear term $h_{sh,j_s} \cdot m_{i,j_s}^{Csteam}$ in strategy 2
Q^{HO}	Process heating requirements that cannot be used/satisfied by steam
Q_s^{HO}	Process heating provided by hot oil system at steam temperature range
Q_T^{HO}	Total process heating provided by hot oil system
$Q_{eq,\theta}^{IS}$	Auxiliary variable to replace the bilinear term $\Delta H_\theta^{IS} \cdot Z_{eq,\theta}$ in strategy 2
Q_{i,j_s}^{STin}	Heat from back-pressure turbine exhausts entering steam main i operating at j_s conditions
Q_{eq}^{exh}	Total heat contain in the exhaust gases used in HRSG unit eq
$Q_{eq,v}^{HRSG}$	Heat of the exhaust gases used in the HRSG unit eq operating at v conditions
$Q_{eq,v}^{loss}$	Heat losses to the ambient of exhaust gases of gas turbine eq after HRSG operating at v conditions
$Q_{eq,v}^{pre}, Q_{eq,v}^{vap}, Q_{eq,v}^{sh}$	Heat transfer in each stage of HRSG (eq): preheating (pre), evaporator (vap) and superheating (sh) for generating steam at v conditions
Q_{i,j_s}^{LD}	Heat from let-down station at steam level j_s
Q_{uc,i,j_s}^{in}	Variable vector representing inlet heat flow at steam main i operating at j_s conditions
$R_{j_s}^C$	Residual sink heat at steam level j_s
$R_{j_s}^H$	Residual source heat at steam level j_s
U_{cmdty}	Variable vector representing site consumption of each commodity
U_{cw}	Cooling water consumption in MW
U_e^{imp}, U_e^{exp}	Electricity import and export, respectively
U_f	Fuel consumption in MW
U_w	Treated water consumption in MW
$T_{sh,v}^{VHP}$	Steam temperature at VHP level operating at v conditions for original MINLP problem and strategy 2
W_{eq,j_s',j_s}^{BP-ST}	Power generated by back-pressure turbine operating between steam level j_s' and level j_s
$W_{v,j_s}^{VHP BP-ST}$	Power generated by BP turbine operating between VHP main level v and steam level j_s
W_{eq}	Variable vector representing power generated by equipment eq
$W_{eq,\theta}^{int}$	Willans line intercept
$x_{eq,\theta}$	Load fraction of unit eq operating at θ conditions
Z	Variable vector representing size and load of equipment
Z_{eq}	Variable vector representing equipment load
$Z_{eq,\theta}$	Equipment load operating at θ conditions
Z_{eq}^{max}	Variable vector representing installed equipment capacity
$Z_{eq,\theta}^{max}$	Installed equipment size operating at θ conditions

Binary variables

y	Variable vector representing binary variables
y_{eq}	Vector representing binary variables that denote the equipment selection
$y_{eq,\theta}$	Binary variables to denote the selection of unit operating at θ conditions
$y_{eq,ns_{eq}}$	Binary variable to denote one domain segment for investment calculation, if the equipment is selected

y_{i,j_s}	Binary variables to denote the selection of steam main i operating at j_s conditions
y_v	Binary variable to denote the selection of VHP steam level
$y_{j_s}^{HO}$	Binary variables to denote the selection of hot oil at steam level j_s
y_{n,i,j_s}^N	Binary variable to denote the selection of one domain segment in j_s
$y_{eq,f}^{SF}$	Binary variable to denote the activation of supplementary firing, using fuel f in equipment eq

Parameters

α	Vent rate in the deaerator
ρ_{eq}	Cost exponent for each equipment
β	Condensate return rate
γ	Blowdown rate
ζ	Upper bound of heat content of gas turbine exhausts
Λ	Vector that represents part of the slope in the modelling of power generation units
ΔT_{sat}	Saturation temperature difference during expansion of steam through a turbine
ΔT_{min}^{HRSG}	Minimum approach temperature difference for HRSG
σ_{θ}^{st}	minimum load fraction of steam turbine operating at θ conditions
$\underline{\Omega}_{eq}$	minimum feasible load operation of each equipment
a,b,c	Regression coefficients for linearization of isentropic enthalpy difference in the original MINLP problema and strategy 2
a^T, b^T, c^T	Regression coefficients for steam superheated temperature nonlinear calculation in the original MINLP problema and strategy 2
a_{sx}^T, b_{sx}^T	Linearization parameters for superheat steam temperature calculation in strategy 2
$\tilde{a}_{eq,\theta}, \tilde{b}_{eq,\theta}$	Model coefficients of equipment eq operating at θ conditions
$\tilde{a}_{11}, \tilde{a}_{12}$	Model coefficients for boilers
$\tilde{a}_{21}, \tilde{a}_{22}, \tilde{a}_{23}, \tilde{a}_{24}$	Model coefficients for power generation units, based on Willans line correlation
C_{eq}^A	Variable cost of equipment depending on its size
C_{eq}^B	Fixed cost of equipment selection
C_{eq}^{ref}	Reference cost for each equipment
$CP_{c_i}^C$	Heat capacity flowrate of cold stream c_i
$CP_{h_i}^H$	Heat capacity flowrate of hot stream h_i
cp_{exh}	Heat capacity of exhaust gases
F_{eq}^{ann}	Annualization factor
F_{eq}^{inst}	Installation factor
$\underline{\Delta h}_{is\theta}, \overline{\Delta h}_{is\theta}$	Lower and upper bound for isentropic enthalpy at conditions θ , for strategy 2
$\underline{h}_{sh,j_s}, \overline{h}_{sh,j_s}$	Lower and upper bound for steam enthalpy at superheated stage for strategy 2
$\tilde{h}_{sh,j_s}^H, \tilde{h}_{sh,j_s}^C$	Enthalpy of superheated process steam generation (H) and use (C) at steam level L
h_i	Enthalpy at operating conditions of steam main i , in the algorithm for calculating steam mains' superheating
\tilde{h}_{l,j_s}	Enthalpy of saturated liquid at steam level j_s
\tilde{h}_{v,j_s}	Enthalpy of saturated vapor at steam level j_s
\tilde{h}^{BFW}	Enthalpy of boiling feed water
\tilde{h}^{Cond}	Enthalpy of returned condensate
$\tilde{\Delta h}_{shn,j_s}$	Boundaries of enthalpy at each domain segment n for enthalpy calculation in strategy 2

\tilde{h}_v	Enthalpy of saturated liquid of steam at VHP level v
$\tilde{h}_{j_s}^C$	Enthalpy of saturated liquid of process steam use at steam level j_s
$\tilde{h}_{sh_{j_s}}^C$	Enthalpy of superheated process steam use at steam level j_s
$\tilde{h}_{sh_{j_s}}^H$	Enthalpy of superheated process steam generation at steam level j_s
$\tilde{h}_{v_{j_s}}$	Enthalpy of saturated vapour of steam at level j_s
h^{vent}	Enthalpy of steam vented
h^W	Enthalpy of treated water
L^H, L^C	Heat losses due to distribution at the source and sink side, respectively
L^e	Electrical losses for transmission to/from the national grid
$\overline{m}_{i_{j_s}}^{Csteam}$	Upper bound for each segment steam consumption at the main i .
η_{mec}	Mechanical efficiency of steam turbines
η_{eff}^{HRSG}	Radiation efficiency of HRSG
P_{cmdty}	Commodity price
P_i	Steam pressure of steam main i
\tilde{Q}_j^C	Process heat sink at level j
Q_{eq}^{exh}	Heat contained in gas turbine exhausts of equipment eq
\tilde{Q}_j^H	Process heat source at level j
T_j	Utility temperature at level j
T_{max}	Maximum temperature allowed for steam generation
T^{*in}, T^{*out}	Shifted inlet and outlet stream temperatures
\tilde{T}_{amb}	Ambient temperature
\tilde{T}_{min}^{stack}	Minimum stack temperature for exhaust gases
\tilde{T}_v^{sat}	Saturated steam temperature at v conditions
$\tilde{T}_{max}^{SF}, \tilde{T}_{max}^{UF}$	Maximum temperature achievable with and without supplementary firing, respectively.
t_{op}	Annual site operating hours
T_s^{HO}	Target temperature of hot oil
T_i^{MIN}	Minimum superheat temperature of steam main i
$\tilde{U}_{max}^{exp}, \tilde{U}_{max}^{imp}$	Upper bound for export and import of grid electricity
x_{vl}	Steam quality
\tilde{W}^{dem}	Power demand
\tilde{Z}_{eq}^{ref}	Equipment reference size for capital cost estimation
$\underline{Z}_{eq}, \overline{Z}_{eq}$	Lower and upper size limits for each equipment

Pseudo-parameters

ΔH_0^{IS}	Isentropic enthalpy difference of steam turbine operating at θ conditions for MILP problem in strategy 1
$h_{sh_{i,j_s}}$	Enthalpy of superheated steam at steam main i operating at j_s conditions for MILP problem in strategy 1
h_{sh_v}	Enthalpy of superheated steam at VHP steam main operating at v conditions for MILP problem in strategy 1
$T_{sh_v}^{VHP}$	Steam temperature at VHP level operating at v conditions for MILP problem in strategy 1

1. Introduction

The necessity to reduce CO₂ emissions has prompted industry to place a greater emphasis on sustainable energy consumption. In the process industry, energy is most often supplied by on-site utility systems with a electricity grid connection. On-site utility systems use steam at multiple conditions (temperature and pressure) to satisfy process heat and power generation requirements. Moreover, process utility systems currently depend strongly on gas turbine and steam turbine technologies, and consequently on the combustion of fossil fuels. There is no doubt that for reducing emissions, and for eventually reaching net zero, industry must embrace a greater reliance on renewable sources. In turn, this will mean radical shifts in how the industrial utility systems are designed and operated. Yet, the current market structure creates significant barriers to greater inclusion of sustainable technologies. This is because market mechanisms are based on high marginal costs and availability, whereas renewable energy sources with low marginal costs are intermittent and are not programmable. As a result, this prevents greater market penetration. Moreover, due to the heterogeneity and conservative nature of the energy intensive industry sector, along with absence of major technological breakthroughs (available at commercial scale), the uptake of research focused on delivering low carbon energy is painstakingly slow. For this reason, as well as to embrace cost-effective de-carbonization efficiency, improvements in the provision and management of process heat and power is crucial, especially in short to mid-term. Efficient process plants that use less energy and emit less CO₂, due to the design and operation of utility systems operating at optimum conditions are rightly gaining more interest from both industry and academia.

The optimum synthesis of energy systems is complex due to the variety of sources and energy conversion technologies. Several studies for the synthesis, design and operation of utility systems have been published in recent years. Various frameworks have concentrated on microgrids (Hawkes and Leach, 2009; Zidan et al., 2015), urban areas (Omu et al., 2013; Brandoni and Renzi, 2015), or district-scale distributed energy networks in general (Rieder et al., 2014; Wang et al., 2015; Wouters et al., 2015). Despite process utility systems being classified as microgrid systems (if electricity export is allowed), its design by comparison presents significant differences. On one hand, district systems are usually designed to supply heat at a single low temperature (usually met by hot water or low pressure steam). While in process utility systems: (i) heat is required at medium to high temperatures, (ii) which are met by multiple steam levels, (iii) heat demand is far higher than the power requirement (heat/power ratio between 3.5 to 5.6)(Picón-Núñez and Medina-Flores, 2013) (iii) process utility systems can be employed as heat recovery systems, and process heat surplus (at different temperatures) can be employed in other plant heat sources via steam generation. Consequently, such systems comprise stronger interactions between end-energy users and the utility system. Energy integration plays a key role for the optimal design and operation of such systems.

Although energy integration through on-site utility system and its synthesis, design and operation has been studied previously, the topic is still the focus of research and development with the end goal of enhancing efficiency (Liew et al., 2017; Klemeš et al., 2018; Klemeš et al., 2019). Indeed, as presented later in the state-of-the-art section, key issues such as the optimum selection of pressure and temperature for steam generation and distribution require further analysis. The temperature and pressure of steam levels are an important design variable. This is because they can be regulated to not only enhance heat integration, but also improve on-site power generation via steam expansion through steam turbines. In turn, this results in an improvement to the overall efficiency of the system. What is more, despite process heating being efficiently carried out using steam latent heat, steam superheating temperature is key for the utility system performance and operation. On the one hand, steam superheating constrains the amount of heat recovered from processes and brings additional complexities that need to be considered for the design. On the other hand, due to its poor heat transfer steam often requires to be de-superheated (by injecting BFW) for the actual process heating. This impacts the site steam requirement and site fuel consumption, whether it is renewable or non-renewable. Finally, steam superheating has an effect on the power generation targets due to its direct correlation with steam turbine efficiency. Due to its relevance to the utility system performance, and to address the research gap identified, the novelty of this work lies in the optimum selection of temperature and pressure for steam generation, and distribution for the design of efficient and cost-effective utility systems. After an analysis of the state-of-the-art of current utility system synthesis and design methods, this work presents a novel MINLP formulation with a solution pool based bilevel decomposition strategy in the methodology section. Later, the applicability of the method to various study cases is proved in the results and discussion section.

2. State of the art

Steam utility systems are widely used in the industrial sector and/or large-scale distribution systems to provide both heat and power (Smith, 2016b; Ma et al., 2018). Steam utility systems allow industrial processes to exploit local fuel resources to satisfy their energy requirement, reducing dependency on external suppliers while improving the reliability of energy supply. As a result, operational expenses and environmental costs may be minimised. However, these benefits may not be achieved without using systematic design methods. Different systematic approaches have been developed to provide methodological frameworks for designing utility systems. The systematic approaches could be classified into two categories: (i) insight approaches and (ii) mathematical approaches.

Steam systems have been analysed via several insight approaches (e.g. graphical methods, algebraic algorithms) to evaluate both the utility requirement and heat and power integration across the site (Liew et al., 2018; Sun et al., 2015). In this context, an extension of pinch analysis (Linnhoff and Vredeveld, 1984), known as total site analysis (TSA) (Dhole and Linnhoff, 1993), is often used to

target the amount of surplus heat produced by one process that may be transferred to a process with a heat deficit through a shared system. Hackl et al. (2011) and Matsuda et al. (2012) applied TSA to industrial clusters in Sweden and Japan respectively. These studies showed that even highly efficient single plants can further improve energy efficiency by total site integration. Further improvements in TSA were presented by Lee et al. (2020). Lee et al. (2020) proposed a pinch-based algebraic methodology to account for energy recovery, and heat and power generation opportunities in clusters connecting industrial, commercial and residential buildings via a steam system. Their work demonstrates the potential of integrated steam systems for enhancing regional sustainability and economy. Their targeting is based on fixed utility level parameters (temperature and pressure) and saturated conditions. Regarding the latter, Sun et al. (2015) highlights relevant insights related to the effect of steam sensible heat (i.e. boiler feed water preheating and steam superheating for process steam generation and steam de-superheating for the process heating) and more practical constraints (e.g. steam temperature limitations and use of flash steam recovery) for energy integration and cogeneration potential in steam systems. Other conceptual approaches (Ghannadzadeh et al., 2012; Khoshgoftar Manesh et al., 2013), have also shown the effect of superheating in the targeting of heat and power of the site. However, the graphical tools do not consider relevant utility components such as gas turbines, let-down stations and deaerators. This leads to inaccurate energy targeting. A general limitation of the insight tools is that they cannot be used for a systematic decision-making method to screen alternative conversion technologies in terms of number, size and load, an essential parameter when designing energy systems. Insight approaches are more suitable for physical targets (i.e. minimising energy consumption) (Sanaei and Nakata, 2012). Despite some studies (Khoshgoftar Manesh et al., 2013; Nemet and Kravanja, 2017; Lee et al., 2020) have introduced economic considerations, the actual trade-off cost-energy cannot be evaluated in a rigorous way (Andiappan, 2017).

Several mathematical approaches have been proposed and used widely as one of the most effective approaches for designing utility systems (Andiappan, 2017). Current mathematical models consider a combination of continuous (operating conditions) and discrete (unit selection) variables, resulting in a mixed integer programming (MIP) framework. Moreover, the synthesis of utility systems involves several nonlinearities derived from full and part-load performance curves and investment costs (economy-of-scale effects) of the energy conversion units, as well as the strict energy balances of the site. In general, the synthesis of utility systems leads to a nonconvex mixed integer non-linear programming (MINLP) problem. Most models in the literature tried to obtain linear model formulations (MILP) (Aguilar et al., 2007; Varbanov, 2004; Mitra et al., 2013; Sun and Liu, 2015) by linearizing the product of variables or by using piecewise linear approximations. First, Papoulias and Grossmann (1983) developed a mixed integer linear programming (MILP) model to select the components available in the utility superstructure. The MILP formulation is obtained by linearizing

the costs and assuming fixed operating conditions for both technologies and steam mains. Additionally, equipment efficiency is assumed as a given parameter. Maréchal and Kalitventzeff (1998) extended the MILP superstructure by combining pinch analysis for the selection of optimal pressure steam levels to satisfy energy requirements at minimum cost. The degree of steam superheating, as well as the efficiency of utility units, are considered as given fixed values. Later, Shang and Kokossis (2004) proposed a superstructure-based MILP formulation for the synthesis of utility systems with steam pressure levels selection, where part-load behaviour is integrated. However, the selection of the potential pressure levels options is not systematic and only steam saturated conditions are considered. Varbanov et al. (2005) presented another MILP model in which investment costs and part-load behaviour analysis for continuous component sizing were integrated. Nevertheless steam sensible heat impact for the unit equipment (steam turbine) and steam mains, as well as steam temperature constraints, were neglected. As highlighted earlier in Manuscript 1, such limitations lead to significant inaccuracies. Sun et al. (2017), presented a mathematical model to optimize utility systems operation under variable demand. In their research, the effect of steam mains superheating on steam distribution and power generation is investigated through a sensitivity analysis. Nonetheless, the model fails to consider the interactions between the steam levels and the site processes by neglecting the potential of process steam generation, while assuming fixed steam mass flowrates.

In spite of the significant contributions achieved via linear (MILP) models, the results obtained are only approximate solutions whose accuracy will vary significantly depending on the assumptions and approximation methods employed. Thus, to provide more accurate models, nonlinearities have been considered in the formulation of design optimization problems of energy systems, chiefly by the employing MINLP. One of the first MINLP models for synthesis of energy systems was presented by Bruno et al. (1998). Bruno's analysis considered non-linear unit performance and capital costs. Due to the complexity of the problem, and the state-of-the-art of the solvers, only one component (operation at full load) for each technology was included in the superstructure. Chen and Lin (2011) introduced an MINLP formulation for designing steam systems with integrated heat recovery systems. Nevertheless, the formulation is limited to small-scale studies and the impact of part-load on equipment performance is not examined in depth. Zhang et al. (2015a) proposed an MINLP approach for the optimal design of a cogeneration plants where integration of process heat was considered in the heat recovery steam generator (HRSG) to maximize the net power output. The superstructure model focussed on the optimization of HRSG configuration, assuming the rest of the utility components (i.e. gas and steam turbines) configuration was fixed and operating at constant efficiency. Due to the complexity of the problem only a limited range of process streams with predefined steam requirements were included. Later, Beangstrom and Majozzi (2016) formulated a MINLP model to optimise multi-level steam systems and power production. However, their study

solely considers process heat deficits, neglecting potential heat recovery of process heat surplus through steam generation, and furthermore, its impact on steam main operating conditions and site energy targets. Overall, the applicability of the proposed MINLP models with state-of-the-art solvers is limited at large scale.

Despite the performance of global MINLP solvers (e.g. BARON(Tawarmalani and Sahinidis, 2005), ANTIGONE(Misener and Floudas, 2014) , LINDOGlobal(Lin and Schrage, 2009)) improving significantly, they still present computational limits for small-scale non-convex MINLP problems (Belotti et al., 2013). Therefore, in order to tackle large size problems, significant research is being undertaken to provide global solutions to MINLP formulations (see Trespalacios and Grossmann (2014)for further details). Decomposition algorithms are one of the most popular approaches for problems with time-consuming integer formulations. For instance, Zhao et al. (2015) breaks down the integrated MINLP of optimal operation of process system couple with a utility system into an MILP and NLP problem in which variables are iteratively exchanged. The system configuration as well as the utility level conditions are predefined and are based on steam operating at saturated conditions. For energy systems for district heating and cooling networks, Goderbauer et al. (2016) developed an adaptive discretization algorithm, employing metaheuristic search algorithms for the upper-level problem to address the choice, size and operation of energy conversion units, while at the same time considering nonlinear costs and performances in the lower problem. Elsidio et al. (2017) also proposed a two-stage algorithm using evolutionary algorithms for solving the design of combined heat and power (CHP) sites. In the first stage, evolutionary algorithms are used to select and size the utility units. Later, in the second stage an MILP formulation is used to define its operational scheduling problem. In similar areas, Kermani et al. (2018) proposed a MINLP model with a decomposition strategy for Organic Rankine Cycle integration. The outer level applied a genetic algorithm to determine the working fluid and its operating conditions. In addition to this, the inner level used a sequential solution strategy to select the ORC architecture and equipment sizes (operating at full load) in a MILP sub-problem. One of the main drawbacks of previous decomposition strategies ahas been the sequential approach required. Consequently, key trade-offs (e.g. energy-costs) may be neglected in the upper level. Importantly, meta-heuristic search algorithms strongly depend on the exploration capability of the algorithm employed and the quality of the starting point. In turn, the quality of the returned solution cannot be assessed, entailing the risk of suboptimal solutions. Moreover, when solving large-scale complex problems, searching for a solution could prove both challenging and time-consuming.

For structures that employ non-linearities (e.g., bilinear, linear fractional, concave separable), relaxation methods can be utilised to formulate lower-bounding MILPs. Later, this can be integrated to optimise the continuous variables in a NLP (or MINLP) subproblem. This type of exact

decomposition algorithms, has been termed bilevel decomposition. Bilevel decomposition strongly depends on the quality of the relaxation. Despite being application-specific, it has been proven highly effective (Lotero et al., 2016; Lara et al., 2018; Elsidio et al., 2019) due to its flexibility nature, providing a formulation of the problem and the capability to evaluate the potential trade-offs simultaneously. For instance, Elsidio et al. (2019) presented an ad-hoc bilevel decomposition for the synthesis of heat exchanger networks with Rankine cycles. In this instance, a bilevel strategy was used to solve the non-linearities involved in the heat exchanger costs. Such a methodology presents significant improvements in the computational time when compared with commercial solver (BARON). However, due to the size and complexity of the problem the steam system configuration options were predefined, and the operating conditions of the utility levels were assumed fixed.

Other MILP and MINLP models are under development to design energy systems at different scales such as district heating (Voll et al., 2013), commercial and industrial buildings (Casisi et al., 2009) and central grids (Zhang et al., 2015b). However, as mentioned in the introduction, most of these systems are designed to provide heat at a single temperature by using hot water or low temperature steam. By contrast, industrial processes require heat from moderate to high temperatures, which in turn requires utilities at different levels. Therefore, industrial utility systems do not only differ in terms of energy conversion technologies options, but also require the consideration of additional aspects including: (i) heat requirement at different qualities across all the site, (ii) potential heat recovery from end-users' heat surplus to produce onsite power and/or to meet other end-users' heat deficits (through an intermediate working fluid) and (iii) the selection of the optimum temperature and pressure of the utility levels to enhance heat integration.

As previously noted, steam superheating temperature plays an important role in system performance. However, the incorporation of steam superheating as a design variable would not lead to a non-convex MINLP formulation due to the bilinear terms involved in the energy balance that are the product of the multiplication between mass-flow rates and enthalpies. Also, it could result in computationally challenges even after its decomposition. This is due to steam properties being defined from steam tables based on experimental measurements and/or approximated through equation-of-state models (IAPWS-97 (Wagner et al., 2000)). While the IAPWS-IF97 is the standard model for steam modelling in many simulators, its application in optimization-based methodologies has been restricted due to its complexity (Wang et al., 2019). To overcome this issue, especially for steam turbine performance models, several previous optimization studies on utility system design have chosen approximation functions (Luo et al., 2011; Luo et al., 2014; Beangstrom and Majozi, 2016; Pyrgakis and Kokossis, 2020). Nevertheless, linear approximation is based on discrete number of predefined steam conditions (scenarios) (Luo et al., 2011) or simplification (Singh, 1997) (e.g. assuming saturated conditions). Inaccurate regressions could lead to non-applicable solutions.

In summary, despite significant efforts to solve the design optimisation problem for energy systems, there is still significant progress to be made. There are several fundamental issues that have not been addressed via current research that are highly relevant to ensure optimal energy efficiency of utility systems -- especially at the industrial level. From recent publications, the following observations were made:

- (i) Energy Integration allows for effective use of fuel and other resources, as well as a decreased carbon footprint compared to stand-alone systems (Serra et al., 2009). Despite its relevance, insightful approaches cannot fully evaluate the vast space for selection of optimal utility level parameters to guarantee optimal energy integration. However, the insight from their application can be coupled with mathematical approaches.
- (ii) Several investigations have focused on design of on-site steam systems with process heat integration. However, a systematic approach for the optimization of the operating conditions is still required. Due to the complexity of the optimization problem, work attempting to address this issue (Varbanov et al., 2005; Shang and Kokossis, 2004) has been limited to considering saturated conditions and omitting the effect of steam sensible heat and other utility constraints for both energy integration and utility system operation.
- (iii) Steam superheating influences in several aspects of the steam system performance, including heat recovery, power generation and process heating. Nevertheless, its integration as design variables results into a non-convex MINLP formulation. Therefore, efficient ways to tackle computationally challenging problems are required.
- (iv) Direct use of steam thermodynamic properties in optimization is rarely employed due to its complexity and high nonlinearities. To overcome this issue, rough and/or case specific approximation functions have been adopted in previous research. Robust and accurate linear approximations for describing steam key thermodynamically properties at a wide range, especially at superheated conditions, are still missing from the existing literature.

In Manuscript 1, an optimization formulation was proposed to address the first two points, considering enthalpy as pseudo-parameter -- which is assumed fixed during the optimisation and recalculated later with an algorithm. With this approach, the non-linearities in the energy balance are avoided and the problem can be formulated as MILP. Despite the benefits of the sequential approach presented in Manuscript 1, -- particularly in comparison with previous research -- the quality of the solution cannot be evaluated. Therefore, to tackle these problems and address the current shortcomings in the design of utility systems, this work presents an MINLP formulation with a bilevel decomposition strategy. Note that while attaining a guaranteed globally optimal solution is ideal, the need of getting good solutions for practical-size problems in reasonable times, even without

guarantee of global optimality is crucial for the development of decision support frameworks to enhance energy-efficient industrial utility systems.

This paper directly addresses the aforementioned limitations via the following contributions:

Practical contributions

- (i) A novel framework is proposed for synthesis and optimization of the process utility system problem, with the aim of enhancing total site energy integration. There is a more robust and realistic approach for the synthesis of process utility systems, accounting for site-wide heat recovery and optimum selection of steam levels parameters (temperature and pressure). The proposed framework considers all relevant steam system components and the variation of efficiency with load. Additionally, utility components such as hot oil system and flash steam recovery are examined. The model accounts for steam sensible heat for potential energy integration with the site, including boiler feed water preheating, steam superheating for process steam generation, and de-superheating for process steam use.
- (ii) Despite the application of the methodology being based on conventional processing sites, the methodology outlined in this paper can be extended to influence the design of any distributed energy system, where heat (steam) is required at multiple levels -- for example, locally integrated energy sectors (LIES). The general framework can be extended to consider alternative technology options, which allows for an impact analysis in relation to the synthesis of future steam system.

Theoretical contributions

- (iii) The development of an MINLP framework for the simultaneous synthesis of industrial utility systems and optimum steam level placement, with a solution pool-based bilevel decomposition strategy. The bilevel algorithm comprises decomposing the original problem in a relaxed MILP problem (master problem) and a NLP problem, enhanced with a solution pool strategy.
- (iv) A selective application for the different linearization methods is used to formulate the master problem. To relax the problem without increasing unnecessarily the size and complexity of the (already complex) issue at hand, three different linearization techniques are employed. To exemplify, bilinear terms derived from steam temperature calculation are relaxed with piece-wise linear approximation (Gounaris et al., 2009), while bilinear terms caused from indirect effect of temperature calculation (i.e. steam turbine performance) are linearized by term wise envelopes (McCormick, 1976). The non-linearities of the steam properties are addressed by developing a linear approximation for the accurate definition of superheated

steam properties across a wide range of temperatures and pressures. Finally, solution pool strategy (Corporation, 2017) is employed to effectively reduce the number of iterations between the MILP problem and NLP subproblem to further enhance the algorithm.

- (v) The applicability of the proposed approach is illustrated with three case studies. To demonstrate the benefits of the MINLP model with the solution pool-based bilevel solution strategy, results are compared to the previous approach (Jimenez-Romero et al., 2022) and state-of-the-art MINLP solver (BARON).

This paper is structured as follows: in Section 1 and 2 a background and previous work done in this field is presented. Section 3 outlines the problem statement for the formulation of the mathematical model. Section 4 then presents the mathematical formulation, where the non-linearities are highlighted. The two approaches for tackling the resulting MINLP formulation are described in Section 5. Section 6 presents and discusses the results of this work. Finally, conclusions and directions for future research are addressed in Section 7.

3. Problem Statement

The problem addressed in this work is the optimal synthesis of utility systems that feature cost-effective supply and management of process heat and power across an industrial process site. A simplified site configuration is shown in Figure 2-1. For this, the problem formulation will determine the following aspects:

- i. The optimal selection, size, and load of the different utility system components.
- ii. The optimum steam main operating conditions (pressure and temperature/enthalpy) to enhance cost-effective site energy integration.
- iii. Energy use/supply by the utility system, such as total site fuel consumption, power generation/import/export, and cooling water.
- iv. Process steam generated and/or process steam used.

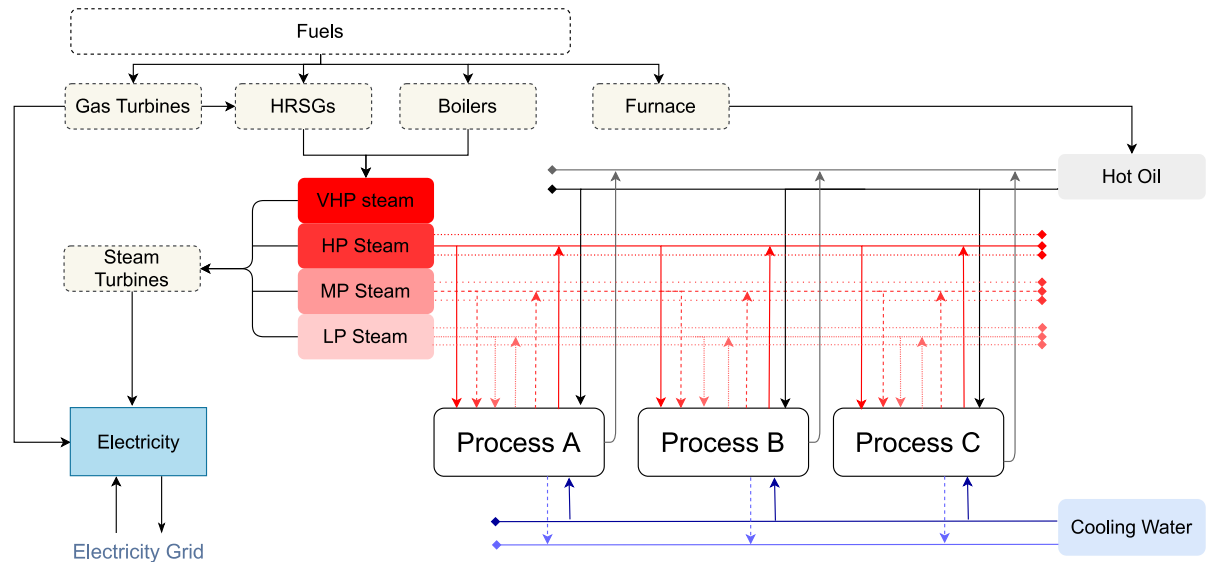


Figure 2-1 Simplified scheme of the superstructure for the synthesis of process utility system (VHP: very high pressure; MP: medium pressure; LP: low pressure; HRSGs: heat recovery steam generators)

The following considerations will be addressed:

- xiv. Process heat demand is mainly satisfied by a steam system. Hot oil circuits and cooling water systems are options for supplementary heating and cooling, respectively.
- xv. Steam main operating pressure and temperature (enthalpy) are degrees of freedom for the optimization. The pressures of steam headers are selected from a set of options based on the total site profile kinks. Enthalpies (temperatures) are continuous variables numerically optimized.
- xvi. Utility steam is raised at VHP conditions and distributed to the different headers -- either passing through steam turbines or let down stations.
- xvii. Let down stations are allowed to maintain the mass and energy balance in each steam main, as well as provide flexibility to the system. Nevertheless, the amount of let-down flow rate is limited to provide a cost-effective utility system configuration operating at maximum cogeneration potential (Varbanov et al., 2004) (Smith, 2016b). If a let-down station is included it should have a minimum flowrate for control purposes and to keep equipment hot.
- xviii. Complex configurations of steam turbines (i.e. multistage turbines) can be modelled as a set of single back-pressure steam turbines operating in series (Sun and Smith, 2015).
- xix. Non-isothermal mixing can occur in distribution headers. At the VHP steam main, all thermal generator units produce steam at the same conditions.
- xx. Process sink heat demand can be satisfied by either hot oil or de-superheated steam.
- xxi. Configuration, utility components selection and sizing, and stream mass flow rates across the steam system are optimization variables.
- xxii. Intra-plant heat recovery (whether optimized or not) is assumed to be inbuilt.
- xxiii. Heat transfer is based on specified minimum temperature approach.

xxiv. Synthesis of heat exchangers is not part of the scope.

The following information is known:

- i. A set of hot and cold process streams is to be integrated by a utility system, with given inlet and outlet temperatures, heat capacities flow, and a specific minimum temperature approach. It is assumed that both temperatures and heat capacity are constant.
- ii. Minimum degree of superheating for steam generation and steam use.
- iii. Set of potential pressure/temperature steam levels associated with each steam header operating conditions.
- iv. Power demands of each process, in addition to electricity import and export limitations and costs.
- v. A set of available conversion units (boilers, steam turbines, gas turbines, etc.) with a practical variety of sizes and loads.
- vi. Cost data relative to the equipment and commodities available.

It is worth noting that at the conceptual stage, it is difficult to define the appropriate configuration of the heat exchangers (e.g. type of heat exchanger, side allocation of fluids, head type), because the network is not yet known, and as such, detailed data analysis can only be completed later in the heat exchanger network (HEN) design. Moreover, film- or overall- heat transfer coefficients are usually difficult to estimate at an early stage due to dependency on several factors (geometry, film transfer coefficient, fouling, pressure drop, fluid velocity, viscosity, temperature difference and so on). In the research literature, constant heat transfer coefficients are commonly assumed to formulate superstructures for its analysis/optimization. Despite its widespread use, rough assumptions of film or overall heat transfer coefficients may result in misleading results in relation to economics. For instance, overall heat transfer coefficient between steam and water can vary from 680-1160 $\text{Wm}^{-2}\text{K}^{-1}$ in relation to construction materials. Additionally, if the different state-phases of water/steam are evaluated, film transfer coefficients could vary from 20-100 $\text{Wm}^{-2}\text{K}^{-1}$ for superheated steam to 3000-15000 $\text{Wm}^{-2}\text{K}^{-1}$ for saturated steam (Xu et al., 2013). While process streams coefficients could vary from 100-3000 $\text{Wm}^{-2}\text{K}^{-1}$ (Smith, 2016a), this increases the uncertainty of the prediction. Heat exchanger area calculations can predict network area typically within 10 % of accuracy if the film coefficients vary less than an order of magnitude (Smith, 2016a). This, in combination with the highly non-linearity comprise in the logarithmic temperature difference and the combinatorial nature of HEN design, make an accurate cost analysis difficult of the HE between the process streams and the utility system, at early stages. For this reason, given that the focus of this work is the synthesis of utility systems, the HEN synthesis and costs are not part of the scope.

4. Model formulation

4.1. Data extraction

The proposed framework is reliant on data extraction. Five types of data are required for the problem: (i) heating and cooling demand, (ii) site power requirement (iii) technology available and (iv) energy market price and (v) site constraints (e.g. maximum electricity import and/or export, minimum superheat required for steam generation, distribution and use). In relation to heating and cooling demand, it is based on the process stream data of all the process requiring utilities. Data should be tabulated in terms of inlet and outlet temperature (T^{in} , T^{out}), heat capacity flowrate (CP) or heat loads and minimum temperature approach between the process and utilities ($\Delta T_{\text{min}}^{\text{PU}}$).

4.2. Superstructure construction

4.2.1. Heat cascades and steam levels superstructure

For optimal heat (and power) integration, the trade-off between recovering heat/steam at certain steam main pressures and producing/using steam at the same level requires analysis. While decreasing the pressure of a particular steam main may be beneficial for higher process steam recovery and power generation (due to an increment in pressure drop), it may be offset by the amount of process heating that actually could be satisfied by that steam. This may lead to a requirement for a greater degree of higher temperature utilities which are usually more expensive. Consequently, operating costs increase. To account for this trade-off, and to define the steam pressure levels for site heat recovery, a transshipment model (first presented in (Papoulias and Grossmann, 1983)) with heat cascades is incorporated. The transshipment model considers heat as commodity which can be transferred from the hot streams (or also termed as heat sources) to the different utility levels and from the utility levels to the cold streams (known as heat sinks). Heat cascades enforce thermodynamic insights by ensuring the energy balance at each level is closed, while allowing heat transfer only from higher to lower temperatures. The proposed framework comprises the two conventional heat cascades (heat sources and heat sink) and incorporates a steam cascade to represent the utility system.

To determine the utility levels -- more specifically the steam levels -- stream data is pre-processed based on problem table algorithm (Klemeš et al., 1997). Each inlet and outlet temperature is shifted according to the minimum temperature approach from process and utilities ($\Delta T_{\text{min}}^{\text{PU}}$). The resulting shifted inlet and outlet temperatures are then considered as relevant utility levels for energy recovery across the site. The relevant temperatures are extracted and sorted from higher to lower to generate a set of discrete temperature levels. In other words, T_1 and T_n represent the highest and lowest temperature of utility levels.

Temperature levels (j) among the site temperature boundaries for steam generation and use are defined as steam level candidates (j_s). Because process heating is mainly done at saturated conditions, in this work, steam level candidates are used to determine the optimal pressure of operation for each steam main. Steam level candidates are further grouped depending on the specified number and pressure ranges of steam mains (denoted by index i).

In addition, heat that cannot be recovered from process can be supplied by utility steam at a very higher pressure (VHP). Utility steam levels are considered as a separate set ($v \in \text{VHP}_L$), which comprises temperature/pressure levels defined by the designer. Note that heat requirements at temperature levels above the maximum pressure allowed for steam distribution (denoted by index j_{ho}), are considered to be satisfied by a hot oil system. In a similar manner, heat sources at temperature levels below the minimum pressure allowed for steam distribution (denoted by index j_{wh}) can be rejected to cooling water.

4.2.2. Utility components superstructure

Process utility systems mainly use steam to meet the heating and power generation demand on the site. Boilers or heat recovery steam generators are used to generate utility steam at VHP level (HRSGs). For steam production, two kinds of boilers are considered -- packaged and field-erected boilers -- which can operate with a set of fossil fuels. HRSGs, fuelled by gas turbine waste gases, can operate in two modes: unfired and with supplementary firing. Steam is distributed through steam mains, in which pressure and temperature are a part of the optimization. Steam is distributed to the different steam mains to provide heat at process streams and/or produce power (via steam turbines). Steam can be expanded from any higher pressure to a lower one through either back-pressure steam turbines or let-down stations. Additionally, depending on the steam main operating conditions, process steam can be recovered/generated at different steam levels. On site-power can be generated by gas turbines (aero-derivative or industrial frame) and steam turbines (i.e. back-pressure or condensing turbines). While back-pressure steam turbines operate between any two pressure levels, condensing turbines expand steam to the condensate steam main to produce additional power. Importing or exporting energy to or from the local grid may be done in the event of an imbalance of power (if allowed). Flash steam recovery systems and deaerators are included in the modelling framework.

A schematic representation of the integrated superstructure is illustrated in Figure 2-2.

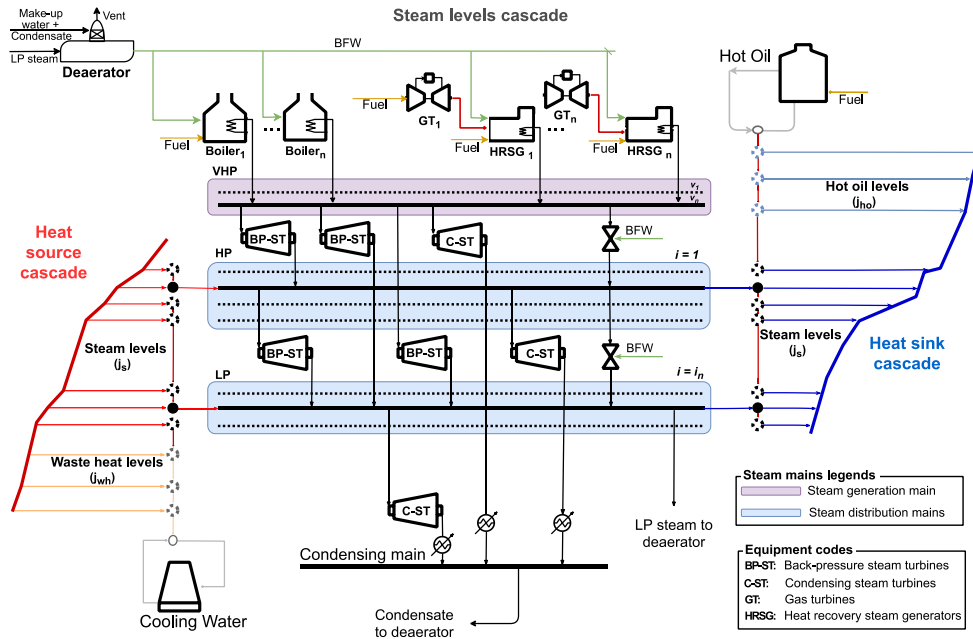


Figure 2-2. Schematic representation of the superstructure
(BFW: boiling feed water, HP: high pressure; LP: low pressure VHP: very high pressure)

4.3. Mathematical model

The general MINLP model for the simultaneous synthesis of utility system with optimal steam level selection comprises the following variables and constraints:

4.3.1. Decision variables:

Variables can be grouped into design and operational variables. Design variables involve discrete and continuous decisions defined by four variable vectors (\mathbf{y} , \mathbf{Z} , \mathbf{m} and λ). The variable vector \mathbf{y} comprises binary variables y_{Eq} , y_L^{HO} , y_L for the selection of conversion technologies, utilities, and steam level pressure respectively. The variable vector \mathbf{Z} contains the continuous variables Z_{eq}^{max} , Z_{eq} that represent the size and load of each equipment. The variable vector \mathbf{m} includes the water/steam flows of utility components (UC) such as steam turbines (m^{ST}), let-down stations (m^{LD}), BFW injected (m^{BFW}), deaerators (m^{deae}) and flash steam recovery (FSR) tanks (m^{FSR}). The variable vector \mathbf{m} also includes process steam generation (m^H) and process steam use (m^C) at the different steam levels L of the energy system. λ contains the operating enthalpy at different distribution steam levels (h_{shL}). Finally, variable vector \mathbf{U}_{cmdty} comprises dependent variables related to commodities consumption such as treated water (U_W), cooling water (U_{CW}), fuels (U_F) and electricity (U_e). Importantly, additional variables may be required to guarantee feasibility of the model.

4.3.2. Constraints

The constraints can be classified into three groups: investment, operational and investment-operational linking constraints.

Investment constraints:

- (i) Equipment selection and sizing.

Operational constraints:

- (ii) Equipment operating load, considering the minimum and maximum allowed load of each conversion unit.
- (iii) Mass and energy balance in each of the steam mains selected, guaranteeing that the energy demand is satisfied.
- (iv) Electricity balance, where the power site demand can be met by power generated on the site or by the grid (if possible). Any additional power generated (if applicable) can be exported to the grid.
- (v) Mass and energy balance at process steam generation and use side, subject to thermodynamic laws.

Investment – operational linking constraints:

- (vi) Equipment performance models at full and part-load.
- (vii) Logical relation between steam levels selected and feasible conversion units operation (guaranteeing that selected equipment can only operate under the conditions selected).

4.4. MINLP model formulation

Based on the problem outlined above and to achieve the best trade-off for system configuration and operation at minimum cost, the problem can be synthetically formulated as follows:

4.4.1. Objective function

The objective function to optimize is given by the minimum total annualised cost (TAC), expressed by the sum of the annualised CAPEX (C^{inv}) and the OPEX of equipment maintenance (C^{main}) and commodities costs for annual site operation (C^{op}), as expressed by Eq. (2.1). Note that *eq* represents the utility equipment for thermal and/or power generation and *comdty* references utility commodities such as fuels, cooling water, treated water and electricity. $F_{\text{eq}}^{\text{ann}}$ identifies the annualization factor of

each equipment, based on an estimated rate of interest and the estimated lifetime of the utility components.

$$\min \text{TAC} = \sum_{\text{eq}} (F_{\text{eq}}^{\text{ann}} \cdot C_{\text{eq}}^{\text{inv}} + C_{\text{eq}}^{\text{main}}) + \sum_{\text{cmdty}} C_{\text{cmdty}}^{\text{op}} \quad (2.1)$$

Investment functions comprise of the purchased cost of the equipment, in addition to their corresponding installation costs (e.g. control systems, contingency, structures, etc.). The installation costs are accounted as a specified factor by term $F_{\text{eq}}^{\text{inst}}$. Capital costs usually increase in relation to the the unit size. Nevertheless, the increment rate tends to decrease as size increases, as illustrated by Figure 2-3. To consider the scale effect (Eq. (2.2a)) and maintain model linearity and robustness, a piecewise affine approximation (PWA) can be used to model the capital cost as a linear dependence with size, as given by Eq. (2.2b). Since the capital cost is a concave function that must be minimized, a binary variable ($y_{\text{eq}, \text{ns}_{\text{eq}}}$) for each linear segment (ns_{eq}) is required to identify the active linear approximation.

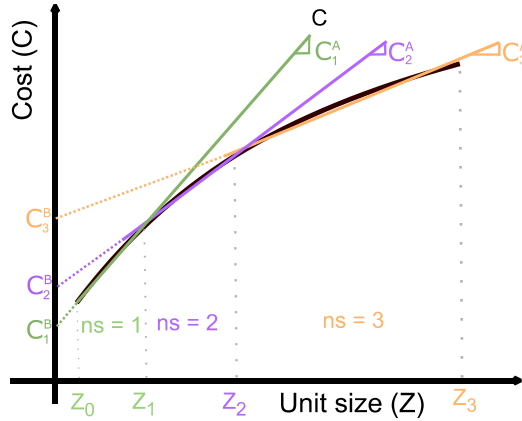


Figure 2-3. Modelling of capital cost of equipment by multiple linear correlations (PWA)

$$C_{\text{eq}}^{\text{inv}} = F_{\text{eq}}^{\text{inst}} \cdot C_{\text{eq}}^{\text{ref}} \left(\frac{Z_{\text{eq}}^{\text{max}}}{Z_{\text{eq}}^{\text{ref}}} \right)^{\rho_{\text{eq}}} \quad \forall \text{eq} \in \text{EEQ} \quad (2.2a)$$

$$C_{\text{eq}}^{\text{inv}} = F_{\text{eq}}^{\text{inst}} \sum_{\text{ns}_{\text{eq}} \in \mathcal{S}_{\text{eq}}} (C_{\text{eq}, \text{ns}_{\text{eq}}}^{\text{A}} \cdot Z_{\text{eq}, \text{ns}_{\text{eq}}}^{\text{max}} + C_{\text{ns}_{\text{eq}}}^{\text{B}} \cdot y_{\text{eq}, \text{ns}_{\text{eq}}}) \quad \forall \text{eq} \in \text{EEQ} \quad (2.2b)$$

In the nonlinear cost function, $C_{\text{eq}}^{\text{ref}}$ is the reference cost for the reference size $Z_{\text{eq}}^{\text{ref}}$ of equipment eq. ρ_{eq} is the exponent for cost calculation, which describe the scale effect of equipment (Eq. (2.2a)). Furthermore, C_{eq}^{A} and C_{eq}^{B} are the model regression coefficients that represent the variable and fixed costs relative to the installed size ($Z_{\text{eq}}^{\text{max}}$) of specific equipment.

Maintenance costs are specified as a fraction ($F_{\text{eq}}^{\text{main}}$) of the annual capital cost.

$$C_{eq}^{main} = F_{eq}^{main} \cdot C_{eq}^{inv} \quad (2.3)$$

The operating costs are given by the sum of the commodity consumption (U_{cmdty}) across the annual site operation (t_{op}) multiplied by its specific cost (P_{cmdty}). Crucially, different fuels can be selected for the range of utility units.

$$C_{cmdty}^{op} = U_{cmdty} \cdot P_{cmdty} \cdot t_{op} \quad (2.4)$$

4.4.2. Equipment selection and sizing

For a specific equipment that is selected, it is assumed that there is a large variety of sizes. Therefore, the size can be assumed to be a continuous variable, constrained by lower and upper limits, as expressed by Eq. (2.5a). Z_{eq}^{max} is a continuous variable representing the installed equipment size (either in MW or t/h, depending on the technology). y_{eq} is a binary variable representing the unit selection, and $\underline{Z}_{eq,ns_{eq}}$ and $\overline{Z}_{eq,ns_{eq}}$ are parameters representing the minimum and maximum equipment capacity at each size range. Note that if the size range is not segmented $S_{n_{eq}}=1$, constraints (2.5b) and (2.5c) are not required, since binary variable $y_{eq,ns_{eq}} = y_{eq}$.

$$\underline{Z}_{eq,ns_{eq}} \cdot y_{eq,ns_{eq}} \leq Z_{eq,ns_{eq}}^{max} \leq \overline{Z}_{eq,ns_{eq}} \cdot y_{eq,ns_{eq}} \quad \forall eq \in EQ \quad (2.5a)$$

$$\sum_{ns_{eq} \in S_{eq}} Z_{eq,ns_{eq}}^{max} = Z_{eq}^{max} \quad \forall eq \in EQ \quad (2.5b)$$

$$\sum_{ns_{eq} \in S_{eq}} y_{eq,ns_{eq}} = y_{eq} \quad \forall eq \in EQ \quad (2.5c)$$

4.4.3. Equipment load

Eq. (2.6) links the installed size of a technology to its actual use and ensures that installed equipment does not operate in unsafe conditions or with low efficiency levels. Under normal circumstances, the equipment efficiency decreases at part load operation. The term $\underline{\Omega}_{eq}$ represents the minimum feasible load operation for the equipment used.

$$\underline{\Omega}_{eq} \cdot Z_{eq}^{max} \leq Z_{eq} \leq Z_{eq}^{max} \quad \forall eq \in EQ \quad (2.6)$$

4.4.4. Electricity balance

Eq. (2.7) ensures that the power demand (θ^e) is met by power generated on-site (W_{eq}) in addition to any grid electricity sold (U_e^{exp}) or purchased (U_e^{imp}). The grid electricity trade may be restricted by limits imposed by the structure of the grid network it is connected to, or alternatively by the contracts

agreed between the site and the grid operator. Either way, limitations are enforced by Eq. (2.8). L^e represents the potential transmission losses

$$U_e^{\text{imp}} - U_e^{\text{exp}} + \sum_{\text{eq} \in \text{EQ}} W_{\text{eq}} = (1+L^e)\widetilde{W}^{\text{dem}} \quad (2.7)$$

$$U_e^{\text{imp}} \leq \widetilde{U}_{\text{max}}^{\text{imp}} \quad \text{and} \quad U_e^{\text{exp}} \leq \widetilde{U}_{\text{max}}^{\text{exp}} \quad (2.8)$$

4.4.5. Steam main mass and energy balance

The different utility components (UC) are connected through steam mains as illustrated in Figure 2-4. The flows from/to UC at steam main i operating at j_s conditions are represented by variables in vectors $m_{\text{UC}_{i,j_s}}^{\text{in}}$ and $m_{\text{UC}_{i,j_s}}^{\text{out}}$. In addition, steam flows related to (indirect) heat integration are described by m_{i,j_s}^{H} and $m_{i,j_s}^{\text{C,steam}}$, representing process steam generation and process steam use at the steam main instant respectively. Moreover, the streams entering the steam header may be introduced at different conditions (e.g. temperature), and consequently an energy balance is required to ensure that the required temperature needed at each steam main is maintained. This is achieved by regulating the injection of either let-down steam or de-superheating water (BFW). In the case of the last steam main, outlet streams to back-pressure steam mains and let-down stations are set to zero and an additional stream is considered to account for the steam directed to the deaerator. Generally, the steam mains' (superheat) temperature is expressed through its corresponding enthalpy ($h_{\text{sh}_{j_s}}$), which in this work is considered as a design variable. The mass and energy balance at each steam main are given by Eqs (2.9) and (2.10). Analogous equations are developed for the VHP steam main.

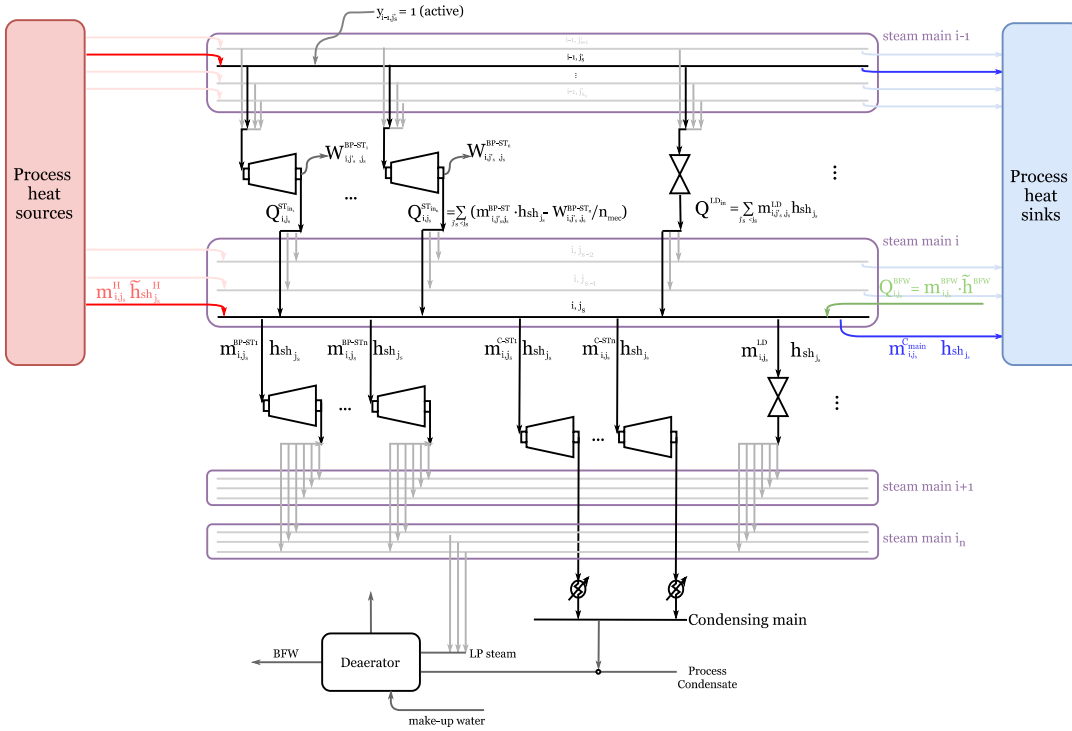


Figure 2-4. Mass balance for i -th steam main
(h_{sh} : superheated steam enthalpy, m : mass flowrate, Q : heat, W : power)

$$m_{i,j_s}^H + \sum_{uc \in UC_L} m_{uc,i,j_s}^{in} = \sum_{uc \in UC_L} m_{uc,i,j_s}^{out} + m_{i,j_s}^{C,steam} \quad \forall i \in I, (i,j_s) \in IJ_s \quad (2.9)$$

$$m_{i,j_s}^H \cdot \widetilde{h}_{sh,j_s}^H + \sum_{uc \in UC} Q_{uc,i,j_s}^{in} = \sum_{uc \in UC} (m_{uc,i,j_s}^{out}) \cdot h_{sh,j_s} + m_{i,j_s}^{C,steam} \cdot h_{sh,j_s} \quad \forall i \in I, (i,j_s) \in IJ_s \quad (2.10)$$

Q_{uc,i,j_s}^{in} represents the heat from the inlet streams to steam main i operating at j_s conditions. For steam turbines and let-down stations, the consideration of different combinations of inlet/outlet conditions is expressed by Eqs. (2.11) and (2.12).

$$Q_{i,j_s}^{LD,in} = \sum_{i' < i} \sum_{(i',j_s') \in IJ_s} (m_{i',j_s',j_s}^{LD} \cdot h_{sh,j_s'}) + \sum_{v \in V} (m_{v,j_s}^{VHP,LD} \cdot h_{sh,v}) \quad \forall i \in I, (i,j_s) \in IJ_s \quad (2.11)$$

$$Q_{i,j_s}^{ST,in} = \sum_{eq \in EQ} \sum_{i' < i} \sum_{(i',j_s') \in IJ_s} Q_{eq,i',j_s',j_s}^{BP-ST} + \sum_{eq \in EQ} \sum_{v \in VHP} Q_{eq,v,j_s}^{VHP, BP-ST} \quad \forall i \in I, (i,j_s) \in IJ_s \quad (2.12)$$

Where: $Q_{eq,i',j_s',j_s}^{BP-ST} = m_{eq,i',j_s',j_s}^{BP-ST} \cdot h_{sh,j_s'} - \frac{W_{eq,i',j_s',j_s}^{BP-ST}}{\eta_{mec}}$ and $Q_{eq,v,j_s}^{VHP, BP-ST} = m_{eq,v,j_s}^{VHP, BP-ST} \cdot h_{sh,v} - \frac{W_{eq,v,j_s}^{VHP, BP-ST}}{\eta_{mec}}$

Index j_s' defines position subset J_s , and is used to restrict heat transfer from higher to lower levels only. For steam turbines the heat contribution comes from the inlet heat minus the work generated considering mechanical efficiency (η_{mec}). In addition, to avoid negative impacts in the blades of turbines due to steam condensation, Eq.(2.13) guarantees that turbine exhausts are superheated or partially condensed. Since steam quality (x_{v1}) should be kept as high as possible -- especially for back pressure steam turbines--, in this work, x_{v1} is limited to be higher than 0.9.

$$Q_{eq, j_s', j_s}^{BP-ST} \geq m_{eq, i', j_s', j_s}^{BP-ST} \cdot x_{vl} \cdot \tilde{h}_{v, j_s} + (1-x_{vl}) \cdot \tilde{h}_{l, j_s} \quad \forall i \in I, i' < i, (i, j_s) \text{ and } (i', j_s') \in IJ_s \quad (2.13)$$

$$Q_{eq, v, j_s}^{BP-ST} \geq m_{eq, v, j_s}^{VHP BP-ST} \cdot x_{vl} \cdot \tilde{h}_{v, j_s} + (1-x_{vl}) \cdot \tilde{h}_{l, j_s} \quad \forall (i, j_s) \in IJ_s$$

4.4.6. Process steam generation and use: heat integration

Figure 2-5 shows a scheme of the heat cascades concept applied for consideration of heat integration. In the heat source cascade, all the heat available is used to generate process steam (m_{i, j_s}^H) at superheated conditions (\tilde{h}_{sh, j_s}^H). Later, it is mixed in the steam main with the other inlet streams at the corresponding steam level. Once the steam main is balanced, generally steam is at an appropriately high temperature to ensure the optimal operation of all utility components across all the steam distribution. However, as previously discussed in the introduction, this is not ideal for process heating itself. For this reason, at the sink side steam should be desuperheated locally prior its use by BFW injection ($m_{i, j_s}^{C BFW}$). Additionally, in this work the potential recovery from flashed steam is considered to further enhance the site energy efficiency. Saturated steam can be recovered from the reduction of condensate pressure at a higher level to meet lower temperature demands. As mentioned in Manuscript 1, although recovering steam directly into the headers (operating at superheated conditions) may benefit power generation, its benefit would likely be offset by the additional energy required to balance the steam mains and prevent excessive condensation. Thus, flash steam recovery (FSR) is assumed to be only used for process heating, as illustrated in Figure 2-5.

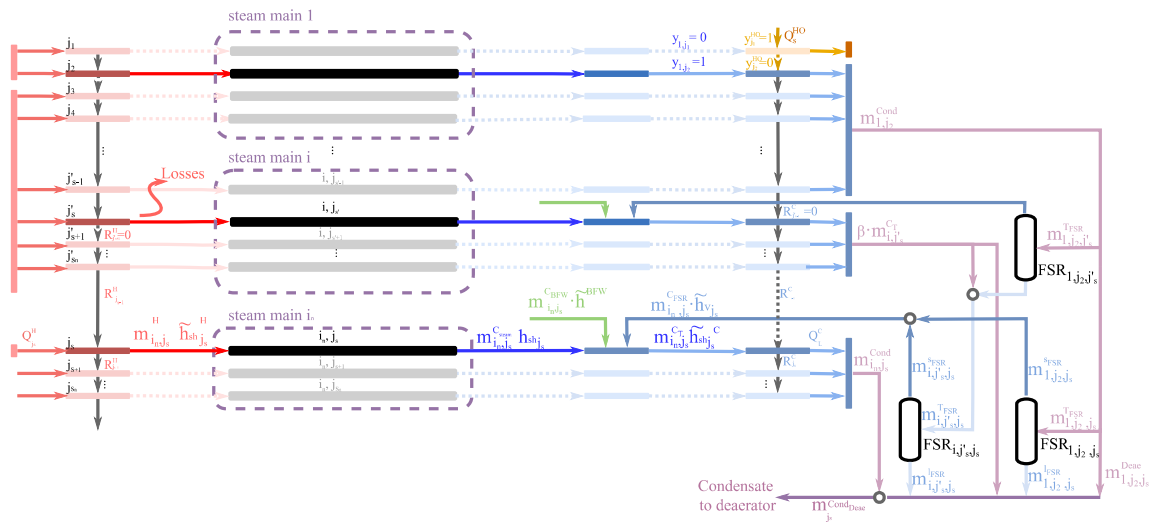


Figure 2-5. Schematic of process steam generation and use (BFW: Boiler feed water, C: heat sinks, Cond: condensate, FSR: flash steam recovery, H: heat sources)

The amount of process steam generated m_{i, j_s}^H and use $m_{i, j_s}^{C steam}$ at each steam level is restricted by thermodynamic constraints, expressed in Eqs.(2.14)-(2.18). Eqs. (2.15) and (2.18) ensure that the energy balance at each level is maintained (first law). Meanwhile, Eqs. (2.14), (2.16) and (2.17) guarantee heat transfer feasibility (second law), while also allowing heat cascading (if required).

Note that due to practical restrictions for steam distribution above 40 bar (Towler and Sinnott, 2013; Smith, 2016b), and to incorporate the option to meet heat demand at high temperature levels, heat flow from hot oil is allowed at the highest steam level, as expressed by Eq. (2.16). Hot oil supply is restricted to the levels where the use of hot oil is favoured by the optimization ($y_{j_s}^{HO} = 1$). Hot oil constraints are based on Manuscript 1 and summarised in Section 4.4.7.

$$\tilde{Q}_{j_s}^H + R_{j_s-1}^H = m_{i,j_s}^H \cdot (1+L^H) \cdot (\tilde{h}_{sh_{j_s}}^H - \tilde{h}^{BFW}) + R_{j_s}^H \quad \forall i \in I, (i, j_s) \in IJ_s \quad (2.14)$$

$$\tilde{Q}_j^H = \sum_{h_i \in H} CP_{h_i}^H \cdot \left(\min(T_{h_i}^{*in}, T_{j-1}) - \max(T_{h_i}^{*out}, T_j) \right) \quad \forall j \in J \quad (2.15)$$

$$m_{i,j_s}^{CT} \cdot (1-L^C) \cdot (\tilde{h}_{sh_{j_s}}^C - \tilde{h}_{i,j_s}^C) + Q_s^{HO} + R_{j_s-1}^C = \tilde{Q}_{j_s}^C + R_{j_s}^C \quad \forall j_s = 1, (i, j_s) \in IJ_s \quad (2.16)$$

$$m_{i,j_s}^{CT} \cdot (1-L^C) \cdot (\tilde{h}_{sh_{j_s}}^C - \tilde{h}_{i,j_s}^C) + R_{j_s-1}^C = \tilde{Q}_{j_s}^C + R_{j_s}^C \quad \forall j_s > 1, (i, j_s) \in IJ_s \quad (2.17)$$

$$\tilde{Q}_j^C = \sum_{c_i \in C} CP_{c_i}^C \cdot \left(\min(T_{c_i}^{*out}, T_j) - \max(T_{c_i}^{*in}, T_{j+1}) \right) \quad \forall j \in J \quad (2.18)$$

$CP_{h_i}^H$ and $CP_{c_i}^C$ are the heat capacity flowrate of hot and cold process streams, respectively. Terms \tilde{Q}_j^H and \tilde{Q}_j^C represent the heat available/required of the process streams involved at each steam level. \tilde{Q}_j^H is defined by heat surplus of all hot streams in the temperature interval $(T_{j-1} - T_j)$, as described in Eq. (2.15). Similarly, \tilde{Q}_j^C is determined by the summation of heat demand of all cold streams in the temperature interval $(T_L - T_{L+1})$, as expressed in Eq. (2.18). Heat that is not used in a particular level flows to the next lower level as residual heat involved in terms $R_{j_s}^H$ and $R_{j_s}^C$. Additionally, heat losses from steam distribution from processes heat sources to the steam system, are accounted by the fixed terms (L^H) in Eq. (2.14). Similarly, losses from the steam system to the processes heat sinks, are considered in term (L^C) in Eq. (2.17).

On the sink side, considerations such as BFW injection (m_{i,j_s}^{CBFW}) and FSR (m_{i,j_s}^{CFSR}) are reflected in the mass and energy balance, given by Eqs. (2.19) and (2.20).

$$m_{i,j_s}^{CT} = m_{i,j_s}^{Csteam} + m_{i,j_s}^{CBFW} + m_{i,j_s}^{CFSR} \quad \forall i \in I, (i, j_s) \in IJ_s \quad (2.19)$$

$$m_{i,j_s}^{CT} \cdot \tilde{h}_{sh_{j_s}}^C = m_L^{Csteam} \cdot h_{sh_{j_s}} + m_{i,j_s}^{CBFW} \cdot \tilde{h}^{BFW} + m_{i,j_s}^{CFSR} \cdot \tilde{h}_{v_{j_s}}^{FSR} \quad \forall i \in I, (i, j_s) \in IJ_s \quad (2.20)$$

Note that, contrary to the steam main enthalpy (h_{sh_L}) -- which is defined by the optimization--, $\tilde{h}_{sh_L}^H$ and $\tilde{h}_{sh_L}^C$ are designer inputs. The degree of superheat at both the sink and source side is an engineering design condition based on the type of heat exchanger design and its limitations. As cited,

high superheat temperatures are not usually preferable due to the poor heat transfer coefficient at superheated conditions.

4.4.7. Equipment performance

For both the thermal and power generator units, the input flows (fuel, supplementary fuel, exhaust gases, and/or electricity) are correlated with output energy (steam for heat and/or power) through the equipment performance curves. Equipment performance curves are usually nonlinear functions that depend on the installed size ($Z_{eq, \theta}^{\max}$), load operation ($Z_{eq, \theta}$) and manufacturer. In this methodology, linear approximations that are widely cited in previous literature (Varbanov, 2004; Shang, 2000; Sun and Smith, 2015) are employed to model equipment performance that accounts for full- and part-load operation. However, other performance models can be easily adapted/included by approximating the performance curves to the form given by Eq.(2.21) using piece wise linear functions, and the state-of-the-art linearization techniques. $\tilde{a}_{eq, \theta}$ and $\tilde{b}_{eq, \theta}$ are model coefficients of equipment eq operating at θ conditions. For instance, in boilers fuel energy (U_f) is used to generate steam from BFW conditions (\tilde{h}^{BFW}) to superheated steam at v conditions ($v \in VHP_L$), as described in Eq. (2.22).

$$U_{cmdty} = \sum_{\theta} \sum_{eq \in EQ} (\tilde{a}_{eq, \theta} \cdot Z_{eq, \theta} + \tilde{b}_{eq, \theta} \cdot Z_{eq, \theta}^{\max}) \quad \forall cmdty \in CMDT \quad (2.21)$$

$$U_f = \sum_{v \in VHP_L} \sum_{eq \in EQ} \left[(h_{sh, v} - \tilde{h}^{BFW}) (\tilde{a}_{11} \cdot Z_{eq, v} + \tilde{a}_{12} \cdot Z_{eq, v}^{\max}) + \gamma \cdot Z_{Eq, v} (\tilde{h}_{1, v} - \tilde{h}^{BFW}) \right] \quad \forall f \in F \quad (2.22)$$

\tilde{a}_{11} and \tilde{a}_{12} involved regressed model coefficients, which account for variations in efficiency. In this work, model coefficients are based on literature data from Varbanov (2004). Additionally, blowdown losses are accounted through the fixed fraction parameter β .

In the case of HRSGs, the remaining heat contained in gas turbine exhausts (Q_{eq}^{exh}) is used to raise steam, as illustrated in Figure 2-6. Part of the heat of the exhaust gases is used in the HRSG ($Q_{eq, v}^{HRSG}$) and the rest is lost to the ambient ($Q_{eq, v}^{loss}$), as expressed by Eq. (2.23). The HRSG comprises three main sections: (i) economizer or preheating stage –pre-, where BFW is heated up to saturation, (ii) evaporator or vaporization –vap-, where saturated water is turned into saturated steam, and (iii) superheater or superheating stage –sh-, where steam is dried and/or superheated to VHP temperature (T_{VHP}).

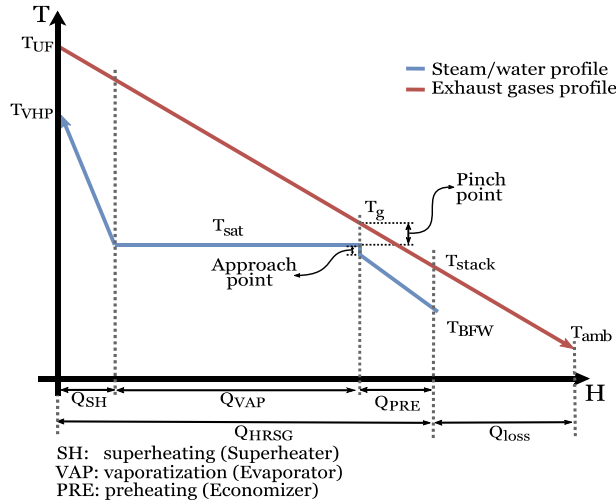


Figure 2-6 Temperature – enthalpy representation of HRSG

$$Q_{eq}^{exh} = \sum_{v \in VHP} [Q_{eq,v}^{loss} + Q_{eq,v}^{HRSG}] \quad \forall eq \in EQ \quad (2.23)$$

$$Q_{eq,v}^{HRSG} = Q_{eq,v}^{sh} + Q_{eq,v}^{vap} + Q_{eq,v}^{pre} \quad \forall eq \in EQ, v \in VHP \quad (2.24)$$

$$Q_{eq,v}^{sh} = \frac{1}{\eta_{eff}^{HRSG}} [(h_{sh_v} - \tilde{h}_{v_v}) \cdot Z_{eq,v}] \quad \forall eq \in EQ, v \in VHP$$

$$Q_{eq,v}^{vap} = \frac{1}{\eta_{eff}^{HRSG}} [(\tilde{h}_{v_v} - \tilde{h}_{l_v}) \cdot Z_{eq,v}] \quad \forall eq \in EQ, v \in VHP$$

$$Q_{eq,v}^{pre} = \frac{1}{\eta_{eff}^{HRSG}} [(\tilde{h}_{pre_v} - \tilde{h}^{BFW}) (1 + \gamma) \cdot Z_{eq,v}] \quad \forall eq \in EQ, v \in VHP$$

The term η_{eff}^{HRSG} comprises the efficiency losses. The subscripts v and l denote the vapor and liquid enthalpy (h) of steam at v pressure level, which are known parameters at the different discrete levels considered ($v \in VHP$).

In contrast with boilers -- where fuel combustion temperature does not present a limitation -- gas turbine exhausts depend on the gas turbine installed size and load. Exhaust gases could only reach temperatures \tilde{T}_{max}^{UF} up to 600 °C (without supplementary firing)(Smith, 2016a). This temperature limitation requires additional constraints to avoid heat transfer infeasibilities at any HRSG section, as expressed by Eqs. (2.25a)- (2.25c).

$$Q_{eq,v}^{loss} \geq m_{exh}^{HRSG} \cdot cp_{exh} (\tilde{T}_{min}^{stack} - \tilde{T}_{amb}) \quad \forall eq \in EQ, v \in VHP \quad (2.25a)$$

$$Q_{eq,v}^{pre} + Q_{eq,v}^{loss} \geq m_{exh}^{HRSG} \cdot cp_{exh} (\tilde{T}_v^{sat} + \Delta T_{min}^{HRSG} - \tilde{T}_{amb}) \quad \forall eq \in EQ, v \in VHP \quad (2.25b)$$

$$Q_{eq,v}^{exh} \geq m_{exh}^{HRSG} \cdot cp_{exh} (T_{sh_v}^{VHP} + \Delta T_{min}^{HRSG} - \tilde{T}_{amb}) \quad \forall eq \in EQ, v \in VHP \quad (2.25c)$$

In many situations, the energy available in gas turbine exhaust gases is insufficient to satisfy the steam requirement. A supplementary burner may be located before the HRSG, where the gases can

be mixed with extra fuel (supplementary firing), as expressed by Eq. (2.26). In this way, the extra fuel energy ($U_{eq,f}^{SF}$) improves the available heat of the gases and the steam generation, without altering the gas turbine's operating load. Because only the extra oxygen in the exhaust gases is utilised, the exhaust gases with additional firing may reach temperatures up to 900°C (T_{max}^{SF}), limited by materials of construction. An extra set of binary variables $y_{eq,f}^{SF}$ is needed to activate a particular fuel (Eq.(2.27)). Temperature constraints are considered by Eq. (2.28), where ζ is an upper bound of the heat which can be provided by exhaust gases. Note that the model assumes that heat capacity of the exhausts (cp_{exh}) and approach temperature (ΔT_{min}^{HRSG}) are pre-specified and constant.

$$\sum_{v \in VHP} Q_{eq,v}^{exh} = Q_{eq}^{exh} + \sum_{f \in F} U_{eq,f}^{SF}, \quad \text{where } U_{eq,f}^{SF} = m_{eq,f}^{SF} \cdot NHV_f \quad \forall eq \in EQ \quad (2.26)$$

$$m_{eq,f}^{SF} \leq \text{Lim}_f y_{eq,f}^{SF} \quad \text{and} \quad \sum_{f \in eq_f} y_{eq,f}^{SF} \leq y_{eq} \quad \forall eq \in EQ, v \in VHP \quad (2.27)$$

$$Q_{eq,v}^{exh} \leq m_{exh}^{HRSG} \cdot cp_{exh} \left(\tilde{T}_{max}^{UF} - \tilde{T}_{amb} \right) + \zeta \cdot \sum_{f \in F} y_{eq,f}^{SF} \quad \forall eq \in EQ, v \in VHP \quad (2.28)$$

$$Q_{eq,v}^{exh} \leq m_{exh}^{HRSG} \cdot cp_{exh} \left(\tilde{T}_{max}^{SF} - \tilde{T}_{amb} \right) + \zeta \cdot \sum_{f \in F} (1 - y_{eq,f}^{SF}) \quad \forall eq \in EQ, v \in VHP$$

Power generated by either gas turbines or steam turbines can be described by Eq. (2.30), based on Willans line correlation (Eq. (2.29)). Λ represents the net heat value (NHV) of gas turbine fuels and the isentropic enthalpy drop (ΔH_{θ}^{IS}) across the steam turbine. $Z_{eq,\theta}$ and $Z_{eq,\theta}^{max}$ are the operating and maximum fuel flow rate for GTs and the steam flowrate for steam turbines. $y_{eq,\theta}$ is the binary variable representing equipment selection at θ operating conditions. For steam mains, θ represents the potential combinations of inlet and outlet level conditions ($\Theta = \{(j_s, j_s') \mid j_s' > j_s\}$), while for gas turbines θ represents the set of fuels available for the gas turbines ($\Theta = GT_F = \{\dots, \text{Natural gas, distillate oil, } \dots\}$). \tilde{a}_{21} , \tilde{a}_{22} , \tilde{a}_{23} and \tilde{a}_{24} comprises the different model coefficients defined by specific inlet conditions and the turbine type. In existing work, the size, load and operating conditions of the utility components are optimized simultaneously.

$$W_{eq} = \sum_{\theta} n_{eq,\theta} \cdot Z_{eq,\theta} + W_{eq,\theta}^{int} \quad \forall eq \in EQ \quad (2.29)$$

$$n_{eq,\theta} = \tilde{a}_{21} \left(\Lambda_{\theta} - \frac{\tilde{a}_{22}}{Z_{eq,\theta}^{max}} \right) \quad \forall eq \in EQ, \theta \in \Theta$$

$$W_{eq,\theta}^{int} = \tilde{a}_{23} \left(\Lambda_{\theta} \cdot Z_{eq,\theta}^{max} + \tilde{a}_{24} \cdot y_{eq,\theta} \right) \quad \forall eq \in EQ, \theta \in \Theta$$

Replacing the slope ($n_{eq,\theta}$) and intercept ($W_{eq,\theta}^{int}$) in Willans Line correlation.

$$W_{eq} = \sum_{\theta} \left[\tilde{a}_{21} \left(\Lambda_{\theta} - \frac{\tilde{a}_{22}}{Z_{eq,\theta}^{max}} \right) Z_{eq,\theta} + \tilde{a}_{23} \left(\Lambda_{\theta} \cdot Z_{eq,\theta}^{max} + \tilde{a}_{24} \cdot y_{eq,\theta} \right) \right] \quad \forall eq \in EQ \quad (2.30)$$

Table 2-1 provides the main equations for the additional utility components, such as flash steam recovery and let-down stations. The equations are based on mass and energy balances of each of the components. Variables m and h represents mass flowrates and enthalpy, respectively.

Table 2-1. Main equations of additional utility components

Component	Equations/Constraints
	Mass balance at the FSR inlet: $\beta \cdot m_{i,j_s}^{CT} + \sum_{i < i'} \sum_{j_s \in IJ_s} m_{i',j_s}^{FSR} = m_{in,i,j_s}^{FSR} \quad (2.31)$
Flash steam recovery (FSR)	Overall mass and energy balance: $\sum_{i > i'} \sum_{(i',j_s) \in IJ_s} (m_{i,j_s}^{FSR} + m_{i',j_s}^{FSR}) = m_{in,i,j_s}^{FSR} \quad (2.32)$ $\sum_{i > i'} \sum_{(i',j_s) \in IJ_s} (m_{i,j_s}^{FSR} \cdot \tilde{h}_{v,j_s} + m_{i',j_s}^{FSR} \cdot \tilde{h}_{l,j_s}') = m_{in,i,j_s}^{FSR} \cdot \tilde{h}_{v,j_s}$
Deaerator (Deae)	Mass and energy balance at the deaerator: $m_T^{BFW} = m^W + \sum_{i \in I} \sum_{(i,j_s) \in IJ_s} m_{i,j_s}^{Cond} + (1-\alpha) \sum_{i'=in} \sum_{(i',j_s) \in IJ_s} m_{i',j_s}^{Deae} \quad (2.33)$ $m_T^{BFW} \cdot \tilde{h}^{BFW} + \sum_{i'=in} \sum_{(i',j_s) \in IJ_s} (\alpha \cdot m_{i',j_s}^{Deae} \cdot \tilde{h}^{vent}) = \sum_{i \in I} \sum_{(i,j_s) \in IJ_s} (m_{i,j_s}^{Cond} \cdot \tilde{h}^{Cond}) + m^W \cdot \tilde{h}^W + \sum_{i'=in} \sum_{(i',j_s) \in IJ_s} (m_{i',j_s}^{Deae} \cdot \tilde{h}_{sh,i,j_s})$
	System mass balance of BFW: $m_T^{BFW} = \sum_{i \in I} \sum_{(i,j_s) \in IJ_s} (m_{i,j_s}^H + m_{i,j_s}^{CBFW} + m_{i,j_s}^{BFW}) + \sum_{eq \in EQ} \sum_{v \in VHP} (m_{eq,v}^{boi} + m_{eq,v}^{HRSG}) \quad (2.34)$
	Overall hot oil supply: $Q_T^{HO} = Q_s^{HO} + Q^{HO} \quad (2.35)$
	Heat provided above T_{max} : $Q^{HO} = \sum_{j \in J^{HO}, T_j \geq T_{max}} \tilde{Q}_j^C \quad (2.36)$
Hot oil system (HO)	Overall energy demand in the sink cascade: $\sum_{i \in I} \sum_{(i,j_s) \in IJ_s} Q_{i,j_s}^{Cin} + Q_T^{HO} = \sum_{j \in J} \tilde{Q}_j^C \quad \text{where } Q_{i,j_s}^{Cin} = m_{i,j_s}^{CT} \cdot (\tilde{h}_{sh,i,j_s}^C - \tilde{h}_{i,j_s}^C) \quad (2.37)$
	$Q_s^{HO} = \sum_{j_s \in J_s, T_{j_s} > T_i^{HO}} (\tilde{Q}_j^C \cdot y_{j_s}^{HO}) \quad (2.38)$
	Logical constraints: $y_{j_s}^{HO} - y_{j_s-1}^{HO} \leq 0 \quad (2.39)$ $y_{j_s}^{HO} + y_{i,j_s} \leq 1$

Note: due to the large number of parameters and variables, the reader is referred to the nomenclature section of this manuscript.

4.4.8. Logical constraints

A simplified version of feasibility constraints are represented by Eq. (2.40). It prevents non-zero flows for non-existing steam level candidates where required. Superscripts in and out represent the inlet and outlet mass (m) and heat (Q) flows at each steam main i operating at j_s conditions. While U^m and U^Q are upper bounds for the steam system, based on the problem specifications. Similar constraints are imposed for the VHP level.

$$m_{i,j_s}^{in} - U^m \cdot y_{i,j_s} \leq 0 \quad \forall i \in I, (i,j_s) \in IJ_s \quad (2.40)$$

$$m_{i,j_s}^{out} - U^m \cdot y_{i,j_s} \leq 0$$

$$Q_{i,j_s}^{in} - U^Q \cdot y_{i,j_s} \leq 0$$

$$Q_{i,j_s}^{\text{out}} - U^Q \cdot y_{i,j_s} \leq 0$$

The VHP main can work only at a single pressure, as expressed in Eq. (2.41). While the option of activating (or not) a steam main is given by Eq. (2.42). Note that only actual steam level candidates L of each steam main can be selected. Thus, for any “forbidden” operating condition $L \notin SL$, y_L is fixed as zero ($y_L = 0$).

$$\sum_{v \in \text{VHP}} y_v = 1 \quad (2.41)$$

$$\sum_{(i,j) \in \text{IJ}_s} y_{i,j_s} \leq 1 \quad \forall i \in I \quad (2.42)$$

Equipment activation depends on the steam level selection. For equipment operating only at one level, such as boilers or HRSG the constraint is given by Eq (2.43). For equipment operating between two levels (e.g. steam turbines), Eq. (2.44) imposes that the unit can only be selected if both inlet and outlet steam mains are active.

$$y_{\text{eq}} \leq y_L \quad \forall L \in \text{IJ}_s \cup \text{VHP}_L \quad (2.43)$$

$$y_{\text{eq}_{L,L'}} \leq \frac{y_L + y_{L'}}{2} \quad \forall \text{eq} \in \text{EQ}, L \in \text{IJ}_s \cup \text{VHP}, L' > L \quad (2.44)$$

Regarding enthalpies, logical boundaries are defined based on the maximum and minimum temperature allowed in each steam main. Eqs. (2.45)-(2.48)

$$\underline{h}_{\text{sh}_v} y_v \leq h_{\text{sh}_v} \leq \overline{h}_{\text{sh}_v} y_v \quad \forall v \in \text{VHP}_L \quad (2.45)$$

$$\underline{h}_{\text{sh}_{j_s}} y_{i,j_s} \leq h_{\text{sh}_{j_s}} \leq \overline{h}_{\text{sh}_{j_s}} y_{i,j_s} \quad \forall i \in I, (i,j_s) \in \text{IJ}_s \quad (2.46)$$

$$h_{\text{sh}_{j_s}} \leq \sum_v h_{\text{sh}_v} \quad \forall j_s \in J_s \quad (2.47)$$

$$h_{\text{sh}_{j_s}} \leq \sum_{(i-1,j_s') \in \text{IJ}_s} [h_{\text{sh}_{j_s}} + \overline{h}_{\text{sh}_{j_s}} (1 - y_{i,j_s}')] \quad \forall i > 1, (i,j_s) \in \text{IJ}_s \quad (2.48)$$

4.4.9. Non-linear terms involved in the MINLP formulation

The presented problem formulation involves several non-linearities in the energy balances and equipment performance models. Table 2-2 highlights the main non-linearities, its type and location.

Table 2-2. Types of non-linearities in the proposed model

No.	Non-linearity	Found in	Type
N ₁	ΔH_0^{IS}	Isentropic enthalpy difference	Non-linear
N ₂	$T_{\text{sh}_v}^{\text{VHP}}$	Temperature of VHP	Non-linear

No.	Non-linearity	Found in	Type
N ₃	$m_{i,j_s}^{C_{steam}} \cdot h_{sh,j_s}$	Steam main and process steam use energy balance	Bilinear
N ₄	$m_{uc,i,j_s}^{out} \cdot h_{sh,j_s}$	Steam main energy balance (outputs)	Bilinear
N ₅	$m_{uc,i,j_s} \cdot h_{sh,j_s}$	Steam level energy balance (inputs)	Bilinear
N ₆	$m_{T_v}^{VHP} \cdot h_{sh,v}$	VHP level energy balance	Bilinear
N ₇	$m_{i,j_s}^{Deae} \cdot h_{sh,j_s}$	Deaerator energy balance	Bilinear
N ₈	$Z_{eq,v}^{max} \cdot h_{sh,v}$	Performance model of thermal generator units	Bilinear
N ₉	$Z_{eq,v} \cdot h_{sh,v}$	Performance model of thermal generator units	Bilinear
N ₁₀	$m_{exh}^{HRSG} \cdot T_{sh,v}^{VHP}$	Performance model of HRSG	Bilinear
N ₁₁	$Z_{eq,\theta} / Z_{eq,\theta}^{max}$	Performance model of power generator units	Fractional
N ₁₂	$\Delta H_{\theta}^{IS} \cdot Z_{eq,\theta}$	Performance model of steam turbine	Bilinear
N ₁₃	$\Delta H_{\theta}^{IS} \cdot Z_{eq,\theta}^{max}$	Performance model of steam turbine	Bilinear
N ₁₄	Z_{eq}^{β}	Objective	Concave

5. MINLP decomposition: Optimization strategy

Due to the combinatorial nature and the nonlinear terms involved in the energy balances of the steam mains, as well as the equipment performance models, the general problem is a nonconvex Mixed Integer Non-Linear Programming (MINLP) formulation. As shown in Table 2-2, most of non-linearities in the proposed problem derive from the definition of steam enthalpy as a variable and its effect on equipment performance. To approach the non-linearities involved and to develop an effective approach, especially for tackling industrial scale problems, the MINLP problem needs to be decomposed. By decomposing the problem, the computational effort can be significantly reduced, while the robustness of the solution can be maintained. For the decomposition two approaches are presented: (1) a sequential MILP followed by simulations, and (2) a bilevel decomposition (rMINLP and NLP decomposition). Notably, while achieving global optimality for these types of nonlinear problems is important and challenging, finding good solutions to practical-scale problems within a reasonable amount of time is crucial for exploring different energy saving opportunities, technology alternatives, and/or scenarios, even if global optimality is not guaranteed. Thus, the authors want to clarify that while the methodology aims to provide the best solutions possible, the aim of this work is not to guarantee global optimality.

5.1. Strategy 1 – STYLE

In the first instance, STYLE model presented in Manuscript 1 is adopted, where the problem is formulated as MILP problem, that replicates the MINLP problem with the exception that steam properties are defined as specified fixed values during the optimization. After the optimisation, the system properties are re-calculated to consider the non-linear effects in the system performance and to calculate the actual steam mains temperatures (and consequently, enthalpies). Once there has been an estimation of new conditions, the optimization parameters are re-defined. This procedure is carried out until the defined and actual values converge. Due to the high degree of non-linearity and the overall complexity involved in the estimation of the steam thermodynamic properties, the simulation stage is carried out in VBA – Excel®. The system thermodynamic properties are calculated by the proposed algorithm for steam main superheating (detailed in Manuscript 1), employing Steam97® Excel Add-In.

5.1.1. MILP formulation

Since the steam enthalpy is fixed (and consequently the T_L^{VHP}) there is no need for linearization of the terms N_1 - N_8 , N_{10} and N_{11} . In addition, the capital costs (N_{12}) of conversion technology are expressed as a linear functions (as shown in Eq. (2.2b)). The fractional term N_{11} (equipment load), can be easily removed by expressing $\left(x_{\theta}^{eq} = \frac{Z_{eq, \theta}}{Z_{eq, \theta}^{max}}\right)$ as a product, and introducing the variable variable $x_{eq, \theta}$, as shown in Eq. (2.49). The resulting nonconvex term is then relaxed into a convex expression, by widely used methodologies, such as McCormick convex envelopes, (Eq. (2.50)). Note that this can be done due to the nature of the fractional term, which has a physical interpretation -- unit load fraction -- , thus the exchange can be easily done. However, this is not always the case for other nonconvexities of this kind. For fractional nonlinearities linearization techniques the reader is referred to Tawarmalani and Sahinidis (2001) and Zamora and Grossmann (1998)

$$x_{eq, \theta} = \frac{Z_{eq, \theta}}{Z_{eq, \theta}^{max}} \text{ or } Z_{eq, \theta} = x_{eq, \theta} \cdot Z_{eq, \theta}^{max} \quad (2.49)$$

$$Z_{eq, \theta} \geq \sigma_{\theta}^{eq} \cdot Z_{eq, \theta}^{max} + \underline{\Omega}_{eq, \theta} \cdot x_{eq, \theta} - \sigma_{\theta}^{eq} \cdot \underline{\Omega}_{eq, \theta} \cdot y_{eq, \theta} \quad (2.50)$$

$$Z_{eq, \theta} \leq Z_{eq, \theta}^{max} + \underline{\Omega}_{eq, \theta} \cdot x_{eq, \theta} - \underline{\Omega}_{eq, \theta} \cdot y_{eq, \theta}$$

$$Z_{eq, \theta} \geq Z_{eq, \theta}^{max} + \overline{\Omega}_{eq, \theta} \cdot x_{eq, \theta} - \overline{\Omega}_{eq, \theta} \cdot y_{eq, \theta}$$

$$Z_{eq, \theta} \leq \sigma_{\theta}^{eq} \cdot Z_{eq, \theta}^{max} + \overline{\Omega}_{eq, \theta} \cdot x_{eq, \theta} - \sigma_{\theta}^{eq} \cdot \overline{\Omega}_{eq, \theta} \cdot y_{eq, \theta}$$

Where σ_0^{eq} represents the steam turbine minimum load, in fraction. $\underline{\Omega}_{\text{eq}, \theta}$ and $\overline{\Omega}_{\text{eq}, \theta}$ define the minimum and maximum equipment capacity in terms of flowrate, respectively. Note that the tightness of the bounds is important due to its impact on the linearization.

Additional, logical constraints are added to ensure the range of the variable $x_{\text{eq}, \theta}$ are included in Eq.(2.51) and (2.52).

$$x_{\text{eq}, \theta} \geq \sigma_0^{\text{eq}} \cdot y_{\text{eq}, \theta} \quad (2.51)$$

$$x_{\text{eq}, \theta} \leq y_{\text{eq}, \theta} \quad (2.52)$$

Based on the above-mentioned modification, Eq. (2.30) can be written as:

$$W_{\text{eq}, \theta} = \widetilde{a}_{21} (\Lambda_{\theta} \cdot Z_{\text{eq}, \theta} - \widetilde{a}_{22} \cdot x_{\text{eq}, \theta}) + \widetilde{a}_{23} (\Lambda \cdot Z_{\text{eq}, \theta}^{\text{max}} + \widetilde{a}_{24} \cdot y_{\text{eq}, \theta}) \quad (2.30a)$$

The resulting MILP problem, defined by Eq. (2.53), is simpler to solve (with state-of-the-art solvers) compared to the original (MINLP) formulation.

$$\text{sMILP} \left\{ \begin{array}{l} \min \text{TAC} \\ \text{s.t. Eqs. (2.2b)-(2.28),(2.30a),(2.31)-(2.44)} \end{array} \right\} \quad (2.53)$$

5.1.2. Calculation of steam mains' superheating

After the optimization stage, the actual superheating can be defined by the mass and energy balances in each steam header. To determine the temperature and superheating needed for each steam main, a top-down iteration is employed, that initialises with the utility steam main (VHP main), assigned in the algorithm as $i = 1$, as illustrated in . The algorithm requires the enthalpies and mass flowrates of all input streams (turbine exhausts, let-down steam, process steam, and BFW) at each steam main. The enthalpy of the turbine exhaust is calculated using the Willans Model of Sun and Smith (2015). On the other hand, the enthalpy of let-down steam are calculated assuming isenthalpic expansion.

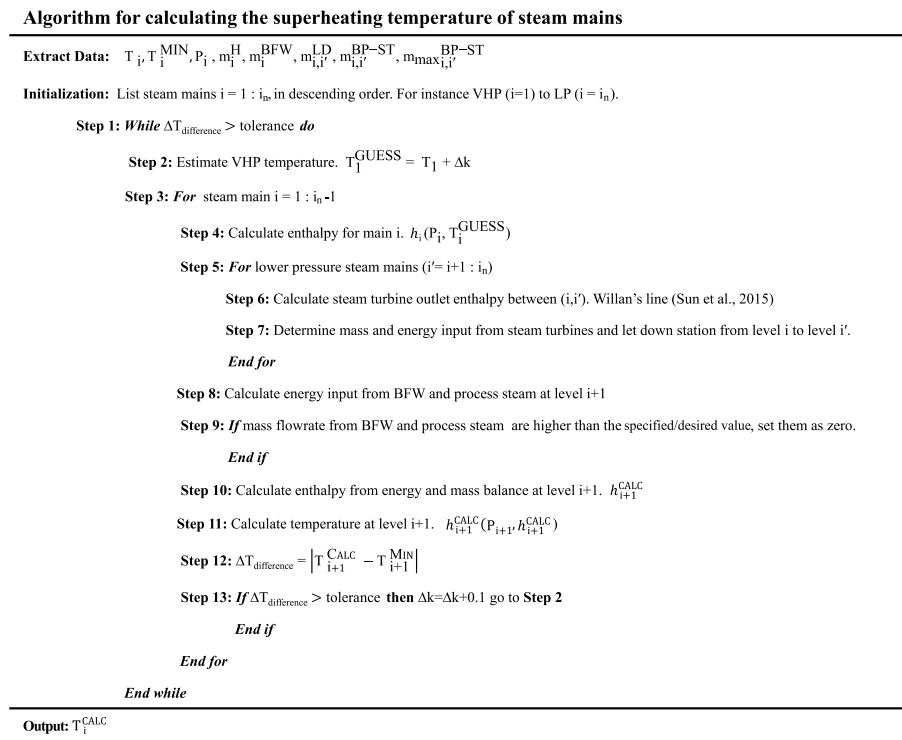


Figure 2-7. Algorithm for calculating steam mains' superheating

The overall strategy 1 (STYLE algorithm) is summarized below

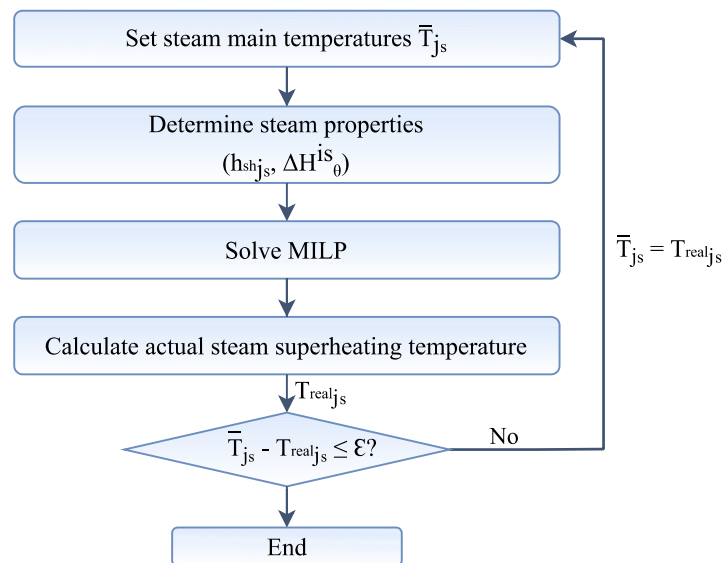


Figure 2-8. STYLE algorithm for synthesis of industrial utility systems taking into account steam mains' operating conditions

5.2. Strategy 2 – BEELINE

The complexity of the MINLP problem comprises not only a large number of discrete decisions but also the non-convex constraints involved. Several global optimization algorithms exist in the literature to address such a complex problem. The most common one (but not the only one) is the

spatial branch-and-bound approach. The success of a spatial branch-and-bound algorithm depends critically on the rate at which the gap between the lower and upper bounds decrease. The convergence rate is closely related to the accuracy (tightness) of the bounds, in addition to the quality and time required to obtain them.

Due to the computational challenges of the problem, spatial branch and bound solvers (i.e. BARON) are less effective for practical-size problems, as shown by the computational results reported later in Section 5. While for small-scale problems, the spatial branch and bound solvers can solve to problem to optimality, for large-scale problems it can present problems to converge. To address this issue, BEELINE, a BilEvel dEcomposition aLgorithm for synthesis of Industrial eNergy systEMs is proposed in this work. Bilevel decomposition, proposed for first time by Iyer and Grossmann (1998), has been widely applied to address large-scale MILP (Dogan and Grossmann, 2006) and MINLP (Lotero et al., 2016; Lara et al., 2018; Elsidio et al., 2019) problems with success. Bilevel decomposition allows the reformulation of the problem into two subproblems: the master subproblem (rMINLP), which is a specific relaxed version of the original problem, and the slave subproblem (NLP), where the continuous variables are (re)optimized. The latter is usually defined as a fixed version of the original problem, which relies on the integer decisions obtained in the master subproblem. The bilevel decomposition is a search algorithm based on the concept that the solution space of a subproblem is part of the feasible region of the original problem. Therefore, the union of all subproblems feasible region should resemble the original feasible region. In this way, the master problem allows for the identification of the subset that contains the optimum solution. The optimal solution, then, is searched in the subset by solving the NLP problem. Each iteration should exclude the explored subsets from the feasible region, until the optimal solution of the full-space model is found. As stated in (Gomes and Mateus, 2017), a master problem can have several quality (near-optimal) solutions, as well as the optimal one. Since the optimal solution of the next iteration may be among these solutions, and with the purpose of reducing the number of iterations, the “solution pool” feature of CPLEX is applied in this work. Solution pool allows for the direct addition of bender cuts during the branch and bound process of the MILP problem. In this way, several quality solutions, in addition to the optimal solution, can be generated when solving the master problem to aid exploring different areas of the solution space in each iteration. These solutions, including the optimal solution, can be ranked, filtered and stored in a set called the solution pool (Corporation, 2017). Finally, in the event that the solution pool is found to be infeasible, then additional integer and logical cuts (described in section 5.4.3) can be added to force the master problem to produce different solutions to those of the solution pool in the next iteration. As a result, this reduces the number of times the master problem must be solved, thereby speeding up the algorithm convergence.

To sum up, the master problem is first solved to generate a pool of feasible solutions (including the master optimal solution), which solutions are ranked and filtered based on the objective value. The best solution provides the lower bound (LB) to the original problem. Next, each one of the solutions are used to locally evaluate the sub problem by fixing the values of binary variables and generates an upper bound UB to the original problem. The iterative process terminates when the optimality condition ($LB \geq (1 - \epsilon) UB$) or no solution improvement is not achieved after a specified number of iterations (e.g. $\max_{iter} = 20$). Otherwise, the solution is removed from the solution pool. Once all the solutions are evaluated, the integer cuts are added to the master problem to exclude previous results and explore different regions.

Note that despite the master (rMINLP) and slave (NLP) problem are easier to solve than the original nonconvex MINLP problem. The NLP sub problem still comprises nonconvex terms, which solution could result in the most expensive part, since global optimization strategies might be still required. Thus, to improve the performance of the algorithm, a good local optimum/feasible solution of the problem is accepted instead, since it still provides a rigorous UB and allows faster convergence (although without guaranteed global optimality).

In the next subsections, the formulation of the master (rMILP) and slave (NLP) problem are presented in detail. Also, some approaches used in the algorithm, such as different linearization techniques and strategies to improve computationally efficiency, are discussed.

5.2.1. rMINLP problem

For convenience, the linearized version of the original MINLP problem is denoted as rMINLP. Based on the non-linearity types presented in Table 2-2, different relaxation techniques are employed to construct the lower bounding MILP problem are presented below.

- i. The bilinear terms of the type (N_3-N_9) in the energy balance of the steam and VHP levels are underestimated using piecewise-linear relaxation (Gounaris et al., 2009) as specified in Section iv.
- ii. The bilinear term N_{10} related to the heat transfer feasibility in the HRSG, as well as the terms N_{12} and N_{13} involved in the turbine performance model, are relaxed using term wise envelopes (McCormick, 1976), according to Section vii.
- iii. The non-linearities of the steam properties (N_1 and N_2) are addressed by linearization of the functions at the superheated stage, as described in Section viii.
- iv. Finally, the non-linearity resulting from the exponential expression of the utility components costs (N_{14}), is linearized using piece-wise affine approximation presented in section 4.4, Eqs. (2.2b) and (2.5).

i. Piecewise MILP relaxation of bilinear terms

As stated earlier, the MILP formulation comprises a linearized and relaxed version of the original MINLP problem. The relaxation involves approximating the feasible region. However, this is at the expense of underestimating the objective function. A relaxation does not replace the original problem, but it provides the lower bound on the optimal objective function (in minimization problems). The relaxation of the bilinear terms plays a key role in the convergence rate of the general problem (Wicaksono and Karimi, 2008). An important factor in the relaxation is the accuracy (tightness) to approximate the original problem and its solution. LP relaxations, such as McCormick (1976) and Al-Khayyal and Falk (1983) are widely used to relax bilinear terms in nonconvex programs. However, LP relaxations are often weak (Wicaksono and Karimi, 2008; Misener and Floudas, 2010). As a remedy, many works have explored the idea of a priori partitioning the search domain leading to a mixed-integer linear program (MILP): a piecewise MILP relaxation (Wicaksono and Karimi, 2008). MILP relaxations have shown to provide superior relaxation tightness compared with not only LP relaxations but also Big-M (BM) and Convex-Hull (CH) formulations (Wicaksono and Karimi, 2008; Misener and Floudas, 2010).

Based on the implications and results presented on the studies of Wicaksono and Karimi (2008) and Misener and Floudas (2010), the **NF4R** formulation (Gounaris et al., 2009) has been used to piecewise-underestimate each of the bilinear terms involved in the energy balances. The bilinear terms are substituted with a placeholder variable Δh_{shL} . Since the enthalpy at each level (h_{shj_s}) is the common variable in most of the bilinear terms, it has been chosen as a partitioning variable. Moreover, a uniformly partition of the enthalpy variables has been selected because it usually produces the tightest relaxation (Gounaris et al., 2009). Each variable is initially partitioned into N segments, as shown in Eq. (2.54). The lower and upper bounds to the enthalpy variables for the energy balances, $\overline{h_{shj_s}}$ and $\underline{h_{shj_s}}$, are given by the minimum superheat temperature required at each level and the limitations of the materials of construction or site specifications, respectively.

$$\widetilde{h_{shn,j_s}} = \underline{h_{shj_s}} + \frac{n}{N} \left(\overline{h_{shj_s}} - \underline{h_{shj_s}} \right) \quad \forall j_s \in J_s, n \in N \quad (2.54)$$

Additionally, an integer variable $y_{n,L}^N$ is introduced to select one singular domain segment, if the steam level is active.

$$y_{n,i,j_s}^N = \begin{cases} 1 & \text{if } \widetilde{h_{shn-1,j_s}} \leq h_{shj_s} \leq \widetilde{h_{shn,j_s}} \\ 0 & \text{else} \end{cases} \quad \forall i \in I, (i, j_s) \in IJ_s, n \in N \quad (2.55)$$

$$\sum_{n \in N} \widetilde{h_{shn-1,j_s}} \cdot y_{n,i,j_s}^N \leq h_{shj_s} \leq \sum_{n \in N} \widetilde{h_{shn,j_s}} \cdot y_{n,i,j_s}^N \quad \forall i \in I, (i, j_s) \in IJ_s \quad (2.56)$$

$$\sum_{n \in N} y_{n, i, j_s}^N = y_{i, j_s} \quad \forall i \in I, (i, j_s) \in IJ_s \quad (2.57)$$

Additionally, Eq. (2.58) restricts the steam main enthalpy to be lower than enthalpy of previous level (if selected)

$$h_{sh, j_s} \leq \sum_{i'=i-1} \sum_{j_s' < j_s} h_{sh, j_s'} + \bar{h}_{sh, j_s} (1 - y_{i', j_s'}) \quad \forall i \in I, (i, j_s) \in IJ_s, (i', j_s') \in IJ_s \quad (2.58)$$

Mass flow rate is defined as a semi-continuous variable. However, due to the combinatorial nature of the problem there is no advantage for determining a nonzero lower bound for m_{n, i, j_s} . The upper bound (\bar{m}_{i, j_s}) was defined based on maximum flows required and/or equipment capacity. Additionally, continuous variables $\Delta m_{n, i, j_s}$ are set as place holders for mass flow rates m_{n, i, j_s} that are nonzero only in the active interval, where they are equal to m_{n, i, j_s} , as shown in Eqs. (2.59)-(2.61).

For simplicity, the logical constraints to linearize the bilinear term necessitated by the steam consumption in the main ($\Delta m_{n, L}^{C_{\text{steam}}}$) are presented. Analogous linearization constraints are applied to the rest of bilinear terms (N₄-N₉).

$$0 \leq \Delta m_{n, i, j_s}^{C_{\text{steam}}} \leq \bar{m}_{i, j_s}^{C_{\text{steam}}} \quad \forall i \in I, (i, j_s) \in IJ_s, n \in N \quad (2.59)$$

$$0 \leq \Delta m_{n, i, j_s}^{C_{\text{steam}}} \leq \bar{m}_{i, j_s}^{C_{\text{steam}}} \cdot y_{n, i, j_s}^N \quad \forall i \in I, (i, j_s) \in IJ_s, n \in N \quad (2.60)$$

$$m_{i, j_s}^{C_{\text{steam}}} = \sum_{n=1}^N \Delta m_{n, i, j_s}^{C_{\text{steam}}} \quad \forall i \in I, (i, j_s) \in IJ_s \quad (2.61)$$

The final relaxation of the bilinear terms is presented in Eqs. (2.62 a) - (2.62 d). Where Eqs. (2.62 a) and (2.62 c), are the under estimators of the function, and Eqs. (2.62 b) and (2.62 d) represent the over estimators.

$$Q_{i, j_s}^{C_{\text{steam}}} \geq \sum_{n=1}^N \bar{\Delta h}_{sh, n, j_s} \cdot \Delta m_{n, i, j_s}^{C_{\text{steam}}} \quad \forall i \in I, (i, j_s) \in IJ_s \quad (2.62 a)$$

$$Q_{i, j_s}^{C_{\text{steam}}} \leq \sum_{n=1}^N \bar{\Delta h}_{sh, n, j_s} \cdot \Delta m_{n, i, j_s}^{C_{\text{steam}}} \quad \forall i \in I, (i, j_s) \in IJ_s \quad (2.62 b)$$

$$Q_{i, j_s}^{C_{\text{steam}}} \geq \bar{m}_{n, i, j_s}^{C_{\text{steam}}} \cdot h_{sh, j_s} + \sum_{n=1}^N \left[\bar{\Delta h}_{sh, n, j_s} \left(\Delta m_{n, i, j_s}^{C_{\text{steam}}} - \bar{m}_{n, i, j_s}^{C_{\text{steam}}} \cdot y_{n, i, j_s}^N \right) \right] \quad \forall i \in I, (i, j_s) \in IJ_s \quad (2.62 c)$$

$$Q_{i, j_s}^{C_{\text{steam}}} \leq \bar{m}_{n, i, j_s}^{C_{\text{steam}}} \cdot h_{sh, j_s} + \sum_{n=1}^N \left[\bar{\Delta h}_{sh, n, j_s} \left(\Delta m_{n, i, j_s}^{C_{\text{steam}}} - \bar{m}_{n, i, j_s}^{C_{\text{steam}}} \cdot y_{n, i, j_s}^N \right) \right] \quad \forall i \in I, (i, j_s) \in IJ_s \quad (2.62 d)$$

It should be noted that when the number of segments is equal to one ($n=1$) the MILP relaxation is equal to the McCormick envelopes, described in the next section.

vii. Convex envelopes relaxation of bilinear terms

As previously stated, LP relaxations such as convex envelopes (McCormick, 1976) can be also used to underestimate bilinear terms. In this work, McCormick (1976) envelopes were preferred to convexify nonlinear terms where prior partitioning of the search domain increase the problem size without a significant change in the objective function. This is the case of bilinear terms involving the isentropic enthalpy difference term (ΔH_{θ}^{IS}), such as $\Delta H_{\theta}^{IS} \cdot Z_{eq, \theta}$ and $\Delta H_{\theta}^{IS} \cdot Z_{eq, \theta}^{max}$. It is important to mention that this simplification is also possible due to the strong correlation between the isentropic enthalpy difference (ΔH_{θ}^{IS}) and the inlet enthalpy of each steam main ($h_{sh\theta}$) – explained in more detail in Section viii -, where piecewise relaxations are already employed to constrain the latter. Besides this, note that both mass flow rate ($Z_{eq, \theta}$) and isentropic enthalpy difference (ΔH_{θ}^{IS}) are semi-continuous variables, which lower bound depends on the selection of the operating conditions θ for unit eq ($y_{eq, \theta}$), involving a mixed-integer bilinear term $\Delta H_{\theta}^{IS} y_{eq, \theta}$. The resultant bilinear term is removed by replacing $\Delta H_{\theta}^{IS} y_{eq, \theta}$ with $\mu_{eq, \theta}$ and adding linear constraints for this term, as described in Eq. (2.64).

$$Q_{eq, \theta}^{IS} \geq Z_{eq, \theta} \cdot \underline{\Delta h}_{is\theta} + \bar{Z}_{eq, \theta} \cdot \mu_{\theta}^{st} - Z_{eq, \theta} \cdot \underline{\Delta h}_{is\theta} \cdot y_{eq, \theta} \quad (2.63)$$

$$Q_{eq, \theta}^{IS} \leq Z_{eq, \theta} \cdot \overline{\Delta h}_{is\theta} + \bar{Z}_{eq, \theta} \cdot \mu_{\theta}^{st} - \bar{Z}_{eq, \theta} \cdot \overline{\Delta h}_{is\theta} \cdot y_{eq, \theta}$$

$$Q_{eq, \theta}^{IS} \geq Z_{eq, \theta} \cdot \overline{\Delta h}_{is\theta} + \bar{Z}_{eq, \theta} \cdot \mu_{\theta}^{st} - \bar{Z}_{eq, \theta} \cdot \overline{\Delta h}_{is\theta} \cdot y_{eq, \theta}$$

$$Q_{eq, \theta}^{IS} \leq Z_{eq, \theta} \cdot \underline{\Delta h}_{is\theta} + \bar{Z}_{eq, \theta} \cdot \mu_{\theta}^{st} - \bar{Z}_{eq, \theta} \cdot \underline{\Delta h}_{is\theta} \cdot y_{eq, \theta}$$

$$\underline{\Delta h}_{is\theta} \cdot y_{eq, \theta} \leq \mu_{eq, \theta}^{st} \leq \overline{\Delta h}_{is\theta} \cdot y_{eq, \theta} \quad (2.64)$$

$$\Delta H_{\theta}^{IS} - \overline{\Delta h}_{is\theta} (1 - y_{eq, \theta}) \leq \mu_{eq, \theta}^{st} \leq \Delta H_{\theta}^{IS}$$

viii. Estimation of steam properties

In general, to define steam properties only two variables are required (e.g. pressure and temperature, temperature and enthalpy, enthalpy and pressure, etc.). In this work, steam operating conditions are defined by pressure and enthalpy. As mentioned before, to reduce the complexity of the problem a discrete number of pressure levels has been assumed. Thus, superheating temperature is involved in the continuous variable of enthalpy. Temperature ($T=f(P, h)$) can be determined after the optimization based on the corresponding pressure and enthalpy. For the VHP steam main only the direct calculation of the temperature is required, but its approximation will be explained in further detail later in this section. In the case of the steam turbine model, Willans line approximation is used to determine its performance at full and part-load. The slope and the

intercept of the Willan's line rely on the isentropic enthalpy change across the steam turbine (ΔH_{is}). ΔH_{is} depends on the inlet and outlet pressure, as well as the inlet temperature/enthalpy. Singh (1997) proposed a regression model based on the saturation temperature difference of expansion (ΔT_{sat}) and the specific heat load of superheated steam contained above saturated liquid ($h_{sh}-h_l$), as given by Eq. (2.65).

$$\Delta H_{is} = \frac{\Delta T_{sat}}{1854 - 1931(h_{sh}-h_l)} \quad (2.65)$$

Singh's correlation is non-linear with respect to the inlet enthalpy, and more importantly presents a deviation up to 10 % with actual steam properties. Therefore, for a turbine with "given" inlet and outlet pressures, a more accurate and linear regression is obtained. The ΔH_{is} term is regressed as a linear function of the specific inlet enthalpy (h_{sh}), as shown in Eq. (2.66). The effects of the operating pressures are introduced through the modelling coefficients a and b, using Eqs. (2.67) and (2.68).

$$\Delta H_{is} = a \cdot h_{sh} + b \quad (2.66)$$

$$a = a_1 \left(\frac{P_{in}}{P_{out}}\right)^6 + a_2 \left(\frac{P_{in}}{P_{out}}\right)^5 + a_3 \left(\frac{P_{in}}{P_{out}}\right)^4 + a_4 \left(\frac{P_{in}}{P_{out}}\right)^3 + a_5 \left(\frac{P_{in}}{P_{out}}\right)^2 + a_6 \left(\frac{P_{in}}{P_{out}}\right) + a_7 \quad (2.67)$$

$$b = b_1 \left(\frac{P_{in}}{P_{out}}\right)^6 + b_2 \left(\frac{P_{in}}{P_{out}}\right)^5 + b_3 \left(\frac{P_{in}}{P_{out}}\right)^4 + b_4 \left(\frac{P_{in}}{P_{out}}\right)^3 + b_5 \left(\frac{P_{in}}{P_{out}}\right)^2 + b_6 \left(\frac{P_{in}}{P_{out}}\right) + b_7 \quad (2.68)$$

The correlating parameters a_1 - a_7 and b_1 - b_7 of Eqs. (2.67) and (2.68) depend on the pressure range considered and it is only valid for inlet steam at superheated conditions.

Table 2-3. shows the modelling coefficients for an operating pressure range between 0.1 and 120 bar and temperatures from saturation to 570 °C. Under these conditions, the correlation estimates the isentropic enthalpy difference with a mean error of 0.8 % and a maximum deviation of 5 %. Overall, the approximation employed to estimate the ΔH_{is} results in sound agreement with the thermodynamic data.

Table 2-3. Modelling coefficients for the estimation of the isentropic enthalpy change across the steam turbine*

Modelling coefficients for linear correlations			
a_1	0.00215130	b_1	-0.00184233
a_2	-0.02287910	b_2	0.01987759
a_3	0.08182395	b_3	-0.07311089
a_4	-0.08098163	b_4	0.08298832
a_5	-0.16623258	b_5	0.09962741
a_6	0.52882032	b_6	-0.2846926
a_7	-0.00008219	b_7	0.00007468
Min error [%]		0.00	
Max error [%]		5.30	
Average error [%]		0.80	

* Operating pressure range between 0.1 and 120 bar, and superheat temperature from steam saturated conditions up to 570 °C.

Regarding the HRSG, and more specifically in the superheating section, it is important to ensure the direct calculation of the steam superheat temperature to guarantee feasible heat transfer, and to estimate the area of the heat exchanger. Superheat temperature ($T=f(P, h)$) could be estimated based on pressure (which is a parameter) and enthalpy (degree of freedom) as shown below. The effect of pressure is included in coefficients a^T , b^T and c^T (detailed in Table 2-4) through Eqs. (2.70) - (2.72).

$$T_{sh_v}^{VHP} = a^T \cdot h_{sh_v}^2 + b^T \cdot h_{sh_v} + c^T \quad (2.69)$$

$$a^T = a_1^T \cdot P_{in} + a_2^T \quad (2.70)$$

$$b^T = b_1^T \cdot P_{in} + b_2^T \quad (2.71)$$

$$c^T = c_1^T \cdot P_{in} + c_2^T \quad (2.72)$$

Table 2-4. Modelling coefficients for the nonlinear calculation of the superheating temperature at VHP level

Modelling coefficients			
a_1^T	9.34150	b_2^T	-586.40561
a_2^T	1225.72724	c_1^T	11.15590
b_1^T	-20.10415	c_2^T	-80.09496
Min error [%]	0.00		
Max error [%]	2.00		
Average error [%]	0.32		

* Operating pressure range between 40 and 120 bar, and superheat temperature from steam saturated conditions up to 570 °C.

Despite the non-linearity, Eq. (2.69) involves a single variable. Therefore, it can easily be replaced by a sufficiently dense set of linear constraints without introducing binary variables, as shown in Eq. (2.73). This leads to a rigorous underestimation of the function of temperature, proposed in this work, which is strictly convex and monotonic in the range applied. Therefore, a lower bounding of convex functions -- as this is -- does not raise the computational complexity. Moreover, this approach is justified since in the HRSG, the heat transfer feasibility is limited by the superheating temperature required (implicitly defined by Eq.(2.25c)). Thus, it is desirable to achieve the minimum superheat temperature possible to increase the steam generation from the same heat flow.

$$T_{sh_v}^{VHP} \geq a_{sx}^T \cdot h_{sh_v} + b_{sx}^T \quad (2.73)$$

Where sx is the index for set S_x , of linearization with parameters a_{sx}^T and b_{sx}^T . These correlating parameters are calculated through Eqs. (2.70) and (2.72). In this methodology, the formulation for superheat temperature of the VHP level is linearized with three intervals, but it can be easily extended to multiple intervals where there will be a trade-off between the accuracy of the approximation and the size of the problem.

Table 2-5. shows the correlating coefficients for an operating pressure range between 40 and 120 bar and temperatures from saturation to 570 °C. Under these conditions, the correlation estimates the VHP temperature with a mean error of 0.3 % and a maximum deviation of 2.3 % in comparison with the thermodynamic values. In general, the estimation used for $T_{sh_v}^{VHP}$ is in a good agreement with real data. Moreover, in the results section a comparison between the power generated by employing state-of-the-art water properties model (IAPWS) and the proposed functions is presented.

Table 2-5. Modelling coefficients for the linear estimation of the superheating temperature at VHP level

	Segment 1	Segment 2	Segment 3
a_{sx1}^T	-5.566	-4.010	-2.621
a_{sx2}^T	1405.353	1660.220	1668.420
b_{sx1}^T	5.520	4.228	2.962
b_{sx2}^T	-889.133	-1106.817	-1114.563
Min error [%]	0.00		
Max error [%]	2.29		
Average error [%]	0.26		

Finally, the rMINLP problem is defined by Eq. (2.74). The rMINLP comprises a relaxed version of the original problem. In addition, integer cuts Eq. (2.76) (further detailed in Section iii) are incorporated to the model to exclude binary solutions already explored in the NLP problem. In this way a lower bound of the original problem is obtained.

$$\text{rMINLP} \left\{ \begin{array}{l} \min \text{TAC} \\ \text{s.t. Eqs. (2.2b)-(2.28),(2.30a),(2.31)-(2.48),(2.54)-(2.68),(2.70),(2.71),(2.73),(2.76)} \end{array} \right\} \quad (2.74)$$

5.2.2. NLP problem

Based on the results of the MILP optimization, continuous variables (i.e. steam mass flow-rates, heat duties, equipment load, steam main superheat) are re-optimized. For this sub problem, discrete variables (i.e. steam pressure level selection and utility system configuration) are assumed to be fixed. The sub-problem involves essentially the bilinear terms of the energy balance, yielding a nonconvex nonlinear program (NLP). To improve the NLP solver convergence, the values of the continuous variables found in the solution pool of the rMINLP master problem are given as starting point. If viable, the NLP solution becomes in a valid upper limit for the original problem (MINLP). Moreover, the values of the variables in the NLP solution are used to update the linearization of the constraints (lower and upper boundaries) adopted in the rMINLP problem.

$$\text{NLP} \left\{ \begin{array}{l} \min \text{TAC} \\ \text{s.t. Eqs. (2.2a)-(2.28),(2.30a),(2.31)-(2.40),(2.45)-(2.48),(2.49)} \end{array} \right\} \quad (2.75)$$

5.2.3. Improving computational efficiency

i. Initialization and bound tightening

To reduce the number of iterations and therefore the convergence time required by the algorithm, to initialize the bilevel decomposition, the MILP problem suggested in strategy 1 (Eq. (2.53)) is solved. From its resolution, a pool of feasible solutions (including the optimal integer solution) is obtained to initialize the continuous variables using the current values of the binary variables, and minimize the NLP subproblem. Note that for the MILP problem, steam properties are fixed, and as a consequence cannot provide a valid lower bound for the MINLP problem. Nevertheless, it allows a first estimate of the energy targets and potential configurations, to define/tight boundaries of the comprising variables.

ii. Solution pool

A solution pool, is a feature of the CPLEX solver that enables the generation and storage of multiple solutions (in addition to the optimal) of mixed integer problems (Corporation, 2017). This feature is particularly useful when relaxing constraints (especially when they are difficult to linearize efficiently). Once the master problem is solved, the solution pool provides multiple (near-optimal) solutions that can be evaluated in the NLP problem. In this way, different subsets of the solution space can be examined in each iteration, thus reducing the computational time. If the solution lies within a tolerance of the lower bound, the algorithm will terminate. Otherwise, the solution is removed from the solution pool and added as an integer cut in the MILP (to avoid exploring suboptimal solutions in the following iterations). Note that the time involved in each generation of the solution pool depends on multiple factors, such as number of solutions to be evaluated, population strategy selected, relative gap, among others. For more information on this, the reader is referred to Corporation (2017).

iii. Setting priorities and integer cuts

Note that in this work, the binary variables involved in the problem reflect choices that fall into two broad categories: (i) selection of utility levels (and their corresponding enthalpy range) and (ii) installation of utility components (equipment). The latter, strongly depends on the selection of the utility levels, not only because it defines the inlet/outlet operating pressures (and therefore its performance), but also because it limits the potential process energy integration, influencing the system energy requirement. For instance, the choice of steam turbine (and its performance) will depend on the inlet and outlet steam pressure selected. Therefore, the selection of utility levels is a key variable due to its impact on the operating costs, but also on the optimal layout and performance of the overall system. Based on this insight of the aforementioned problem, and to help structure the

problem, an order priority is imposed to ensure that selection of the utility levels is completed before the selection of utility components. The model option “prioropt” (prioropt = 1) in CPLEX/GAMS is used to specify that binary variables must be branched first while solving the master problem. High priority variables (lower values of .prior attribute), are branched on before those with lower priorities (Corporation, 2017). In this way, the number of nodes searched can be dramatically reduced without sacrificing performance, leading to time savings. Even though priorities are seldom required, preliminary results (not reported here for sake of conciseness) indicate that the optimization without them requires greater computational time and may provide inferior solutions. Note that priority is only assigned to the binary variables related to the utility level selection ($y_{n,L}^N, y_L$), no priority is given to the conversion technologies.

Once the NLP sub-problem is solved, additional constraints (called cuts)(Iyer and Grossmann, 1998), are added to the master problem to integrate information provided in the previous master problem and the last slave sub problem, to exclude previous feasible solutions and derive an alternative solution. Eqs. (2.76) and (2.77) are used as integer cuts

$$\sum_{y_{Eq} \in \tilde{y}_{Eq}^{ite}=1} y_{Eq} - \sum_{y_L \in \tilde{y}_{Eq}^{ite}=0} y_{Eq} \leq \sum_{y_{Eq}} \tilde{y}_{Eq}^{ite} - 1 \quad (2.76)$$

$$\sum_{y_{n,L} \in \tilde{y}_{n,L}^{ite}=1} y_{n,L} - \sum_{y_{n,L} \in \tilde{y}_{n,L}^{ite}=0} y_{n,L} \leq \sum_{y_L} \tilde{y}_{n,L}^{ite} - 1 \quad (2.77)$$

$\tilde{y}_{n,L}^{ite}$ and \tilde{y}_{Eq}^{ite} represent the selection of utility level node and equipment selection at iteration *iter*, respectively. Note that the integer cuts accumulate along the iterations.

A scheme of the proposed strategy 2 is shown in Figure 2-9

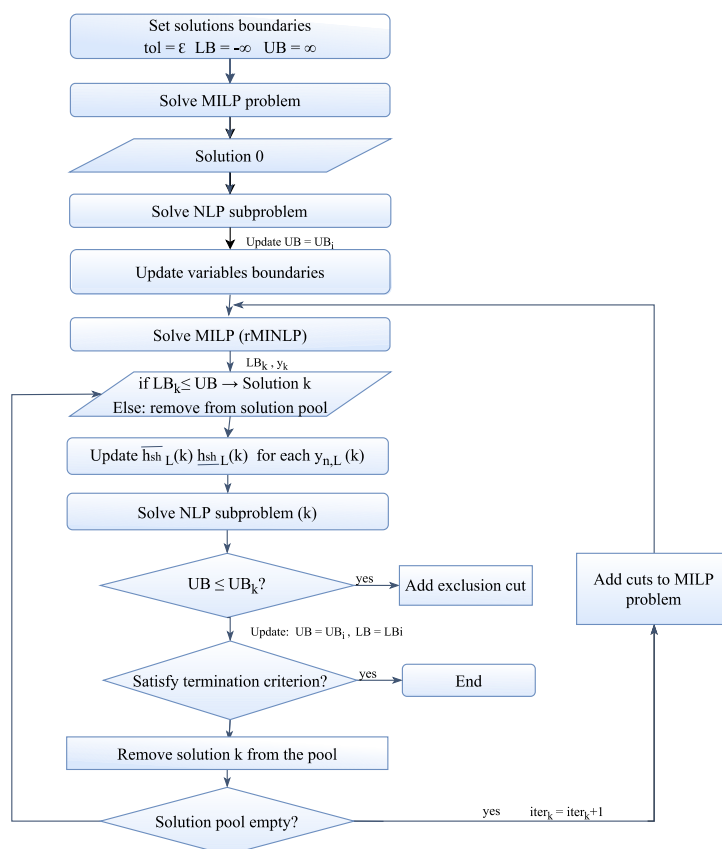


Figure 2-9. Scheme of optimization strategy 2

To sum up, two strategies are proposed to reduce the complexity of the nonconvex MINLP problem. In the first case -- strategy 1, a sequential MILP formulation -- comprising a MILP optimization for the steam levels and equipment selection, followed by a simulation stage where the steam properties are recalculated to provide a feasible solution where the superheat temperature of the steam is included. Note that although the quality of the solution cannot be determined, it provides a fast alternative to explore potential site heat recovery through the utility system, while also allowing different energy conversion technologies. In the second case, strategy 2, aims to provide a more rigorous methodology by employing a solution pool based bilevel decomposition, where the original MINLP problem is decomposed in a relaxed version of the MINLP problem and a NLP subproblem. For the bilevel decomposition, steam properties calculations are approximated with greater accuracy for the superheated zone (which is convex in the analysed zone).

6. Case studies

To illustrate the applicability and power of the proposed framework and solution strategy, 12 examples of different scales are considered in this section. The examples correspond to three case studies taken from the literature (Varbanov et al., 2005) and real-world cases (Sun et al., 2015; Oluleye, 2015). The different case studies are detailed below:

- Tests 1-4 are based on the (Varbanov et al., 2005) case study, which provides the total site profiles (TSP) of an industrial process. The TSP comprise 20 temperature intervals/levels. Process energy can be recovered through steam across 10 potential steam pressure levels based on the kink points. Site power demand is 25 MW, and is assumed operated 8640 h y⁻¹.
- Tests 5-8 are based on the real-world example presented in (Sun et al., 2015). The industrial site comprises 5 chemical processes, where 23 hot streams require a cold utility and 13 cold streams require hot utility. Steam mains can be allocated across 24 potential steam operating pressures based on the kink points. The site has a power demand of 40 MW, and is assumed to operate for the entire year (8760 h y⁻¹)
- Finally, Tests 9-12 are based on the real-world example presented in (Oluleye, 2015) in which heat from 4 chemical processes is recovered through a utility system. The site involves 51 hot streams connected to a cold utility, while 23 cold streams require hot utility. Steam mains can be allocated among 35 potential steam level candidates. The site requires 15 MW of power, and operates 8640 h y⁻¹.

In addition, each of the case studies are analysed under two different scenarios which can affect the synthesis of the utility systems and/or the optimum operating conditions. Importantly, in relation to the problem formulation, the different scenarios described below only affect the interactions with the electricity grid (expressed by Eqs. (2.7) and (2.8)). The scenario analysis does not affect the number of variables involved in the formulation of each case study (summarized in Table 2-6).

Scenario 1: The utility system acts as a stand-alone system. This means that interactions between the utility system and the grid are not considered. The utility system must be designed to meet the site energy demand.

Scenario 2: The utility system acts as a microgrid, which is connected to the national electricity grid. Electricity from the macro grid can be imported to meet the electricity demand that cannot be satisfied via onsite power generation. Furthermore, revenues from selling electricity are possible. Since in practical situations, the import/export of electricity is usually restricted to an agreed value, in this work 10 and 5 MW are assumed as limits for import and export of electricity, respectively.

Capital and technical data of utility components considered for the synthesis of the utility system, as well as additional data of the site, are detailed in Supplementary Information P2.A

For all tests, the MILP and the rMINLP problems are solved with CPLEX 20.1.0.0 (Corporation, 2017), while the NLP subproblem is solved CONOPT 3 (Drud, 1985). Although the NLP subproblem still includes nonconvexities, local optimal solutions provide rigorous upper bounds - potentially higher than those attained with global solvers. Moreover, despite the algorithm

converging, it cannot be guaranteed that a global optimal solution will be reached. For this reason, preliminary tests were carried out to assess the computational time and upper bound quality yield. For this formulation -- where the nonlinearities mainly arise from bilinear terms -- the preliminary computational tests (see Supplementary Information P2.B) showed that, despite the use a local solver, there is no significant difference in the results. Crucially however, the subproblem is solved at lower computational costs.

6.1. Model comparison

The results of the two strategies are compared with the direct solution of the nonconvex MINLP problem solved directly with the global MINLP solver BARON 19.12.7 (Tawarmalani and Sahinidis, 2005). Table 2-6 summarizes the test examples to be evaluated and their corresponding model statistics. Computational results are reported in Table 2-6. The best solution found (TAC), best solution possible and the computational time of the different strategies are set out.

Table 2-6 Model parameters and statistics of the six test examples

Test	Reference	No. steam mains	Power site demand [MW]	Integration HO and FSR	No. variables	No. equations
1		2		no	1327 (113 binaries)	1331
2	Varbanov et al. (2005)	2	25	yes	1544 (141 binaries)	1485
3		3		no	18052 (132 binaries)	1588
4		3		yes	2106 (168 binaries)	1789
5		3		no	8 165 (512 binaries)	5 816
6	Sun et al. (2015)	3	40	yes	9 550 (709 binaries)	6 879
7		4		no	10 404 (542 binaries)	6 340
8		4		yes	11 123 (757 binaries)	7 522
9		3		no	16 048 (957 binaries)	10 713
10	Oluleye (2015)	3	15	yes	18 457 (1354 binaries)	12 147
11		4		no	20 080 (1107 binaries)	11 282
12		4		yes	21 817 (1442 binaries)	13 561

Table 2-7. Computational results of the test problems

Test Case	BARON	sMILP	Bilevel decomposition
Test 1. Scenario 1			
Best solution found, M€/y	30.487	30.090	30.487
Best possible, M€/y	30.456	N/A	30.456
Computational time, s	319.1	31.2	190.2
Test 1. Scenario 2			
Best solution found, M€/y	27.638	28.651	27.641
Best possible, M€/y	27.610	N/A	27.610
Computational time, s	224.8	33.1	106.7
Test 2. Scenario 1			
Best solution found, M€/y	24.989	25.479	24.989
Best possible, M€/y	24.974	N/A	24.963
Computational time, s	612.3	32.4	307.1
Test 2. Scenario 2			
Best solution found, M€/y	24.901	24.832	24.901
Best possible, M€/y	24.876	N/A	24.874
Computational time, s	497.4	30.2	382.2
Test 3. Scenario 1			
Best solution found, M€/y	27.182	28.025	27.182
Best possible, M€/y	27.082	N/A	27.081
Computational time, s	5631.2	23.4	515.0
Test 3. Scenario 2			
Best solution found, M€/y	25.514	26.717	25.511
Best possible, M€/y	26.489	N/A	25.489
Computational time, s	6482.1	26.5	789.1
Test 4. Scenario 1			
Best solution found, M€/y	24.164	25.201	24.164
Best possible, M€/y	24.140	N/A	24.138
Computational time, s	5144.2	38.1	877.3
Test 4. Scenario 2			
Best solution found, M€/y	22.919	23.927	22.919
Best possible, M€/y	22.896	N/A	22.897
Computational time, s	8930.7	33.5	959.1
Test 5. Scenario 1			
Best solution found, M€/y	66.993	66.380	66.738
Best possible, M€/y	34.506	N/A	63.047
Computational time, s	(20000 limit)	77.8	1716.3
Test 5. Scenario 2			
Best solution found, M€/y	65.593	64.460	64.863

Test Case	BARON	sMILP	Bilevel decomposition
Best possible, M€/y	37.118	N/A	60.211
Computational time, s	(20000 limit)	102.7	1643.2
Test 6. Scenario 1			
Best solution found, M€/y	55.395	56.010	55.167
Best possible, M€/y	31.540	N/A	54.271
Computational time, s	(20000 limit)	104.5	2120.2
Test 6. Scenario 2			
Best solution found, M€/y	54.859	54.718	53.891
Best possible, M€/y	30.848	N/A	52.659
Computational time, s	(20000 limit)	85.3	2613.3
Test 7. Scenario 1			
Best solution found, M€/y	66.002	65.481	65.136
Best possible, M€/y	32.914	N/A	62.742
Computational time, s	(20000 limit)	81.4	2124.1
Test 7. Scenario 2			
Best solution found, M€/y	64.657	63.98	64.221
Best possible, M€/y	31.156	N/A	62.192
Computational time, s	(20000 limit)	94.3	2350.5
Test 8. Scenario 1			
Best solution found, M€/y	57.418	56.178	55.289
Best possible, M€/y	30.695	N/A	54.223
Computational time, s	(20000 limit)	98.1	2410.3
Test 8. Scenario 2			
Best solution found, M€/y	56.283	54.901	53.844
Best possible, M€/y	29.286	N/A	52.857
Computational time, s	(20000 limit)	101.3	2603.2
Test 9. Scenario 1			
Best solution found, M€/y	12.301	12.386	12.16
Best possible, M€/y	9.281	N/A	10.02
Computational time, s	(20000 limit)	61.5	1442.1
Test 9. Scenario 2			
Best solution found, M€/y	11.667	12.351	11.65
Best possible, M€/y	8.431	N/A	9.924
Computational time, s	(20000 limit)	58.7	1541.2
Test 10. Scenario 1			
Best solution found, M€/y	11.981	12.303	11.891
Best possible, M€/y	9.059	N/A	10.247
Computational time, s	(20000 limit)	142.2	1829.8
Test 10. Scenario 2			

Test Case	BARON	sMILP	Bilevel decomposition
Best solution found, M€/y	12.315	12.112	11.405
Best possible, M€/y	8.281	N/A	9.987
Computational time, s	(20000 limit)	420.3	1951.7
Test 11. Scenario 1			
Best solution found, M€/y	11.890	12.103	11.788
Best possible, M€/y	8.592	N/A	10.068
Computational time, s	(20000 limit)	58.1	2130.9
Test 11. Scenario 2			
Best solution found, M€/y	11.715	11.781	11.475
Best possible, M€/y	8.658	N/A	10.504
Computational time, s	(20000 limit)	62.1	2411.3
Test 12. Scenario 1			
Best solution found, M€/y	11.981	12.012	11.842
Best possible, M€/y	8.276	N/A	9.440
Computational time, s	(20000 limit)	145.2	2511.3
Test 12. Scenario 2			
Best solution found, M€/y	11.738	11.624	11.252
Best possible, M€/y	7.414	N/A	9.235
Computational time, s	(20000 limit)	306.9	2621.2

As observed in Table 2-7 the state-of-the-art solver is able to solve to global optimality in tests 1 to 4 with finite computational time (up to three hours). Nevertheless, for real-case studies (tests 5-12) the global solver has a slow converge and requires large computational times reaching the maximum computational time limit (20000 seconds). Moreover, the optimality gap between the best solutions found and the best possible is at least 40 %, reaching 100 % for some cases (e.g Tests 5 and 7). On the other hand, the bilevel decomposition algorithm presents similar results and computational times for small scale cases, without a significant difference in the solution quality and/or computational time. Nevertheless, for large-scale MINLP cases, the bilevel decomposition algorithm provides solutions with superior quality to the state-of-the art global solver BARON, and with at least one order of magnitude reduction of the computational time.

Note that although the sequential approach sMILP (strategy 1) cannot be considered as rigorous, an estimation of the lower bounds of the original problem (since temperature/enthalpy are assumed fixed during the optimization and are only simulated), it can provide a feasible solution with a good estimation of the most promising objective functions so far found (up to ± 10 % from the best objective function found). An added benefit is low computational time (minutes). This is relevant since for large-scale problems the global solver could spend considerable time (up to 2 hours) trying to find a feasible initial point.

For the comparison of the system configurations reached by strategy 1 and strategy 2, the best solution attained for Case Study 2 (Test 6. Scenario 2) are illustrated in Figure 2-10 and Figure 2-11 for the system configuration of strategy 1 and 2, respectively. Both optimization strategies favour the integration of a hot oil system for the higher temperature levels, requiring only 2 steam mains. In relation to the equipment, both employ a gas turbine coupled with a HRSG and two steam turbines. Nevertheless, the configuration obtained by the successive MILP favours steam operation at 14 bar for the MP header and steam expansion from the VHP level for both turbines, while the bilevel decomposition best solution achieved selects the MP steam main operating at 20 bar, and steam turbines operating in series. This, in combination with the incorporation of the steam enthalpy headers as an optimization variable in the bilevel decomposition strategy, results in a 1.3 % increment of the total costs. A brief analysis, optimizing the utility system at the steam pressures provided by the sMILP formulation shows that one of the challenges of such problems is the high combinatorial nature of the system, where not only different equipment configurations, but enthalpy-pressure combinations, and steam generation/use trade-offs can lead to feasible and yet non-optimal solutions when minimizing or maximising a single variable. Figure 2-12 illustrates how completely different operating conditions for the MP steam main (operating at 14 bar and 267 °C in Figure 2-10) from the best obtained solution found (operating at 20 bar and 295.5 °C in Figure 2-11) has a total cost difference of only 0.3%, and 2.6 % of the best known lower cost. For this reason, and despite the use of the MILP formulation as a good initial guess to obtain promising solutions, generating diverse enough solutions of the rMINLP is still computationally expensive.

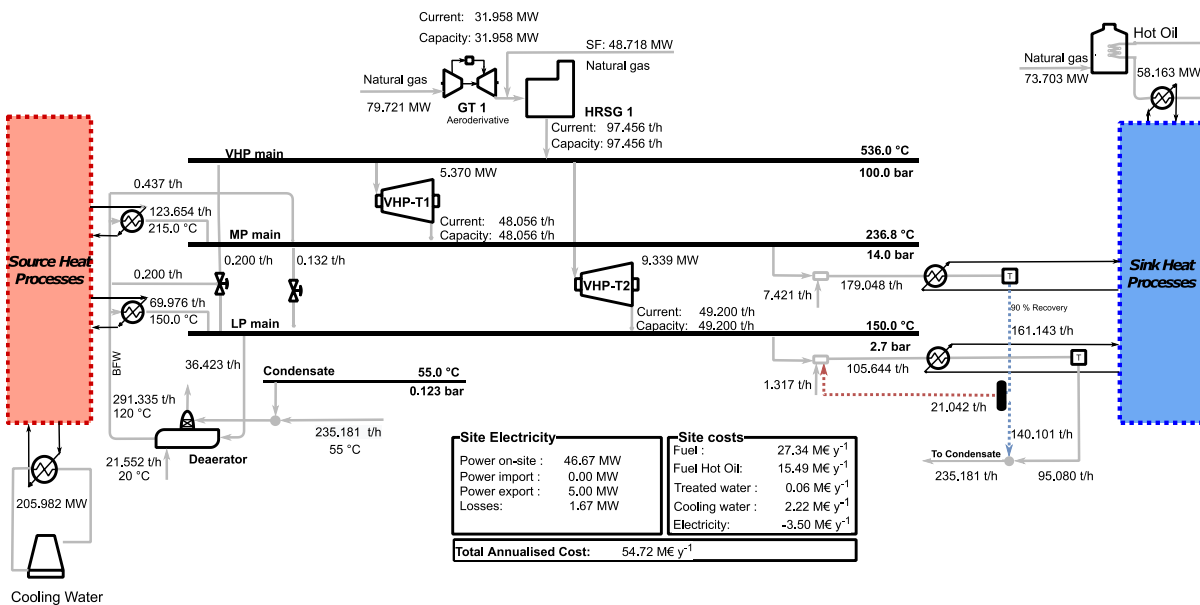


Figure 2-10. Utility system configuration obtained with a successive MILP strategy or test 6 under scenario 2

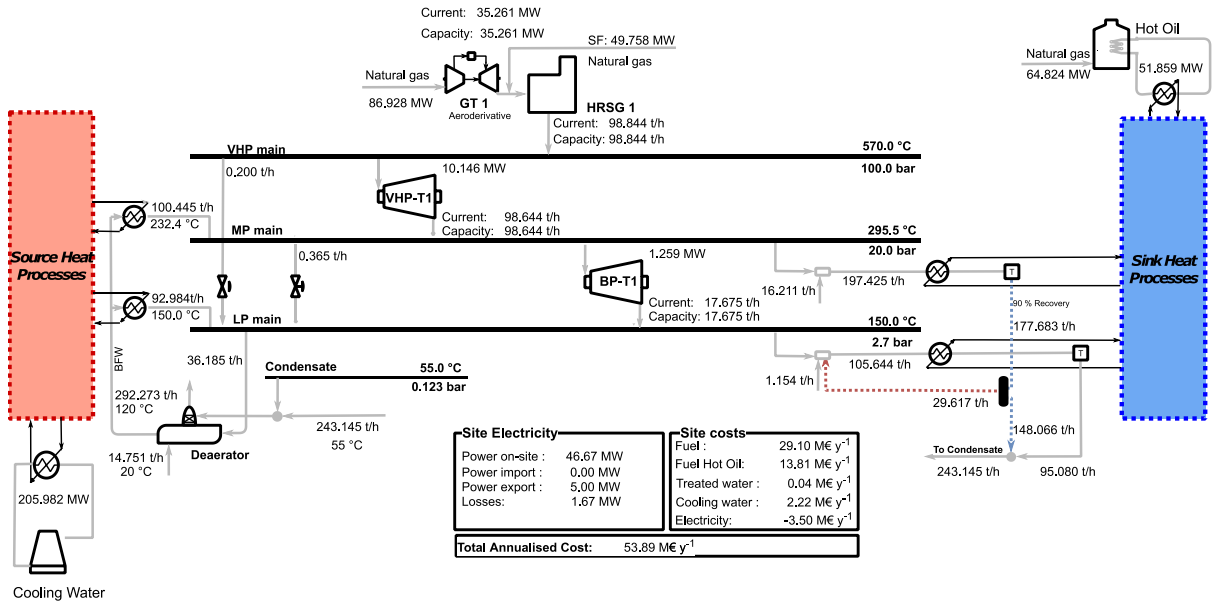


Figure 2-11. Utility system configuration obtained with the bilevel decomposition strategy for test 6 under scenario 2

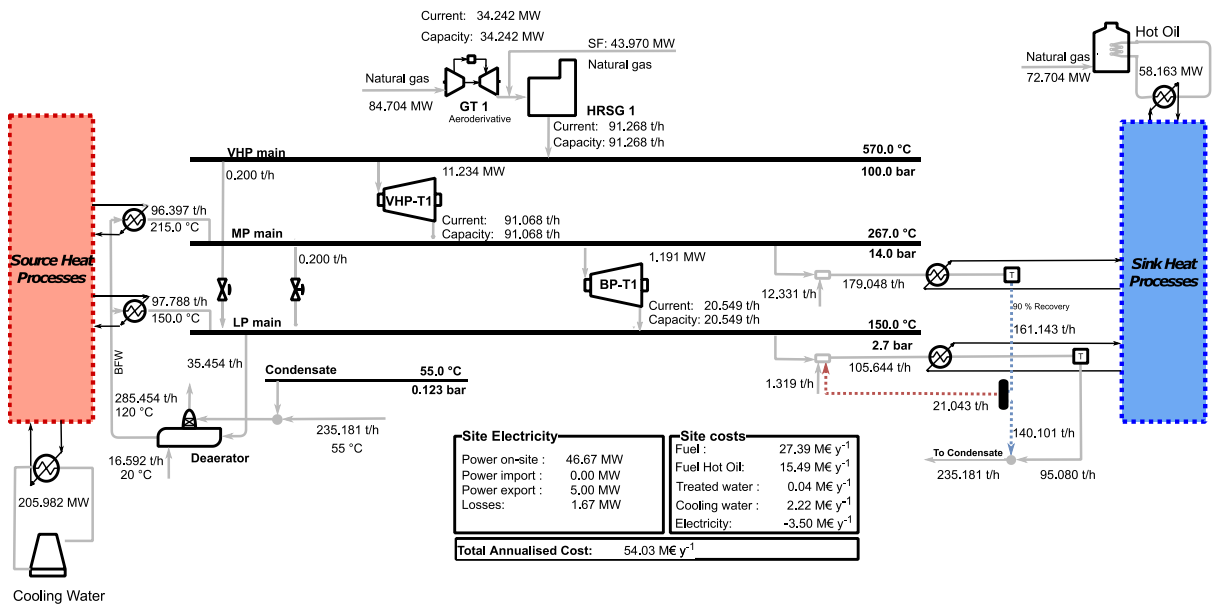


Figure 2-12. Optimized utility system configuration obtained by fixing the steam main pressures based on the information given by strategy 1

Finally, steam generation obtained by employing and the steam properties linearization proposed in this work is validated against the state-of-the-art model for steam properties – IAPWS (Wagner et al., 2000) .

Table 2-8 Comparison of the steam properties values calculated with the presented model against the real values.

Description	Steam turbine	Operating conditions			His [MW]		Steam turbine power generation [MW]*	
		Tin [C]	Pin [bar]	Pout [bar]	Real	This work	IAPWS model	This work
Best obtained configuration	VHP-ST 1	570.0	100.0	20.0	0.1385	0.1367	10.29	10.15
	BP-ST 1	295.5	20.0	2.7	0.1126	0.1152	1.22	1.26
	Total						11.51	11.41
Configuration with fixed steam main pressures	VHP-ST 1	570.0	100.0	20.0	0.1385	0.1367	9.45	9.32
	BP-ST 1	267.0	14.0	2.7	0.0915	0.0936	1.16	1.19
	Total						10.61	10.51

Calculated using turbine model.

As observed in Table 2-8, results obtained with the proposed steam properties approximations for the superheated region present a good agreement with the real values, resulting in an overall variation of less than a 1 %. Note that explicit values of temperatures are not calculated/used during the optimization, except for the VHP steam main. For test 6- scenario 2, the calculated temperature is 572 °C, resulting in 0.35 % discrepancy from the real value. Result analysis

For the analysis of the system configurations among the different scenarios for the synthesis of utility systems, the results of Case Study 2 (tests 5-8) are presented in Table 2-9.

Table 2-9. Best solution found for 's case study with three steam mains

Results	Utility system		Utility system with HO and FSR integration	
	Stand-alone	Micro grid	Stand-alone	Micro grid
VHP Pressure , [bar]	100	100	100	100
VHP Temperature, [°C]	570.0	570.0	570.0	570.0
Steam mains	HP/MP/LP	HP/MP/LP	MP / LP	MP/LP
Pressure, [bar]	37.8 / 12.3 / 2.7	37.8 / 12.3 / 2.7	14 / 2.7	20 / 2.7
Temperature, [°C]	442.6 / 288.2 / 150.0	441.3 / 285.1 / 150.0	273.1 / 150	295.5 / 150
Process steam use*, [t h ⁻¹]	104.3 / 155.6 / 103.9	104.2 / 155.6 / 103.9	165.77 / 83.28	181.21 / 74.87
Flash steam, [t h ⁻¹]	- / - / -	- / - / -	- / 21.04	- / 29.62
Process steam generation, [t h ⁻¹]	- / 42.3 / 153.8	- / 42.4 / 153.7	76.4 / 118.5	100.4 / 93.0
Utility steam generation, [t h ⁻¹]	217.78	217.78	137.09	136.67
Boiler, [t h ⁻¹]	128.76	115.45	-	-
HRSG, [t h ⁻¹]	89.02	102.33	89.438	136.67
Hot oil system, [MW]	-	-	58.16	51.86
Fuel consumption, [MW]	239.97	245.04	121.96	175.03
Power generation, [MW]	41.67	46.67	41.67	46.67

Results	Utility system		Utility system with HO and FSR integration	
	Stand-alone	Micro grid	Stand-alone	Micro grid
Steam turbines, [MW]	20.89	20.88	11.02	11.41
Gas turbines, [MW]	20.78	25.79	30.65	35.26
Costs				
Operating costs, [M€ y ⁻¹]	52.83	50.49	43.71	41.66
Fuel costs, [M€ y ⁻¹]	50.60	51.78	25.96	29.10
HO operating costs	-	-	13.81	13.81
Power revenue, [M€ y ⁻¹]	-	-3.50	-	-3.50
Maintenance costs, [M€ y ⁻¹]	3.53	3.59	2.46	2.63
Capital costs, [M€ y ⁻¹]	10.38	10.78	8.99	9.60
Total costs, [M€ y⁻¹]	66.74	64.86	55.17	53.89

*At the exit of the steam main

In both scenarios -- with and without integration of hot oil circuits and FSR -- the results demonstrate the benefit of designing the process utility system as a microgrid network. For the utility system without integration, the revenue of selling electricity results in an overall cost reduction of 2.8 %. In this case, the additional power is provided by the gas turbine, for which installed capacity increases 24 %. Note that despite the fact that size increment results in higher capital costs, maintenance and fuel consumption, these cost increments (1.64 M€ y⁻¹) are offset by the revenue from exporting electricity (3.50 M€ y⁻¹). Concerning the operating conditions of steam mains, note that the operating conditions of the steam mains (in terms of pressure and temperature) are the same for the stand-alone system and the microgrid. This can be explained by the additional gas exhaust flow rates available, resulting in a switch of heat duties from boilers to heat recovery steam generators, while maintaining the overall amount of utility steam generated. In this way, higher power generation is achieved without affecting the balance across the steam mains.

In the case of utility systems with hot oil circuit and FSR integration, a similar trend can be observed, with the microgrid configuration providing major benefits. Regarding the steam mains operating conditions, the same VHP and LP steam pressure is selected (in comparison to the system without integration). However, the optimization favours a two steam main system coupled with a hot oil system and a flash tank. The latter option allows heat recovery from process condensates, where the flashed steam (at saturation) from the MP main can reduce the steam requirement at the lowest level. This, in combination with process heating at high temperatures supplied by a hot oil system, results in further reduction of the costs in comparison to the systems without their use. The integration of this utility option decreases only the site heat demand, while the site power requirement still needs to be satisfied. This, in addition to the higher heat to power ratio that gas turbines provide, also explains the gradual switch of power generated by steam turbines (from 20.89 MW to 11.21 MW) to power generated by the gas turbines (from 25.79 MW to 35.45 MW). The integration of the hot oil

system and FRS results in operating and capital costs savings of 16.7 % and 10.7 % respectively, compared with the solution found for the microgrid system without integration. Thus, the overall costs are reduced by 15.8 %.

It is important to note that in this analysis the costs of heat exchangers and piping are not part of the scope, which could reduce or even offset the cost savings presented above. The focus of this study is to provide a high-level analysis of the effect of different scenarios, as well as the integration of practical utility alternatives/options in the system configuration and its optimal operating conditions for total site energy integration (through steam systems). Future research where costs of heat exchangers and piping are included in the optimization framework are required. However, as presented in Elsidó et al. (2019)’s work, the synthesis of utility systems including heat exchangers, even for sites involving few streams and an energy system operating at fixed conditions, could be computationally challenging and expensive.

For the Case Study 2 presented above the optimum temperature for the VHP main is 570 °C (the maximum possible). Steam at higher superheat temperature can result in a higher process heating capacity (after de-superheating), consequently reducing the utility steam requirement, fuel consumption and installed capacity of the thermal generators. Moreover, higher temperatures benefit steam turbine efficiency and therefore power generation. Nevertheless, these results cannot be generalized for all utility sites. As discussed below, the optimum utility steam temperature for Case Study 3 site is 477 °C. For sake of illustration, the best design for a utility system operating with 3 steam mains (Tests studies 9 and 10) is presented in Figure 2-13.

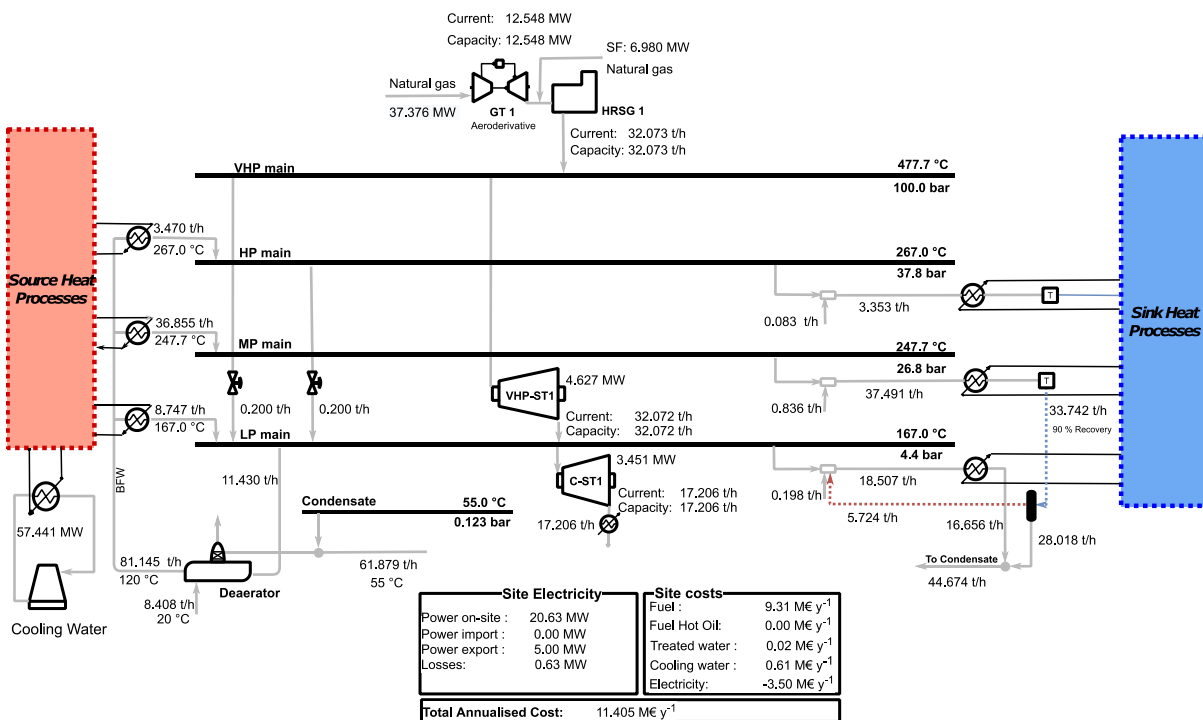


Figure 2-13 Best utility system configuration for Case Study 3, operating with 3 steam mains

Figure 2-13 shows the best utility system configuration for Case Study 3. The most economic utility system benefits from operating as microgrid, generating 20.625 MW on site. While on-site power is mainly provided by a gas turbine (12.55 MW), the additional power is generated by steam expansion through a back-pressure steam turbine (4.67 MW) and a condensing turbine (3.45 MW) at the LP header. Site heating requirement (31.73 MW) is met by utility steam raised in a HRSG unit (25.558 MW), and process steam recovered within the 3 steam mains. Since steam turbines are only connected at the last steam main, all the steam headers operate with the minimum degree of superheat to avoid excessive condensation (assumed in this work as 20 °C). Note that although hot oil system and flash steam tanks are available as utility options in the design framework, the optimum design benefits only from recovery of LP saturated steam.

7. Conclusions

This work proposes a novel framework for synthesising process utility systems with optimal steam level selection. Motivated by practical site issues and the need for more realistic and accurate frameworks for cost-effective process utility system transition, this methodology proposes a systematic approach to analysing site-wide heat recovery and the part-load performance of the various utility components to synthesise steam systems operating at optimum conditions, while taking the sensible heat of steam into account (e.g. steam superheating and de-superheating and boiler feed water preheating). In addition, to ensure technical and practical distribution of steam, temperature restrictions on the generation and use of steam are also included.

Due to the challenging problem that results from simultaneously synthesising utility systems and steam level placement, a bilevel decomposition technique is proposed that consists of a linearized mixed-integer master problem and a nonlinear sub problem. The master problem is linearized using a variety of techniques. For instance, piecewise relaxation of bilinear components in energy balancing constraints, convex envelopes for dependent variables, and linearization of steam characteristics within the superheating zone have been explored. Additionally, the algorithm's performance is enhanced by the inclusion of a solution pool, which allows for the exploration of several plausible solutions during each iteration.

This research was applied to three test cases taken from the literature and real-world examples and compared against a commercial MINLP solver. The results demonstrate that for large scale problems, the problem may become intractable if approached directly with commercial solvers. Thus, it is of fundamental importance to develop strategies to address the synthesis of utility systems. The results presented demonstrate that the bilevel decomposition, combined with a solution pool strategy, is an effective algorithm due to its rapid convergence and good solution quality. Additionally, the proposed algorithm can simultaneously evaluate trade-offs between energy integration, cogeneration

potential, and capital expenses. This is essential for the transition of current process utility systems into more energy-efficient utility systems. The framework presented accounts for multiple levels of heat supply/integration, considering the interactions between the on-site utility system and processes (industrial clusters), alongside more practical issues such as steam sensible heat. Consequently, the framework can be used as the foundation for future work where many conversion technologies can be easily incorporated into the formulation.

The future development of the methodology will focus on expanding its application to the design and operation of process utility systems considering variable energy demand and supply (multi-period version). Another point of focus, as mentioned previously, is the integration of a wider range of energy sources and conversion technologies, including thermal and electrical energy storage.

References

- Aguilar, O., Perry, S. J., Kim, J. K. & Smith, R. (2007) 'Design and Optimization of Flexible Utility Systems Subject to Variable Conditions: Part 2: Methodology and Applications', *Chemical Engineering Research and Design*, 85(8), pp. 1149-1168.
- Al-Khayyal, F. A. & Falk, J. E. (1983) 'Jointly Constrained Biconvex Programming', *Mathematics of Operations Research*, 8(2), pp. 273-286.
- Andiappan, V. (2017) 'State-Of-The-Art Review of Mathematical Optimisation Approaches for Synthesis of Energy Systems', *Process Integration and Optimization for Sustainability*, 1(3), pp. 165-188.
- Beangstrom, S. G. & Majozi, T. (2016) 'Steam system network synthesis with hot liquid reuse: II. Incorporating shaft work and optimum steam levels', *Computers & Chemical Engineering*, 85, pp. 202-209.
- Belotti, P., Kirches, C., Leyffer, S., Linderoth, J., Luedtke, J. & Mahajan, A. (2013) 'Mixed-integer nonlinear optimization', *Acta Numerica*, 22, pp. 1-131.
- Brandoni, C. & Renzi, M. (2015) 'Optimal sizing of hybrid solar micro-CHP systems for the household sector', *Applied Thermal Engineering*, 75, pp. 896-907.
- Bruno, J. C., Fernandez, F., Castells, F. & Grossmann, I. E. (1998) 'A Rigorous MINLP Model for the Optimal Synthesis and Operation of Utility Plants', *Chemical Engineering Research and Design*, 76(3), pp. 246-258.
- Casisi, M., Pinamonti, P. & Reini, M. (2009) 'Optimal lay-out and operation of combined heat & power (CHP) distributed generation systems', *Energy*, 34(12), pp. 2175-2183.
- Chen, C.-L. & Lin, C.-Y. (2011) 'A flexible structural and operational design of steam systems', *Applied Thermal Engineering*, 31(13), pp. 2084-2093.

- Corporation, I. (2017). V12. 8: IBM ILOG CPLEX Optimization Studio CPLEX User's Manual: International Business Machines Corporation.
- Dhole, V. R. & Linnhoff, B. (1993) 'Total site targets for fuel, co-generation, emissions, and cooling', *Comput Chem Eng.*, 17, pp. 101-109.
- Dogan, M. E. & Grossmann, I. E. (2006) 'A Decomposition Method for the Simultaneous Planning and Scheduling of Single-Stage Continuous Multiproduct Plants', *Industrial & Engineering Chemistry Research*, 45(1), pp. 299-315.
- Drud, A. (1985) 'CONOPT: A GRG code for large sparse dynamic nonlinear optimization problems', *Mathematical Programming*, 31(2), pp. 153-191.
- Elsido, C., Bischi, A., Silva, P. & Martelli, E. (2017) 'Two-stage MINLP algorithm for the optimal synthesis and design of networks of CHP units', *Energy*, 121, pp. 403-426.
- Elsido, C., Martelli, E. & Grossmann, I. E. (2019) 'A bilevel decomposition method for the simultaneous heat integration and synthesis of steam/organic Rankine cycles', *Computers & Chemical Engineering*, 128, pp. 228-245.
- Ghannadzadeh, A., Perry, S. & Smith, R. (2012) 'Cogeneration targeting for site utility systems', *Applied Thermal Engineering*, 43, pp. 60-66.
- Goderbauer, S., Bahl, B., Voll, P., Lübbecke, M. E., Bardow, A. & Koster, A. M. C. A. (2016) 'An adaptive discretization MINLP algorithm for optimal synthesis of decentralized energy supply systems', *Computers & Chemical Engineering*, 95, pp. 38-48.
- Gomes, F. R. A. & Mateus, G. R. (2017) 'Improved Combinatorial Benders Decomposition for a Scheduling Problem with Unrelated Parallel Machines', *Journal of Applied Mathematics*, 2017, pp. 9452762.
- Gounaris, C. E., Misener, R. & Floudas, C. A. (2009) 'Computational Comparison of Piecewise-Linear Relaxations for Pooling Problems', *Industrial & Engineering Chemistry Research*, 48(12), pp. 5742-5766.
- Hackl, R., Andersson, E. & Harvey, S. (2011) 'Targeting for energy efficiency and improved energy collaboration between different companies using total site analysis (TSA)', *Energy*, 36(8), pp. 4609-4615.
- Hawkes, A. D. & Leach, M. A. (2009) 'Modelling high level system design and unit commitment for a microgrid', *Applied Energy*, 86(7), pp. 1253-1265.
- Iyer, R. R. & Grossmann, I. E. (1998) 'A Bilevel Decomposition Algorithm for Long-Range Planning of Process Networks', *Industrial & Engineering Chemistry Research*, 37(2), pp. 474-481.
- Kermani, M., Wallerand, A. S., Kantor, I. D. & Maréchal, F. (2018) 'Generic superstructure synthesis of organic Rankine cycles for waste heat recovery in industrial processes', *Applied Energy*, 212, pp. 1203-1225.

- Khoshgoftar Manesh, M. H., Abadi, S. K., Amidpour, M. & Hamed, M. H. (2013) 'A new targeting method for estimation of cogeneration potential and total annualized cost in process industries', *Chemical Engineering Research and Design*, 91(6), pp. 1039-1049.
- Klemeš, J., Dhole, V. R., Raissi, K., Perry, S. J. & Puigjaner, L. (1997) 'Targeting and design methodology for reduction of fuel, power and CO₂ on total sites', *Applied Thermal Engineering*, 17(8), pp. 993-1003.
- Klemeš, J. J., Varbanov, P. S., Walmsley, T. G. & Foley, A. (2019) 'Process Integration and Circular Economy for Renewable and Sustainable Energy Systems', *Renewable and Sustainable Energy Reviews*, 116, pp. 109435.
- Klemeš, J. J., Varbanov, P. S., Walmsley, T. G. & Jia, X. (2018) 'New directions in the implementation of Pinch Methodology (PM)', *Renewable and Sustainable Energy Reviews*, 98, pp. 439-468.
- Lara, C. L., Trespalacios, F. & Grossmann, I. E. (2018) 'Global optimization algorithm for capacitated multi-facility continuous location-allocation problems', *Journal of Global Optimization*, 71(4), pp. 871-889.
- Lee, P. Y., Liew, P. Y., Walmsley, T. G., Wan Alwi, S. R. & Klemeš, J. J. (2020) 'Total Site Heat and Power Integration for Locally Integrated Energy Sectors', *Energy*, 204, pp. 117959.
- Liew, P. Y., Theo, W. L., Wan Alwi, S. R., Lim, J. S., Abdul Manan, Z., Klemeš, J. J. & Varbanov, P. S. (2017) 'Total Site Heat Integration planning and design for industrial, urban and renewable systems', *Renewable and Sustainable Energy Reviews*, 68, pp. 964-985.
- Liew, P. Y., Wan Alwi, S. R., Ho, W. S., Abdul Manan, Z., Varbanov, P. S. & Klemeš, J. J. (2018) 'Multi-period energy targeting for Total Site and Locally Integrated Energy Sectors with cascade Pinch Analysis', *Energy*, 155, pp. 370-380.
- Lin, Y. & Schrage, L. (2009) 'The global solver in the LINDO API', *Optimization Methods and Software*, 24(4-5), pp. 657-668.
- Linnhoff, B. & Vredeveld, R. (1984) 'Pinch technology has come of age', *Chemical Engineering Progress*, 80, pp. 33-40.
- Lotero, I., Trespalacios, F., Grossmann, I. E., Papageorgiou, D. J. & Cheon, M.-S. (2016) 'An MILP-MINLP decomposition method for the global optimization of a source based model of the multiperiod blending problem', *Computers & Chemical Engineering*, 87, pp. 13-35.
- Luo, X., Hu, J., Zhao, J., Zhang, B., Chen, Y. & Mo, S. (2014) 'Multi-objective optimization for the design and synthesis of utility systems with emission abatement technology concerns', *Applied Energy*, 136, pp. 1110-1131.
- Luo, X., Zhang, B., Chen, Y. & Mo, S. (2011) 'Modeling and optimization of a utility system containing multiple extractions steam turbines', *Energy*, 36(5), pp. 3501-3512.
- Ma, J., Chang, C., Wang, Y. & Feng, X. (2018) 'Multi-objective optimization of multi-period interplant heat integration using steam system', *Energy*, 159, pp. 950-960.

- Maréchal, F. & Kalitventzeff, B. (1998) 'Process integration: Selection of the optimal utility system', *Computers & Chemical Engineering*, 22, pp. S149-S156.
- Matsuda, K., Tanaka, S., Endou, M. & Iiyoshi, T. (2012) 'Energy saving study on a large steel plant by total site based pinch technology', *Applied Thermal Engineering*, 43, pp. 14-19.
- McCormick, G. P. (1976) 'Computability of global solutions to factorable nonconvex programs: Part I — Convex underestimating problems', *Mathematical Programming*, 10(1), pp. 147-175.
- Misener, R. & Floudas, C. A. (2010) 'Global Optimization of Large-Scale Generalized Pooling Problems: Quadratically Constrained MINLP Models', *Industrial & Engineering Chemistry Research*, 49(11), pp. 5424-5438.
- Misener, R. & Floudas, C. A. (2014) 'ANTIGONE: Algorithms for coNTinuous / Integer Global Optimization of Nonlinear Equations', *Journal of Global Optimization*, 59(2), pp. 503-526.
- Mitra, S., Sun, L. & Grossmann, I. E. (2013) 'Optimal scheduling of industrial combined heat and power plants under time-sensitive electricity prices', *Energy*, 54, pp. 194-211.
- Nemet, A. & Kravanja, Z. (2017) 'Synthesis of More Sustainable Total Site', *CHEMICAL ENGINEERING TRANSACTIONS*, 56, pp. 19-24.
- Oluleye, O. (2015) *Integration of Waste Heat Recovery in Process Sites*. PhD, University of Manchester, Manchester.
- Omu, A., Choudhary, R. & Boies, A. (2013) 'Distributed energy resource system optimisation using mixed integer linear programming', *Energy Policy*, 61, pp. 249-266.
- Papoulias, S. A. & Grossmann, I. E. (1983) 'A structural optimization approach in process synthesis—I: Utility systems', *Computers & Chemical Engineering*, 7(6), pp. 695-706.
- Picón-Núñez, M. & Medina-Flores, J. M. (2013) '16 - Process Integration Techniques for Cogeneration and Trigeneration Systems', in Klemeš, J. J. (ed.) *Handbook of Process Integration (PI)*: Woodhead Publishing, pp. 484-504.
- Pyrgakis, K. A. & Kokossis, A. C. (2020) 'Total Site Synthesis: Selection of Processes to Save Energy and Boost Cogeneration', in Pierucci, S., Manenti, F., Bozzano, G. L. & Manca, D. (eds.) *Computer Aided Chemical Engineering*: Elsevier, pp. 1345-1350.
- Rieder, A., Christidis, A. & Tsatsaronis, G. (2014) 'Multi criteria dynamic design optimization of a small scale distributed energy system', *Energy*, 74, pp. 230-239.
- Sanaei, S. M. & Nakata, T. (2012) 'Optimum design of district heating: Application of a novel methodology for improved design of community scale integrated energy systems', *Energy*, 38(1), pp. 190-204.
- Serra, L. M., Lozano, M.-A., Ramos, J., Ensinas, A. V. & Nebra, S. A. (2009) 'Polygeneration and efficient use of natural resources', *Energy*, 34(5), pp. 575-586.
- Shang, Z. (2000) *Analysis and Optimisation of Total Site Utility Systems*. Ph.D, Manchester, U.K.

- Shang, Z. & Kokossis, A. (2004) 'A transshipment model for the optimisation of steam levels of total site utility system for multiperiod operation', *Computers & Chemical Engineering*, 28(9), pp. 1673-1688.
- Singh, H. (1997) *Flue Gas Minimisation From Total Sites*. Ph.D., UK.
- Smith, R. (2016a). *Chemical Process Design and Integration* (2nd ed. ed.): Wiley.
- Smith, R. (2016b) 'Steam Systems and Cogeneration', *Chemical Process: Design and Integration*. Second ed. Chichester: John Wiley & Sons, Ltd, pp. 583-646.
- Sun, L., Doyle, S. & Smith, R. (2015) 'Heat recovery and power targeting in utility systems', *Energy*, 84, pp. 196-206.
- Sun, L., Gai, L. & Smith, R. (2017) 'Site utility system optimization with operation adjustment under uncertainty', *Applied Energy*, 186, pp. 450-456.
- Sun, L. & Liu, C. (2015) 'Reliable and flexible steam and power system design', *Applied Thermal Engineering*, 79, pp. 184-191.
- Sun, L. & Smith, R. (2015) 'Performance Modeling of New and Existing Steam Turbines', *Industrial & Engineering Chemistry Research*, 54(6), pp. 1908-1915.
- Tawarmalani, M. & Sahinidis, N. V. (2001) 'Semidefinite Relaxations of Fractional Programs via Novel Convexification Techniques', *Journal of Global Optimization*, 20(2), pp. 133-154.
- Tawarmalani, M. & Sahinidis, N. V. (2005) 'A polyhedral branch-and-cut approach to global optimization', *Mathematical Programming*, 103(2), pp. 225-249.
- Towler, G. & Sinnott, R. (2013) 'Utilities and Energy Efficient Design', *Chemical engineering design, principles, practice and economics of plant and process design*. Second ed. Oxford, UK: Elsevier, pp. 103-160.
- Trespalacios, F. & Grossmann, I. E. (2014) 'Review of Mixed-Integer Nonlinear and Generalized Disjunctive Programming Methods', *Chemie Ingenieur Technik*, 86(7), pp. 991-1012.
- Varbanov, P., Perry, S., Klemeš, J. & Smith, R. (2005) 'Synthesis of industrial utility systems: cost-effective de-carbonisation', *Applied Thermal Engineering*, 25(7), pp. 985-1001.
- Varbanov, P., Perry, S., Makwana, Y., Zhu, X. X. & Smith, R. (2004) 'Top-level Analysis of Site Utility Systems', *Chemical Engineering Research and Design*, 82(6), pp. 784-795.
- Varbanov, P. S. D., S.; Smith, R. (2004) 'Modelling and Optimization of Utility Systems', *Chem. Eng. Res. Des.*, 82, pp. 561-578.
- Voll, P., Klaffke, C., Hennen, M. & Bardow, A. (2013) 'Automated superstructure-based synthesis and optimization of distributed energy supply systems', *Energy*, 50, pp. 374-388.
- Wagner, W., Cooper, J., Dittmann, A., Kijima, J., Kretzschmar, H.-J., Kruse, A., Mareš, R., Oguchi, K., Sato, H., Stoecker, I., Šifner, O. & Takaishi, Y. (2000) 'The IAPWS Industrial

- Formulation 1997 for the Thermodynamic Properties of Water and Steam', *Journal of Engineering for Gas Turbines and Power-transactions of The Asme - J ENG GAS TURB POWER-T ASME*, 122.
- Wang, H., Yin, W., Abdollahi, E., Lahdelma, R. & Jiao, W. (2015) 'Modelling and optimization of CHP based district heating system with renewable energy production and energy storage', *Applied Energy*, 159, pp. 401-421.
- Wang, L., Yang, Z., Sharma, S., Mian, A., Lin, T.-E., Tsatsaronis, G., Maréchal, F. & Yang, Y. (2019) 'A Review of Evaluation, Optimization and Synthesis of Energy Systems: Methodology and Application to Thermal Power Plants', *Energies*, 12(1), pp. 73.
- Wicaksono, D. S. & Karimi, I. A. (2008) 'Piecewise MILP under- and overestimators for global optimization of bilinear programs', *AIChE Journal*, 54(4), pp. 991-1008.
- Wouters, C., Fraga, E. S. & James, A. M. (2015) 'An energy integrated, multi-microgrid, MILP (mixed-integer linear programming) approach for residential distributed energy system planning – A South Australian case-study', *Energy*, 85, pp. 30-44.
- Xu, A. Z., Mu, L. X., Wu, X. H., Fan, Z. F. & Zhao, L. (2013) 'Superiority of Superheated Steam Flooding in Development of High Water-Cut Heavy Oil Reservoir', *Advanced Materials Research*, 616-618, pp. 992-995.
- Zamora, J. M. & Grossmann, I. E. (1998) 'A global MINLP optimization algorithm for the synthesis of heat exchanger networks with no stream splits', *Computers & Chemical Engineering*, 22(3), pp. 367-384.
- Zhang, B. J., Liu, K., Luo, X. L., Chen, Q. L. & Li, W. K. (2015a) 'A multi-period mathematical model for simultaneous optimization of materials and energy on the refining site scale', *Applied Energy*, 143, pp. 238-250.
- Zhang, D., Evangelisti, S., Lettieri, P. & Papageorgiou, L. G. (2015b) 'Optimal design of CHP-based microgrids: Multiobjective optimisation and life cycle assessment', *Energy*, 85, pp. 181-193.
- Zhao, H., Rong, G. & Feng, Y. (2015) 'Effective Solution Approach for Integrated Optimization Models of Refinery Production and Utility System', *Industrial & Engineering Chemistry Research*, 54(37), pp. 9238-9250.
- Zidan, A., Gabbar, H. A. & Eldessouky, A. (2015) 'Optimal planning of combined heat and power systems within microgrids', *Energy*, 93, pp. 235-244

SUPPLEMENTARY INFORMATION P2

BEELINE: Bilevel dEcomposition aLgorithm for synthesis of Industrial eNergy systEms

Julia Jiménez-Romero^{a,b,*}, Adisa Azapagic^b, Robin Smith^a

^a Centre for Process Integration, Department of Chemical Engineering and Analytical Science, University of Manchester, Manchester, M13 9PL, United Kingdom

^b Sustainable Industrial Systems Group, Department of Chemical Engineering and Analytical Science, University of Manchester, Manchester, M13 9PL, United Kingdom

* Julia Jiménez-Romero. Email: julia.jimenezromero@manchester.ac.uk, nataly.jimenezr@hotmail.com

SUPPLEMENTARY INFORMATION P2.A

Site data

Table P2.A 1. Site configuration and operating conditions

Parameter	Value
Interest rate [%]	8
Plant life [y]	25
Capital installation factor [-]	4
ΔT_{CW} [°C]	10
T_{BFW} [°C]	120

Table P2.A 2. Temperature specifications for the steam system

Constraints	Temperature [°C]
Maximum boiler steam superheated temperature	570
Maximum process steam usage temperature (saturation)	250
Minimum process steam generation temperature (saturation)	134
Minimum steam main superheating	20
Degree of superheating for process steam generation	20
Degree of superheating for process heating	3

Table P2.A 3. Economic indicators

Parameter	Value
CEPCI 2000 [-]	394.1
CEPCI 2008 [-]	575.4
CEPCI 2010 [-]	532.9
CEPCI 2014 [-]	576.1
CEPCI 2019 [-]	607.5
Energy CPI 2002 [-]	59.2
Energy CPI 2019 [-]	109.3
USD to EURO 2019	0.8931

Table P2.A 4. Model coefficients of equipment costs

Resource	Variable/units	Z_{eq}^{ref}	C_{eq}^{ref} [€]	ρ_{eq}	C_{nEq}^A [€/unit]	C_{nEq}^B [€]	Range	F_{eq}^{main} [%]	Reference
Boiler									
Packaged*	$m_{n_b, t_b, f_b, v}^b$, [t/h]	50	2,548,770.98	0.960	46,432.32	318,715.66	50 - 350	5	Smith (2016)
Field-erected*	$m_{n_b, t_b, f_b, v}^b$, [t/h]	20	1,801,717.41	0.810	57,059.40	843,282.30	20 - 154.2	5	Smith (2016)
					40,411.71	3,948,425.00	154.2 - 800		
Steam turbine	W_{θ}^{st} , [MW]	-	-	-	345,101.63	44,057.43	1 - 200	3	Fleiter et al. (2016)
Gas turbine									
Aeroderivative	$W_{n_{gt}}^{gt}$, [MW]	1	827,490.91	0.777	417,061.85	764,213.50	2 - 13.1		Pauschert (2009)
					299,924.77	2,497,065.00	13.1 - 51	3	
Industrial	$W_{n_{gt}}^{gt}$, [MW]	1	720,016.47	0.770	282,115.02	1,463,097.00	6 - 34.1		Pauschert (2009)
					204,104.04	4,439,144.00	34.1 - 125		
HRSG**	m_{exh}^{HRSG} , [t/h]	120	481,845.69	1.163	5,147.91	114,719.42	33.5 - 800	5	Corporation (2000)
HO Furnace	Q^{HO} , [MW]	5	465,365.00	0.748	67,821.29	135,275.97	5 - 11.4	5	Towler and Sinnott (2013)
					44,447.73	403,443.62	11.4 - 60		
Condenser	Q_{θ}^{st} , [MW]	-	-	-	6,885.26	209,311.81	1 - 2000	1	Varbanov (2004)
Deaerator	m_{Γ}^{BFW} , [t/h]	-	-	-	602.21	64,962.22	10 - 300	1	Varbanov (2004)
					430.22	115,452.82	300 - 600		
Flash tank***	m_{in}^{FSR} , [t/h]	1	4,205.99	0.506	309.45	13,679.76	20 - 100	1	Loh et al. (2002)
					142.52	32,057.92	100 - 400		

Note: costs adjusted to 2019

* Pressure reference 100 bar, $f_{p_{ref}} = 1.9$, ** Pressure reference 11.34 bar, $f_{p_{ref}} = 1.1$

*** Horizontal vessel, residence time = 5 min, density = $0.9 \text{ t} \cdot \text{m}^{-3}$, Pressure = 10 bar, $f_{p_{ref}} = 1.1$

For boilers, HRSG and flash tanks, capital cost should involve the pressure factor f_p

$$f_p = 0.0090943 \cdot P_v^{VHP} + 1.012986 \quad (C.1)$$

$$CC_{nEq} = \left(C_{nEq}^A \cdot Z_{nEq, tEq}^{Eq} + C_{nEq}^B \cdot y_{nEq, tEq}^{Eq} \right) \frac{f_p}{f_{p_{ref}}} \quad (C.2)$$

Table P2.A 5. Resources data

Resource	LHV ^a [MWh·t ⁻¹]	Cost [€·MWh ⁻¹]	Reference
Natural gas	13.08	24.30 ^b	Eurostat (2020b)
Distillate oil	11.28	39.65	Comission (2019)
Fuel gas	13.03	23.87	Author's estimation ^d
Fuel oil	10.83	39.40	Comission (2019)
Hot oil	-	30.40	Author's estimation ^e
Electricity import	-	88.65 ^b	Eurostat (2020a)
Electricity export	-	79.79	Author's estimation ^f
Cooling water		1.230	Turton et al. (2018)
Treated water		0.301 ^c	Turton et al. (2018)

^a Source : Engineering ToolBox (2008)

^b Prices for XL scale industries: Band I6 for natural gas (>4 000 000 MWh y-1)
Band IG for electricity (>150 000 MWh y-1)

^c Cost per ton [€·t⁻¹]

^d Based on energy inflation (CPI) (OECD, 2021)

^e Price related to the furnace fuel (Natural gas). Assuming 80 % efficiency (Towler and Sinnott, 2013)

^f Assuming 10 % of distribution losses

References

- Corporation, O. S. E. (2000) *The Market and Technical Potential for Combined Heat and Power in the Industrial Sector*, Washington, DC: ONSITE SYCOM Energy Corporation.
- Fleiter, T., Steinbach, J. & Ragwitz, M. (2016) *Mapping and analyses of the current and future (2020 - 2030) heating/cooling fuel deployment (fossil/renewables)*, Germany: European Commission.
- Loh, H. P., Lyons, J. & Chales W. White, I. (2002) *Process Equipment Cost Estimation Final Report*, Pittsburgh, PA: NETL, US Department of Energy (DOE/NETL-2002/1169. Available at: <https://www.osti.gov/servlets/purl/797810/>.
- Pauschert, D. (2009) *Study of Equipment Prices in the Power Sector*, Washington, D.C.: Energy Sector Management Assistance ProgramESMAP Technical Paper 122/09).
- Smith, R. (2016). *Chemical Process Design and Integration* (2nd ed. ed.): Wiley.
- Towler, G. & Sinnott, R. (2013) 'Utilities and Energy Efficient Design', *Chemical engineering design, principles, practice and economics of plant and process design*. Second ed. Oxford, UK: Elsevier, pp. 103-160.
- Varbanov, P. (2004) *Optimisation and Synthesis of Process Utility Systems*. PhD, University of Manchester, Manchester, UK [Online] Available at: <https://books.google.co.uk/books?id=9Ff4xQEACAAJ> (Accessed).
- Comission, E. (2019) *Consumer prices of petroleum products inclusive of duties and taxes: European Commission*. Available at: https://ec.europa.eu/energy/observatory/reports/2019_01_07_with_taxes_1933.pdf.
- Engineering ToolBox. (2008). *Fossil and Alternative Fuels Energy Content*. [Online]. Available at: https://www.engineeringtoolbox.com/fossil-fuels-energy-content-d_1298.html [Accessed 2021].

- Eurostat (2020a) 'Electricity prices for non-household consumers - bi-annual data (from 2007 onwards)'. Available at: https://ec.europa.eu/eurostat/databrowser/view/NRG_PC_205_custom_494574/default/table [Accessed].
- Eurostat (2020b) 'Gas prices for non-household consumers - bi-annual data (from 2007 onwards)'. Available at: https://ec.europa.eu/eurostat/databrowser/view/NRG_PC_203_custom_494286/default/table?lang=en [Accessed].
- OECD. (2021). *Inflation (CPI)* [Online]. Organisation for Economic Co-operation and Development. Available at: <https://data.oecd.org/> [Accessed 2021].
- Towler, G. & Sinnott, R. (2013) 'Utilities and Energy Efficient Design', *Chemical engineering design, principles, practice and economics of plant and process design*. Second ed. Oxford, UK: Elsevier, pp. 103-160.
- Turton, R., Shaeiwitz, J. A., Bhattacharyya, D. & Whiting, W. B. (2018). *Analysis, Synthesis, and Design of Chemical Processes* (5 ed.): Pearson.

SUPPLEMENTARY INFORMATION P2.B

Computational tests

Table P2.B 1 Computational performance of solvers CONOPT3 and BARON

	CONOPT3		BARON	
	Objective function	CPU time (s)	Objective function	CPU time (s)
Run 1	67.431	4.00	67.431	352.93
Run 2	67.308	4.31	67.308	353.14
Run 3	67.367	4.64	67.367	353.25
Run 4	67.431	4.12	67.431	352.98
Run 5	67.295	5.23	67.295	353.15

CHAPTER 4

Design of Flexible Utility Systems

Overview

The scope of this paper aims to introduce time-dependency to capture the dynamic behavior of industrial sites (product variation, plant maintenance, shut-down), which is directly related to its energy requirement. Moreover, market opportunities -due to electricity price fluctuations- are also explored. In this way, the methodology attempts to guarantee flexible operation of the process utility systems. This research also analyze the effect of energy price market on the energy systems design choices to satisfy the industrial energy demands, and whether energy storage influences the design and operation of process utility systems. This is achieved by investigating how the optimal design of process utility systems would vary under different energy pricing scenarios.

This contribution develops a multi-period MINLP model to simultaneously optimize system configuration and operation accounting for time-dependent energy demands, steam level selection and part-load efficiency. To address the challenging MINLP problem with nonconvex terms, BEELINE methodology for single-period (presented in Contribution 2) is extended to incorporate time-dependent demand and the integration of energy storage.

To limit the computational complexity in multi-period methodology some considerations were required:

- i. Time scale is reduced by determining representative periods and inter-time periods resolution. For this, a time-series aggregation of energy demand profiles and electricity prices is carried out prior the optimization.
- ii. Steam pressure levels are fixed to those obtained after an initial running of the multiperiod version of STYLE methodology. This assumption is supported by the findings of Contribution 2, where two near-optimal designs may differ in steam pressure level but present only marginal costs differences and thus are practically equally good.

Finally, Contribution 3 outcomes show that technology and operational thresholds are heavily reliant on energy price market conditions, demonstrating that there is no "one size fits all" solution. As a result, the importance of tools that enable the identification of the most cost-effective design in a given scenario is critical.

4.1 Contribution 3

Title: Next generation of industrial steam systems: A decision support framework for an efficient and evolving process utility system

Authors: Julia Jimenez-Romero, Adisa Azapagic and Robin Smith

To be submitted to: Applied Energy

Year: 2021

Next generation of industrial steam systems: A decision support framework for an efficient and evolving process utility system

Julia Jiménez-Romero^{a,b,*}, Adisa Azapagic^b, Robin Smith^a

^a Centre for Process Integration, Department of Chemical Engineering and Analytical Science, University of Manchester, Manchester, M13 9PL, United Kingdom

^b Sustainable Industrial Systems Group, Department of Chemical Engineering and Analytical Science, University of Manchester, Manchester, M13 9PL, United Kingdom

* Julia Jiménez-Romero. Email: julia.jimenezromero@manchester.ac.uk

Abstract

Process utility systems have emerged as a cost-effective measure for increasing industrial energy efficiency via site energy integration and cost fuel savings. Additionally, process utility systems can enhance grid flexibility through on-site power generation. Nonetheless, the design and operation of cross-sectoral energy systems is a challenging task. Site utility systems can compromise a wide range of energy resources and conversion technologies. Moreover, utility components are often highly linked to energy users and the utility market. Therefore, its design and operation require the use of rigorous optimization frameworks. On top of this, increasing market volatility and variable energy demand require that utility system operate at greater adaptability in process utility systems' operations. This work introduces a multi-period design approach for optimizing process utility systems and steam primary operational parameters concurrently to achieve a cost-effective design that takes advantage of system interactions with the site. The proposed framework supports boiler feed water pre-heating, steam superheating and desuperheating, load-dependent unit efficiency, and flash steam recovery. The synthesis procedure is based on the heating and cooling site profiles, variable across the time horizon (one year).

The framework also incorporates thermal and electrical energy storage to balance energy supply and demand. To consider the transition from current to sustainable energy resources, a mix of fossil and renewable energy sources are integrated. The resulting problem is formulated as a nonconvex mixed-integer nonlinear programming (MINLP). Due to the size and complexity of the problem, the direct use of general-purpose MINLP solvers could be computationally restrictive, therefore in this work, a bilevel decomposition technique based on solution pools is specifically developed. Despite the large number of hot/cold streams and technical design/operational constraints, the proposed method can identify very good solutions with cost-effective designs. The main findings indicate that a holistic optimization of the utility system design, taking steam main conditions into account and incorporating flash steam recovery (FSR), could result in a 27.9 % reduction in fuel consumption

and a 24.5 % total cost savings, compared to the baseline scenario. Furthermore, an assessment of energy pricing and variations on the electricity/natural gas price ratio highlights the effect of the energy market on the optimal utility design, operation, and technological transitions.

Highlights

- Design framework considering both conventional and renewable energy sources
- Integration of both thermal and electrical energy storage in an industrial site
- Site time-variant energy integration through the selection of steam main conditions
- Specific multi-period bilevel decomposition strategy to design process utility systems
- Industrial demand-side flexibility provides energy and cost savings
- Sensitivity analysis of energy prices to define optimal utility system design and operation

Keywords

Superstructure, nonconvex mixed integer problem model, bilevel decomposition, site heat recovery, industrial steam systems, energy storage.

Nomenclature

Abbreviations

BFW	Boiler feed water
comdy	Commodity
FSR	Flash steam recovery
HO	Hot oil
HRSG	Heat recovery steam generator
HS	Hydrogen storage
LiB	Lithium-ion battery
MILP	Mixed integer linear programming
MINLP	Mixed integer non liner programming
MS	Molten salt system
NaS	Sodium sulphur battery
NHV	Net heat value
sh	superheated
SA	Steam accumulator
SSE	Sum of squared errors
ST	Steam turbine
TAC	Total Annualized Cost
UC	Utility components
VHP	Very High Pressure

Sets

CMDTY	Set of utility commodities
C	Set of cold streams
ES	Set of energy storage units
EQ	Set of utility equipment for thermal and/or power generation (subset of utility components)
F_{eq}	Set of fuels for each equipment
H	Set of hot streams
I	Set of steam mains
IJ	Set of steam levels j_s that belong to steam main i (i, j_s)
J	Set of temperature/pressure intervals
J_{HO}	Set of temperature/pressure intervals for hot oil (subset of temperature intervals)
J_s	Set of temperature/pressure intervals for steam main (subset of temperature intervals)
J_{WH}	Set of temperature/pressure intervals for waste heat (subset of temperature intervals)
K	Set of design periods
MS	Set of molten salt systems (subset of energy storage ES)
SA	Set of steam accumulators (subset of energy storage ES)
T	Set of intra design periods
UC	Set of utility components
VHP_L	Set of VHP steam levels

Variables

C_{cmdty}^{op}	Operating costs of commodities
TAC	Total annualized costs

Positive variables

$\delta_{eq,\theta,k,t}^{start}$	Continuous variable with values between 0 and 1, that indicates if equipment eq operating at θ conditions is started-up at time t
C_{uc}^{inv}	Investment cost of utility component uc
C_{uc}^{main}	Maintenance cost of each utility component uc
C^{start}	Start-up costs
$E_{es,d,t}^{es}$	Energy stored in unit es at any given time step
h_{shj_s}	Enthalpy of of superheated steam at steam level j_s
h_{shv}	Enthalpy of superheated steam at VHP steam main operating at v conditions
$L_{es,d,t}$	Losses of storage unit es at any given time period
$m_{i,j_s,k,t}^{CBFW}$	Steam mass flow rate of BFW injected to desuperheated steam operating at j_s conditions, at any given time period
$m_{i,j_s,j_s',k,t}^{C_{ch-SA}}$, $m_{i,j_s,j_s',k,t}^{C_{dch-SA}}$	Charging and discharging steam mass flow of steam accumulator operating between steam level j_s to level j_s' , at any given time period
$m_{i,j_s,k,t}^{CFSR}$	Steam mass flow rate of FSR injected to desuperheated steam operating at j_s conditions, at any given time period
$m_{i,j_s,k,t}^{C_{steam}}$	Process steam use at steam main i instant operating at level j_s , at any given time period
$m_{i,j_s,k,t}^{CT}$	Process steam use at the process use instant at level j_s , at any given time period
$m_{eq,f_{eq},k,t}^F$	Fuel flowrate of type fuel f_{eq} in unit eq at a specific time period
$m_{i,j_s,k,t}^{in}$, $m_{i,j_s,k,t}^{out}$	Variable vector representing inlet and outlet mass flowrates at steam main i operating at level j_s , at any given time period
$m_{UC,i,j_s,k,t}^{in}$	Variable vector representing mass flows from unit component UC to steam main i (operating at j_s), at any given time period
$m_{UC,i,j_s,k,t}^{out}$	Variable representing mass flows from steam main i (operating at j_s) to unit component UC, at any given time period
$m_{i,j_s,k,t}^H$	Mass flow rate of process steam generation for steam level j_s at any given time period
$m_{i,j_s,k,t}^{MS}$	Steam mass flowrate from molten salt system to steam main i operating at j_s conditions at any given time period
$m_{v,k,t}^{VHP-MS}$	Steam mass flow rate from VHP level v to molten salt system at any given time period
$P_{es,k,t}^{ch}$, $P_{es,k,t}^{dch}$	Charging and discharging power of storage unit es at any given time period
$Q_{eq,k,t}^B$	Fuel consumption of boiler eq at period t of design day k
$Q_{eq,k,t}^F$	Fuel consumed in unit eq at a specific time period
$Q_{s,k,t}^{HO}$	Process heating provided by hot oil system at steam temperature range, at any given time period
$Q_{i,j_s,k,t}^{in}$, $Q_{i,j_s,k,t}^{out}$	Variable vector representing inlet and outlet energy at steam main i operating at j_s conditions, at any given time period
$Q_{uc,i,j_s,k,t}^{in}$	Variable vector representing inlet heat flow at steam main i operating at j_s conditions, at any given time period
$Q_{eq,f,k,t}^{start}$	Consumption of fuel f required for start-up of equipment eq
$R_{j_s,k,t}^C$	Residual sink heat at steam level j_s , at any given time period
$R_{j_s,k,t}^H$	Residual source heat at steam level j_s , at any given time period

$U_{\text{comdy},k,t}$	Variable vector representing site consumption of each commodity, at any given time period
$U_e^{\text{exp}}_{k,t}, U_e^{\text{imp}}_{k,t}$	Electricity export and import at any given time period, respectively
$W_{k,t}^{\text{EB}}$	Power required by the electrode boiler at specific time period
$W_{T,k,t}^{\text{EB}}$	Total power required by electrode boiler and electric superheater (if selected) at a specific time period
$W_{k,t}^{\text{shEB}}$	Power required by the electric superheater at specific time period
$W_{\text{eq},k,t}$	Variable vector representing power generated by equipment eq at specific time period
$Z_{\text{eq},\theta,k,t}$	Equipment load operating at θ conditions at a specific time period
$Z_{\text{es}}^{\text{es}}$	Energy storage capacity of unit es
$Z_{\text{eq},\theta,k,t}^{\text{m}}$	Auxiliary variable to represent equipment load if unit eq is operation at a specific time period
$Z_{\text{uc}}^{\text{max}}$	Variable vector representing installed capacity of utility component uc
$Z_{\text{eq},\theta}^{\text{max}}$	Installed equipment size operating at θ conditions
$Z_{\text{eq},v,k,t}^{\text{sh}}$	Electric superheater load operating at v conditions at a specific time period

Binary variables

y_{es}	Binary variable to denote the activation of energy storage es
$y_{\text{UC},L,L',k,t}$	Variable vector representing equipment operating between level L and L' , at any given time period
y_{i,j_s}	Binary variables to denote the selection of steam main i operating at j_s conditions
y_v	Binary variable to denote the selection of VHP steam level
$y_{\text{eq},f_{\text{eq}},k,t}^{\text{f}}$	Binary variable to denote selection of fuel f_{eq} for unit eq at a specific time period
$y_{\text{eq},\theta,k,t}^{\text{op}}$	Binary variables to denote the activation of equipment eq operating at θ conditions at a specified time period
$y_{\text{eq},\theta}^{\text{s}}$	Binary variable to denote the selection of equipment eq operating at θ conditions
$y_{\text{eq},v,k,t}^{\text{sh}}$	Binary variable to denote the activation of electric superheater eq operating at θ conditions in a specific time period

Parameters

Ψ_{uc}	Cost exponent for each utility component
γ	Blowdown rate
$\sigma(d)$	Function that correlates the design day k corresponding to day of the year d
Λ	Vector that represents part of the slope in the modelling of power generation units
Δt_t	Duration of the time interval t
$\Delta t_{\text{eq}}^{\text{start}}$	Duration of start-up of equipment eq
$g_{\text{es}}^{\text{loss}}$	Self-discharge coefficient of storage unit es
$\underline{\Omega}_{\text{eq}}$	minimum feasible load operation of each equipment
τ_{es}	time required to fully charge/discharge the unit es
$\widetilde{a}_{11}, \widetilde{a}_{12}$	Model coefficients for boilers
$\widetilde{a}_{21}, \widetilde{a}_{22}, \widetilde{a}_{23}, \widetilde{a}_{24}$	Model coefficients for power generation units, based on Willan's line correlation
$C_{\text{eq}}^{\text{ref}}$	Reference cost for each equipment
$CP_{k,t}^{\text{C}} c_i$	Heat capacity flowrate of cold stream c_i , at any given time period
$CP_{h_i,k,t}^{\text{H}}$	Heat capacity flowrate of hot stream h_i , at any given time period
DoD_{es}	Depth of discharge of energy storage unit es

F_{uc}^{ann}	Annualization factor of utility component uc
F_{uc}^{inst}	Installation factor of utility component uc
F_{uc}^{main}	Maintenance factor of utility component uc
F_{eq}^{start}	Fraction of fuel used per start-up of equipment eq
$\underline{h}_{sh}, \overline{h}_{sh}$	Lower and upper bound for steam enthalpy at superheated stage
$\widetilde{h}_{shj_s}^H, \widetilde{h}_{shj_s}^C$	Enthalpy of superheated process steam generation (H) and use (C) at steam level L
$\widetilde{h}_l, \widetilde{h}_v$	Enthalpy of saturated liquid and vapour, respectively
\widetilde{h}^{BFW}	Enthalpy of boiling feed water
\widetilde{h}^{Cond}	Enthalpy of returned condensate
L^H, L^C	Heat losses due to distribution at the source and sink side, respectively
L^e	Electrical losses for transmission to/from the national grid
$\underline{m}_{f_{eq,k,t}}^F, \overline{m}_{f_{eq,k,t}}^F$	Lower and upper bound of fuel at a specific time period
$NHV_{f_{eq}}$	Net heat value of fuel f_{eq}
$N_{max_{eq}}^{start}$	Maximum number of start-ups permissible per day corresponding to unit eq
$\eta_{es}^{ch}, \eta_{es}^{dch}$	Charging and discharging efficiency of storage unit es
η_{shEB}	Efficiency of electric superheater of electrode boiler EB
$P_{comdy_{k,t}}$	Commodity price at specific time period
P_{EB}^{max}	Maximum steam pressured allowed in electrode boiler EB
P_v	Steam pressure at v conditions
$\widetilde{Q}_{j,k,t}^C$	Process heat sink at level j , at any given time period
$\widetilde{Q}_{j,k,t}^H$	Process heat source at level j , at any given time period
T_j	Utility temperature at level j
T^{*in}, T^{*out}	Shifted inlet and outlet stream temperatures
$t_{op_{k,t}}$	Duration of specific time period
$\widetilde{U}_{max}^{exp}, \widetilde{U}_{max}^{imp}$	Upper bound for export and import of grid electricity
U_{es}	Representative parameter of the upper boundaries of storage unit es variables
$U_{k,t}^m, U_{k,t}^Q$	Parameter vector representing upper bounds for mass and energy vectors of variables, at any given time period
$\widetilde{W}_{k,t}^{dem}$	Power demand at any given time period
\widetilde{Z}_{eq}^{ref}	Equipment reference size for capital cost estimation
$\underline{Z}_{eq}, \overline{Z}_{eq}$	Lower and upper size limits for each equipment

1. Introduction

To curtail CO₂ emissions and achieve the goals of Paris Agreement, sustainable energy use has prompted as one of the main focus of energy intensive industries. Industrial utility systems can significantly enhance the sustainability of chemical and manufacturing processes by accomplishing step changes in energy efficiency, cost reduction, and environmental impact mitigation via total site heat recovery, energy-efficient supply, and on-site power generation. To fully benefit from the potential of industrial energy systems, the systems must be accurately designed, considering the most relevant design parameters (e.g., energy sources and technologies, size, load, among others) to guarantee efficient performance. These parameters will become even more important as energy demand and/or supply varies over time. Energy variations in industry may stem from several factors such as the variation of the production level, production shifts or batches, start-up or shut down of equipment or processes, energy price fluctuations and availability (Marechal and Kalitventzeff, 2003; Elsidio et al., 2021). The latter two have become more crucial in the recent years due to the increasing share of intermittent renewable sources in the power sector. For this, an accurate and flexible design is fundamental to ensure system stability and supply reliability. Utility systems must be able to respond to change in demand and supply while maintaining stable and efficient performance, as well as rapid load adjustments (Elsido et al., 2021).

In relation to industrial utility systems, there are a range of different approaches to enhance flexibility, such as demand side management, flexible energy supply and conversion technologies, energy storage integration, or production scheduling adapted to market tariffs (Heffron et al., 2020). However, the design of utility systems with operational flexibility presents the following challenges: (i) several conversion and storage technologies options, (ii) each of them with several decision variables (e.g., selection, operational status) and (iii) technical and operational characteristics (e.g., costs, sizes, and load). Additionally, (iv) design optimization problems usually require long-term analysis (time horizons of at least one year long), while for integration of (v) electricity price fluctuations, as well as energy storage nature, a detailed model with discretization at hourly level may be required. For short-term operation optimization with a small number of time steps, models with a great degree of detail (e.g., operational constraints) increase the model accuracy. Nonetheless, the complexity and computational costs involved in design optimization models with a large number of time steps and decision variables reach the limit of practical applicability. It is then computationally intractable to apply a scheduling model to the entire time horizon (Zhang et al., 2018).

Several methods are proposed in the literature to optimally design and operate energy systems (Andiappan, 2017; Frangopoulos, 2018; Ganschinetz, 2021). These designs can be based on linear or non-linear mathematical models, characterized by single or multi-objective optimization

frameworks that capture the behavior of the different system components in different levels of detail. Concerning time resolution and horizon, some studies have recently tackled the complexity of the optimization problem by using time series aggregation methods, reducing the number of time intervals while retaining a level of detail sufficient to describe the dynamics of the energy system (Domínguez-Muñoz et al., 2011; Schütz et al., 2018). Despite several studies investigating the optimal design and operation of energy systems, and the potential integration of energy storage, several aspects remain unresolved. On the one hand, such studies are mainly based on residential, district heating, or power generation systems, in which the study of industrial systems and their characteristics receive little attention. The industrial sector -- in contrast with district heating -- requires heat at different temperature levels, where site heat recovery and optimization of utility levels play an important role in the design and operation of the system (as demonstrated in Chapter 3). On the other hand, the system behavior of industrial utility systems has been investigated in a small number of scenarios (Shang and Kokossis, 2005; Sun and Liu, 2015; Sun et al., 2017; Fernandes, 2017). However, the selection of the representative periods -- as well as the interaction between and within them -- has not been fully accounted for. Therefore, to exploit the full potential of the industrial utility systems, properly representing the system's physical behavior across the time, a novel optimization framework is presented in this work. This framework attempts to retain a level of detail sufficient to describe the dynamics of the energy system with a reduced number of time intervals, while accounting for: (i) short- and long-term dynamics of energy demand, storage and supply, (ii) systematic selection of (different) utility temperature levels (iii) steam sensible heat (i.e. steam superheating and de-superheating) influence on system design and operation (iv) part-load performance models of the conversion technologies involved in the industrial site, and (v) both thermal and electrical energy storage, as alternatives to help level out the imbalance between energy demand and supply.

Therefore, the proposed problem is formulated as a mixed-integer nonlinear program (MINLP) problem. The MINLP model is then linearized - to a mixed-integer linear program (MILP) - to capture the most important elements, while maintaining a manageable computing complexity. The relaxed MILP model allows for the determination of the lower bound of the original optimization problem and defines the value of the binary variables to then re-optimize the continuous variables considering the non-linearities in a non-convex linear (NLP) program model, which yield an upper bound. This sequence of MILP and NLP optimization is defined as a bilevel decomposition, which is presented in more detail in Contribution 2 (Chapter 3).

The rest of the paper is organized as follows: After the problem statement and main assumptions are stated in section 3, the methodology used for the optimal design problem of process utility systems and the solution strategy employed are described in section 4. The methodology comprises the

definition of design days, the model formulation and solution approach employed to solve it. In section 5, a relevant case study and potential scenarios are defined. Section 6 presents the main results from the optimization model and discusses the main findings of the different scenarios analysis. Finally, in section 7, the concluding remarks of this study are drawn.

2. Relevant literature

Among the possible approaches to address variable demand, multi-period optimization has been proven as an effective approach to consider time-based energy demand variability, different operating modes and conditions (Sun et al., 2017). More recently, multi-period optimization has also been employed to consider the integration of energy storage (Gabrielli et al., 2018a). Based on this, the most relevant literature focus in multi-period approaches is presented below.

One of the first utility systems synthesis considering variable demand was presented by Iyer and Grossmann (1998). The design problem was decomposed in design and operating levels. Energy demand was discretized (averaged) monthly and considering day and night modes. In their work, thermal demand was specified at each period, as steam mass flowrate at pre-defined values. Marechal and Kalitventzeff (2003) extended Iyer and Grossmann (1998) work by including part-load equipment performance and a non-linear optimization to identify and classify the data into typical loads. The optimization comprises the minimization of error between the averaged value and the real heat demand. Nevertheless, energy prices are not included in the clustering. Moreover, authors do not specify how the number of periods were defined nor the sequence of the data. Later, Mian et al. (2016) extended the approach of Marechal and Kalitventzeff (2003) propose a sequential algorithm for the design of heat exchanger networks considering the utility system synthesis. Due to the complexity, several simplifications are required. For instance, steam main pressure and temperature are assumed pre-defined and fixed, and utility components operate at constant efficiency. Varbanov et al. (2005) also presented multi-period methodologies for the synthesis of industrial utility systems, considering equipment part-load performance and site energy integration. The MINLP formulation synthesizes a utility system considering heating and cooling site profiles and steam level selection and was addressed by an iterative procedure of rigorous simulation and MILP optimization. In Aguilar et al. (2007) and Aguilar et al. (2008) flexibility and reliability concepts were introduced to assess industrial utility system design and operation performance under energy demand variation. The MILP methodology is based on fixed steam main conditions and mass flowrates. In similar way, Sun and Liu (2015) integrated load transitions into the design and operation of steam power systems -- considering a year time-horizon --. The proposed methodology allowed to consider equipment reliability and additional operating costs due to operation mode variation (on/off) of the utility components. Sun and Liu (2015) work highlighted the importance of utility system operating flexibility to adjust to variable demand and in this way reduce operational costs. However, a

limitation of the works (Varbanov et al., 2005; Aguilar et al., 2007; Sun and Liu, 2015) is that the periods are treated as single time intervals with separated operational variables. This approach is not suitable for modelling *complicated constraints* such as start-up rates or energy storages. Moreover, in Varbanov et al. (2005) and Sun and Liu (2015) the energy demand variability and its effect on the system performance is only analyzed under two extreme periods: winter and summer.

Luo et al. (2012) developed a multi-period model to include environmental concerns in the utility system by assuming costs for green houses emissions. The variability of the energy demand is represented by average month variations of the steam flows requirement of each unit. Sun et al. (2017) proposed a multi-period optimization strategy for conventional utility system operation adjustments under energy demand uncertainty. In the proposed methodology, operation scheduling is specified at the design stage based on six pre-specified steam and power demands. Although energy demand variability is represented with larger number of periods, and uncertainty of this demands is considered, the utility system is analyzed and design in isolation, without considering interactions between the utility system and the site. Moreover, the effect of significant demand variation -- due to a site plant starting-up or shutting down -- is not accounted for. Zhang et al. (2015) presented a mathematical model for the optimization of refining complex with on-site energy system. In their work, interactions between the refinery plants and the energy system are accounted for. Nevertheless, only optimal short-term operational schedule of utility plants is considered (three representative periods of an hour length each). Moreover, constant efficiency of the different utility components is assumed.

Previous work has focused on improving utility system flexibility based on fossil fuel technologies. However, due to the increasing requirement of low carbon technologies, recent studies have included additional technologies into the utility system design. In Panuschka and Hofmann (2019), an MILP formulation is proposed to assess the integration of steam accumulators in industrial utility system operating under varying electricity and emissions prices. Panuschka and Hofmann (2019) showed that the integration of thermal storages can reduce electricity import. But findings were based only on operating costs (capital cost was not part of the scope). Moreover, optimization of size of steam accumulators was not part of the scope of the problem. Elsidio et al. (2021), investigated the integration of molten salt energy systems in the design of utility systems with heat exchanger network. Findings in their work suggest that molten salt system can enhanced on site power generation and utility system flexibility. Nevertheless, due to the complexity of the model formulation, the case study is only based on a representative week, considering six time periods. Regarding the integration of renewable sources, Lok et al. (2020) proposed a fuzzy optimization approach for the optimization of an existing cogeneration system operation, taking into account start-up and shutdown costs. In their work, biomass sources and technologies were considered. However,

the variable energy demand and the periods employed for the optimization were not specified by the authors. Pérez-Uresti et al. (2020) proposed a multi-period MILP model to design a flexible renewable-based steam plant. The plant is design to supply domestic electricity demand and low-pressure steam to a bioethanol plant. The design framework considers biomass, wind and solar sources and technologies. The optimization is carried out based on averaged weekly and monthly power demand, obtaining different configurations for each time-resolution. Moreover, authors shown that monthly-based system design is not able to capture the utility demands predicted in a shorter-time discretization, and therefore not able to meet the energy requirements under weekly variations. To address the discrepancy, an economic analysis is carried out considering electrical energy storages integration (Li-ion battery and pump hydro storage). Energy size and operation are estimated under the worst-case scenario and not as degrees of freedom in the design framework.

Regarding the interactions between site and utility systems, several numerical approaches (Varbanov and Klemeš, 2011 ; Liew et al., 2018; Yong et al., 2021) have also been developed to consider site energy demand variability. Moreover, these approaches have also considered renewable sources and energy storage, particularly for local integrated energy systems (LIES). Varbanov and Klemeš (2011) developed time slice total site composite curves and site profiles to address renewables variability with time. Liew et al. (2018) extended their work by considering thermal storage. Jamaluddin et al. (2020) coupled pinch technology with a trigeneration storage cascade table for the sizing of power, heating and cooling energy systems under variable demand. More recently Yong et al. (2021) have integrated both thermal and electric energy storage and gas turbines. Although numerical approaches consider interactions between the utility system and the process site and could determine minimum energy requirements, they cannot provide a rigorous assessment of the trade-offs of utility system costs related to different size and load of the utility units, as well as the use of different fuels. In consequence, its effect on system configuration and performance cannot be fully assessed. Moreover, most of studies are based on saturated conditions for site-energy integration.

Most of the previous methodologies assumes pre-specified steam main temperature and pressure conditions, neglecting the high correlation between the utility system and the site processes, leading to possible missing potential energy-saving options. It is important to note that most effective heat transfer is done at saturated conditions. Nevertheless, steam superheating is required to avoid equipment damage and/or excessive condensation. Thus, the degree of superheat in steam mains is closely related to the utility components selection. For instance, if steam turbines are not required only a minimum degree of superheat (defined by the designer) to avoid condensation is required, while if steam turbines are operating between steam mains, a higher degree of superheat might be required to avoid equipment damage and to increase power generation. Moreover, based on the same idea -- heat transfer is more effective close to steam saturated conditions--, steam de-superheating

(by water injection) prior its use results in a reduction of the site steam requirement, as demonstrated in Manuscript 1. Therefore, an *a priori* decision regarding steam main conditions could result in misleading energy targets and suboptimal designs.

In similar areas such as district energy systems, variability of energy demand and integration of energy storage has been also studied. For instance, Elsidio et al. (2017) proposed a two-stage MINLP algorithm for the optimal synthesis and design of networks of cogeneration units for district heating with thermal storage (hot water tank). Elsidio et al. (2017) decompose a year demand through three typical weeks. While the approach allows analyzing intraday storage, its strictly cyclic schedules do not allow analyzing seasonal operation --since continuity between the periods is not accounted for--. Gabrielli et al. (2018a) presented a MILP model for the synthesis of district heating and cooling systems focusing in seasonal storage. Findings in their work show the relevance of considering chronology in the time series to exploit the benefits of long-term storage and therefore achieve higher energy and operational cost savings. Moreover, the relevance of achieving a good compromise between number of representative periods and computational time is shown. A major limitation of these methodologies, as mentioned in the introduction, is that heat requirement is only at a single (low) temperature. If cooling is required, this is at a much lower temperature than the heating requirement. Therefore, there are not energy integration possibilities within the system and the energy users. Moreover, if cogeneration technologies are evaluated, they can only provide heat at a single temperature, so heat cascade for further power generation while satisfying heat requirements are not required. Utility temperature is pre-specified, there is no need to evaluate the trade-offs between heat and power generation, and thermal storage at a unique temperature is required (usually the same as the utility temperature).

In summary, although several pieces of research have included variable energy demand in the design of utility systems, there is no agreement in the level of discretization required to reflect its variability and effect on the system configuration and performance. Moreover, the integration of start-up constraints and more specifically energy storage involve *complicating variables* and *constraints*, relating the design variables with the operational ones in all the time periods. This complicates the solution of the problem due to time-series coupling and the need of considering chronology between time-series. In addition, connections among the process site and steam system operating conditions are usually overlooked. Selection of steam main operating conditions prior its optimization could result in missing opportunities for energy savings. Moreover, the degree of superheat of steam mains needs to be consider simultaneously with the utility system synthesis.

2.1. Contribution of this work

The analysis above shows the remarkable complexity of the optimization problem. It identifies a clear knowledge gap on providing a systematic approach for cost-effective solutions for industrial symbiosis by optimizing the design and operation of the utility system and the energy integration opportunities simultaneously, accounting for the variability of energy demands through time. To the best of the authors' knowledge, none of the available approaches considers simultaneously the technical constraints (site heat integration, steam temperature limitations, steam superheating and de-superheating) and operational issues (part-load performance, multi-component resolution, start-up constraints) for the design of industrial utility systems with operational flexibility requirements. To address these challenges, in this work, the methodology proposed in Manuscript 2 is adapted to incorporate the energy demand variability across the time horizon and all the technical features required guaranteeing the industrial relevance of the solution. In addition, the proposed methodology integrates thermal and electrical storage systems, as well as some low-carbon fuels and technologies alternatives (e.g., biomass and electrode boilers). For this purpose, an MINLP model dealing with time-variable loads and tariffs and energy storage (if required) is formulated. The MINLP formulation is decomposed into MILP and NLP sub problems. The study aims at answering the following questions:

- (i) How can the variation of the energy requirements within time influence the optimal energy system configuration and operating conditions?
- (ii) To what extent is the deployment of thermal and electrical storage practical/beneficial in industrial utility systems?
- (iii) How the utility's (e.g., electricity) price fluctuation affects the design and operation of industrial utility system?
- (iv) What temporal resolution (i.e., time step size) is required to obtain accurate and meaningful optimization results without compromising computational costs?

Providing answers to these open questions is highly relevant for future model development in industrial utility system design and optimization. The proposed model also considers the following issues: (i) effect of part load performance of utility components, derived from experimental data or provided by the manufacturer (ii) start-up phase of some units requires a non-negligible time and also implies a significant energy penalization due to the warm-up phase of the machines and (iii) multiple components for reliability. The present tool is based on grassroots design of utility systems. However, by adding the relevant constraints from the existing system, the decision support tool provides benefits at different levels:

Operations and planning

- Optimum equipment operation (on/off)
- Optimum equipment load allocation (exploit differences in efficiency)
- Reduced of energy consumption/waste

Management

- Provide decision support information for utility contract negotiation
- Site management over different time horizons, considering anticipated demands and equipment availability

Advisory

- What-if scenario analyses for developing road maps to evolve existing systems to future demands, based on plant demands, utilities prices and equipment availability

Compared to previous works, the proposed model in this work, not only systematically incorporate all the features above mentioned for the effective design of flexible industrial utility systems, but also includes:

- Design of industrial utility systems with heat (steam) supply/demand at least at three steam levels. The steam levels are associated to the saturated pressure, therefore: High-pressure (HP), Medium pressure (MP) and Low-pressure (LP).
- Determination of appropriate pressure/temperature of each steam level for total site energy integration.
- Integration of both thermal and electrical storage systems in the optimization of industrial utility systems.
- Integration of low-carbon sources and technologies such as electrode and biomass boilers, as well as gas turbines operating with biogas or syngas.
- Consideration of the effect of chronological time periods for the design and operation of seasonal energy storage.

3. Problem statement and challenges

In process industrial sites, utility systems are usually employed to produce steam to satisfy heat and power site requirements. Additionally, the site can interact by recovering heat surplus of a process to use it in other process required, through the steam system (indirect heat recovery). The main energy requirement of the industrial site are heating and cooling and at multiple temperatures and power. For this, different energy conversion technologies can be selected, from conventional fossil fuel-based technologies (e.g. gas boilers, gas turbines, steam turbines, heat recovery steam generators) to cleaner alternatives (such as biomass boilers and electrode boilers). In addition, electrical energy

storage units such as Lithium ion (Li-ion) and Sodium Sulphur (NaS) batteries, hydrogen storage system. Also, thermal storage units such as steam accumulators (SA) and molten salt systems (MSS), are considered as options to smooth the imbalance between the energy demand and supply. The framework considers additional utility features such as deaerator, let-down stations, flash steam recovery (FSR), and supplementary utilities such as hot oil and cooling water. A schematic representation of the process utility system, its interaction with the site and the different energy sources and technologies available are shown in Figure 3-1.

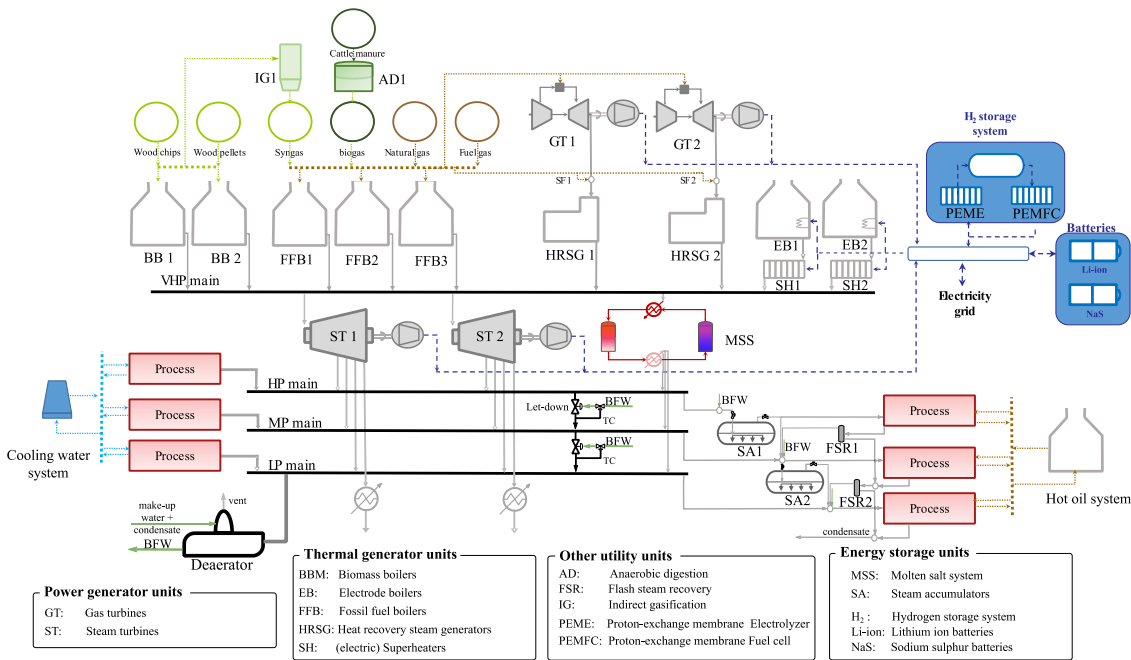


Figure 3-1 Schematic representation of the proposed process utility system

This study analyses the optimal design of the process utility system for such industrial site, defining the mix of energy technologies and storage (in terms of size and load operation) to allow cost-effective supply of the variable energy demands over a representative timespan. Importantly, the methodology considers the selection of different steam levels (in terms of pressure and temperature) to explore the site-wide energy integration and cogeneration potential to achieve an energy-efficient industrial site. System flexible operation is considered in terms of fuel options, equipment part-load operation, as well as potential short and mid-term energy storage to smooth the imbalance between the energy supply and demand.

3.1. Main assumptions

- (i) There is a linear correlation between the production profiles and the heating and cooling requirements of the process. Although the efficiency of process plant operation is also affected when operating at part load, the recollection of exact heat load of each heat exchanger every day of the year could be quite complex (even more when considering the integration of several

process plants involving a large number of streams). For this reason, a linear correlation has been assumed in this work for estimating the heating and cooling site demand.

- (ii) The supply and target temperatures of process streams is assumed constant across the year. While this assumption could simplify the problem significantly, it is not always available the detailed data about temperature variation of processes across the year, since it depends on several factors (such as ambient conditions, product specifications, market variations, among others).
- (iii) Inter-plant heat recovery can be achieved through on-site utility system, while intra-plant heat recovery (whether optimized or not) is assumed to be inbuilt. Design of heat exchanger network is out of the scope of this work.
- (iv) Process heating and cooling requirement can be satisfied mainly by superheated steam, by either generating process steam or using it. Note that while the degree of superheating for both process steam generation and use is a designer input parameter, steam main superheating is a design variable in the optimization framework.
- (v) Steam main operating conditions are assumed constant across the time horizon. While temperature could easily vary depending on the circumstances, steam main pressure is constrained by the capacity of pipes and valves. Moreover, (continuous) drastic temperature changes can cause thermomechanical stress in the equipment. As a result, steam mains working at single operating conditions are assumed in this work. Nonetheless, the problem formulation allows for assessing the most appropriate steam mains temperature and pressure for maximum heat recovery under different conditions.
- (vi) Supplementary heating and cooling can be meet by hot oil and cooling water systems.
- (vii) Utility steam is raised at VHP conditions and distributed to the different headers -- either passing through steam turbines or let down stations.
- (viii) Steam provided by either FSR or steam accumulators is at saturated conditions. Thus, it is assumed to be only used for heating purposes and not considered for steam expansion through steam turbines. Recovering saturated steam into the superheated steam main may result in a greater energy demand to balance the headers and prevent excessive condensation.

4. Methodology

In the following, the clustering approach employed to define the appropriate number of design days and time resolution is presented. Then, the MINLP formulation for the synthesis of process utility systems under time-variant energy demand and prices is presented. The formulation and its solution strategy are based on the solution bi-level decomposition model for a single period, proposed in Contribution 2. Note that continuous variables in this model must be nonnegative unless otherwise stated.

4.1. Definition of design days - clustering approach

In this problem, the operation modes of the utility system components depend on the process operating profile and the utility price fluctuations expected during a time horizon. Process operating profiles exhibit different behaviors for different days of the year and could be zero when a specified plant is shut down (due to product scheduling or maintenance). To reduce the amount of data (and the computational effort) while maintaining variability and accuracy, the planning horizon (assumed here as an operational year) is divided in typical/design days, denoted by index k . Each design day k consists of a representative set of time periods, t , which starts at time point t_l . Time periods considered before time t_l are used to track previous day. The length of time (Δt) will depend on the results of the clustering, (e.g., an hour). This makes it simpler to describe certain features, such as electricity prices, which fluctuate hourly but also show daily/seasonal variations (Aguilar et al., 2008).

In this framework, clustering involves two general steps: (1) normalization and weight, and (2) assignment and representation. Figure 3-2 shows an illustrative example of clustering.

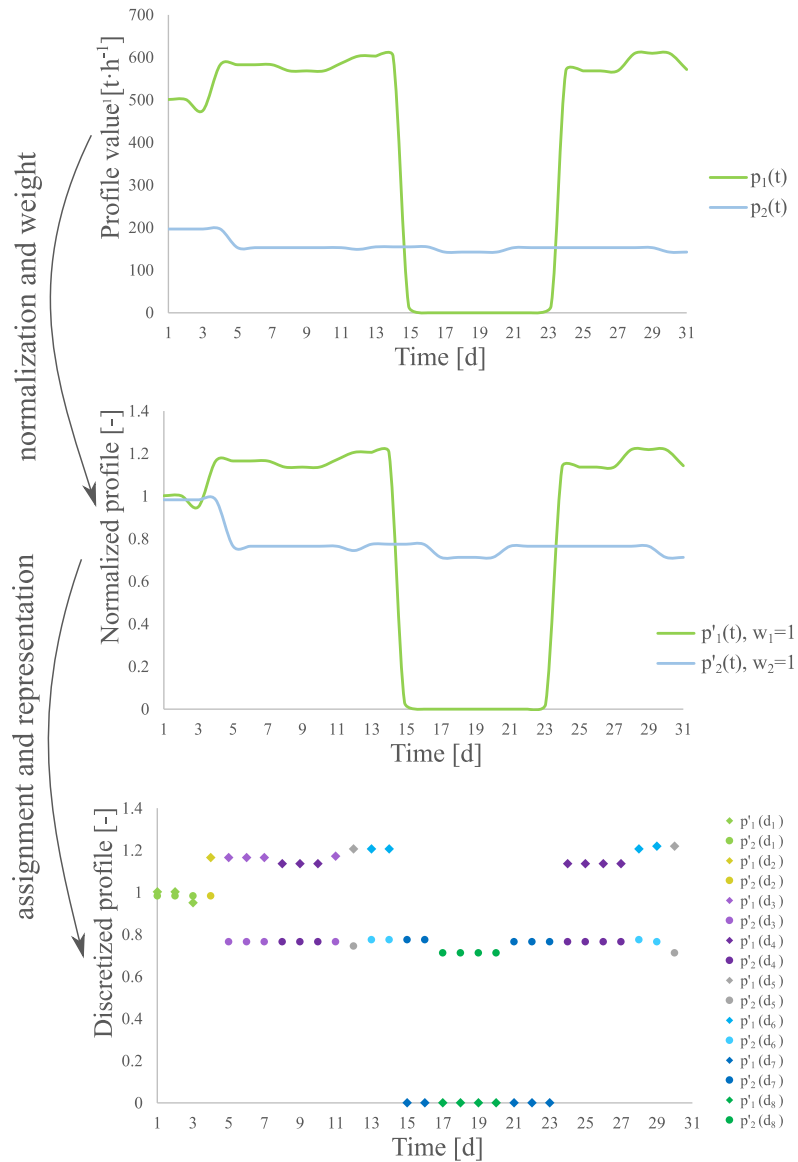


Figure 3-2 Illustrative example of data set clustering for finding representative periods for the optimization of utility systems

4.1.1. Normalization and weight

Prior data clustering, data needs to be normalized in order to avoid any potential biased due to different scales among the key drivers of variation. Once normalized the data, the relevance of each driver in the system behavior can be evaluated by adding weight coefficients (if required). For instance, in Elsidio et al. (2017) stated that the correct heightening of the main drivers can reduce the inaccuracies from 10 to 3%.

4.1.2. Assignment and representation

Following normalization, the assignment stage allocates similar periods to clusters. Assignment can be performed by a number of clustering methods. Most of these algorithms can fall into two categories: partitional and hierarchical (Domínguez-Muñoz et al., 2011). The most relevant partitional clustering (but not the only ones) are k -means and k -medoids. k -means algorithm is the most common clustering technique, which tries to find a user specified number of clusters (k) by minimizing the distance between the k -data and the k -centroid. k -centroid are initially determined randomly and refined iteratively. Thus, k -centroids do not necessarily agree with values in the data and could be quite sensitive to initial values of the centers. Alternatively, k -medoids algorithm select as k -centroid actual data-points to then, in a similar way as k -means algorithm, minimize the distance within the points assigned in the k cluster. In literature this two algorithms as well as hierarchical approach. For instance, Kotzur et al. (2018) analyzed the performance of the three clustering methodologies and compared it with averaging periods. Kotzur et al. (2018) concluded that averaging periods provide incorrect findings, and that no aggregation technique outperforms all others in every case study. The k -medoids algorithm provides somewhat greater performance. In a similar manner, Teichgraber and Brandt (2019) study compared k -means, k -medoids, and hierarchical clustering for approximating power price series. Overall, k -means can forecast the operational domain better than medoid-based methods. Schiefelbein et al. (2015) applied a k -medoid algorithm to determine the typical demand days in a city district with five buildings. Based on their findings, the authors suggest that after a minimum number of typical days (in their case study established as seven) the optimal energy system configuration does not change however, it strongly influences the computational time.

Based on this analysis, the k -means and k -medoids algorithms are applied to determine the best fit and design days for the annual data. The clustering algorithms k -means and k -medoids from package *sklearn* (Pedregosa et al., 2011) in Python (Rossum, 1995) are employed. Since clustering algorithms tend to smooth the demand profiles, an extreme period is included to ensure the system operational feasibility across the entire time horizon (Gabielli et al., 2018a). There is no widespread agreement on the optimal method to selecting extreme periods, although it seems that choosing peak values is one of the most effective (Fazlollahi et al., 2014). Based on the assumption that, in the worst-case scenario, site power requirement can be met by electricity grid import, and any additional cooling demand can be satisfied by rejecting heat to cooling water. The stricter constraint of the system is set to always to meet site-heating requirement. Thus, the days with lowest heat integration potential are identified as extreme points; in other words, among the data points with the highest heating requirements, the points with lowest cooling requirements are selected.

To achieve the necessary data reduction, each cluster must be aggregated using representative characteristics. The representation must be specified in such a manner that data within each cluster

are comparable yet vary among the different clusters. Thus, it is critical to establish the appropriate number of clusters for this purpose. In this work, to determine the appropriate number of typical days for the mean typical year data and/or assess the quality of the clustering, the widely known elbow (Thorndike, 1953) and silhouette (Rousseeuw, 1987) methods in cluster analysis are applied in this work. Elbow method consists in calculate the sum of squared errors (SSE) within a cluster k and plotting the SSE against the number of clusters. Note that the higher the number of clusters considered the lower the SSE will be. Nevertheless, the curve tend to have an exponential decrement, thus the inflection point of the curve (the elbow) can show a good compromise between the number of clusters and the SSE. To identify the elbow point programmatically, the function *kneelocator* of Python package *kneed* (Satopaa et al., 2011) is used. In addition to this, silhouette method is also considered. The Silhouette method consist of measuring the separation distance between the resulting clusters. Silhouette distances are usually determined based on Euclidean distance and values range between -1 and +1, where higher (positive) values are desirable, as indicates greater agreement of the points to the allocated cluster k . Silhouette scores were determined using the function *Silhouette.scores* from *skitlearn* (Pedregosa et al., 2011). In this work, design periods were considered from 2 to 52 (assuming weekly design periods) considering 42 random starting points. A similar approach was applied considering k -medoids algorithm, to evaluate the best fit to the available data.

4.2. MINLP model formulation

4.2.1. Objective function

The problem formulation is based on minimum total annualized costs (TAC) as the objective function. TAC comprises investments (C^{inv}), maintenance costs (C^{main}), operating costs (C^{op}) and start-up costs (C^{start}). To annualize the investment costs an annuity factor (F^{ann}) is used. $uc \in UC$ denotes the utility components and $cmdty \in CMDTY$ the commodities (i.e., cooling water, fuels, electricity, treated water).

$$\min TAC = \sum_{uc \in UC} (F_{uc}^{ann} \cdot C_{uc}^{inv} + C_{uc}^{main}) + \sum_{cmdty} C_{cmdty}^{op} + C^{start} \quad (3.1)$$

The investment cost comprises the cost of the purchased equipment. Installation costs are considered by the factor F_{uc}^{inst} . The scale dependency of the utility component costs is expressed by the power function Eq. (3.64)

$$C_{uc}^{inv} = F_{uc}^{inst} \cdot C_{uc}^{ref} \left(\frac{Z_{uc}^{max}}{Z_{uc}^{ref}} \right)^{\psi_{uc}} \quad \forall uc \in UC \quad (3.2)$$

Where C_{uc}^{inv} is the investment cost of the uc unit, whose size is Z_{uc}^{max} . C_{uc}^{ref} denotes the reference cost for the reference size of the same unit \tilde{Z}_{uc}^{ref} , and term ψ_{uc} is the scale law cost exponent.

The maintenance cost is assumed as a proportion of the investment cost, as given by Eq.(2.3).

$$C_{uc}^{main} = F_{uc}^{main} \cdot C_{uc}^{inv} \quad \forall uc \in UC \quad (3.3)$$

Frequent start-ups and shutdowns of equipment are not ideal for its operation due to: (i) increase of the fuel consumption --equipment warm-up--, and (ii) reduction of component lifetime -- material stress and worn --. This in particular can be considered in technologies such as boilers, gas turbines and HRSGs (Sun and Liu, 2015). Therefore, equipment start-up costs are given by the additional fuel consumption required ($Q_{eq,f}^{start}$) during the time of the start-up (Δt_{eq}^{start}).

$$C^{start} = \sum_{eq} \sum_{f \in F_{eq}} U_f \cdot Q_{eq,f}^{start} \cdot \Delta t_{eq}^{start} \quad \forall eq \in \{FBB, BB, GT, HRSG\} \quad (3.4)$$

The operating costs are given by the sum of the multiplication of the commodity consumption (U_{comdty}) by its specific cost (P_{comdty}) at each period (t) of the design day (k), weighted on the basis of the duration of the period t_{op} . Note that operating costs also involves the potential revenues from exporting electricity in which case selling price is assumed as a negative value.

$$C_{comdty}^{op} = \sum_{k \in K} \sum_{t \in T} U_{comdty_{k,t}} \cdot P_{comdty_{k,t}} \cdot t_{op_{k,t}} \quad (3.5)$$

All the technical and capital specification are detail in Supplementary Information P3.A.

4.2.2. Utility components

i. Selection, sizing and load

For a set of available technologies denoted by eq , the nominal size (Z_{eq}^{max}) can be considered as a continue variable, limited by the minimum (\underline{Z}_{eq}) and maximum (\overline{Z}_{eq}) nominal capacities available in the market. Whether the specific equipment eq , is installed is given by the binary variable $y_{eq,\theta}^s$.

$$\underline{Z}_{eq} \cdot y_{eq,\theta}^s \leq Z_{eq,\theta}^{max} \leq \overline{Z}_{eq} \cdot y_{eq,\theta}^s \quad \forall eq \in EQ \quad (3.6)$$

Many technologies (e.g boilers and gas turbines) cannot operate below certain load specifications (minimum part-load) due to either poor efficiency performance or unsafety issues. Therefore, Eq. (2.6) ensures that equipment used operates between the minimum ($\underline{\Omega}_{eq}$) and maximum load each

period. Note that for electrical units such as electric boiler, their operation is barely constrained by part-load limitations. Manufactures

$$\underline{\Omega}_{\text{eq}} \cdot Z_{\text{eq},\theta}^{\text{max}} \leq Z_{\text{eq},\theta,k,t} \leq Z_{\text{eq},\theta}^{\text{max}} \quad \forall \text{eq} \in \text{EQ} \quad (3.7)$$

Note that a selected equipment ($y_{\text{eq},\theta}^{\text{s}} = 1$) can be shut down at certain periods. Thus, a set of binary variables $y_{\text{eq},\theta,k,t}^{\text{op}}$ is required to indicate whether a technology is operating during a specific time period. $y_{\text{eq},\theta,k,t}^{\text{op}}$ is constrained by Eq. (3.8).

$$y_{\text{eq},\theta,k,t}^{\text{op}} \leq y_{\text{eq},\theta}^{\text{s}} \quad \forall \text{eq} \in \text{EQ}, k \in \text{K}, t \in \text{T} \quad (3.8)$$

Additionally, $Z_{\text{eq},\theta,k,t}$ is treated as a semi-continuous variable, where the lower boundary varies depending if it is operating or not. In other words, lower bound of $Z_{\text{eq},\theta,t}$ is zero if the equipment is not operating at time t, and is $\underline{\Omega}_{\text{eq}} \cdot Z_{\text{eq},\theta}^{\text{max}}$ if it is operating. Auxiliary variable $Z_{\text{eq},\theta,k,t}^{\text{m}}$ and Glover (1975) linear formulations (Eq. (3.9)) are implemented to avoid mixed-integer term ($Z_{\text{eq},\theta,k,t}^{\text{max}} \cdot y_{\text{eq},\theta,k,t}^{\text{op}}$) and ensure $Z_{\text{eq},\theta,t}$ is zero if the equipment is not operating. Eq. (3.7) is replaced by Eq. (3.7a).

$$\underline{\Omega}_{\text{eq}} \cdot Z_{\text{eq},\theta,t}^{\text{m}} \leq Z_{\text{eq},\theta,t} \leq Z_{\text{eq},\theta,t}^{\text{m}} \quad \forall \text{eq} \in \text{EQ}, k \in \text{K}, t \in \text{T} \quad (3.7a)$$

$$\underline{Z}_{\text{eq}} \cdot y_{\text{eq},\theta,k,t}^{\text{op}} \leq Z_{\text{eq},\theta,t}^{\text{m}} \leq \overline{Z}_{\text{eq}} \cdot y_{\text{eq},\theta,k,t}^{\text{op}} \quad \forall \text{eq} \in \text{EQ}, k \in \text{K}, t \in \text{T} \quad (3.9)$$

$$Z_{\text{eq},\theta}^{\text{max}} - \overline{Z}_{\text{eq}} (1 - y_{\text{eq},\theta,k,t}^{\text{op}}) \leq Z_{\text{eq},\theta,k,t}^{\text{m}} \leq Z_{\text{eq},\theta}^{\text{max}} \quad \forall \text{eq} \in \text{EQ}, k \in \text{K}, t \in \text{T}$$

ii. Equipment performance

Equipment performance can vary significantly when operating at part-load. Thus, part-load performance is important to be considered for the system design. This variation usually comprises nonlinear functions. Nevertheless, affine and piecewise affine correlations with high accuracy are widely available in the literature. While piecewise models can improve the accuracy of the models, the inclusion of additional binary variables to describe variable efficiency may increase the complexity of the optimization problem. Therefore, in this work, linear correlations presented in previous works (Varbanov, 2004; Shang, 2000; Sun and Smith, 2015) are employed to model equipment performance of boilers, gas turbines and steam turbines. Part-load performance of heat recovery steam generators are neglected since additional supplementary firing can be used to compensate gas turbine part-load operation.

- Fossil fuel boilers (FFB) and Biomass (BB)

The Varbanov (2004)'s linear approach was used in this work to describe variable efficiency of boilers. The model comprises losses related to the operation load level and blowdowns. Moreover, the same correlation was used to derive the relation for solid biomass boilers, as presented in Supplementary Information P3.A.

Biomass and fossil fuel boilers performance can be described by Eq (3.10)

$$Q_{eq,k,t}^B = \sum_{v \in VHP_L} \left[(h_{sh,v} - \tilde{h}^{BFW}) (\tilde{a}_{11} \cdot Z_{eq,v,t} + \tilde{a}_{12} \cdot Z_{eq,v,k,t}^m) + \gamma \cdot Z_{Eq,v,t} (\tilde{h}_{l,v} - \tilde{h}^{BFW}) \right] \quad \begin{array}{l} \forall eq \in \{BB, FFB\}, \\ k \in K, t \in T \end{array} \quad (3.10)$$

Term $Q_{eq,k,t}^B$ represent the fuel consumption (in MW) of each boiler eq at period t of design day k . \tilde{a}_{11} , \tilde{a}_{12} are the modelling coefficient specific for each kind of boiler. γ is the blowdown percentage and $h_{sh,v}$, $\tilde{h}_{l,v}$, \tilde{h}^{BFW} are the water enthalpy at superheating, saturated liquid and boiler feed water conditions, respectively.

- Electrode boilers (EB)

In contrast to biomass and fossil fuel boilers, electric boilers operate in a more flexible way. According to manufacturers, electrode boilers can change load rate in less than 30 seconds, without efficiency variation over the operation range (Parat Halvorsen AS, 2021). Electrode boilers are assumed to be almost 100 % efficient, where the only losses come from the blowdown (ACME, 2009a). Note that industrial electrode boilers are suitable as water heaters and steam generators, being the latter of interest in this work. Current electric steam generators can generate only saturated steam at pressures up to 85 bar_a (Parat Halvorsen AS, 2021). However, superheating can be achieved by the integration of electrical superheaters. These limitations are considered in Eqs. (3.12) and (3.13), where saturated steam can be generated on electric boilers only if VHP steam main operates at pressures (P_v) below the maximum allowed by the equipment ($P_{EB}^{\max} = 85 \text{ bar}_a$). Moreover, electric superheating can be activated through auxiliary binary variable $y_{eq,v,k,t}^{sh}$, to superheat steam (if required). The overall power required by electrode boilers ($W_{T,k,t}^{EB}$) is the summation of the power required by the boiler ($W_{k,t}^{EB}$) and the superheater ($W_{k,t}^{shEB}$).

$$W_{T,k,t}^{EB} = W_{k,t}^{EB} + W_{k,t}^{shEB} \quad \forall k \in K, t \in T \quad (3.11)$$

$$W_{k,t}^{EB} = \sum_{P_v \leq P_{EB}^{\max}} \sum_{eq \in EB} Z_{eq,v,k,t} (\tilde{h}_{v,v} - \tilde{h}^{BFW}) + \gamma \cdot Z_{Eq,v,k,t} (\tilde{h}_{l,v} - \tilde{h}^{BFW}) \quad \begin{array}{l} \forall k \in K, t \in T, \\ v \in VHP_1 \end{array} \quad (3.12)$$

$$W_{k,t}^{\text{shEB}} = \frac{1}{\eta_{\text{shEB}}} \sum_{v: P_v \leq P_{\text{EB}}^{\text{max}}} \sum_{\text{eq} \in \text{EB}} (h_{\text{sh}_v} - \tilde{h}_{v,v}) Z_{\text{eq},v,k,t}^{\text{sh}} \quad \forall k \in K, t \in T \quad (3.13)$$

Term η_{shEB} represent the efficiency of the superheater, in this work assumed $\eta_{\text{shEB}} = 0.89$ based on manufacturer specifications (ACME, 2009b). Note that if electric boiler is selected, the superheater can be activated or not. To ensure the steam flowrate passing through the superheater $Z_{\text{eq},v,k,t}^{\text{sh}}$ is non-zero only if the superheater is selected ($y_{\text{eq},v,k,t}^{\text{sh}}=1$), the set of equations given by Eq. (3.14)(3.16) are applied.

$$Z_{\text{eq},v,k,t} - \overline{Z_{\text{eq}}^{\text{sh}}} \cdot \sum_{v: P_v \leq P_{\text{EB}}^{\text{max}}} (1 - y_{\text{eq},v,k,t}^{\text{sh}}) \leq Z_{\text{eq},v,k,t}^{\text{sh}} \leq Z_{\text{eq},v,k,t} \quad \forall \text{eq} \in \text{EB}, v \in \text{VHP}_1, k \in K, t \in T \quad (3.14)$$

$$Z_{\text{eq},v,k,t}^{\text{sh}} \leq \overline{Z_{\text{eq}}^{\text{sh}}} \cdot y_{\text{eq},v,k,t}^{\text{sh}}$$

Eq. (3.15) imposes that electrode boilers cannot be selected for VHP pressure levels above the maximum pressure allowed by the equipment.

$$Z_{\text{eq},v,k,t}, Z_{\text{eq},v}^{\text{max}} = 0 \quad \forall \text{eq} \in \text{EB}, v = \{v \mid P_v \geq P_{\text{shEB}}^{\text{max}}\}, k \in K, t \in T \quad (3.15)$$

Finally, the nominal size (or capacity) of the electric boiler is defined as the maximum steam required from the electric boiler among all the periods, as expressed in Eq. (3.16). Note that feasible sizes are already constrained by Eq. (3.6).

$$Z_{\text{eq},v,k,t} \leq Z_{\text{eq},v}^{\text{max}} \quad \forall k \in K, t \in T, \text{eq} \in \text{EB}, v = \{v \mid P_v \leq P_{\text{shEB}}^{\text{max}}\} \quad (3.16)$$

- Steam (ST) and gas (GT) turbines

On site power generation can be reached by steam turbines (e.g. back-pressure, condensing) and/or gas turbines (e.g. Aeroderivative, industrial). The power generated depends on the load and capacity of the equipment, this correlation can be described by Willans correlation. For sake of brevity, a compact formulation given in Eq. (3.17) is used to represent the performance of both equipment. Nevertheless, the terms employed have different interpretations depending on the equipment. For instance, term Λ represents the net fuel heat value (NHV) for gas turbine fuels, while for steam turbines Λ represents the isentropic enthalpy drop ($\Delta H_{\theta}^{\text{IS}}$) across the unit. $Z_{\text{eq},\theta}$ and $Z_{\text{eq},\theta}^{\text{max}}$ are the operating and maximum fuel flow rate for GT and the steam flowrate for steam turbines. Subindex θ represents the set of fuel available for gas turbines, whereas for steam turbines represents the set of inlet and outlet pressure (j_s, j'_s) combinations allowed. Finally, \tilde{a}_{21} , \tilde{a}_{22} , \tilde{a}_{23} and \tilde{a}_{24} involves the specific model coefficients of each turbine type. It is important to mention that in this work model coefficients were taken from Varbanov (2004) and Contribution 1 for gas turbines, and from Sun and Smith (2015) for steam turbines. Nevertheless, in practice, such coefficients depend on the design and operation of the turbines and the manufacturer.

$$W_{eq, k, t} = \sum_{\theta} \left[\widetilde{a}_{21} \left(\Lambda_{\theta} - \frac{\widetilde{a}_{22}}{Z_{eq, \theta, k, t}^m} \right) Z_{eq, \theta, k, t} + \widetilde{a}_{23} \left(\Lambda \cdot Z_{eq, \theta, k, t}^m + \widetilde{a}_{24} \cdot y_{eq, \theta, k, t}^{op} \right) \right] \quad \forall eq \in \{GT, ST\}, \quad (3.17)$$

$$k \in K, t \in T$$

Note that despite Willans correlation is linear, due to the simultaneous optimization of size, load and operating conditions of the equipment, the power generation involve nonlinear terms $\left(\frac{Z_{eq, \theta, k, t}}{Z_{eq, \theta, k, t}^m} \right)$ for both type of turbines and $\Lambda \cdot Z_{eq, \theta, k, t}$ and $\Lambda \cdot Z_{eq, \theta, k, t}^m$ for steam turbines only).

The correlations of additional utility components, such as heat recovery steam generators (HRSG), hot oil systems, let-down stations, deaerator and FSR, are reported in Supplementary Information P3.B.

- Electrolyzer and Fuel Cell (Power-to-gas system)

Proton exchange membrane electrolyzers (PEME) and fuel cells (PEMFC) are included to investigate the potential use of electrical energy to generate hydrogen (and oxygen), store it, and then convert it back to electricity as needed. For both equipment, Gabrielli et al. (2018b)'s piecewise linear approximations are employed to describe equipment performance, as expressed by Eq. (3.18).

$$P_{eq, k, t} \leq \alpha_{eq, n_{eq}} Z_{eq, k, t} + \beta_{eq, n_{eq}} Z_{eq, k, t}^m \quad \forall eq \in \{PEME, PEMFC\}, \quad (3.18)$$

$$k \in K, t \in T$$

Here, $\alpha_{eq, n_{eq}}$ and $\beta_{eq, n_{eq}}$ are modelling coefficients for each approximate line segment. For electrolyzer, $Z_{eq, k, t}$ and $P_{eq, k, t}$ represent the electrical power absorbed and the generated hydrogen (in MW), respectively. While for the fuel cell, $Z_{eq, k, t}$ and $P_{eq, k, t}$ represent the inlet hydrogen (in MW) and the electrical power generated. Additionally, Fuel cells can produce at the same time electrical and thermal power, which can be related using Eq. (3.19). Due to the low temperature of PEMFC operation, the thermal power produced is assumed to be used to heat up the make-up water in the deaerator.

$$Q_{PEMFC, k, t} = \gamma_{PEMFC} P_{PEMFC, k, t} + \beta_{PEMFC} Z_{PEMFC, k, t}^m \quad \forall k \in K, t \in T \quad (3.19)$$

It is important to note that, like in Gabrielli et al. (2018a)'s work, fuel cells are designed to operate using air oxygen. This enables to compensate for the oxygen mismatch between the electrolyzer ($H_2:O_2$ ratio of 2:1) and the fuel cell ($H_2:O_2$ ratio of 1.15:1). While this assumption has an influence on fuel cell performance, it also avoids oversizing the electrolyzer and storage tanks, as well as the injection of excess hydrogen into the natural gas system.

iv. Fuel selection and consumption

$$Q_{eq,k,t}^F = \sum_{f_{eq} \in F_{eq}} m_{eq, f_{eq},k,t}^F \text{NHV}_{f_{eq}} \quad \forall eq \in EQ \quad (3.20)$$

$Q_{eq,k,t}^F$ represents the fuel consumption (in MWh) in unit eq at a specific time period, while $m_{eq, f_{eq},k,t}^F$ and $\text{NHV}_{f_{eq}}$ the mass flowrate and net heat value of fuel f_{eq} . Note that certain equipment, such as gas turbines and HRSGs, can only use one kind of fuel at a time, resulting in the introduction of a set of binary variables ($y_{eq, f_{eq},k,t}^F$) to ensure that one type of fuel is chosen, as expressed in Eq. (3.21).

$$\underline{m}_{f_{eq},k}^F \cdot y_{eq, f_{eq},k,t}^f \leq m_{eq, f_{eq},k,t}^F \leq \overline{m}_{f_{eq},k}^F \cdot y_{eq, f_{eq},k,t}^f \quad \forall eq \in \{GT, HRSG\}, f_{eq} \in F_{eq}, k \in K, t \in T \quad (3.21)$$

Fuel availability can be represented by allowing the fuel consumption rates to fluctuate within a range, as given by Eq. (3.22).

$$\underline{m}_{f_{eq},k}^F \leq \sum_{eq \in EQ \setminus \{EB\}} \sum_{t \in T} m_{eq, f_{eq},k,t}^F \leq \overline{m}_{f_{eq},k}^F \quad \forall f_{eq} \in F_{eq}, k \in K \quad (3.22)$$

- Lignocellulose biomass

Lignocellulose biomass can be burned directly in a boiler or it can be processed to produce syngas. Syngas can be used as raw material for producing chemicals such as hydrogen, methanol, ethanol, or more complex ones. However, in this work only direct use of syngas for heat and power is investigated. Syngas production involves four stages: drying, gasification, reforming, and cleaning, as summarized in Figure 3-3. Further details about the process can be found in Supplementary Information P3.A.

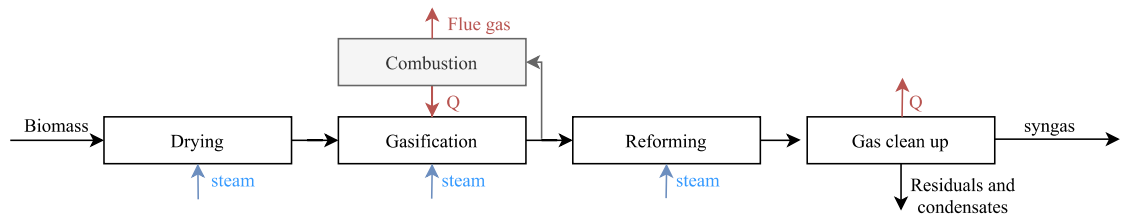


Figure 3-3 Block diagram of syngas processing

Prior gasification, biomass is dried with LP steam. Steam demand is given by Eq. (3.23).

$$\sum_{i=i_n} \sum_{j_s \in IJs} m_{i,j_s,k,t}^{S_{dry}} \cdot h_{sh_{j_s}} = \sum_{f_{eq} \in BIO} \Delta h^{dry} \cdot k_{f_{eq},k,t}^{dry} \cdot m_{IG, f_{eq},k,t}^F \quad \forall k \in K, t \in T \quad (3.23)$$

Once biomass is dried, gasification is carried out in a fluidized bed gasifier, where biomass is converted to syngas ($m_{f_{eq},k,t}^{SG}$) by using steam ($m_{k,t}^{IG}$). This process is endothermic, therefore, the heat

required at the gasifier is provided by the combustion of the char formed during the gasification. Combustor flue gas ($m_{k,t}^{fg}$) is then send to a HRSG to produce steam. While this scheme emits less CO₂ gases, it generates a higher distribution of tars and light hydrocarbons (Pérez-Uresti et al., 2019). Thus, in the reforming stage, steam ($m_{j_s, f_{eq}, k, t}^{SSR}$) is employed to convert tars and light hydrocarbons in CO and H₂, as a result syngas yield increase. It is important to note that the syngas production process is able to meet its thermal demands, and further use of available heat is used to interact with the utility system. The steam requirement, as well as the resultant flue gas and syngas flow are given by Eqs. (3.24)-(3.27). The parameters are based on the values reported in Phillips et al. (2007) and Pérez-Uresti et al. (2019).

$$m_{k,t}^{IG} = \sum_{f_{eq} \in F_{IG}} k^{IG} \cdot m_{IG, f_{eq}, k, t}^F \quad \forall k \in K, t \in T \quad (3.24)$$

$$m_{k,t}^{fg} = \sum_{f_{eq} \in F_{IG}} k^{fg} \cdot m_{IG, f_{eq}, k, t}^F \quad \forall k \in K, t \in T \quad (3.25)$$

$$m_{k,t}^{SR} = \sum_{f_{eq} \in F_{IG}} k_{f_{eq}}^{SR} \cdot m_{IG, f_{eq}, k, t}^F \quad \forall k \in K, t \in T \quad (3.26)$$

$$m_{f_{eq}, k, t}^{SG} = k_{f_{eq}}^{SG} \cdot m_{IG, f_{eq}, k, t}^F \quad \forall k \in K, t \in T, f_{eq} \in F_{IG} \quad (3.27)$$

Steam requirements of gasification and reforming stages are provided by the distribution steam mains. Due to superheating requirements for operation of the steam mains, if required, steam is expanded and cooled down to reach the operating conditions of the process, as expressed in Eqs. (3.28)-(3.31).

$$\sum_{i=1}^n \sum_{j_s \in IJs} m_{i, j_s, k, t}^{S_{IG}} + m_{k, t}^{BFW_{IG}} = m_{k, t}^{IG} \quad \forall k \in K, t \in T \quad (3.28)$$

$$\sum_{i=1}^n \sum_{j_s \in IJs} m_{i, j_s, k, t}^{S_{IG}} \cdot h_{sh_{j_s}} + m_{k, t}^{BFW_{IG}} \tilde{h}^{BFW} = m_{k, t}^{IG} \tilde{h}^{IG} \quad \forall k \in K, t \in T \quad (3.29)$$

$$\sum_{P_i \geq P_{SR}} \sum_{j_s \in IJs} m_{i, j_s, k, t}^{S_{SR}} + m_{k, t}^{BFW_{SR}} = m_{k, t}^{SR} \quad \forall k \in K, t \in T \quad (3.30)$$

$$\sum_{P_i \geq P_{SR}} \sum_{j_s \in IJs} m_{i, j_s, k, t}^{S_{SR}} \cdot h_{sh_{j_s}} + m_{k, t}^{BFW_{SR}} \tilde{h}^{BFW} = m_{k, t}^{SR} \tilde{h}^{SR} \quad \forall k \in K, t \in T \quad (3.31)$$

Finally, if biomass gasification process is selected, the heat available from the gas cleanup process is included in the heat cascade (See section 4.2.4), based on the mass of syngas generated ($m_{f_{eq}, k, t}^{SG}$), the heat capacity of the gas (\tilde{C}_p^{SG}) and the temperature difference required (ΔT^{SG}). The parameters \tilde{C}_p^{SG} and ΔT^{SG} are based on the values reported in Ayub et al. (2020) and Phillips et al. (2007).

$$Q_{T, k, t}^{SG} = m_{f_{eq}, k, t}^{SG} \cdot \tilde{C}_p^{SG} \cdot \Delta T^{SG} \quad \forall k \in K, t \in T, f_{eq} \in F_{IG} \quad (3.32)$$

The amount of syngas used in the utility system is limited to the operation of gasifier ($y_{IG,k,t}^o$) and the amount of biomass available.

$$m_{f_{eq},k,t}^{SG} \leq \overline{m_{f_{eq},k}^F} \cdot y_{IG,k,t}^o \quad \forall k \in K, t \in T, f_{eq} \in F_{IG} \quad (3.33)$$

$$m_{f_{eq},k,t}^{SG} \leq \overline{m_{f_{eq},k}^F} \cdot y_{IG,k,t}^o \quad \forall k \in K, t \in T, f_{eq} \in F_{IG} \quad (3.34)$$

$$m_{FFB,f_{eq},k,t}^F + m_{GT,f_{eq},k,t}^F + m_{HRSG,f_{eq},k,t}^F \leq m_{f_{eq},k,t}^{SG} \quad \forall k \in K, t \in T, f_{eq} \in F_{IG} \quad (3.35)$$

- Biogas

Biogas can be obtained by anaerobic digestion. In Europe, the main feedstock for biogas production is energy crops and livestock waste (Scarlat et al., 2018). Due to concerns related to the use of energy crops and more restricted European policies, only biogas obtained from livestock manure is considered in this work. Biogas composition depends on the feedstock and the operating conditions, however, on average biogas contains between CH₄ (50 – 70 %), CO₂ (25 – 45 %), H₂O (2 – 7 %), and other residual components (O₂, N₂, NH₃, H₂, H₂S) . Once obtained, biogas is cleaned and separated from the residual components (Figure 3-4) prior its use in either boiler or gas turbine. Digester data was obtained from yield data reported in Martín-Hernández et al. (2018). Further details about the process can be found in Supplementary Information P3.A.

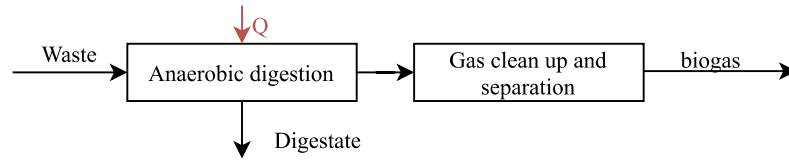


Figure 3-4 Block diagram of biogas processing

According to León and Martín (2016), digester operating with thermophilic bacteria at 55 °C maximize methane production. To keep this temperature, LP steam is used to heat up the digester. The amount of BFW required is given by Eq. (3.36). The amount of biogas (and its composition) and by-product (digestate) produced is given by (3.37)

$$m_{AD,k,t}^{SAD} = k^{SAD} m_{W,AD,k,t}^{AD} \quad \forall k \in K, t \in T \quad (3.36)$$

$$m_{AD,k,t}^{biogas_{AD}} = k^{biogas_{AD}} m_{AD,k,t}^{AD} \quad \forall k \in K, t \in T \quad (3.37)$$

$$m_{AD,k,t}^{CH4_{AD}} = k^{CH4_{AD}} m_{AD,k,t}^{biogas_{AD}}$$

$$m_{AD,k,t}^{CO2_{AD}} = k^{CO2_{AD}} m_{AD,k,t}^{biogas_{AD}}$$

$$m_{AD,k,t}^{dig_{AD}} = k^{dig_{AD}} m_{AD,k,t}^{AD}$$

Like syngas, biogas production is limited to the selection of the anaerobic digester and the amount of bio-waste available. Therefore, analogous constraints to Eqs. (3.33)-(3.35) can be used to model biogas availability.

v. *Start-up costs*

To take into account start-up limitations, the modeling approach by Bischi et al. (2014) is used to consider start-up costs for boilers, HRSGs and both gas and steam turbines. The maximum number of start-ups permissible per day for each unit is denoted as $N_{\max_{\text{eq}}}^{\text{start}}$. Additionally, a set of auxiliary variables $\delta_{\text{eq},\theta,k,t}^{\text{start}}$ is introduced for modeling if a utility component is started up during a time interval t ($\delta_{\text{eq},\theta,k,t}^{\text{start}}=1$).

$$\sum_{t \in T} \delta_{\text{eq},\theta,k,t}^{\text{start}} \leq N_{\max_{\text{eq}}}^{\text{start}} \quad \forall \text{eq} \in \text{EQ} \setminus \{\text{EB}\}, k \in K \quad (3.38)$$

To avoid introducing more integer variables $\delta_{\text{eq},\theta,k,t}^{\text{start}}$ is defined as a continuous variable, which can take values between 0 and 1 ($\delta_{\text{eq},\theta,k,t}^{\text{start}} \in [0,1]$), and is subject to Eqs. (3.39) and (3.40). Note that these set of constraints are also required to ensure variable $\delta_{\text{eq},\theta,k,t}^{\text{start}}$ is active ($\delta_{\text{eq},\theta,k,t}^{\text{start}}=1$) if, and only if, the unit was *off* the previous period (t-1) and is *on* at period t.

$$\delta_{\text{eq},\theta,k,t}^{\text{start}} \leq y_{\text{eq},\theta,k,t}^{\text{op}} \quad \forall \text{eq} \in \text{EQ} \setminus \{\text{EB}\}, k \in K, t \in T \setminus \{t_1\} \quad (3.39)$$

$$\begin{aligned} \delta_{\text{eq},\theta,k,t}^{\text{start}} &\geq y_{\text{eq},\theta,k,t}^{\text{op}} - y_{\text{eq},\theta,k,t-1}^{\text{op}} \\ \delta_{\text{eq},\theta,k,t}^{\text{start}} &\leq 1 - y_{\text{eq},\theta,k,t-1}^{\text{op}} \end{aligned} \quad \forall \text{eq} \in \text{EQ} \setminus \{\text{EB}\}, k \in K, t \in T \setminus \{t_1\} \quad (3.40)$$

To account for instances when equipment is turned off at the end of the day but start running at the first hour of the following day, Eqs. (3.41) and (3.42) are added. Eq. (3.41) connects the end of each day d ($1 \leq d \leq 365$) to the start of the following day, while Eq. (3.42) connect the last period t_n of D^{th} day to the first time step t_1 of the first day --periodicity condition. Additionally, Gabrielli et al. (2018a)'s assignment function $\sigma(d)$ is included to consider two consecutive days, represented by design day k . The function σ returns the design day k corresponding to each day of the year d , $\sigma(d)=k$.

$$\delta_{\text{eq},\theta,\sigma(d),t_1}^{\text{start}} \geq y_{\text{eq},\theta,\sigma(d),1}^{\text{op}} - y_{\text{eq},\theta,\sigma(d-1),t_n}^{\text{op}} \quad \forall \text{eq} \in \text{EQ} \setminus \{\text{EB}\}, d > 1 \quad (3.41)$$

$$\begin{aligned} \delta_{\text{eq},\theta,\sigma(d),t_1}^{\text{start}} &\leq 1 - y_{\text{eq},\theta,\sigma(d-1),t_n}^{\text{op}} \\ \delta_{\text{eq},\theta,\sigma(1),t_1}^{\text{start}} &\geq y_{\text{eq},\theta,\sigma(1),1}^{\text{op}} - y_{\text{eq},\theta,\sigma(D),t_n}^{\text{op}} \\ \delta_{\text{eq},\theta,\sigma(1),t_1}^{\text{start}} &\leq 1 - y_{\text{eq},\theta,\sigma(D),t_n}^{\text{op}} \end{aligned} \quad \forall \text{eq} \in \text{EQ} \setminus \{\text{EB}\} \quad (3.42)$$

The additional fuel consumption required for the start-up ($Q_{\text{eq},f,k,t}^{\text{start}}$) is estimated to be a fraction ($F_{\text{eq}}^{\text{start}}$) of the fuel used in full load operation, which is given by Eq. (3.43) In this work, it is assumed that $F_{\text{eq}}^{\text{start}} = 5\%$ (Sun and Liu, 2015).

$$Q_{\text{eq},f,k,t}^{\text{start}} \geq F_{\text{eq}}^{\text{start}} Q_{\text{eq},\theta}^{\text{Fmax}} - F_{\text{eq}}^{\text{start}} \overline{m_{\text{eq},k,t}^{\text{F}}} (1 - \delta_{\text{eq},\theta,k,t}^{\text{start}}) \quad \forall \text{eq} \in \{\text{FFB}, \text{BB}, \text{GT}, \text{HRSG}\}, f \in F_{\text{eq}}, k \in K, t \in T \quad (3.43)$$

$$Q_{eq,f,k,t}^{start} \leq F_{eq}^{start} Q_{eq,\theta}^F \quad \forall eq \in \{FFB, BB, GT, HRSG\}, f \in F_{eq},$$

$$k \in K, t \in T$$

4.2.3. Storage technologies

iii. Performance of energy storage technologies

All energy storage units are described through the following linear equations (Eqs. (3.44) and (3.45)), stating that the energy stored in any given time step ($E_{d,t}$) is equal to the energy that was stored in the previous time step ($E_{d,t-1}$), plus energy inputs, and minus output that can result from either discharging or losses.

$$E_{es,d,t}^{es} = E_{es,d,t-1}^{es} + \eta_{es}^{ch} \cdot P_{es,\sigma(d),t}^{ch} \cdot \Delta t_t - \frac{P_{es,\sigma(d),t}^{dch}}{\eta_{es}^{dch}} \cdot \Delta t_t - L_{es,d,t} \cdot \Delta t_t \quad \forall es \in ES, d \in D, t \in T \setminus \{t_1\} \quad (3.44)$$

$$L_{es,d,t} = \vartheta_{es}^{loss} \cdot E_{es,d,t-1}^{es} \quad \forall es \in ES, d \in D, t \in T \setminus \{t_1\} \quad (3.45)$$

So, the charging/discharging behaviour of the energy storages can be described by Eq. (3.46)

$$E_{es,d,t}^{es} = E_{es,d,t-1}^{es} (1 - \vartheta_{es}^{loss} \cdot \Delta t_t) + \eta_{es}^{ch} \cdot P_{es,\sigma(d),t}^{ch} \cdot \Delta t_t - \frac{P_{es,\sigma(d),t}^{dch}}{\eta_{es}^{dch}} \cdot \Delta t_t \quad \forall es \in ES, d \in D, t \in T \setminus \{t_1\} \quad (3.46)$$

Here P^{ch}, P^{dch} represents charging and discharging power, respectively; ϑ_{es}^{loss} is a self-discharge parameter, characteristic of each storage unit. η_{es} indicates the specified charging/discharging efficiencies; Δt_t is the duration of the time interval t .

To ensure that the energy level between two days is connected, Eq. (3.47) is enforced. Additionally, Eq. (3.48), resumes storage unit initial state/level at the end of the time horizon – periodicity constraint.

$$E_{es,d,t_1}^{es} = E_{es,d-1,t_n}^{es} (1 - \vartheta_{es}^{loss} \cdot \Delta t_t) + \eta_{es}^{ch} \cdot P_{es,\sigma(d),t_1}^{ch} \cdot \Delta t_t - \frac{P_{es,\sigma(d),t_1}^{dch}}{\eta_{es}^{dch}} \cdot \Delta t_t \quad \forall es \in ES, d > 1 \quad (3.47)$$

$$E_{es,1,t_1}^{es} = E_{es,D,t_n}^{es} (1 - \vartheta_{es}^{loss} \cdot \Delta t_t) + \eta_{es}^{ch} \cdot P_{es,\sigma(1),t_1}^{ch} \cdot \Delta t_t - \frac{P_{es,\sigma(1),t_1}^{dch}}{\eta_{es}^{dch}} \cdot \Delta t_t \quad \forall es \in ES, d \in D, t \in T \setminus \{t_1\} \quad (3.48)$$

Storage units, and specially batteries, require that there is a minimum amount of energy store in the unit to avoid adverse effects on the unit's life. This is usually known as depth of discharge (DoD). The DoD refers to the percentage a storage unit can safely discharge to. Eq. (3.49) accounts for the depth of discharge restriction.

$$E_{es,d,t}^{es} \geq (1 - DoD_{es}) \cdot Z_{es}^{es} \quad \forall es \in ES, d \in D, t \in T \setminus \{t_1\} \quad (3.49)$$

The charge and discharge rate of the storage unit is limited by the unit capacity (Z_{es}^{es}) and time required to fully charge/discharge the unit (τ_{es}), as expressed in Eq.(3.50)

$$0 \leq P_{es, \sigma(d), t}^{ch}, P_{es, \sigma(d), t}^{dch} \leq \frac{Z_{es}^{es}}{\tau_{es}} \quad \forall es \in ES, d \in D, t \in T \quad (3.50)$$

Additional logical constraints for sizing and selection of the storage technology are expressed by Eqs. (3.51) and (3.52), respectively.

$$E_{es, \sigma(d), t}^{es} \leq Z_{es}^{es} \quad \forall es \in ES, d \in D, t \in T \quad (3.51)$$

$$Z_{es}^{es}, P_{es, \sigma(d), t}^{ch}, P_{es, \sigma(d), t}^{dch} \leq U_{es} \cdot y_{es} \quad \forall es \in ES, d \in D, t \in T \quad (3.52)$$

The binary variable y_{es} represents the activation of the energy storage, while U_{es} represents the upper boundaries for each variable. It is worth noting that energy storage units add additional complexity to the problem, since their design variables are connected to all operating periods. This precludes a simple time-based decomposition.

- Thermal energy storage

Thermal storage requires additional constraints, according to the type of technology employed. In this work, two currently commercial alternatives have been considered: (i) molten salt systems and (ii) steam accumulators.

Molten salt has been proven as an effective heat transfer fluid in systems such as concentrated solar power due to its high thermal storage. The most common molten salts used are the so-called Solar Salts, which are a binary nitrate mixture of 60 wt% NaNO_3 and 40 wt% KNO_3 . The mixture has widely used, nevertheless its applicability can be limited in utility systems due to its high melting point (≈ 220 °C) and corrosivity at high temperatures (González-Roubaud et al., 2017). Due to higher demand in recent years, ternary nitrate mixtures (e.g., LiNaK, Hitec, Hitec XL, among others) with lower melting point (120 - 142 °C) had become available in the market. However, its maximum operating temperature also decreases (500 °C compared with 600 °C of Solar Salts). Based on the (saturated) temperatures of the VHP main and the distribution mains (temperature range: 130 – 330 °C), in this work, the ternary mixture LiNaK (30 wt% LiNO_3 -18 wt% NaNO_3 – 52 wt% KNO_3) (Ibrahim et al., 2021) has been considered as an option for storing heat from the VHP main and use it to raise steam from BFW conditions to a minimum superheat degree (20 °C) at the different distribution steam mains (i, j_s). These considerations are expressed in Eqs. (3.53) and (3.54).

$$\sum_{MS} P_{MS, k, t}^{ch} = \sum_{v \in VHP_L} m_{v, k, t}^{VHP-MS} (\tilde{h}_{v_v} - \tilde{h}_{l_v}) \quad \forall k \in K, t \in T \quad (3.53)$$

$$\sum_{MS} P_{MS, k, t}^{dch} = \sum_{i \in I} \sum_{j_s \in IJ_s} m_{i, j_s, k, t}^{MS} (\tilde{h}_{sh_{j_s}}^{MS} - \tilde{h}^{BFW}) \quad \forall k \in K, t \in T \quad (3.54)$$

It is important to note that in this work utility steam at saturated conditions it is assumed to be stored. This assumption is introduced to be able to define the supply and target temperature of the molten

salt system (for variable VHP pressure options), without increasing the complexity of the challenging MINLP (already featuring a large number of variables and nonconvex terms). Due to the large number of variables involved, state-of-the-art MINLP solvers (such as BARON) cannot solve the problem. Therefore, the assumption allows to adopt the bilevel decomposition algorithm and explore the potential of molten salt systems as thermal storage. Finally, although the assumption affects the temperature gradient between the hot salt and the cold salt, this can be offset by the amount of steam required to storage the heat. This can be explained by the increased mass flowrate (due to BFW injection to de-superheat VHP steam) and since the larger heat provided by steam is latent heat.

On the other hand, steam accumulators are considered the current state-of-the-art technology for steam storage, which can be used directly and therefore, eliminating the need of intermediate heat transfer fluid and the corresponding heat exchangers. For the same reason, high discharge rates are possible. However, storage capacity is limited by the pressure vessel volume. Steam accumulators are pressurized vessels that accumulate water at saturated conditions, to later release it as saturated steam. Typical steam accumulator pressure ranges for industrial plants are between 5 and 40 bar (Spirax Sarco, 2021). However, in power plants steam accumulators operating up to 150 bar can be found (Spirax Sarco, 2021). According to González-Roubaud et al. (2017), at charging stages, saturated steam is preferred over superheated steam. The latter could cause a gradual loss of stored water due to evaporation. At the discharge stage, flashed steam is produced by pressure difference. In other words, steam can be recovered only at a lower (pressure) level. This is expressed by Eqs. (3.55) and (3.56), where steam accumulators can be located within the distribution levels (if activated). For instance, the steam accumulator operating between levels j_s and j_s' is charged by de-superheated steam at j_s pressure ($m_{i,j_s,j_s',k,t}^{C_{ch-SA}}$) and discharged at j_s' pressure.

$$\sum_{SA} P_{SA,i,j_s,j_s',k,t}^{ch} = m_{i,j_s,j_s',k,t}^{C_{ch-SA}} \cdot \widetilde{h}_{sh_{j_s}}^C \quad \forall k \in K, t \in T, i \in I, (i,j_s) \in IJ_s, i' > i, (i',j_s') \in IJ_s \quad (3.55)$$

$$\sum_{SA} P_{SA,i,j_s,j_s',k,t}^{dch} = m_{i,j_s,j_s',k,t}^{C_{dch-SA}} \cdot \widetilde{h}_{v_{j_s'}} \quad \forall k \in K, t \in T, i \in I, (i,j_s) \in IJ_s, i' > i, (i',j_s') \in IJ_s \quad (3.56)$$

It is important to mention that although thermochemical and phase-change materials (PCM) technologies are promising thermal storage systems, most of these technologies are still in development stage. Thus, the aforementioned options were not included in this study. Moreover, sensible thermal storage such as hot water tank has not been considered since the focus of this work is medium-high temperatures (100 - 400 °C), where its applicability is out of the scope.

- Electrical energy storage

For electrical energy storage, batteries and hydrogen storage have been included for short- and medium-term electricity compensations. There are a number of battery types that can be used at utility scale, including but not limiting to Lithium-ion (LiB), Sodium Sulphur (NaS), and Lead-acid. Nevertheless, the most widely used in recent years has been Li-ion batteries. Nevertheless, due to low energy losses, fast response and longer period of operation, NaS have also been considered as a promising alternative to meet short-term electric imbalances (Luo et al., 2015). On the other hand, even though hydrogen storage (HS) has a low round-trip efficiency of 42 %, its negligible energy losses and larger storage capacity result in a higher round-trip efficiency over the long term, making it a feasible alternative for storing energy for extended times. The HS system comprises an electrolyzer, storage tank and a fuel cell, to generate, store and use the hydrogen. In addition to the period able to store energy, and depending on its use, it is important to consider also charging and discharging efficiencies and rates (see Table 3-1).

Table 3-1 Technical characteristics of energy storage technologies considered in this work

Technology	Z_{\min} [MW]	Z_{\max} [MW]	η_{es}^{ch} [-]	η_{es}^{dch} [-]	ϑ_{es}^{loss} [h ⁻¹]	τ^* [h]	DoD	T_{\min} [°C]	T_{\max} [°C]	Ref.
Steam accumulator	0.5	100	0.97	0.98	0.001	4	0.5	130	250*	[1][2]
Molten salts	0.5	100	0.95	0.95	0.001	4	0.8*	150* ($T_m=120$)	550*	[3]
Li-ion Battery	1	100	0.92	0.85	0.001	4	0.8	-	-	[4][5]
NaS Battery	0.05	8	0.85	0.85	-	4	0.8	-	-	[4][5]
Hydrogen storage	0.5	150	1.00	0.99	-	4	0.8	-	-	[4][5]

[1]Hofmann et al. (2019), [2]González-Roubaud et al. (2017), [3] Ibrahim et al. (2021), [4] Luo et al. (2015), [5] Breeze (2019)

Z_{\min} and Z_{\max} minimum and maximum sizes; η_{es}^{ch} and η_{es}^{dch} : charging and discharging rates; ϑ_{es}^{loss} : self-loss; τ : time required to fully charge/discharge; DoD: Depth of discharge; T_{\min} and T_{\max} : minimum and maximum temperature allowed; T_m : melting point

* Assumed data

4.2.4. Heat integration and steam distribution constraints

For optimum heat (and power) integration, the trade-off between recovering heat/steam and producing/using steam at the same level must be evaluated. As shown in Manuscript 2, this trade-off can be accounted for by employing heat cascades concept and a LP transshipment formulation (Papoulias and Grossmann, 1983). In this way, thermodynamic feasibility is guaranteed by enforcing heat transfer only from higher to lower utility intervals of the heat cascade and closing energy balances at each level.

Utility intervals are defined as stated in Manuscript 2, where the shifted inlet and outlet temperature of the process streams are extracted and sorted in descendent order. Thus, a set of discrete number

of utility level candidates are generated, which are defined by sub index j . The utility levels corresponding to the temperature/pressure range for steam distribution are indexed as j_s and further classified depending on the number and pressure range of steam mains (indexed as i) pre-specified by the designer. Heat requirements above the maximum steam distribution pressure are assumed to be satisfied by hot oil systems, while heat available below the minimum pressure for steam distribution are assumed to be rejected to cooling water.

In similar way to Manuscript 2, in this work utility steam is assumed to be generated only at the very high pressure (VHP) steam main, which operates at temperatures/pressures above any heat sink or source. Therefore, an additional set of steam levels, denoted by index v are included, based on designer inputs, to determine the appropriate operating conditions for the VHP main.

Based on the specifications stated above, the main constraints for heat integration and steam distribution are mentioned below:

i. Heat cascades

To consider site-wide heat integration, the formulation comprises three heat cascades: heat source cascade, steam cascade and heat sink cascade. Heat source and sink cascades covers the site heat surplus (\tilde{Q}^H) and deficits (\tilde{Q}^C) at each utility level j across the time horizon, as given by Eqs. (3.57) and (3.58). Moreover, heat cascades restrict the amount of the amount of process steam generated $m_{i,j_s,k,t}^H$ and use $m_{i,j_s,k,t}^C$ at each steam level, as expressed in Eqs. (3.60)-(3.62). Note that the degree of superheating at the process steam generation and use is implicitly involved in designer parameters $\tilde{h}_{sh_{j_s}}^H$ and $\tilde{h}_{sh_{j_s}}^C$.

$$\tilde{Q}_{j,k,t}^H = \sum_{h_i \in H} CP_{h_i,k,t}^H \cdot \left(\min(T_{h_i}^{*in}, T_{j-1}) - \max(T_{h_i}^{*out}, T_j) \right) \quad \forall j \in J, k \in K, t \in T \quad (3.57)$$

$$\tilde{Q}_{j,k,t}^C = \sum_{c_i \in C} CP_{c_i,k,t}^C \cdot \left(\min(T_{c_i}^{*out}, T_j) - \max(T_{c_i}^{*in}, T_{j+1}) \right) \quad \forall j \in J, k \in K, t \in T \quad (3.58)$$

Note that if biomass gasification is selected, heat from the gas cooling process can be recovered to generate steam at different levels. This is expressed by the variable $Q_{j,k,t}^{SG}$ and Eq. (3.59)

$$Q_{j,k,t}^{SG} = \sum_{f_{eq} \in FIG} m_{f_{eq},k,t}^{SG} \cdot \tilde{C}P^{SG} \cdot \left(\min(T_{in}^{BG}, T_{j-1}) - \max(T_{out}^{BG}, T_j) \right) \quad \forall j \in J, k \in K, t \in T \quad (3.59)$$

$$Q_{T,k,t}^{SG} = \sum_{j \in J} Q_{j,k,t}^{SG} \quad \forall j \in J, k \in K, t \in T$$

$$\tilde{Q}_{j_s,k,t}^H + Q_{j_s,k,t}^{SG} + R_{j_s-1,k,t}^H = m_{i,j_s,k,t}^H \cdot (1+L^H) \cdot \left(\tilde{h}_{sh_{j_s}}^H - \tilde{h}^{BFW} \right) + R_{j_s,k,t}^H \quad \forall i \in I, (i, j_s) \in IJ_s, k \in K, t \in T \quad (3.60)$$

$$m_{i,j_s,k,t}^{C_T} \cdot (1-L^C) \cdot (\widetilde{h}_{shj_s}^C - \widetilde{h}_{j_s}) + Q_{s,k,t}^{HO} + R_{j_s-1,k,t}^C = \widetilde{Q}_{j_s,k,t}^C + R_{j_s,k,t}^C \quad \forall j_s = 1, (i, j_s) \in IJ_s, \quad (3.61)$$

$$k \in K, t \in T$$

$$m_{i,j_s,k,t}^{C_T} \cdot (1-L^C) \cdot (\widetilde{h}_{shj_s}^C - \widetilde{h}_{j_s}) + R_{j_s-1,k,t}^C = \widetilde{Q}_{j_s,k,t}^C + R_{j_s,k,t}^C \quad \forall j_s > 1, (i, j_s) \in IJ_s, \quad (3.62)$$

$$k \in K, t \in T$$

Heat that is not used in a particular level flows to the next lower level as residual heat involved in terms $R_{j_s,k,t}^H$ and $R_{j_s,k,t}^C$. Heat losses from steam distribution between the utility system and the site processes, are accounted by the fixed terms L^H and L^C . Finally, as mentioned in the assumptions, hot oil systems is included through term $Q_{s,k,t}^{HO}$ for supplementary heating (if applicable). Further constraints regarding, hot oil system is condensed in Supplementary Information P3.B

ii. Mass and energy balance

Constraints in Eqs. (3.63) and (3.64) link the utility components (UC) with the site mass flowrates, through the steam mains in each period (k,t). Additionally, steam flows related to energy storage in molten salt tanks are described are included here, as illustrated in Figure 3-1. Note that streams entering the steam header may be introduced at different temperatures, and consequently an energy balance is required to ensure that the temperature needed at each steam main is maintained. Generally, the steam mains' (superheat) temperature is expressed through its corresponding enthalpy (\widetilde{h}_{shj_s}), which in this work is considered as a design variable. Similar constraints are formulated for the VHP steam main.

$$m_{i,j_s,k,t}^H + m_{i,j_s,k,t}^{MS} + \sum_{uc \in UC_L} m_{uc,i,j_s,k,t}^{in} = \sum_{uc \in UC_L} m_{uc,i,j_s,k,t}^{out} + m_{i,j_s,k,t}^{C_{steam}} \quad \forall i \in I, \quad (3.63)$$

$$(i, j_s) \in IJ_s$$

$$m_{i,j_s,k,t}^H \cdot \widetilde{h}_{shj_s}^H + m_{i,j_s,k,t}^{MS} \cdot \widetilde{h}_{shj_s}^{MS} + \sum_{uc \in UC} Q_{uc,i,j_s,k,t}^{in} = \sum_{uc \in UC} (m_{uc,i,j_s,k,t}^{out}) \cdot \widetilde{h}_{shj_s} + m_{i,j_s,k,t}^{C_{steam}} \cdot \widetilde{h}_{shj_s} \quad \forall i \in I, \quad (3.64)$$

$$(i, j_s) \in IJ_s$$

$m_{uc,i,j_s,k,t}^{in}$ comprises the inlet streams at each steam main i operating at j_s condition, such as BFW, let-down steam and steam turbine exhausts. $m_{uc,i,j_s,k,t}^{out}$ involves outputs like steam to either back-pressure or condensing turbines, let-down stations or in case of the last steam main, steam to the deaerator. $Q_{uc,i,j_s,k,t}^{in}$ represents the heat from the inlet streams to steam main i operating at j_s conditions.

While for the heat source side there is only the input of process streams (including biomass gasification –if applicable-) for steam generation, on the heat sink side it is required to consider several streams, such as BFW injection ($m_{i,j_s,k,t}^{C_{BFW}}$) for steam de-superheating, saturated steam from FSR tanks, and any amount of steam discharging(charging) from(to) steam accumulators units (if

activated). The mass and energy balance of the different streams involved are reflected in Eqs. (3.65) and (3.66).

$$m_{i,j_s,k,t}^{C_T} = m_{i,j_s,k,t}^{C_{\text{steam}}} + m_{i,j_s,k,t}^{C_{\text{BFW}}} + m_{i,j_s,k,t}^{C_{\text{FSR}}} + \sum_{i' < i} \sum_{(i',j_s) \in IJ_s} m_{i',j_s,j_s,k,t}^{C_{\text{dch-SA}}} - \sum_{i' > i} \sum_{(i',j_s) \in IJ_s} m_{i,j_s,j_s,k,t}^{C_{\text{ch-SA}}} \quad \forall i \in I, \quad (i, j_s) \in IJ_s \quad (3.65)$$

$$m_{i,j_s,k,t}^{C_T} \cdot \widetilde{h}_{sh_{j_s}}^C = m_{i,j_s,k,t}^{C_{\text{steam}}} \cdot h_{sh_{j_s}} + m_{i,j_s,k,t}^{C_{\text{BFW}}} \cdot \widetilde{h}^{\text{BFW}} + m_{i,j_s,k,t}^{C_{\text{FSR}}} \cdot \widetilde{h}_{v_{j_s}}^{\text{FSR}} + \sum_{i' < i} \sum_{(i',j_s) \in IJ_s} m_{i',j_s,j_s,k,t}^{C_{\text{dch-SA}}} \cdot \widetilde{h}_{v_{j_s}}^{\text{SA}} - \sum_{i' > i} \sum_{(i',j_s) \in IJ_s} m_{i,j_s,j_s,k,t}^{C_{\text{ch-SA}}} \cdot \widetilde{h}_{sh_{j_s}}^C \quad \forall i \in I, \quad (i, j_s) \in IJ_s \quad (3.66)$$

4.2.5. Electricity balance

The electricity balance at time t comprises the site power demand (θ^c), on-site power generation, electricity import (export) from (to) the grid and the charging (discharging) from(to) the electrical energy storage, as expressed in Eq. (3.67).

$$U_{e,k,t}^{\text{imp}} + \sum_{eq \in \{\text{GT}, \text{ST}\}} W_{eq,k,t} + P_{es,k,t}^{\text{dch}} = (1+L^e) \cdot \widetilde{W}_{k,t}^{\text{dem}} + W_{T,k,t}^{\text{EB}} + P_{es,k,t}^{\text{ch}} + U_{e,k,t}^{\text{exp}} \quad \forall k \in K, \quad t \in T \quad (3.67)$$

Additionally, practical limits for import and export of electricity are given by Eq.(3.68).

$$U_{e,k,t}^{\text{imp}} \leq \widetilde{U}_{\text{max}}^{\text{imp}} \quad \text{and} \quad U_{e,k,t}^{\text{exp}} \leq \widetilde{U}_{\text{max}}^{\text{exp}} \quad \forall k \in K, \quad t \in T \quad (3.68)$$

Note that in this work a single value to restrict the power import and export is assumed, nevertheless this could be easily adapted to represent restrictions during peak and off-peak demand times.

4.2.6. Logical constraints

A simplified version of the logical constraints are presented below

i. Steam level selection and forbidden operating conditions

Constraints in Eqs. (3.69) and (3.70) restrict to single operating conditions for the steam mains. In the case of distribution steam mains, the selection(activation) or not of steam main i , is consider by the inequality of Eq. (3.70). In addition, any steam level candidate j_s that do not correspond to set IJ_s , is fixed as zero. In other words, if $(i,j_s) \notin IJ_s$ then $y_{i,j_s} = 0$.

$$\sum_{v \in \text{VHP}_L} y_v = 1 \quad (3.69)$$

$$\sum_{(i,j_s) \in IJ_s} y_{i,j_s} \leq 1 \quad \forall i \in I \quad (3.70)$$

Moreover, the selection of steam level determines equipment activation. Only if steam level L is selected, equipment activation can be considered. In this context, there are two main cases: (i) equipment that only operates at one level (i.e. boilers and HRSG), where the constraint is imposed

by Eq. (3.71), and (ii) equipment operating between two levels such as: steam turbines, molten salt system, steam accumulators and FSR, where Eq. (3.72) is applied.

$$y_{eq,L,k,t} \leq y_L \quad \forall eq \in EQ, L \in IJ_s \cup VHP_L, k \in K, t \in T \quad (3.71)$$

$$y_{UC,L',k,t} \leq \frac{y_L + y_{L'}}{2} \quad \forall UC \in \{ST, FSR, MSS, SA\}, L \in IJ_s \cup VHP, L' > L \quad (3.72)$$

ii. Feasibility constraints

Eq. (3.73) represents links the mass and energy flows with the steam level selected. Note that U^m and U^Q denotes the upper bounds for mass and energy vectors of variables, based on problem specifications. Analogous constraints are formulated for the VHP level.

$$\begin{aligned} m_{i,j_s,k,t}^{in} - U_{k,t}^m \cdot y_{i,j_s} &\leq 0 \\ m_{i,j_s,k,t}^{out} - U_{k,t}^m \cdot y_{i,j_s} &\leq 0 \\ Q_{i,j_s,k,t}^{in} - U_{k,t}^Q \cdot y_{i,j_s} &\leq 0 \\ Q_{i,j_s,k,t}^{out} - U_{k,t}^Q \cdot y_{i,j_s} &\leq 0 \end{aligned} \quad \forall i \in I, (i,j_s) \in IJ_s, k \in K, t \in T \quad (3.73)$$

iii. Enthalpy (temperature) constraints

Based on allowed temperature range for each steam main (specified by the designer), upper and lower boundaries for steam main enthalpies are imposed by Eqs. (3.74)-(3.77)

$$\underline{h}_{sh_v} y_v \leq h_{sh_v} \leq \overline{h}_{sh_v} y_v \quad \forall v \in VHP_L \quad (3.74)$$

$$\underline{h}_{sh_j_s} y_{i,j_s} \leq h_{sh_j_s} \leq \overline{h}_{sh_j_s} y_{i,j_s} \quad \forall i \in I, (i,j_s) \in IJ_s \quad (3.75)$$

$$h_{sh_j_s} \leq \sum_v h_{sh_v} \quad \forall j_s \in J_s \quad (3.76)$$

$$h_{sh_j_s} \leq \sum_{(i-1,j_s) \in IJ_s} \left[h_{sh_j_s} + \overline{h}_{sh_j_s} (1 - y_{i,j_s}') \right] \quad \forall i > 1, (i,j_s) \in IJ_s \quad (3.77)$$

The multi-period optimization problem resulting from combining superstructure of steam levels and utility component is a nonconvex MINLP. It comprises binary variables for the selection of: (i) steam levels, (ii) fuel, (iii) equipment and (iv) energy storage, as well as the activation of equipment operating at specific period. Continues variables are involved in thermal and power generation, size and load of conversion and storage units, enthalpies, and water/steam mass flowrates. The main nonlinearities result from the consideration of steam enthalpy/temperature ($h_{sh_j_s}$ and h_{sh_v}) as a design variable, leading to bilinear products in energy balances at each steam main, and in the performance models of the conversion units. Additionally, non linearities result from economy of scale law in the investment cost of equipment and steam functions --e.g., isentropic enthalpy difference and VHP temperature calculation --, see Manuscript 2 for further details. In summary, the nonconvex MINLP formulation can be synthesize as below:

Objective function	{min Total Annualized Cost	Eq. (3.1)
Subject to:		
Costs	{ Investment	Eq. (3.2)
	{ Maintenance	Eq. (3.3)
	{ Operation	Eq. (3.5)
	{ Start-up	Eq. (3.4)
Utility component constraints	{ Selection, sizing and load	Eqs. (3.6),(3.7a),(3.8) & (3.9)
	{ Equipment performance	Eqs. (3.10) - (3.19)
	{ Fuel selection and consumption	Eqs. (3.20) - (3.37)
	{ Start-up costs	Eqs. (3.38) - (3.43)
Energy units constraints	{ Performance of energy storage	Eqs. (3.44) - (3.48)
	{ Charging and discharging constraints	Eqs. (3.49) & (3.50)
	{ Selection and sizing	Eqs. (3.51) & (3.52)
Heat integration and steam distribution	{ Heat cascades	Eqs. (3.57) - (3.62)
	{ Mass and energy balance	Eqs. (3.63) - (3.66)
Electricity import/export constraint	{Electricity balance	Eqs. (3.67) & (3.68)
Additional constraints to avoid infeasibilities	{ Steam level selection	Eqs. (3.69) - (3.72)
	{ Feasibility constraints	Eq. (3.73)
	{ Enthalpy constraints	Eqs. (3.74) - (3.77)

4.3. Optimization strategy

According to preliminary computational experiments, the proposed nonconvex MINLP model cannot be solved using general-purpose MINLP solvers such as BARON, due to the large number of decision variables and nonlinearities involved in this class of mathematical optimization problems. Therefore, the MINLP model is solved through an adaption of the BEELINE model presented in Manuscript 2. The adopted strategy incorporates time dependency of energy demands and electricity prices, in addition to the energy storage options and additional sources and technologies. The implemented optimization algorithm, summarized in Figure 3-5, proceeds as below:

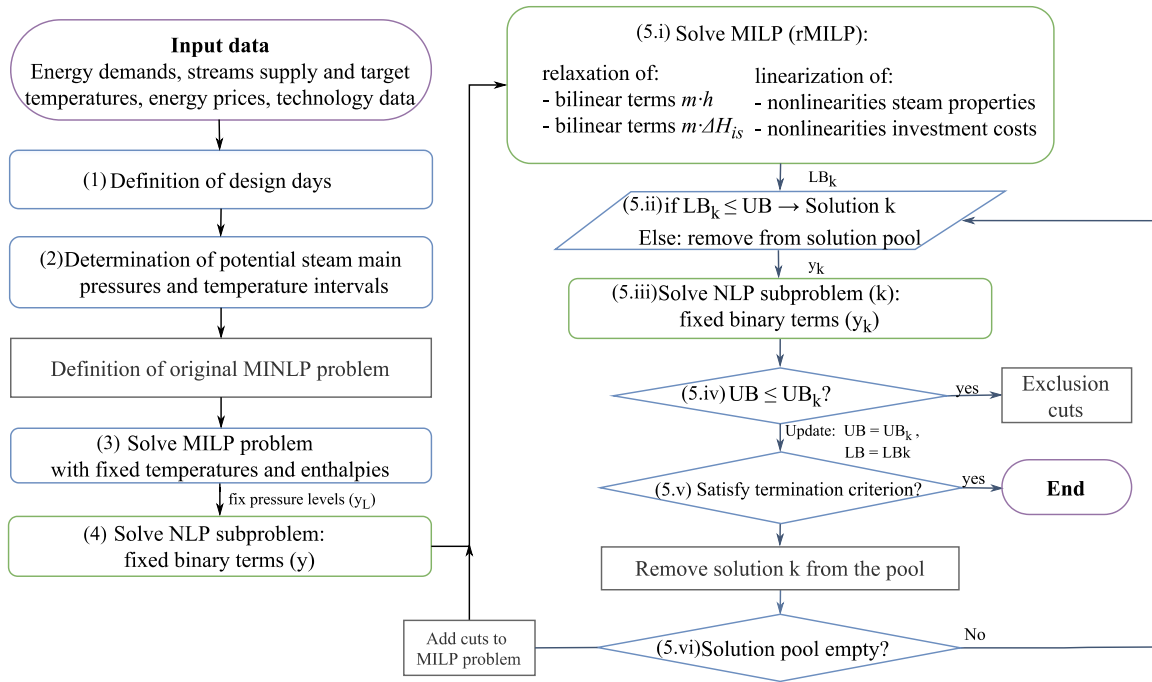


Figure 3-5 Summary of the optimization framework to determine utility system design and operation, considering variable demand and energy price fluctuations

- (1) **Definition of design days.** To reduce the computational effort while retaining variability and accuracy, the appropriate fit and design days for the annual data are identified using the procedure outlined in Section 4.1
- (2) **Determination of potential steam main pressures and temperature intervals.** To keep the formulation simple and avoid adding unnecessary complexities, the steam header pressures are chosen from a discrete set of options determined by the kinks in the heat sink and source profiles. The kinks are obtained based on the shifted supply and target temperatures, listed in descending order (for more information see Contribution 1). Moreover, additional heating and cooling utilities are determined depending on the minimum and maximum allowed steam distribution pressures. For instance, heat requirements over the maximum steam saturated temperature are provided by hot oil systems, while heat available below the minimum steam saturated temperature is rejected to cooling water.

Based on steps (1) and (2), in addition of the input data, the original MINLP problem is formulated.

- (3) and (4) To reduce the convergence time required by the algorithm, a MILP version of the original MINLP is used for initialization. The MILP formulation obtained by setting steam enthalpies and temperatures offers a good initial point of the steam main pressures and potential configurations (at lower computational effort) and minimize the NLP subproblem. Due to the fact that steam properties are set for the MILP version, the computed solution

cannot be used as lower bound (LB) for the original MINLP problem. Nevertheless, it enables the estimation of the energy targets and possible configurations, as well as the definition/tightening of the comprising variables limits.

- (5) The bilevel algorithm comprises a MILP problem (upper level) and a NLP sub problem (lower level). The upper-level problem, also referred as master problem, is a linearized and relaxed version of the original problem. The MILP problem is first solved to generate a pool of feasible solutions (including the master optimal solution), which are then ranked and filtered according to their objective value. The best solution provides the lower bound (LB) to the original problem. Then, the solutions of binary variables are passed to the NLP sub problem, which re-optimizes the continuous variables, and in this way obtain the MINLP upper bound. After the assessment of all the solutions, the integer cuts are applied to the master problem to exclude prior results and explore new solution spaces.

(5.i) The master problem, rMILP, is obtained using the following linearization techniques (detailed formulation is presented in Manuscript 2):

- Piecewise MILP linearization (Gounaris et al., 2009) of bilinear terms directly involving steam main enthalpies (h_{sh_j} and h_{sh_v}). To provide a higher tightness to the relaxation, the bilinear terms resulting from the multiplication of mass flow rates and steam enthalpies, as is the case of energy balances of steam mains and the performance model of the boilers, are addressed with Gounaris et al. (2009)'s NF4R formulation.
- Convex envelopes (McCormick, 1976) are used to linearize bilinear terms where the addition of piecewise-MILP relaxations increased the problem size without a significant change in the objective function. For instance, the HRSG and turbines performance models.
- Polynomial approximation of steam properties. Steam temperature and isentropic enthalpy difference can accurately be described by linear or quadratic approximations respect to enthalpy (see Supplementary Information P3.C). It is important to note that the validity of these correlations is restricted to steam superheated stage.
- Piece-wise affine approximation of investment costs. To consider the scale effect, investment cost can be expressed as a set of linear segments respect to the size.

(5.ii) Notably, the optimal values of the objective function of rMILP provides a rigorous lower bound of the MINLP, however, since the rMILP has a larger feasibility space than the original MINLP. Its solution may be unfeasible when used as input to the original MINLP. Therefore, the rMILP model is solved with CPLEX solver with solution pool option active. If the solutions obtained are lower than the upper bound UB, they are part of solution pool

(5.iii) The solutions stored in the CPLEX solution pool are used to fix the values of the binary variables and used as starting points for the continuous variables in the NLP subproblem.

(5.iv) If any of the computed solutions is feasible and has a smaller objective function value than the previous upper bound (UB), then UB is updated with this value. Otherwise, the combination of integer variables is considered as an exclusion cut.

(5.v) The algorithm is carried out until the difference between the UB and the LB is less than a predetermined tolerance (denoted as ϵ), or if the number of iterations is greater than the maximum defined ITmax. Otherwise, the solution is removed from pool and continue to Step (5.vi).

(5.vi) If all the solutions stored in the solution pool are evaluated, all the integer cuts are added to the rMILP (step (5.i)) to combine prior master and sub problem information, to exclude binary solutions already assessed and generate an alternate solution.

The optimization problem is encoded GAMS (Bussieck and Meeraus, 2004). The initialization stage and the master problem are solved with CPLEX 20.1.0.0 (Corporation, 2017), while the NLP subproblem is solved with CONOPT 4 (Drud, 1985). Despite the use of a local solver cannot guarantee global solutions, the results obtained are promising and at lower computational time compared against global solver BARON (Tawarmalani and Sahinidis, 2005).

5. Case study definition

The proposed methodology is applied to an illustrative case study based on Sun et al. (2015) nominal data of a petrochemical plant. In this work it is assumed that the production profile of the different site plants across the year is similar to the one provided for the petrochemical plant in Bungener et al. (2015) study. The objective function is the Total Annual Cost (TAC).

5.1. Energy demands parameters

The industrial site is composed by five industrial plants with different heating, cooling, and power demands. It is assumed that industrial energy requirements can be accurately defined by a linear correlation with the production profile of each plant, expressed daily for a whole year of operation. Heating and cooling requirements are given by heating and cooling site profiles.

Figure 3-6 represents the nominal heating and cooling profiles for each plant, while Figure 3-7 shows their production profile. Note that a key assumption in this work is that supply and target temperature of streams are constant across the time horizon. Although, the assumption simplifies the problem, this consideration results are practical due to the complexity of having registers of hourly or daily process temperature changes.

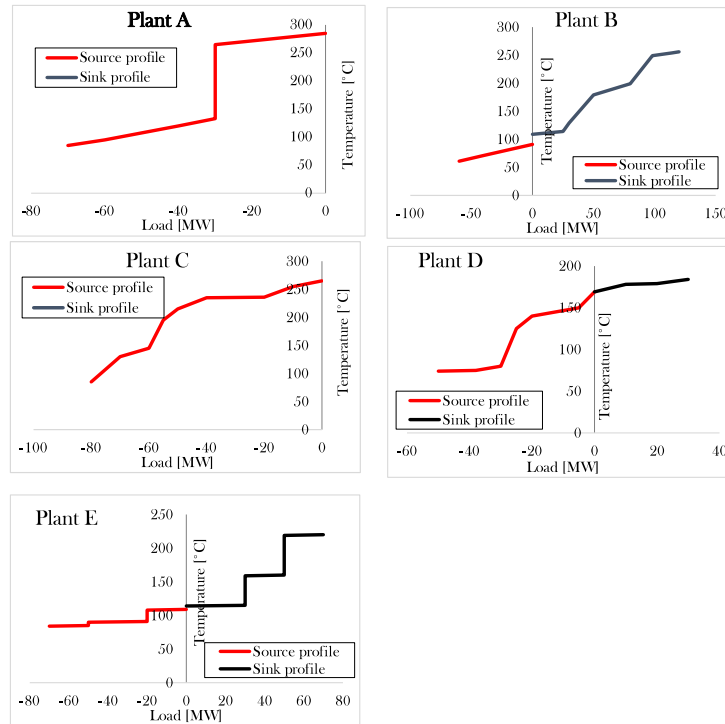


Figure 3-6 Nominal heating and cooling profile of each plant [based on Contribution 1]

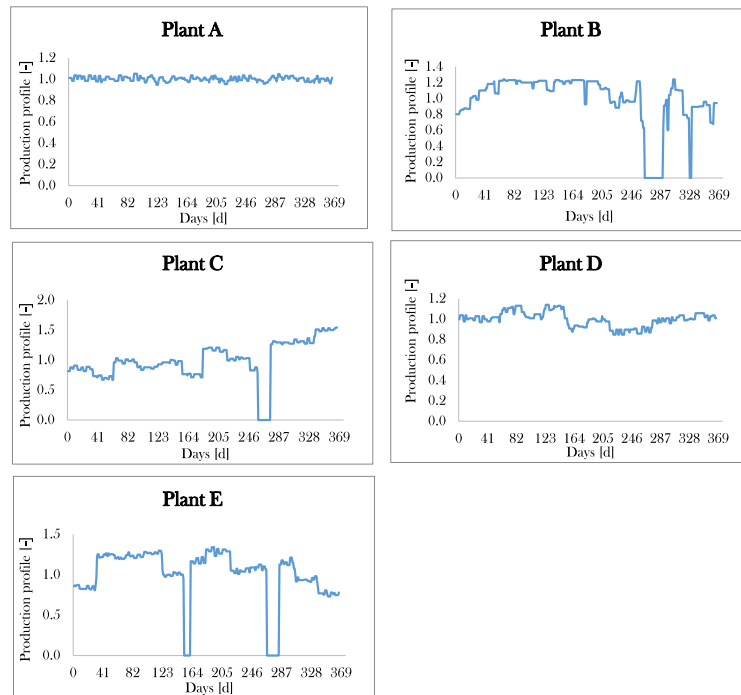


Figure 3-7 Production profile of each plant across an operational year with daily resolution [adapted from Bungener et al. (2015) study]

5.2. Technical and cost parameters

Another relevant time-variant parameter is the hourly electricity price fluctuation. Although industries can usually have fixed contracts for weeks up to three years. Wholesale market and its variability across time can affect the tariffs in the industry, especially for selling electricity to the

grid. In this work, electricity price fluctuation is based on data from 2019, available with hourly resolution in (Pool, 2020) and illustrated in Figure 3-8. Power requirements, minimum temperature approach and other site specifications are presented in Table 3-2.

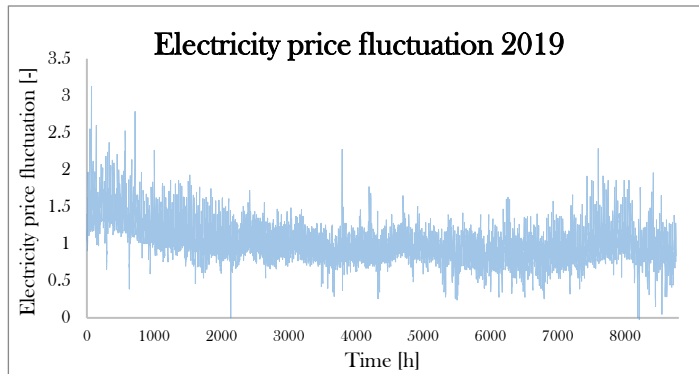


Figure 3-8 Electricity profile across the year with hourly resolution

Table 3-2. Site specifications for the steam system

Parameter	Unit	Value
Nominal power requirement plant A	MW	13
Nominal power requirement plant B	MW	11
Nominal power requirement plant C	MW	7
Nominal power requirement plant D	MW	6
Nominal power requirement plant E	MW	3
Site minimum steam main superheating	°C	20
Degree of superheating for process steam generation	°C	20
Degree of superheating for process heating	°C	3

It is important to note that while average purchasing costs of electricity and natural gas can be defined for Europe, in practice, the cost of electricity and fuels can vary considerably -- depending on several factors including the geopolitical location, tax structure, network charges and industry scale. Figure 3-9 illustrates the energy prices for several European countries in 2019. Energy prices influence the utility system operating costs and selection of equipment (as detailed later in the results). As a result, the impact of various electricity/fuel price ratios is investigated through a sensitivity analysis of the proposed scenarios, considering as reference the electricity and fuel prices registered in 2019.

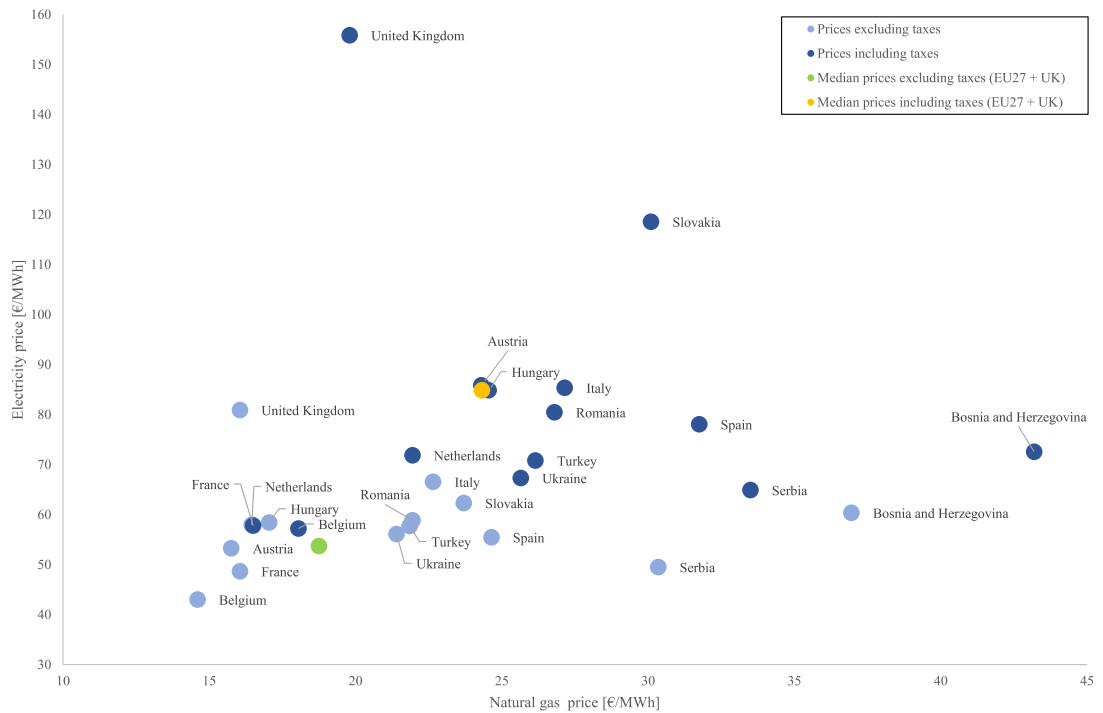


Figure 3-9 Electricity and natural gas purchase prices for European countries in 2019 Eurostat (2020)

5.3. Scenarios definition

The present methodology allows us to analyze different scenarios. For first analysis, a set of two scenarios is established to examine the effect of energy storage on the design and operation of the utility system. Scenario I comprise only conversion technologies, whereas Scenario II includes FSR and energy storage integration options. Moreover, a comparison with the suggested operating conditions for steam mains in Sun et al. (2015)’s study is made to evaluate the benefits of temperature and pressure selection for steam mains. The scenarios under study in this work are summarized in Table 3-3.

Table 3-3.Scenario specifications for sensitivity analysis

		Steam main conditions selection	Integration of FSR and energy storage	
			Yes	No
Base case	Scenario I	No		✓
Case 1	Scenario II	No	✓	
Case 2	Scenario I	Yes		✓
Case 3	Scenario II	Yes	✓	

Furthermore, a sensitivity analysis is performed to determine how the utility system design choices, and thus its costs and primary energy consumption patterns, would vary across a broader range of energy prices. The electricity/natural gas price ratio is varied between 1 and 7, with the 2019 nominal price as a reference, as presented in

Table 3-4. Additionally, the effect of potential increase of fossil fuels either due to increasingly heavier carbon pricing levels or to evolving market conditions is also evaluated.

Table 3-4. Test levels for electricity and natural gas nominal prices and variations

Energy parameter	Variation
Electricity*	1, 1.25, 1.50, 1.75, 2.0, 2.25, 2.50 3.0, 4.0, 5.0 , 6.0, 7.0
Fossil fuels (Fuel gas, Natural gas, Distillate oil, Fuel oil)	1.05, 1.10, 1.25, 1.50, 2.00, 3.64**

*Having as reference 2019 nominal purchase price of natural gas as 24.30 [€·MWh⁻¹]

** Price variation for similar natural gas and electricity nominal purchase price (85.6 €·MWh⁻¹)

6. Results and discussion

To select the most representative typical periods *k*-means and *k*-medoids algorithm are applied by considering $k \in \{2, \dots, 52\}$ to approach a maximum period of a week, and a maximum of 3000 iterations was assumed. Additionally, for *k*-means method 300 random starting points were considered. The results obtained are presented in Figure 3-10.

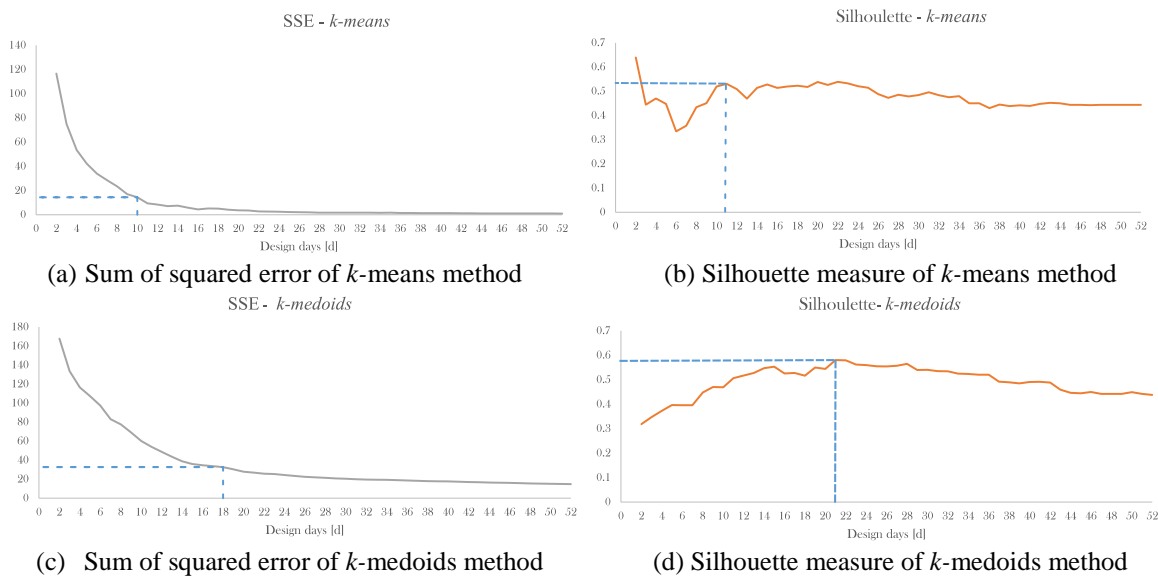


Figure 3-10 SSE and Silhouette measures as function of the number of typical design days using *k*-means and *k*-medoids methods

Based on Figure 3-10 (a) and (c) it can be determined that for the particular case study *k*-means algorithm presents a better performance than *k*-medoids. The latter not only requires a higher minimum number of design days (18) compared to the *k*-means algorithm (10), but also presents a lower agreement between the clusters. SSE for *k*-means becomes close to 0 after 24 clusters while for *k*-medoids only reaches values around 9. Therefore, for the case *k*-means clustering is employed to define the design days.

It is important to note that although increasing the number of design periods to 24 would reduce the error to less than 1.5 %, this leads to an exponential increased size of the optimization model.

Therefore, a minimum of 10 design periods are required to represent the data. The highest values of silhouette measure (inter-cluster distance) are obtained at 11, 23, 25 design periods, as shown in Figure 3-10 (b). Therefore, 11 design days plus 1 extreme period are chosen as the best qualified number of typical periods.

In a similar way, the electricity price fluctuation within design days has been analyzed, defining 4-time steps of varying length as shown in Figure 3-11.

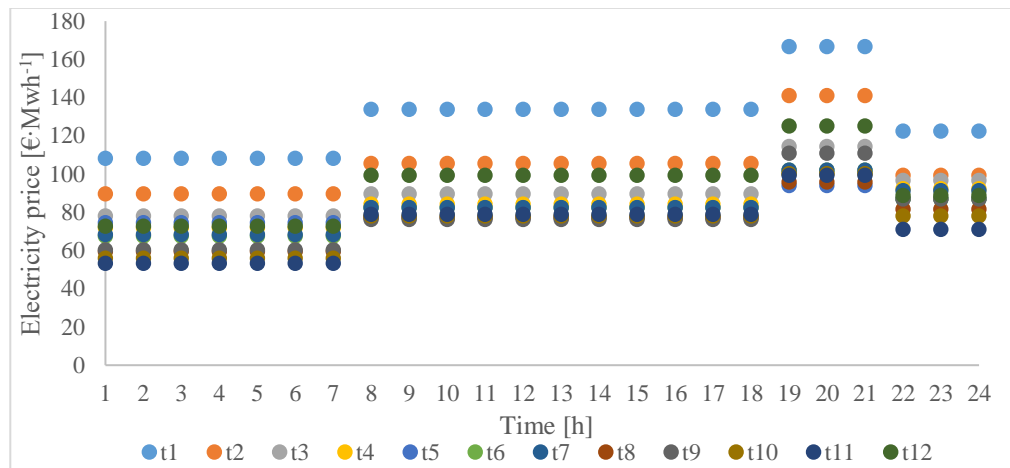


Figure 3-11 Electricity price fluctuation for the different design days

6.1. Case study results

The resulting MINLP problem consists of 14 286 decision variables (1 424 binary) and 35 623 equations. Note that the number of variables depends on the number of intervals for the piece wise linearization adopted for the models. In this work, three intervals have been considered. The number of variables depends on the number of intervals of the PWL adopted to model the characteristic curves of the units. The tests were carried out on an Intel i7 with 211 GHz CPUs and 16 GB of RAM. The computational time required is about 11 259 s. Table 3-5 summarizes the main findings of the case study under scenarios I and II, taking into account steam main operating conditions. The findings indicate that operating expenses are the dominant costs. This explains why, under given energy market conditions, economic optimal designs rely entirely on fossil fuels to meet heat and power requirements. Moreover, all the designs benefit from revenues generated by power export to the grid (denoted as negative costs).

Table 3-5. Costs and equipment capacities for the base case and optimized case under different scenarios

		Optimized design with predefined steam main conditions*		Optimized design with steam main conditions selection	
		Scenario I (Baseline)	Scenario II	Scenario I	Scenario II
Steam mains		VHP / HP / MP / LP		VHP / HP / MP / LP	
Temperature	[° C]	560 / 270.4 / 232.4 / 171.8		570 / 267.0 / 209.1 / 150.0	
Pressure	[bar]	85.0 / 40.0 / 20.0 / 5.0		85.0 / 37.8 / 12.3 / 2.7	
Total Annualized cost	[m€·y ⁻¹]	79.53	71.44 (-10.2 %)	68.52 (-13.8 %)	60.02 (-24.5 %)
Operating cost	[m€·y ⁻¹]	63.82	56.33 (-11.7 %)	53.72 (-15.8 %)	45.91 (-28.1 %)
Maintenance cost	[m€·y ⁻¹]	4.23	3.92 (-7.3 %)	3.89 (-8 %)	3.53 (-16.4 %)
Start cost	[m€·y ⁻¹]	0.02	0.01 (-20.7 %)	0.02 (-10.4 %)	0.02 (+11.6 %)
Capital cost	[m€·y ⁻¹]	11.47	11.17 (-2.6 %)	10.89 (-5 %)	10.56 (-7.9 %)
Operating costs					
Electricity	[m€·y ⁻¹]	-1.46	-1.45 (-0.5 %)	-1.55 (6.7 %)	-1.51 (3.9 %)
Fuel	[m€·y ⁻¹]	62.79	55.3 (-11.9 %)	53.12 (-15.4 %)	45.26 (-27.9 %)
Cooling water	[m€·y ⁻¹]	2.37	2.37 (0 %)	2.05 (-13.8 %)	2.05 (-13.8 %)
Make-up water	[m€·y ⁻¹]	0.12	0.12 (0 %)	0.11 (-0.9 %)	0.11 (-0.9 %)
Site fuel consumption					
Fuel gas	[GWh·y ⁻¹]	1, 088.3	1,050.60 (-3.5 %)	1,014.20 (-6.8 %)	568.3 (-47.8 %)
Natural gas	[GWh·y ⁻¹]	1, 514.3	1,214.60 (-19.8 %)	1,113.20 (-26.5 %)	1223.3 (-19.2 %)
Equipment selection /capacities					
Packaged boiler (fuel gas)	[t·h ⁻¹]	216.37	176.8 (-18.3 %)	175.01 (-19.1 %)	138.29 (-36.1 %)
HRSR (natural gas)	[t·h ⁻¹]	147.32	147.08 (-0.2 %)	147.09 (-0.2 %)	141.6 (-3.9 %)
Steam turbine	[MW]	2.06	2.06 (0 %)	2.06 (0 %)	4.12 (+100.6 %)
Gas turbine (natural gas)	[MW]	48.20	48.2 (0 %)	48.2 (0 %)	46.16 (-4.2 %)
Total FSR	[t·h ⁻¹]	-	124.08	-	120.34
Molten salt system	[MWh]	-	-	-	-
Steam accumulator	[MWh]	-	-	-	-
Li-ion battery	[MWh]	-	-	-	-
NaS battery	[MWh]	-	-	-	-
Hydrogen storage	[MWh]	-	-	-	-

*based on Sun et al. (2015)'s steam main conditions

In terms of steam main conditions, determining the appropriate operating pressure and temperature for steam headers results in a reduction not only in the fuel consumption (15.4 %) and cooling requirements

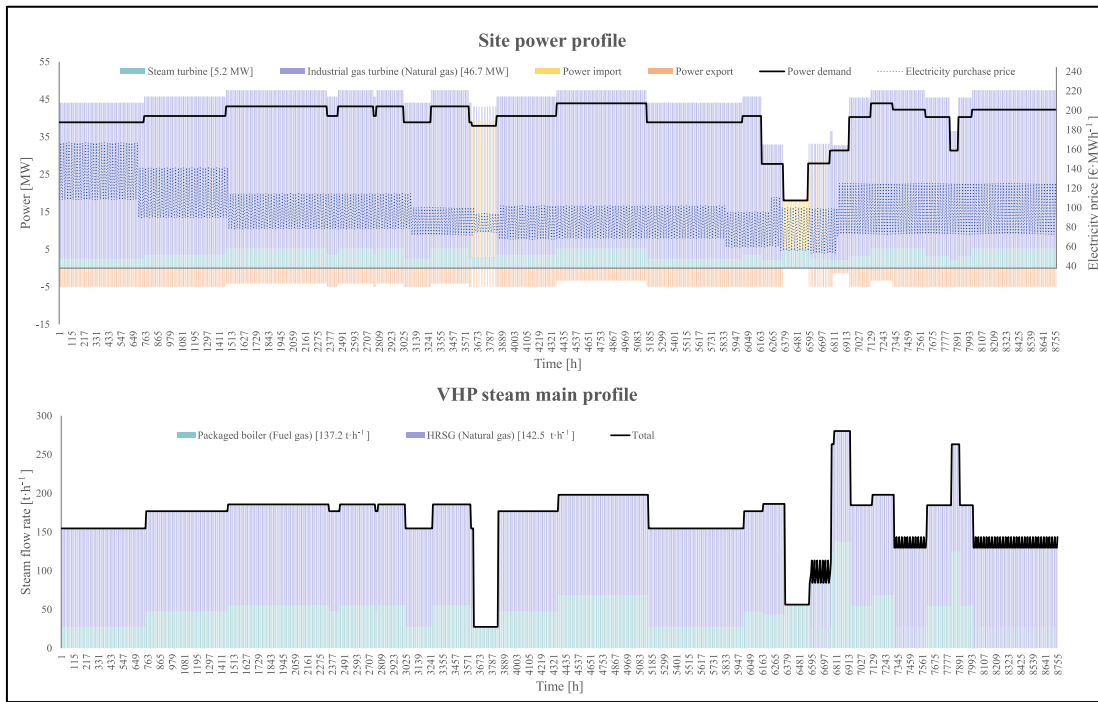
(13.8 %), but also a decrease in boiler duty (19.1 %) when compared to the optimum design with predefined steam levels (presented here as baseline). This leads to a total cost savings of 13.8 %.

When FSR and energy storage are included as utility options (Scenario II), the optimal design maximizes energy savings by recovering condensate heat via flash tanks. Integration of FSR can result in a decrease of fuel usage by 11.9 %, leading to a 10.2 % reduction in total costs compared to the baseline. Furthermore, compared to the baseline scenario, a holistic optimization that takes steam main conditions into account and incorporates FSR may result in 27.8 % fuel savings and a 24.5 % reduction in total costs. This highlights the advantage of holistic optimization in terms of energy savings and cost benefits.

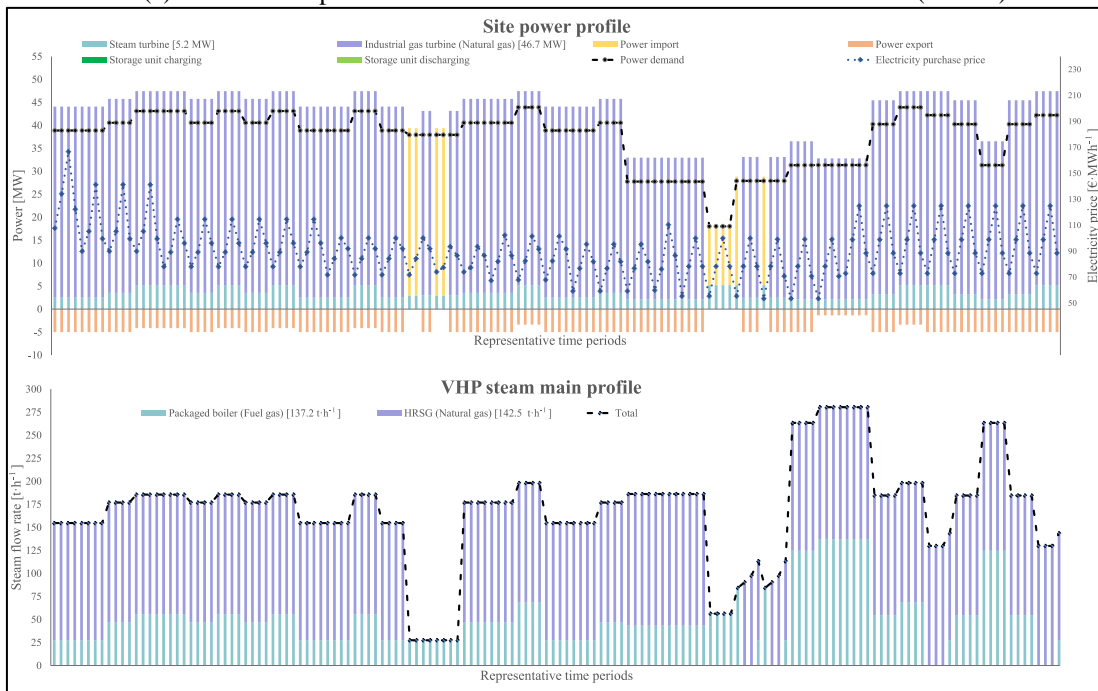
It is important to note that in none of the situations, energy storage units were adopted. The lack of energy storage may be attributed to the system's ability to supply site heat and electricity while generating revenues by exporting to the grid. The absence of electrical energy storage can be attributed to two factors. First, the cost of generating 1 MWh of electricity varies between 78.37 and 83.62 €·MWh⁻¹, depending on the load (for industrial gas turbines), but the cost of purchasing electricity fluctuates between 53.19 and 166.66 €·MWh⁻¹, with an average of 86.88 €·MWh⁻¹ (see Figure 3-11). Consequently, it is more cost-effective to generate electricity on-site to satisfy the power requirement, most of the time. Additionally, it is worth noting that heat demand is far greater than power demand, making cogeneration (from gas turbines coupled with HRSG) a more cost-effective alternative than steam generation from boilers and purchasing electricity from the grid (as it can be observed later in Figure 3-13). A second reason is that the capacity of exporting electricity to the grid (assumed in this work to be a maximum of 5 MW) enables revenue from injecting electricity into the distribution grid (particularly during peak times), rather than storing it for later consumption, which would entail both round-trip losses (in addition to self-losses) and costs associated with the purchase of storage units.

The thermal and power profiles of the site over the term of an operational year are shown in Figure 3-12 (a). For analysis purposes, annual characterization is displayed in representative periods, as seen in Figure 3-12 (b). As seen in Figure 3-12 (b) purchasing electricity is only justifiable when both the cost of electricity is less than the cost of onsite generation and the thermal/power demand ratio is less than three. As mentioned before, although electricity grid prices might be much lower (53.19 MWh⁻¹ compared to 83.62 €·MWh⁻¹ from gas turbine¹) at certain times of the year, due to the necessity to meet thermal requirements, cogeneration presents a more cost-effective solution than separate heat and power supply. Additionally, the system is sufficiently flexible to offset energy purchases by exporting power during periods of increased electricity rates.

¹Gas turbine capacity of 46.7 MW operating at ≈70 % load



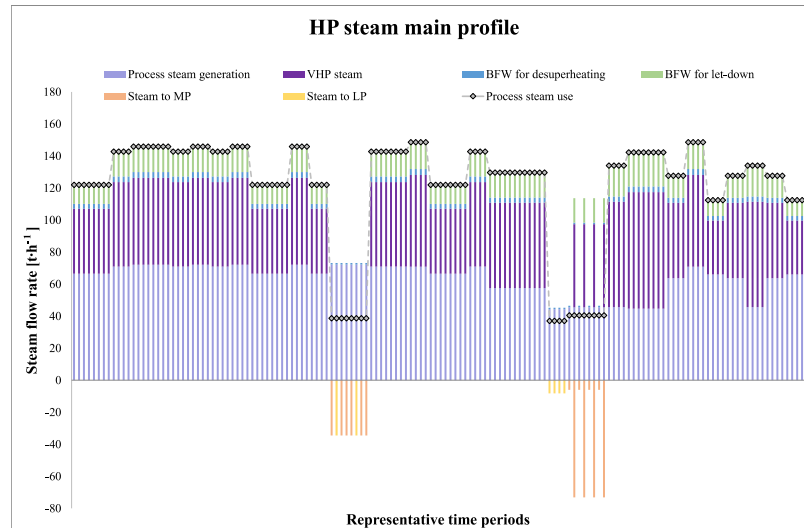
(a) Annual site power and thermal levels across the entire time horizon (8760 h)



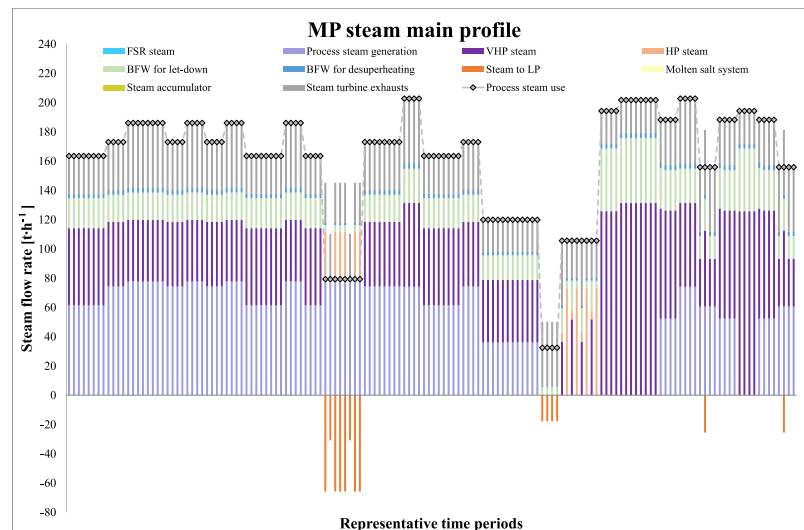
(b) Annual site power and thermal levels represented by the design time periods
 Figure 3-12 Energy site level across the time horizon for optimized case scenario II

Figure 3-13 illustrates the operating schedule for the distribution steam main: (a) high pressure –HP-, (b) medium pressure –MP- and (c) low pressure –LP-. It can be observed from Figure 3-13, that process steam generation plays a key role in meeting thermal demand. Along these, flashed steam delivers about 40 % of process steam consumption at LP steam mains. It is

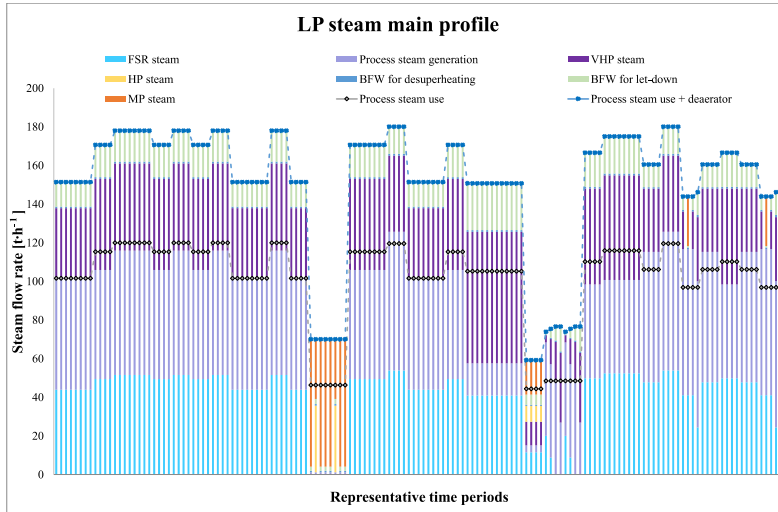
important to note that in periods of low thermal demand, the HRSG is shut off and heat requirement is mainly provided by process steam generation and boiler steam. Additionally, during periods of low thermal demand, flashed steam is lowered to minimum, as process steam generation is sufficient to meet heat requirements at MP and LP steam levels. In addition to the site's steam consumption, the deaerator is a major steam consumer at the LP steam main. Deaerator demand is approximately 30.2 % of the LP steam requirement, reaching up to 63.1 % of the LP demand at low thermal demands but “normal” power requirements.



(a) High pressure (HP) steam profile across the time horizon



(b) Medium pressure (MP) steam profile across the time horizon



(c) Low pressure (LP) steam profile across the time horizon

Figure 3-13 Thermal site level across the time horizon for optimized case scenario II

6.2. Sensitivity analysis

6.2.1. Electricity and natural gas (fossil fuels) price ratio

As previously stated in Section 6.1, the principal expenditures of an industrial utility plant are operating costs. Consequently, changes in energy prices have a significant influence on the system configuration and operation. Therefore, this subsection studies the impact of the price ratio between electricity and natural gas (fossil fuels) on the system total costs sustained and more important on the optimal design configuration. For this, interactions with the grid are also analyzed, considering the availability to export electricity to the grid (up to 5 MW). The main results are summarized in Figure 14 and Figure 3-15. Figure 3-14 presents first the total costs (in millions of euros per year), and second the electricity costs as function of the electricity/natural gas price ratio, where negative values represent revenues from exporting electricity to the grid. Figure 15 shows the installed capacity of the main energy conversion units selected for the different electricity/natural gas price ratio.

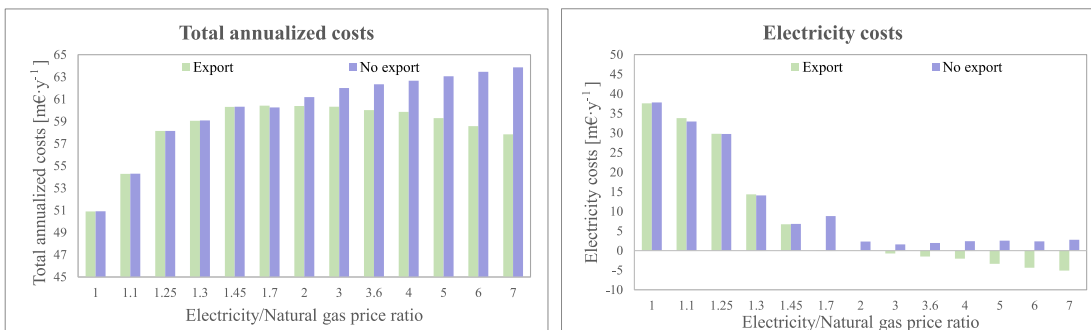


Figure 3-14 Total (left) and electricity (right) annual costs for a range of electricity/natural gas price ratios from 1 to 7 and two scenarios characterized by interactions with the grid (with and without electricity export)

Total annualized costs, as shown in Figure 3-14, vary with the electricity/natural gas price ratio. For scenarios where electricity export is not allowed, total annualized presents an increasing trend as the

electricity price increases, as expected. On the other hand, when the system is able to interact with the grid, total annualized costs reach a peak at a price ratio of 1.7. This peak can be explained by the system configuration and operation strategy, reflected in the site electricity costs. At price ratios between 1.7 to 2, export electricity stops being profitable, therefore the system is mainly designed to satisfy site power demands. In contrast, when the electricity/natural gas ratio is greater than 1.7, the optimal system design maximizes onsite power production, and any surplus electricity is exported to the grid to generate revenue.

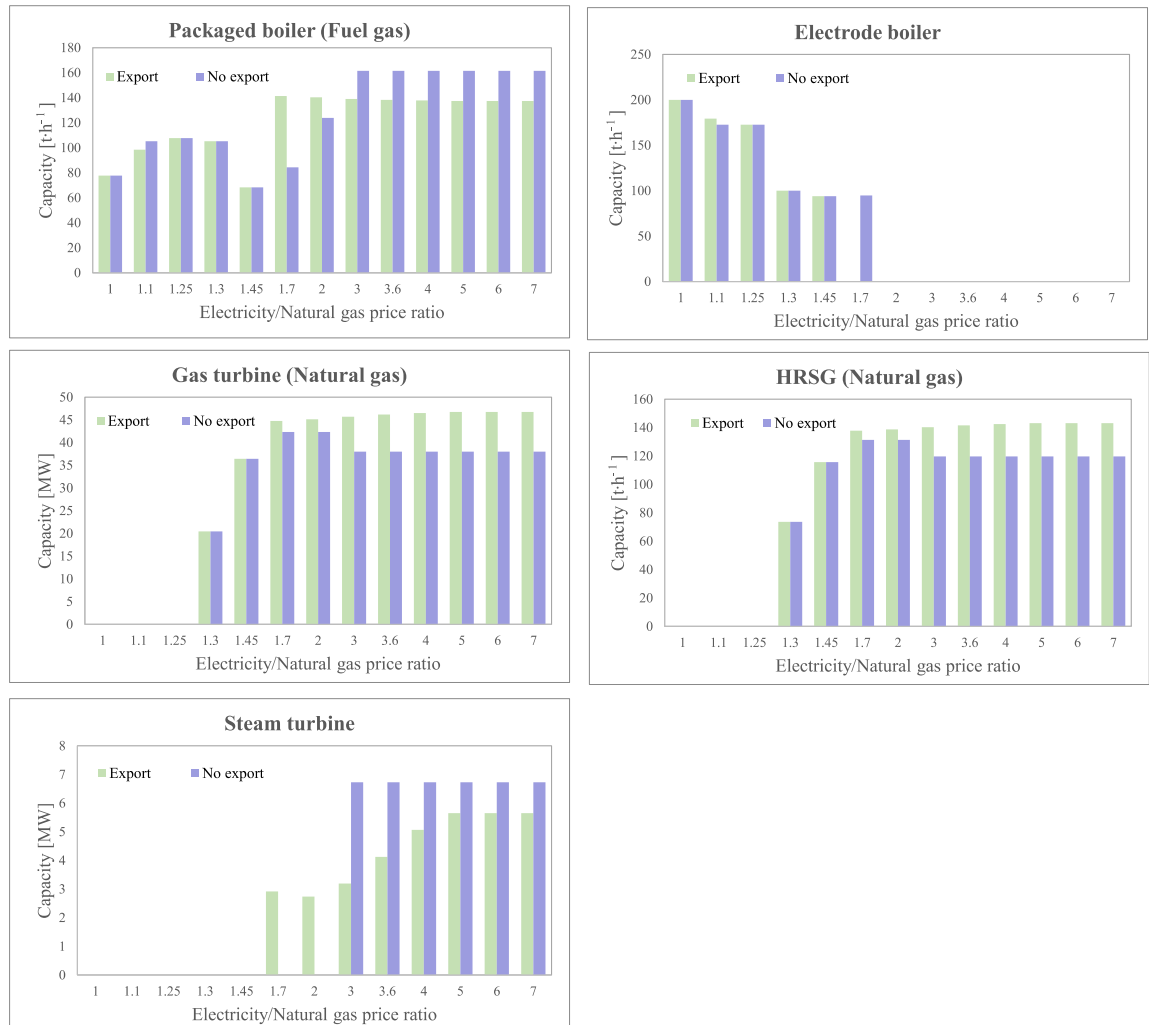


Figure 3-15 Results for the optimal process utility systems design based on the electricity/natural price and two scenarios characterized by hydrogen storage (HS) investment costs

Furthermore, the electricity/natural gas price ratio also affects the utility system configuration and the installed size of the technologies, as illustrated in Figure 3-15. Based on results a few considerations can be made:

- i. Regardless of the interactions with the electricity grid (export or no export allowed), the power generation in most of the optimal designs is mainly driven by natural gas turbine coupled with HRSG. However, technology sizes and technology threshold may vary

depending on the electricity export restriction. This may be explained by the higher gas turbines heat to power efficiency when compared against steam turbines. Resulting in the same amount of VHP steam supply delivered either by HRSG or boiler, but different power generation depending on the thermal unit favored.

- ii. Electrode boilers are only cost-competitive in scenarios where the nominal price of electricity is relatively low: (i) Natural gas/ electricity price ratio less than 1.70 if electricity export is not allowed and (ii) price ratio below 1.45 if surplus electricity can be traded. This may be caused by the variability of the electricity price across the year, resulting in be more convenient to produce electricity onsite most of the time and import electricity only in specific periods.
- iii. For scenarios where electricity prices are close to natural gas (price ratio <1.3), onsite power generation is not beneficial. However, for energy price ratios above 1.3 utility system design benefits from generating its own electricity and/or exporting electricity to the grid. For this reason, gas turbines with a size higher than the peak power demand (43.8 MW) are usually installed. Moreover, additional power is provided by steam turbines.
- iv. With respect to short-term storage technologies, such as batteries, molten salt systems and steam accumulators, storage units are never installed, independently of the of the electricity/natural gas price ratio and/or electricity export feasibility. This can be explained by its self-energy losses and high capital costs, which outweigh the potential energy savings obtained in certain time periods (e.g. electricity peak time).

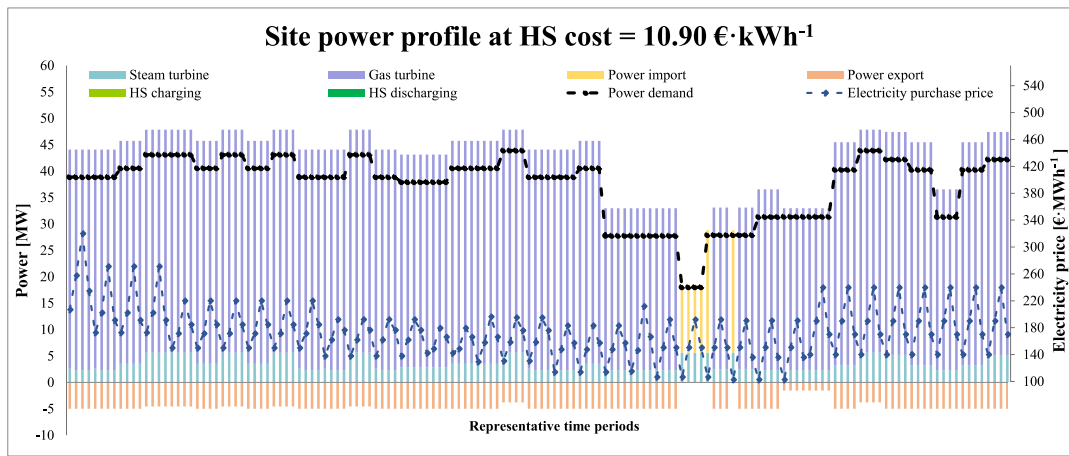
Further analysis on the long-term energy storage, determined that hydrogen storage is not a economically optimal option at the current investment costs ($\approx 10.90 \text{ €}\cdot\text{kWh}^{-1}$). However, if the capital cost of hydrogen storage is reduced to $3.3 \text{ €}\cdot\text{kWh}^{-1}$, hydrogen storage is chosen in scenarios where electricity costs are at least seven times greater than natural gas prices, as is the case in the United Kingdom. According to Guerra et al. (2020), the cost of hydrogen storage can be reduced to $3.30 \pm 1.65 \text{ €}\cdot\text{kWh}^{-1}$ by 2025. Further improvement in power to gas technologies and cost reductions in hydrogen storage installation could lead to its installation in scenarios where electricity is at least four times the price of natural gas. As a result, its deployment should be examined further.

For purpose of illustration, Table 3-6 and Figure 3-16 presents a detailed analysis of system costs and power profile at different hydrogen storage costs for electricity/natural gas price ratio = 7. The main results show that the deployment of hydrogen storage could result in around 0.6 % operating cost reduction. Moreover, due to the capital expenditure required and the losses due to the roundtrip efficiency, the overall benefit from installing hydrogen storage is less than 0.2 %,

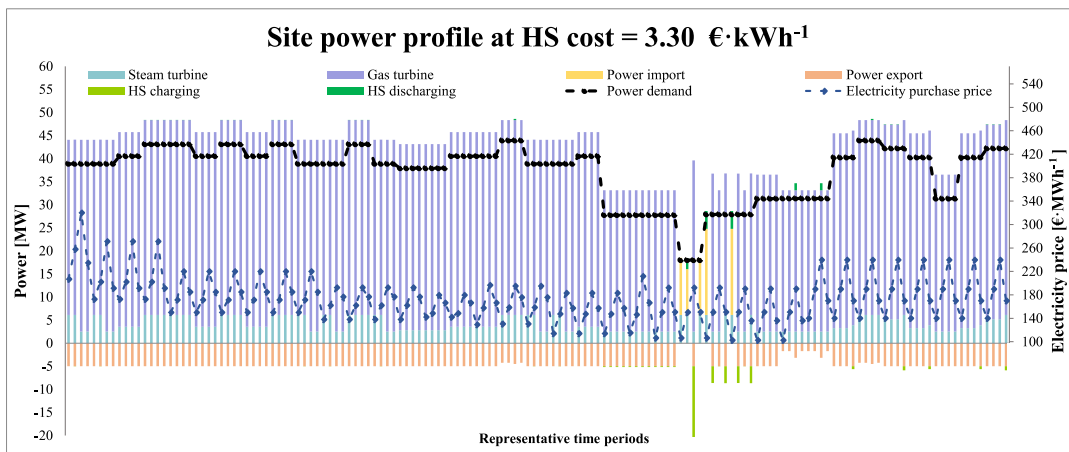
even when the investment cost of hydrogen is as low as $1.65 \text{ €}\cdot\text{kWh}^{-1}$. This is because, when electricity export is allowed, the system is flexible enough to compensate any electricity purchase by exporting electricity, making unnecessary the investment and additional capital expenditures required for the purchase of the equipment, as observed in Figure 3-16.

Table 3-6. Utility system costs as a function of the investment costs of hydrogen storage at electricity/natural gas price ratio = 7

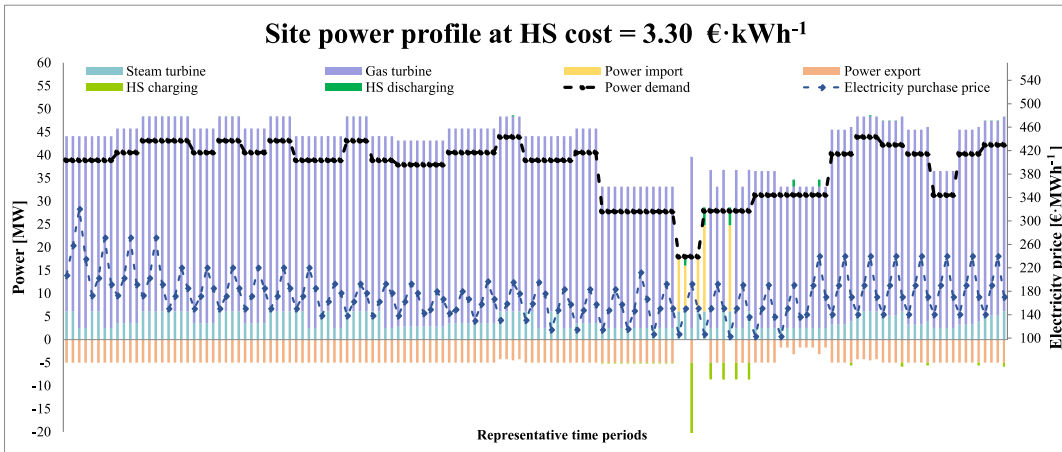
		HS investment costs [$\text{€}\cdot\text{kWh}^{-1}$]		
		10.90	3.30	1.65
Hydrogen capacity	[MWh]	-	39.51	140.98
Operating cost	[$\text{m€}\cdot\text{y}^{-1}$]	43.56	43.32 (-0.5 %)	43.31 (-0.6 %)
Maintenance cost	[$\text{m€}\cdot\text{y}^{-1}$]	3.59	3.63 (1.1 %)	3.62 (0.9 %)
Start cost	[$\text{m€}\cdot\text{y}^{-1}$]	0.017	0.019 (11.8 %)	0.019 (11.8 %)
Capital cost	[$\text{m€}\cdot\text{y}^{-1}$]	10.80	10.95 (1.4 %)	10.92 (1.1 %)
Total Annualized cost	[$\text{m€}\cdot\text{y}^{-1}$]	57.96	57.92 (-0.1 %)	57.87 (-0.2 %)



(a)



(b)



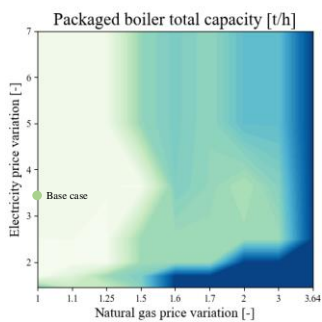
(c)

Figure 3-16 Annual site power profile represented by the design time periods at electricity/natural gas price ratio = 7 and three scenarios characterized by hydrogen storage (HS) installed costs

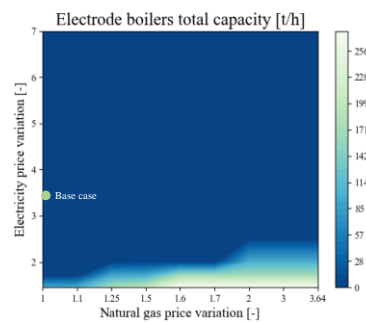
Overall, the results show that under current natural gas price scenarios neither biomass-based technologies nor energy storage are cost-competitive. In the next subsection, a sensitivity analysis on the impact of potential increase of fossil fuels either due to increasingly heavier carbon pricing levels or to evolving market conditions, on the system configuration is carried out.

6.2.2. Fossil fuel price rise

Figure 3-17 shows the optimal design configurations under a range of natural gas and electricity price variations, x- and y- axis respectively. For purpose of clarity, the axis is presented as a proportion of the nominal purchase price of natural gas (24.30 €·MWh⁻¹). The color scale represents the overall capacity installed of each design choice. Note that Figure 3-17 focuses only on the design choices selected in any of the scenarios. Technologies such as biomass gasification or anaerobic digestion, as well as energy storage, are not represented since they were not favored under any of the scenarios considered in this analysis. Figure 3-18 presents the site annual energy consumption of the different fuels. Additionally, the on-site power generation and the interaction with the grid (import/export) are also represented. The current European average energy prices are marked in each subfigure of both Figure 3-17 and Figure 3-18 to show how their design and primary energy usage patterns compare with other potential scenarios.



(a)



(b)

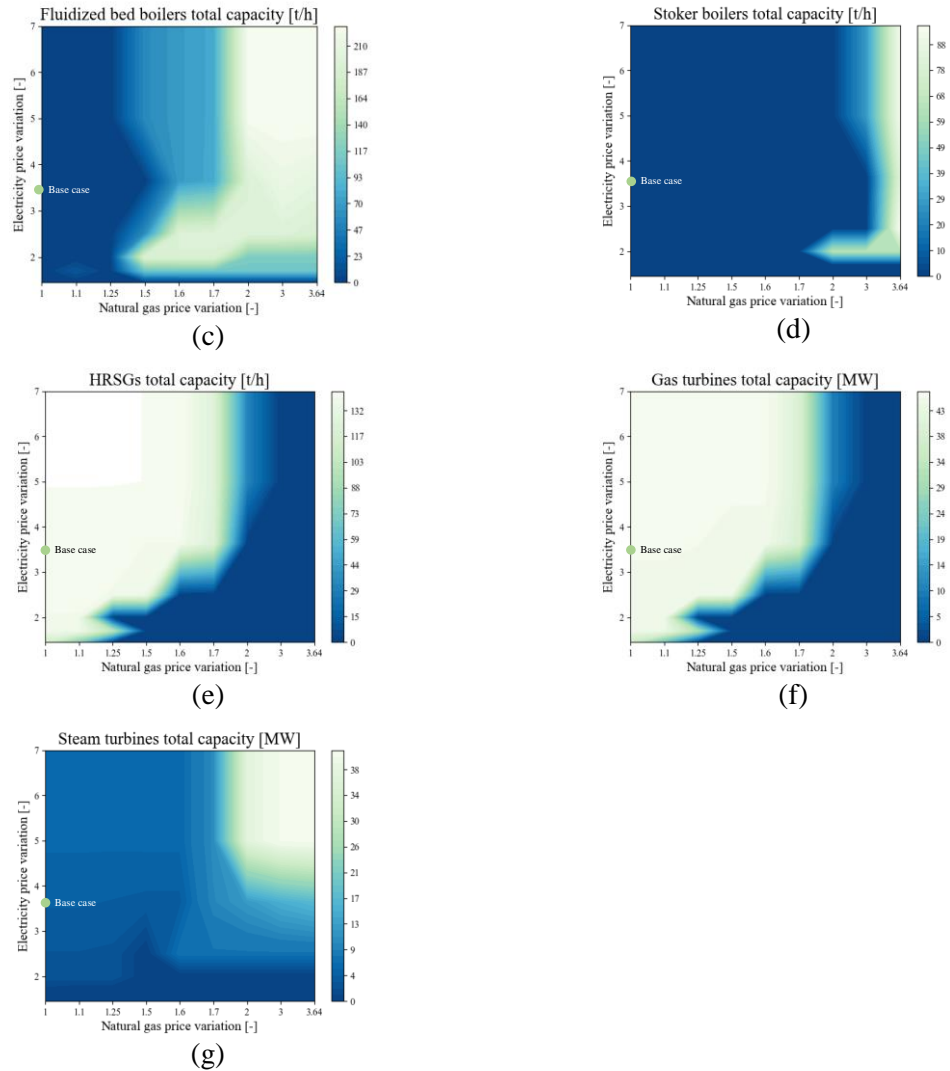


Figure 3-17 Results for the optimal systems design for a range of natural gas and electricity price variations (price reference: 24.30 [€·MWh⁻¹]). Subfigures show the total capacities of the selected technologies (a) packaged boilers, (b) electrode boilers, (c) fluidized bed, (d) stoker boiler, (e) heat recovery steam generators and (f) gas turbines and (g) steam turbines.

In Figure 3-17 can be observed how as the fossil fuel price increases, the optimal system design shifts to biomass and/or electricity-based technologies, depending on the nominal electricity price. For low electricity price scenarios, electrode boilers may represent a cost-competitive alternative (Figure 3-17 (b)). Nevertheless, its applicability is still limited due to its high operation costs compared to other fuel-based options (e.g., biomass-based boilers). Figure 3-17 (c) and (d) show how under higher electricity price scenarios, the optimal design leverages more a biomass-based system, when natural gas price increases.

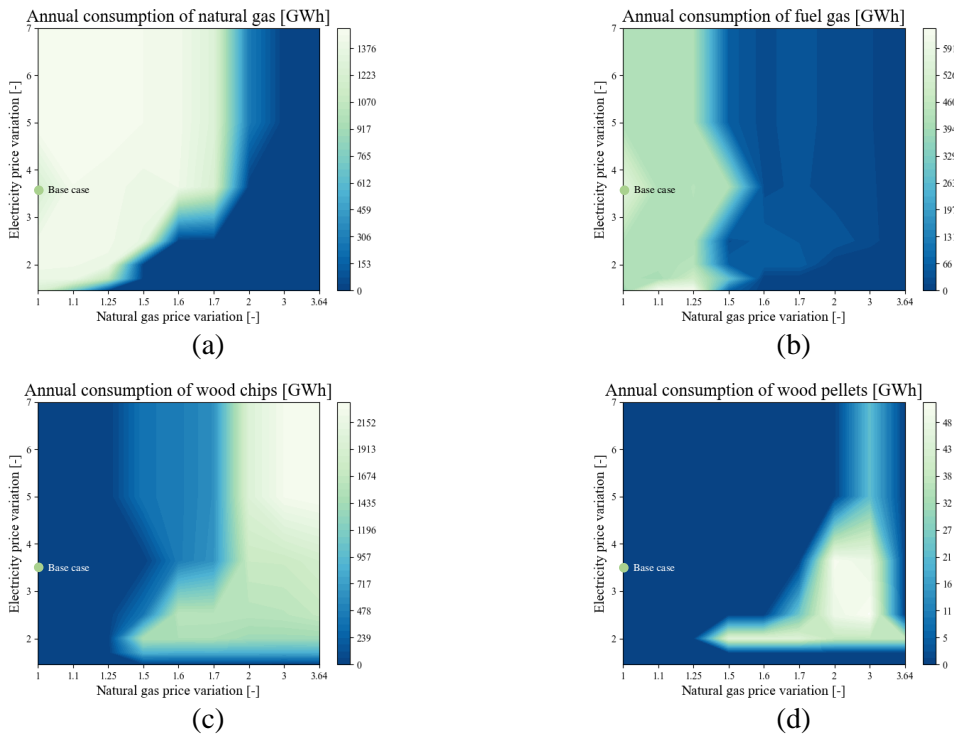
In comparison with fossil fuel-based technologies, the optimal size of the biomass-based technologies (in particular fluidized bed boilers operating with wood chips) gradually increases at the expense of packaged boilers (Figure 3-17 (a)). It has also to be noticed that although packaged boilers are still selected when natural gas price doubles, its annual operation is reduced, operating

mainly as a back-up boiler, as can be observed by the significant reduction of annual consumption of fuel gas in Figure 3-18(b).

Regarding power generation, most scenarios favour on-site power generation. Although fossil fuel price increments, the system is mainly driven by natural gas turbines coupled with HRSG. Only for scenarios where the fossil fuel price doubles, power generation drops gas turbines to operate mainly with steam turbines. This can be explained by the higher cogeneration efficiency that gas turbines coupled with HRSG present, in comparison with steam turbines.

While biomass gasification or anaerobic digestion may be a viable alternative to renewable-based gas turbines in this context, these technologies were not favored in any of the scenarios. This might be explained by multiple factors. First, due to the low efficiency of biomass gasification ($\approx 50\%$) and the higher operation and capital costs involved, direct combustion of biomass may result more cost competitive than syngas production. On the other hand, anaerobic digestion economic viability may be limited by the availability and costs of feedstock (including collection and transportation).

Regarding energy storage, none of the options was selected in any of the scenarios, even for the highest natural gas prices. The results show that the system is flexible enough to guarantee that any electricity purchase can be offset by power exporting revenues rather than storing it for later use, which would involve both round-trip losses and capital expenses associated with energy storage implementation.



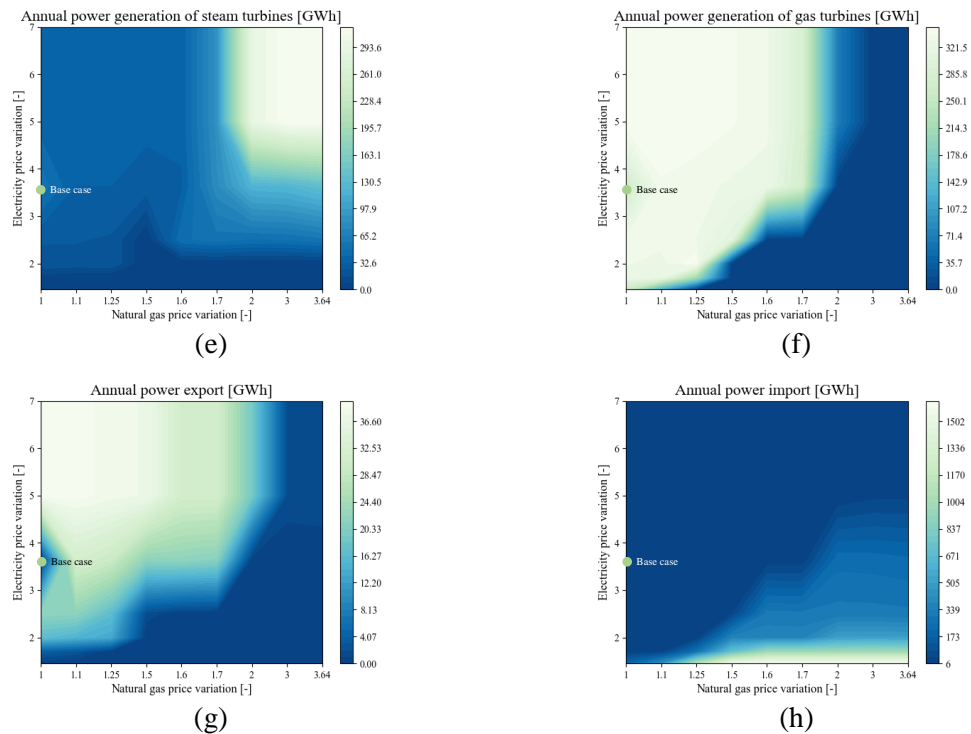


Figure 3-18 Annual site primary energy consumption/generation for a range of natural gas and electricity price variations (price reference: $24.30 \text{ [€·MWh}^{-1}\text{]}$).

In general, the results indicate that increasing the cost of fossil fuels may result in a reduction in fossil fuel consumption at the utility site. However, fossil fuel prices would have to nearly double before fossil fuels could be phased out. Additionally, as natural prices rise, the results suggest that there are two broad types of designs that can be distinguished by their nominal electricity prices. For low electricity costs, the optimal design relies heavily on electrode boilers and power import (bottom-right corner). While for high electricity prices, the design relies mainly on biomass boilers and steam turbines (top-right corner).

7. Conclusions

This work established a mathematical framework for designing efficient and cost-effective process utility systems capable of meeting industrial demand for both heat and power concurrently, while taking time-varying energy demand and electricity prices into account. The proposed framework takes into account the following: (i) the appropriate selection of steam main pressures and temperatures, taking into account interplant heat recovery opportunities; (ii) the integration of thermal and electrical storage systems in the optimization of industrial utility systems; and (iv) reliance on an efficient (though not guaranteed global convergence) MINLP decomposition method.

By considering potential fluctuations in electricity and fossil fuel prices, the effect of energy market prices on the design and operation of process utility systems was investigated. Sensitivity analysis aided in the understanding of the impact of energy price markets on industrial energy transition. The

findings indicated that the optimal design is extremely dependent on external variables such as energy prices. For example, electrification of utility systems is cost-competitive only when the cost of electricity is roughly equivalent to the cost of fossil fuels and biomass. Otherwise, the utility system is designed in such a way that it favors on-site generation to meet energy consumption while also exporting excess electricity to the grid to generate revenue (if allowed). Additionally, under current energy prices energy storage could be avoided. Nonetheless, if the installation costs of hydrogen storage systems are reduced by approximately two-thirds of their current levels, potential benefits may be realized in scenarios with high increasing grid electricity costs.

An additional insight regards the impact of fossil fuel prices suggests that while an increase in the price of fossil fuels may enhance a shift to renewable energy sources, this alone may not be sufficient to ensure significant reductions of the fossil fuel consumption. Moreover, the required price increment on fossil fuels is highly dependent on external conditions such as electricity and biomass costs. As a result, other alternatives driven by actual emissions should be investigated in order to develop cost-effective strategies for decarbonizing industrial utility systems.

Future research will focus on optimizing utility system design, considering the environmental impact of utility components throughout their life cycle in order to accurately assess any potential for carbon footprint reduction.

References

- ACME (2009a) *Electric steam boilers*. INC., A. E. P.
- ACME (2009b) *Large electric steam superheaters*. INC., A. E. P.
- Aguilar, O., Kim, J.-K., Perry, S. & Smith, R. (2008) 'Availability and reliability considerations in the design and optimisation of flexible utility systems', *Chemical Engineering Science*, 63(14), pp. 3569-3584.
- Aguilar, O., Perry, S. J., Kim, J. K. & Smith, R. (2007) 'Design and Optimization of Flexible Utility Systems Subject to Variable Conditions: Part 2: Methodology and Applications', *Chemical Engineering Research and Design*, 85(8), pp. 1149-1168.
- Andiappan, V. (2017) 'State-Of-The-Art Review of Mathematical Optimisation Approaches for Synthesis of Energy Systems', *Process Integration and Optimization for Sustainability*, 1(3), pp. 165-188.
- Ayub, H. M. U., Park, S. J. & Binns, M. (2020) 'Biomass to Syngas: Modified Non-Stoichiometric Thermodynamic Models for the Downdraft Biomass Gasification', *Energies*, 13(21), pp. 5668.
- Bischi, A., Taccari, L., Martelli, E., Amaldi, E., Manzolini, G., Silva, P., Campanari, S. & Macchi, E. (2014) 'A detailed MILP optimization model for combined cooling, heat and power system operation planning', *Energy*, 74, pp. 12-26.

- Breeze, P. (2019) 'Chapter 10 - Power System Energy Storage Technologies', in Breeze, P. (ed.) *Power Generation Technologies (Third Edition)*: Newnes, pp. 219-249.
- Bungener, S., Hackl, R., Van Eetvelde, G., Harvey, S. & Marechal, F. (2015) 'Multi-period analysis of heat integration measures in industrial clusters', *Energy*, 93, pp. 220-234.
- Bussieck, M. R. & Meeraus, A. (2004) 'General Algebraic Modeling System (GAMS)', in Kallrath, J. (ed.) *Modeling Languages in Mathematical Optimization*. Boston, MA: Springer US, pp. 137-157.
- Corporation, I. (2017). *V12. 8: IBM ILOG CPLEX Optimization Studio CPLEX User's Manual*: International Business Machines Corporation.
- Domínguez-Muñoz, F., Cejudo-López, J. M., Carrillo-Andrés, A. & Gallardo-Salazar, M. (2011) 'Selection of typical demand days for CHP optimization', *Energy and Buildings*, 43(11), pp. 3036-3043.
- Drud, A. (1985) 'CONOPT: A GRG code for large sparse dynamic nonlinear optimization problems', *Mathematical Programming*, 31(2), pp. 153-191.
- Elsido, C., Bischi, A., Silva, P. & Martelli, E. (2017) 'Two-stage MINLP algorithm for the optimal synthesis and design of networks of CHP units', *Energy*, 121, pp. 403-426.
- Elsido, C., Martelli, E. & Grossmann, I. E. (2021) 'Multiperiod optimization of heat exchanger networks with integrated thermodynamic cycles and thermal storages', *Computers & Chemical Engineering*, 149, pp. 107293.
- Eurostat (2020) 'Electricity prices for non-household consumers - bi-annual data (from 2007 onwards)'. Available at: https://ec.europa.eu/eurostat/databrowser/view/NRG_PC_205_custom_494574/default/table [Accessed].
- Fazlollahi, S., Bungener, S. L., Mandel, P., Becker, G. & Maréchal, F. (2014) 'Multi-objectives, multi-period optimization of district energy systems: I. Selection of typical operating periods', *Computers & Chemical Engineering*, 65, pp. 54-66.
- Fernandes, J. (Year). Multi-period optimisation of a utility plant model in gPROMS. *In*, 2017.
- Frangopoulos, C. A. (2018) 'Recent developments and trends in optimization of energy systems', *Energy*, 164, pp. 1011-1020.
- Gabrielli, P., Gazzani, M., Martelli, E. & Mazzotti, M. (2018a) 'Optimal design of multi-energy systems with seasonal storage', *Applied Energy*, 219, pp. 408-424.
- Gabrielli, P., Gazzani, M. & Mazzotti, M. (2018b) 'Electrochemical conversion technologies for optimal design of decentralized multi-energy systems: Modeling framework and technology assessment', *Applied Energy*, 221, pp. 557-575.
- Ganschietz, D. C. (2021) 'Design of on-site energy conversion systems for manufacturing companies – A concept-centric research framework', *Journal of Cleaner Production*, 310, pp. 127258.
- Glover, F. (1975) 'Improved Linear Integer Programming Formulations of Nonlinear Integer Problems', *Management Science*, 22(4), pp. 455-460.

- González-Roubaud, E., Pérez-Osorio, D. & Prieto, C. (2017) 'Review of commercial thermal energy storage in concentrated solar power plants: Steam vs. molten salts', *Renewable and Sustainable Energy Reviews*, 80, pp. 133-148.
- Gounaris, C. E., Misener, R. & Floudas, C. A. (2009) 'Computational Comparison of Piecewise-Linear Relaxations for Pooling Problems', *Industrial & Engineering Chemistry Research*, 48(12), pp. 5742-5766.
- Guerra, O. J., Zhang, J., Eichman, J., Denholm, P., Kurtz, J. & Hodge, B.-M. (2020) 'The value of seasonal energy storage technologies for the integration of wind and solar power', *Energy & Environmental Science*, 13(7), pp. 1909-1922.
- Heffron, R., Körner, M.-F., Wagner, J., Weibelzahl, M. & Fridgen, G. (2020) 'Industrial demand-side flexibility: A key element of a just energy transition and industrial development', *Applied Energy*, 269, pp. 115026.
- Hofmann, R., Panuschka, S. & Beck, A. (2019) 'A simultaneous optimization approach for efficiency measures regarding design and operation of industrial energy systems', *Computers & Chemical Engineering*, 128, pp. 246-260.
- Ibrahim, A., Peng, H., Riaz, A., Abdul Basit, M., Rashid, U. & Basit, A. (2021) 'Molten salts in the light of corrosion mitigation strategies and embedded with nanoparticles to enhance the thermophysical properties for CSP plants', *Solar Energy Materials and Solar Cells*, 219, pp. 110768.
- Iyer, R. R. & Grossmann, I. E. (1998) 'Synthesis and operational planning of utility systems for multiperiod operation', *Computers & Chemical Engineering*, 22(7), pp. 979-993.
- Jamaluddin, K., Wan Alwi, S. R., Hamzah, K. & Klemeš, J. J. (2020) 'A Numerical Pinch Analysis Methodology for Optimal Sizing of a Centralized Trigeneration System with Variable Energy Demands', *Energies*, 13(8).
- Kotzur, L., Markewitz, P., Robinius, M. & Stolten, D. (2018) 'Impact of different time series aggregation methods on optimal energy system design', *Renewable Energy*, 117, pp. 474-487.
- León, E. & Martín, M. (2016) 'Optimal production of power in a combined cycle from manure based biogas', *Energy Conversion and Management*, 114, pp. 89-99.
- Liew, P. Y., Wan Alwi, S. R., Ho, W. S., Abdul Manan, Z., Varbanov, P. S. & Klemeš, J. J. (2018) 'Multi-period energy targeting for Total Site and Locally Integrated Energy Sectors with cascade Pinch Analysis', *Energy*, 155, pp. 370-380.
- Lok, W. J., Ng, L. Y. & Andiappan, V. (2020) 'Optimal decision-making for combined heat and power operations: A fuzzy optimisation approach considering system flexibility, environmental emissions, start-up and shutdown costs', *Process Safety and Environmental Protection*, 137, pp. 312-327.
- Luo, X., Wang, J., Dooner, M. & Clarke, J. (2015) 'Overview of current development in electrical energy storage technologies and the application potential in power system operation', *Applied Energy*, 137, pp. 511-536.
- Luo, X., Zhang, B., Chen, Y. & Mo, S. (2012) 'Operational planning optimization of multiple interconnected steam power plants considering environmental costs', *Energy*, 37, pp. 549-561.

- Marechal, F. & Kalitventzeff, B. (2003) 'Targeting the integration of multi-period utility systems for site scale process integration', *Applied Thermal Engineering*, 23(14), pp. 1763-1784.
- Martín-Hernández, E., Sampat, A. M., Zavala, V. M. & Martín, M. (2018) 'Optimal integrated facility for waste processing', *Chemical Engineering Research and Design*, 131, pp. 160-182.
- McCormick, G. P. (1976) 'Computability of global solutions to factorable nonconvex programs: Part I — Convex underestimating problems', *Mathematical Programming*, 10(1), pp. 147-175.
- Mian, A., Martelli, E. & Maréchal, F. (2016) 'Framework for the Multiperiod Sequential Synthesis of Heat Exchanger Networks with Selection, Design, and Scheduling of Multiple Utilities', *Industrial & Engineering Chemistry Research*, 55(1), pp. 168-186.
- Panuschka, S. & Hofmann, R. (2019) 'Impact of thermal storage capacity, electricity and emission certificate costs on the optimal operation of an industrial energy system', *Energy Conversion and Management*, 185, pp. 622-635.
- Papoulias, S. A. & Grossmann, I. E. (1983) 'A structural optimization approach in process synthesis—I: Utility systems', *Computers & Chemical Engineering*, 7(6), pp. 695-706.
- Parat Halvorsen AS. (2021). *PARAT IEH: High Voltage Electrode boiler for Steam and Hot water* [Online]. Available at: <https://parat.no/ieh/> [Accessed].
- Pedregosa, F., Varoquaux, G., Gramfort, A., Michel, V., Thirion, B., Grisel, O., Blondel, M., Prettenhofer, P., Weiss, R., Dubourg, V., Vanderplas, J., Passos, A., Cournapeau, D., Brucher, M., Perrot, M. & Duchesnay, E. (2011) 'Scikit-learn: Machine Learning in Python', *Journal of Machine Learning Research*, 12(85), pp. 2825-2830.
- Pérez-Uresti, S. I., Martín, M. & Jiménez-Gutiérrez, A. (2019) 'Superstructure approach for the design of renewable-based utility plants', *Computers & Chemical Engineering*, 123, pp. 371-388.
- Pérez-Uresti, S. I., Martín, M. & Jiménez-Gutiérrez, A. (2020) 'A Methodology for the Design of Flexible Renewable-Based Utility Plants', *ACS Sustainable Chemistry & Engineering*, 8(11), pp. 4580-4597.
- Phillips, S., Aden, A., Jechura, Dayton, D. & Eggeman, T. (2007) *Thermochemical Ethanol Via Indirect Gasification and Mixed Alcohol Synthesis of Lignocellulosic Biomass*, Golden, Colorado: National Renewable Energy Lab. (NREL)No. NREL/TP-510-41168).
- Pool, N. (2020). *Historical Market Data* [Online]. Available at: <https://www.nordpoolgroup.com/historical-market-data/> [Accessed 2020].
- Rossum, G. v. (1995) *Python tutorial* Amsterdam: Centrum voor Wiskunde en Informatica (CWI)Technical Report CS-R9526).
- Rousseeuw, P. J. (1987) 'Silhouettes: A graphical aid to the interpretation and validation of cluster analysis', *Journal of Computational and Applied Mathematics*, 20, pp. 53-65.
- Satopaa, V., Albrecht, J., Irwin, D. & Raghavan, B. (Year). Finding a "Kneedle" in a Haystack: Detecting Knee Points in System Behavior. *In: 2011 31st International Conference on Distributed Computing Systems Workshops*, 20-24 June 2011 2011. 166-171.
- Scarlat, N., Dallemand, J.-F. & Fahl, F. (2018) 'Biogas: Developments and perspectives in Europe', *Renewable Energy*, 129, pp. 457-472.

- Schiefelbein, J., Tesfaegzi, J., Streblow, R. & Mueller, D. (2015). *Design of an Optimization Algorithm for the Distribution of Thermal Energy Systems and Local Heating Networks within a City District*.
- Schütz, T., Schraven, M. H., Fuchs, M., Remmen, P. & Müller, D. (2018) 'Comparison of clustering algorithms for the selection of typical demand days for energy system synthesis', *Renewable Energy*, 129, pp. 570-582.
- Shang, Z. (2000) *Analysis and Optimisation of Total Site Utility Systems*. Ph.D, Manchester, U.K.
- Shang, Z. & Kokossis, A. (2005) 'A systematic approach to the synthesis and design of flexible site utility systems', *Chemical Engineering Science*, 60(16), pp. 4431-4451.
- Spirax Sarco. (2021). *The boiler house: steam accumulators* [Online]. Available at: <https://www.spiraxsarco.com/learn-about-steam/the-boiler-house/steam-accumulators#article-top> [Accessed].
- Sun, L., Doyle, S. & Smith, R. (2015) 'Heat recovery and power targeting in utility systems', *Energy*, 84, pp. 196-206.
- Sun, L., Gai, L. & Smith, R. (2017) 'Site utility system optimization with operation adjustment under uncertainty', *Applied Energy*, 186, pp. 450-456.
- Sun, L. & Liu, C. (2015) 'Reliable and flexible steam and power system design', *Applied Thermal Engineering*, 79, pp. 184-191.
- Sun, L. & Smith, R. (2015) 'Performance Modeling of New and Existing Steam Turbines', *Industrial & Engineering Chemistry Research*, 54(6), pp. 1908-1915.
- Tawarmalani, M. & Sahinidis, N. V. (2005) 'A polyhedral branch-and-cut approach to global optimization', *Mathematical Programming*, 103(2), pp. 225-249.
- Teichgraeber, H. & Brandt, A. R. (2019) 'Clustering methods to find representative periods for the optimization of energy systems: An initial framework and comparison', *Applied Energy*, 239, pp. 1283-1293.
- Thorndike, R. L. (1953) 'Who belongs in the family?', *Psychometrika*, 18(4), pp. 267-276.
- Varbanov, P., Perry, S., Klemeš, J. & Smith, R. (2005) 'Synthesis of industrial utility systems: cost-effective de-carbonisation', *Applied Thermal Engineering*, 25(7), pp. 985-1001.
- Varbanov, P. S. & Klemeš, J. J. (2011) 'Integration and management of renewables into Total Sites with variable supply and demand', *Computers & Chemical Engineering*, 35(9), pp. 1815-1826.
- Varbanov, P. S. D., S.; Smith, R. (2004) 'Modelling and Optimization of Utility Systems', *Chem. Eng. Res. Des.*, 82, pp. 561-578.
- Yong, W. N., Liew, P. Y., Woon, K. S., Wan Alwi, S. R. & Klemeš, J. J. (2021) 'A pinch-based multi-energy targeting framework for combined chilling heating power microgrid of urban-industrial symbiosis', *Renewable and Sustainable Energy Reviews*, 150, pp. 111482.
- Zhang, B. J., Liu, K., Luo, X. L., Chen, Q. L. & Li, W. K. (2015) 'A multi-period mathematical model for simultaneous optimization of materials and energy on the refining site scale', *Applied Energy*, 143, pp. 238-250.

Zhang, Q., Bremen, A. M., Grossmann, I. E. & Pinto, J. M. (2018) 'Long-Term Electricity Procurement for Large Industrial Consumers under Uncertainty', *Industrial & Engineering Chemistry Research*, 57(9), pp. 3333-3347.

SUPPLEMENTARY INFORMATION P3

Next generation of industrial steam systems: A decision support framework for an efficient and evolving process utility system

Julia Jiménez-Romero^{a,b,*}, Adisa Azapagic^b, Robin Smith^a

^a Centre for Process Integration, Department of Chemical Engineering and Analytical Science, University of Manchester, Manchester, M13 9PL, United Kingdom

^b Sustainable Industrial Systems Group, Department of Chemical Engineering and Analytical Science, University of Manchester, Manchester, M13 9PL, United Kingdom

* Julia Jiménez-Romero. Email: julia.jimenezromero@manchester.ac.uk, nataly.jimenezr@hotmail.com

SUPPLEMENTARY INFORMATION P3.A

Technical and capital specifications

Nomenclature

ΔT_{CW}	Cooling water temperature approach
ρ_{ss}	Stainless steel density
ρ_{SA}^l	Density of liquid phase in steam accumulator <i>SA</i>
Ψ_{eq}	Scaling law exponent
C_p	Heat capacity
C_{eq}^{ref}	Specific cost of reference equipment <i>eq</i>
D_d	internal diameter
f_p	Pressure factor
$f_{p,ref}$	Pressure factor of reference
F_{eq}^{ins}	Installation factor of equipment <i>eq</i>
F_{eq}^{main}	Maintenance factor of equipment <i>eq</i>
l	length of the steam accumulator
m_{ss}	Stainless steel mass
P_d	Design internal pressure
P_{j_s}	Distribution pressure corresponding to set j_s
P_v^{VHP}	Very high pressure steam main pressure corresponding to set v
T_{BFW}	Boiler feed water temperature
T_{ref}	Reference temperature
T_v^{sat}	Saturated temperature at v conditions
t_w	Wall thickness
S	Maximum allowable stress
S_{ss}	Maximum allowable stress of stainless steel
V_{SA}	Volume of steam accumulator tank <i>SA</i>
V_{SA}^l	Liquid volume of steam accumulator <i>SA</i>
Z_{eq}^{ref}	Reference capacity size of equipment <i>eq</i>

A.I. Site general specifications

Table P3.A. 1. Site configuration and operating conditions

Parameter	Value
Interest rate [%]	8
Plant life [y]	25
ΔT_{CW} [°C]	10
T_{BFW} [°C]	120

Table P3.A. 2. Boiler efficiency at full load

Parameter	Full load efficiency [%]	Reference
Electrode boiler	99	Parat Halvorsen AS (2021)
Field-erected boiler	85	Varbanov (2004)
Packaged boiler	81	Varbanov (2004)
Stoker boiler*	71	EPA (2015)
Fluidized bed boiler*	75	EPA (2015)

*Moisture content 30%

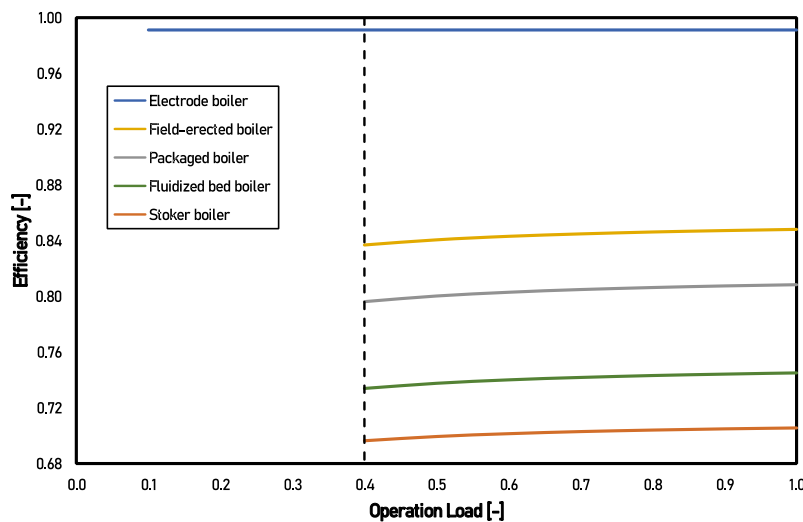


Figure P3. A. 1 Boiler efficiency as a function of load

A.II. Equipment economical specifications

Equipment economical specifications are detailed in Table P3.A. 3. C_{eq}^{ref} specific cost of reference size unit (Z_{eq}^{ref}), ψ_{eq} scaling law exponent and F_{eq}^{ins} and F_{eq}^{main} the installation and maintenance factor, respectively.

Table P3.A. 3. Model coefficients of equipment costs

Resource	Z_{eq}^{ref}	C_{eq}^{ref} [€]	Ψ_{eq}	Range	F_{eq}^{ins} [%]	F_{eq}^{main} [%]	Reference
Boiler							
Packaged*, [t/h]	50	2,548,770.98	0.960	50 - 350	4	5	Smith (2016)
Field-erected*, [t/h]	20	1,801,717.41	0.810	20 - 800	4	5	Smith (2016)
Biomass stoker ^f , [t/h]	1	1,177,937.852	0.751	4 - 300	1	3	EPA (2015)
Biomass fluidized bed ^f , [t/h]	1	(variable) 369,759.0 (fixed) 9,966,103.0	1.000	0 - 300	1	3	EPA (2015)
Electrode, [MW]	70	62,350.33	0.700 ⁺	3 - 70	2.5	1	Marsidi (2018) Jaspers and Afman (2017)
Electric superheater, [MW]	70	135,092.37 (variable)	0.700 ⁺	3 - 70	1	1	Jaspers and Afman (2017)
Steam turbine, [MW]	-	345,101.63 (fixed) 44,057.43	1.000	1 - 200	4	3	Fleiter et al. (2016)
Gas turbine							
Aeroderivative, [MW]	1	827,490.91	0.777	2 - 51	4	3	Pauschert (2009)
Industrial, [MW]	1	720,016.47	0.770	6 - 125	4	3	Pauschert (2009)
HRSG**, [t/h] ^x	120	481,845.69 (variable)	1.163	33.5 - 800	4	5	Corporation (2000)
PEM Fuel cell	-	{2,160,000; 1,680,000; 1,320,000} (fixed)	1	0-10 {0 - 0.2; 0.2-0.8; 0.8-10}	1.5	8	Gabrielli et al. (2018b)
PEM Electrolyzer	1	{0; 320,000; 800,000} (variable) {2,693,000; 1,727,000; 1,354,000 } (fixed)	1	0-10 {0 - 0.2; 0.2-0.8; 0.8-10}	1.5	8	Gabrielli et al. (2018b)
Gasifier, [t/h]	5	1,600,000	0.917	5-500	4	3	Martín and Grossmann (2022)
Anaerobic digester, [t/h]	-	345.75	1	1041.2 - 6247.20	4	3	Martín and Grossmann (2022)

Resource	Z_{eq}^{ref}	C_{eq}^{ref} [€]	Ψ_{eq}	Range	F_{eq}^{ins} [%]	F_{eq}^{main} [%]	Reference
PSA,[t/h]	-	3093.2	1	1 - 500	2	1	Andiappan (2016)
HO Furnace, [MW]	5	465,365.00	0.748	5 - 60	4 ⁺	5	Towler and Sinnott (2013)
Condenser, [MW]	-	-	-	1 - 2000	4 ⁺	1	Varbanov (2004)
Deaerator, [t/h]	-	-	-	10 - 300 300 - 600	4 ⁺ 4 ⁺	1	Varbanov (2004)
Flash tank ^{***} , [t/h]	1	4,205.99	0.506	20 - 100 100 - 400	4 ⁺	1	Loh et al. (2002)

Note: costs adjusted to 2019

* Pressure reference 100 bar, $f_{p,ref} = 1.9$, ** Pressure reference 11.34 bar, $f_{p,ref} = 1.1$, *** Horizontal vessel, residence time = 5 min, density = $0.9 \text{ t} \cdot \text{m}^{-3}$, Pressure = 10 bar, $f_{p,ref} = 1.1$

^x based on exhaust gases, ^f Installed cost, including biomass storage

⁺ Assumed

For boilers, HRSG and flash tanks, capital cost should involve the pressure factor f_p

$$f_p = 0.0090943 \cdot P_v^{VHP} + 1.012986 \quad (\text{P3.A. 1})$$

$$C_{eq} = C_{eq}^{ref} \left(\frac{Z_{eq}^{Eq}}{Z_{eq}^{ref}} \right)^{\Psi_{eq}} \frac{f_{p,eq}}{f_{p,ref,eq}} \quad (\text{P3.A. 2})$$

A.II.1. Biomass gasification

Prior gasification, the feedstock is firstly dried by low pressure steam to remove any excess moisture above 10 %. Then, dried biomass is converted into producer gas by thermochemical gasification using steam as gasifying agent. In this study, the gasifier is assumed to be operated at 1.6 bar and over the gasification temperature of 890 °C. Gasification is an endothermic process, therefore here 27 kg of olivine/kg dry biomass are used to provide the heat required. Olivine is reheated by the combustion of char (at 950 °C) obtained by the gasification.

To increase the biomass conversion to syngas, the usage of a downstream reforming unit to convert tar and other hydrocarbons into H₂ and CO is used. Steam reforming (SR) operating at 25 bar was considered in this work as alternative to decompose the light hydrocarbons generated in the gasification process. The process requires about 0.4 kg saturated steam/ kg dry biomass. Finally, gas is cleaned up from impurities such as tar; metals and sulphur are removed by cold gas cleaning and filters. For this syngas stream requires to be cold down from 850 °C to 150 °C and pressurized at various stages (Susmozas et al., 2013) (Dutta and Phillips, 2009), which can be used for process steam generation. On top of this, flue gas exiting the combustor (at 950 °C) can be used to recover heat by producing steam in an HRSG.

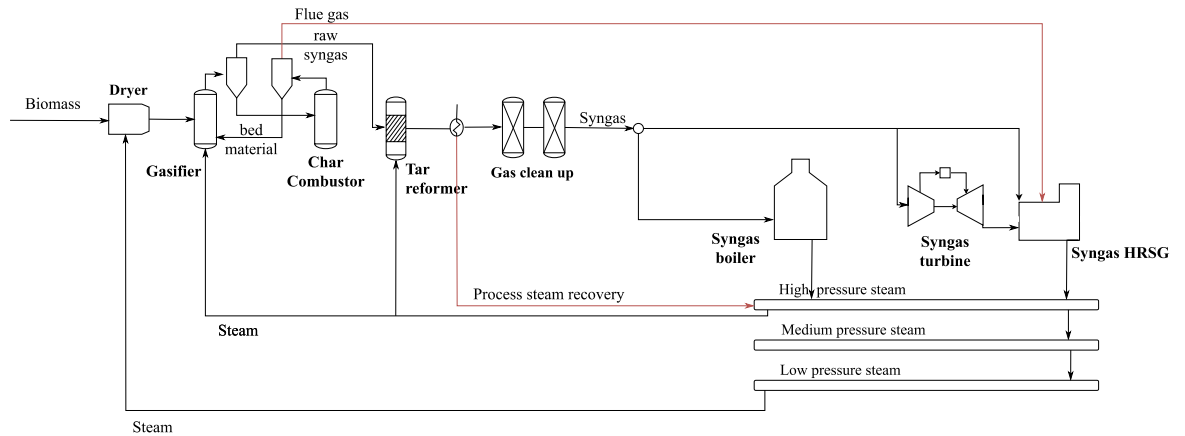


Figure P3. A. 2 Biomass process scheme

Table P3.A. 4 Composition of syngas from lignocellulosic biomass

Feedstock	Wood chips	Wood pellets
Moisture	30 %	10 %
Gas yield [$t \cdot t^{-1}$]	0.5776 ^a	0.5776 ^a
Flue gas [$t \cdot t^{-1}$]	2.7129 ^a	2.7129 ^a
molar ratio H ₂ :CO	1.2 ^b	1.2 ^b

^aPérez-Uresti et al. (2019)

^bDutta and Phillips (2009)

A.II.2. Anaerobic Digestion

Anaerobic digestion breaks down the biogenic carbon in wet biomass and releases it as biogas. With the aid of appropriate bacteria, anaerobic wet biomass digestion takes place in four stages: hydrolysis, acidogenesis, acetogenesis and methanogenesis. The energy efficiency of the digester and the production of methane is closely tied to the digested biomass and the operating conditions (bacteria and temperature). According to Martín-Hernández et al. (2018) the use of mesophilic bacteria at 55 °C enhance the yield of methane for its use as fuel. Therefore, feedstock is assumed to be preheated from 15 to 55 °C with low pressure steam. To determine the heat required, the thermal properties given by Chen (1983) are assumed. Once obtained the biogas, traces of H₂S needs to be removed. For this the biogas is sent to a fixed bed reactor of Fe₂O₃. Furthermore, the CO₂ (and other traces).are removed by a Pressure Swing Adsorption (PSA) process at 25 °C (Hernández et al., 2017). Once the biogas is mainly methane it can be used in the gas turbines or gas boilers.

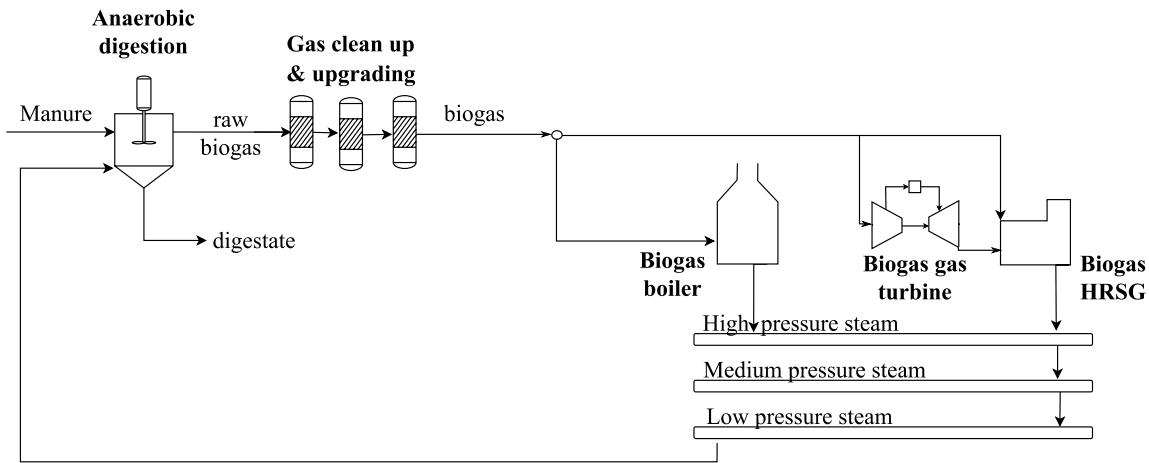


Figure P3. A. 3 Biogas process scheme

Table P3.A. 5 Composition of biogas from cattle manure

Feedstock	Cattle Manure
Gas yield [$t \cdot t^{-1}$]	0.0208 ^a
Dry matter [% wt]	8 ^a
Raw biogas composition [% wt]	
CH ₄	56.8 ^b
CO ₂	25.2 ^b
H ₂ O	15.7 ^b
O ₂	0.4 ^b
N ₂	1.7 ^b
K, P, N index ^a	1.017/1.932/3.051

^aHernández et al. (2017), ^bMartín-Hernández et al. (2020)

Additionally, by-product digestate comprises both undigested biomass and important nutrients from the feed stream. So, digestate streams can provide a benefit as soil fertilizers today. Both the biogas composition as well as the nutrients available in the digestate are obtained by (Martín-Hernández et al., 2018)

A.III. Energy storage specifications

Table P3.A. 6. Model coefficients of energy storage costs

Resource	Z_{eq}^{ref}	C_{eq}^{ref} [€ unit ⁻¹]	Ψ_{eq}	Range	F_{eq}^{ins} [-]	F_{eq}^{main} [%]	Reference
Steam accumulator, [t/h] ^a	6	98,400.00	0.82	6 - 100	2.5	2	Smith (2016)
Molten salt systems ^b , [kWh]	1	19.22	1	0 - 10000	1	2	Glatzmaier (2011) Caraballo et al. (2021)

Resource	Z_{eq}^{ref}	C_{eq}^{ref} [€ unit ⁻¹]	Ψ_{eq}	Range	F_{eq}^{ins} [-]	F_{eq}^{main} [%]	Reference
Li-ion Battery, [kWh]	1	(400-1100) 750	1	1-100000	1.5	2	Gabrielli et al. (2018a)
NaS Battery, [kWh]	1	(250-900) 575	1	50 - 8000	1.5	2	Breeze (2019)
Hydrogen tank, [kWh]	-	13.6 (fixed)	1	500 - 5500	1.5	3	Gabrielli et al. (2018a)
	-	2,350 (variable)	1	5500-15000	1.5	3	Gabrielli et al. (2018a)
		10.9 (fixed)					
		94,500					

^a Cost related per ton of stainless steel of the pressure vessel

^b Price included installation. Supply temperature (T_{ref}) 400 °C, target temperature 150 °C and $C_p = 1.58$ J/gK (Caraballo et al., 2021)

A.III.1. Molten salt system

In molten salt systems, temperature difference between the supply and target temperature influences the amount of working fluid and size of the tanks (Glatzmaier, 2011). Therefore, supply temperature is considered as correction factor in the costs, as expressed in Eq. (P3.A. 3). Note that in this work, supply temperature is assumed as saturated temperature at v conditions (T_v^{sat}) and target temperature is defined as 150 °C.

$$C_{MS} = Z_{MS} \cdot C_{MS}^{ref} \cdot \left(\frac{T_v^{sat}}{T_{ref}} \right)^{-1.701} \quad (P3.A. 3)$$

A.III.2. Steam accumulator calculations for capital cost estimation

To define the capital cost of the steam accumulator, it is assumed that the main cost driver is the pressure vessel (Beck et al., 2021). The pressure vessels costs correlation are calculated as a function of the construction material, in this work assumed as stainless steel (m_{ss}).

To determine the material mass the wall thickness is required (t_w), which in this work is calculated under the pressure vessel norm ASME BPV Code Sec. VIII D.1 (The American Society of Mechanical Engineers, 2017), as expressed in Eq. (P3.A. 4).

$$t_w = \frac{P_d(D_d + t_w)}{2S} \quad (P3.A. 4)$$

Where S is the maximum allowable stress (in $N\ mm^{-2}$) and P_d is the internal pressure (design pressure, in MPa) and D_d is the internal diameter (in mm).

$$t_w = \frac{P_d D_d}{2S - P_d} \quad (P3.A. 5)$$

Moreover, assuming cylindrical storage vessels the material mass can be calculated as a function of the wall thickness (t_w), the diameter of the vessel (D_i), the length of the storage (l), and the density of the material (ρ). In this work stainless steel has being assumed as storage material.

$$V_{ss} = \frac{m_{ss}}{\rho_{ss}} = D_d \pi l \cdot t_w \quad (P3.A. 6)$$

Replacing (P3.A. 5) in (P3.A. 6):

$$m_{ss} = D_d^2 \pi l \cdot \frac{P_d}{2S_{ss} - P_d} \rho_{ss} \quad (P3.A. 7)$$

If assumed that 90 % of the storage tank is filled with saturated water, water volume can be expressed as:

$$V_{SA}^l = 0.9 \cdot V_{SA} = 0.9 \frac{D_d^2 \pi l}{4} \quad (P3.A. 8)$$

$$\text{where } V_{SA}^l = \frac{m_{SA}^l}{\rho_{SA}^l} \quad (P3.A. 9)$$

Combining Eqs. (P3.A. 7), (P3.A. 8) and (P3.A. 9) and rearranging gives:

$$m_{ss} = 4.44 \cdot \frac{P_d}{2S_{ss} - P_d} \cdot \frac{\rho_{ss}}{\rho_{SA}^l} m_{SA}^l \quad (P3.A. 10)$$

For the given problem formulation:

$$m_{ss_{i j_s j'_s}} = 4.44 \cdot \frac{0.1 P_{j_s}}{2S_{ss_{j_s}} - 0.1 P_{j_s}} \cdot \frac{\rho_{ss}}{\rho_{SA_{j_s}}^l} m_{SA_{i j_s j'_s}}^l \quad (P3.A. 11)$$

Subindexes $i j_s j'_s$ indicates unit i operating at j_s conditions and releasing steam at j'_s conditions. P_{j_s} is the pressure (in bar) at steam level j_s . ρ_{ss} is stainless steel density ($\rho_{ss} = 8000 \text{ kg/m}^3$) and $\rho_{SA_{j_s}}^l$ is the water density at j_s conditions. $S_{ss_{j_s}}$ represents the maximum allowable stress for stainless steel at j_s conditions, which can be defined by Eq. (P3.A. 12) and coefficients detailed in Table P3.A. 7.

$$S_{ss_{j_s}} = s_{ss4} T_{j_s}^4 + s_{ss3} T_{j_s}^3 + s_{ss2} T_{j_s}^2 + s_{ss1} T_{j_s} + s_{ss0} \quad (P3.A. 12)$$

Table P3.A. 7. Modelling coefficients for the estimation of stainless steel stress (Turton et al.)

Parameter	Value
s_{ss4}	$2.63987 \cdot 10^{-9}$
s_{ss3}	$-3.83482E \cdot 10^{-6}$
s_{ss2}	0.002139213
s_{ss1}	-0.609233667
s_{ss0}	158.0701695

Finally, the water content ($m_{SA_{i,j_s,j'_s}}^l$) required in the steam accumulator (operating between j_s and j'_s conditions) is calculated based on the energy capacity required ($Z_{SA_{i,j_s,j'_s}}^{es}$) and the water enthalpy (\tilde{h}_l) difference between the operating conditions.

$$Z_{SA_{i,j_s,j'_s}}^{es} = m_{SA_{i,j_s,j'_s}}^l (\tilde{h}_{l_{j_s}} - \tilde{h}_{l_{j'_s}}) \quad (P3.A. 13)$$

A.IV. Resource specifications

Table P3.A. 8. Resources data

Resource	LHV	Cost	Reference
	[MWh·t ⁻¹]	[€·MWh ⁻¹]	
Natural gas	13.08 ^a	24.30 ^c	Eurostat (2020b)
Distillate oil	11.28 ^a	39.65	Comission (2019)
Fuel gas	13.03 ^a	23.87	Author's estimation ^e
Fuel oil	10.83 ^a	39.40	Comission (2019)
Woodchip	3.5 ^b	29.3	Duić et al. (2017) ^e
Wood pellets	4.8 ^b	39.7	Duić et al. (2017) ^e
Cattle manure	*	6.05 ^d	Author's estimation ^f
Digestate	-	P/ K / N/ ^d 1408/1056/682/	Nussbaum (2021)
Syngas	1.94 ^{**}	-	Author's estimation
Biogas	13.1	-	Martín-Hernández et al. (2018)
Hot oil	-	30.40	Author's estimation ^g
Electricity import	-	88.65 ^c	Eurostat (2020a)
Electricity export	-	70.92	Author's estimation ^h
Cooling water		1.230	Turton et al. (2018)
Treated water		0.301 ^d	Turton et al. (2018)

* Cp = 4.19 - 0.0275(DM) [J kg·K⁻¹] (Chen, 1983), ** 7 MJ/Nm³

^a Source : Engineering ToolBox (2008)

^b Source: Research (2020)Wood chips (30% moisture content), wood pellets (10% moisture content)

^c Prices for XL scale industries: Band I6 for natural gas (>4 000 000 MWh y⁻¹)
Band IG for electricity (>150 000 MWh y⁻¹)

^d Cost per ton [€·t⁻¹]

^e Based on energy inflation (CPI) (OECD, 2021)

^f Assuming Andersen (2016)'s correlation and 10 mile (16 km) distance

^g Price related to the furnace fuel (Natural gas). Assuming 80 % efficiency (Towler and Sinnott, 2013)

^h Assuming 20 % of distribution losses

Reference

- Andersen, D. (2016). *What does manure application cost?* [Online]. Iowa State University. Available at: <https://themanurescoop.blogspot.com/2016/05/what-does-manure-application-cost.html> [Accessed].
- Andiappan, V. (2016) *SYSTEMATIC APPROACHES FOR SYNTHESIS, DESIGN AND OPERATION OF BIOMASS-BASED ENERGY SYSTEMS*. PhD, University of Nottingham, Nottingham.
- Beck, A., Sevault, A., Drexler-Schmid, G., Schöny, M. & Kauko, H. (2021) 'Optimal Selection of Thermal Energy Storage Technology for Fossil-Free Steam Production in the Processing Industry', *Applied Sciences*, 11(3), pp. 1063.
- Breeze, P. (2019) 'Chapter 10 - Power System Energy Storage Technologies', in Breeze, P. (ed.) *Power Generation Technologies (Third Edition)*: Newnes, pp. 219-249.
- Caraballo, A., Galán-Casado, S., Caballero, Á. & Serena, S. (2021) 'Molten Salts for Sensible Thermal Energy Storage: A Review and an Energy Performance Analysis', *Energies*, 14(4), pp. 1197.
- Chen, Y. R. (1983) 'Thermal properties of beef cattle manure', *Agricultural Wastes*, 6(1), pp. 13-29.
- Comission, E. (2019) *Consumer prices of petroleum products inclusive of duties and taxes*: European Comission. Available at: https://ec.europa.eu/energy/observatory/reports/2019_01_07_with_taxes_1933.pdf.
- Corporation, O. S. E. (2000) *The Market and Technical Potential for Combined Heat and Power in the Industrial Sector*, Washington, DC: ONSITE SYCOM Energy Corporation.
- Duić, N., Štefanić, N., Lulić, Z., Krajačić, G., Pukšec, T. & Novosel, T. (2017) *EU28 fuel prices for 2015, 2030 and 2050*, Croatia: Heat Roadmap Europe695989).
- Dutta, A. & Phillips, S. D. (2009) *Thermochemical Ethanol via Direct Gasification and Mixed Alcohol Synthesis of Lignocellulosic Biomass* Golden, Colorado: National Renewable Energy Lab (NREL)NREL/TP-510-45913).
- Engineering ToolBox. (2008). *Fossil and Alternative Fuels Energy Content*. [Online]. Available at: https://www.engineeringtoolbox.com/fossil-fuels-energy-content-d_1298.html [Accessed 2021].
- EPA (2015) *Biomass CHP Catalog*: U.S. Environmental Protection Agency. Available at: https://www.epa.gov/sites/default/files/2015-07/documents/biomass_combined_heat_and_power_catalog_of_technologies_5_biomass_conversion_technologies.pdf.
- Eurostat (2020a) 'Electricity prices for non-household consumers - bi-annual data (from 2007 onwards)'. Available at: https://ec.europa.eu/eurostat/databrowser/view/NRG_PC_205_custom_494574/default/table [Accessed].
- Eurostat (2020b) 'Gas prices for non-household consumers - bi-annual data (from 2007 onwards)'. Available at: https://ec.europa.eu/eurostat/databrowser/view/NRG_PC_203_custom_494286/default/table?lang=en [Accessed].

- Fleiter, T., Steinbach, J. & Ragwitz, M. (2016) *Mapping and analyses of the current and future (2020 - 2030) heating/cooling fuel deployment (fossil/renewables)*, Germany: European Commission.
- Gabrielli, P., Gazzani, M., Martelli, E. & Mazzotti, M. (2018a) 'Optimal design of multi-energy systems with seasonal storage', *Applied Energy*, 219, pp. 408-424.
- Gabrielli, P., Gazzani, M. & Mazzotti, M. (2018b) 'Electrochemical conversion technologies for optimal design of decentralized multi-energy systems: Modeling framework and technology assessment', *Applied Energy*, 221, pp. 557-575.
- Glatzmaier, G. (2011) *Developing a Cost Model and Methodology to Estimate Capital Costs for Thermal Energy Storage*: NREL/NREL/TP-5500-53066).
- Hernández, B., León, E. & Martín, M. (2017) 'Bio-waste selection and blending for the optimal production of power and fuels via anaerobic digestion', *Chemical Engineering Research and Design*, 121, pp. 163-172.
- Jaspers, D. & Afman, M. (2017) *Electrification in the Dutch process industry*: Berenschot.
- Loh, H. P., Lyons, J. & Chales W. White, I. (2002) *Process Equipment Cost Estimation Final Report*, Pittsburgh, PA: NETL, US Department of Energy (DOE/NETL-2002/1169). Available at: <https://www.osti.gov/servlets/purl/797810/>.
- Marsidi, M. (2018) *Electric Industrial boiler - Technology Factsheet*. Energy.nl.
- Martín-Hernández, E., Guerras, L. S. & Martín, M. (2020) 'Optimal technology selection for the biogas upgrading to biomethane', *Journal of Cleaner Production*, 267, pp. 122032.
- Martín-Hernández, E., Sampat, A. M., Zavala, V. M. & Martín, M. (2018) 'Optimal integrated facility for waste processing', *Chemical Engineering Research and Design*, 131, pp. 160-182.
- Martín, M. & Grossmann, I. E. (2022) 'Chapter 2 - Mathematical modeling for renewable process design', in Martín, M. (ed.) *Sustainable Design for Renewable Processes*: Elsevier, pp. 35-100.
- Nussbaum, M. (2021). *Fertilizer Costs Make Manure Look Better* [Online]. Ohio. [Accessed 2021].
- OECD. (2021). *Inflation (CPI)* [Online]. Organisation for Economic Co-operation and Development. Available at: <https://data.oecd.org/> [Accessed 2021].
- Parat Halvorsen AS. (2021). *PARAT IEH: High Voltage Electrode boiler for Steam and Hot water* [Online]. Available at: <https://parat.no/ieh/> [Accessed].
- Pauschert, D. (2009) *Study of Equipment Prices in the Power Sector*, Washington, D.C.: Energy Sector Management Assistance ProgramESMAP Technical Paper 122/09).
- Pérez-Uresti, S. I., Martín, M. & Jiménez-Gutiérrez, A. (2019) 'Superstructure approach for the design of renewable-based utility plants', *Computers & Chemical Engineering*, 123, pp. 371-388.
- Research, F. (2020). *Typical calorific values of fuels* [Online]. Available at: <https://www.forestresearch.gov.uk/tools-and-resources/fthr/biomass-energy-resources/reference-biomass/facts-figures/typical-calorific-values-of-fuels/> [Accessed August 2020].

- Smith, R. (2016). *Chemical Process Design and Integration* (2nd ed. ed.): Wiley.
- Susmozas, A., Iribarren, D. & Dufour, J. (2013) 'Life-cycle performance of indirect biomass gasification as a green alternative to steam methane reforming for hydrogen production', *International Journal of Hydrogen Energy*, 38(24), pp. 9961-9972.
- The American Society of Mechanical Engineers. (2017). *ASME Boiler and Pressure Vessel Code (BPVC), Section VIII, Rules for Construction of Pressure Vessels - Division 1*. ASME International.
- Towler, G. & Sinnott, R. (2013) 'Utilities and Energy Efficient Design', *Chemical engineering design, principles, practice and economics of plant and process design*. Second ed. Oxford, UK: Elsevier, pp. 103-160.
- Turton, R., Shaeiwitz, J. A., Bhattacharyya, D. & Whiting, W. B. (2018). *Analysis, Synthesis, and Design of Chemical Processes* (5 ed.): Pearson.
- Varbanov, P. (2004a) *Optimisation and Synthesis of Process Utility Systems*. PhD, University of Manchester, Manchester, UK [Online] Available at: <https://books.google.co.uk/books?id=9Ff4xQEACAAJ> (Accessed).
- Varbanov, P. S. D., S.; Smith, R. (2004b) 'Modelling and Optimization of Utility Systems', *Chem. Eng. Res. Des.*, 82, pp. 561-578.

SUPPLEMENTARY INFORMATION P3.B

Correlations of additional utility components

Nomenclature

B.I.1. Abbreviation

amb	ambient
BFW	Boiler feed water
boi	boiler
C	Heat sink side
C_{BFW}	Boiler feed water used at the heat sink side
C_T	Total process steam use (at the heat sink side)
Cond	condensate
Deae	deaerator
eq	equipment
exh	Exhaust gases
FSR	Flash steam recovery
H	Heat source side
HO	Hot oil
HRSG	Heat recovery steam generator
loss	Heat losses
SF	Supplementary firing
sh	Superheating stage - superheater
stack	Stack gases
vap	Evaporation stage - evaporator
pre	Preheating stage - economizer
w	Treated water

Sets

EQ	Set of utility equipment for thermal and/or power generation (subset of utility components)
F	Set of fuels
I	Set of steam mains
I_{j_s}	Set of steam levels j_s that belong to steam main i (i, j_s)
J	Set of temperature/pressure intervals
k	Set of representative days
t	Set of intra time-periods
v	Set of VHP steam levels

Parameters

α	Vent rate in the deaerator
β	Condensate return rate

γ	Blowdown rate
$\Delta T_{\min}^{\text{HRSG}}$	Minimum approach temperature difference for HRSG
ζ	Upper bound of heat content of gas turbine exhausts
$\eta_{\text{eff}}^{\text{HRSG}}$	Radiation efficiency of HRSG
$c_{p,\text{exh}}$	Heat capacity of exhaust gases
\tilde{h}_{l,j_s}	Enthalpy of saturated liquid at steam level j_s
\tilde{h}_{v,j_s}	Enthalpy of saturated vapor at steam level j_s
\tilde{h}^{BFW}	Enthalpy of boiling feed water
$\tilde{h}_{l,j_s}^{\text{C}}$	Enthalpy of saturated liquid of process steam use at steam level j_s
$\tilde{h}_{\text{sh},j_s}^{\text{C}}$	Enthalpy of superheated process steam use at steam level j_s
\tilde{h}^{Cond}	Enthalpy of returned condensate
\tilde{h}^{vent}	Enthalpy of steam vented
\tilde{h}^{W}	Enthalpy of treated water
Lim_f	Upper limit of fuel f
NHV_f	Net heat value of fuel f
\tilde{T}_{amb}	Ambient temperature
\tilde{T}_{FG}	Inlet temperature of flue gas from indirect gasification
\tilde{T}_v^{sat}	Saturated steam temperature at v conditions
$\tilde{T}_{\min}^{\text{stack}}$	Minimum stack temperature for exhaust gases
$\tilde{T}_{\max}^{\text{SF}}, \tilde{T}_{\max}^{\text{UF}}$	Maximum temperature achievable with and without supplementary firing, respectively.
$\tilde{Q}_{j,k,t}^{\text{C}}$	Process heat sink at level j at any given time period

Positive variables

h_{sh,j_s}	Enthalpy of superheated steam at steam level j_s
$h_{\text{sh},v}$	Enthalpy of superheated steam at VHP steam main operating at v conditions
$m_{\text{T},k,t}^{\text{BFW}}$	Total mass flowrate of boiler feed water in the site at any given time period
$m_{i,j_s,k,t}^{\text{CBFW}}$	Steam mass flow rate of BFW injected to desuperheated steam operating at j_s conditions, at any given time period
$m_{i,j_s,k,t}^{\text{Cond}}$	Condensate mass flow rate from steam main i operating at level j_s , at any given time period
$m_{i,j_s,k,t}^{\text{CT}}$	Process steam use at steam level j_s , at any given time period
$m_{i,j_s,k,t}^{\text{Deae}}$	Steam mass flowrate from LP steam main operating at j_s conditions to deaerator, at any given conditions
$m_{\text{G},k,t}^{\text{FG}}$	Mass flowrate of flue gas from indirect gasification
$m_{i,j_s,k,t}^{\text{FSR}}$	Inlet mass flow rate at FSR drum i operating at j_s conditions, at any given time periods
$m_{i,j_s,j_s',k,t}^{\text{FSR}}$	Liquid mass flow rate of FSR i operating from pressure j_s to j_s' , at any given time periods
$m_{s,j_s,j_s',k,t}^{\text{FSR}}$	Steam mass flow rate of FSR i operating from pressure j_s to j_s' , at any given time period
$m_{i,j_s,k,t}^{\text{H}}$	Process steam generation at steam main i instant operating at level j_s , at any given time period
$m_{\text{exh},eq,v,k,t}^{\text{HRSG}}$	Mass flow rate of gas exhausts of unit eq , to generate steam in a HRSG operating at v conditions, at any given time period
$m_{i,j_s,k,t}^{\text{MS}}$	Steam mass flowrate from molten salt system to steam main i operating at j_s conditions at any given time period
$m_{\text{eq},f,k,t}^{\text{SF}}$	Fuel flowrate of supplementary firing at any given time period
$m_{k,t}^{\text{W}}$	Mass flow rate of treated water at any given time period
$T_{\text{sh},v}^{\text{VHP}}$	Steam temperature at VHP level operating at v conditions

$Q_{i,j_s,k,t}^{Cin}$	Heat available for process heating from steam main i operating at j_s conditions, at any given time period
$Q_{k,t}^{HO}$	Process heating requirements that cannot be used/satisfied by steam at any given time period
$Q_{s,k,t}^{HO}$	Process heating provided by hot oil system at steam temperature range at any given time period
$Q_{T,k,t}^{HO}$	Total process heating provided by hot oil system at any given time period
$Q_{eq,v,k,t}^{HRSG}$	Heat of the exhaust gases used in the HRSG unit eq operating at v conditions, at any given time period
$Q_{eq,v,k,t}^{loss}$	Heat losses to the ambient of exhaust gases of gas turbine eq after HRSG operating at v conditions, at any given time period
$Q_{eq,v,k,t}^{pre}, Q_{eq,v,k,t}^{vap}, Q_{eq,v,k,t}^{sh}$	Heat transfer in each stage of HRSG (eq): preheating (pre), evaporation (vap) and superheating (sh) for generating steam at v conditions, at any given time period
$U_{eq,f,k,t}^{SF}$	Fuel consumption of supplementary firing at any given time period
$Z_{eq,v,k,t}^{boi}$	Boiler load operation v conditions at any given time period, in [t/h]
$Z_{eq,v,k,t}^{HRSG}$	HRSG load operation v conditions at any given time period, in [t/h]

Binary variables

y_{i,j_s}	Binary variables to denote the selection of steam main i operating at j_s conditions
y_{eq}	Binary variables to denote the selection of equipment
$y_{j_s}^{HO}$	Binary variables to denote the selection of hot oil at steam level j_s
$y_{eq,f,k,t}^{SF}$	Binary variable to denote activation of supplementary firing at any given time period

Table P3.B. 1. Main equations of additional utility components

Component	Equations/Constraints
	Energy balance at each stage:
	$Q_{eq,k,t}^{exh} = \sum_v [Q_{eq,v,k,t}^{loss} + Q_{eq,v,k,t}^{HRSG}] \quad (P3.B. 1)$
	$Q_{eq,v,k,t}^{HRSG} = Q_{eq,v,k,t}^{sh} + Q_{eq,v,k,t}^{vap} + Q_{eq,v,k,t}^{pre}$ $Q_{eq,v,k,t}^{sh} = \frac{1}{\eta_{eff}^{HRSG}} [(h_{sh,v} - \tilde{h}_{v,v}) \cdot Z_{eq,v,k,t}^{HRSG}]$ $Q_{eq,v,k,t}^{vap} = \frac{1}{\eta_{eff}^{HRSG}} [(\tilde{h}_{v,v} - \tilde{h}_{l,v}) \cdot Z_{eq,v,k,t}^{HRSG}] \quad (P3.B. 2)$ $Q_{eq,v,k,t}^{pre} = \frac{1}{\eta_{eff}^{HRSG}} [(\tilde{h}_{pre,v} - \tilde{h}^{BFW}) (1 + \gamma) \cdot Z_{eq,v,k,t}^{HRSG}]$
Heat recovery steam generator (HRSG)	Heat transfer feasibility: $Q_{eq,v,k,t}^{loss} \geq m_{exh}^{HRSG} \cdot cp_{exh} (\tilde{T}_{min}^{stack} - \tilde{T}_{amb}) \quad (P3.B. 3)$ $Q_{eq,v,k,t}^{pre} + Q_{eq,v,k,t}^{loss} \geq m_{exh}^{HRSG} \cdot cp_{exh} (\tilde{T}_v^{sat} + \Delta T_{min}^{HRSG} - \tilde{T}_{amb})$ $Q_{eq,v,k,t}^{exh} \geq m_{exh}^{HRSG} \cdot cp_{exh} (T_{sh,v}^{VHP} + \Delta T_{min}^{HRSG} - \tilde{T}_{amb})$
	Supplementary firing: $\sum_v Q_{eq,v,k,t}^{exh} = Q_{eq,k,t}^{exh} + \sum_{IG} m_{IG,k,t}^{FG} \cdot cp_{exh} (\tilde{T}_{FG} + \Delta T_{min}^{HRSG} - \tilde{T}_{amb}) + \sum_f U_{eq,f,k,t}^{SF} \quad (P3.B. 4)$
	where $U_{eq,f,k,t}^{SF} = m_{eq,f,k,t}^{SF} \cdot NHV_f$ $m_{eq,f,k,t}^{SF} \leq \text{Lim}_f \cdot y_{eq,f,k,t}^{SF} \quad \text{and} \quad \sum_f y_{eq,f,k,t}^{SF} \leq y_{eq} \quad (P3.B. 5)$
	$Q_{eq,v,k,t}^{exh} \leq m_{exh}^{HRSG} \cdot cp_{exh} (\tilde{T}_{max}^{UF} - \tilde{T}_{amb}) + \zeta \cdot \sum_{f \in F} y_{eq,f,k,t}^{SF} \quad (P3.B. 6)$ $Q_{eq,v,k,t}^{exh} \leq m_{exh}^{HRSG} \cdot cp_{exh} (\tilde{T}_{max}^{SF} - \tilde{T}_{amb}) + \zeta \cdot \sum_{f \in F} (1 - y_{eq,f,k,t}^{SF})$

Component	Equations/Constraints
	<p>Mass balance at the FSR inlet:</p> $\beta \cdot m_{i,j_s,k,t}^{C_T} + \sum_{i < i'} \sum_{j_s \in IJ_s} m_{i',j_s,k,t}^{FSR} = m_{i,j_s,k,t}^{FSR} \quad (P3.B. 7)$
Flash steam recovery (FSR)	<p>Overall mass and energy balance:</p> $\sum_{i > i'} \sum_{(i',j_s) \in IJ_s} (m_{i',j_s,k,t}^{FSR} + m_{i',j_s,k,t}^{FSR}) = m_{i,j_s,k,t}^{FSR} \quad (P3.B. 8)$ $\sum_{i > i'} \sum_{(i',j_s) \in IJ_s} (m_{i',j_s,k,t}^{FSR} \cdot \tilde{h}_{v_{j_s}} + m_{i',j_s,k,t}^{FSR} \cdot \tilde{h}_{j_s}) = m_{i,j_s,k,t}^{FSR} \cdot \tilde{h}_{v_{j_s}}$
	<p>Mass and energy balance at the deaerator:</p> $m_{k,t}^{BFW} = m_{k,t}^W + \sum_{i \in I} \sum_{(i,j_s) \in IJ_s} m_{i,j_s,k,t}^{Cond} + (1-\alpha) \sum_{i=i_n} \sum_{(i,j_s) \in IJ_s} m_{i,j_s,k,t}^{Deac} \quad (P3.B. 9)$
Deaerator (Deae)	$m_{k,t}^{BFW} \cdot \tilde{h}^{BFW} + \sum_{i=i_n} \sum_{(i,j_s) \in IJ_s} (\alpha \cdot m_{i,j_s,k,t}^{Deac} \cdot \tilde{h}^{vent}) = \sum_{i \in I} \sum_{(i,j_s) \in IJ_s} (m_{i,j_s,k,t}^{Cond} \cdot \tilde{h}^{Cond}) + m_{k,t}^W \cdot \tilde{h}^W + \sum_{i=i_n} \sum_{(i,j_s) \in IJ_s} (m_{i,j_s,k,t}^{Deac} \cdot h_{sh_{j_s}})$ <p>System mass balance of BFW:</p> $m_{k,t}^{BFW} = \sum_{i \in I} \sum_{(i,j_s) \in IJ_s} (m_{i,j_s,k,t}^H + m_{i,j_s,k,t}^{C-BFW} + m_{i,j_s,k,t}^{BFW}) + \sum_{eq \in EQ} \sum_{v \in VHP} (Z_{eq,v,k,t}^{boi} + Z_{eq,v,k,t}^{HRSG}) + \sum_{i \in I} \sum_{j_s \in IJ_s} m_{i,j_s,k,t}^{MS} \quad (P3.B. 10)$
	<p>Overall hot oil supply:</p> $Q_{k,t}^{HO} = Q_{k,t}^{HO} + Q_{k,t}^{HO} \quad (P3.B. 11)$
	<p>Heat provided above T_{max}:</p> $Q_{k,t}^{HO} = \sum_{j \in J_{HO}, T_j \geq T_{max}} \tilde{Q}_{j,k,t}^C \quad (P3.B. 12)$
Hot oil system (HO)	<p>Overall energy demand in the sink cascade:</p> $\sum_i \sum_{(i,j_s) \in IJ_s} Q_{i,j_s,k,t}^{C_{in}} + Q_{k,t}^{HO} = \sum_j \tilde{Q}_{j,k,t}^C \quad \text{where} \quad Q_{i,j_s,k,t}^{C_{in}} = m_{i,j_s,k,t}^{C_T} \cdot (\tilde{h}_{sh_{j_s}}^C - \tilde{h}_{j_s}^C) \quad (P3.B. 13)$
	$Q_{k,t}^{HO} = \sum_{j_s, T_{j_s} > T_1^{HO}} (\tilde{Q}_{j_s,k,t}^C \cdot y_{j_s}^{HO}) \quad (P3.B. 14)$
	<p>Logical constraints:</p> $y_{j_s}^{HO} - y_{j_s-1}^{HO} \leq 0 \quad (P3.B. 15)$ $y_{j_s}^{HO} + y_{i,j_s} \leq 1$

SUPPLEMENTARY INFORMATION P3.C

Estimation of steam properties

Nomenclature

ΔH_{is}	Isentropic enthalpy difference
h_{sh}	Superheating enthalpy (at the inlet of steam turbine)
$h_{sh\nu}$	Superheating enthalpy at the VHP steam main operating at ν conditions
P_{in}, P_{out}	Inlet and outlet pressure of steam turbine
P_{ν}	Pressure of VHP steam main ν
T_{sh}^{VHP}	Superheating temperature at the VHP steam main
a, b	Modelling coefficients for the calculation of isentropic enthalpy difference
a^T, b^T, c^T	Modelling coefficients for the calculation of superheating temperature

C.I. Isentropic enthalpy difference (ΔH_{is})

Isentropic enthalpy difference can be linearly correlated to enthalpy through Eq. (P3.C. 1), where the effect of pressure is included in coefficients a and b , as expressed in Eqs. (P3.C. 2) and (P3.C. 3). Table P3.C. 1 summarizes the coefficient values for a pressure range between 0.1 and 120 bar, and superheat temperature from steam saturated conditions up to 570 °C.

$$\Delta H_{is} = a \cdot h_{sh} + b \quad (P3.C. 1)$$

$$a = a_1 \left(\frac{P_{in}}{P_{out}}\right)^6 + a_2 \left(\frac{P_{in}}{P_{out}}\right)^5 + a_3 \left(\frac{P_{in}}{P_{out}}\right)^4 + a_4 \left(\frac{P_{in}}{P_{out}}\right)^3 + a_5 \left(\frac{P_{in}}{P_{out}}\right)^2 + a_6 \left(\frac{P_{in}}{P_{out}}\right) + a_7 \quad (P3.C. 2)$$

$$b = b_1 \left(\frac{P_{in}}{P_{out}}\right)^6 + b_2 \left(\frac{P_{in}}{P_{out}}\right)^5 + b_3 \left(\frac{P_{in}}{P_{out}}\right)^4 + b_4 \left(\frac{P_{in}}{P_{out}}\right)^3 + b_5 \left(\frac{P_{in}}{P_{out}}\right)^2 + b_6 \left(\frac{P_{in}}{P_{out}}\right) + b_7 \quad (P3.C. 3)$$

Table P3.C. 1. Modelling coefficients for the estimation of the isentropic enthalpy change across the steam turbine

Modelling coefficients for linear correlations			
a_1	0.00215130	b_1	-0.00184233
a_2	-0.02287910	b_2	0.01987759
a_3	0.08182395	b_3	-0.07311089
a_4	-0.08098163	b_4	0.08298832
a_5	-0.16623258	b_5	0.09962741
a_6	0.52882032	b_6	-0.2846926
a_7	-0.00008219	b_7	0.00007468
Min error [%]		0.00	
Max error [%]		5.30	
Average error [%]		0.80	

C.II. Superheating steam temperature (T_{sh}^{VHP})

Superheat temperature ($T = f(P, h)$) could be estimated based on pressure (which is a parameter) and enthalpy (degree of freedom) as shown below. The polynomial correlation is given by Eqs. (P3.C. 4) - (P3.C. 7) and correlation coefficients detailed in Table P3.C. 2.

$$T_{sh_v}^{VHP} = a^T \cdot h_{sh_v}^2 + b^T \cdot h_{sh_v} + c^T \quad (P3.C. 4)$$

$$a^T = a_1^T \cdot P_v + a_2^T \quad (P3.C. 5)$$

$$b^T = b_1^T \cdot P_v + b_2^T \quad (P3.C. 6)$$

$$c^T = c_1^T \cdot P_v + c_2^T \quad (P3.C. 7)$$

Table P3.C. 2. Modelling coefficients for the nonlinear calculation of the superheating temperature at VHP

Modelling coefficients			
a_1^T	9.34150	b_2^T	-586.40561
a_2^T	1225.72724	c_1^T	11.15590
b_1^T	-20.10415	c_2^T	-80.09496
Min error [%]	0.00		
Max error [%]	2.00		
Average error [%]	0.32		

* Operating pressure range between 40 and 120 bar, and superheat temperature from steam saturated conditions up to 570 °C.

For linear problems Eq. (2.73) is employed to consider superheat steam temperature constraint. In this work, superheat steam temperature involves a strictly convex and monotonic, which needs to be minimized. Therefore, a sufficiently dense set of linear constraints given by Eq. (P3.C. 8) can rigorously underestimate the temperature function.

$$T_{sh_v}^{VHP} \geq a_{sx}^T \cdot h_{sh_v} + b_{sx}^T \quad (P3.C. 8)$$

Where sx is the index for set S_x , of linearization with parameters a_{sx}^T and b_{sx}^T . These correlating parameters are calculated through similar Eqs. to (P3.C. 5) - (P3.C. 7).

Table P3.C. 3. Modelling coefficients for the linear estimation of the superheating temperature at VHP level

	Segment 1	Segment 2	Segment 3
a_{sx1}^T	-5.566	-4.010	-2.621
a_{sx2}^T	1405.353	1660.220	1668.420
b_{sx1}^T	5.520	4.228	2.962
b_{sx2}^T	-889.133	-1106.817	-1114.563
Min error [%]	0.00		
Max error [%]	2.29		
Average error [%]	0.26		

CHAPTER 5

Integration of Sustainability Criterion in the Design of Utility Systems

Overview

This chapter discusses a manuscript intended for submission to the journal "Cleaner Production". The environmental impact is included in this manuscript to determine the true potential for decarbonizing the process utility system. This is accomplished by employing a lifecycle assessment of the main utility technologies (boilers, HRSG, gas turbines, steam turbines) and energy storage options (lithium-ion and sodium sulphur batteries, hydrogen storage system, steam accumulators and molten salt systems). The resources considered were fuel gas, natural gas, woodchip, wood pellets, cattle manure, water and electricity grid.

The environmental and economic impacts are integrated using an epsilon constraint approach, having as driving forces the total annualized cost and global warming potential. Moreover, other relevant environmental issues such as ecotoxicity, air, water and soil pollution, resource depletion and human health are also assessed for the obtained designs. The resulting set of Pareto solutions where system designs capable of achieving significant CO₂ reductions at a marginal cost increment can be identified

The results show that by selecting appropriate utility levels and enhancing site heat integration, it is possible to save up to 9 and 27.6 % on costs and CO₂ emissions, compared to an optimal design with fixed conditions. Moreover, all the environmental impacts are also reduced between 6 and 67 %. Further decarbonization is possible and will require a gradual transition away from natural gas-based technologies. However, as the CO₂ emissions target becomes more aggressive, the cost of abatement increases significantly.

Overall, this contribution allows to explore trade-offs between economic and environmental to provide cost-effective industrial utility designs, on a sustainable basis.

5.1 Contribution 4

Title: Roadmap to low-carbon industrial utility systems: Design of cost-effective process utility systems considering environmental life-cycle assessment

Authors: Julia Jimenez-Romero, Adisa Azapagic and Robin Smith

To be submitted to: Cleaner Production

Year: 2022

Roadmap to low-carbon industrial utility systems: Design of cost-effective process utility systems considering environmental life-cycle assessment

Julia Jiménez-Romero^{a,b,*}, Adisa Azapagic^b, Robin Smith^a

^a Centre for Process Integration, Department of Chemical Engineering and Analytical Science, University of Manchester, Manchester, M13 9PL, United Kingdom

^b Sustainable Industrial Systems Group, Department of Chemical Engineering and Analytical Science, University of Manchester, Manchester, M13 9PL, United Kingdom

* Julia Jiménez-Romero. Email: julia.jimenezromero@manchester.ac.uk

Abstract

In industrial sites, a steam system is often built to meet the site heat and power requirements. Current utility systems strongly rely on fossil fuels. Switching from fossil fuels to renewables can decrease CO₂ emissions; however, different aspects such as investment costs, energy demands, energy market and economic efficiency play a key role in the decision-making. Thus, to provide a cost-effective transition from current to future sustainable energy systems require the development of systematic approaches for selecting the most appropriate utility system configuration and operation. Synthesis approaches based on economic criteria can reduce energy consumption and CO₂ emissions due to a reduction of utilities consumption with a cost-optimal design. However, to achieve further decarbonisation the environmental impact has to be assessed simultaneously. This paper proposes an optimization framework to design cost-effective utility system, exploring trade-offs between decarbonisation goals and total costs, using ϵ -constraint method. The model considers indirect energy integration through the site (process steam generation), as well as the heat recovery from condensates through flash steam recovery system. To smooth the imbalance between energy demands and supply the integration of both thermal and electric storage units is also analysed. The environmental assessment of both the equipment's material and utility consumption in the system using the life cycle assessment approach. To show the applicability of the proposed framework, an illustrative petrochemical site is used as a case study. The method developed efficiently achieves near-Pareto fronts of economic and environmental goals, where the main results indicate simultaneous optimization of utility system configuration and site heat recovery can successfully minimise both the economic and environmental implications of the site.

Highlights

- Optimization framework to explore cost-effective sustainable industrial system.
- The framework include heat integration, multiple units, and energy storage systems.
- Up to 27.6 % CO₂ emissions can be reduced by enhancing site heat integration
- Costs of CO₂ mitigation increase rapidly when the emissions target is increased.
- Emission abatement above 90 % is feasible, but will need targeted finance support.

Keywords

Superstructure, multi-objective optimization, nonconvex mixed integer problem model, hybrid energy system, site heat recovery, industrial steam systems, energy storage, life-cycle assessment

Nomenclature

Abbreviations

BFW	Boiler feed water
cmdty	Commodity
FSR	Flash steam recovery
HO	Hot oil
HRSG	Heat recovery steam generator
HS	Hydrogen storage
LiB	Lithium-ion battery
MILP	Mixed integer linear programming
MINLP	Mixed integer non liner programming
MS	Molten salt system
NaS	Sodium sulphur battery
NHV	Net heat value
sh	superheated
SA	Steam accumulator
SSE	Sum of squared errors
ST	Steam turbine
TAC	Total Annualized Cost
UC	Utility components
VHP	Very High Pressure

Sets

CMDTY	Set of utility commodities
C	Set of cold streams
ES	Set of energy storage units
EQ	Set of utility equipment for thermal and/or power generation (subset of utility components)
F _{eq}	Set of fuels for each equipment
H	Set of hot streams
I	Set of steam mains
IJ	Set of steam levels j_s that belong to steam main i (i, j_s)

J	Set of temperature/pressure intervals
J_{HO}	Set of temperature/pressure intervals for hot oil (subset of temperature intervals)
J_s	Set of temperature/pressure intervals for steam main (subset of temperature intervals)
J_{WH}	Set of temperature/pressure intervals for waste heat (subset of temperature intervals)
K	Set of design periods
MS	Set of molten salt systems (subset of energy storage ES)
SA	Set of steam accumulators (subset of energy storage ES)
T	Set of intra design periods
UC	Set of utility components
VHP_L	Set of VHP steam levels

Variables

C_{comdty}^{op}	Operating costs of commodities
TAC	Total annualized costs

Positive variables

$\delta_{eq,\theta,k,t}^{start}$	Continuous variable with values between 0 and 1, that indicates if equipment eq operating at θ conditions is started-up at time t
C_{uc}^{inv}	Investment cost of utility component uc
C_{uc}^{main}	Maintenance cost of each utility component uc
C^{start}	Start-up costs
$E_{es,d,t}^{es}$	Energy stored in unit es at any given time step
h_{shj_s}	Enthalpy of of superheated steam at steam level j_s
h_{shv}	Enthalpy of superheated steam at VHP steam main operating at v conditions
$L_{es,d,t}$	Losses of storage unit es at any given time period
$m_{i,j_s,k,t}^{CBFW}$	Steam mass flow rate of BFW injected to desuperheated steam operating at j_s conditions, at any given time period
$m_{i,j_s,j_s',k,t}^{C_{ch-SA}}, m_{i,j_s,j_s',k,t}^{C_{dech-SA}}$	Charging and discharging steam mass flow of steam accumulator operating between steam level j_s to level j_s' , at any given time period
$m_{i,j_s,k,t}^{CFSR}$	Steam mass flow rate of FSR injected to desuperheated steam operating at j_s conditions, at any given time period
$m_{i,j_s,k,t}^{C_{steam}}$	Process steam use at steam main i instant operating at level j_s , at any given time period
$m_{i,j_s,k,t}^{C_T}$	Process steam use at the process use instant at level j_s , at any given time period
$m_{eq}^F, f_{eq,k,t}$	Fuel flowrate of type fuel f_{eq} in unit eq at a specific time period
$m_{i,j_s,k,t}^{in}, m_{i,j_s,k,t}^{out}$	Variable vector representing inlet and outlet mass flowrates at steam main i operating at level j_s , at any given time period
$m_{UC}^{in}_{i,j_s,k,t}$	Variable vector representing mass flows from unit component UC to steam main i (operating at j_s), at any given time period
$m_{UC}^{out}_{i,j_s,k,t}$	Variable representing mass flows from steam main i (operating at j_s) to unit component UC, at any given time period
$m_{i,j_s,k,t}^H$	Mass flow rate of process steam generation for steam level j_s at any given time period
$m_{i,j_s,k,t}^{MS}$	Steam mass flowrate from molten salt system to steam main i operating at j_s conditions at any given time period
$m_{v,k,t}^{VHP-MS}$	Steam mass flow rate from VHP level v to molten salt system at any given time period
$P_{es,k,t}^{ch}, Pd_{es,k,t}^{ch}$	Charging and dischargin power of storage unit es at any given time period
$Q_{eq,k,t}^B$	Fuel consumption of boiler eq at period t of design day k

$Q_{eq,k,t}^F$	Fuel consumed in unit eq at a specific time period
Q_s^{HO}	Process heating provided by hot oil system at steam temperature range, at any given time period
$Q_{i,j_s,k,t}^{in}, Q_{i,j_s,k,t}^{out}$	Variable vector representing inlet and outlet energy at steam main i operating at j_s conditions, at any given time period
$Q_{uc,i,j_s,k,t}^{in}$	Variable vector representing inlet heat flow at steam main i operating at j_s conditions, at any given time period
$R_{j_s,k,t}^C$	Residual sink heat at steam level j_s , at any given time period
$R_{j_s,k,t}^H$	Residual source heat at steam level j_s , at any given time period
$U_{comdty,k,t}$	Variable vector representing site consumption of each commodity, at any given time period
U_e^{exp}, U_e^{imp}	Electricity export and import at any given time period, respectively
$W_{k,t}^{EB}$	Power required by the electrode boiler at specific time period
W_T^{EB}	Total power required by electrode boiler and electric superheater (if selected) at a specific time period
$W_{k,t}^{shEB}$	Power required by the electric superheater at specific time period
$W_{eq,k,t}$	Variable vector representing power generated by equipment eq at specific time period
$Z_{eq,\theta,k,t}$	Equipment load operating at θ conditions at a specific time period
Z_{es}^{es}	Energy storage capacity of unit es
$Z_{eq,\theta,k,t}^m$	Auxiliary variable to represent equipment load if unit eq is operation at a specific time period
Z_{uc}^{max}	Variable vector representing installed capacity of utility component uc
$Z_{eq,\theta}^{max}$	Installed equipment size operating at θ conditions
$Z_{eq,v,k,t}^{sh}$	Electric superheater load operating at v conditions at a specific time period

Parameters

Ψ_{uc}	Cost exponent for each utility component
γ	Blowdown rate
$\sigma(d)$	Function that correlates the design day k corresponding to day of the year d
Λ	Vector that represents part of the slope in the modelling of power generation units
Δt_t	Duration of the time interval t
g_{es}^{loss}	Self-discharge coefficient of storage unit es
$\underline{\Omega}_{eq}$	minimum feasible load operation of each equipment
τ_{es}	time required to fully charge/discharge the unit es
$\widetilde{a}_{11}, \widetilde{a}_{12}$	Model coefficients for boilers
$\widetilde{a}_{21}, \widetilde{a}_{22}, \widetilde{a}_{23}, \widetilde{a}_{24}$	Model coefficients for power generation units, based on Willan's line correlation
C_{eq}^{ref}	Reference cost for each equipment
$CP_{k,t}^C c_i$	Heat capacity flowrate of cold stream c_i , at any given time period
$CP_{h_i,k,t}^H$	Heat capacity flowrate of hot stream h_i , at any given time period
DoD_{es}	Depth of discharge of energy storage unit es
F_{uc}^{ann}	Annualization factor of utility component uc
F_{uc}^{inst}	Installation factor of utility component uc
F_{uc}^{main}	Maintenance factor of utility component uc
F_{eq}^{start}	Cost per start-up of equipment eq
$\underline{h}_{sh}, \overline{h}_{sh}$	Lower and upper bound for steam enthalpy at superheated stage

$\tilde{h}_{shj_s}^H, \tilde{h}_{shj_s}^C$	Enthalpy of superheated process steam generation (H) and use (C) at steam level L
\tilde{h}_l, \tilde{h}_v	Enthalpy of saturated liquid and vapour, respectively
\tilde{h}^{BFW}	Enthalpy of boiling feed water
\tilde{h}^{Cond}	Enthalpy of returned condensate
L^H, L^C	Heat losses due to distribution at the source and sink side, respectively
L^e	Electrical losses for transmission to/from the national grid
$\underline{m}_{feq,k,t}^F, \overline{m}_{feq,k,t}^F$	Lower and upper bound of fuel at a specific time period
NHV_{feq}	Net heat value of fuel f_{eq}
$N_{max_{eq}}^{start}$	Maximum number of start-ups permissible per day corresponding to unit eq
$\eta_{es}^{ch}, \eta_{es}^{dch}$	Charging and discharging efficiency of storage unit es
η_{shEB}	Efficiency of electric superheater of electrode boiler EB
$P_{comdy_{k,t}}$	Commodity price at specific time period
P_{EB}^{max}	Maximum steam pressured allowed in electrode boiler EB
P_v	Steam pressure at v conditions
$\tilde{Q}_{j,k,t}^C$	Process heat sink at level j , at any given time period
$\tilde{Q}_{j,k,t}^H$	Process heat source at level j , at any given time period
T_j	Utility temperature at level j
T^{*in}, T^{*out}	Shifted inlet and outlet stream temperatures
$t_{op_{k,t}}$	Duration of specific time period
$\tilde{U}_{max}^{exp}, \tilde{U}_{max}^{imp}$	Upper bound for export and import of grid electricity
U_{es}	Representative parameter of the upper boundaries of storage unit es variables
$U_{k,t}^m, U_{k,t}^Q$	Parameter vector representing upper bounds for mass and energy vectors of variables, at any given time period
$\tilde{W}_{k,t}^{dem}$	Power demand at any given time period
\tilde{Z}_{eq}^{ref}	Equipment reference size for capital cost estimation
$\underline{Z}_{eq}, \overline{Z}_{eq}$	Lower and upper size limits for each equipment

1. Introduction

With rising energy demand, resource depletion, and environmental consequences, there is a need for urgent and significant action in the industry sector is required. The Industrial sector consumes around 37% of global demand and produces 36 % of CO₂ emissions (IEA, 2018). Since energy is a non-replaceable and necessary input of industrial processes (Gahm et al., 2016), it must be used as efficiently as possible to save resources both ecologically and economically.

In most industrial sites, energy (heat and power) are mainly met by on-site utility systems with electricity grid connection. On the one hand, process utility system is the main consumer of industrial primary energy and, therefore, the main producer of industrial CO₂ emissions, especially when driven by fossil fuels. On the other hand, process utility systems also represent an effective solution for enhancing process industries sustainability via total site heat recovery, energy-efficient supply, and on-site power generation. For these reasons, process utility systems are becoming the focus of attention for industrial and researchers to reduce primary energy use and carbon emissions. Moreover, process utility systems are promising options to increase reliability and flexibility in the energy supply.

Furthermore, several factors, including (i) heat recovery from energy conversion technologies and/or excess heat from process streams at different temperatures depending on-site requirements and topology; (ii) variable energy demand and costs from industry to industry and over time; and (iii) different energy conversion options to meet energy demand could all have an impact on-site heat and power generation efficiency, fuel consumption, and CO₂ emissions. Moreover, as the energy market evolves and the share of renewables in the energy sector grows, process utility sites may shift from consumers to prosumers, with excess electricity sold to neighboring consumers or the grid. As a result, determining the optimal design and operation of the utility system accounting for the different potential scenarios and their boundary constraints becomes more and more critical. Nonetheless, due to a large number of decision variables, optimization may be technically challenging, particularly for large-scale sites. This has accentuated the need to develop specific decision-making tools to determine the optimal design of energy systems.

In terms of optimal design and operation of energy systems, techno-economic aspects such as total annualized costs and technical feasibility have been prioritized as design criteria (for detailed information, the reader is recommended to the reviews paper paper (Andiappan, 2017; Frangopoulos, 2018; Ganschietz, 2021). Although several studies have recognized the importance of energy security and environmental impacts in recent years, the design and optimization of energy systems are mainly based on economic objectives. Even when environmental implications are taken into account, they are frequently used as a benchmark (Pérez-Uresti et al., 2020) or translated into

economic terms, attributing an economical penalty on fossil fuels and/or unintended emissions (Sun and Liu, 2015). While the approach may result in a shift toward greener solutions (as mentioned in Contribution 3), it does not investigate trade-offs between economic efficiency and environmental benefits associated with various energy conversion technologies, which may result in missed opportunities for cost-effective solutions.

Multi-objective optimization (MOO), where more than one objective function is evaluated, may be used in this context to provide a set of optimal solutions that reflect different trade-offs between the competing objectives. Among the mathematical methods used in MOO are the ε -constraint approach, the weighted sum method, and evolutionary algorithm, among others.

One of the first multi-objective studies on utility systems is presented by Chang and Hwang (1996). Chang and Hwang (1996) incorporated the Smith (1991) concept of global emissions to a MILP model to synthesise utility plants with heat recovery. Oliveira Francisco and Matos (2004) proposed a multi-objective formulation based on the multiperiod model of Iyer and Grossmann (1998) for the synthesis and operational planning of utility systems that included emissions from fuel combustion. One limitation of these studies is the consideration of only CO, NO_x, and SO_x emissions, with particular emphasis on direct emissions from the combustion of fossil fuels.

To avoid a narrow outlook on environmental impact, Papandreou and Shang (2008) and Eliceche et al. (2007) introduced the use of life cycle assessment (LCA) in utility design framework to evaluate different environmental impacts other than air pollution (i.e. acidification and ecotoxicity potential). Papandreou and Shang (2008) presented a MILP model to generate a set of optimal solutions, while Eliceche et al. (2007) proposed a utility plant synthesis framework using bi-objective mixed-integer nonlinear programming (MINLP). Due to the computational complexity at the time, simple correlations, assuming constant efficiency, were employed. Moreover, in both cases, without considering process integration and focusing on on-site emissions. Later, Vaskan et al. (2014) provided a multi-objective MILP model with a dimensionality reduction approach to assess multiple objective functions without increasing the problem complexity. Vaskan et al. (2014)'s findings suggest that the best combination of two objectives is the total cost and global warming potential (carbon emissions).

Different alternatives to reduce environmental impact and achieve standard CO₂ have also been studied. Luo et al. (2014) proposed a MINLP model with an ε -constraint approach to synthesize a steam plant coupled with pollutant abatement processes. In Luo et al. (2014)'s work, gas emissions are reduced by considering desulfurization and denitrification processes, operating at fixed efficiencies. To overcome this issue, Xiao et al. (2021) provided a multi-objective genetic algorithm that considers variable efficiency. Wu et al. (2016) explored the environmental impact of steam diver

selection (i.e. electric motors or steam turbines) based on a multi-objective optimization with epsilon constraint technique. A drawback of these studies is that they only consider fossil fuel technologies working under nominal operating conditions.

Renewable energy sources in utility systems have also been investigated for CO₂ emissions reduction in energy systems. Pérez-Uresti et al. (2019) presented a MILP model to design renewable utility systems at industrial sites. The CO₂ emissions generated by the utility system are provided, yet the utility configuration is based only on the economics. In similar research areas, such as steam power plants, Gutiérrez-Arriaga et al. (2013) presented a multi-objective model for the optimal fuel selection (fossil fuel-based or renewable) for a steam power plant with a fixed flowsheet structure. The methodology employs LCA to quantify the carbon emission resulting from a combination of different primary energy sources. Fazlollahi et al. (2014) presented a MINLP model coupled with an evolutionary algorithm to integrate biomass resources into distributed energy systems for urban areas. Zheng et al. (2018) introduced an MINLP multi-objective optimization model to determine the optimal mix of renewable energy technologies for an urban utility system. Gabrielli et al. (2018a) proposed a MILP formulation with a ϵ -constraint approach to assessing the trade-offs between total annualized cost and CO₂ emissions of a low-carbon energy system, including energy storage units. While Zheng et al. (2018) and Gabrielli et al. (2018a) approach enables analysis of utility system topologies for a range of emission levels and boundary constraints, the environmental assessment is restricted to CO₂ emission caused by fuel combustion or electricity import.

In terms of energy integration as an effective measure of reducing carbon emission, several studies on heat recovery networks inside industrial facilities have also been conducted. Hipólito-Valencia et al. (2014) developed a site heat integration framework to synthesize a heat exchanger network coupled with a trigeneration utility system. The model considers the economic, environmental and social impact of different sources to generate steam. Although the methodology considers utility temperature optimization depending on the source used, steam generation is only evaluated at low-pressure steam conditions. Isafiade et al. (2017) proposed the synthesis of a heat exchanger network considering multiple levels of saturated steam generated by different energy sources. Isafiade et al. (2017)'s work emphasized the critical role of multi-energy approaches in achieving cost-effective, sustainable industrial systems. While the authors make reference to the potential impact of power generation/use on the site in their analysis of the site environmental-economic trade-offs, this is not included in the scope. Additionally, neither the technologies nor their configuration for utility generation was specified. Liu et al. (2020) proposed a MINLP optimization model to synthesize a cross-plant heat exchanger network interconnected with a fossil fuel-based utility system. Liu et al. (2020) conclude that steam generation from surplus heat in process streams reduces

not only utility system fuel usage but also HEN costs. Additionally, highlight the need for appropriate steam distribution to balance the industrial site's environmental and economic impact.

Notably, due to the remarkable complexity of the HEN-utility system synthesis problem, significant model simplifications have been required. For instance, only focus on a few utility components operating at fixed efficiency factors. Another common approach is to assume that steam mains operate at saturated steam conditions and/or at a single pressure level. As shown in Contribution 1, these assumptions can lead to inaccurate and/or impractical energy targets and thus incorrect analysis of the utility system design and its corresponding emissions.

In summary, the following points can be drawn based on the prior analysis:

- Increasing demand for industrial decarbonization requires a paradigm change in the design and operation of process utility systems. There are several alternatives for reducing carbon emission in process utility systems. A decision support tool is required to develop the roadmap for transitioning from current fossil-fuel-based utility systems to future process utility systems. A systematic approach is still needed to analyze the different process energy system configurations in relation to a range of emission levels and boundary constraints.
- Due to the mathematical complexity of utility systems with intra heat exchanger networks, previous research has either neglected site-wide energy integration opportunities or simplified the utility system configuration to the point where only a few utility components with fixed efficiencies and/or operating conditions have been considered, omitting critical practical issues (e.g. equipment part-load performance and limits).
- Depending on the topology and requirements of the site, industrial heat supply/use can be met at a wide range of temperatures. Heat recovery under steam fixed conditions (without a prior site evaluation) may miss not only potential heat recovery opportunities but also the trade-off between heat recovery and power generation potential in process utility systems (Contribution 1). Furthermore, taking into account steam sensible heat (i.e. boiler water preheating, steam superheating, and desuperheating) is critical to improving energy target accuracy.
- Energy storage systems are frequently overlooked to reduce time-coupling constraints and the complexity of the problem.
- Conducting an environmental analysis purely based on emissions from fossil fuel combustion may result in an inaccurate assessment of the environmental impact of a given system configuration. While most emissions from fossil-fuel-based units are associated with the use phase, emissions from renewable technologies are primarily associated with the construction and disposal phases of the

equipment. As a result, a life cycle assessment is required to quantify the site's true environmental impact and avoid emissions leakage to other stages.

2. Scope of the paper and contributions

This paper addresses the discussed issues and presents a holistic design approach through multi-objective optimization of process utility systems considering both economic and environmental objectives. The framework considers a variety of heat and power generation units, electric and thermal energy storage units and site-wide heat recovery measures. In addition, the design framework also considers operational issues (i.e. part-load performance and limits, start-up constraints) and practical constraints (i.e. steam temperature limitations, steam latent heat). To the knowledge of the authors, there is no previous study of optimal design of process utility systems considering both renewable and non-renewable technologies, energy storage units and site-wide energy integration. The methodology can determine not only the optimal system configuration but also the appropriate steam main conditions to exploit the trade-off between site-wide energy integration and power generation potential. The mathematical model is based on the extended version of BEELINE model presented in Contribution 3. The optimization framework is adapted by integrating a ϵ -constraint approach to consider both economic and environmental objectives. For the environmental performance, a life cycle assessment of the technologies and resources is conducted. The study aims at answering the following questions:

- What is the environmental impact of a process utility system from entire life-cycle perspective?
- Is carbon neutrality a feasible and cost-effective target for process utility systems?

3. Problem statement

The problem addressed in this work is as follows. Several independent plants located in the same industrial cluster are linked to an on-site utility system to meet their corresponding heat and power requirements. To improve site energy efficiency, the utility system can also function as heat recovery system, with excess heat from one plant can be used to generate steam and then be used in another. Since heat can be recovered/used at a wide temperature range, the most appropriate operating conditions (in terms of temperature and pressure) for steam distribution system must be selected, considering the trade-off between fuel consumption and power generation.

Different conversion technologies (renewable or non-renewable) can be selected to satisfy the energy demands. The framework also includes utility features such as deaerator, let-down stations and flash steam recovery (FSR). Additionally, supplementary utilities such as hot oil and cooling water can be used to meet thermal requirements that cannot be met by steam. Finally, electrical and thermal energy

storage units are being considered as alternatives for balancing the energy supply and demand. The different options considered in this framework are depicted in Figure 4-1.

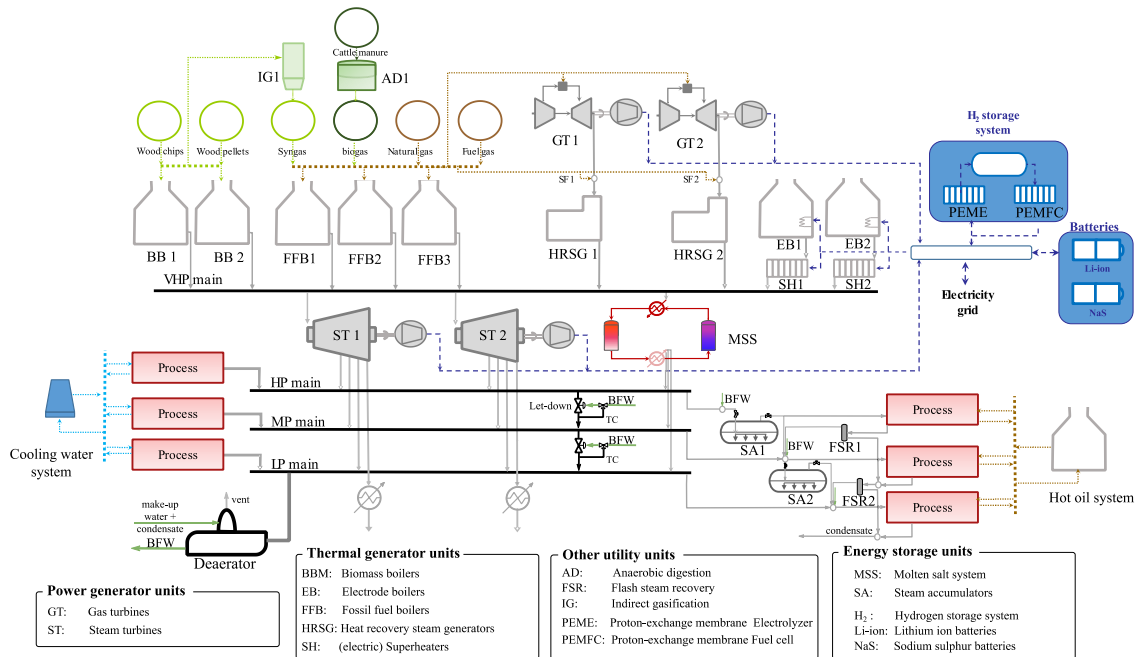


Figure 4-1 Schematic representation of the proposed process utility system superstructure

The selection of the most appropriate system configuration (in terms of size and load operation) is based on two criteria: total annualized costs and global warming potential (CO₂ equivalent emissions) (Vaskan et al., 2014) considering the following information:

- Power and thermal demand profiles of each plant for the considered time horizon. Thermal requirement is defined based on hot and cold process streams of each plant, with their corresponding supply and target temperatures, heat capacity flow rates, and specific minimum temperature approach.
- Catalogue of potentially available conversion and storage units.
- Degree of superheating for steam generation and steam use.
- Market data, list of fuels (e.g. natural gas, fuel gas) available with their corresponding prices, in addition to the hourly price of import and export electricity costs.

Note that the two objectives are conflictive, so a set of optimal solutions based on the features of the aforementioned synthesis task is produced. The set of optimal solutions, known also as Pareto set, is established with the ϵ -constraint strategy, while a case analysis provide some useful insights. Additional assumptions made include the following:

- Thermal demand profiles can be determined based on the nominal input and output temperatures.

- Direct process heat is not allowed. Due to the complexity in data recollection, only streams requiring utilities are considered. Therefore, in this work intra plant heat recovery is assumed fixed -either optimized or not- (Smith, 2016a). Moreover, direct heat integration between independent plants may not only economically viable, since each stream involved requires a separate pipeline, in addition to the operability, controllability, safety issues (Wang and Feng, 2017).
- Heat exchanger network is not considered. At conceptual stage, it is complex to determine the heat transfer coefficients of each stream, since they not only depend on the properties of the fluid, but also heat exchanger type, topology due to its dependence on the type of heat exchanger and fluids involved. Moreover, that the cost of heat exchanger network in comparison with the utility systems is much lower, becoming the driver of the capital cost (Elsido et al., 2021a).
- The cost of steam transportation is deemed negligible in comparison to the other costs.
- Pseudo steady state is assumed. The time required for ramp-up or ramp-down load is assumed negligible in comparison time interval considered in this work (hours).
- Although several environmental impact indicators of the utility system are determined. To avoid additional complexity to the problem, the optimal design is based on two criteria: total annualized costs and global warming potential (CO₂ equivalent emissions). This assumption is supported by the current need of system decarbonization and based on (Vaskan et al., 2014)findings.

The rest of paper is structured as follows. Section 3 describes the features of the investigated process utility system. Section 4 presents the results. Finally, in Section 5 conclusions are drawn.

4. Methodology

The aim of this work is to provide a decision support system for the design and operation of process utility systems that incorporates economic and environmental aspects. Key system aspects, such as environmental assessment, model formulation and optimization approach, are covered in the following subsections.

4.1. Environmental assessment

The life cycle assessment (LCA) has been used to determine the environmental impact of the different utility system configurations. The LCA has been conducted following the guidelines in ISO 14040 (Principles and Framework) (ISO, 2006b) and ISO 14044 (Requirements and Guidelines)(ISO, 2006a), and carried out by means of the commercial software GaBi v7.3(Thinkstep, 2019). Within this software, the impact assessment method chosen was Recipe 2016 V1.1 method.

The goal and scope of the study, as well as the data and assumptions, are all defined in the following sections.

4.1.1. Goal and scope

The goal of this study is to quantify the environmental impacts and economic costs of energy supply by process utility systems. The scope of the study is from ‘cradle to grave’, The system boundaries are illustrated in Figure 4-2. The life cycle stages considered include the production, assembly, transport, operation and disposal of resources and components of the system. The analysis is based on the functional unit defined as ‘generation of site energy (electricity and heat) over a year’. The study is based on European conditions (excluding Switzerland).

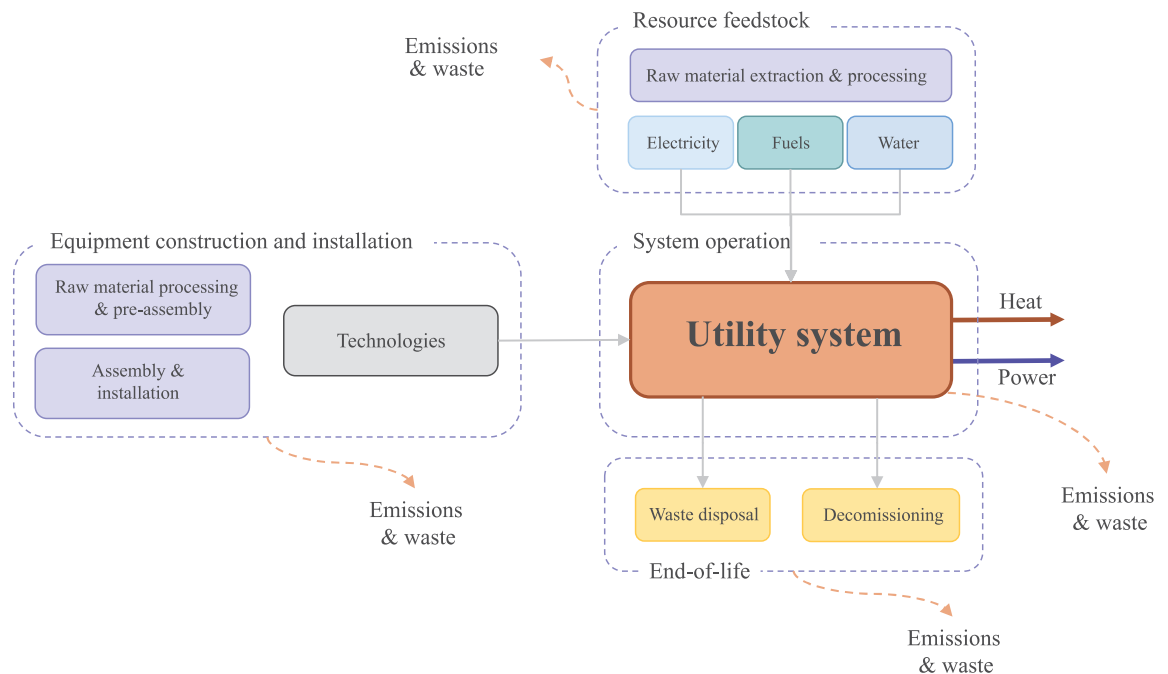


Figure 4-2 Scheme of the considerations for the industrial utility systems assessment

4.1.2. Life cycle inventory data and assumptions

Along with the lifecycle inventory of the fuel combustion, the environmental impact of the conversion technologies is taken into consideration. The inventory is based on the utility components assessed in the techno-economic model, such as steam turbines, gas turbines, HRSGs, boilers, gasifiers, anaerobic digesters, fuel cells, electrolyzers, as well as electric and thermal energy storage and flash tanks. To ensure consistency, auxiliary equipment, as well as heat exchangers and pipes are not included in the lifecycle assessment, since they are not involved directly in the optimization of the process.

i. *Utility equipment*

A scheme of the boundaries for the analysis of equipment in the utility system is shown in Figure 4-3. The raw materials processing, assembly, and installation data for the energy conversion technologies, have been sourced from the Ecoinvent 3.5 database (Wernet et al., 2016) and manufacturing data from literature. Data sources and main assumptions considered are listed in Table 4-1. Additional information can be found in Supplementary Information P4.A.

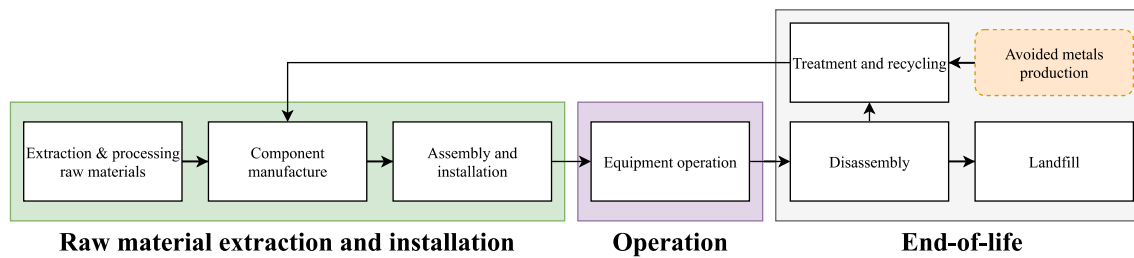


Figure 4-3 Boundaries for the equipment of the utility systems

Table 4-1 Inventory of the main components of the utility system

Component	Reference	Lifetime [y]	Reference size [unit]	Scaling factor [-]
Steam turbines	Kelly et al. (2014)	20	60 MW	1 ^a
Gas turbines	Wernet et al. (2016)	20	10 MW	0.77 ^b
Anaerobic digester	Wernet et al. (2016)	20	500 t ^{**}	1 ^c
Pressure swing adsorption (PSA)	Jungbluth et al. (2007), yield Martín- Hernández et al. (2018) and Bauer et al. (2013)	20	1 t h ^{-1**}	1 ^d
Gasifier	Adams (2011)	20	0.2 t h ⁻¹⁺	0.92 ^c
HRSB	Kelly et al. (2014)	20		1.163 ^e
Gas boiler	Wernet et al. (2016)	20	1 MW	0.96 ^f
Wood chip boiler	Wernet et al. (2016)	20	5 MW	1 ^g
Wood pellet boiler	Wernet et al. (2016)	20	1 MW	1 ^g
Electrode boiler	Adapted from Abbas (2015), using dimensions of Parat Halvorsen AS (2021)	20	60 MW	0.70 ^h
PEM Electrolyzer	BareiB et al. (2019)	10	1 MW	1 ⁱ
PEM Fuel cell	Stropanik et al. (2019)	10	0.01MW	1 ⁱ
Hydrogen tank	Agostini et al. (2018) & Hua et al. (2010)	20	0.01 MWh	1 ⁱ
NaS battery	Peters et al. (2016)	15	1 kg	1 ^j
Li-ion battery	Majeau-Bettez et al. (2011)	10	1 kg	1 ⁱ
Steam accumulator	Wernet et al. (2016)	20	-	0.82 ^f
Flash tanks	Wernet et al. (2016)	20	-	1 ^f

Component	Reference	Lifetime [y]	Reference size [unit]	Scaling factor [-]
Deaerator	Wernet et al. (2016)	20	-	-
Molten salt system	(Kelly et al., 2010)	20	1 MWh	1 ^k

* Construction and installation components are assumed to be supplied locally for conversion technologies.

** Converted with assuming a manure density of 1.041 t/m³(Martín-Hernández et al., 2018)

+ per tonne of dry biomass

^a Fleiter et al. (2016), ^b Pauschert (2009), ^c Martín and Grossmann (2022), ^d Andiappan (2016), ^e Corporation (2000), ^f Smith (2016a), ^g EPA (2015), ^h Assumed, ⁱ Gabrielli et al. (2018b), ^j Breeze (2019), ^k Glatzmaier (2011)

ii. Resources

Utility system uses three main resources: fuel, electricity and water. In the following sections the inventory and main assumptions for each resource has being detailed.

- Feedstock/fuel supply

Fuel gas, natural gas, waste woodchips, wood pellets and and livestock manure has been considered as fuels. While electricity can be imported from the grid or generated on-site. Figure 4-4 presents a representation of the stages considered for the feedstock/fuel supply.

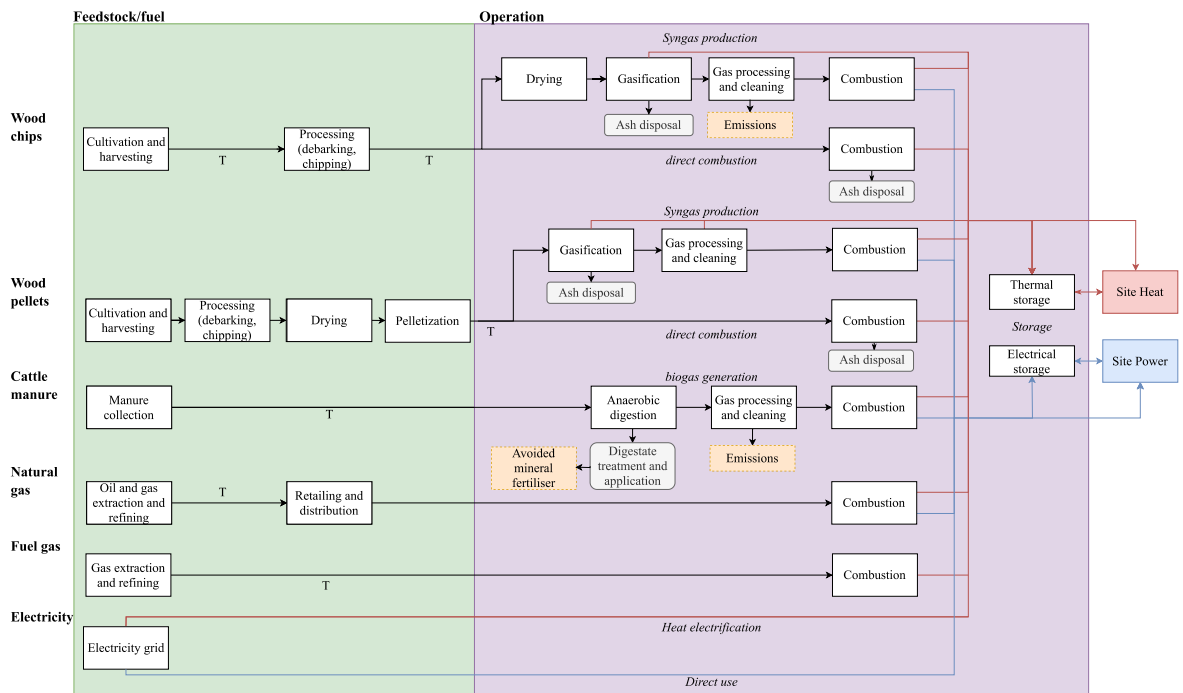


Figure 4-4 System boundaries for the feedstock of the utility system

By 2019, European natural gas is provided by Russia (41.1%), Norway (16.2 %), Algeria (7.6 %), Qatar (5.2 %) and others (29.9 %) (Eurostat, 2020a). Note that these ranges could vary significantly depending on the country. For instance, Qatar shippes liquefied natural gas to Belgium, France, Netherlands, while Algeria provides natural gas to Spain and Poturgal through pipelines. For general

purpose of the methodology the natural gas mix of Germany has been considered as the average for European natural gas, which is transported via pipelines. The mix supply is: 40 % Russia, 21 % Norway, 29 % Netherlands and 10 % domestic production. Inventory data is taken from Ecoinvent 3.5 (Ecoinvent Association, 2018).

Waste wood chips are assumed to be provided locally, with a moisture content of 30 %. Regarding wood pellets, the shares of locally produced and imported feedstocks are heterogenic across Europe (Calderón et al., 2019). Nevertheless, Europe, as whole, is net importer of wood pellets (Zwolinski, 2015). This agrees with the data reported by (Calderón et al., 2019), where United Kingdom (43 %), Denmark (21%) and Belgium (6%) heavily rely on the import of biomass to meet their industrial renewable requirements. For the same countries, the main wood pellets trader is United States (60 %), Canada and Russia. Therefore, a conservative assumption of 30% of locally sourced feedstock and 70 % wood pellet import.

- Water

Raw water is fed to the system, to raise steam and/or cool streams. Although water is usually recirculated within the system, due to contamination or losses across the processes the system require constant freshwater makeup. Depending on the quality of the water and the use within the system, water need to be pre-treated prior its use.

Cooling water is used to cool and/or condensate streams. Cooling water is usually returned to its source without any contamination. However, around 1 % water is lost due to evaporation in cooling towers (Vengateson, 2017). As a result, a makeup of 1% of the circulating rate is considered. This water is usually pretreated to remove any suspended solids and avoid any fouling, but no further treatment is required. Therefore, softened water has been assumed to be employed for cooling processes. Data has been sourced from Ecoinvent 3.5

In contrast to cooling water, for most site boilers operating at high pressures removing hardness is not enough, but also require that other dissolved solids, in particular inorganic salts are removed (Smith, 2016b). Therefore, deionised water for boiler feedwater has been assumed. Moreover, the steam condensate return rate can be as high as 90 %. Higher levels of condensate return might not be economically feasible owing to pipe costs. Additionally, potential contamination and/or direct injection of steam during the heating process can also restrict the condensate return (Smith, 2016b). Therefore, a return rate of 90% is anticipated in this study.

- Grid electricity

The environmental impacts of European electricity grid have been estimated using the generation mix reported in (IEA, 2020) for 2019. Data for the individual electricity technologies present in the mix have been sourced from Ecoinvent 3.5 (Ecoinvent Association, 2018).

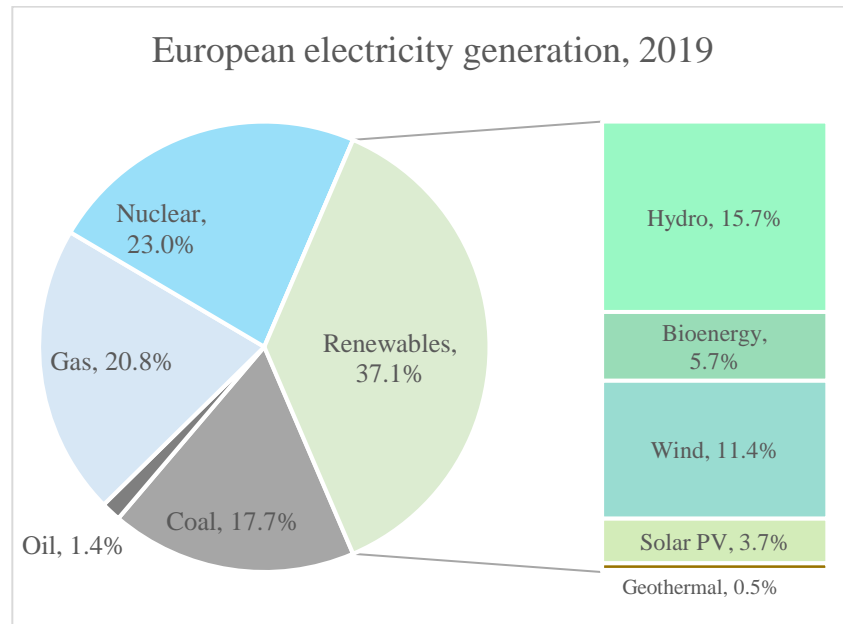


Figure 4-5 European electricity mix IEA (IEA, 2020)

iii. System Operation

Emissions from the combustion of fuels have been sourced from Ecoinvent 3.5 (Ecoinvent Association, 2018) and literature. Additional operational requirement of each equipment are detailed in Supplementary Information P4.A. Table 4-2 summarises the emissions in kilograms per MWh of fuel input.

Table 4-2 Emissions from fuel combustion

Components [kg·MWh ⁻¹]	Fuel gas	Natural gas ^c	Wood chips ^d	Wood pellets ^d	Syngas ^d	Biogas ^{e, c}
CO ₂	226.3 ^a	214.1	N/A	N/A	N/A	214.1
CO	0.054 ^b	-	0.93	0.93	0.1	-
NO _x	0.90 ^{**}	0.36	0.34	0.76	0.12	0.18 ⁺
N ₂ O	-	-	0.02	0.02	-	-
SO ₂	0.10 ^b	-	0.04	0.04	-	-
CH ₄	0.02 ^b	-	0.04	0.04	0.02	-
PM ₁₀	-	-	0.31	0.42	-	-
PM _{2.5}	0.02 ^b	-	0.19	0.25	-	-
VOCs [*]	17.89 ^b	-	26.37	26.37	-	-
Zn [*]	-	-	0.65	0.65	-	-

Components [kg·MWh ⁻¹]	Fuel gas	Natural gas ^c	Wood chips ^d	Wood pellets ^d	Syngas ^d	Biogas ^{e, c}
Cu [*]	-	-	0.08	0.08	-	-
Other metals [*]	0.005 ^b	-	1.08	1.08	-	-

N/A: Not applicable, since the CO₂ emitted from combustion is balanced by the uptake of CO₂ during the biomass growth. Thus, considered carbon neutral

^{*} g MWh⁻¹

^{**} Depend on the content of hydrogen and can be up to 2.5 times the NO_x of natural gas (Department for Business, 2021).

Due to the lack of information a conservative assumption of the maximum of NO_x emissions is considered

[†] Methane based fuels can produce 50 % less NO_x emissions due to lower temperatures of combustion (Department for Business, 2021)

^a Author's calculation based on Herold (2003)'s emissions factor

^b Ecoinvent Association (2018)

^c Department for Business (2021)

^d Group (2001)

^e Assumed similar to natural gas due to its similar heat capacity

Note that fuel gas composition and its corresponding combustion emissions will vary depending on the refinery/process but usually comprises a mixture of non-condensable gases (hydrogen, methane, ethane, and olefins). Due to the lack of information about fuel gas composition, a correlation between the emission factor of natural gas and fuel gas is used to define the emissions of combustion from Herold (2003) and Department for Business (2021).

- Ash and digestate management

Although cattle manure is considered waste, it has been allocated environmental burden or credit based on their current disposal practices. Cattle manure is either used as fertilizer or left on the ground. According to Bacenetti et al. (2016), approximately 58 % of cattle manure is believed to be utilised as fertiliser, with the remainder being left on the ground. Therefore, the effect of fertiliser is included in the analysis, and the system is credited for the avoided use of chemical fertilisers. Data for the production of fertiliser are taken from Ecoinvent, while emissions from their management have been considered following the IPCC guidelines (Hongmin et al., 2006). The by-products of biomass are listed in Table 4-3.

Table 4-3 By-products from waste biomass

	Wood pellet ash	Wood chip ash	Cattle digestate
By-product, [t·MWh ⁻¹]	0.6 ^a	3.2 ^b	0.08 ^{*c}
Composition [t per t of by-product]			
Nitrogen	0.15	0.15	0.065 ^c
Phosphorus	0.53	0.53	0.010 ^c
Potassium	2.6	2.6	0.068 ^c

^a Bandara et al. (2021), ^b Pedišius et al. (2021), ^c Martín-Hernández et al. (2018)

^{*} t per t⁻¹ manure

iv. Transport

As the study considers a generic system in Europe, transport distances have been generic. Raw materials have been assumed to be transported to the factory in a 16–32 t Euro 3 truck over a distance of 150 km.

Natural gas is assumed to be processed and refined in the place and then transported. Most natural gas is transported by pipelines, considering average distances to from the plant of 1,222 km (Russia – Nord stream), 440 km (Norway - Norpipe) and 372 km (Netherlands - METG).

On the other hand, the imported wood pellet is shipped to Europe by transoceanic freight ships, considering a distance of 7728.0 km. Based on the assumption of US as the main supplier and port Allen and Rotterdam as the main wood pellet bulk terminals in US and Europe, respectively. Then, wood pellet is delivered by 16–32 t Euro 5 trucks to a storage facility in Munich (830 km), chosen as European geographical centre.

For end-of-life, waste is transported by 16–32 t Euro 5 truck, assuming 100 km distance to the waste treatment facility.

v. End-of-life waste management

The end-of-life phase comprises the direct recycling and disposal of the utility components. The direct recycling comprises efforts to disassembling and use of recyclable materials in other process stages. Metal waste (i.e. steel, steel alloys, copper and aluminum) is assumed to be recyclable at 90 % rate, according to available dataset (EuRIC, 2020). The recycling process is modelled in GaBi, based on the ‘net scrap’ approach (PE international, 2014) to credit the system. This method takes into account the environmental effects of recycling and attribute any credits only for the additional quantity of virgin material replaced. For instance, European steel is fabricated by 44% crude steel and 56 % steel scrap, therefore the system is credited for recycling 34 % of steel (90 % - 56 %). The rest of materials (e.g. concrete, waste oil, ashes) are assumed to be landfilled or incinerated (e.g. waste oil).

Regarding batteries, there is limited real-world experience associated with cost-effective recycling pathways. This is because the technology is still in early stages of application, with the majority of utility-scale batteries deployed within the last 5 years (still within their expected lifetime -10 years-). Due to the lack of available uniform information (in terms of distances and energy requirement during the recycling), this study assumes only recycling of waste metals from the casing. Despite the rough assumption, prior researches (Pellow et al., 2020; da Silva Lima et al., 2021) have reveal that potential recover of cobalt and lithium carbonate through pyro- and/or hydrometallurgical processes has little effect on the overall climate change impact (although it can reduce the effect of other environmental factors). Moreover, while it is technically feasible to recover phosphate or titanium,

existing industrial recycling methods do not prioritize the recovery of these metals, which is why it is not pursued further (Weber et al., 2018).

4.1.3. Quantification

Economic performance of the utility design is assessed in terms of total annualized costs metrics. For this, both annualized capital and operating expenses are considered. On the other hand, environmental impact is quantified through equivalent CO₂ emissions using the Global Warming Potential impact category (GWP_{100a}).

The emissions and impacts of the equipment depend on the equipment size. Emissions are likely to be proportional to employed in the process equipment's manufacture, as shown in Gerber et al. (2011). Therefore, to minimize the inaccuracies when scaling emissions, the non-linear approach used for scaling the capital costs at different sizes ('economies of scale' method) is adapted to the emissions (Greening and Azapagic, 2013), as shown in Eq. (4.1).

$$E_2 = E^{\text{ref}} \left(\frac{Z_2}{Z_{\text{eq}}^{\text{ref}}} \right)^{\beta} \quad (4.1)$$

E_2 denotes the environmental impacts of , E^{ref} represents the environmental impacts of the reference size of the same equipment ($Z_{\text{eq}}^{\text{ref}}$) and β is the scaling factor. To determine the scaling factor, Gerber et al. (2011)'s approach is adopted in this work. In case that datasets for (at least) two different scales are accessible, the scaling exponent is calculated directly, if not the same exponents used for the cost estimation are employed.

4.1.4. Assessment

A multi-objective optimization framework is used to examine the environmental impact and find the most cost-effective options that could enhance environmental performance (e.g. reduction of CO₂-eq emissions).

It is important to note that although only reduction of GHGs emissions are used as indicator for the environmental impact in the optimization, the other midpoint indicators in the ReCiPE method are also measured. Therefore, for the evaluation the indicators have been grouped in the following environmental issues:

- climate change: global warming potential (GWP);
- air pollution: ozone depletion (ODP) and particulate matter formation potentials (PMFP);

- water and soil pollution: freshwater and marine eutrophication potentials (FEP and MEP, respectively) and terrestrial acidification potential (TAP);
- ecotoxicity: freshwater, marine and terrestrial ecotoxicity potentials (FETP, METP and TETP, respectively);
- resource depletion: fossil, mineral and water depletion potentials (FDP, MDP and WDP, respectively); and
- human health: human toxicity (HTP)

4.2. Model Formulation

A multi-objective, multiperiod MINLP model is proposed to address the problem in this work. The MINLP formulation and its solution strategy are based on the BEELINE2 model proposed in Contribution 3. An example of a utility system superstructure is shown in Figure 4-1. All possible combinations are allowed, start-up and part-load efficiency effect are taken into account and potential heat integration from process heat sources a. Further details of this model can be found in Contribution 3.

For brevity, the complete mathematical formulation of the model is given in Supplementary information P4.B. In the next section the equations used for determining the economic and environmental performance of the utility system are described.

4.2.1. Economic objective—minimizing annualized total cost

The economic objective is to minimize the total annual costs (TAC), including the total annualized investment cost (C^{inv}), maintenance cost (C^{main}), operating cost (C^{op}) and start-up cost (C^{start}).

$$\min TAC = C^{inv} + C^{main} + C^{op} + C^{start} \quad (4.2)$$

The investment cost equals the total installation costs for utility components (i.e. energy conversion technologies and storage units). The investment costs of unit uc , with size Z_{uc}^{max} is determined by employing economic scale law, considering a reference size unit and its corresponding cost. Moreover the installation costs are included by the parameter F_{uc}^{inst} . Investment costs are annualized through the annualization factor F_{uc}^{ann} .

The investment cost includes the purchase cost (C_{uc}^{inv}) of the different utility components (i.e. energy conversion technologies and storage units) and the installation expenses associated with their deployment. Installation costs are considered in the term F_{uc}^{inst} . The costs of purchasing unit uc of size

Z_{uc}^{max} are determined by using economic scaling law, taking into account a reference size unit (Z_{uc}^{ref}), its associated cost (C_{uc}^{ref}) and the scale law exponent (ψ_{uc}). The investment costs are expressed on a yearly basis by employing annualization factor F_{uc}^{ann} .

$$C_{uc}^{inv} = \sum_{uc \in UC} F_{uc}^{ann} \cdot C_{uc}^{inv} = \sum_{uc \in UC} F_{uc}^{ann} \cdot F_{uc}^{inst} \cdot C_{uc}^{ref} \left(\frac{Z_{uc}^{max}}{Z_{uc}^{ref}} \right)^{\psi_{uc}} \quad (4.2a)$$

The maintenance cost (C_{uc}^{main}) is calculated as a proportion of the investment cost, as given by Eq. (4.2b)

$$C_{uc}^{main} = F_{uc}^{main} \cdot C_{uc}^{inv} \quad \forall uc \in UC \quad (4.2b)$$

The operating costs are calculated by multiplying the commodity consumption (U_{comdty}) by its specific cost (P_{comdty}) for each period (t) of the design day (k), weighted by the length of the period t_{op} . Operating expenses include potential revenues from exporting power, where the selling price is assumed to be negative.

$$C^{op} = \sum_{comdty} \sum_{k \in K} \sum_{t \in T} U_{comdty_{k,t}} \cdot P_{comdty_{k,t}} \cdot t_{op_{k,t}} \quad (4.2c)$$

Finally, additional costs regarding equipment start-ups are included to minimize additional fuel consumption and reduced equipment life. Equipment start-up costs are given by Eq. The term F_{eq}^{start} is a parameter that represents the cost per start-up of unit eq , and $\delta_{eq,\theta,k,t}^{start}$ is a continuous variable with values between 0 and 1 ($\delta_{eq,\theta,k,t}^{start} \in [0,1]$), that indicates whether a equipment eq operating at θ conditions is started-up at period t .

$$C^{start} = \sum_{eq \in \{boi,gt,st\}} F_{eq}^{start} \sum_{\theta} \sum_{k \in K} \sum_{t \in T} \delta_{eq,\theta,k,t}^{start} \quad (4.2d)$$

Tables Table 4-4 - Table 4-6 summarize the main cost coefficients of equipment, energy storage and resources.

Table 4-4 Model coefficients of equipment costs

Resource	Z_{eq}^{ref}	C_{eq}^{ref} [€]	ψ_{eq}	Range	F_{eq}^{ins} [%]	F_{eq}^{main} [%]	Reference
Boiler							
Packaged*, [t/h]	50	2,548,770.98	0.960	50 - 350	4	5	Smith (2016a)
Field-erected*, [t/h]	20	1,801,717.41	0.810	20 - 800	4	5	Smith (2016a)
Biomass stoker ^f , [t/h]	1	1,177,937.852	0.751	4 - 300	1	3	EPA (2015)

Resource	Z_{eq}^{ref}	C_{eq}^{ref} [€]	Ψ_{eq}	Range	F_{eq}^{ins} [%]	F_{eq}^{main} [%]	Reference
Biomass fluidized bed ^f , [t/h]	1	(variable) 369,759.0 (fixed) 9,966,103.0	1.000	0 - 300	1	3	EPA (2015)
Electrode, [MW]	70	62,350.33	0.700 ⁺	3 - 70	2.5	1	Marsidi (2018) Jaspers and Afman (2017)
Electric superheater, [MW]	70	135,092.37	0.700 ⁺	3 - 70	1	1	Jaspers and Afman (2017)
Steam turbine, [MW]	-	(variable) 345,101.63 (fixed) 44,057.43	1.000	1 - 200	4	3	Fleiter et al. (2016)
Gas turbine							
Aeroderivative, [MW]	1	827,490.91	0.777	2 - 51	4	3	Pauschert (2009)
Industrial, [MW]	1	720,016.47	0.770	6 -125	4		Pauschert (2009)
HRSG**, [t/h] ^x	120	481,845.69	1.163	33.5 - 800	4	5	Corporation (2000)
PEM Fuel cell	-	(variable) {2,160,000; 1,680,000; 1,320,000} (fixed) {0; 320,000; 800,000}	1	0-10 {0 - 0.2; 0.2-0.8; 0.8-10}	1.5	8	Gabrielli et al. (2018b)
PEM Electrolyzer	1	(variable) {2,693,000; 1,727,000; 1,354,000 } (fixed) {0; 96,700; 24,600 }	1	0-10 {0 - 0.2; 0.2-0.8; 0.8-10}	1.5	8	Gabrielli et al. (2018b)
Gasifier, [t/h]	5	1,600,000	0.917	5-500	4	3	Martín and Grossmann (2022)
Anaerobic digester, [t/h]	-	345.75	1	1041.2 - 6247.20	4	3	Martín and Grossmann (2022)
PSA,[t/h]	-	3093.2	1	1 - 500	2	1	Andiappan (2016)
HO Furnace, [MW]	5	465,365.00	0.748	5 - 60	4	5	Towler and Sinnott (2013)
Condenser, [MW]	-	-	-	1 - 2000	4	1	Varbanov (2004)
Deaerator, [t/h]	-	-	-	10 - 300 300 - 600	4 ⁺ 4 ⁺	1	Varbanov (2004)

Resource	Z_{eq}^{ref}	C_{eq}^{ref} [€]	Ψ_{eq}	Range	F_{eq}^{ins} [%]	F_{eq}^{main} [%]	Reference
Flash tank ^{***} , [t/h]	1	4,205.99	0.506	20 - 100 100 - 400	4 ⁺	1	Loh et al. (2002)

Note: costs adjusted to 2019

* Pressure reference 100 bar, $f_{p_{ref}} = 1.9$, ** Pressure reference 11.34 bar, $f_{p_{ref}} = 1.1$, *** Horizontal vessel, residence time = 5 min, density = $0.9 \text{ t} \cdot \text{m}^{-3}$, Pressure = 10 bar, $f_{p_{ref}} = 1.1$

^x based on exhaust gases, ^f Installed cost, including biomass storage

⁺ Assumed

Table 4-5 Model coefficients of energy storage costs

Resource	Z_{eq}^{ref}	C_{eq}^{ref} [€ unit ⁻¹]	Ψ_{eq}	Range	F_{eq}^{ins} [-]	F_{eq}^{main} [%]	Reference
Steam accumulator, [t/h] ^a	6	98,400.00	0.82	6 - 100	2.5	2	Smith (2016a)
Molten salt systems ^b , [kWh]	1	19.22	1	0 - 10000	1	2	Glatzmaier (2011) Caraballo et al. (2021)
Li-ion Battery, [kWh]	1	(400-1100) 750	1	1-100000	1.5	2	Gabrielli et al. (2018a)
NaS Battery, [kWh]	1	(250-900) 575	1	50 - 8000	1.5	2	Breeze (2019)
	-	(variable) 13.6 (fixed)	1	500 - 5500	1.5	3	Gabrielli et al. (2018a)
Hydrogen tank, [kWh]	-	2,350 (variable) 10.9 (fixed)	1	5500-15000	1.5	3	Gabrielli et al. (2018a)
	-	94,500					

Table 4-6 Fuels and resources prices

Resource	LHV	Cost	Reference
	[MWh·t ⁻¹]	[€·MWh ⁻¹]	
Natural gas	13.08 ^a	24.30 ^c	Eurostat (2020b)
Fuel gas	13.03 ^a	23.87	Author's estimation ^e
Woodchip	3.5 ^b	29.3	Duić et al. (2017) ^e
Wood pellets	4.8 ^b	39.7	Duić et al. (2017) ^e
Cattle manure	*	6.05 ^d	Author's estimation ^f
Digestate	-	P/ K / N/ ^d 1408/1056/682/	Nussbaum (2021)
Syngas	1.94 ^{**}	-	Author's estimation
Biogas	13.1	-	Martín-Hernández et al. (2018)
Electricity import	-	88.65 ^c	Eurostat (2020a)
Electricity export	-	70.92	Author's estimation ^g
Cooling water		1.230	Turton et al. (2018)
Treated water		0.301 ^d	Turton et al. (2018)

* $C_p = 4.19 - 0.0275(\text{DM})$ [J kg·K⁻¹] (Chen, 1983), ** 7 MJ/Nm³

^a Source : Engineering ToolBox (2008)

^b Source: Research (2020) Wood chips (30% moisture content), wood pellets (10% moisture content)

^c Prices for XL scale industries: Band I6 for natural gas (>4 000 000 MWh y⁻¹)

Band IG for electricity (>150 000 MWh y⁻¹)

^d Cost per ton [€·t⁻¹]

^e Based on energy inflation (CPI) (OECD, 2021)

^f Assuming Andersen (2016)'s correlation and 10 mile (16 km) distance

^g Assuming 20 % of distribution losses

The remaining utility system equations of the model are provided in Supplementary Information P3.B. These include mass, energy and electricity balances, heat integration cascades, equipment selection, sizing and performance, fuel selection and logic constraints.

4.2.2. Environmental objective—minimizing GWP (CO₂-eq·y⁻¹)

As discussed previously, the environmental objective is to minimize the total annual global warming potential (TAGWP). The TAGWP is defined as the sum of the emissions at the following stages: (i) extraction, processing and transportation of resources, (ii) installation and decommissioning of equipment, and (iii) operation (and waste disposal) of the utility system, as expressed by Eq (4.3).

$$\min \text{TAGWP} = E^{\text{re}} + E^{\text{eq}} + E^{\text{op}} \quad (4.3)$$

E^{re} represents the emissions generated by the resources (e.g. water, fuels and electricity) considering the emissions related to the extraction, processing, transportation. E^{re} involves the fuel ($Q_{\text{eq},f_eqk,t}^{\text{F}}$) and (imported) electricity consumed ($W_{k,t}^{\text{imp}}$) at time step t of design day k , multiplied by the corresponding emission burden (e) and the duration of the time step t_{op} .

$$E^{\text{re}} = \sum_{k \in K} \sum_{t \in T} \left[e_f^{\text{re}} \cdot Q_{\text{eq},f_eqk,t}^{\text{F}} + e^{\text{re}} \cdot W_{k,t}^{\text{imp}} \right] t_{\text{op},k,t} \quad (4.3a)$$

E^{eq} denotes the emissions related to the installation and decommissioning of equipment – i.e. energy conversion technologies and storage units -.

$$E^{\text{eq}} = \sum_{uc \in UC} \frac{e_{uc}^{\text{eq}} \cdot \tau_{uc}^{\text{max}}}{\text{lifetime} \cdot t_{\text{op}}} \quad UC \in EQ \cup ES \cup TES \cup SA \quad (4.3b)$$

E^{op} represents the emissions generated in the use phase (fuel combustion (e.g. water, fuels and electricity) considering the emissions related to the extraction, processing, transportation. In this work, E^{op} involve direct (scope I) and indirect (scope II) emissions produced at time step t of design day k , multiplied by the corresponding emission burden (e) and the duration of the time step t_{op} . Direct emissions are the ones corresponding to the fuel consumption ($Q_{k,t}^{\text{f}}$), while indirect emissions are the ones related to electric purchased ($W_{k,t}^{\text{imp}}$).

$$E^{\text{op}} = \sum_{k \in K} \sum_{t \in T} \left[e_f^{\text{op}} \cdot Q_{k,t}^{\text{f}} + e^{\text{elec}} \cdot W_{k,t}^{\text{imp}} \right] t_{\text{op},k,t} \quad (4.3c)$$

The values of emission factors can be obtained from ecoinvent, Aspen Plus process models, and relevant literature, after grouping the GHG gases emissions into a single indicator in terms of carbon dioxide equivalent emissions ($\text{CO}_2\text{-eq}\cdot\text{y}^{-1}$).

4.3. The solution approach

The proposed model results in a mixed integer nonlinear problem (MINLP). The MINLP problem incorporates three sources of difficulty in terms of (i) variable type (mixed integer), (ii) constraint type (non-linear), and (iii) objective function (bi-criteria). Thus, the problem could be computationally intensive when applied to practical size problems. Therefore, the following strategies have been implemented in order to sort the problem.

4.3.1. Dealing with non-linearity

The nonlinearity arises from the equipment cost functions, the environmental impact quantification and the selection of steam main operating conditions. While the two first type of non-linearity, can be easily handled by piecewise affine approximations of the functions, the third type is much more difficult to address. This derive from the integration of steam temperature as a design variable, where bilinear terms are introduced in the energy balance and some equipment performance and moreover in the actual calculation of the steam properties (which are highly non linear). In order to solve this, the BEELINE strategy presented in Contribution 2 and extended in Contribution 3 is applied in this work. BEELINE strategy comprises a bilevel decomposition of the problem, where the master problem is a relaxed version of the mixed-integer linear programme (MILP). In the MILP problem the value of the binary variables are defined, to then re-optimize the continues variables considering the non-linearities in a non-convex linear (NLP) program model.

4.3.2. Dealing with the objective function

To determine the Pareto-optimal curve and define the trade-off between economic and environmental performance, the ϵ -constraint approach (Mavrotas, 2009) is employed. The ϵ -constraint approach begins by establishing minimum and maximum values for the objective functions TAC and TAGWP, which are determined using the lexicographic optimization. Minimum value of TAC, denoted as TAC_{\min} , is obtained by solving the proposed model with the objective to minimize TAC only. While the maximum value of TAC (TAC_{\max}), is generated by fixing $\text{TAC}=\text{TAC}_{\min}$ and re-solving the proposed model with the objective to minimize TAGWP. The same process is followed to obtain TAGWP_{\min} and TAGWP_{\max} .

Once defined the upper and lower bounds of the objective functions, the rest of Pareto-optimal points are obtained by solving the proposed model with the objective of minimizing Eq.(4.4)

$$\min: \text{TAC} + \delta \cdot \left(\frac{s_2}{r_2} \right) \quad (4.4)$$

δ is a small number (on the order of $[10^{-6}, 10^{-3}]$), s_2 is a nonnegative slack variable for the objective function TAGWP, defined by Eq.(4.5). r_2 is a parameter, which is equal to the difference between the upper and lower bound of TAGWP (Eq (4.6))

$$\text{TAGWP} + s_2 = \varepsilon_2 \quad (4.5)$$

$$r_2 = \text{TAGWP}_{\max} - \text{TAGWP}_{\min} \quad (4.6)$$

Note that the set of pareto solutions are obtained by solving the proposed model for different ε_2 . ε_2 is a parameter defined by Eq (4.7), where n comprises the number of interval points to be evaluated $n \in (0, 1, 2, \dots, N)$.

$$\varepsilon_{2n} = \text{TAGWP}_{\min} + \frac{\text{TAGWP}_{\max} - \text{TAGWP}_{\min}}{N} n \quad (4.7)$$

As a result, the Pareto front for the proposed model and optimum solutions for different emission values (TAGWP) can be determined.

The optimization problem is encoded GAMS (Bussieck and Meeraus, 2004). The initialization stage and the master problem are solved with CPLEX 20.1.0.0 (Corporation, 2017), while the NLP subproblem is solved with CONOPT 4 (Drud, 1985). All the calculation are solved employing an Intel(R) Core(TM) i7-8650U @ 2.1 GHz and 16.0 GB of RAM.

5. Case study definition

The proposed methodology is applied to the illustrative case study presented in Contribution 3. The industrial site comprises five industrial plants with an annual heating, cooling and power demands (expressed on a daily basis). Figure 4-6 refers to the mean typical annual site energy demand. Moreover, the electricity price fluctuation is given in an hourly resolution (Pool, 2020) To reduce the size of the problem, the whole year energy demand of the site is represented by 11 typical days and 1 extreme day, based on a k -means algorithm, as detailed in Contribution 3. Furthermore, the electricity tariffs were aggregated in 4 segments.

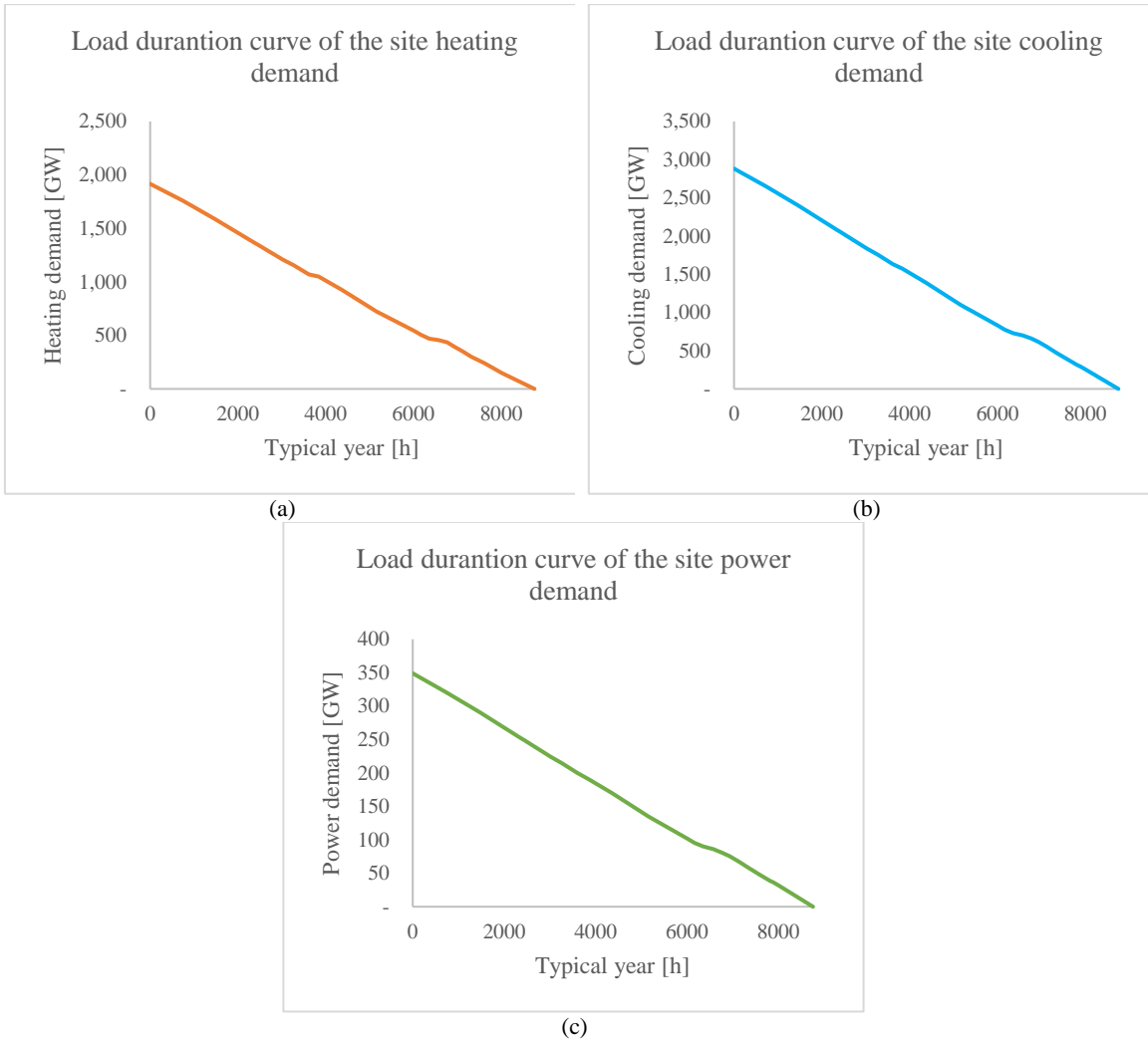


Figure 4-6 Load duration curves of site energy demand for a typical year

To illustrate the applicability of the proposed methodology, the case study is analysed under different scenarios. To illustrate the applicability of the proposed methodology, the case study is analysed under different scenarios. First, the optimal configuration is pursued with different objectives (minimum total annualized cost and minimum global warming potential) under two scenarios. The scenarios are described below:

- *Scenario 1.* Process utility system steam main operating conditions are predefined and are not part of the optimization. The system is allowed to exchange electricity with the grid (buying/selling).
 - Heat recovery from condensates is not considered (w/o FSR)
 - Heat recovery from condensates through flash tanks is considered (w FSR)
- *Scenario 2* Steam main operating conditions are part of the design optimization.
 - Heat recovery from condensates is not considered (w/o FSR)
 - Heat recovery from condensates through flash tanks is considered (w FSR)

6. Results and discussion

6.1. Total annualized costs oriented optimal design

Table 4-7 summarizes the main findings of the case study under scenarios 1 and 2, taking into account steam main operating conditions and the integration of flash steam recovery (FSR). The results show that the selection of operating conditions of steam mains not only allow reducing at least 13.6 % annualized costs, but also the annual CO₂ emissions by 15.2%. Moreover, the integration of FSR for condensate heat recovery enables further emissions abatement, reaching a reduction up to 27.6 %, when compared to the Scenario 1 without FSR (used here as a reference). It is important to note that in this work, heat exchanger network is not considered, so the economic and environmental impact of heat exchangers is not taken into account. Nevertheless, previous research works have shown that the impact of heat exchangers is minimal in comparison with costs of utility equipment (Elsido et al., 2021b) and environmental impact of the primary energy consumption (Liu et al., 2020).

Table 4-7 Optimization results based on minimum total annualized cost (TAC)

	Scenario 1		Scenario 2	
	w/o FSR	w FSR	w/o FSR	w FSR
Steam mains	VHP / HP / MP / LP		VHP / HP / MP / LP	
Temperature [° C]	560 / 270.4 / 232.4 / 171.8		570 / 267.0 / 209.1 / 150.0	
Pressure [bar]	85.0 / 40.0 / 20.0 / 5.0		85.0 / 37.8 / 12.3 / 2.7	
Total annualized cost [m€·y ⁻¹]	79.44	71.51	68.61	60.04
	-	(-10.0 %)	(-13.6 %)	(-24.4 %)
GWP [kt CO ₂ ·y ⁻¹]	665.02	609.24	563.92	481.78
	-	(-8.4 %)	(-15.2 %)	(-27.6 %)

Figure 4-7 (a) presents the contribution of the different site costs (in million euros per year). As can be seen, the operating costs, more specifically fuel costs, are the dominant costs. This emphasizes the key role of heat recovery (either by FSR or process steam generation) in reducing not only the duty of the thermal units and their associated fuel requirement, but also in the utility system costs.

Figure 4-7 (b) depicts the primary energy consumption of the four different optimal designs. It is worth noting that all of the designs share a common configuration: fuel gas boiler, natural gas turbine coupled with HRSG, and steam turbine. The main difference is given by the duty of each unit. Note that although thermal and electrical energy storage are considered in the optimization, storage units are not cost-competitive. As shown in Contribution 3, under current European energy costs, for most countries utility system design benefits from on-site power generation, and can be flexible enough to offset any electricity import requirement. Moreover, storage self-energy losses and current high capital costs can outweigh the potential energy savings obtained at electricity peak times.

When compared to the reference system, the integration of FSR and higher process steam generation can result in a reduction of 47.8 and 19.2 % in fuel gas and natural gas consumption per year, respectively. This can be reflected in the GHGs emissions of the system. Along with CO₂-eq emissions, a range of other direct and indirect emissions occur throughout all processes, from raw material extraction for fuel, infrastructure, and other materials required through waste treatment and disposal. For purpose of brevity and since all the systems present similar configurations, a comparison only between the best design (Scenario 2 with FSR) and the reference are presented in Figure 4-8.

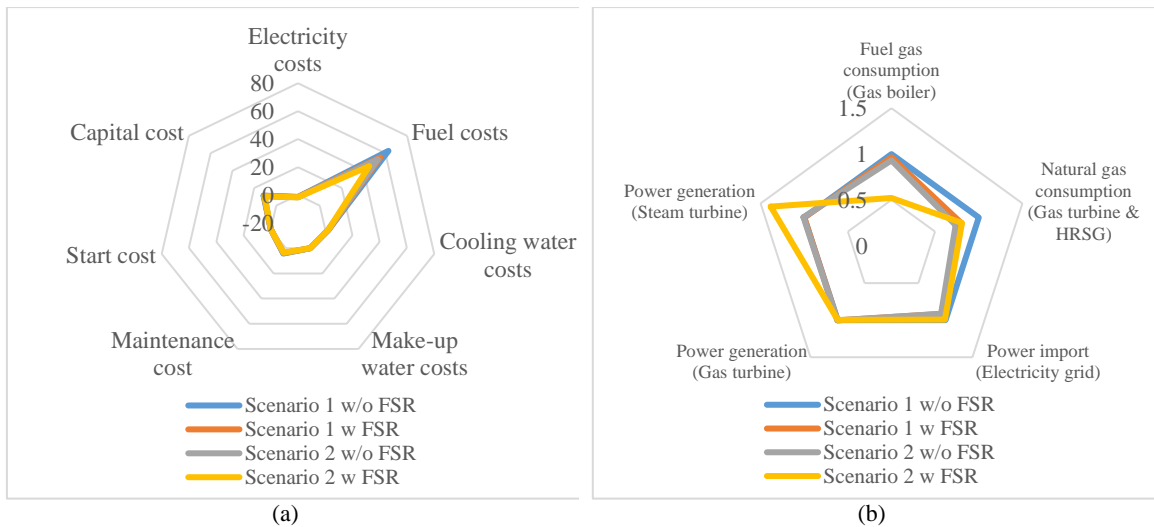


Figure 4-7 TAC oriented optimal design per year of operation: (a) Costs contribution (in m€·y⁻¹) and (b) electricity and fuel consumption, having as reference Scenario 1 w/o FSR design.

[Energy consumption in GWh·y⁻¹. Fuel gas consumption: 1088.30, Natural gas consumption: 1514.30, Power import: 12.18, Power generation - Gas turbine: 355.58, Power generation - Steam turbine: 14.87]

In general, the TAC oriented design of scenario 2 with FSR outperforms in all the environmental impacts to the reference system (Scenario 1 without FSR). The impacts are unevenly distributed over different utility components, but overall the main contribution for lower emissions of the utility site are the lower combustion emissions and the reduced cooling water consumption. As mentioned before, the higher site heat integration reduces the duty from the thermal units, leading to lower fuel consumption which not only reduces the emission of GHG emissions, but also the air pollution related impacts due to lower emission of NO_x during fuel combustion. Moreover, higher site heat integration also allows to reduce the the cooling requirements supplied by cooling water, this is reflected in a lower water depletion. In terms of life cycle environmental impacts, the optimization of the utility system considering heat recovery lead to an improvement of 3 to 67 % on all environmental impacts assessed in this work.

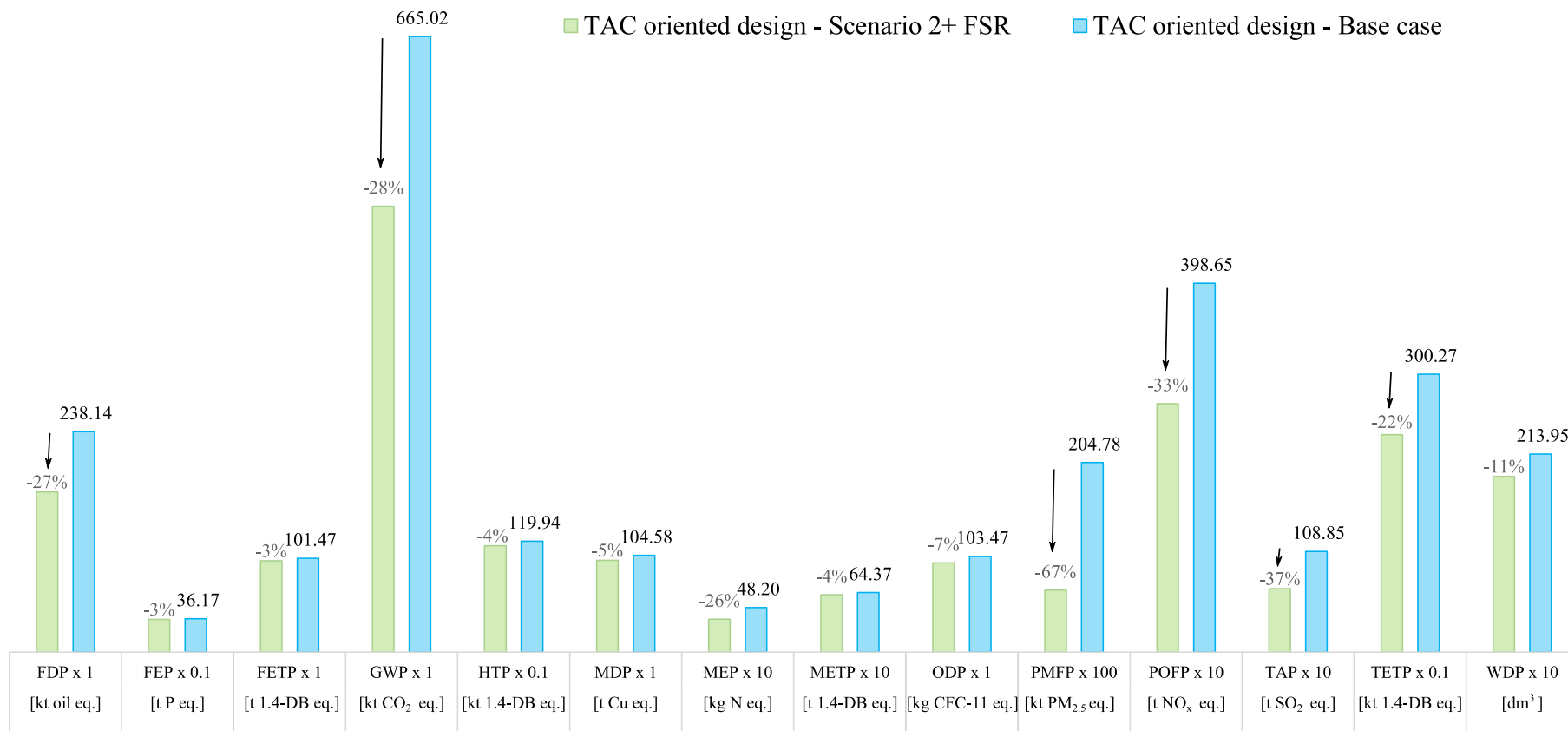
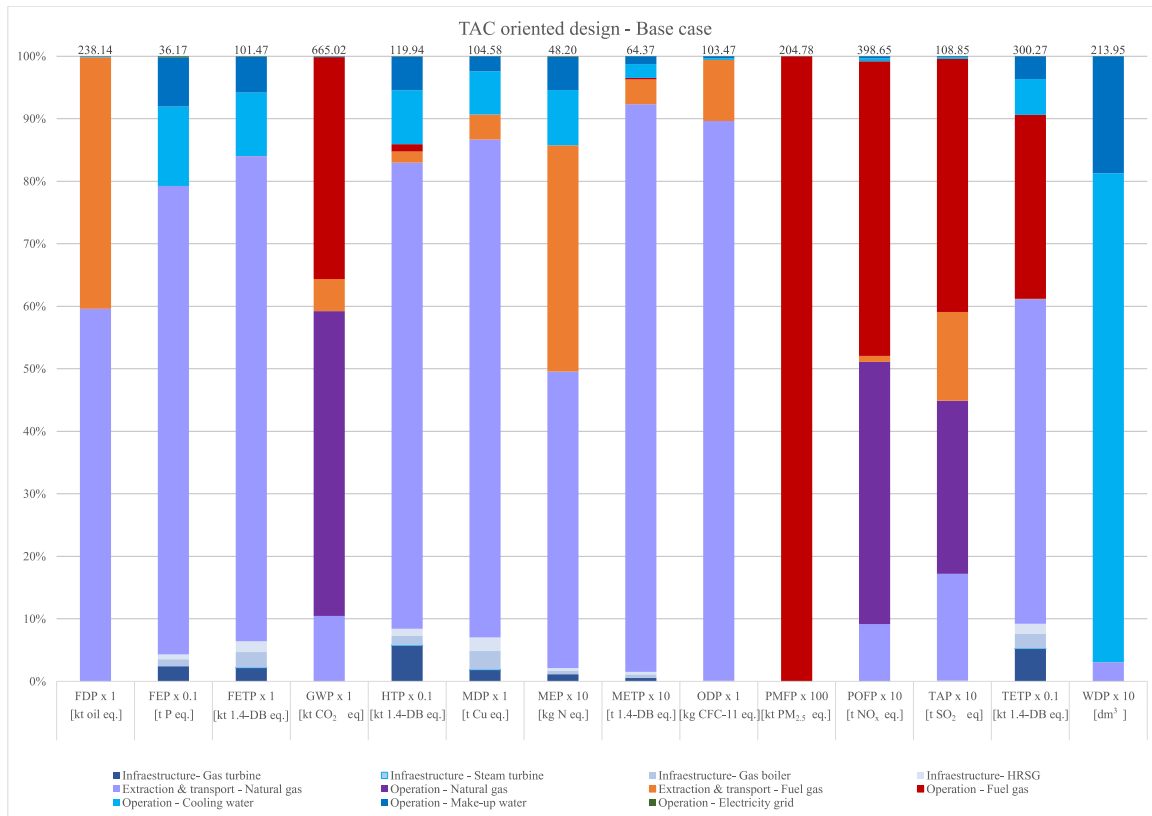
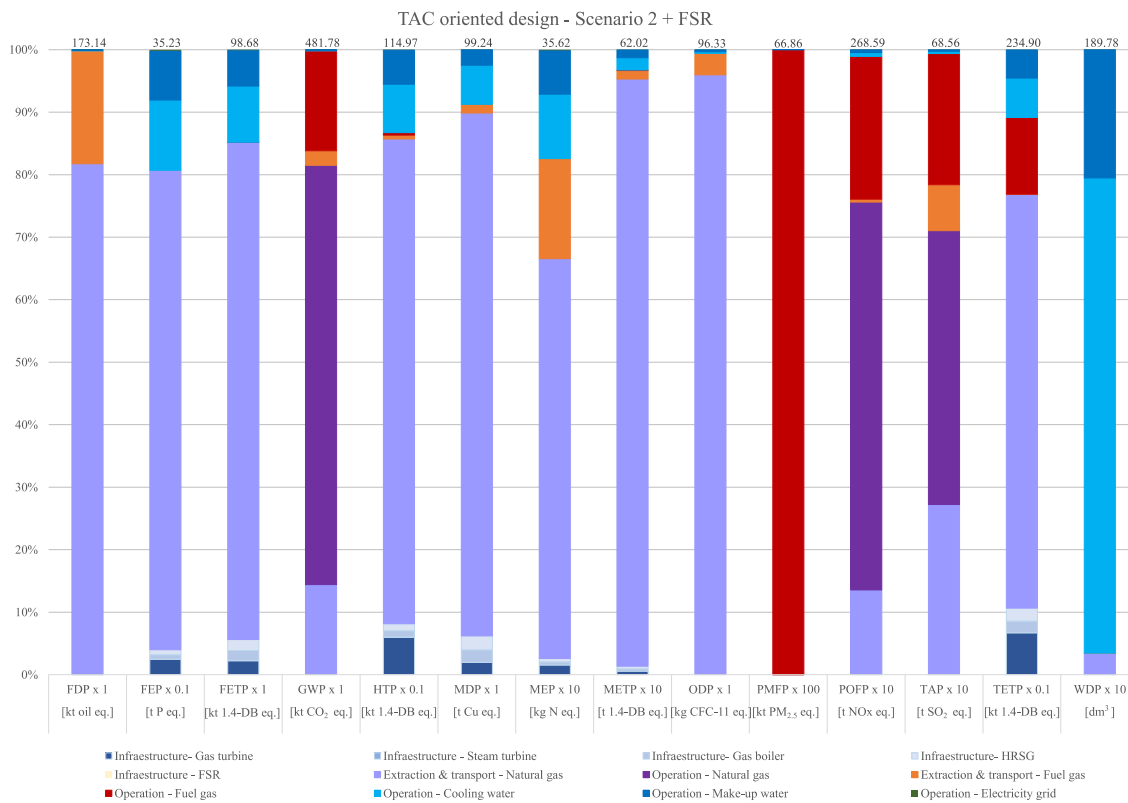


Figure 4-8 Environmental lifecycle assessment of best TAC-oriented design (Scenario 2 with FSR), considering a year of operation

[All impacts are expressed by the energy generated by the utility system to meet the annual heat and power demand of the site. Data label are the environmental impacts. FDP: fossil depletion potential; FEP: freshwater eutrophication potential; FETP: freshwater ecotoxicity potential; GWP: global warming potential; HTP: human toxicity potential; MDP: mineral depletion potential; MEP: marine eutrophication potential; METP: marine ecotoxicity potential; ODP: ozone depletion potential; PMFP: particulate matter formation potential; TAP: terrestrial acidification potential; TETP: terrestrial ecotoxicity potential]. Note that some of the values have been scaled. To obtain the original value of the data label, multiply the values shown in the graph with the scaling factor on the x-axis



(a)



(b)

Figure 4-9 Contribution analysis of: (a) Base case design and (b) TAC- oriented – Scenario 2 + FSR, considering a year of operation (For impact nomenclature see Figure 4-8)

The following sections discuss in more detail the individual impacts, which are classified according to the corresponding environmental issues.

- Climate change (GWP): In both designs, the main contributors to the global warming potential (GWP) is the consumption of fossil fuel, in particular the gas turbine coupled with the HRSG, which burn natural gas for their operation. Due to the higher heat to power potential, most power requirement is satisfied by gas turbines coupled with HRSG. Moreover, HRSG has the flexibility to burn additional fuel (supplementary firing) to raise the steam generation. Overall, this leads to the gas turbine coupled with the HRSG contribute around 82 % and 59 % for the Scenario 2 + FSR and reference case, respectively. However, it is important to note that although most of the natural gas contribution is due to combustion emissions, between 10 and 14 % are sourced by the extraction and transport of natural gas, due to the significant share of natural gas import and related distribution gas losses.

Due to the higher energy integration in Scenario 2 + FSR design, the boiler size and operational load, reducing its annual fuel consumption by 49.1 %. As a result, the GWP impact from fuel gas combustion in gas boilers decreases from 236 kt CO₂ per year to 77 kt CO₂ per year.

- Air pollution (ODP, PMFP): Ozone depletion potential (ODP) impact is only estimated to be 96.3 and 103.5 kg CFC-11 eq. per year for the best design and the reference systems, respectively. The main contributions are from natural gas import. Regarding particulate matter formation (PMFP), while particulate matter is not present in natural gas, fuel gas emits fine particulate matter, being the source of the emissions.

As mentioned in previous impact, the reduction of boiler contribution for steam generation, explains the 67 % reduction of PMPF emitted by the Scenario 2 with FSR system.

- Water and soil pollution (FEP, MEP, TAP): For fresh eutrophication (FEP) the main source of emissions is the primary energy required for the extraction of natural gas, while 20 % is sourced by process required to pretreat utility water. Marine eutrophication (MEP), the nitrogen and ammonia released to the air during the processing of fuel gas contribute to 24 and 36 % of the emissions from the optimum and reference case, respectively. On the other hand, terrestrial acidification (TAP) is mainly sourced by the use of fossil fuels. Around 65 % of the emissions are related to the NO_x emitted during fuel combustion, while the rest (44 %) correspond to indirect emissions related to the extraction of the fossil fuels.

- Ecotoxicity (FETP, METP, TETP) and human health (HTP): For freshwater ecotoxicity (FETP) the main contributor are the heavy metals released during the extraction of natural gas. Around 15 % of the emissions are associated with the electricity and chemicals used during water

pre-treatment. Equipment construction contributes with less than 6 % of the emissions in both cases. Additionally, for terrestrial ecotoxicity (TETP), heavy metals released to the soil during fuel gas combustion contribute to between 12 and 29% of the emissions.

Resource depletion (FDP, MDP, WDP): Although both systems are fossil fuel based, site heat recovery enhancement of Scenario 2 + FSR design can reduce the negative impact in fossil fuel (FDP) and mineral (MDP) depletion by 27 % and 5%, respectively. While for water depletion (WDP), results highlight the significant impact of industrial sites not only in terms of fossil fuel consumption and their corresponding impacts, but also in terms of water resources. This is due to the large amount of water (2,139.5 dm³ per year) required to satisfy the heating and cooling demand.

As mentioned before, optimal selection of steam mains for site recovery do not only reduce the fuel consumption, but also diminish the amount of cooling water requirement, reducing the water depletion impact by 11 %.

6.2. Total annual global warming potential oriented optimal design

However, when the system is driven by environmental forces, the system favours the use of biomass, more specifically woodchips, due to its low environmental impact. Figure 4-10 summarizes the costs distribution of the TAGWP systems and the site primary energy consumption/generation.

Table 4-8 shows the results of the case study under scenarios 1 and 2, considering total annual global warming potential as objective function. As in previous section, the integration of FSR and enhanced heat recovery can lead to up to 24.1 % further CO₂ emissions than systems where these parameters have not being considered. However, when the system is driven by environmental forces, the system favours the use of biomass, more specifically woodchips, due to its low environmental impact. Figure 4-10 summarizes the costs distribution of the TAGWP systems and the site primary energy consumption/generation.

Table 4-8 Optimization results based on minimal total annual global warming potential (TAGWP)

	Scenario 1		Scenario 2	
	w/o FSR	w FSR	w/o FSR	w FSR
Steam mains	VHP / HP / MP / LP		VHP / HP / MP / LP	
Temperature [° C]	560 / 270.4 / 232.4 / 171.8		570 / 267.0 / 209.1 / 150.0	
Pressure [bar]	85.0 / 40.0 / 20.0 / 5.0		85.0 / 37.8 / 12.3 / 2.7	
Total annualized cost	156.02	131.55	133.85	119.91
[m€·y ⁻¹]	-	-15.7%	-14.2%	-23.1%
GWP [kt CO ₂ ·y ⁻¹]	48.21	43.34	41.35	36.59
	-	-10.1%	-14.2%	-24.1%

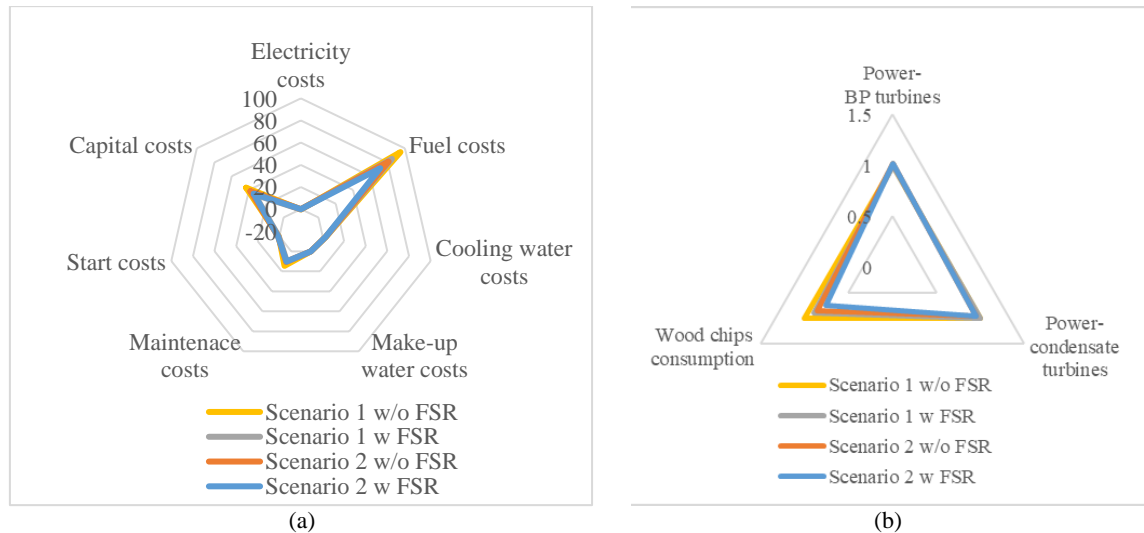


Figure 4-10 TAGWP oriented optimal design per year of operation: (a) Costs contribution (in m€·y⁻¹) and (b) electricity and fuel consumption, having as reference Scenario 1 w/o FSR design.

[Energy consumption in GWh·y⁻¹. Wood chips consumption: 3234.8, Power import: 0.00, Power generation – back-pressure turbine: 350.19, Power generation – condensate turbine: 87.03]

Figure 4-10(b) depicts the primary energy consumption of the four different optimal designs. As in the TAC oriented designs, system share a common configuration: biomass boilers, back-pressure steam turbines and condensate turbines. It is worth nothing that due to the relative high GWP of the current electricity system (444 kg CO₂ eq. per MWh) system do not import electricity, but favours on site power generation. Since power generation through back-pressure turbines is limited by the amount of site steam requirement, the deployment of condensate turbines is required to satisfy the annual power demand. In contrast to TAC oriented designs, the system only selects biomass boilers as thermal generators, where the main difference between the different scenarios is the boiler duty. For this reason, the contribution analysis only of the best TAGWP oriented design is discussed below.

- Climate change (GWP): As shown in Figure 4-11 the system with min TAGWP emits 36.59 kt CO₂-eq per year. Note that carbon dioxide emissions from combustion of biomass are not considered (due to its biogenic nature). Emissions due to NO_x represent 4 % of the emissions. The preparation and transport of biomass resulting in 89 % of the GWP emissions. This is mainly due to the diesel used for wood chipping.
- Air pollution (ODP, PMFP): Ozone depletion potential (ODP) is estimated to be 11.7°kt CFC-11 eq. per year. For particulate matter formation (PMFP), only 29 % of the impact in the TAGWP system originates from the combustion of wood chips, specially SO₂ emissions.
- Water and soil pollution (FEP, MEP, TAP): Although use of ash as fertilizer could displace the production of chemical fertilisers, its application to soil leads to fresh water

eutrophication (FEP) via leaching and runoff. For marine eutrophication (MEP) and terrestrial acidification, SO₂ and NO_x emissions from the energy used for wood preparation and transport are the main source.

- Ecotoxicity (FETP, METP, TETP) and human health (HTP): Disposal of ash is the main contributor to fresh water ecotoxicity potential (FETP). Although, displacement of fertiliser provide credits for METP and TETP, these may be offset by the heavy metals present in the ashes. Regarding human toxicity potential (HTP): The combustion of wood chips contributes to source due to the release of phosphorus and heavy metals to air.
- Resource depletion (FDP, MDP, WDP): the fuel associated with the preparation and transport of woodchips is the main source of fossil depletion. Boiler equipment contributes to 33 % of the mineral depletion, due to the mineral used in the construction system. Regarding WDP, water consumed by the feedstock represents the 8 %.

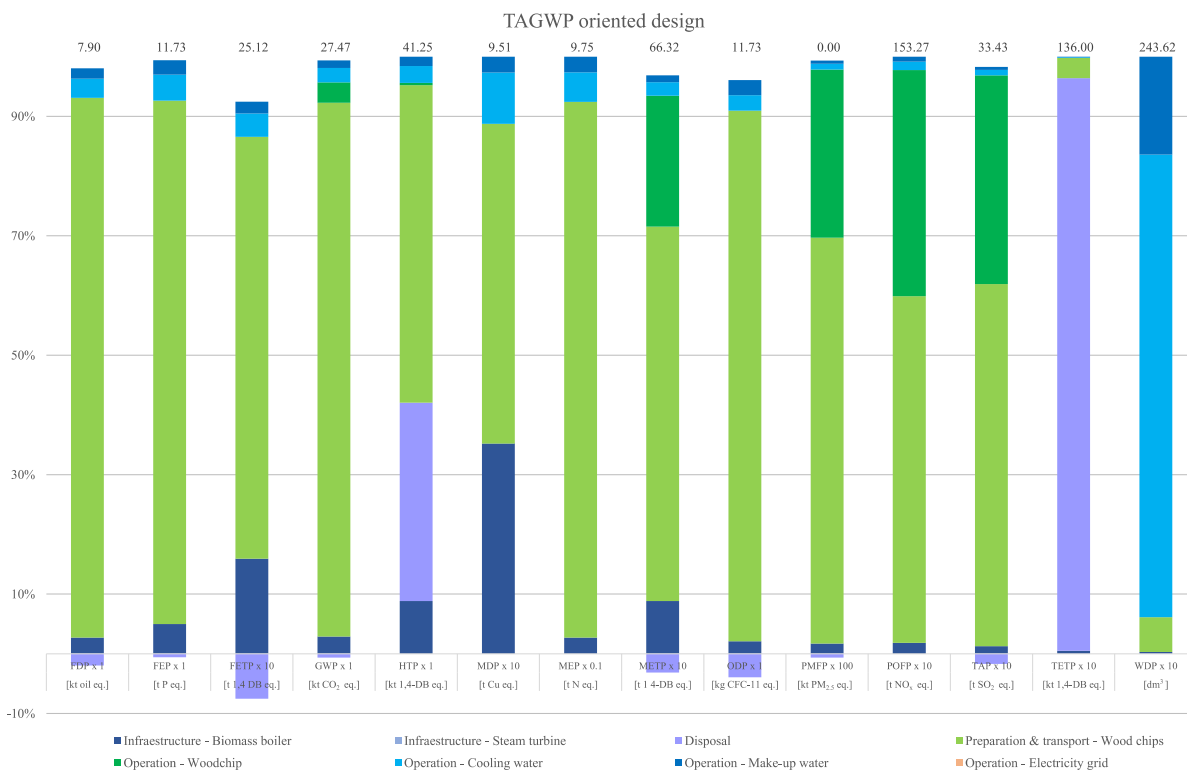


Figure 4-11 Contribution analysis of the TAGWP oriented design (For impact nomenclature see Figure 4-8)

6.3. Comparison of environmental impacts for the TAGWP and TAC designs

A comparison of the environmental impact of TAGWP oriented design and the TAC design is shown in Figure 4-12.

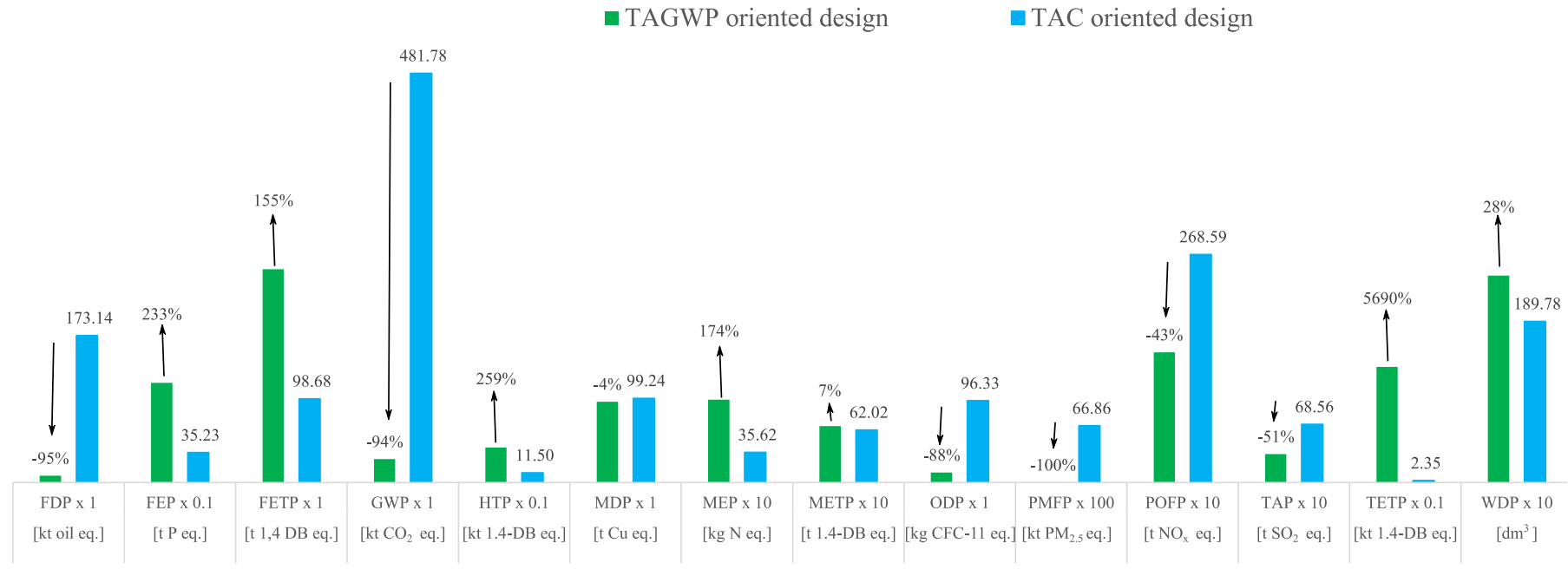


Figure 4-12 Life cycle environmental impacts of industrial utility systems per year of operation (For impact nomenclature see Figure 4-8)

The TAGWP oriented design (operating with biomass boilers) reduces the GWP impact by 94 % (compared to the optimum design for min TAC). Moreover, the TAGWP design outperform the TAC system for the three impacts considered a priority for government policies for reducing climate change (GWP: -94 %), fossil fuel use (FDP: -95%) and ozone layer depletion (ODP: -88%). However, this reduction is at the expense of significantly increasing other impacts such as human health (HTP: +259 %), water pollution (FEP: +233 % and MEP: +174 %), ecotoxicity This may be explained by the lower combustion emissions of natural and fuel gas (except for GHGs and particulate matter -fuel gas-) and the impact from ash disposal. Moreover, the water need for the biomass increase the negative impact in water depletion (+ 28%).

6.4. Multiobjective optimization results aiming minimum TAC and TAGWP

Figure 4-13, 4-13 and 4-14 present multiple optimal solutions for different ranges of the two objective functions. For purpose of illustration, 20 points have been selected to set the Pareto curve. Figure 4-13 shows the variation in GWP and TAC for each of the design points from the best TAC oriented design (Scenario 2 + FSR) until reach the extreme point in the right, which represents the optimal design with minimum TAGWP. Figure 4-14 (a) and (b) show the thermal and power energy conversion technologies shift as the amount of CO₂ emissions allowed become more and more strict.

As expected, the reduction of GWP can only be achieved at the cost of TAC. However, it is important to note that by generating the Pareto set, the trade-off between the two objective functions can be obtained. For instance, Design in point 3, can achieve a CO₂-eq emissions reduction of 19.5 % by switching fuel gas to natural gas in the gas boiler. This reduction only increases the total annualized costs in 3.45 %.

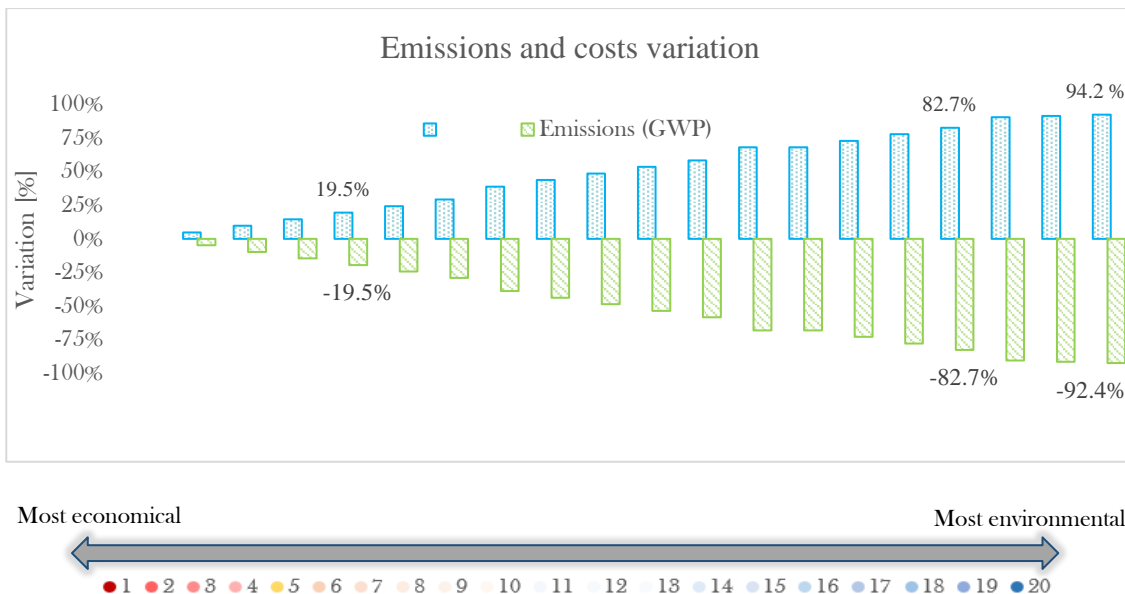


Figure 4-13 Pareto curve of the multiobjective optimization. Representation of the TAC and TAGWP variation with respect to the best TAC oriented design

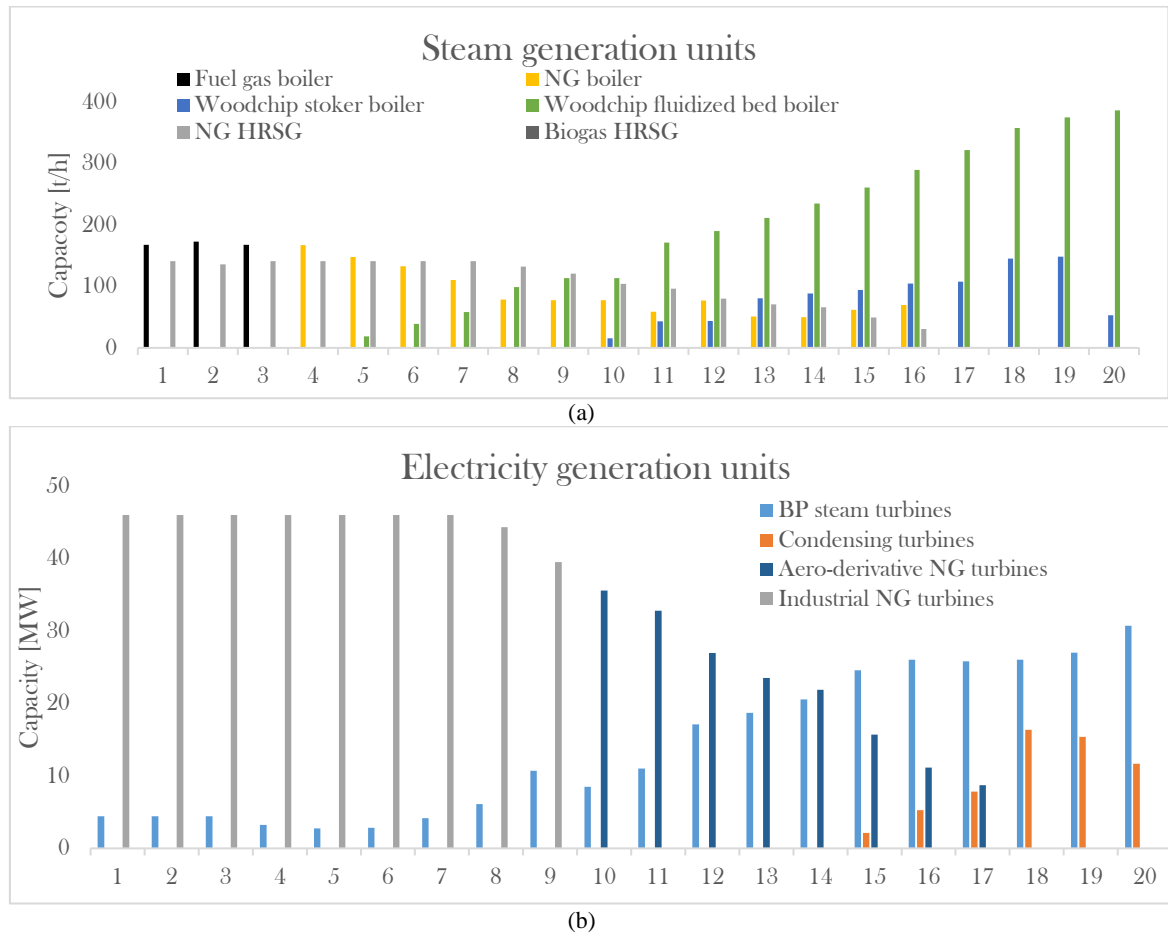


Figure 4-14 Pareto curve of the multiobjective optimization: (a) thermal generation units capacity (b) Power generation units capacity, at each design point,

As can be observed in Figure 4-14 the system gradually shift from use of fossil fuel, to a mix of natural gas and biomass up to a emission reduction of 82.7%. Notably, as the CO₂ emission restrictions increases, onsite power generated by steam turbines increases. This can be explained by the operation of steam turbines based on heat available from the HRSG and boiler, without requiring additional fuel combustion. However, power generation through back-pressure steam turbines also depend on the site thermal heating requirement. Consequently, as the power requirement from steam turbine increases, the deployment of condensate turbines is necessary. This is more clear at high decarbonisation levels above 82.7 %, where due to its is necessary to fully exploit the renewable generation, condensate turbines with greater capacities are deployed.

7. Conclusions

This study provided a methodology for the cost-effective design of industrial utility systems considering environmental impacts. Based on the BEELINE model presented in Contribution 3, a multi-objective approach was introduced to consider the environmental impacts of industrial utility

systems while providing cost-effective solutions. The proposed framework comprises general constraints of the system such as mass and energy balances, part-load equipment performance, time-dependent energy demand and electricity prices. Moreover, the model considers the selection of the steam main operating conditions to exploit the close interrelation between the site processes and the utility system at multiple temperature levels. This allows not only improving the energy efficiency and reducing the fuel consumption of the site, but also reducing its environmental impact as shown in the first part of the results.

The resulting MO-MINLP mathematical model is established with minimum total annualized cost and minimum global warming potential as driving forces for the design of utility systems. To determine the environmental impact of the system a life cycle assessment approach was employed. Although only global warming potential is considered during the optimization, the solutions obtained were assessed considering other environmental issues such as air, water and soil pollution, ecotoxicity and resource depletion.

The results highlight the relevance of optimization tools for the design and operation of industrial utility systems, accounting for site heat integration and operating conditions. By considering steam main conditions as part of the optimization, the system can reduce the total annual costs and the GHGs emissions by 24.4 % and 27.6 %, respectively. Moreover, results show that other environmental impacts can also be reduced simultaneously. This is due to a better energy utilization, resulting in the requirement of smaller size equipment, lower full consumption and diminution in the water usage as well.

To achieve further CO₂ reductions a gradual shift away from fossil fuel sources and technologies, as expected. However, this is not only done at the expenses of higher total annualized costs. Moreover, although the environmental design reduces the three impacts considered a priority for government policies for reducing climate change, fossil fuel use and ozone layer depletion, it is at the expense of other environmental impacts such as human toxicity, ecotoxicity, water pollution and depletion.

Electrical and thermal systems are not selected in any of the scenarios, since the renewable sources considered in this study (biomass) are as flexible as fossil fuel. Nevertheless, these results cannot be extrapolated to all systems or scenarios. If more intermittent renewable sources (such as wind and solar) become available for industrial use, energy storage have been proven useful to compensate its intermittency and benefit from lower CO₂ emissions. Therefore, future work would involve integrating other energy source and low-carbon technologies to explore different scenarios.

References

- Andiappan, V. (2017) 'State-Of-The-Art Review of Mathematical Optimisation Approaches for Synthesis of Energy Systems', *Process Integration and Optimization for Sustainability*, 1(3), pp. 165-188.
- Bacchetti, J., Sala, C., Fusi, A. & Fiala, M. (2016) 'Agricultural anaerobic digestion plants: What LCA studies pointed out and what can be done to make them more environmentally sustainable', *Applied Energy*, 179, pp. 669-686.
- Bandara, J. C., Jaiswal, R., Nielsen, H. K., Moldestad, B. M. E. & Eikeland, M. S. (2021) 'Air gasification of wood chips, wood pellets and grass pellets in a bubbling fluidized bed reactor', *Energy*, 233, pp. 121149.
- Bareiß, K., de la Rúa, C., Möckl, M. & Hamacher, T. (2019) 'Life cycle assessment of hydrogen from proton exchange membrane water electrolysis in future energy systems', *Applied Energy*, 237, pp. 862-872.
- Bussieck, M. R. & Meeraus, A. (2004) 'General Algebraic Modeling System (GAMS)', in Kallrath, J. (ed.) *Modeling Languages in Mathematical Optimization*. Boston, MA: Springer US, pp. 137-157.
- Calderón, C., Colla, M., Jossart, J.-M., Nathalie Hemeleers, G. C., Aveni, N. & Caferra, C. (2019) *Report Pellet: Bioenergy Europe*.
- Chang, C.-T. & Hwang, J.-R. (1996) 'A multiobjective programming approach to waste minimization in the utility systems of chemical processes', *Chemical Engineering Science*, 51(16), pp. 3951-3965.
- Corporation, I. (2017). *V12. 8: IBM ILOG CPLEX Optimization Studio CPLEX User's Manual: International Business Machines Corporation*.
- da Silva Lima, L., Quartier, M., Buchmayr, A., Sanjuan-Delmás, D., Laget, H., Corbisier, D., Mertens, J. & Dewulf, J. (2021) 'Life cycle assessment of lithium-ion batteries and vanadium redox flow batteries-based renewable energy storage systems', *Sustainable Energy Technologies and Assessments*, 46, pp. 101286.
- Department for Business, E. I. S. (2021) *Combined Heat and Power – Environmental A detailed guide for CHP developers – Part 3*, UK: Department for Business, Energy & Industrial Strategy.
- Drud, A. (1985) 'CONOPT: A GRG code for large sparse dynamic nonlinear optimization problems', *Mathematical Programming*, 31(2), pp. 153-191.
- Eliceche, A. M., Corvalán, S. M. & Martínez, P. (2007) 'Environmental life cycle impact as a tool for process optimisation of a utility plant', *Computers & Chemical Engineering*, 31(5), pp. 648-656.
- Elsido, C., Cremonesi, A. & Martelli, E. (2021) 'A novel sequential synthesis algorithm for the integrated optimization of Rankine cycles and heat exchanger networks', *Applied Thermal Engineering*, 192, pp. 116594.
- EuRIC (2020) *Metal Recycling Factsheet*, Brussels: EuRIC AISBL – Recycling: Bridging Circular Economy & Climate Policy.

- Fazlollahi, S., Bungener, S. L., Mandel, P., Becker, G. & Maréchal, F. (2014) 'Multi-objectives, multi-period optimization of district energy systems: I. Selection of typical operating periods', *Computers & Chemical Engineering*, 65, pp. 54-66.
- Frangopoulos, C. A. (2018) 'Recent developments and trends in optimization of energy systems', *Energy*, 164, pp. 1011-1020.
- Gabrielli, P., Gazzani, M., Martelli, E. & Mazzotti, M. (2018) 'Optimal design of multi-energy systems with seasonal storage', *Applied Energy*, 219, pp. 408-424.
- Ganschinetz, D. C. (2021) 'Design of on-site energy conversion systems for manufacturing companies – A concept-centric research framework', *Journal of Cleaner Production*, 310, pp. 127258.
- Gerber, L., Gassner, M. & Maréchal, F. (2011) 'Systematic integration of LCA in process systems design: Application to combined fuel and electricity production from lignocellulosic biomass', *Computers & Chemical Engineering*, 35(7), pp. 1265-1280.
- Greening, B. & Azapagic, A. (2013) 'Environmental impacts of micro-wind turbines and their potential to contribute to UK climate change targets', *Energy*, 59, pp. 454-466.
- Gutiérrez-Arriaga, C. G., Serna-González, M., Ponce-Ortega, J. M. & El-Halwagi, M. M. (2013) 'Multi-objective optimization of steam power plants for sustainable generation of electricity', *Clean Technologies and Environmental Policy*, 15(4), pp. 551-566.
- Hipólito-Valencia, B. J., Lira-Barragán, L. F., Ponce-Ortega, J. M., Serna-González, M. & El-Halwagi, M. M. (2014) 'Multiobjective design of interplant trigeneration systems', *AIChE Journal*, 60(1), pp. 213-236.
- Hongmin, D., Mangino, J., McAllister, T., Hatfield, J., Johnson, D. & Lassey, K. (2006) *Emissions from Livestock and Manure Management. IPCC Guidel. Natl. Greenh. Gas Invent.*
- IEA (2018) *CO2 Emissions from Fuel Combustion 2018*: International Energy Agency.
- IEA (2020) *CO2 Emissions from Fuel Combustion: Overview*, Paris: IEA. Available at: <https://www.iea.org/reports/co2-emissions-from-fuel-combustion-overview>.
- Isafiade, A. J., Short, M., Bogataj, M. & Kravanja, Z. (2017) 'Integrating renewables into multi-period heat exchanger network synthesis considering economics and environmental impact', *Computers & Chemical Engineering*, 99, pp. 51-65.
- ISO (2006a) *ISO14044:2006 Environmental management—Life cycle assessment—Requirements and guidelines*. . BSI, London.
- ISO (2006b) *ISO 14040:2006 Environmental management—Life cycle assessment—Principles and framework*. . BSI, London.
- Iyer, R. R. & Grossmann, I. E. (1998) 'Synthesis and operational planning of utility systems for multiperiod operation', *Computers & Chemical Engineering*, 22(7), pp. 979-993.
- Kelly, K. A., McManus, M. C. & Hammond, G. P. (2014) 'An energy and carbon life cycle assessment of industrial CHP (combined heat and power) in the context of a low carbon UK', *Energy*, 77, pp. 812-821.
- Liu, L., Sheng, Y., Zhuang, Y., Zhang, L. & Du, J. (2020) 'Multiobjective Optimization of Interplant Heat Exchanger Networks Considering Utility Steam Supply and Various Locations of

- Interplant Steam Generation/Utilization', *Industrial & Engineering Chemistry Research*, 59(32), pp. 14433-14446.
- Luo, X., Hu, J., Zhao, J., Zhang, B., Chen, Y. & Mo, S. (2014) 'Multi-objective optimization for the design and synthesis of utility systems with emission abatement technology concerns', *Applied Energy*, 136, pp. 1110-1131.
- Martín-Hernández, E., Sampat, A. M., Zavala, V. M. & Martín, M. (2018) 'Optimal integrated facility for waste processing', *Chemical Engineering Research and Design*, 131, pp. 160-182.
- Mavrotas, G. (2009) 'Effective implementation of the ϵ -constraint method in Multi-Objective Mathematical Programming problems', *Applied Mathematics and Computation*, 213(2), pp. 455-465.
- Oliveira Francisco, A. P. & Matos, H. A. (2004) 'Multiperiod synthesis and operational planning of utility systems with environmental concerns', *Computers & Chemical Engineering*, 28(5), pp. 745-753.
- Papandreou, V. & Shang, Z. (2008) 'A multi-criteria optimisation approach for the design of sustainable utility systems', *Computers & Chemical Engineering*, 32(7), pp. 1589-1602.
- PE international (2014) *Best Practice LCA: End-of-Life Modelling*. Available at: https://gabi.sphera.com/uploads/media/Webinar_End_of_Life_Oct2014.pdf.
- Pedišius, N., Praspaliauskas, M., Pedišius, J. & Dzenajavičienė, E. F. (2021) 'Analysis of Wood Chip Characteristics for Energy Production in Lithuania', *Energies*, 14(13), pp. 3931.
- Pellow, M. A., Ambrose, H., Mulvaney, D., Betita, R. & Shaw, S. (2020) 'Research gaps in environmental life cycle assessments of lithium ion batteries for grid-scale stationary energy storage systems: End-of-life options and other issues', *Sustainable Materials and Technologies*, 23, pp. e00120.
- Pérez-Uresti, S. I., Martín, M. & Jiménez-Gutiérrez, A. (2019) 'Superstructure approach for the design of renewable-based utility plants', *Computers & Chemical Engineering*, 123, pp. 371-388.
- Pérez-Uresti, S. I., Martín, M. & Jiménez-Gutiérrez, A. (2020) 'A Methodology for the Design of Flexible Renewable-Based Utility Plants', *ACS Sustainable Chemistry & Engineering*, 8(11), pp. 4580-4597.
- Pool, N. (2020). *Historical Market Data* [Online]. Available at: <https://www.nordpoolgroup.com/historical-market-data/> [Accessed 2020].
- Smith, R. (2016). *Chemical Process Design and Integration* (2nd ed. ed.): Wiley.
- Smith, R., & Delaby, O. (1991) 'Targeting flue gas emissions', *Chemical Engineering Research and Design*.
- Sun, L. & Liu, C. (2015) 'Reliable and flexible steam and power system design', *Applied Thermal Engineering*, 79, pp. 184-191.
- Author (2019) *Thinkstep Lifecycle Assessment LCA Software: GaBi Software*. . Available at: <http://www.gabi-software.com>.
- Vaskan, P., Guillén-Gosálbez, G., Turkay, M. & Jiménez, L. (2014) 'Multiobjective Optimization of Utility Plants under Several Environmental Indicators Using an MILP-Based Dimensionality

- Reduction Approach', *Industrial & Engineering Chemistry Research*, 53(50), pp. 19559-19572.
- Wang, Y. & Feng, X. (2017) 'Heat Integration Across Plants Considering Distance Factor', in Kopanos, G. M., Liu, P. & Georgiadis, M. C. (eds.) *Advances in Energy Systems Engineering*. Cham: Springer International Publishing, pp. 621-648.
- Weber, S., Peters, J. F., Baumann, M. & Weil, M. (2018) 'Life Cycle Assessment of a Vanadium Redox Flow Battery', *Environmental Science & Technology*, 52(18), pp. 10864-10873.
- Wernet, G., Bauer, C., Steubing, B., Reinhard, J., Moreno-Ruiz, E. & Weidema, B. (2016) 'The ecoinvent database version 3 (part I): overview and methodology', *The International Journal of Life Cycle Assessment*, 21(9), pp. 1218-1230.
- Wu, L., Liu, Y., Liang, X. & Kang, L. (2016) 'Multi-objective optimization for design of a steam system with drivers option in process industries', *Journal of Cleaner Production*, 136, pp. 89-98.
- Xiao, W., Cheng, A., Li, S., Jiang, X., Ruan, X. & He, G. (2021) 'A multi-objective optimization strategy of steam power system to achieve standard emission and optimal economic by NSGA-II', *Energy*, 232, pp. 120953.
- Zheng, X., Wu, G., Qiu, Y., Zhan, X., Shah, N., Li, N. & Zhao, Y. (2018) 'A MINLP multi-objective optimization model for operational planning of a case study CCHP system in urban China', *Applied Energy*, 210, pp. 1126-1140.
- Zwolinski, D. (2015) *UK and EU trade of wood pellets: DECC*.

SUPPLEMENTARY INFORMATION P4

Roadmap to low-carbon industrial utility systems: Design of cost-effective process utility systems considering environmental life-cycle assessment

Julia Jiménez-Romero^{a,b,*}, Adisa Azapagic^b, Robin Smith^a

^a Centre for Process Integration, Department of Chemical Engineering and Analytical Science, University of Manchester, Manchester, M13 9PL, United Kingdom

^b Sustainable Industrial Systems Group, Department of Chemical Engineering and Analytical Science, University of Manchester, Manchester, M13 9PL, United Kingdom

* Julia Jiménez-Romero. Email: julia.jimenezromero@manchester.ac.uk, nataly.jimenezr@hotmail.com

SUPPLEMENTARY INFORMATION P4.A

Life Cycle Assessment Assumptions

A.I. Resources

A.I.1. Wood chips and wood pellets

Data from Ecoinvent 3.5 (Ecoinvent Association, 2018) was considered. The LCA model for wood chips comprises: harvesting operations and chipping. Chipping energy consumption depends on the bulk density of the waste wood. In this work diesel consumption of 33.7 MJ and 23.8 MJ per 1 m³ of dry wood, for hardwood and softwood respectively (Tagliaferri et al., 2018). On the other hand, wood pellets environmental estimation considers wood residue from sawmills and woodchips as raw materials. The wood pellets LCA model comprises: harvesting operations, pre-treatment, drying and pelletisation.

A.I.2. Cattle manure

In Europe, around 92% of manure is usually re-applied to soil (“raw application”), while less than 8% has any kind of pre-treatment prior its application as fertilizer (Königer et al., 2021). The impacts of chemical fertilisers have been added to the system, while the system has been credited for the avoided emissions to soil.

Table P4. A.1 Properties of cattle manure

Properties	Units	Value
Manure production	[t dry matter·head day]	$4.68 \cdot 10^{-3}$ ^a
Moisture content	[%]	92 ^b
Composition	[per t dry matter]	
N	[t]	0.065 ^b
P	[t]	0.010 ^b
K	[t]	0.068 ^b
As	[g]	0.15 ^c
Cd	[g]	0.16 ^c
Cr	[g]	1.28 ^c
Cu	[g]	30.0 ^c
Pb	[g]	0.25 ^c
Zn	[g]	180.0 ^c
Management		
Raw application	[%]	92 ^d

Properties	Units	Value
Costs		
Manure at the plant	[€·t ⁻¹]	6.05 ^e
		K: 1,056
Digestate	[€·t ⁻¹]	P: 1,408
		N: 682

^a Velthof (2014), considering a median of 111 kg N output per dairy cattle head

^b Martín-Hernández et al. (2018), ^c Hejna et al. (2019), ^d Köninger et al. (2021)

^e Own calculation based on Andersen (2016) and assuming a distance of 10 miles

A.II. Utility components

A.II.1. Gas turbine

Construction materials and installation of gas turbine are sourced by Ecoinvent 3.5(Ecoinvent Association, 2018) for a 10 MW gas turbine, where 95 % of the turbine mass is reinforcing steel and the remaining 5% chromium (stainless) steel. In (Kelly et al., 2014) masses are given for a 40 MW gas turbine, and are used to calculate the scaling exponent ($\beta = 0.8$). The functional parameter for the gas turbine is the electric power MW.

Table P4. A.2 Inventory data for a gas turbine 10 MW

Item	Unit	Value
Raw materials		
Reinforcing steel	[kg]	47.5
Chromium steel	[kg]	2.5
Poliethylene, high density	[kg]	15
Assembly and installation		
Concrete	[m ³]	50
Cooper	[t]	5
Electricity	[MJ]	1.69·10 ⁵
Heat	[MJ]	7.21·10 ⁵
Diesel	[kg]	7.59·10 ⁵
Transport		
Transport lorry (raw material)	[km]	100 ^c
Transport freight train	[km]	542 ^c

A.II.2. Steam turbine

The analysis of the steam turbine was performed as dependent of the material composition. The material data set of Kelly et al. (2014). For the scaling, the same cost coefficient is employed.

Table P4. A.3 Inventory data for a steam turbine 40 MW

Item	Unit	Value
Raw materials		
Reinforcing steel	[kg]	47.5
Low alloyed steel	[kg]	2.5
Transport		
Transport lorry (raw material)	[km]	100 °
Transport freight train	[km]	542 °

A.II.3. Boilers

A.II.3.1. Gas boiler

Manufacture of gas boilers are sourced by Ecoinvent 3.5 . In (Kelly et al., 2014) masses are given for a 40 MW gas turbine, and are used to calculate the scaling exponent ($\beta = 0.8$). The functional parameter for the gas turbine is the electric power MW.

Table P4. A.4 Inventory data for a gas boiler

Item	Unit	Value
Reference size		1 MW
Raw materials		
Alkyd paint, white, without solvent, in 60% solution state	[kg]	5
Aluminium, cast alloy	[kg]	30
Brass	[kg]	0.05
Cast iron	[kg]	4200
Copper	[kg]	0.03
Polyethylene, high density, granulate	[kg]	0.40
Refractory, fireclay, packed	[kg]	70.00
Steel, chromium steel 18/8, hot rolled	[kg]	230.00
Steel, low-alloyed, hot rolled	[kg]	190.00
Stone wool	[kg]	40.00
Assembly and installation		
Heat, natural gas	[MWh]	4.00
Heat, other than natural gas	[MWh]	2.24
Electricity, medium voltage	[MWh]	2.78
Tap water	[kg]	6190

A.II.3.2. Biomass boiler

Manufacture of biomass boilers has been defined based on the models provided in Ecoinvent 3.5 (Ecoinvent Association, 2018). Boilers with storage silos has been taken into account.

Table P4. A.5 Inventory data for biomass boilers

Item	Unit	Wood chips	Wood pellet
Reference size		5 MW	0.3 MW
Raw materials			
alkyd paint, white, without solvent, in 60% solution state	[kg]	12.00	3.50
Aluminum, wrought alloy	[kg]	104.00	9.50
Cast iron	[kg]	1120.00	0.00
Concrete, normal	[m ³]	56.00	16.90
Copper	[kg]	46.00	4.50
Drawing of pipe, steel	[kg]	70.00	0.00
Electronics, for control units	[kg]	12.00	4.00
Iron-nickel-chromium alloy	[kg]	528.00	0.00
Lubricating oil	[kg]	32.00	3.00
Polyethylene, high density, granulate	[kg]	18.00	5.50
Polystyrene foam slab	[kg]	361.00	52.00
Refractory, fireclay, packed	[kg]	41200.00	686.00
Sheet rolling, steel	[kg]	2000.00	184.00
Steel, chromium steel 18/8, hot rolled	[kg]	70.00	30.00
Steel, low-alloyed, hot rolled	[kg]	7480.00	2890.00
Stone wool	[kg]	1850.00	266.00
Assembly and installation			
Heat, other than natural gas	[MWh]	2.66	2.50
Electricity, low voltage	[MWh]	5.87	1.33

A.II.3.3. Electrode boilers

Due to the lack of detailed information about the electrodes, electrode boiler inventory is based on an electric boiler source (Abbas, 2015). This assumption is based on the similarity in infrastructure. The materials are adapted for the dimensions and mass of a 60 MW electrode boiler provided by manufacturer Parat Halvorsen AS (2021).

Table P4. A.6 Inventory data for a 60 MW electrode boiler

Item	Unit	Value
Raw materials		
Metals		
Stainless steel	[t]	3.17
Brass	[t]	0.81
Galvanized steel	[t]	5.26
Low alloyed	[t]	4.45
Mild unalloyed	[t]	3.18
Cast iron	[t]	2.74
Insulation		
Glass fibre	[t]	0.16

Item	Unit	Value
Rock wool	[t]	0.1
Ceramics		0.24
Electronics		
Cables	[t]	2.26
Clamps	[t]	0.22
Electronic board		0.32
Plastics		
Handles	[t]	0.05
Gaskets	[t]	0.02
Sealing	[t]	0.03
Assembly and installation		
Electricity	[MWh]	38.1
Heat	[MWh]	17.8

A.II.4. Biomass gasifier

Biomass infrastructure materials have taken from Adams (2011), which is sourced by manufacturers.

Table P4. A.7 Inventory data for a 0.2 t h⁻¹ biomass gasifier

Item	Unit	Value
Raw materials		
Feed air pre-heater		
Chromium steel	[kg]	95
Gasifier		
Chromium steel	[kg]	740
Rock wool	[kg]	20
Ash disposal system		
Reinforcing steel	[kg]	449
Chromium steel	[kg]	8
Copper	[kg]	0.2
Gas cleaning system		
Aluminum, cast alloy	[kg]	3.7
Aluminum, wrought alloy	[kg]	1.5
Magnetite	[kg]	0.8
chromium	[kg]	508.8
Reinforced glass	[kg]	0.8
Copper	[kg]	0.2
Tetrafluoroethylene film	[kg]	0.2
Operation		
Olivine	[kg]	5.4
Electricity	[MWh]	0.01

Adams (2011)

A.II.5. Anaerobic digester

The data for construction of anaerobic digester is sourced from Ecoinvent, corresponding a plant of 500 m³.

Table P4. A.8 Inventory data for an anaerobic digester 500 m³, with methane recovery

Item	Unit	Value
Raw materials		
Anaerobic digester		
Concrete	[m ³]	1.20·10 ²
Reinforcing steel	[kg]	1.08·10 ⁴
Chromium steel	[kg]	2.50·10 ²
Copper	[kg]	1.30·10 ³
Laminated timber	[m ³]	80
High-density polyethylene	[kg]	1.70·10 ²
High-impact polystyrene	[kg]	5.70·10 ²
Polyvinyl chloride	[kg]	3.30·10 ²
Synthetic rubber	[kg]	1.20·10 ³

Additional fugitive emissions of methane during the anaerobic digestion process have been considered. Fugitive emissions range from 1 to 3% of the amount of biogas produced (Bernstad and la Cour Jansen, 2012; Naroznova et al., 2016). Therefore, a conservative approach has been consider the mean value of 2%. This emissions to the air account for the storage of the substrate prior the anaerobic digestion.

A.II.6. Pressure swing adsorption

The desulphurization step is based on Stucki et al. (2011). The generic value of infrastructure facilities is taken from Jungbluth et al. (2007). Raw biogas and biogas yield is obtained from Martín-Hernández et al. (2018) and Bauer et al. (2013) operating with zeolite 5A. The amount of zeolite 5A required is based on Alonso-Vicario et al. (2010). The methane emissions are assumed 2 % (Bauer et al., 2013) from the raw biogas. It is assumed that the retained H₂S is oxidised to sulphur dioxide and emitted into air (Stucki et al., 2011)

Table P4. A.9 Inventory data for a PSA with 1t processed biogas

Item	Unit	Value
Infrastructure		
Plant	[unit]	2.67·10 ⁻¹⁰ a
Operation		
Lubricating oil	[t]	2.05·10 ⁻⁴ b
Zeolite 5A	[t]	4.866 c
Electricity	[MWh]	0.3 b

Item	Unit	Value
Emissions to air*		
CO ₂	[t]	1.331 ^b
CH ₄	[t]	0.012 ^d
SO ₂	[t]	9.02·10 ⁻⁶ ^b

^a Jungbluth et al. (2007), ^b Stucki et al. (2011),

^c Alonso-Vicario et al. (2010), ^d (Bauer et al., 2013).

* CH₄ content: raw biogas = 70% Martín-Hernández et al. (2018)
 processed biogas = 96% Bauer et al. (2013);

Density: CH₄ = 0.708 kg/m³, CO₂ = 1.977 kg/m³

Lower Heating Value: CH₄ = 32.52 MJ/m³

A.II.7. Pressurized vessels (Steam accumulators and flash tank)

Pressurized vessels are used for steam accumulators. The cylindrical vessels are predominantly made from stainless steel. Glass wool is used for insulation. To determine the material mass the wall thickness is required (t_w), which in this work is calculated under the pressure vessel norm ASME BPV Code Sec. VIII D.1 Detailed calculation of the steel mass requirement is given in Supplementary Information P3.A.III.2

A.II.8. Li-Ion Battery

Two different Li-ion chemistries were considered in this work: Iron Phosphate (LFP) and Manganese Oxide (LMO). The mass distribution for the manufacturing of an industrial battery is mainly given by Majeau-Bettez et al. (2011), where only Notter et al. (2010) materials for the LMO cathode were considered. Note that despite these two studies are based on electric vehicles (EV) application, utility scale Li-ion batteries use the same chemistries, and in some cases the same cells, its mass distribution for the battery cell is relevant (Pellow et al., 2020) and has been used in several utility-scale studies (Hiremath et al., 2015). Nevertheless, the container housing and battery management system are different for stationary storage from for EV application. For instance, the utility scale-battery require considering concrete foundations, as well as an inverter and a fire suppression system to control the environment of the system and avoid potential thermal runaways (Pellow et al., 2020). Material components from (Pellow et al., 2020) are assumed to model the container housing and battery management system. For transportation, standard transport distances for Europe according to the Ecoinvent standards are assumed (Frischknecht, 2007).

Inventory for the assembly of Li-ion batteries is listed in Table P4. A.10. Based on the energy density of the total battery packs (88 KWh/t and 112 KWh/t of LFP and LMO, respectively). For complete detailed inventory on sub-processes for battery cell, the reader is referred to Majeau-Bettez et al. (2011) and Notter et al. (2010)

Table P4. A.10 Raw materials, assembly and installation data per 1 kg of Li-ion battery

Item	Unit	Type of battery	
		Li-ion (LFP)	Li-ion (LMO)
Raw materials			
Battery cell			
Anode	[kg]	0.163 ^a	0.179 ^d
Cathode	[kg]	0.284 ^a	0.268 ^d
Separator	[kg]	0.033 ^a	0.033 ^a
Electrolyte	[kg]	0.120 ^a	0.120 ^a
Cell container	[kg]	0.201 ^a	0.201 ^a
Module and battery packaging	[kg]	0.170 ^b	0.170 ^b
Battery management system (BMS)	[kg]	0.03 ^b	0.03 ^b
Assembly and installation			
Electricity	[MJ]	27 ^a	27 ^a
Heat	[MJ]	24.9 ^a	24.9 ^a
Water	[kg]	380 ^a	380 ^a
Infrastructure	[unit]	1.9·10 ^{-8a}	1.9·10 ^{-8a}
Transport			
Transport lorry (battery cell components)	[km]	100 ^c	100 ^c
Transport freight train	[km]	542 ^c	542 ^c
Air emissions			
Waste heat	[MJ]	52 ^a	52 ^a

LFP: Iron Phosphate; LMO: Manganese Oxide

^a Majeau-Bettez et al. (2011) ^b Pellow et al. (2020) ^c Wernet et al. (2016), ^d Notter et al. (2010)**A.II.9. Na-S battery**

For the analysis of Na-S batteries the manufacturer composition provided by Peters et al. (2016) is employed. In similar way to the Li-ion batteries, two options are analysed for the Na-S battery. Based on Peters et al. (2016)'s findings, two different precursors for the anode construction are evaluated: sugar and petro coke. Battery pack is assumed to be of similar layout like that Li-ion battery. Therefore the same components and mass distribution is considered, where 60 % wt is the battery cell, and the casing 34.5 % and BMS 5.5% (Pellow et al., 2020). Inventory for the assembly of Na-S batteries is listed in Table P4. A.11.

Table P4. A.11 Raw materials, assembly and installation data per 1 kg of Na-S battery

Item	Unit	Na-S*
Raw materials		
Battery cell		
Anode	[kg]	0.155 ^a
Cathode	[kg]	0.209 ^a
Separator	[kg]	0.012 ^a

Item	Unit	Na-S*
Electrolyte	[kg]	0.085 ^a
Cell container	[kg]	0.139 ^a
Module and battery packaging	[kg]	0.345 ^b
Battery management system (BMS)	[kg]	0.055 ^b
Assembly and installation		
Electricity	[kWh]	3.64 ^a
Heat	[MJ]	26.31 ^a
Water	[kg]	380 ^a
Infrastructure	[unit]	4·10 ^{-10a}
Transport		
Transport lorry (battery cell components)	[km]	100 ^c
Transport freight train	[km]	542 ^c
Air emissions		
Waste heat	[MJ]	0.469 ^a

* Sugar precursor

^a Peters et al. (2016) ^b Pellow et al. (2020) ^c Wernet et al. (2016)

A.II.10. H₂ storage system

This section describes a hydrogen storage system that uses electrolysis to generate hydrogen from the power grid or from on-site sources. There are various water electrolysis-based hydrogen generation technologies available, with the most market-mature being alkaline water electrolyzer (AWE) and polymer-electrolyte-membrane (PEMWE) (Grigoriev et al., 2020). Hydrogen storage option include pressurized vessels, geological storage, and other underground storage. Despite the benefits of using geologic bulk storage in the natural gas industry, its geographical applicability is limited, and more research is needed to determine its broad applicability. As a result, pressurised vessels are taken into account in this study. Finally, once hydrogen has been compressed and stored, it can be used to generate electricity via gas turbines or fuel cells. Because of their reliability and higher performance, the latter are preferred for research. As a result, the main components of hydrogen storage are: (i) water electrolyzer, (ii) a hydrogen storage tank, and (iii) a fuel cell. Figure 2 illustrates a high-level schematic. in **Error! Reference source not found.**

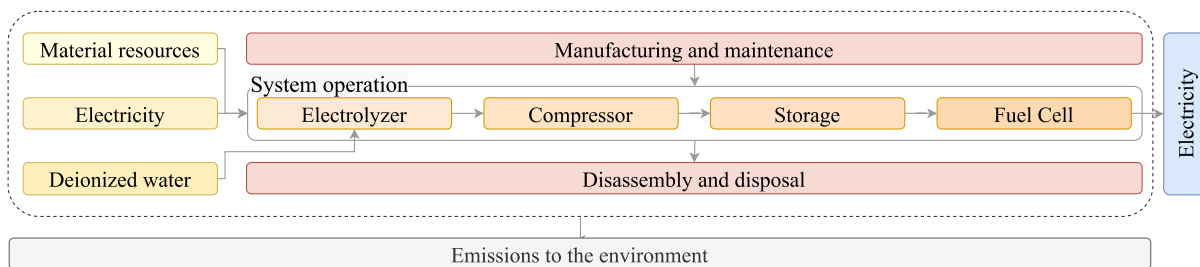


Figure P4.1. System boundaries for the hydrogen storage based on hydrogen production via electrolysis

A.II.10.1. Electrolyzer

Data was adopted from Bareiß et al. (2019), from a 1 MW power PEM electrolyzer, since the author's use laboratory and manufacturer sources. The cell comprises and iridium anode, platinum cathode and a titanium bipolar plate. Nafion composes the polysulfonic acid membrane mainly.

Note that balance of plant (BOP) components, such as gas purifier, heat exchanger, pumps, are not part of the scope, as Bareiß et al. (2019) shows that they have a minor impact in comparison to the electricity consumption.

Table P4. A.12 Raw materials, assembly and installation data per 1 MW of PEMEW

Item	Unit	Value
Raw materials		
Cell stack		
Titanium	[kg]	528 ^a
Aluminium	[kg]	27 ^a
Stainless steel	[kg]	100 ^a
Copper	[kg]	4.5 ^a
Nafion@*	[kg]	16 ^a
Activated carbon	[kg]	9 ^a
Iridium	[kg]	0.75 ^a
Platinum	[kg]	0.075 ^a
Assembly and installation	[kg]	200
Electricity***	[MWh]	5.36 ^b
Infrastructure	[unit]	1.9·10 ⁻⁸
Operation		
De-ionized water	[t]	273.46 ^c
Silica gel heat	[MWh]	0.05 ^c
Transport		
Transport lorry (cell stack components)	[km]	100 ^c
Transport freight train	[km]	542 ^c

*Nafion is assumed as Polytetrafluoroethylene granulate (PTFE)

**Iridium impact is assumed as Platinum

*** Assumed that PEM fuel cell and PEM electrolyzer production requires the same amount of electricity

^a Bareiß et al. (2019)

^c Assuming de-ionized water 9.1 kg/kg H₂ and 119 800 kJ/kg H₂

A.II.10.2. Storage tank

The hydrogen produced is stored in gas cylinders at a pressure of 40 bar, which corresponds the outlet pressure of the electrolyzer. The materials for the hydrogen tank are sourced from Agostini et al. (2018) and Hua et al. (2010)

Table P4. A.13 Raw materials data per 10 kWh of hydrogen storage

Item	Unit	Value
Raw materials		
Pressure vessel liner		
Aluminium alloy	[kg]	15.00
Overwrap		
Carbon fiber	[kg]	12.60
Epoxy resin		8.40
Bosses		
Stainless steel	[kg]	0.50
Insulation		
Glass fiber	[kg]	0.41
Balance of plant		
Stainless steel	[kg]	0.93

^aAgostini et al. (2018) and ^bHua et al. (2010)
Considering 33.3 MWh t⁻¹ H₂

A.II.10.3. Fuel cell

Fuel cell materials are taken from Stropnik et al. (2019)

Table P4. A.14 Raw materials, assembly and installation data per 0.01 MW of PEMFC

Item	Unit	Value
Raw materials		
Cell stack		
Graphite	[kg]	1.8
Polyvinylidene chloride (PVdC)	[kg]	0.5
Aluminum	[kg]	0.6
Chromium steel	[kg]	0.04
Glass fibers	[kg]	0.5
Nafion®*	[kg]	12
Carbon black	[kg]	0.15
Platinum	[kg]	1.4
Balance of plant		
Polyethylene high density granulate (HDPE)	[kg]	1.5
Chromium steel	[kg]	1.1
Cast iron	[kg]	4.5
Aluminum	[kg]	0.75
Polypropylene granulate (PP)	[kg]	0.25
Assambly and installation		
Electricity	kWh	16.9
Infrastructure	[unit]	1.9·10 ⁻⁸

Item	Unit	Value
Transport		
Transport lorry (cell stack components)	[km]	100 °
Transport freight train	[km]	542 °

*Nafion is assumed as Polytetrafluoroethylene granulate (PTFE)

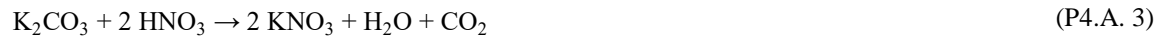
A.II.11. Molten salt system

Molten salt system comprises two tank storages, which contain the hot and cold molten salt. Due to the higher temperature, hot storage tank is usually made of stainless steel, while cold storage is made of carbon steel (Kelly, 2010). For both tanks, LCA data was found in the ecoinvent database.

In this work, nitrate salt LiNaK is employed as heat transfer fluid. The nitrate salt comprises: 30 %wt Lithium nitrate (LiNO_3), 18 %wt sodium nitrate (NaNO_3) and 52 %wt potassium nitrate (KNO_3) (Ibrahim et al., 2021). As no detailed LCA dataset was available for the salts, the modelling of each component was made by performing a stoichiometric calculation. Lithium nitrate is synthesized industrially by neutralizing nitric acid with lithium carbonate.



Analogous reactions can be found for sodium nitrate and potassium nitrate production:



LCA data can be found in Ecoinvent database, while heat requirement to melt the salt was given by (Viebahn et al., 2008), and accounts for 0.38 MJ/kg.

Table P4. A.15 1 kg of reactants per kg of nitrate salt

	XCO_3 [kg]	HNO_3 [kg]
LiNO_3 , [1 kg]	0.54	0.91
NaNO_3 , [1 kg]	0.62	0.74
KNO_3 , [1 kg]	0.68	0.62

Structural steel in form of low-alloyed steel and chromium steel. Moreover, the elevated platforms in the thermal storage system are made of heavy structural steel. The storage tanks are insulated using a 12" (cold tank) to 16" (hot tank) thick lagging made of calcium silicate and mineral wool.

The concrete work and the site work of the storage system stems from the construction of elevated platforms and the construction of the storage foundations. This includes the excavation and backfill

works, concrete, embedded metals, reinforced steel and foam glass, sand and refractory bricks for the tank foundations.

Table P4. A.16 Raw materials, assembly and installation data per 1 MWh of molten salt system

Item	Unit	Value
Raw materials		
Storage tanks		
Reinforcing steel	[kg]	117.46
Stainless steel	[kg]	127.49
Mineral wool	[kg]	88.11
Molten salt		
Lithium nitrate (LiNO ₃)		
Lithium carbonate (Li ₂ CO ₃)	[kg]	1088.23
Nitric acid (HNO ₃)	[kg]	1833.87
Sodium nitrate (NaNO ₃)		
Sodium carbonate (Na ₂ CO ₃)	[kg]	749.67
Nitric acid (HNO ₃)	[kg]	894.77
Potassium nitrate (KNO ₃)		
Potassium carbonate (K ₂ CO ₃)	[kg]	2375.30
Nitric acid (HNO ₃)	[kg]	2165.71
Elevated Platform		
Reinforcing steel	[kg]	30.58
Assembly and installation		
Reinforce steel	[kg]	4.4
Concrete	[m ³]	34.06
Foam glass	[kg]	21.61
Heat (initial salt melting)	[MJ]	31.2

Reference

- Abbas, A. M. (2015) *Life Cycle Assesment of Water Heating Systems Used in Health Clubs*. MSc, An-Najah National University, Nablus-Palestine.
- Alonso-Vicario, A., Ochoa-Gómez, J. R., Gil-Río, S., Gómez-Jiménez-Aberasturi, O., Ramírez-López, C. A., Torrecilla-Soria, J. & Domínguez, A. (2010) 'Purification and upgrading of biogas by pressure swing adsorption on synthetic and natural zeolites', *Microporous and Mesoporous Materials*, 134(1), pp. 100-107.
- Andiappan, V. (2016) *SYSTEMATIC APPROACHES FOR SYNTHESIS, DESIGN AND OPERATION OF BIOMASS-BASED ENERGY SYSTEMS*. PhD, University of Nottingham, Nottingham.
- Barei, K., de la Rua, C., Mckl, M. & Hamacher, T. (2019) 'Life cycle assessment of hydrogen from proton exchange membrane water electrolysis in future energy systems', *Applied Energy*, 237, pp. 862-872.

- Frischknecht, R. J., N.; Althaus, H.-J.; Doka, G.; Heck, T.; Hellweg, S.; Hirschier, R.; Nemecek, T.; Rebitzer, G.; Spielmann, M.; Wernet, G.; Frischknecht, R.; Jungbluth, N. (2007) *Overview and Methodology. Ecoinvent report No. 1*, Dübendorf, Switzerland: Swiss Centre for Life Cycle Inventories.
- Grigoriev, S. A., Fateev, V. N., Bessarabov, D. G. & Millet, P. (2020) 'Current status, research trends, and challenges in water electrolysis science and technology', *International Journal of Hydrogen Energy*, 45(49), pp. 26036-26058.
- Hiremath, M., Derendorf, K. & Vogt, T. (2015) 'Comparative Life Cycle Assessment of Battery Storage Systems for Stationary Applications', *Environmental Science & Technology*, 49(8), pp. 4825-4833.
- Ibrahim, A., Peng, H., Riaz, A., Abdul Basit, M., Rashid, U. & Basit, A. (2021) 'Molten salts in the light of corrosion mitigation strategies and embedded with nanoparticles to enhance the thermophysical properties for CSP plants', *Solar Energy Materials and Solar Cells*, 219, pp. 110768.
- Kelly, K. A., McManus, M. C. & Hammond, G. P. (2014) 'An energy and carbon life cycle assessment of industrial CHP (combined heat and power) in the context of a low carbon UK', *Energy*, 77, pp. 812-821.
- Majeau-Bettez, G., Hawkins, T. R. & Strømman, A. H. (2011) 'Life cycle environmental assessment of lithium-ion and nickel metal hydride batteries for plug-in hybrid and battery electric vehicles', *Environ Sci Technol*, 45(10), pp. 4548-54.
- Martín-Hernández, E., Sampat, A. M., Zavala, V. M. & Martín, M. (2018) 'Optimal integrated facility for waste processing', *Chemical Engineering Research and Design*, 131, pp. 160-182.
- Notter, D. A., Gauch, M., Widmer, R., Wäger, P., Stamp, A., Zah, R. & Althaus, H.-J. (2010) 'Contribution of Li-Ion Batteries to the Environmental Impact of Electric Vehicles', *Environmental Science & Technology*, 44(17), pp. 6550-6556.
- Parat Halvorsen AS. (2021). *PARAT IEH: High Voltage Electrode boiler for Steam and Hot water* [Online]. Available at: <https://parat.no/ieh/> [Accessed].
- Pellow, M. A., Ambrose, H., Mulvaney, D., Betita, R. & Shaw, S. (2020) 'Research gaps in environmental life cycle assessments of lithium ion batteries for grid-scale stationary energy storage systems: End-of-life options and other issues', *Sustainable Materials and Technologies*, 23, pp. e00120.
- Peters, J., Buchholz, D., Passerini, S. & Weil, M. (2016) 'Life cycle assessment of sodium-ion batteries', *Energy & Environmental Science*, 9(5), pp. 1744-1751.
- Tagliaferri, C., Evangelisti, S., Clift, R. & Lettieri, P. (2018) 'Life cycle assessment of a biomass CHP plant in UK: The Heathrow energy centre case', *Chemical Engineering Research and Design*, 133, pp. 210-221.
- Wernet, G., Bauer, C., Steubing, B., Reinhard, J., Moreno-Ruiz, E. & Weidema, B. (2016) 'The ecoinvent database version 3 (part I): overview and methodology', *The International Journal of Life Cycle Assessment*, 21(9), pp. 1218-1230.

SUPPLEMENTARY INFORMATION P4.B

Mathematical model

Abbreviation

amb	ambient
BFW	Boiler feed water
boi	boiler
C	Heat sink side
CBFW	Boiler feed water used at the heat sink side
cmdty	Commodity
Cond	condensate
CT	Total process steam use (at the heat sink side)
Deae	deaerator
eq	equipment
exh	Exhaust gases
FSR	Flash steam recovery
H	Heat source side
HO	Hot oil
HRSG	Heat recovery steam generator
HS	Hydrogen storage
LiB	Lithium-ion battery
loss	Heat losses
MILP	Mixed integer linear programming
MINLP	Mixed integer non liner programming
MS	Molten salt system
NaS	Sodium sulphur battery
NHV	Net heat value
pre	Preheating stage - economizer
SA	Steam accumulator
SF	Supplementary firing
sh	superheated
SSE	Sum of squared errors
ST	Steam turbine
stack	Stack gases
TAC	Total Annualized Cost
UC	Utility components
vap	Evaporation stage - evaporator
VHP	Very High Pressure
w	Treated water

Sets

C	Set of cold streams
CMDTY	Set of utility commodities
EQ	Set of utility equipment for thermal and/or power generation (subset of utility components)
ES	Set of energy storage units
F _{eq}	Set of fuels for each equipment
H	Set of hot streams
I	Set of steam mains
IJs	Set of steam levels js that belong to steam main i (i,js)
J	Set of temperature/pressure intervals
J _{HO}	Set of temperature/pressure intervals for hot oil (subset of temperature intervals)
J _s	Set of temperature/pressure intervals for steam main (subset of temperature intervals)
J _{WH}	Set of temperature/pressure intervals for waste heat (subset of temperature intervals)
k	Set of representative days
MS	Set of molten salt systems (subset of energy storage ES)
SA	Set of steam accumulators (subset of energy storage ES)
t	Set of intra time-periods
UC	Set of utility components
VHP _L	Set of VHP steam levels

Parameters

α	Vent rate in the deaerator
β	Condensate return rate
γ	Blowdown rate
$\Delta T_{\min}^{\text{HRSG}}$	Minimum approach temperature difference for HRSG
ζ	Upper bound of heat content of gas turbine exhausts
$\eta_{\text{eff}}^{\text{HRSG}}$	Radiation efficiency of HRSG
$c_{p_{\text{exh}}}$	Heat capacity of exhaust gases
ψ_{uc}	Cost exponent for each utility component
γ	Blowdown rate
$\sigma(d)$	Function that correlates the design day k corresponding to day of the year d
Λ	Vector that represents part of the slope in the modelling of power generation units
Δt_t	Duration of the time interval t
$\Delta t_{\text{eq}}^{\text{start}}$	Duration of start-up of equipment eq
$g_{\text{es}}^{\text{loss}}$	Self-discharge coefficient of storage unit es
$\underline{\Omega}_{\text{eq}}$	minimum feasible load operation of each equipment
τ_{es}	time required to fully charge/discharge the unit es
$\widetilde{a}_{11}, \widetilde{a}_{12}$	Model coefficients for boilers
$\widetilde{a}_{21}, \widetilde{a}_{22}, \widetilde{a}_{23}, \widetilde{a}_{24}$	Model coefficients for power generation units, based on Willan's line correlation
$C_{\text{eq}}^{\text{ref}}$	Reference cost for each equipment
$CP_{k,t}^C c_i$	Heat capacity flowrate of cold stream c_i , at any given time period
$CP_{h_i,k,t}^H$	Heat capacity flowrate of hot stream h_i , at any given time period
DoD_{es}	Depth of discharge of energy storage unit es
$F_{\text{uc}}^{\text{ann}}$	Annualization factor of utility component uc
$F_{\text{uc}}^{\text{inst}}$	Installation factor of utility component uc
$F_{\text{uc}}^{\text{main}}$	Maintenance factor of utility component uc
$F_{\text{eq}}^{\text{start}}$	Fraction of fuel used per start-up of equipment eq

$\underline{h}_{sh}, \overline{h}_{sh}$	Lower and upper bound for steam enthalpy at superheated stage
$\widetilde{h}_{sh_j^H}, \widetilde{h}_{sh_j^C}$	Enthalpy of superheated process steam generation (H) and use (C) at steam level L
$\widetilde{h}_l, \widetilde{h}_v$	Enthalpy of saturated liquid and vapour, respectively
\widetilde{h}^{BFW}	Enthalpy of boiling feed water
\widetilde{h}^{Cond}	Enthalpy of returned condensate
\widetilde{h}^{vent}	Enthalpy of steam vented
\widetilde{h}^W	Enthalpy of treated water
L^H, L^C	Heat losses due to distribution at the source and sink side, respectively
L^e	Electrical losses for transmission to/from the national grid
Lim_f	Upper limit of fuel f
$\underline{m}_{f_{eq,k,t}}^F, \overline{m}_{f_{eq,k,t}}^F$	Lower and upper bound of fuel at a specific time period
$NHV_{f_{eq}}$	Net heat value of fuel f_{eq}
$N_{max_{eq}}^{start}$	Maximum number of start-ups permissible per day corresponding to unit eq
$\eta_{es}^{ch}, \eta_{es}^{dch}$	Charging and discharging efficiency of storage unit es
η_{shEB}	Efficiency of electric superheater of electrode boiler EB
$P_{cmdty_{k,t}}$	Commodity price at specific time period
P_{EB}^{max}	Maximum steam pressured allowed in electrode boiler EB
P_v	Steam pressure at v conditions
$\widetilde{Q}_{j,k,t}^C$	Process heat sink at level j , at any given time period
$\widetilde{Q}_{j,k,t}^H$	Process heat source at level j , at any given time period
T_j	Utility temperature at level j
T^{*in}, T^{*out}	Shifted inlet and outlet stream temperatures
$t_{op_{k,t}}$	Duration of specific time period
\widetilde{T}_{amb}	Ambient temperature
\widetilde{T}_{FG}	Inlet temperature of flue gas from indirect gasification
\widetilde{T}_v^{sat}	Saturated steam temperature at v conditions
$\widetilde{T}_{min}^{stack}$	Minimum stack temperature for exhaust gases
$\widetilde{T}_{max}^{SF}, \widetilde{T}_{max}^{UF}$	Maximum temperature achievable with and without supplementary firing, respectively.
$\widetilde{U}_{max}^{exp}, \widetilde{U}_{max}^{imp}$	Upper bound for export and import of grid electricity
U_{es}	Representative parameter of the upper boundaries of storage unit es variables
$U_{k,t}^m, U_{k,t}^Q$	Parameter vector representing upper bounds for mass and energy vectors of variables, at any given time period
$\widetilde{W}_{k,t}^{dem}$	Power demand at any given time period
\widetilde{Z}_{eq}^{ref}	Equipment reference size for capital cost estimation
$\underline{Z}_{eq}, \overline{Z}_{eq}$	Lower and upper size limits for each equipment

Variables

C_{cmdty}^{op} Operating costs of commodities

Positive variables

$\delta_{eq,\theta,k,t}^{start}$ Continuous variable with values between 0 and 1, that indicates if equipment eq operating at θ conditions is started-up at time t

C_{uc}^{inv} Investment cost of utility component uc

C_{uc}^{main} Maintenance cost of each utility component uc

C^{start} Start-up costs

$E_{es,d,t}^{es}$ Energy stored in unit es at any given time step

h_{sh,j_s} Enthalpy of of superheated steam at steam level j_s

$h_{sh,v}$ Enthalpy of superheated steam at VHP steam main operating at v conditions

$L_{es,d,t}$ Losses of storage unit es at any given time period

$m_{T,k,t}^{BFW}$ Total mass flowrate of boiler feed water in the site at any given time period

$m_{i,j_s,k,t}^{CBFW}$ Steam mass flow rate of BFW injected to desuperheated steam operating at j_s conditions, at any given time period

$m_{i,j_s,k,t}^{Cond}$ Condensate mass flow rate from steam main i operating at level j_s , at any given time period

$m_{i,j_s,k,t}^{CT}$ Process steam use at steam level j_s , at any given time period

$m_{i,j_s,k,t}^{Deae}$ Steam mass flowrate from LP steam main operating at j_s conditions to deaerator, at any given conditions

$m_{i,j_s,k,t}^{CBFW}$ Steam mass flow rate of BFW injected to desuperheated steam operating at j_s conditions, at any given time period

$m_{i,j_s,j_s',k,t}^{Ch-SA}, m_{i,j_s,j_s',k,t}^{Deh-SA}$ Charging and discharging steam mass flow of steam accumulator operating between steam level j_s to level j_s' , at any given time period

$m_{i,j_s,k,t}^{CFSR}$ Steam mass flow rate of FSR injected to desuperheated steam operating at j_s conditions, at any given time period

$m_{i,j_s,k,t}^{Csteam}$ Process steam use at steam main i instant operating at level j_s , at any given time period

$m_{i,j_s,k,t}^{CT}$ Process steam use at the process use instant at level j_s , at any given time period

$m_{eq,f_{eq},k,t}^F$ Fuel flowrate of type fuel f_{eq} in unit eq at a specific time period

$m_{i,j_s,k,t}^{in}, m_{i,j_s,k,t}^{out}$ Variable vector representing inlet and outlet mass flowrates at steam main i operating at level j_s , at any given time period

$m_{UC,i,j_s,k,t}^{in}$ Variable vector representing mass flows from unit component UC to steam main i (operating at j_s), at any given time period

$m_{UC,i,j_s,k,t}^{out}$ Variable representing mass flows from steam main i (operating at j_s) to unit component UC, at any given time period

$m_{i,j_s,k,t}^H$ Mass flow rate of process steam generation for steam level j_s at any given time period

$m_{i,j_s,k,t}^{MS}$ Steam mass flowrate from molten salt system to steam main i operating at j_s conditions at any given time period

$m_{v,k,t}^{VHP-MS}$ Steam mass flow rate from VHP level v to molten salt system at any given time period

$m_{IG,k,t}^{FG}$ Mass flowrate of flue gas from indirect gasification

$m_{in,i,j_s,k,t}^{FSR}$ Inlet mass flow rate at FSR drum i operating at j_s conditions, at any given time periods

$m_{i,j_s,j_s',k,t}^{FSR}$ Liquid mass flow rate of FSR i operating from pressure j_s to j_s' , at any given time periods

$m_{s,i,j_s,j_s',k,t}^{FSR}$ Steam mass flow rate of FSR i operating from pressure j_s to j_s' , at any given time period

$m_{i,j_s,k,t}^H$ Process steam generation at steam main i instant operating at level j_s , at any given time period

$m_{\text{exh}}^{\text{HRSG}}_{eq, v, k, t}$	Mass flow rate of gas exhausts of unit eq , to generate steam in a HRSG operating at v conditions, at any given time period
$m_{i, j_s, k, t}^{\text{MS}}$	Steam mass flowrate from molten salt system to steam main i operating at j_s conditions at any given time period
$m_{\text{eq}, f, k, t}^{\text{SF}}$	Fuel flowrate of supplementary firing at any given time period
$m_{k, t}^{\text{W}}$	Mass flow rate of treated water at any given time period
$P_{\text{es}, k, t}^{\text{ch}}, P_{\text{es}, k, t}^{\text{ch}}$	Charging and discharging power of storage unit es at any given time period
$Q_{\text{eq}, k, t}^{\text{B}}$	Fuel consumption of boiler eq at period t of design day k
$Q_{\text{eq}, k, t}^{\text{F}}$	Fuel consumed in unit eq at a specific time period
$Q_{i, j_s, k, t}^{\text{in}}, Q_{i, j_s, k, t}^{\text{out}}$	Variable vector representing inlet and outlet energy at steam main i operating at j_s conditions, at any given time period
$Q_{uc, i, j_s, k, t}^{\text{in}}$	Variable vector representing inlet heat flow at steam main i operating at j_s conditions, at any given time period
$Q_{\text{eq}, f, k, t}^{\text{start}}$	Consumption of fuel f required for start-up of equipment eq
$Q_{i, j_s, k, t}^{\text{Cin}}$	Heat available for process heating from steam main i operating at j_s conditions, at any given time period
$Q_{k, t}^{\text{HO}}$	Process heating requirements that cannot be used/satisfied by steam at any given time period
$Q_{s, k, t}^{\text{HO}}$	Process heating provided by hot oil system at steam temperature range, at any given time period
$Q_{\text{T}, k, t}^{\text{HO}}$	Total process heating provided by hot oil system at any given time period
$Q_{\text{eq}, v, k, t}^{\text{HRSG}}$	Heat of the exhaust gases used in the HRSG unit eq operating at v conditions, at any given time period
$Q_{\text{eq}, v, k, t}^{\text{loss}}$	Heat losses to the ambient of exhaust gases of gas turbine eq after HRSG operating at v conditions, at any given time period
$Q_{\text{eq}, v, k, t}^{\text{pre}}, Q_{\text{eq}, v, k, t}^{\text{vap}}, Q_{\text{eq}, v, k, t}^{\text{sh}}$	Heat transfer in each stage of HRSG (eq): preheating (pre), evaporation (vap) and superheating (sh) for generating steam at v conditions, at any given time period
$R_{j_s, k, t}^{\text{C}}$	Residual sink heat at steam level j_s , at any given time period
$R_{j_s, k, t}^{\text{H}}$	Residual source heat at steam level j_s , at any given time period
$T_{\text{sh}, v}^{\text{VHP}}$	Steam temperature at VHP level operating at v conditions
$U_{\text{cmdty}, k, t}$	Variable vector representing site consumption of each commodity, at any given time period
$U_{e, k, t}^{\text{exp}}, U_{e, k, t}^{\text{imp}}$	Electricity export and import at any given time period, respectively
$U_{\text{eq}, f, k, t}^{\text{SF}}$	Fuel consumption of supplementary firing at any given time period
$W_{k, t}^{\text{EB}}$	Power required by the electrode boiler at specific time period
$W_{\text{T}, k, t}^{\text{EB}}$	Total power required by electrode boiler and electric superheater (if selected) at a specific time period
$W_{k, t}^{\text{shEB}}$	Power required by the electric superheater at specific time period
$W_{\text{eq}, k, t}$	Variable vector representing power generated by equipment eq at specific time period
$Z_{\text{eq}, \theta, k, t}$	Equipment load operating at θ conditions at a specific time period
$Z_{\text{eq}, v, k, t}^{\text{boi}}$	Boiler load operation v conditions at any given time period, in [t/h]
$Z_{\text{es}}^{\text{es}}$	Energy storage capacity of unit es
$Z_{\text{eq}, v, k, t}^{\text{HRSG}}$	HRSG load operation v conditions at any given time period, in [t/h]
$Z_{\text{eq}, \theta, k, t}^{\text{m}}$	Auxiliary variable to represent equipment load if unit eq is operation at a specific time period
$Z_{\text{uc}}^{\text{max}}$	Variable vector representing installed capacity of utility component uc
$Z_{\text{eq}, \theta}^{\text{max}}$	Installed equipment size operating at θ conditions

$Z_{eq, v, k, t}^{sh}$ Electric superheater load operating at v conditions at a specific time period

Binary variables

y_{es} Binary variable to denote the activation of energy storage es

$y_{UC, L, L', k, t}$ Variable vector representing equipment operating between level L and L' , at any given time period

$y_{j_s}^{HO}$ Binary variables to denote the selection of hot oil at steam level j_s

y_{i, j_s} Binary variables to denote the selection of steam main i operating at j_s conditions

y_v Binary variable to denote the selection of VHP steam level

$y_{eq, f, eq, k, t}^f$ Binary variable to denote selection of fuel f_{eq} for unit eq at a specific time period

$y_{eq, \theta, k, t}^{op}$ Binary variables to denote the activation of equipment eq operating at θ conditions at a specified time period

$y_{eq, \theta}^s$ Binary variable to denote the selection of equipment eq operating at θ conditions

$y_{eq, v, k, t}^{sh}$ Binary variable to denote the activation of electric superheater eq operating at θ conditions in a specific time period

$y_{eq, f, k, t}^{SF}$ Binary variable to denote activation of supplementary firing at any given time period

B.I. Costs

Table P4.B. 1 Cost equations

Component	Equations/Constraints	
Maintenance	$C_{uc}^{main} = F_{uc}^{main} \cdot C_{uc}^{inv}$	(B.1)
Start-up	$C_{eq}^{start} = \sum_{eq} \sum_{f \in F_{eq}} U_f \cdot Q_{eq, f}^{start} \cdot \Delta t_{eq}^{start}$	(B.2)
Operation	$C_{cmdty}^{op} = \sum_{k \in K} \sum_{t \in T} U_{cmdty, k, t} \cdot P_{cmdty, k, t} \cdot t_{op, k, t}$	(B.3)

B.II. Mass, energy and electricity balance

Table P4.B. 2 Mass, energy and electricity balance equations

Component	Equations/Constraints	
Mass balance	$m_{i, j_s, k, t}^H + m_{i, j_s, k, t}^{MS} + \sum_{uc \in UC_L} m_{uc, i, j_s, k, t}^{in} = \sum_{uc \in UC_L} m_{uc, i, j_s, k, t}^{out} + m_{i, j_s, k, t}^{C-steam}$	(B.4)
Energy balance	$m_{i, j_s, k, t}^H \cdot \tilde{h}_{sh, j_s}^H + m_{i, j_s, k, t}^{MS} \cdot \tilde{h}_{sh, j_s}^{MS} + \sum_{uc \in UC} Q_{uc, i, j_s, k, t}^{in} = \sum_{uc \in UC} (m_{uc, i, j_s, k, t}^{out} \cdot h_{sh, j_s} + m_{i, j_s, k, t}^{C-steam} \cdot h_{sh, j_s})$	(B.5)
Electricity balance	$U_{e, k, t}^{imp} + \sum_{eq \in \{GT, ST\}} W_{eq, k, t} + P_{es, k, t}^{del} = (1+L^e) \cdot \tilde{W}_{k, t}^{dem} + W_{T, k, t}^{EB} + P_{es, k, t}^{ch} + U_{e, k, t}^{exp}$	(B.6)
	Restriction: $U_{e, k, t}^{imp} \leq \tilde{U}_{max}^{imp}$ and $U_{e, k, t}^{exp} \leq \tilde{U}_{max}^{exp}$	
Heat cascades	Heat source cascade: $\tilde{Q}_{j_s, k, t}^H + Q_{j_s, k, t}^{SG} + R_{j_s-1, k, t}^H = m_{i, j_s, k, t}^H \cdot (1+L^H) \cdot (\tilde{h}_{sh, j_s}^H - \tilde{h}^{BFW}) + R_{j_s, k, t}^H$	(B.7)
	Heat sink cascade: $m_{i, j_s, k, t}^{CT} \cdot (1-L^C) \cdot (\tilde{h}_{sh, j_s}^C - \tilde{h}_{j_s}^C) + Q_{s, k, t}^{HO} + R_{j_s-1, k, t}^C = \tilde{Q}_{j_s, k, t}^C + R_{j_s, k, t}^C$ $m_{i, j_s, k, t}^{CT} \cdot (1-L^C) \cdot (\tilde{h}_{sh, j_s}^C - \tilde{h}_{j_s}^C) + R_{j_s-1, k, t}^C = \tilde{Q}_{j_s, k, t}^C + R_{j_s, k, t}^C$	(B.8)

B.III. Utility components

Table P4.B. 3 Equations of equipment performance and constraints

Component	Equations/Constraints	
Selecting, sizing and load	Selection and sizing	(B.9)
	$\underline{Z}_{eq} \cdot y_{eq,\theta}^s \leq Z_{eq,\theta}^{max} \leq \overline{Z}_{eq} \cdot y_{eq,\theta}^s$ $\underline{\Omega}_{eq} \cdot Z_{eq,\theta}^{max} \leq Z_{eq,\theta,k,t} \leq Z_{eq,\theta}^{max}$	
	Operation:	(B.10)
	$y_{eq,\theta,k,t}^{op} \leq y_{eq,\theta}^s$	
	Load:	(B.11)
	$\underline{\Omega}_{eq} \cdot Z_{eq,\theta,t}^m \leq Z_{eq,\theta,t} \leq Z_{eq,\theta,t}^m$ $\underline{Z}_{eq} \cdot y_{eq,\theta,k,t}^{op} \leq Z_{eq,\theta,t}^m \leq \overline{Z}_{eq} \cdot y_{eq,\theta,k,t}^{op}$ $Z_{eq,\theta}^{max} - \overline{Z}_{eq} (1 - y_{eq,\theta,k,t}^{op}) \leq Z_{eq,\theta,k,t}^m \leq Z_{eq,\theta}^{max}$	
Start-up	Maximum start-ups	(B.12)
	$\sum_{t \in T} \delta_{eq,\theta,k,t}^{start} \leq N_{max,eq}^{start}$	
	Logical constraints:	(B.13)
	$\delta_{eq,\theta,k,t}^{start} \leq y_{eq,\theta,k,t}^{op}$ $\delta_{eq,\theta,k,t}^{start} \geq y_{eq,\theta,k,t}^{op} - y_{eq,\theta,k,t-1}^{op}$ $\delta_{eq,\theta,k,t}^{start} \leq 1 - y_{eq,\theta,k,t-1}^{op}$ $\delta_{eq,\theta,\sigma(d),t_1}^{start} \geq y_{eq,\theta,\sigma(d),1}^{op} - y_{eq,\theta,\sigma(d-1),t_n}^{op}$ $\delta_{eq,\theta,\sigma(d),t_1}^{start} \leq 1 - y_{eq,\theta,\sigma(d-1),t_n}^{op}$ $\delta_{eq,\theta,\sigma(1),t_1}^{start} \geq y_{eq,\theta,\sigma(1),1}^{op} - y_{eq,\theta,\sigma(D),t_n}^{op}$ $\delta_{eq,\theta,\sigma(1),t_1}^{start} \leq 1 - y_{eq,\theta,\sigma(D),t_n}^{op}$	
	Start-up fuel consumption	(B.14)
	$Q_{eq,f,k,t}^{start} \geq F_{eq}^{start} Q_{eq,\theta}^{F,max} - F_{eq}^{start} m_{eq,k,t}^F (1 - \delta_{eq,\theta,k,t}^{start})$ $Q_{eq,f,k,t}^{start} \leq F_{eq}^{start} Q_{eq,\theta}^F$	
Fossil fuel and biomass boilers	$Q_{eq,k,t}^B = \sum_{v \in VHP_L} \left[(h_{sh,v} - \tilde{h}^{BFW}) (\tilde{a}_{11} \cdot Z_{eq,v,t} + \tilde{a}_{12} \cdot Z_{eq,v,k,t}^m) + \gamma \cdot Z_{Eq,v,t} (\tilde{h}_{1v} - \tilde{h}^{BFW}) \right]$	(B.15)
Electrode boilers	Total electricity requirement:	(B.16)
	$W_{T,k,t}^{EB} = W_{k,t}^{EB} + W_{k,t}^{shEB}$	
	Electrode boiler:	(B.17)
	$W_{k,t}^{EB} = \sum_{P_v \leq P_{EB}^{max}} \sum_{eq \in EB} Z_{eq,v,k,t} (\tilde{h}_{v,v} - \tilde{h}^{BFW}) + \gamma \cdot Z_{Eq,v,k,t} (\tilde{h}_{1v} - \tilde{h}^{BFW})$	
	Superheater:	(B.18)
	$W_{k,t}^{shEB} = \frac{1}{\eta_{shEB}} \sum_{v: P_v \leq P_{EB}^{max}} \sum_{eq \in EB} (h_{sh,v} - \tilde{h}_{v,v}) Z_{eq,v,k,t}^{sh}$	
	Logical constraints	(B.19)
	$Z_{eq,v,k,t} - \overline{Z}_{eq}^{sh} \sum_{v: P_v \leq P_{EB}^{max}} (1 - y_{eq,v,k,t}^{sh}) \leq Z_{eq,v,k,t}^{sh} \leq Z_{eq,v,k,t}$ $Z_{eq,v,k,t}^{sh} \leq \overline{Z}_{eq}^{sh} y_{eq,v,k,t}^{sh}$	
Heat recovery steam generator (HRSG)	Energy balance at each stage:	(B.20)
	$Q_{eq,k,t}^{exh} = \sum_v [Q_{eq,v,k,t}^{loss} + Q_{eq,v,k,t}^{HRSG}]$ $Q_{eq,v,k,t}^{HRSG} = Q_{eq,v,k,t}^{sh} + Q_{eq,v,k,t}^{vap} + Q_{eq,v,k,t}^{pre}$ $Q_{eq,v,k,t}^{sh} = \frac{1}{\eta_{eff}^{HRSG}} [(h_{sh,v} - \tilde{h}_{v,v}) \cdot Z_{eq,v,k,t}^{HRSG}]$ $Q_{eq,v,k,t}^{vap} = \frac{1}{\eta_{eff}^{HRSG}} [(\tilde{h}_{v,v} - \tilde{h}_{1v}) \cdot Z_{eq,v,k,t}^{HRSG}]$ $Q_{eq,v,k,t}^{pre} = \frac{1}{\eta_{eff}^{HRSG}} [(\tilde{h}_{pre,v} - \tilde{h}^{BFW}) (1 + \gamma) \cdot Z_{eq,v,k,t}^{HRSG}]$	(B.21)
	Heat transfer feasibility:	(B.22)
	$Q_{eq,v,k,t}^{loss} \geq m_{exh,eq,v,k,t}^{HRSG} \cdot cp_{exh} (\tilde{T}_{min}^{stack} - \tilde{T}_{amb})$	

Component	Equations/Constraints
	$Q_{eq,v,k,t}^{pre} + Q_{eq,v,k,t}^{loss} \geq m_{exh,eq,v,k,t}^{HRSG} \cdot cp_{exh} \left(\tilde{T}_v^{sat} + \Delta T_{min}^{HRSG} - \tilde{T}_{amb} \right)$ $Q_{eq,v,k,t}^{exh} \geq m_{exh,eq,v,k,t}^{HRSG} \cdot cp_{exh} \left(T_{sh_v}^{VHP} + \Delta T_{min}^{HRSG} - \tilde{T}_{amb} \right)$
	<p>Supplementary firing:</p> $\sum_v Q_{eq,v,k,t}^{exh} = Q_{eq,k,t}^{exh} + \sum_{IG} m_{IG,k,t}^{FG} \cdot cp_{exh} \left(\tilde{T}_{FG} + \Delta T_{min}^{HRSG} - \tilde{T}_{amb} \right) + \sum_f U_{eq,f,k,t}^{SF}$ <p>where $U_{eq,f,k,t}^{SF} = m_{eq,f,k,t}^{SF} \cdot NHV_f$</p> $m_{eq,f,k,t}^{SF} \leq \text{Lim}_f y_{eq,f,k,t}^{SF} \quad \text{and} \quad \sum_f y_{eq,f,k,t}^{SF} \leq y_{eq}$
	$Q_{eq,v,k,t}^{exh} \leq m_{exh,eq,v,k,t}^{HRSG} \cdot cp_{exh} \left(\tilde{T}_{max}^{UF} - \tilde{T}_{amb} \right) + \zeta \cdot \sum_{f \in F} y_{eq,f,k,t}^{SF}$
	$Q_{eq,v,k,t}^{exh} \leq m_{exh,eq,v,k,t}^{HRSG} \cdot cp_{exh} \left(\tilde{T}_{max}^{SF} - \tilde{T}_{amb} \right) + \zeta \cdot \sum_{f \in F} \left(1 - y_{eq,f,k,t}^{SF} \right)$
Turbines	$W_{eq,k,t} = \sum_{\theta} \left[\tilde{a}_{21} \left(\Lambda_{\theta} - \frac{\tilde{a}_{22}}{Z_{eq,\theta,k,t}^m} \right) Z_{eq,\theta,k,t} + \tilde{a}_{23} \left(\Lambda \cdot Z_{eq,\theta,k,t}^m + \tilde{a}_{24} \cdot y_{eq,\theta,k,t}^{op} \right) \right]$
Biomass gasifier	<p>Steam requirement:</p> $\sum_{i \in I_n} \sum_{j_s \in J_s} m_{i,j_s,k,t}^{dry} \cdot h_{sh_{j_s}} = \sum_{f_{eq} \in \text{BIO}} \Delta h^{dry} \cdot k_{f_{eq,k,t}}^{dry} \cdot m_{IG,f_{eq,k,t}}^F$ $m_{k,t}^{IG} = \sum_{f_{eq} \in \text{FIG}} k_{f_{eq}}^{IG} \cdot m_{IG,f_{eq,k,t}}^F$ $m_{k,t}^{SR} = \sum_{f_{eq} \in \text{FIG}} k_{f_{eq}}^{SR} \cdot m_{IG,f_{eq,k,t}}^F$
	<p>Flue gas:</p> $m_{k,t}^{fg} = \sum_{f_{eq} \in \text{FIG}} k_{f_{eq}}^{fg} \cdot m_{IG,f_{eq,k,t}}^F$
	<p>Syngas generation:</p> $m_{f_{eq,k,t}}^{SG} = k_{f_{eq}}^{SG} \cdot m_{IG,f_{eq,k,t}}^F$
	<p>Steam desuperheating:</p> $\sum_{i \in I_n} \sum_{j_s \in J_s} m_{i,j_s,k,t}^{S_{IG}} + m_{k,t}^{BFW_{IG}} = m_{k,t}^{IG}$ $\sum_{i \in I_n} \sum_{j_s \in J_s} m_{i,j_s,k,t}^{S_{IG}} \cdot h_{sh_{j_s}} + m_{k,t}^{BFW_{IG}} \cdot h^{BFW} = m_{k,t}^{IG} \cdot h^{IG}$ $\sum_{P_i \geq P_{SR}} \sum_{j_s \in J_s} m_{i,j_s,k,t}^{S_{SR}} + m_{k,t}^{BFW_{SR}} = m_{k,t}^{SR}$ $\sum_{P_i \geq P_{SR}} \sum_{j_s \in J_s} m_{i,j_s,k,t}^{S_{SR}} \cdot h_{sh_{j_s}} + m_{k,t}^{BFW_{SR}} \cdot h^{BFW} = m_{k,t}^{SR} \cdot h^{SR}$
	<p>Fuel constraint:</p> $m_{f_{eq,k,t}}^{SG} \leq \overline{m_{f_{eq,k,t}}^F} \cdot y_{IG,k,t}^o$ $m_{f_{eq,k,t}}^{SR} \leq \overline{m_{f_{eq,k,t}}^F} \cdot y_{IG,k,t}^o$ $m_{FFB,f_{eq,k,t}}^F + m_{GT,f_{eq,k,t}}^F + m_{HRSG,f_{eq,k,t}}^F \leq m_{f_{eq,k,t}}^{SG}$
Anaerobic Digester	$m_{AD,k,t}^{SAD} = k^{SAD} m_{AD,k,t}^{WAD}$ $m_{AD,k,t}^{biogasAD} = k^{biogasAD} m_{AD,k,t}^{AD}$ $m_{AD,k,t}^{CH_4AD} = k^{CH_4AD} m_{AD,k,t}^{biogasAD}$ $m_{AD,k,t}^{CO_2AD} = k^{CO_2AD} m_{AD,k,t}^{biogasAD}$ $m_{AD,k,t}^{digAD} = k^{digAD} m_{AD,k,t}^{AD}$
Electrolyzer and Fuel cell	$P_{eq,k,t} \leq \alpha_{eq} Z_{eq,k,t} + \beta_{eq} Z_{eq,k,t}^m$
	<p>Heat from fuel cell:</p> $Q_{PEMFC,k,t} = \gamma_{PEMFC} P_{PEMFC,k,t} + \beta_{PEMFC} Z_{PEMFC,k,t}^m$
Flash steam recovery (FSR)	<p>Mass balance at the FSR inlet:</p> $\beta \cdot m_{i,j_s,k,t}^{CT} + \sum_{i < j_s} \sum_{j_s' \in I_{j_s}} m_{i,j_s',k,t}^{FSR} = m_{i,j_s,k,t}^{FSR}$
	<p>Overall mass and energy balance:</p> $\sum_{T > i} \sum_{(j_s') \in I_{j_s}} \left(m_{s,i,j_s',k,t}^{FSR} + m_{h,i,j_s',k,t}^{FSR} \right) = m_{in,i,j_s,k,t}^{FSR}$ $\sum_{T > i} \sum_{(j_s') \in I_{j_s}} \left(m_{s,i,j_s',k,t}^{FSR} \cdot \tilde{h}_{v,j_s'} + m_{h,i,j_s',k,t}^{FSR} \cdot \tilde{h}_{j_s'} \right) = m_{in,i,j_s,k,t}^{FSR} \cdot \tilde{h}_{v,j_s}$
Deaerator	<p>Mass and energy balance at the deaerator:</p>

Component	Equations/Constraints
(Deae)	$m_{T,k,t}^{BFW} = m_{k,t}^W + \sum_{i \in I} \sum_{(i,j) \in I_s} m_{i,j_s,k,t}^{Cond} + (1-\alpha) \sum_{i \in I_n} \sum_{(i,j) \in I_s} m_{i,j_s,k,t}^{Deae}$ $m_{T,k,t}^{BFW} \cdot \tilde{h}^{BFW} + \sum_{i \in I_n} \sum_{(i,j) \in I_s} (\alpha \cdot m_{i,j_s,k,t}^{Deae} \cdot \tilde{h}^{vent}) = \sum_{i \in I} \sum_{(i,j) \in I_s} (m_{i,j_s,k,t}^{Cond} \cdot \tilde{h}^{Cond}) + m_{k,t}^W \cdot \tilde{h}^W + \sum_{i \in I_n} \sum_{(i,j) \in I_s} (m_{i,j_s,k,t}^{Deae} \cdot h_{shj_s})$ <p>System mass balance of BFW:</p> $m_{T,k,t}^{BFW} = \sum_{i \in I} \sum_{(i,j) \in I_s} (m_{i,j_s,k,t}^H + m_{i,j_s,k,t}^{CBFW} + m_{i,j_s,k,t}^{BFW}) + \sum_{eq \in EQ} \sum_{v \in VHP} (Z_{eq,v,k,t}^{boi} + Z_{eq,v,k,t}^{HRSG}) + \sum_{i \in I} \sum_{j_s \in I_s} m_{i,j_s,k,t}^{MS}$
Hot oil system (HO)	<p>Overall hot oil supply:</p> $Q_{T,k,t}^{HO} = Q_{s,k,t}^{HO} + Q_{k,t}^{HO}$ <p>Heat provided above T_{max}:</p> $Q_{k,t}^{HO} = \sum_{j \in J_{HO}, T_j \geq T_{max}} \tilde{Q}_{j,k,t}^C$ <p>Overall energy demand in the sink cascade:</p> $\sum_i \sum_{(i,j) \in I_s} Q_{i,j_s,k,t}^{Cin} + Q_{T,k,t}^{HO} = \sum_j \tilde{Q}_{j,k,t}^C \quad \text{where} \quad Q_{i,j_s,k,t}^{Cin} = m_{i,j_s,k,t}^{CT} \cdot (\tilde{h}_{shj_s}^C - \tilde{h}_{i,j_s}^C)$ $Q_{s,k,t}^{HO} = \sum_{j_s, T_{j_s} > T_{i,j_s}^{HO}} (\tilde{Q}_{j,k,t}^C \cdot y_{j_s}^{HO})$ <p>Logical constraints:</p> $y_{j_s}^{HO} - y_{j_s-1}^{HO} \leq 0$ $y_{j_s}^{HO} + y_{i,j_s} \leq 1$

B.IV. Energy storage

Table P4.B. 4 Equations of energy storage main constraints

Item	Equations/Constraints
Balance:	$E_{es,d,t}^{es} = E_{es,d,t-1}^{es} (1 - \vartheta_{es}^{loss} \cdot \Delta t_t) + \eta_{es}^{ch} \cdot p_{es,\sigma(d),t}^{ch} \cdot \Delta t_t - \frac{p_{es,\sigma(d),t}^{dch}}{\eta_{es}^{dch}} \cdot \Delta t_t$
Periodicity:	$E_{es,d,t_1}^{es} = E_{es,d-1,t_1}^{es} (1 - \vartheta_{es}^{loss} \cdot \Delta t_t) + \eta_{es}^{ch} \cdot p_{es,\sigma(d),t_1}^{ch} \cdot \Delta t_t - \frac{p_{es,\sigma(d),t_1}^{dch}}{\eta_{es}^{dch}} \cdot \Delta t_t$
	$E_{es,1,t_1}^{es} = E_{es,D,t_1}^{es} (1 - \vartheta_{es}^{loss} \cdot \Delta t_t) + \eta_{es}^{ch} \cdot p_{es,\sigma(1),t_1}^{ch} \cdot \Delta t_t - \frac{p_{es,\sigma(1),t_1}^{dch}}{\eta_{es}^{dch}} \cdot \Delta t_t$
Depth of discharge (DoD)	$E_{es,d,t}^{es} \geq (1 - DoD_{es}) \cdot Z_{es}^{es}$
Sizing and logical constraints	$E_{es,\sigma(d),t}^{es} \leq Z_{es}^{es}$ $Z_{es}^{es} \cdot p_{es,\sigma(d),t}^{ch} \leq p_{es,\sigma(d),t}^{dch} \leq U_{es} \cdot y_{es}$
Molten salt constraints	$\sum_{MS} p_{MS,k,t}^{ch} = \sum_{v \in VHP_L} m_{v,k,t}^{VHP-MS} (\tilde{h}_{v_v} - \tilde{h}_{1_v})$ $\sum_{MS} p_{MS,k,t}^{dch} = \sum_{i \in I} \sum_{j_s \in I_s} m_{i,j_s,k,t}^{MS} (\tilde{h}_{shj_s}^{MS} - \tilde{h}^{BFW})$
Steam accumulator constraints	$\sum_{SA} p_{SA,i,j_s,j_s',k,t}^{ch} = m_{i,j_s,j_s',k,t}^{C_{ch-SA}} \cdot \tilde{h}_{shj_s}^C$ $\sum_{SA} p_{SA,i,j_s,j_s',k,t}^{dch} = m_{i,j_s,j_s',k,t}^{C_{dch-SA}} \cdot \tilde{h}_{v_{j_s}}$

B.V. Logical constraints

Table P4.B. 5 Logical constraints of the model

Item	Equations/Constraints
Steam level selection	$\sum_{v \in VHP_L} y_v = 1 ; \sum_{(i,j) \in I_s} y_{i,j_s} \leq 1 ,$ $y_{eq,L,k,t} \leq y_L$ $y_{UC,LL,k,t} \leq \frac{y_L + y_{L'}}{2}$

Feasibility constraint	$m_{i,j_s,k,t}^{\text{in}} - U_{k,t}^m \cdot y_{i,j_s} \leq 0$ $m_{i,j_s,k,t}^{\text{out}} - U_{k,t}^m \cdot y_{i,j_s} \leq 0$ $Q_{i,j_s,k,t}^{\text{in}} - U_{k,t}^Q \cdot y_{i,j_s} \leq 0$ $Q_{i,j_s,k,t}^{\text{out}} - U_{k,t}^Q \cdot y_{i,j_s} \leq 0$	(B.52)
Enthalpy constraints	$\underline{h}_{\text{sh}_v} y_v \leq h_{\text{sh}_v} \leq \overline{h}_{\text{sh}_v} y_v m_{i,j_s,k,t}^{\text{out}} - U_{k,t}^m \cdot y_{i,j_s} \leq 0$ $\underline{h}_{\text{sh}_{j_s}} y_{i,j_s} \leq h_{\text{sh}_{j_s}} \leq \overline{h}_{\text{sh}_{j_s}} y_{i,j_s}$ $h_{\text{sh}_{j_s}} \leq \sum_v h_{\text{sh}_v}$ $h_{\text{sh}_{j_s}} \leq \sum_{(i-1,j_s') \in I_{j_s}} [h_{\text{sh}_{j_s}} + \overline{h}_{\text{sh}_{j_s}} (1 - y_{i,j_s'})]$	(B.53)

Conclusions and future work

Overview

This chapter provides a thesis summary by highlighting the main contributions, outcomes and limitations. In addition, several guidelines for future research direction are stated.

6.1 Conclusions

This work aimed to assist process industries in reducing their energy consumption and greenhouse gas emissions to contribute to sustainable development in the industry sector. In this context, a comprehensive and flexible process utility system design decision-making tool has been developed, encompassing engineering, economic and environmental aspects. The key outputs of this work are summarized according to the general objectives of this thesis (Section 1.4), which are detailed as follows:

6.1.1 Modelling and optimization of industrial energy systems, accounting for heat integration and more realistic and accurate conditions and targets

In Chapter 3 (Contribution 1 and Contribution 2) the need for considering steam main operating conditions as part of design and optimization of utility systems was proved. Nevertheless, its integration into the optimization model increases the complexity of the model, resulting in a nonconvex MINLP problem. For small-scale cases, the problem can be solved directly through state-of-the-art solvers such as BARON. However, due to the high combinatorial nature and size of real-world utility site problems, a direct approach could be computationally challenging even for systems that only consider conventional technologies, as demonstrated in Contribution 2. Therefore, two strategies were formulated to approach the issue. The first strategy involves a sequential approach of MILP and simulation stages, presented in Contribution 1, while the second strategy comprises a solution pool based bilevel decomposition.

The work presented in Contribution 1 allowed identifying the following insights:

- The synthesis of utility systems considering allocation of steam (pressure) levels can reduce not only fuel consumption but also cold utility requirements. In Contribution 1, two optimizations for the synthesis of a utility system for an industrial case study, one considering fixed pressures (as referred in the literature) and another considering steam pressure level optimization were used for the analysis. The comparison demonstrated that optimization of pressure levels increased site heat recovery (process steam generation) by 35.3 %, for the particular case study. This results in a reduction of 15.8 % and 13.3 % of fuel and cooling water consumption, respectively.
- Site-wide energy integration based on steam mains at saturated conditions results in significant inaccuracies of the potential heat recovery and cogeneration. The results from a case study showed that the assumption of saturated conditions for the steam distribution results in a 12.9 % higher demand of utility steam, in addition to a 34.7 % lower power generation per unit of utility steam flow.
- The inclusion of practical considerations as maximum steam temperature permitted - especially for steam distribution and/or process heating - not only avoid prohibitively expensive and unsafe configurations, but also allow for the obtaining of more realistic energy targets. Moreover, Contribution 1 highlights the need to consider additional utility options such as fired heating in the design of utility systems. Hot oil systems demonstrated to be a cost-effective utility for meeting several relatively small amounts of heat at relatively high-temperatures (up to 400 °C).
- Contribution 1 highlights that heat recovery options, such as recovery of steam condensates through flash steam systems, could further reduce the industrial site demand. The results of the case study showed that the integration of flash steam tanks result in an additional 15.7 % fuel reduction, at a marginal cost.
- Contribution 1 also demonstrates that a higher number of steam mains reduces energy requirements, due to a higher site heat integration. However, its economic viability could limit the number of steam mains. A high-level economic analysis (were piping costs were not included) showed that the economic benefit also decreases with the number of steam mains.

Due to the generation of good feasible solutions at a low computational effort (in a range of few minutes) as demonstrated in Contribution 2, the methodology developed in Contribution 1 was used as a starting point to develop systematic approach presented in Contribution 2. In Contribution 2, a solution pool based bilevel decomposition strategy was proposed for the simultaneous optimization of utility system configuration and steam main temperature.

The proposed methodology was compared against state-of-the-art solver BARON. The results presented from three different case studies under different scenarios, that the bilevel decomposition

combined with a solution pool strategy, provides better results in terms of solution quality and computational time.

Furthermore, the presented work demonstrates that one of the challenges of such problems is the high combinatorial nature of the system, where not only different equipment configurations, but enthalpy-pressure combinations, and strong interactions among the system and the site processes, could result in different near-optimal solutions. The results in Contribution 2 shown how two utility systems designs -- where one of the steam mains pressure differ -- can present a total cost difference of only 0.3%, and within 2.6 % of the best known lower cost.

6.1.2 Synthesis of flexible industrial utility system, able to operate under variable demand and supply, accounting for energy price fluctuations

Contribution 3 considers the impact of energy demand variations on the design of process utility systems and in the reduction of energy consumption. The effect of potential shift in the primary energy sources prices is also analyzed to define how the optimal design would vary consequently to such shifts. To do so, the methodology developed in Contribution 2 is adapted to consider multi-period analysis and the integration thermal and electrical storage. The superstructure also integrates low carbon technologies such as biomass boilers, gasifiers and biogas turbines.

The case-study results of Contribution 3 provide the following insights:

- Under current investment costs and considering median European energy prices, the results show that the optimal design heavily relies on fossil fuel units to meet the energy needs of the site. Nevertheless, on-site heat and power generation enables around 20 % savings of primary energy (without considering heat recovery) in comparison with separate heat and power generation standards.
- The integration of low carbon technologies and energy storage require further attention of policy makers, as the increase of fossil fuel prices could incentive the deployment of low-carbon technologies; however, it still cannot yet compete against their fossil-based counterparts.
- If the system is capable of exporting energy, investment in energy storage is not an economically optimal choice. Flexible design minimizes costs by exporting power to the grid rather than storing it for later use. This could be explained as energy storage are round-trip losses (and energy leakage), in addition to the capital costs associated with its implementation. Nonetheless, if installation costs for hydrogen storage systems are reduced by approximately two-thirds of their current levels, potential benefits may be found in scenarios with increasing grid electricity costs or in scenarios where electricity export is not possible.
- The optimal design of utility systems is heavily influenced by external factors such as energy tariffs, which can define technology and operational thresholds. When electricity prices are

comparable to natural gas prices (price ratio of 1.75), the optimal system operation shifts only to import electricity. Moreover, as the electricity nominal price falls, heat electrification becomes cost-competitive, where for prices as low as 1.15 times the current natural gas price (≈ 24 €/MWh) fossil fuel units are phased-out.

- On the other side, for increasingly expensive electricity prices (above 1.75 times the cost of fuel), the utility system is designed in such a way that onsite generation meets energy consumption and generates revenues by exporting excess electricity to the grid. It is important to mention that at this point the price difference between fossil gas and biomass may influence the fuel choice for thermal and power generation units.

6.1.3 Integration of economic and environmental sustainability criteria to the conceptual design of industrial utility systems

In previous chapters, different technologies and scenarios were assessed for the design of cost-effective industrial energy systems. While significant energy savings can be achieved through energy efficiency and economic objectives, further CO₂ mitigation requires the use of a multi-objective optimization approach to assess the trade-offs between economic and environmental impacts. As a result, in Chapter 5, the design and optimization framework is extended to achieve cost-effective designs that are sustainable. Due to the widespread acceptance of CO₂-eq emissions as a proxy for environmental impact in the design of low-carbon energy systems, industrial designs based on total annualized cost and CO₂-eq emissions are carried out in Chapter 5. Nonetheless, the remaining environmental indicators are also measured.

Based on the results of Contribution 4, the following conclusions can be drawn:

- Hollistic optimization of the system can lead to not only higher energy efficiency and cost savings but also can reduce the overall environmental impact of the system. For the case study presented, GHGs emissions can be reduced. Based on cost oriented designs, GHGs emissions can be reduced up to 26 % by enhancing site heat recovery. Moreover, environmental issues such as air, water and soil pollution, ecotoxicity and resources depletion can be also reduced between 6 and 67 %.
- - To achieve further reductions, a gradual shift away from fossil fuel sources and technologies is required. The framework allows to explore different trade-offs between economic and environmental impacts. For instance, fuel switching from fuel gas to natural gas boilers could result in a 15% reduction in emissions at a marginal cost ($\approx 1\%$).
- - Further constraints on system CO₂ emissions promotes the shift from natural gas to biomass technologies. This highlights the relevance of CO₂ targets as an effective decarbonization strategy in industrial energy systems. Nevertheless, it is important to note that the use of natural

gas remains significant up to 80% CO₂ emissions reduction. This can be explained by the high flexibility and cogeneration potential of gas turbines.

- To meeting ambitious GHG reduction targets (above 80% CO₂ abatement), two elements are key: phase-out of natural gas technologies and deployment of storage units. Moreover, the findings show that energy transition is technically feasible, but that total costs will increase by a factor of three. More important, certain environmental categories, such as human toxicity, terrestrial ecotoxicity and mineral resource depletion, are rapidly deteriorating as the CO₂ emissions restrictions are increased.

Overall, it is feasible to design low-carbon industrial energy systems. However, it is done at the expense of total costs and deterioration of other environmental impact factors. While the former is largely dependent on technological advancements and their associated impact on operational costs, potential burden-shifting could be avoided by considering environmental impacts other than only fossil fuel depletion and CO₂-equivalent emissions. In this context, government strategies should take into account the aforementioned environmental effects, rather than focusing exclusively on climate change and fossil fuel depletion.

6.2 Future work

While this thesis addresses a number of issues concerning the optimal design of industrial utility systems integrating site heat recovery and a variety of different types of energy conversion technologies and energy storage, it also lays the groundwork for the exploration and integration of emerging low-carbon technologies and energy sectors. Additionally, areas for further exploration into the optimal design of industrial utility systems using sustainable criterion are identified. The next subsections outline some future research directions that could expand the range of applicability of the proposed modelling framework by incorporating model features that were not included in this work. However, it should be noted that the addition of further model details is expected to increase the size and complexity of the problem significantly, thus requiring preliminary enhancement of the current synthesis methodology to guarantee its practical applicability at a reasonable computational effort.

6.2.1 Incorporation of emerging technologies to the framework

The methods and tools developed in this work could enable the assessment of diverse emerging technologies and energy storage options. Future research should include emerging low carbon technologies such as high temperature heat pumps, concentrated solar power and power-to-gas systems to evaluate its potential implementation on the utility system, and put

in perspective with different technology options. Similarly, additional seasonal electrical and thermal energy storage alternatives can be integrated to the optimization framework.

6.2.2 Extending the framework to include other end-user sectors

The optimization framework was limited to industrial steam systems, where low temperature heat was assumed to be rejected to cooling water. Future work should consider other opportunities to exploit industrial waste heat, such as (i) generation of hot water for district heating, and (ii) further electricity generation through Organic Rankine Cycles. Moreover, inclusion of energy demands of transport and residential sectors should be considered.

6.2.3 Extending the framework to take into account location and piping

For large sites, long distances between processes might result in poor mixing and significant pressure drop along the main. Thus, conditions inside a single main might vary considerably in different parts of the site. If this turns out to be a significant problem, virtual steam mains will need to be added to the model to represent the varying conditions in different geographic locations. Moreover, it could also imply additional constraints to the site heat recovery.

6.2.4 Extending the framework to account uncertainty in the conceptual design of industrial utility systems

The optimization framework presented in this thesis is based on deterministic variation of certain parameter such as energy price markets and site operating profiles. A sensitivity analysis with respect to different energy prices and potential scenarios highlighted the strong dependence of the optimal design to this parameter. However, there is highly uncertainty regarding energy pricing, technological development, and regulatory frameworks on the long term. Inclusion of uncertainties for future scenarios in the optimization framework could increase the robustness (and complexity) of the utility design.

Stochastic and robust optimization techniques have been proposed to tackle uncertainty problems. The major issue here is the trade-off between model accuracy and computational tractability. Both approaches usually required large amount of information and increase the computational burden (due to the increment in the size of the problem). For this, mathematical enhancements may be required to tighter convex relaxations, improve the speed of convergence, and reduce the computational costs.

6.2.5 Integration of other sustainability criteria for the design and optimization of industrial utility systems

In this thesis, the optimal utility system design has considered the life cycle of CO₂ equivalent emissions of conversion and storage technologies. However, integrating other environmental (i.e. acidification, ecotoxicity, resource depletion) and social impacts (i.e. job

creation, local economic benefits, social acceptance) into the optimization framework may provide a more comprehensive overview for the sustainable development of process utility systems. Including many objective functions in system design, on the other hand, complicates the decision-making process and increases the computational effort. Tools like principal component analysis (PCA) and multiple criteria decision-making (MCDM) may be applied to reduce the problem dimension.

6.3 Concluding remarks

In this thesis, a methodological framework for the optimization-based design of process utility systems is proposed to reduce industrial primary energy requirements and enhance sustainable development.

The proposed framework identifies promising process utility systems that can significantly reduce industrial energy demand and CO₂ emissions at marginal cost variations for the real-world problems considered in this thesis. The findings of this study show the importance of a holistic approach where site-wide heat recovery and energy carrier's quality levels are taken into account to achieve further reductions in industrial energy demand. In fact, due to the highly combinatorial nature of the synthesis problem, several near-optimal solutions can be obtained with minor variations in the objective function and thus be practically equally good. While the design engineer may question the absolute need for an optimization-based synthesis tool that includes energy quality, it is essential to note that it is nearly impossible to identify solutions such as those presented in this thesis without considering all of these factors simultaneously. Not only because the design could differ in terms of energy quality level selection but also in terms of equipment configuration, sizing, and operation. While the results of this study are based on a specific set of components and technologies, the proposed methodology can be helpful to design engineers, industrials, and policymakers in exploring different energy sources and technologies and making more informed decisions.

Finally, it is hoped that the general public can gain an appreciation that there is no "one-size-fits-all" solution, mainly due to the strong interrelationships between the utility system design/operation and the scenario conditions (e.g. site energy demands, available sources and technologies, energy prices and policies). Therefore, optimization-based frameworks are essential to enhance industrial energy transition in a cost-effective way.